

AD-A037 334

ADVISORY GROUP FOR AEROSPACE RESEARCH AND DEVELOPMENT--ETC F/G 20/1
AERODYNAMIC NOISE.(U)

JAN 77

UNCLASSIFIED

AGARD-LS-80

NL

1 OF 4
AD
A037334



ADA037334

AD NO. —
DDC FILE COPY

B.S. 
AGARD-LS-80

AGARD

ADVISORY GROUP FOR AEROSPACE RESEARCH & DEVELOPMENT

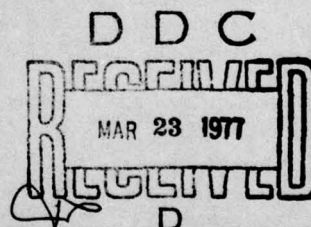
7 RUE ANCELLE 92200 NEUILLY SUR SEINE FRANCE

COPY AVAILABLE TO DDC DOES NOT
PERMIT FULLY LEGIBLE PRODUCTION

AGARD LECTURE SERIES No. 80

on

Aerodynamic Noise



NORTH ATLANTIC TREATY ORGANIZATION



DISTRIBUTION AND AVAILABILITY
ON BACK COVER

DISTRIBUTION STATEMENT A
Approved for public release;
Distribution Unlimited

ACCESSION TAG	
White Section	<input checked="" type="checkbox"/>
Buff Section	<input type="checkbox"/>
Per Hrs. on file	
AVAILABILITY CODES	
AVAIL. CODE/SPECIAL	
A	

14 AGARD-LS-80

NORTH ATLANTIC TREATY ORGANIZATION
 ADVISORY GROUP FOR AEROSPACE RESEARCH AND DEVELOPMENT
 (ORGANISATION DU TRAITE DE L'ATLANTIQUE NORD)

AGARD Lecture Series No.80

6 AERODYNAMIC NOISE

11 Jan 77

12 307p.

DDC
 RECEIVED
 MAR 23 1977
 RECEIVED
 D

DISTRIBUTION STATEMENT A
 Approved for public release
 Distribution Unlimited

The material in this book has been assembled to support a Lecture Series under the sponsorship of the Fluid Dynamics Panel, the von Kármán Institute and the Consultant and Exchange Program of AGARD, presented at the von Kármán Institute, Rhode St Genèse, Belgium in December 1976.

400 043

LB

THE MISSION OF AGARD

The mission of AGARD is to bring together the leading personalities of the NATO nations in the fields of science and technology relating to aerospace for the following purposes:

- Exchanging of scientific and technical information;
- Continuously stimulating advances in the aerospace sciences relevant to strengthening the common defence posture;
- Improving the co-operation among member nations in aerospace research and development;
- Providing scientific and technical advice and assistance to the North Atlantic Military Committee in the field of aerospace research and development;
- Rendering scientific and technical assistance, as requested, to other NATO bodies and to member nations in connection with research and development problems in the aerospace field;
- Providing assistance to member nations for the purpose of increasing their scientific and technical potential;
- Recommending effective ways for the member nations to use their research and development capabilities for the common benefit of the NATO community.

The highest authority within AGARD is the National Delegates Board consisting of officially appointed senior representatives from each member nation. The mission of AGARD is carried out through the Panels which are composed of experts appointed by the National Delegates, the Consultant and Exchange Program and the Aerospace Applications Studies Program. The results of AGARD work are reported to the member nations and the NATO Authorities through the AGARD series of publications of which this is one.

Participation in AGARD activities is by invitation only and is normally limited to citizens of the NATO nations.

The content of this publication has been reproduced
directly from material supplied by AGARD or the authors.

Published January 1977

Copyright © AGARD 1977
All Rights Reserved

ISBN 92-835-0180-2



*Printed by Technical Editing and Reproduction Ltd
Harford House, 7-9 Charlotte St, London, W1P 1HD*

PREFACE

This Lecture Series 80 on 'Aerodynamic Noise' has been co-sponsored by the Fluid Dynamics Panel of AGARD and by the von Kármán Institute for Fluid Dynamics, and implemented by the Consultant and Exchange Programme of AGARD together with VKI.

The aim here is to provide an up-to-date account and an authoritative appraisal of aerodynamic noise concepts, theory and experiments. Particular emphasis is given to practical methods for the prediction, measurement and reduction of external noise from jet/fan aircraft. Following a brief overview of relevant aircraft design and operational considerations, the main lectures include detailed presentations on the fundamental theory of aerodynamic noise generation and propagation, basic aero-acoustics of jet efflux noise, engine exhaust noise characteristics, fan noise, airframe self-noise, airframe/engine interaction effects, aero-acoustic measurement and analysis techniques, aircraft flyover noise measurement, noise-source identification and location methods, and ground-based facilities with forward-speed representation.

The specialist lecturers from Europe and the USA deserve much appreciation for their extensive efforts and cooperation, in providing such valuable studies and preparing such comprehensive lecture notes for advance publication. Our acknowledgements are also due to the official and private organisations through whose help and courtesy it was possible to offer appropriate technical experts as lecturers. Finally, Professor John Sandford, the VKI Coordinator, warrants special mention for his local organisation of the Short Course at VKI, Rhode-St-Genèse (Belgium) from 6 to 9 December 1976.

John WILLIAMS
Lecture Series Director

LIST OF SPEAKERS

- Lecture Series Director: Professor J. Williams
Aerodynamics Department
Royal Aircraft Establishment
Farnborough
Hampshire, GU14 6TD
UK
- Speakers:
- Dr K.W. Bushell
Noise Department
Rolls-Royce (1971) Limited
P.O. Box 31
Derby DE2 8BJ
UK
- Dr M.J. Fisher
Institute for Sound and Vibration Research
University of Southampton
Highfield
Southampton SO9 5NH
UK
- Dr H.V. Fuchs
Institut für Turbulenz Forschung, DFVLR
Müller-Breslaustrasse 8
1 Berlin 12
Germany
- Dr J.C. Hardin
NASA Langley Research Center
Hampton
Virginia 23665
USA
- Dr M.E. House
Institute for Sound and Vibration Research
University of Southampton
Highfield
Southampton SO9 5NH
UK
- Dr B. Lowrie
Noise Department
Rolls-Royce (1971) Limited
P.O. Box 31
Derby DE2 8BJ
UK
- Professor M. Perulli
ONERA
92320 Châtillon-sous-Bagneux
France

CONTENTS

	Page
PREFACE	iii
LIST OF SPEAKERS	iv
	Reference
INTRODUCTORY COMMENTS ON AERODYNAMIC NOISE CONSIDERATIONS IN AIRCRAFT DESIGN AND OPERATION by J.Williams	1
BASIC AERODYNAMIC NOISE THEORY by H.V.Fuchs	2
JET NOISE by M.J.Fisher and C.L.Morfev	3
GAS TURBINE ENGINE EXHAUST NOISE by K.W.Bushell	4
FAN NOISE by B.W.Lowrie	5
AIRFRAME SELF-NOISE - FOUR YEARS OF RESEARCH by J.C.Hardin	6
PAPER NOT AVAILABLE	7
AERO-ACOUSTIC MEASUREMENT AND ANALYSIS TECHNIQUES by M.E.House	8
AIRCRAFT FLYOVER MEASUREMENTS by M.E.House	9
COMPARAISON DE DIFFERENTES METHODES DE LOCALISATION ET D'IDENTIFICATION DE SOURCES SONORES DE TURBOREACTEURS par M.Perulli	10
GROUND-BASED FACILITIES WITH FORWARD-SPEED REPRESENTATION FOR AIRCRAFT NOISE RESEARCH by J.Williams	11
BIBLIOGRAPHY	B

INTRODUCTORY COMMENTS ON AERODYNAMIC NOISE CONSIDERATIONS
IN AIRCRAFT DESIGN AND OPERATION

by

John Williams

Aerodynamics Department, Royal Aircraft Establishment,
 Farnborough, Hants, GU14 6TD, England

1 BASIC AIRCRAFT DESIGN FACTORS AND INTERACTIONS

The designers of even quieter aircraft will have to exploit and carefully integrate a number of modern R&D techniques simultaneously, in order to avoid unacceptable economic penalties, taking into account rising fuel costs and environmental constraints, while still meeting complementary demands for maintaining or improving operational and airworthiness standards. In particular from our present viewpoint (Fig 1), the engine design, the airframe design, the aircraft flight performance, and possible engine/airframe aero-acoustic interference all have to be analysed with a significant bias towards the reduction of noise annoyance (on the ground) caused by take-off, landing and other low-altitude subsonic operations. The problem of achieving economically much lower noise levels (order of 10 PNdB reduction) outside airport boundaries is also now aggravated by the need to predict and guarantee the noise field from future aircraft projects to a much greater accuracy than hitherto (within ± 1 PNdB). While this applies primarily to civil transport operations, similar reductions and predictions are also desirable for some military operations; not merely for transports but also for low-level search and reconnaissance aircraft, and for the avoidance of detection as well as annoyance. The allied topics of helicopter external noise, sonic bangs from high-speed operations, and cabin internal noise are also important but will not be discussed further here.

From an engine-noise viewpoint (Fig 2), a more comprehensive engine-cycle parameter than Bypass-ratio (BPR) is the Static Specific Thrust, namely,

$$SST = (\text{Static Take Off Thrust}) / (\text{Total Air Mass Flow Rate}) \dots \text{N/kg/s.}$$

This represents sensibly the mean jet velocity, V_j m/s. For a prescribed take-off thrust, the unsilenced efflux noise generally reduces with decreasing SST and with increasing BPR. For the low bypass-ratio engines still employed on many subsonic transport aircraft ($BPR < 2$), the noise generated by mixing of the high-speed jet efflux ($SST > 500$ N/kg/s) with the atmosphere has usually predominated. This is of course equally true for both supersonic transports and combat aircraft, often incorporating exhaust reheat in order to further increase the specific thrust. Some suppression of exhaust noise has been achieved by a variety of methods such as special nozzle shapes to modify jet-mixing or to provide shielding, and by acoustic lining/absorber treatments; but usually associated with loss of thrust, higher specific fuel consumption (sfc) and extra weight. More elaborate approaches can involve engine re-fanning to increase the bypass-ratio for present-day subsonic transports, typically $BPR \approx 3$ for a fixed-pitch fan, or much higher with a variable-pitch fan; but the resulting advantages and disadvantages as regards performance and retrofit costs have to be carefully assessed and balanced.

The more modern engines of increased bypass-ratio ($BPR \approx 5$), facilitated by the considerable advances in high-temperature technology, aerodynamics and mechanical design, have provided not only profitable decreases in engine sfc and useful augmentation of the ratio of available take-off thrust to cruise thrust, but also substantial reductions in jet-mixing noise because of the much lower jet-efflux speed ($SST \approx 300$ N/kg/s). Internally generated noise from such sources as the fan, compressor, turbine and combustion system then became relatively important at some flight conditions, although a modest amount of acoustic lining in relevant ducts sufficed to alleviate this - by the order of 5 PNdB then demanded - without significant cost penalties.

The development of even quieter turbo-fan engines is already projected, partly through the more elaborate use of absorbent liners and splitters in engine ducts (Fig 3), through designing components so as to further minimise noise generation at source, and through some engine cycle modifications to reduce core-jet speed from 400 m/s to about 270 m/s - ie to roughly the same as the bypass-jet speed. About 5 PNdB further reduction in engine noise has been foreseen without any substantial increase in bypass-ratio or large decrease in specific thrust, but the resulting growths in engine weight, sfc and costs are together likely to be significant, while associated nacelle/airframe installation factors still need careful appreciation. More generally, although further reduction in engine noise is required if aircraft are to achieve noise levels some 5 to 10 EPNdB below the present standards of ICAO Annex 16 and FAR Part 36 (Fig 4), a careful synthesis of the engine and airframe combination for low noise as well as for other operational requirements becomes vital to avoid unacceptable penalties on aircraft operating costs and safety (Fig 1).

Firstly the aircraft performance characteristics, while still meeting the mission operational requirements, may also be exploited for aircraft noise reduction and smaller noise footprints at take-off and landing (Figs 5 and 6). For example, minimisation of thrust required for airfield performance can signify less noise generated at source; or steeper take-off and landing paths can provide greater separation from the ground and thereby greater distance for noise attenuation. Shorter field lengths can imply a shorter noise footprint (though probably wider) and possibly less duration of objectionable noise levels. Also, even some relaxation of en-route operational demands may permit optimisation of the engine/airframe combination towards a quieter aircraft; eg if maximum speed subsonic not transonic/supersonic.

Next, particular airframe design features (Fig 7) can be significant either indirectly or directly for aircraft noise reduction. For example, the choice of aerodynamic/structural design parameters such as wing aspect-ratio and sweep, in conjunction with the high-lift device arrangements, can reduce in particular the thrust required and allow steeper flight-path gradients. Minimisation of the airframe self-noise, associated particularly with the deployment of the high-lift devices and the undercarriage for landing (Fig 8), may be needed if the engine noise levels are even further reduced. Airframe-surface shielding of engine noise sources (Fig 9a) can be achieved by reflection of radiated sound away from rather than towards the observer on the ground, though penetration into the geometric shadow becomes important because of the edge-diffraction effects at the lower frequencies. Airframe flow-field shielding of engine noise sources (Fig 9b) by refraction of the propagated sound waves also can be significant, such as with trailing vortices located to the side of and below the noise source.

Finally, the aero-acoustic interference between the engine airflow and the neighbouring airframe surface should be minimised (or tailored) to preclude excess noise (or even reduce noise). For example, airframe-surface proximity to the engine intake-flow or jet-exhaust can interact with the engine flow development, thus augmenting or modifying the engine noise sources. Correspondingly, engine exhaust-flow interaction with the local airframe surface can cause extra airframe noise from surface scrubbing or edge-discontinuity effects. This is particularly significant with the increased diameter of the higher bypass-ratio engines compared with wing-chord and ground-clearance dimensions, or with powered-lift applications (eg Fig 10).

Noise technology is the scientific/engineering discipline to which our attention has to be concentrated primarily here. Nevertheless, the effects of any advances in noise technology on the design and operation of economic quiet aircraft cannot be assessed in isolation from the advances in other technologies or from new operational requirements. Even preliminary aircraft design studies must involve many interacting factors drawn from a wide range of aeronautical disciplines; including aerodynamics, structures, propulsion and materials. Fortunately, researches in these areas as well as in noise continue to offer significant technological advances towards achieving better compatible standards of aircraft flight performance, operational economics, airworthiness and noise characteristics.

These general comments on aerodynamic noise considerations in aircraft design and operation can be amplified usefully during the spoken lecture, by appropriate simplified analysis and synthesis of some basic concepts concerning external noise generation and propagation, to help expedite appreciation of the practical significance of the subsequent main lecture topics. Important engine/airframe design interactions and possible costs implications of noise reductions may also be illustrated conveniently by typical results from some exploratory parametric studies for preliminary design optimisation of subsonic swept-wing transports.

2 PURPOSE AND SCOPE OF MAIN LECTURES

The major targets of the present lecture series might reasonably be summarised as follows, with special reference of course to aircraft noise characteristics (engine + airframe):-

- 1) To critically review available prediction/optimisation methods and associated noise data, particularly with a view to clarifying recent advances towards noise reduction.
- 2) To formulate more comprehensive frameworks for the analysis and synthesis of noise data, so that the latter can be more readily appreciated and more readily applied for aircraft design purposes.
- 3) To assess the major deficiencies in the state of knowledge on noise characteristics and noise alleviation treatments, and to suggest appropriate noise research and related development studies bearing in mind possible future aircraft operational requirements.
- 4) To indicate the most profitable steps towards complementary systematic utilisation of and further improvement of theoretical treatments, ground-based testing facilities and flight testing techniques for the reliable prediction and efficient reduction of aircraft noise.

Obviously, it would be unrealistic to claim that any of these goals could be achieved to our satisfaction by this lecture series alone. However, I hope that these published papers, together with any supplementary contributions during discussions, will provide a reasonably comprehensive basis, stimulate further evaluation of the issues raised, and encourage useful exchanges of relevant information and ideas.

The following main lectures therefore aim to provide overall an up-to-date account and an authoritative appraisal of aerodynamic noise concepts, theory and experiments; particular emphasis being devoted to practical methods for the prediction, measurement and reduction of external noise from jet/fan aircraft. Detailed presentations are made on the ten specific topics, ranging from basic aerodynamic noise theory through engine/airframe noise considerations to relevant experimental methods, as given in the 'List of Contents'. These individual topics could have been selected in a variety of ways, but the present arrangement offered a logical choice to cover both theoretical and experimental aspects, along with both research and application interests, without much repetition. Additionally, it expedited agreement by official and industrial establishments in several countries to provide acknowledged experts, not only with special knowledge of their own selected topic, but also with considerable interest and experience in some of the others. This should help encourage profitable discussions throughout the Short Course, including exchange of recent experience, particularly to clarify novel problem areas where divergent opinions may arise. Indeed we should express our appreciation to AGARD, VKI and the contributing technical organisations for meeting the demand to have nine appropriate lecturers to attend from the USA, UK, Germany and France.

Most of the lectures published here contain useful lists of reports for further reference on the particular topics, while a general bibliography with abstracts has also been prepared in the UK by the Defence Research Information Centre of MOD(PE), to support AGARD LS 80. At this stage therefore, perhaps I need refer only to two sets of AGARD papers relating to aerodynamic noise, which in many respects are complemented and up-dated by the present Lecture Series:-

- 1) 'Noise mechanisms'. AGARD CP 131 (Sept 1973).
- 2) 'Aircraft noise generation, emission and reduction'. AGARD LS 77 (June 1975).

To those further interested in the wider implications of aircraft noise reduction on aircraft design and operation, I would also recommend the collection of ten papers which I had the privilege and pleasure of organising for a Royal Aeronautical Society Symposium last year, namely:

- 3) 'The impact of economics on the design and operation of quieter aircraft'. Proc. RAeS Sympos., London (April 1975).

The opinions expressed by the author in this lecture are personal and do not necessarily represent official views.

Copyright © Controller, Her Majesty's Stationery Office, London 1976.

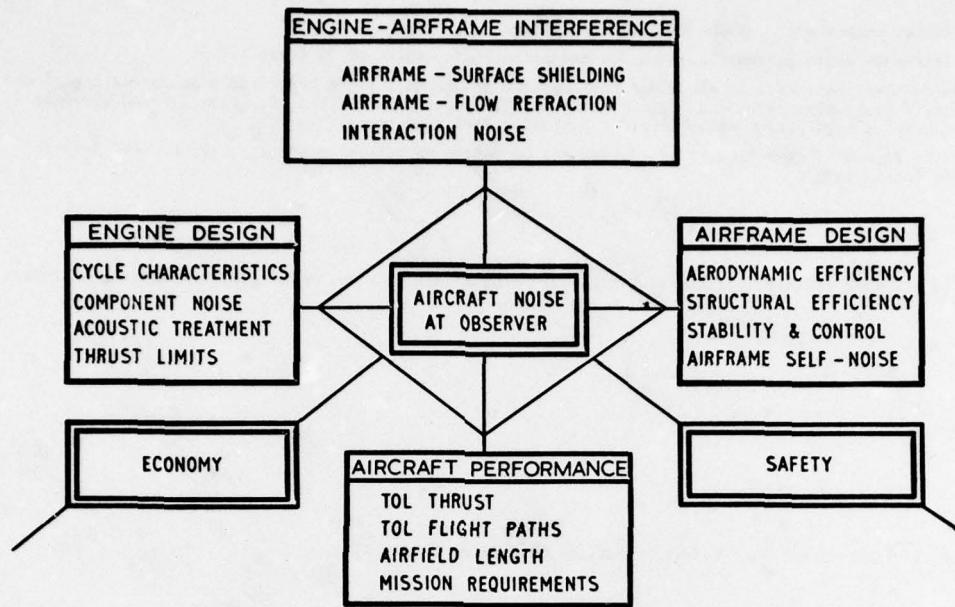
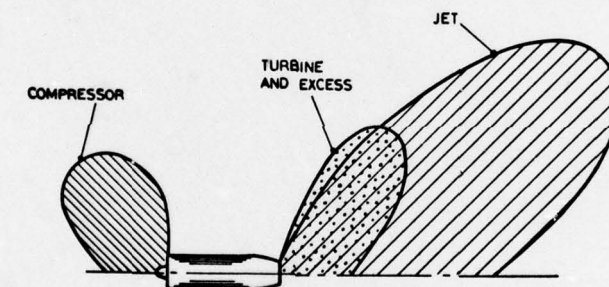
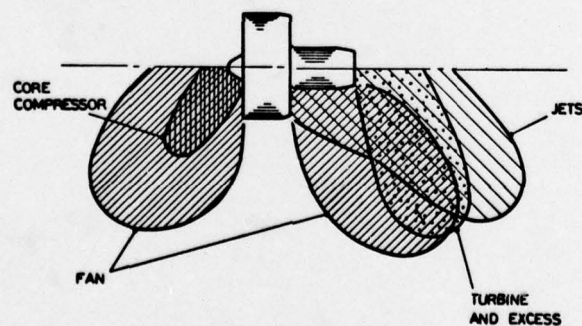


Fig.1 Aircraft design factors influencing noise

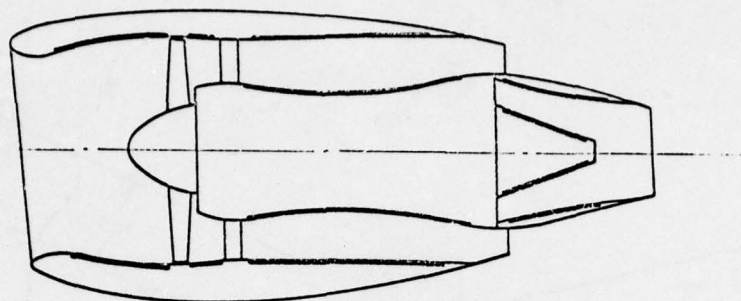


SIMPLE JET ENGINE

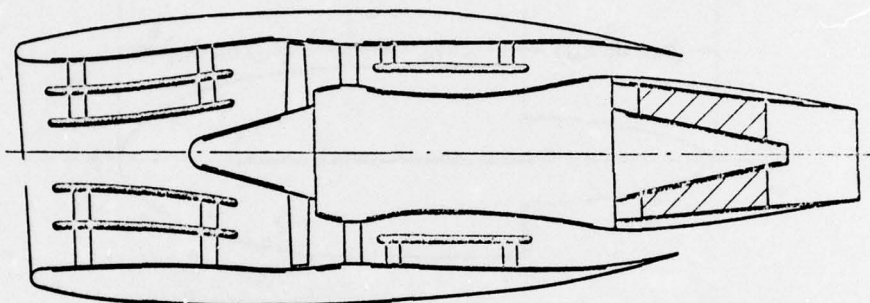


MODERN TURBO-FAN ENGINE

Fig.2 Ingredients of engine noise



TYPICAL CURRENT POWERPLANT



LAYOUT WITH EXTENSIVE TREATMENT

Fig.3 Powerplant layouts with acoustic treatment

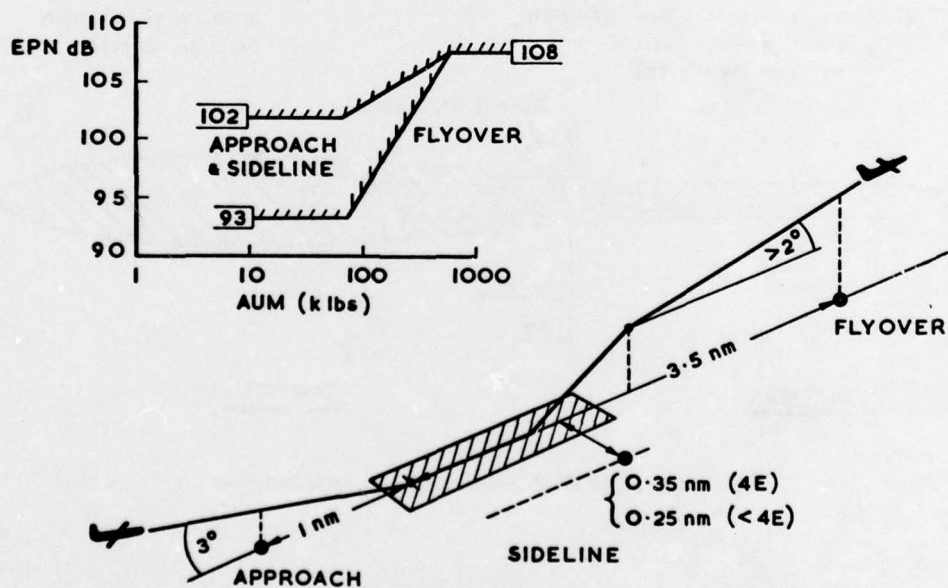


Fig.4 CTOL noise certification (1972)

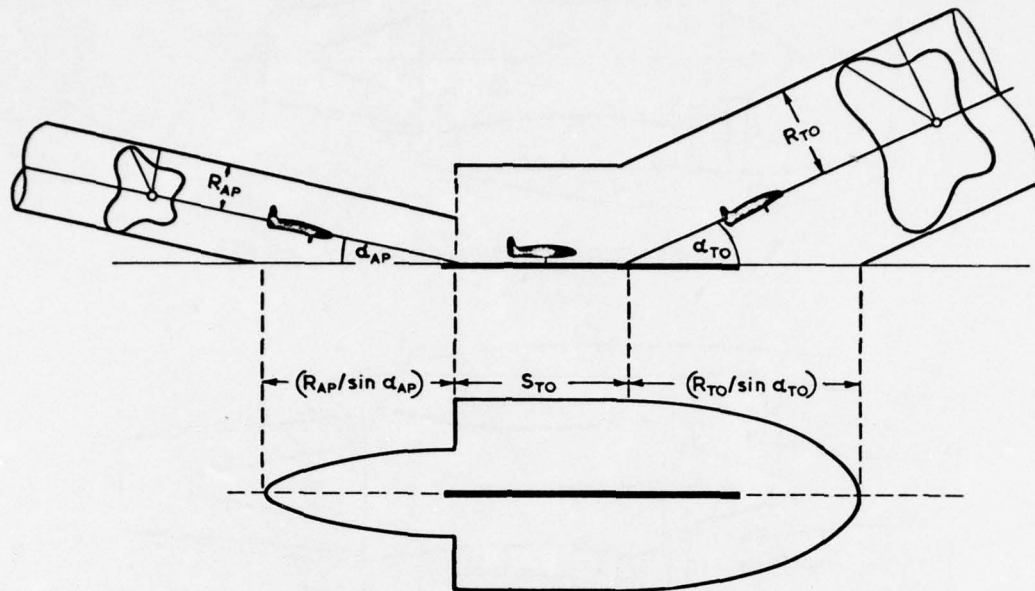




Fig.5 Noise footprint area $\approx \frac{1}{2}(\pi R_{AP}^2/\sin \alpha_{AP}) + 2R_{TO}S_{TO} + \frac{1}{2}(\pi R_{TO}^2/\sin \alpha_{TO})$

 Aircraft with current high by-pass ratio engines

 Aircraft with engines 10 PNdB quieter (without weight or performance penalties)

AIRCRAFT FEATURES:

Twin engines
2000 km range
2000 m field length
200 passengers

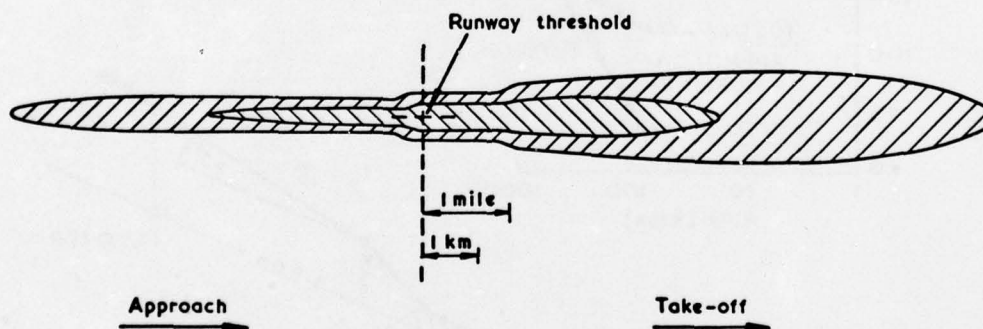


Fig.6 Effect of 10 PNdB noise reduction on noise footprints

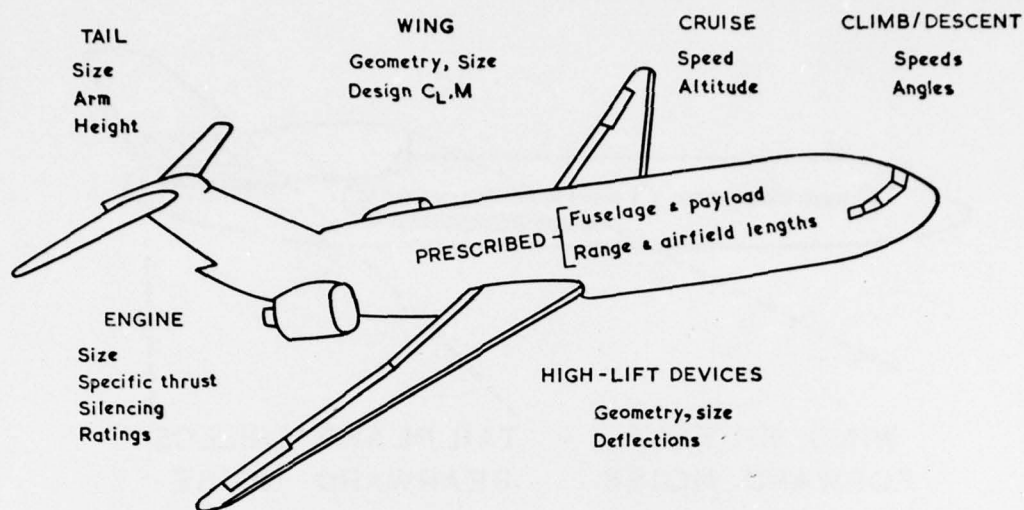


Fig.7 Typical performance variables

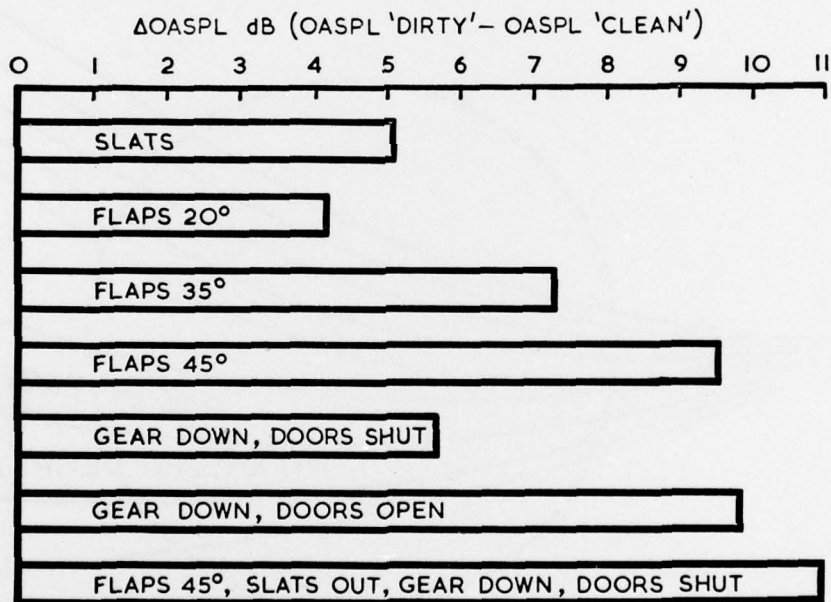


Fig.8 VC10 noise increases due to changes from the 'clean' aircraft configuration (residual engine noise extracted)

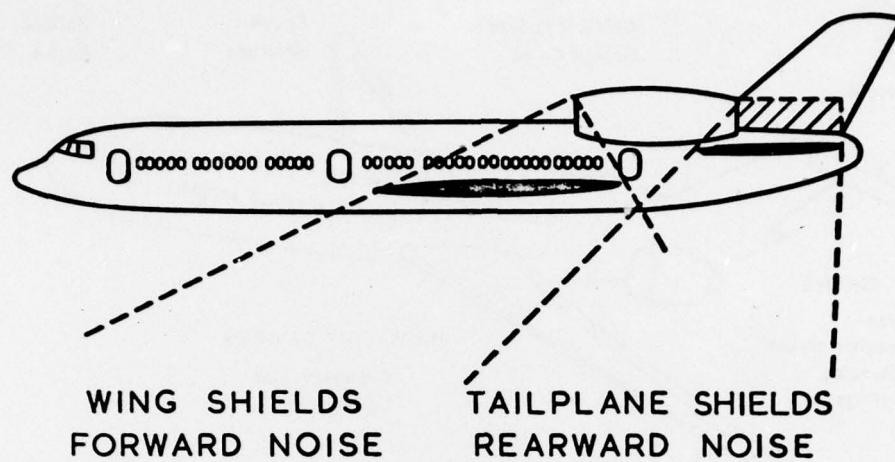


Fig.9(a) Airframe surface shielding engine noise

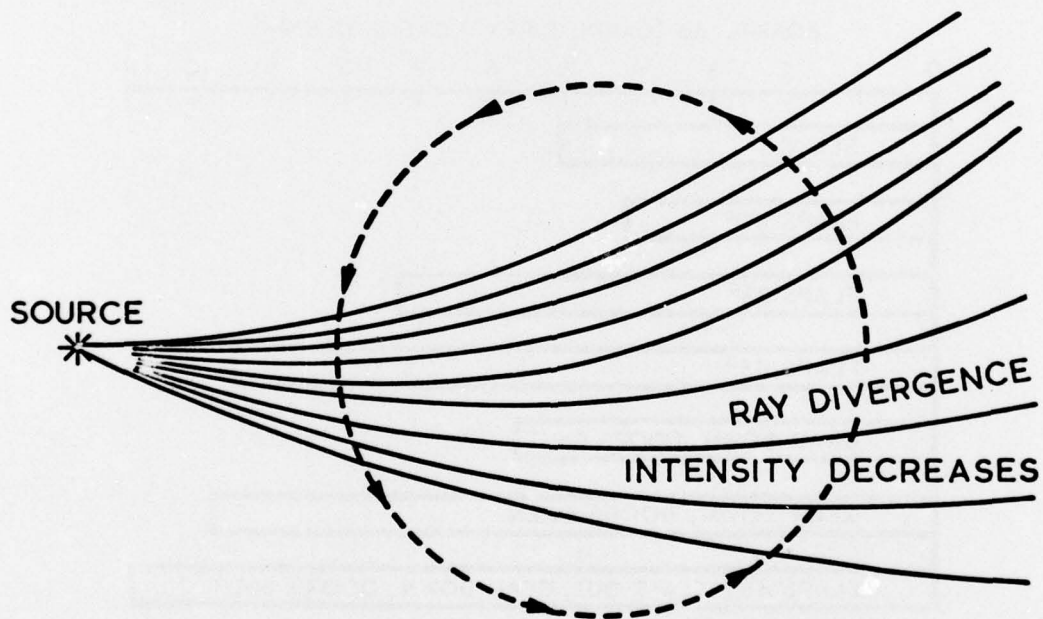


Fig.9(b) Ray paths through a vortex

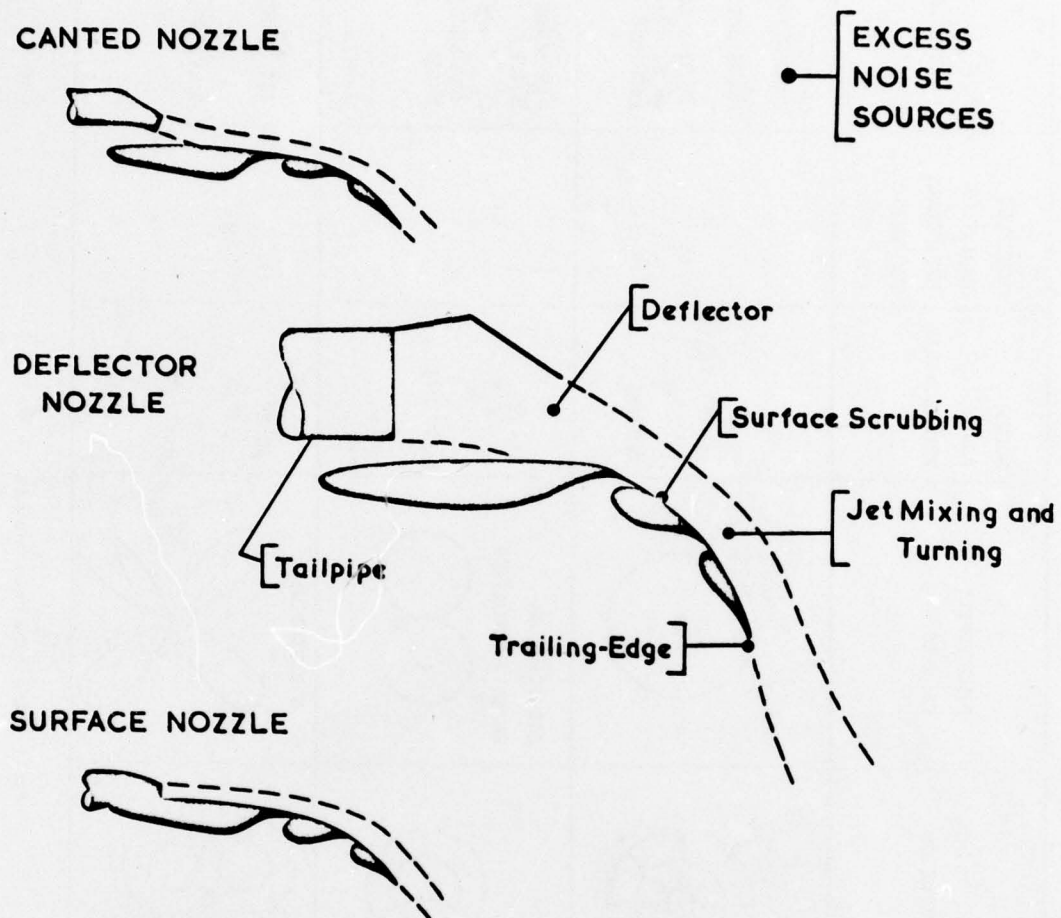


Fig.10 Externally blown flap: over-wing jet


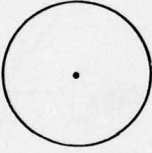
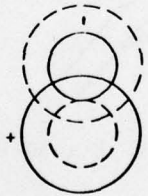
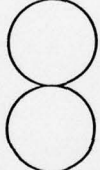
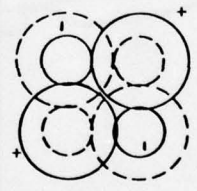
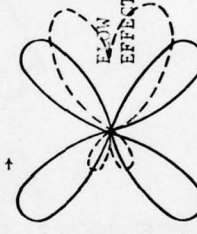
SOURCE TYPE	SOURCE ASSOCIATED WITH:	SOURCE ACOUSTIC REPRESENTATION	DIRECTIVITY PATTERN	SOUND POWER RELATIONSHIP	ACOUSTIC RADIATION EFFICIENCY PROPORTIONAL TO:	EXAMPLES
MONOPOLE	PULSATING FLOW			$\rho L^2 v^4 / a_o$ ($\rho a v^3 M$)	M	DROPLET COMBUSTION - PULSE JETS - INLET & EXHAUSTS OF RECIPROCATING MACHINES
DIPOLE	UNSTEADY FLOWS CLOSE TO SURFACES			$\rho L^2 v^6 / a_o^3$ ($\rho a v^3 M^3$)	M ³	FAN BLADE NOISE - BOUNDARY LAYER NOISE
QUADRUPOLE	FREE MIXING OF EXHAUST FLOWS INTO ATMOSPHERE			$\rho L^2 v^8 / a_o^5$ ($\rho a v^3 M^5$)	M ⁵	JET NOISE - VALVE NOISE

Fig. 11 Basic source characteristics

BASIC AERODYNAMIC NOISE THEORY

by

Helmut V. Fuchs

Deutsche Forschungs- und Versuchsanstalt für Luft- und Raumfahrt E.V.
 Institut für Turbulenzforschung
 1000 Berlin 12, Müller-Breslau-Strasse 8

SUMMARY

These lecture notes may help attendees of this Short Course to assess the present state of knowledge in the theory of aerodynamic noise generation and propagation. The emphasis is on the identification and the physical and analytical modelling of the major sound sources associated with turbulent airflows. Some of the fairly fundamental developments reproduced here may serve as basic frameworks for the subsequent lectures. This review succeeds an earlier one which is herein frequently referred to as ref. [1] since that covers in more mathematical detail the concepts common in Lighthill's now classical theory. More recently two excellent review papers were published in the field of aerodynamic noise theory (ref. [3, 15]). Though none of them claims to be comprehensive, they may be used as course material to assist comprehension of the problem areas, which are numerous.

The present paper reveals a few deficiencies of existing theories with respect to the turbulent source models employed. The importance of source coherency with regard to flow inhomogeneities is outlined, and the relevance of studies into the sound propagation from acoustic singularities embedded in a sheared flow is discussed with respect to the jet noise problem.

Not all known approaches to aerodynamic noise theory could possibly be covered by this lecture; the list of references is by no means complete, either.

LIST OF CONTENTS

	<u>Page</u>
1. Introduction	2-3
2. Fluid dynamics equations	2-3
3. Linear acoustics equations	2-3
3.1 Sound propagation in a nonuniform flow	2-3
3.2 Sound propagation in a unidirectional transversely sheared flow	2-4
3.3 Sound propagation in uniform flow	2-4
3.4 Sound propagation in a homogeneous medium at rest	2-5
3.5 Acoustic point source in uniform motion	2-5
4. Acoustic analogy theories	2-8
4.1 Lighthill's inhomogeneous wave equation	2-8
4.2 Curle's general source integral	2-9
4.3 Turbulent pressure as source quantity	2-9
5. 'True source' identification theories	2-11
5.1 Introduction of a convective amplification Doppler factor	2-11
5.2 Phillips' convected wave equation	2-11
5.3 Pao's linearized convected wave equation	2-13
5.4 Lilley's shear-refraction equation	2-14
5.5 Solutions to Lilley's equation	2-15
6. Models of turbulent source-mechanisms	2-16
6.1 The various concepts of stationary or moving turbulent sources	2-16
6.2 Lighthill's multi-pole source expansion	2-17
6.3 The idealized model of small-scale isotropic turbulence	2-18
6.4 Michalke's multi-mode expansion for noise of cylindrical flows	2-18
6.5 The large-scale coherent turbulence model in jet noise prediction	2-20
6.6 Powell's vortex model of aerodynamic noise	2-21
6.7 Howe's vorticity and entropy-gradient model	2-22
7. Final remarks	2-24
References	2-25

LIST OF SYMBOLS

a, a_0	speed of sound
$A, (dA)$	surface (element)
A_0, A_1, A_2	functions defined by eq. (6.25)
B	specific stagnation enthalpy
c_i, \vec{c}	velocity (vector)
c_p, c_v	specific heats at constant pressure or volume
C	Doppler amplification factor
D	jet nozzle diameter
f	frequency
f_i	externally applied force density (eq. 2.4)
F_r, m	radial interference function (eq. 6.23)
F_x	axial interference function (eq. 6.22)
He	Helmholtz number
I	far-field sound intensity (par. 6.3)
J	sound intensity from unit volume of turbulence (par. 6.3)
J_m	Bessel function of first kind and order m
m	mass injection density (eq. 2.2)
M	Mach number
n_i	outward normal to surface
p	pressure
P	observer position
q	source function
Q	source location
r	logarithm of pressure (par. 5.3)
r, \vec{r}, r_0	distances denoted in Figs. 1 or 4
R, \vec{R}, R_0	normalized distances (par. 6.5)
Re	Reynolds number
s	entropy
St	Strouhal number
t	time
T	temperature
T_{ij}	Lighthill's source tensor (eq. 4.7)
U	normalized axial velocity in a jet flow
U_0	jet exit velocity
u_i	convection velocity (vector)
v	normalized radial velocity in a jet flow
$V, (dV)$	source volume (element)
w	specific enthalpy
W	power spectral density of radiated pressure
W_{12}	cross spectral density of turbulent pressure
$x_i, (y_i)$	Cartesian field (source) coordinates
Z_m	function defined by eq. (6.25)
δ	Dirac delta function
δ_{ij}	Kronecker delta
∇_j	Nabla operator
Y	ratio of specific heats
θ, Θ	angles defined in pars. 3.5 or 6.4
λ	acoustic wave length
ν	kinematic viscosity
ρ	fluid density
σ, τ	functions defined in par. 6.4
τ_{ij}	viscous stress tensor (eq. 2.5)
Φ, ϕ	velocity potential
ϕ, ϕ'	azimuth angle (Fig. 4)
ω	radian frequency
$\vec{\omega}$	vorticity vector (eq. 6.29)

1. INTRODUCTION

Most of the theoretical concepts developed in this field of aero-acoustics start from the equations of mass and momentum conservation and an equation of state (par. 1.1). The various approaches differ in the way they manipulate (differentiate and somehow combine) and in the way they approximate these equations. There seem to be just as many different models as there are investigators tackling one and the same aerodynamic noise problem. This is particularly so in the field of jet noise, although hardly any of these theories can claim to have brought us much closer to a solution or understanding of this problem than Lighthill's first approach. It appears to be not only personal ambition, taste or mathematical skill that created new analyses but also a matter of philosophy of how sound might be generated in and propagated through a turbulent flow. Since most of the proposed models were inspired by acoustic wave equations of one sort or another, it may be worthwhile to briefly recall some basic linear acoustics. This will facilitate understanding of the various attempts to couple far-field noise and turbulent flow characteristics.

2. FLUID DYNAMICS EQUATIONS

The equation of mass conservation in a volume element of a continuous medium may be written, in differential form and Cartesian coordinates x_i , as

$$\frac{\partial \rho}{\partial t} + \frac{\partial \rho c_i}{\partial x_i} = m(x_i, t) \quad (2.1)$$

or

$$\frac{D\rho}{Dt} + \rho \frac{\partial c_i}{\partial x_i} = m(x_i, t) \quad (2.2)$$

with

$$\frac{D}{Dt} \equiv \frac{\partial}{\partial t} + c_i \frac{\partial}{\partial x_i} \quad (2.3)$$

The second flow equation describes the conservation of momentum of a fluid element:

$$\rho \frac{\partial c_i}{\partial t} + \rho c_j \frac{\partial c_i}{\partial x_j} + \frac{\partial p}{\partial x_i} - \frac{\partial \tau_{ij}}{\partial x_j} = f_i(x_i, t) \quad (2.4)$$

or

$$\rho \frac{Dc_i}{Dt} + \frac{\partial p}{\partial x_i} - \frac{\partial \tau_{ij}}{\partial x_j} = f_i(x_i, t) \quad (2.5)$$

A comment on the introduction of a mass injection density and an externally applied force density distribution (m and f_i , respectively) was given in ref. [1]. Finally, an equation of state may be postulated which relates differentials of the density ρ , pressure p and entropy s :

$$d\rho = \left(\frac{\partial \rho}{\partial p}\right)_s dp + \left(\frac{\partial \rho}{\partial s}\right)_p ds \quad d\rho = \frac{1}{a^2} dp - \frac{\rho}{c_p} ds \quad (2.6)$$

or

$$\frac{D\rho}{Dt} = \frac{1}{a^2} \frac{Dp}{Dt} - \frac{\rho}{c_p} \frac{Ds}{Dt} \quad (2.7)$$

with $a^2 = \gamma \frac{p}{\rho}$ local speed of sound squared, $\gamma = c_p/c_v$.

Provided that m and f_i are given and τ_{ij} can be related to the velocity field, a complete description of a general flow situation requires, additionally, the introduction of an energy equation.

3. LINEAR ACOUSTICS EQUATIONS

The equations describing the propagation of small disturbances through an otherwise unperturbed (laminar) flow may be derived from the fluid dynamics equations under a number of simplifying assumptions. Three degrees of simplification are possible which will be treated consecutively in the following subsections:

3.1 Sound propagation in a nonuniform flow

First, the fluid dynamics equations are simplified by the following assumptions,

- a) The density distributions of mass and force sources in eqs. (2.2) and (2.5) are set to zero,

$$m = 0; f_i = 0 \quad (3.1)$$

- b) The viscosity of the medium may be neglected,

$$\tau_{ij} = 0 \quad (3.2)$$

- c) The time-averaged properties of the medium, i.e. the mean pressure, density and temperature, are assumed constant throughout the flow

$$\begin{aligned} \bar{p} &= p(x_i, t) - p'(x_i, t) = p_0 = \text{const} \\ \bar{\rho} &= \rho(x_i, t) - \rho'(x_i, t) = \rho_0 = \text{const} \end{aligned} \quad (3.3)$$

d) The fluctuating (primed) quantities are small compared to the mean values enabling a linearisation of the differential equations.

e) Changes in pressure and density are assumed to be isentropic to the extent that

$$\frac{Dp}{Dt} - \frac{1}{a^2} \frac{Dp}{Dt} = 0 \quad (3.4)$$

Introducing mean and fluctuating quantities into eqs. (2.2) and (2.5) yields the differential equations for the disturbances:

$$\frac{Dp'}{Dt} + \bar{\rho} \frac{\partial c'_i}{\partial x_i} + \rho' \frac{\partial \bar{c}_i}{\partial x_i} = 0 \quad (3.5)$$

$$\bar{\rho} \frac{\partial c'_i}{\partial t} + \frac{\partial p'}{\partial x_i} + (\bar{\rho} c'_j + \rho' \bar{c}_j) \frac{\partial \bar{c}_i}{\partial x_j} = 0 \quad (3.6)$$

When the operator

$$\frac{D}{Dt} = \frac{\partial}{\partial t} + \bar{c}_j \frac{\partial}{\partial x_j} \quad (3.7)$$

is applied to eq. (3.5), $\partial/\partial x_i$ applied to eq. (3.6) and the latter equation is subtracted from the former we obtain a very complicated equation which involves all three fluctuating quantities: p' , ρ' and c'_i ,

$$\frac{\partial^2 p'}{\partial t^2} - \frac{\partial^2 p'}{\partial x_i^2} - \frac{Dp'}{Dt} \frac{\partial \bar{c}_i}{\partial x_i} - \bar{\rho} c'_j \frac{\partial^2 \bar{c}_i}{\partial x_i \partial x_j} - (2 \bar{\rho} \frac{\partial c'_j}{\partial x_i} + \bar{c}_j \frac{\partial \rho'}{\partial x_i} + \rho' \frac{\partial \bar{c}_j}{\partial x_i}) \frac{\partial \bar{c}_i}{\partial x_j} = 0 \quad (3.8)$$

The obvious impossibility to derive some kind of wave equation for p' means there is no easy way of handling sound propagation problems in any non-uniform flow even if one neglects gradients of mean quantities other than the mean velocity.

3.2 Sound propagation in a unidirectional transversely sheared flow

The situation is considerably improved when one assumes a mean flow in only one direction;

$$\bar{c}_i = \{ \bar{c}_1(x_2); 0; 0 \}, \quad (3.9)$$

with finite gradients of \bar{c}_1 occurring only normal to the flow direction. In this very special case the conservation equations of mass and momentum reduce to

$$\frac{Dp'}{Dt} + \bar{\rho} \frac{\partial c'_i}{\partial x_i} = 0 \quad (3.10)$$

$$\bar{\rho} \frac{\partial c'_i}{\partial t} + \frac{\partial p'}{\partial x_i} + \bar{\rho} c'_j \frac{\partial \bar{c}_i}{\partial x_j} = 0 \quad (3.11)$$

and under the assumption e) we may write eq. (3.8) in terms of the pressure p' and the transverse velocity c'_2 as the time dependent variables,

$$\frac{1}{a^2} \frac{\partial^2 p'}{\partial t^2} - \frac{\partial^2 p'}{\partial x_i^2} - 2 \bar{\rho} \frac{\partial \bar{c}_1}{\partial x_2} \frac{\partial c'_2}{\partial x_1} = 0 \quad (3.12)$$

Since c'_2 is related to p' by the transverse component of the momentum equation (3.11),

$$\bar{\rho} \frac{D}{Dt} \frac{\partial c'_2}{\partial x_1} + \frac{\partial^2 p'}{\partial x_1 \partial x_2} = 0,$$

c'_2 may be eliminated from eq. (3.12) leaving a third-order differential equation for the pressure only,

$$\frac{D}{Dt} \left(\frac{1}{a^2} \frac{\partial^2 p'}{\partial t^2} - \frac{\partial^2 p'}{\partial x_i^2} \right) + 2 \frac{\partial \bar{c}_1}{\partial x_2} \frac{\partial^2 p'}{\partial x_1 \partial x_2} = 0 \quad (3.14)$$

This equation, though of higher order than an ordinary wave equation, may at least in principle be solved for the pressure field under given boundary conditions. An analytical solution is possible if the mean velocity is assumed to vary only little over distances x_2 of the order of a wave length of the sound. This is the limiting case of 'geometrical acoustics' which was treated in Blokhintsev's [27] book on the acoustics in moving media. Another solution to (3.14) for constant shear is discussed in Goldstein's excellent review [37]. We shall return to eq. (3.14) when Lilley's theory of noise generation in sheared flows is discussed (par. 5.4).

3.3 Sound propagation in uniform flow

For a constant uniform flow in only one direction the acoustic field equations of par. 3.2 simplify considerably,

$$\frac{Dp'}{Dt} + \bar{\rho} \frac{\partial c'_i}{\partial x_i} = 0 \quad (3.15)$$

$$\bar{\rho} \frac{Dc'_i}{Dt} + \frac{\partial p'}{\partial x_i} = 0 \quad (3.16)$$

with a second-order differential equation being valid for the pressure,

$$\begin{aligned} \frac{\partial^2 p'}{\partial t^2} - a_o^2 \frac{\partial^2 p'}{\partial x_i^2} &= \frac{\partial^2 p'}{\partial t^2} + 2\bar{c}_j \frac{\partial^2 p'}{\partial x_j \partial t} + \bar{c}_i \bar{c}_j \frac{\partial^2 p'}{\partial x_i \partial x_j} - a_o^2 \frac{\partial^2 p'}{\partial x_i^2} \\ &= \frac{\partial^2 p'}{\partial t^2} + 2\bar{c}_j \frac{\partial^2 p'}{\partial x_j \partial t} + (\bar{c}_i \bar{c}_j - a_o^2 \delta_{ij}) \frac{\partial^2 p'}{\partial x_i \partial x_j} = 0 \end{aligned} \quad (3.17)$$

Eq. (3.17) differs from the ordinary wave equation (par. 3.4) only in the fact that the partial time derivatives are replaced by the substantive derivatives \bar{D}/Dt . It is the basis for treating all kinds of relative motion between the sound source, the receiver and the medium which carries the acoustic waves. We shall use it when discussing the various Doppler factors accounting for frequency shifts, amplification and attenuation of sound at the observer. The latter will help to understand why in some aerodynamic noise theories convective Doppler factors were introduced (par. 5.1) to account for source convection by the flow. Eq. (3.17) will also be recalled in the context of convected wave equation approaches to aerodynamic noise problems due to Phillips, Pao and others (par. 5.2 and 5.3).

3.4 Sound propagation in a homogeneous medium at rest

It is not merely for completeness that we finally write down the ordinary acoustic field equations for $\bar{c}_i = 0$, i.e. for a medium which is at rest except for the small perturbations propagating from one or more sound sources,

$$\frac{\partial p'}{\partial t} + \bar{p} \frac{\partial c_i'}{\partial x_i} = 0 \quad (3.18)$$

$$\bar{p} \frac{\partial c_i'}{\partial t} + \frac{\partial p'}{\partial x_i} = 0 \quad (3.19)$$

The reason is that still the most widely accepted concept in aerodynamic noise theory namely that due to Lighthill (par. 4), is based on a wave equation which very closely resembles that valid for a medium at rest,

$$\frac{\partial^2 p'}{\partial t^2} - a_o^2 \frac{\partial^2 p'}{\partial x_i^2} = 0 \quad (3.20)$$

It is noted that identical equations may be written down for the fluctuating density or velocity potential ϕ .

3.5 Acoustic point source in uniform motion

The inhomogeneous linear wave equation,

$$\frac{\partial^2 \phi}{\partial t^2} - a_o^2 \frac{\partial^2 \phi}{\partial x_i^2} = q(x_i, t) \quad (3.21)$$

where q is a prescribed sound source distribution of finite extent may readily be solved via Kirchhoff's integral formula. The procedure was demonstrated, e.g., in ref. [1] for three specific source elements concentrated in an infinitesimal volume element fixed in x_i -space: an acoustic monopole, dipole and quadrupole type of singularity.

If now the fluid flow velocity \bar{c}_i is non-zero and the source is given as travelling at a speed \bar{u}_i (Fig. 1), then eq. (3.17) is valid outside the source itself. By a Galilean transformation of the type

$$x_i = \bar{x}_i + \alpha_{ij} x_j' + \bar{c}_i t' ; t = t' \quad (3.22)$$

which includes a translation, rotation and dilatation of the coordinates in this order, an ordinary wave equation could be obtained,

$$\frac{\partial^2 \phi}{\partial t'^2} - a_o^2 \frac{\partial^2 \phi}{\partial x_i'^2} = 0 \quad (3.23)$$

In this system of coordinates, however, the source would still be moving at a speed $\bar{u}_i - \bar{c}_i$.

A second, Lorentz type of transformation,

$$\begin{aligned} x_1^* &= \frac{x_1' - c^* t^*}{\sqrt{1 - (c^*/a_o)^2}} , x_2^* = x_2' , x_3^* = x_3' \\ t^* &= \frac{t' - c^* x_1'/a_o^2}{\sqrt{1 - (c^*/a_o)^2}} \end{aligned} \quad (3.24)$$

may be shown (refer, e.g., to [2]) to yield again an ordinary wave equation in the new coordinates

$$\frac{\partial^2 \phi}{\partial t^{*2}} - a_o^2 \frac{\partial^2 \phi}{\partial x_i^{*2}} = 0 \quad (3.25)$$

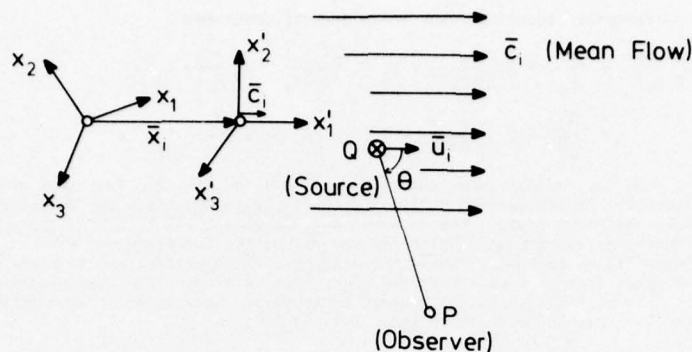


Fig. 1: Acoustic source (Q) moving relative to the observer (P) and the mean flow.

If now the velocity vectors \bar{c}_i and \bar{u}_i are assumed to be parallel and their difference in magnitude to be c^* ,

$$c^* = \bar{c} - \bar{u} ; M = \bar{c}/a_0, M_c = c^*/a_0 = (\bar{c} - \bar{u})/a_0, \quad (3.26)$$

then the starred system of coordinates may be shown to be one whose origin moves at a speed \bar{u} in the original system just as our source point does. One can thus solve the sound problem in the starred system and then re-transform back to the physically more meaningful original or to the primed system. This was done in ref. [4] for a simple harmonic point source. In order to demonstrate the various Doppler effects we may write the corresponding pressure field in the following form

$$p'(x_i, t) = \left\{ \frac{\omega^c}{a_0(1-M_c^2)} (1-M_c \cos \theta) + i M_c \frac{\cos \theta}{r} \right\} \frac{i \rho_0 a_0 A}{r} \exp i \frac{\omega^c}{1-M_c^2} \left[(1-M_c) t + M_c \frac{x_1}{a_0} - \frac{r}{a_0} \right] \quad (3.27)$$

Herein the amplitude A may be related to the total sound flux from the source. The abbreviations $\cos \theta$ and r stand for the following expressions,

$$\cos \theta = (x_1 - \bar{u}t)/r$$

$$r = [(x_1 - \bar{u}t)^2 + (1-M_c^2) [(x_2 - \bar{x}_2)^2 + (x_3 - \bar{x}_3)^2]]^{1/2} \quad (3.28)$$

ω^c is the frequency of the source as measured in a system moving with the source.

The Doppler effects are most readily obtained for the source and the observer both being located on the x_1 -axis,

$$r = |x_1 - \bar{u}t|$$

$$\cos \theta = +1 \text{ for } x_1 > \bar{u}t \text{ (source moving towards the observer)}$$

$$= -1 \text{ for } x_1 < \bar{u}t \text{ (source moving away from the observer)}$$

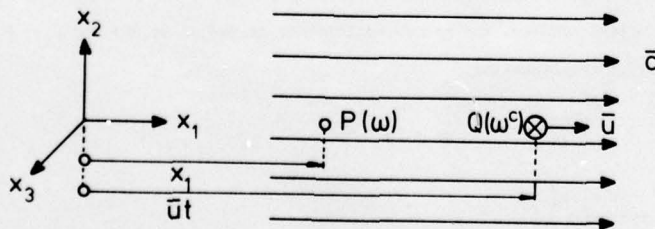


Fig. 2: Sketch illustrating relative motion of source, observer and flow when Q and P are in line.

The situation illustrated by Fig 2 is physically indistinguishable from that of a source moving with $-(\bar{c} - \bar{u})$ and the observer moving with $-\bar{c}$.

The frequency shift is under these conditions easily deducible from the exponential function in eq. (3.27) as

$$\frac{\omega}{\omega^c} = \frac{1 + M}{1 + M_c} \quad \text{for} \quad x_1 > \bar{u}t \quad (3.29)$$

$$\frac{\omega}{\omega^c} = \frac{1 - M}{1 - M_c} \quad \text{for} \quad x_1 < \bar{u}t \quad (3.30)$$

The corresponding Doppler factor in the amplitude due to the relative motion may be derived from eq. (3.27) for the acoustic far-field ($r \gg a_0/\omega^c$):

$$C = \frac{1 - M_c}{1 - M_c^2} = \frac{1}{1 + M_c} \quad \text{for} \quad x_1 > \bar{u}t \quad (3.31)$$

$$C = \frac{1 + M_c}{1 - M_c^2} = \frac{1}{1 - M_c} \quad \text{for} \quad x_1 < \bar{u}t \quad (3.32)$$

Apart from the trivial case $M_c = 0$ three special cases may be of practical interest:

1. The source moves while the observer is at rest ($M = 0$; $M_c = -\bar{u}/a_0$)

a) for $x_1 > \bar{u}t$:

$$\frac{\omega}{\omega^c} = \frac{1}{1 - \bar{u}/a_0} \quad ; \quad C = \frac{1}{1 - \bar{u}/a_0} \quad (3.33)$$

b) for $x_1 < \bar{u}t$:

$$\frac{\omega}{\omega^c} = \frac{1}{1 + \bar{u}/a_0} \quad ; \quad C = \frac{1}{1 + \bar{u}/a_0} \quad (3.34)$$

2. The observer moves while the source is at rest (which case is physically indistinguishable from that with $M_c = 0$; $\bar{c} = \bar{u}$)

a) for $x_1 > \bar{u}t$:

$$\frac{\omega}{\omega^c} = 1 + \bar{u}/a_0 \quad ; \quad C = 1 \quad (3.35)$$

b) for $x_1 < \bar{u}t$:

$$\frac{\omega}{\omega^c} = 1 - \bar{u}/a_0 \quad ; \quad C = 1 \quad (3.36)$$

3. Source and observer move at the same speed (which case is physically indistinguishable from that with $M = M_c = \bar{c}/a_0$; $\bar{u} = 0$)

a) for $x_1 > 0$:

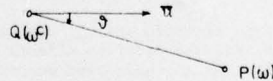
$$\frac{\omega}{\omega^c} = 1 \quad ; \quad C = \frac{1}{1 + \bar{c}/a_0} \quad (3.37)$$

b) for $x_1 < 0$:

$$\frac{\omega}{\omega^c} = 1 \quad ; \quad C = \frac{1}{1 - \bar{c}/a_0} \quad (3.38)$$

The three cases are seen to produce completely different Doppler effects. For the important case 1 we know from standard text books that the more general Doppler factor reads

$$C = \frac{\omega}{\omega^c} = \frac{1}{1 - \bar{u} \cos \vartheta / a_0} \quad (3.39)$$



where now the angle ϑ defines the radiation angle (sketch) at the time of the emission of the sound. It is in the form (3.39) that the Doppler factor will enter the aerodynamic noise theory (compare par. 5.1) to account for source convection. Corresponding Doppler amplification factors could be derived in the form C^n for higher-order acoustic sources like dipoles and quadrupoles with the exponent n depending on the order of these sources.

In this par. 3.5 the source and the observer were idealized to be concentrated at a point with no interaction with the flow. Oestreicher [5] already considered the field of a spatially extended source interacting with a viscous flow. Morfey and Tanna [6] described the sound field of sources in circular motion.

4. ACOUSTIC ANALOGY THEORIES

The preceding paragraph 3 was to illustrate that, from the point of view of an acoustician, one can principally solve any flow noise problem if only a clever aerodynamicist would provide some detailed information about the distribution of acoustic sources which are carried with the flow. Even if the mean flow were highly inhomogeneous and foreign bodies were immersed, one could still apply tools like ray theory, reflection principles and scattering analysis to predict the radiated sound field.

Unfortunately, in most aerodynamic or hydrodynamic noise problems the main problem is how to identify the actual sources in the flow. For such complex sources like jet flows it is extremely difficult to even isolate the turbulent source mechanisms from the secondary effects of source convection and sound diffraction by the flow. In this situation, aerodynamic noise theories differ mainly in the way their authors feel that in some distant future these sources will best be described by theory or experiment. Some theorists will be seen to rely on a possibility of somehow separating the secondary effects. Others follow Lighthill's [7] original idea by drawing a formal analogy between the full nonlinear flow and turbulence phenomena and the linear theory of classical acoustics in a homogeneous medium at rest. This approach intends to keep the mathematical procedures as simple as possible for as long as our understanding of the turbulent flow structure is meager or does not explicitly require an especially adjusted mathematical form of the equations.

4.1 Lighthill's inhomogeneous wave equation:

Taking the time derivative of the continuity eq. (2.1),

$$\frac{\partial^2 \rho}{\partial t^2} + \frac{\partial^2 \rho c_i}{\partial x_i \partial t} = \frac{\partial m}{\partial t} \quad (4.1)$$

then adding to the momentum eq. (2.4) c_i times the eq. (2.1),

$$\frac{\partial \rho c_i}{\partial t} + \frac{\partial \rho c_i c_j}{\partial x_j} + \frac{\partial p}{\partial x_i} - \frac{\partial \tau_{ij}}{\partial x_j} = f_i + m c_i \quad (4.2)$$

taking the divergence of the latter,

$$\frac{\partial^2 \rho c_i}{\partial x_i \partial t} + \frac{\partial^2 \rho c_i c_j}{\partial x_i \partial x_j} + \frac{\partial^2 p}{\partial x_i^2} - \frac{\partial^2 \tau_{ij}}{\partial x_i \partial x_j} = \frac{\partial}{\partial x_i} (f_i + m c_i) \quad (4.3)$$

and finally subtracting (4.3) from (4.1) yields

$$\frac{\partial^2 \rho}{\partial t^2} - \frac{\partial^2 p}{\partial x_i^2} = \frac{\partial^2}{\partial x_i \partial x_j} (\rho c_i c_j - \tau_{ij}) - \frac{\partial}{\partial x_i} (f_i + m c_i) + \frac{\partial m}{\partial t} \quad (4.4)$$

In order to formally obtain an inhomogeneous wave equation for either the pressure or the density, one has to add a term $a_0^2 \partial^2 p / \partial t^2$ or subtract a term $a_0^2 \partial^2 \rho / \partial x_i^2$ on both sides of eq. (4.4):

$$\frac{1}{a_0^2} \frac{\partial^2 p}{\partial t^2} - \frac{\partial^2 p}{\partial x_i^2} = \frac{\partial^2}{\partial x_i \partial x_j} (\rho c_i c_j - \tau_{ij}) - \frac{\partial}{\partial x_i} (f_i + m c_i) + \frac{\partial m}{\partial t} + \frac{1}{a_0^2} \frac{\partial^2}{\partial t^2} (p - a_0^2 \rho) \quad (4.5)$$

$$\frac{\partial^2 \rho}{\partial t^2} - a_0^2 \frac{\partial^2 \rho}{\partial x_i^2} = \frac{\partial^2}{\partial x_i \partial x_j} (\rho c_i c_j - \tau_{ij}) - \frac{\partial}{\partial x_i} (f_i + m c_i) + \frac{\partial m}{\partial t} + \frac{\partial^2}{\partial x_i^2} (p - a_0^2 \rho) \quad (4.6)$$

A full account of Lighthill's subsequent derivations was given in [1]. Here only a few essentials of this approach are underlined:

- The wave equations (4.5) and (4.6) are exact. Neither equation involves the restrictive assumption that the fluid obeys an equation of state. Being no more than a statement of mass and momentum conservation, in fact all continuous flows satisfy a wave equation like (4.5) or (4.6).
- All four terms on the right-hand side vanish individually outside a limited volume occupied by the turbulent flow. With a_0 arbitrarily chosen to equal the ambient speed of sound in the surrounding, inviscid medium, eqs. (4.5) and (4.6) outside the flow reduce to ordinary linear wave equations of the type (3.20).
- As is typical for the acoustic analogy theory, the medium is taken as being homogeneous and at rest at any point in space. All the decisive effects due to the presence of the turbulent flow are viewed as inhomogeneities, i.e. as an equivalent acoustic source distribution within the flow region.
- The original Lighthill source term,

$$\frac{\partial^2 \tau_{ij}}{\partial x_i \partial x_j} = \frac{\partial^2}{\partial x_i \partial x_j} \{ \rho c_i c_j - \tau_{ij} + (p - a_0^2 \rho) \delta_{ij} \} \quad (4.7)$$

does not only incorporate the actual turbulent sources but also - though not explicitly - the secondary effects of source convection by the flow and the diffraction, absorption, refraction and scattering of sound on its way from the emission point in x_i - space to the observer who is also at a fixed x_i .

- Only if $\rho c_i c_j$ (or other relevant source terms) were prescribed in some useful sense, would it be possible to integrate eqs. (4.5) and (4.6) with the aid of Kirchhoff's formula. Many of the conclusions so far were based on features of specific source elements (like single eddies) instead of the space-time structure of an extended source distribution.

4.2 Curle's general source integral

Curle [8] extended Lighthill's analogy by introducing solid boundaries which may or may not take actively part in the sound generating process. Again these boundary surfaces A are thought of as being fixed in x_i -space. The following integral to eq. (4.5) was derived in [1]:

$$\begin{aligned} (p - p_0)_{,4} = \frac{\partial^2}{\partial x_i \partial x_j} \int_V \frac{1}{r} [\rho c_i c_j - \tau_{ij}] dV - \frac{\partial}{\partial x_i} \int_V \frac{1}{r} [f_i + m c_i] dV + \int_V \frac{1}{r} \left[\frac{\partial}{\partial t} \left\{ m + \frac{1}{a_0^2} \frac{\partial}{\partial t} (p - a_0^2 \rho) \right\} \right] dV \\ + \frac{\partial}{\partial x_i} \int_A \frac{1}{r} [p n_i - \tau_{ij} n_j] dA \\ + \frac{\partial}{\partial x_i} \int_A \frac{1}{r} [\rho c_i c_n] dA - \int_A \frac{1}{r} \left[\frac{\partial \rho c_n}{\partial t} \right] dA \end{aligned} \quad (4.8)$$

Here c_n denotes the (fluctuating) flow velocity as normal to the bounding surface A ,

$$c_i dA_i = c_i n_i dA = c_n dA \quad (4.9)$$

For practical applications one may considerably reduce the number of integral terms contributing to the radiation pressure field. The first is the celebrated Lighthill integral for an unbounded turbulent flow with the fluctuating velocities or Reynolds stresses forming the actual source quantity. The second surface integral represents the back-reaction of a solid body to the flow adjacent to it. It includes pressures due to the impact of sound waves generated elsewhere in the flow as well as hydrodynamic flow pressures acting directly as a source distribution. The last two integrals contribute only if the surfaces are compliant or driven externally.

It is pointed out here that both the differential representation (par. 4.1) and the integral representation (par. 4.2) are hardly more than a framework for actual aeroacoustic theories which remain to be based on physical models of the source mechanisms involved. Only if one can identify one source term as dominating and if one knows its space-time development a priori (e.g., from measurements) does the Lighthill-Curle approach offer the solution for a particular flow noise problem.

4.3 Turbulent pressure as source quantity

Several approximations and modifications to Lighthill's approach were put forward over the years. Many of them deal with

$$\tau_{ij} \approx \rho_0 c_i c_j \quad (\rho_0 = \text{const}) \quad (4.10)$$

as the dominant source distribution for an unbounded turbulent flow at low Mach numbers. This approximation cannot be strictly valid since incompressible flow could not generate any sound. It nevertheless helped to further develop the theoretical concepts and arrive at some general conclusions. Some investigators have found it more convenient to replace the Reynolds stresses by a scalar function as source quantity before proceeding any further:

a) Meecham and Ford [9] first employed Poisson's differential equation,

$$\frac{\partial^2 p}{\partial x_i^2} = -\rho_0 \frac{\partial^2 c_i c_j}{\partial x_i \partial x_j} \quad (4.11)$$

which couples pressure and velocity in an incompressible flow and thus wrote Kirchhoff's solution to eq. (4.6) in the form

$$p(x_i, t) - p_0 = -\frac{1}{4\pi a_0^2} \int_V \frac{1}{r} \left[\frac{\partial^2 p}{\partial y_i^2} \right] dV \quad (4.12)$$

(Brackets [] indicate evaluation at retarded times). For an unbounded flow (no surface integrals, eqs. I(35) and I(47) of [1]) this may then be written as

$$p - p_0 = -\frac{1}{4\pi a_0^2} \frac{\partial^2}{\partial x_i^2} \int_V \frac{1}{r} [p] dV \quad (4.13)$$

In the radiated far-field (eqs. II(11), II(2 a), I(17) of [1]) the following expression is equivalent to (4.13):

$$p - p_0 = -\frac{1}{4\pi a_0^4} \int_V \frac{1}{r} \left[\frac{\partial^2 p}{\partial t^2} \right] dV \quad (4.14)$$

This concept is equivalent to Lighthill's only within approximation (4.10),

b) Ribner [10] in a slightly different approach introduced a pressure p^0 by setting

$$\frac{\partial^2 p^0}{\partial x_i^2} = -\frac{\partial^2 \rho c_i c_j}{\partial x_i \partial x_j} \quad (4.15)$$

and inserting this into the wave equation (4.5)

$$\frac{1}{a_0^2} \frac{\partial^2 p}{\partial t^2} - \frac{\partial^2 p}{\partial x_i^2} = - \frac{\partial^2 p^0}{\partial x_i^2} \quad (4.16)$$

He then attaches a very specific meaning to the new source function p^0 by interpreting it as 'pseudosound' which accounts for the quasi-incompressible features of the flow with the total pressure perturbation

$$p - p_0 = p^0 + p' \quad (4.17)$$

being the sum of the 'pseudosound' and the acoustic pressure p' .

With these definitions Ribner rewrote the wave equation in the form

$$\frac{1}{a_0^2} \frac{\partial^2 p'}{\partial t^2} - \frac{\partial^2 p'}{\partial x_i^2} = - \frac{1}{a_0^2} \frac{\partial^2 p^0}{\partial t^2} \quad (4.18)$$

Although $\partial^2 p^0 / \partial x_i^2$ was originally a quasi-incompressible substitute for $\partial^2 \rho c_i c_j / \partial x_i \partial x_j$, Ribner derived his dilatation equation from eq. (4.16):

$$\frac{1}{a_0^2} \frac{\partial^2 p'}{\partial t^2} - \frac{\partial^2 p'}{\partial x_i^2} = \frac{\partial^2 \rho}{\partial t^2} \quad (4.19)$$

with density fluctuations ρ^0 associated with the 'pseudosound' pressure. An equation like (4.19) would relate sound generation by free turbulence to volume pulsations in the fluid.

- c) Lighthill's $\overline{11}$ view of Ribner's alternative again differs from the foregoing in that he defined a new source function ϑ by setting

$$T_{ij} = \vartheta \delta_{ij} ; \quad \frac{\partial^2 \vartheta}{\partial x_i^2} = \frac{\partial^2 \rho c_i c_j}{\partial x_i \partial x_j} \quad (4.20)$$

This, when introduced into the wave equation (4.6),

$$\frac{\partial^2 \rho}{\partial t^2} - a_0^2 \frac{\partial^2 \rho}{\partial x_i^2} = \frac{\partial^2 \vartheta}{\partial x_i^2} \quad (4.21)$$

does not establish a new theory as long as no specific meaning other than that in eq. (4.20) is attached to ϑ . The far-field integral of eq. (4.21),

$$\rho - \rho_0 = \frac{1}{4\pi a_0^4} \int_V \frac{1}{r} \left[\frac{\partial^2 \vartheta}{\partial t^2} \right] dV \quad (4.22)$$

is strictly equivalent to and is equally exact as Lighthill's original integral (eq. II(13) of $\overline{11}$),

$$\rho - \rho_0 = \frac{1}{4\pi a_0^4} \frac{x_i x_j}{|x_i|} \int_V \left[\frac{\partial^2 T_{ij}}{\partial t^2} \right] dV \quad (4.23)$$

- d) In his original theory $\overline{12}$ Lighthill, too, introduced the flow pressure, but on completely different grounds:

$$\frac{\partial^2 T_{ij}}{\partial t^2} \approx \left(\frac{\partial \bar{c}_i}{\partial x_j} + \frac{\partial \bar{c}_j}{\partial x_i} \right) \frac{\partial p}{\partial t} + \frac{\partial p}{\partial t} \left(\frac{\partial \bar{c}_i}{\partial x_j} + \frac{\partial \bar{c}_j}{\partial x_i} \right) \quad (4.24)$$

Though the above expansion of $\partial^2 T_{ij} / \partial t^2$ (eq. III (11) of $\overline{11}$) is not an exact one it helps to illustrate two different mechanisms by which sound may be generated aerodynamically. In the first term the pressure inside the flow acts as the actual source function with an amplification by gradients of the mean-flow velocity \bar{c}_i . The second term involves products of fluctuations, instead (note that $p = p'$). Terms like these are often referred to as 'shear-noise' and 'self-noise', respectively.

- e) Finally, Michalke and Fuchs $\overline{13}$ have thoroughly discussed the mechanisms by which a turbulent pressure field in a sheared flow may, very efficiently, generate sound. Michalke (eq. (2.7) of $\overline{13}$) rewrote Lighthill's source integral (4.23) for the sound pressure in the far-field as due to the mean flow-turbulence interaction (neglecting the non-linear fluctuation terms):

$$p_{MT} = \frac{1}{4\pi a_0^2 r} \int_V dV \left\{ \frac{2}{(1 - \bar{M}_r)^3} \frac{\partial \bar{c}_r}{\partial y_r} \left[\frac{\partial p}{\partial t} \right] + \frac{\bar{M}_r (2 - \bar{M}_r)}{(1 - \bar{M}_r)^2} \left[\frac{\partial^2 p}{\partial t^2} \right] \right\} \quad (4.25)$$

with

$$\bar{M}_r = \frac{x_i \bar{c}_i}{r a_0} = \frac{\bar{c}_r}{a_0} < 1 ; \quad \frac{\partial \bar{c}_r}{\partial y_r} = \frac{x_i x_j}{r^2} \frac{\partial \bar{c}_i}{\partial y_j} \quad (4.26)$$

This source integral (4.25) was found particularly suitable for treating noise from circular jets. The author feels that it has three main advantages over other pressure models discussed before:

- The Mach number M_r of the (local) mean velocity component pointing towards the observer (at distance r) may take on arbitrary values not exceeding unity. The model is therefore less restrictive than approximation (4.10) or Meecham and Ford's source integral (4.12).
- The pressure p in eq. (4.25) is just the pressure fluctuation in the source region with no specifications like Ribner's needed. In particular, it is not necessary to define a pseudosound (or incompressible) pressure field inside as distinct from the sound (or compressible) pressure field outside the flow region as done by Ribner [10]. It thus avoids certain complications when direct measurements are made in the flow and its near-field.
- The weighting functions in (4.25) multiplying the time derivatives of the pressure provide that the relevant source region over which the integration is performed ends where the mean flow tends to zero. Thus Lighthill's objection (1) in the Appendix B of ref. [11] that in pressure source models noise generation from outside the flow has, rather artificially, to be postulated does not apply in this case.

The application of the last-described approach to the problem of jet mixing noise will be elaborated a bit in par. 6.5.

5. 'TRUE SOURCE' IDENTIFICATION METHODS

In the above described acoustic analogy theories the aerodynamic noise sources are taken as being prescribed in an acoustic medium at rest. After Lighthill had concentrated on the acoustic characteristics of just a single volume element of turbulence in free space it was only logical to proceed and take into account that such a turbulent eddy would somehow be convected with the mean flow at a speed U_c which may differ from the local flow velocity. A fixed observer or probe would realize apparent time rates of change in the turbulent field which are partly due to the effect of sources travelling past the observer whereas only the 'intrinsic' rates of change in a co-moving system of coordinates were significant. Several attempts were therefore made to identify the turbulent sources in a convected system.

Some of these attempts remain within the frame-work of Lighthill's acoustic analogy theory, others start from modified or completely new differential equations. Most of them have in common that they assume the actual turbulent sources to be known a priori and then try to describe how the sound originating from some kind of an eddy is modified by convection, refraction or any other kind of mean-flow / acoustic interactions. These methods do not provide any new information about the turbulent source structure itself and about how it generates sound under varying mean flow conditions. Rather they try adjusting the theory to a biased source model in order to make this model more realistic, e.g., to justify the assumption of acoustically compact quadrupoles in jet turbulence.

5.1 Introduction of a convective amplification factor

The first extension of the acoustic analogy approach is due to Lighthill [12], Ribner [10] and Ffowcs Williams [14]. They multiplied the original source integrals as derived for a stationary source distribution by an additional factor C^n where in the simplest case C equals the Doppler factor from equation (3.39). The exponent n depends critically on the nature of the sources involved, i.e. on the model of the turbulence employed.

On the assumption of an isotropic eddy structure convected at constant speed from minus to plus infinity the results of refs. [10, 14] for a modified Doppler factor,

$$C = \{ (1 - U_c \cos \theta / a_0)^2 + \alpha^2 \}^{-1/2}, \quad (5.1)$$

were re-derived in ref. [1]. It was noted there that the introduction of C as an amplification (or attenuation) factor is of not much help if the turbulent source distribution is not isotropic. The isolation and explicit estimation of the source convection effect obviously suffers from the fact that there is no general agreement on the source structure in a specific flow like, e.g., a turbulent jet.

The parameter α in eq. (5.1) has been given different physical meaning by Ribner and Ffowcs Williams. The most plausible interpretation of α is that due to Crighton [15], as an acoustic compactness ratio of the turbulent sources, with $\alpha \ll 1$ for a compact eddy or acoustic point source.

5.2 Phillips' convected wave equation

One may not be convinced that a simple Doppler factor C^n could account for the effect of source convection in turbulent flow in analogy to features of acoustic point sources in uniform motion as described under par. 3.5. But if one, yet, agrees that source convection and sound refraction are important effects which should not be left hidden in the forcing terms of Lighthill's wave equation, it is necessary to abandon the whole concept by which equivalent sound sources are defined in a homogeneous medium at rest in analogy to par. 3.4. Instead one may want to tackle the aerodynamic noise problem with differential equations resembling those for the propagation of sound through non-uniform flow (par. 3.1 or 3.2) with correspondingly modified forcing terms on their right-hand sides.

The work of Phillips [16] was the first major departure from the Lighthill point of view and an early attempt to derive a convected wave equation.

We follow Phillips' idea when writing the fluid dynamics equation of par. 2 in the following form:

$$\frac{1}{\rho} \frac{\partial p}{\partial t} + \frac{\partial c_i}{\partial x_i} = \frac{m}{\rho} \quad (5.2)$$

$$\frac{\partial c_i}{\partial t} + \frac{1}{\rho} \frac{\partial p}{\partial x_i} - \frac{1}{\rho} \frac{\partial \tau_{ij}}{\partial x_j} = \frac{f_i}{\rho} \quad (5.3)$$

$$\frac{1}{a_0^2 \rho} \frac{\partial^2 p'}{\partial t^2} - \frac{1}{\rho} \frac{\partial^2 p'}{\partial x_1^2} = 2 \gamma \frac{\partial \bar{c}_1}{\partial x_2} \frac{\partial c'_2}{\partial x_1} \quad (5.13)$$

When this is compared to eq. (3.12) of par. 3.2 one may, in fact, question if the right-hand side which Phillips considered to be the dominant source term represents a real source mechanism, at all.

It thus remains to be stated that, at least, Phillips successfully eliminated the fluid density ρ from the source function of his inhomogeneous non-linear wave equation. This is an obvious advantage over Lighthill's equation (4.6), in which the same variable ρ appears on both sides. It enabled Phillips to derive asymptotic solutions for two-dimensional shear flows in the limit of very high supersonic speeds and to describe the radiation of 'eddy Mach waves'.

5.3 Pao's linearized convected wave equation

Before deriving Pao's [19] equation, one may first expand the second material derivative in Phillips' equation (5.10),

$$\frac{D^2}{Dt^2} \equiv \frac{\partial^2}{\partial t^2} + 2 c_i \frac{\partial^2}{\partial x_i \partial t} + \frac{\partial c_i}{\partial t} \frac{\partial}{\partial x_i} + c_i c_j \frac{\partial^2}{\partial x_i \partial x_j} + c_i \frac{\partial c_j}{\partial x_i} \frac{\partial}{\partial x_j}, \quad (5.14)$$

for a unidirectional transversely sheared flow with

$$c_i = \bar{c}_i + c'_i; \quad \bar{c}_i = \{\bar{c}_1(x_2); 0; 0\} \quad (5.15)$$

yielding the following identity:

$$\begin{aligned} \frac{D^2}{dt^2} &\equiv \frac{\partial^2}{\partial t^2} + 2 \bar{c}_1 \frac{\partial^2}{\partial x_1 \partial t} + \bar{c}_1^2 \frac{\partial^2}{\partial x_1^2} \\ &\quad + 2 c'_i \frac{\partial^2}{\partial x_i \partial t} + 2 \bar{c}_1 c'_i \frac{\partial^2}{\partial x_1 \partial x_i} \\ &\quad + \frac{\partial c'_i}{\partial t} \frac{\partial}{\partial x_i} + \bar{c}_1 \frac{\partial c'_i}{\partial x_1} \frac{\partial}{\partial x_i} \\ &\quad + c'_i c'_j \frac{\partial^2}{\partial x_i \partial x_j} + c'_i \frac{\partial c'_j}{\partial x_i} \frac{\partial}{\partial x_j} \\ &\equiv \frac{\bar{D}^2}{Dt^2} + \frac{\partial \bar{c}_1}{\partial t} \frac{\partial}{\partial x_1} + 2 c'_i \frac{\bar{D}}{Dt} \frac{\partial}{\partial x_i} + c'_i c'_j \frac{\partial^2}{\partial x_i \partial x_j} + c'_i \frac{\partial c'_j}{\partial x_i} \frac{\partial}{\partial x_j} \end{aligned} \quad (5.16)$$

Phillips' first source term q_1 may be similarly expanded to yield

$$\gamma \frac{\partial c_j}{\partial x_i} \frac{\partial c_i}{\partial x_j} = 2 \gamma \frac{\partial \bar{c}_1}{\partial x_2} \frac{\partial c'_2}{\partial x_1} + \frac{\partial c'_j}{\partial x_1} \frac{\partial c'_i}{\partial x_j}. \quad (5.17)$$

From the resulting form of Phillips' equation,

$$\begin{aligned} \frac{\bar{D}^2 r}{Dt^2} - \frac{\partial}{\partial x_i} (a^2 \frac{\partial r}{\partial x_i}) + \frac{\partial \bar{c}_1}{\partial t} \frac{\partial r}{\partial x_1} + 2 c'_i \frac{\bar{D}}{Dt} \frac{\partial r}{\partial x_i} + c'_i c'_j \frac{\partial^2 r}{\partial x_i \partial x_j} + c'_i \frac{\partial c'_j}{\partial x_i} \frac{\partial r}{\partial x_j} = \\ = 2 \gamma \frac{\partial \bar{c}_1}{\partial x_2} \frac{\partial c'_2}{\partial x_1} + \gamma \frac{\partial c'_j}{\partial x_1} \frac{\partial c'_i}{\partial x_j}, \end{aligned} \quad (5.18)$$

one may derive Pao's linearized convected wave equation. Though he did not give the full eq. (5.18), one may surmise from his paper [19] that he neglected the terms

$$c'_i c'_j \frac{\partial^2 r}{\partial x_i \partial x_j}; \quad c'_i \frac{\partial c'_j}{\partial x_i} \frac{\partial r}{\partial x_j} \quad \text{as being small of higher order}$$

$$2 c'_i \frac{\bar{D}}{Dt} \frac{\partial r}{\partial x_i} \quad \text{by reason of } |c'_i| \ll \bar{c}_1$$

$$\frac{\partial c'_i}{\partial t} \frac{\partial r}{\partial x_i} \quad \text{since } \partial c'_i / \partial t \approx - \bar{c}_1 \partial c'_i / \partial x_1$$

$$\frac{1}{\rho} \frac{Dp}{Dt} = \frac{1}{\rho a^2} \frac{Dp}{Dt} - \frac{1}{c_p} \frac{Ds}{Dt} \quad (5.4)$$

Subtracting eq. (5.4) from (5.2) yields

$$\frac{\partial c_i}{\partial x_i} = -\frac{1}{\rho a^2} \frac{Dp}{Dt} + \frac{1}{c_p} \frac{Ds}{Dt} + \frac{m}{\rho} \quad (5.5)$$

Operating with $\gamma \partial/\partial x_i$ on eq. (5.3) and with $\gamma D/Dt$ on (5.5) results in

$$\frac{\partial}{\partial x_i} \left(\frac{\gamma}{\rho} \frac{\partial p}{\partial x_i} \right) = -\gamma \frac{\partial}{\partial x_i} \frac{D c_i}{Dt} + \frac{\partial}{\partial x_i} \left(\frac{\gamma}{\rho} \frac{\partial \tau_{ij}}{\partial x_j} \right) + \frac{\partial}{\partial x_i} \left(\frac{\gamma f_i}{\rho} \right) \quad (5.6)$$

$$\frac{D}{Dt} \left(\frac{\gamma}{\rho a^2} \frac{Dp}{Dt} \right) = -\gamma \frac{D}{Dt} \frac{\partial c_i}{\partial x_i} + \frac{D}{Dt} \left(\frac{\gamma}{\rho} \frac{Ds}{Dt} \right) + \frac{D}{Dt} \left(\frac{\gamma m}{\rho} \right) \quad (5.7)$$

where γ is the constant ratio of the specific heats of the medium. By means of the identities

$$\frac{\partial}{\partial x_i} \frac{D}{Dt} - \frac{D}{Dt} \frac{\partial}{\partial x_i} \equiv \frac{\partial c_j}{\partial x_i} \frac{\partial}{\partial x_j} \quad (5.8)$$

and

$$\frac{D}{Dt} \left(\frac{1}{\rho} \frac{Dp}{Dt} \right) - \frac{\partial}{\partial x_i} \left(\frac{a^2}{\rho} \frac{\partial p}{\partial x_i} \right) \equiv \frac{D^2}{Dt^2} \ln p/p_0 - \frac{\partial}{\partial x_i} \left(a^2 \frac{\partial}{\partial x_i} \ln p/p_0 \right) \quad (5.9)$$

we may derive a kind of wave equation in terms of the logarithm of the pressure, $r = \ln p/p_0$, by subtracting eq. (5.6) from (5.7),

$$\begin{aligned} \frac{D^2 r}{Dt^2} - \frac{\partial}{\partial x_i} \left(a^2 \frac{\partial r}{\partial x_i} \right) &= \gamma \frac{\partial c_j}{\partial x_i} \frac{\partial c_i}{\partial x_j} + \frac{D}{Dt} \left(\frac{\gamma}{c_p} \frac{Ds}{Dt} \right) - \frac{\partial}{\partial x_i} \left(\frac{\gamma}{\rho} \frac{\partial \tau_{ij}}{\partial x_j} \right) \\ &\quad + \frac{D}{Dt} \left(\frac{\gamma}{\rho} m \right) - \frac{\partial}{\partial x_i} \left(\frac{\gamma}{\rho} f_i \right) \end{aligned} \quad (5.10)$$

The five source terms on the right side of the generalized Phillips' equation (5.10) may be identified as

$$q_1 = \gamma \frac{\partial c_j}{\partial x_i} \frac{\partial c_i}{\partial x_j} \quad \text{due to turbulent velocity field}$$

$$q_2 = \frac{D}{Dt} \left(\frac{\gamma}{c_p} \frac{Ds}{Dt} \right) \quad \text{due to entropy fluctuations}$$

$$q_3 = -\frac{\partial}{\partial x_i} \left(\frac{\gamma}{\rho} \frac{\partial \tau_{ij}}{\partial x_j} \right) \quad \text{due to viscosity effects}$$

$$q_4 = \frac{D}{Dt} \left(\frac{\gamma}{\rho} m \right) \quad \text{due to mass injection}$$

$$q_5 = -\frac{\partial}{\partial x_i} \left(\frac{\gamma}{\rho} f_i \right) \quad \text{due to body forces.}$$

Phillips did not include the external sources, q_4 and q_5 , neglected the diffusion terms, q_2 and q_3 , and ultimately concentrated on q_1 as the dominant source.

Phillips claimed that in his convected wave equation the effects of convection and of refraction of sound by the mean flow and by the variations in the local speed of sound were included in the left-hand side whereas in Lighthill's acoustic analogy these effects had to be described as equivalent sources on the right.

For the special case $a = a_0 = \text{const}$ Phillips' equation,

$$\frac{D^2 r}{Dt^2} - a_0^2 \frac{\partial^2 r}{\partial x_i^2} = \gamma \frac{\partial c_j}{\partial x_i} \frac{\partial c_i}{\partial x_j} ; \quad \frac{D}{Dt} = \frac{\partial}{\partial t} + c_i \frac{\partial}{\partial x_i} \quad (5.11)$$

indeed very closely resembles the wave equation (3.17) of par. 3.3 for the sound propagation in uniform flow ($\bar{c}_i = \text{const}$) or acoustic sources in uniform motion:

$$\frac{\bar{D}^2 p'}{\bar{D}t^2} - a_0^2 \frac{\partial^2 p'}{\partial x_i^2} = 0 ; \quad \bar{D} = \frac{\partial}{\partial t} + \bar{c}_i \frac{\partial}{\partial x_i} \quad (5.12)$$

A comparison of the homogeneous part of eq. (5.11) with the linear acoustic equations valid in non-uniform flows (refer to pars. 3.1 and 3.2) immediately shows that the former cannot possibly model the complete effects of source convection and sound refraction by the mean flow. Lilley [17] and Doak [18] first showed that the right-hand side of (5.11) must contain terms which one ought to take to the left if one had to identify a 'true source' distribution on the right. For a transversely sheared flow (refer to par. 3.2), a linearized version of Phillips' equation would read:

$$\frac{1}{a_0^2 \rho} \frac{\partial^2 p'}{\partial t^2} - \frac{1}{\rho} \frac{\partial^2 p'}{\partial x_i^2} = 2 \gamma \frac{\partial \bar{c}_1}{\partial x_2} \frac{\partial c'_1}{\partial x_1} \quad (5.13)$$

When this is compared to eq. (3.12) of par. 3.2 one may, in fact, question if the right-hand side which Phillips considered to be the dominant source term represents a real source mechanism, at all.

It thus remains to be stated that, at least, Phillips successfully eliminated the fluid density ρ from the source function of his inhomogeneous non-linear wave equation. This is an obvious advantage over Lighthill's equation (4.6), in which the same variable ρ appears on both sides. It enabled Phillips to derive asymptotic solutions for two-dimensional shear flows in the limit of very high supersonic speeds and to describe the radiation of 'eddy Mach waves'.

5.3 Pao's linearized convected wave equation

Before deriving Pao's [19] equation, one may first expand the second material derivative in Phillips' equation (5.10),

$$\frac{D^2}{Dt^2} \equiv \frac{\partial^2}{\partial t^2} + 2 c_i \frac{\partial^2}{\partial x_i \partial t} + \frac{\partial c_i}{\partial t} \frac{\partial}{\partial x_i} + c_i c_j \frac{\partial^2}{\partial x_i \partial x_j} + c_i \frac{\partial c_j}{\partial x_i} \frac{\partial}{\partial x_j}, \quad (5.14)$$

for a unidirectional transversely sheared flow with

$$c_i = \bar{c}_i + c'_i; \quad \bar{c}_i = \{\bar{c}_1(x_2); 0; 0\} \quad (5.15)$$

yielding the following identity:

$$\begin{aligned} \frac{D^2}{Dt^2} &\equiv \frac{\partial^2}{\partial t^2} + 2 \bar{c}_1 \frac{\partial^2}{\partial x_1 \partial t} + \bar{c}_1^2 \frac{\partial^2}{\partial x_1^2} \\ &\quad + 2 c'_i \frac{\partial^2}{\partial x_i \partial t} + 2 \bar{c}_1 c'_i \frac{\partial^2}{\partial x_1 \partial x_i} \\ &\quad + \frac{\partial c'_i}{\partial t} \frac{\partial}{\partial x_i} + \bar{c}_1 \frac{\partial c'_i}{\partial x_1} \frac{\partial}{\partial x_i} \\ &\quad + c'_i c'_j \frac{\partial^2}{\partial x_i \partial x_j} + c'_i \frac{\partial c'_j}{\partial x_i} \frac{\partial}{\partial x_j} \\ &\equiv \frac{\partial^2}{\partial t^2} + \frac{\partial c'_i}{\partial t} \frac{\partial}{\partial x_i} + 2 c'_i \frac{\partial}{\partial t} \frac{\partial}{\partial x_i} + c'_i c'_j \frac{\partial^2}{\partial x_i \partial x_j} + c'_i \frac{\partial c'_j}{\partial x_i} \frac{\partial}{\partial x_j} \end{aligned} \quad (5.16)$$

Phillips' first source term q_1 may be similarly expanded to yield

$$\gamma \frac{\partial c_j}{\partial x_i} \frac{\partial c_i}{\partial x_j} = 2 \gamma \frac{\partial \bar{c}_1}{\partial x_2} \frac{\partial c'_1}{\partial x_1} + \frac{\partial c'_1}{\partial x_1} \frac{\partial c'_1}{\partial x_j}. \quad (5.17)$$

From the resulting form of Phillips' equation,

$$\begin{aligned} \frac{D^2 r}{Dt^2} - \frac{\partial}{\partial x_i} (a^2 \frac{\partial r}{\partial x_i}) + \frac{\partial c'_i}{\partial t} \frac{\partial r}{\partial x_i} + 2 c'_i \frac{\partial}{\partial t} \frac{\partial r}{\partial x_i} + c'_i c'_j \frac{\partial^2 r}{\partial x_i \partial x_j} + c'_i \frac{\partial c'_j}{\partial x_i} \frac{\partial r}{\partial x_j} = \\ = 2 \gamma \frac{\partial \bar{c}_1}{\partial x_2} \frac{\partial c'_1}{\partial x_1} + \gamma \frac{\partial c'_1}{\partial x_1} \frac{\partial c'_1}{\partial x_j}, \end{aligned} \quad (5.18)$$

one may derive Pao's linearized convected wave equation. Though he did not give the full eq. (5.18), one may surmise from his paper [19] that he neglected the terms

$$c'_i c'_j \frac{\partial^2 r}{\partial x_i \partial x_j}; \quad c'_i \frac{\partial c'_j}{\partial x_i} \frac{\partial r}{\partial x_j} \quad \text{as being small of higher order}$$

$$2 c'_i \frac{\partial}{\partial t} \frac{\partial r}{\partial x_i} \quad \text{by reason of } |c'_i| \ll \bar{c}_1$$

$$\frac{\partial c'_i}{\partial t} \frac{\partial r}{\partial x_i} \quad \text{since } \partial c'_i / \partial t \equiv - \bar{c}_1 \partial c'_i / \partial x_1$$

Pao considered both $\partial/\partial t$ and $\bar{c}_1 \partial/\partial x_1$ of the fluctuating velocity components to be large quantities, but he justified the last assumption since "their combination represents the evolution of the turbulence in the moving frame of reference which is known to be slow" (Taylor's hypothesis).

In his own convected wave equation,

$$\frac{\partial^2 r}{\partial t^2} - \frac{\partial}{\partial x_i} (a^2 \frac{\partial r}{\partial x_i}) = 2\gamma \frac{\partial \bar{c}_1}{\partial x_2} \frac{\partial c'_2}{\partial x_1} + \gamma \frac{\partial c'_j}{\partial x_i} \frac{\partial c'_i}{\partial x_j} \quad (5.19)$$

Pao only retained one source term quadratic in fluctuating velocities and one linear. He considered the corresponding 'self-noise' and 'shear-noise' contributions as statistically independent and known a priori in the usual sense.

Pao derived solutions to a generalized Fourier transform of eq. (5.19) for $a = a(x_2)$ in the form of plane wave elements in the x_2 direction. In his attempt to study the effects of refraction, convection, Mach number and temperature variations in the noise emission processes of subsonic and supersonic idealized shear layers, Pao was restricted to sound wave lengths λ not exceeding a certain multiple of the shear layer thickness,

$$\frac{L}{\lambda} = \frac{fL}{a} = \frac{fL}{U} \frac{U}{a} = St M > \frac{1}{2\pi} \quad (5.20)$$

5.4 Lilley's shear refraction equation

For a critique of all the above described theoretical approaches to the aerodynamic noise problem the reader may refer to Doak's paper / 18 /. Concerning the Phillips-Pao concept Doak argues that only the non-linear ('self-noise') term of eq. (5.18) can properly be regarded as a 'true source' term, and that the linear ('shear-noise') term should really be expressed in terms of r and included in the differential operator on the left as a so-called 'shear refraction' term.

This can be done by taking D/Dt of eq (5.10),

$$\begin{aligned} \frac{D}{Dt} \left\{ \frac{\partial^2 r}{\partial t^2} - \frac{\partial}{\partial x_i} (a^2 \frac{\partial r}{\partial x_i}) \right\} &= \gamma \frac{D}{Dt} \left(\frac{\partial c_j}{\partial x_i} \frac{\partial c_i}{\partial x_j} \right) + \frac{D}{Dt} (q_2 + q_3 + q_4 + q_5) \\ &= 2\gamma \frac{\partial c_j}{\partial x_i} \frac{D}{Dt} \left(\frac{\partial c_i}{\partial x_j} \right) + \frac{D}{Dt} (q_2 + q_3 + q_4 + q_5) \end{aligned} \quad (5.21)$$

and by using the identity (5.8),

$$\frac{D}{Dt} \frac{\partial c_i}{\partial x_j} = \frac{\partial}{\partial x_j} \frac{D c_i}{Dt} - \frac{\partial c_k}{\partial x_j} \frac{\partial c_i}{\partial x_k}, \quad (5.22)$$

and the momentum equation (5.3),

$$\frac{D c_i}{Dt} = - \frac{a^2}{\gamma} \frac{\partial r}{\partial x_i} + \frac{1}{\rho} \frac{\partial \tau_{ik}}{\partial x_k} + \frac{f_i}{\rho} \quad (5.23)$$

in order to split the first term on the right of eq. (5.21) into one which represents the shear refraction and as such is taken to the left and into one which in Lilley's / 17 / view more likely represents a 'true source' term and as such is retained on the right:

$$\begin{aligned} \frac{D}{Dt} \left\{ \frac{\partial^2 r}{\partial t^2} - \frac{\partial}{\partial x_i} (a^2 \frac{\partial r}{\partial x_i}) \right\} + 2 \frac{\partial c_j}{\partial x_i} \frac{\partial}{\partial x_j} (a^2 \frac{\partial r}{\partial x_i}) &= - 2\gamma \frac{\partial c_j}{\partial x_i} \frac{\partial c_k}{\partial x_j} \frac{\partial c_i}{\partial x_k} \\ &+ \frac{D}{Dt} (q_2 + q_3 + q_4 + q_5) + q_6 + q_7 \end{aligned} \quad (5.24)$$

with

$$\begin{aligned} q_6 &= 2 \frac{\partial c_j}{\partial x_i} \frac{\partial}{\partial x_j} \left(\frac{\gamma}{\rho} \frac{\partial \tau_{ik}}{\partial x_k} \right) \\ q_7 &= 2 \frac{\partial c_j}{\partial x_i} \frac{\partial}{\partial x_j} \left(\frac{\gamma}{\rho} f_i \right) \end{aligned}$$

This third-order non-linear differential equation may again be linearized about a transversely sheared flow to yield

$$\frac{D}{Dt} \left\{ \frac{\partial^2 r}{\partial t^2} - \frac{\partial}{\partial x_i} (a^2 \frac{\partial r}{\partial x_i}) \right\} + 2 \frac{\partial \bar{c}_1}{\partial x_2} \frac{\partial}{\partial x_1} (a^2 \frac{\partial r}{\partial x_2}) = \Lambda(x_i, t) \quad (5.24)$$

with $\Lambda(x_i, t)$ representing a great variety of source terms of different order of magnitude but with no terms linear in fluctuating velocities being present on the right side of eq. (5.24).

In the special case of $a = a_0 = \text{const}$ the left side of eq. (5.24) indeed very closely resembles eq. (3.14) for sound propagation in a transversely sheared flow. It may be noted that Lilley's equation takes on a similar form as (5.24) when in a cylindrical shear flow the mean axial velocity distribution varies radially,

$$\bar{c}_i = \{0; 0; \bar{c}_z(R)\}; \quad \frac{\partial}{\partial t} \equiv \frac{\partial}{\partial t} + \bar{c}_z \frac{\partial}{\partial z}. \quad (5.25)$$

It should be borne in mind, however, that both density fluctuations ρ' and pressure fluctuations p' are hidden in $a^2 = a^2 + (a^2)'$ and that writing $\Lambda(x_i, t)$ in terms of just the turbulent velocity field c_i' assumes that interactions between c_i' and p' or ρ' are weaker than those involving c_i' (cf. Lilley's [17] approximation (4.14)).

At this point the reader may like to read Doak's [18] emphatic appreciation of Lilley's theory, particularly his par. 2.4. One of his objections against the concepts of Lighthill and Phillips seems to have been the following. On the assumption of very small, compact 'eddies' radiating sound of a given directivity through a shear layer, the far-field sound of any individual eddy would be strongly affected by the shear-refraction effect. It would thus be necessary to use a linearized wave operator like that in eq. (5.24) with, e.g., $a^2 = a^2(x_2)$ if temperature gradients are present in order to predict the propagation of the sound from the source through the shear layer to the observer. An experimenter would find it difficult to trace this refracted sound field in the vicinity of the eddy since the propagation and refraction terms would be swamped in the disturbed flow by the presence of the neighbouring 'eddies'. Thus, according to Doak and the model he employed, "the experimenter is quite unable to provide the theoretician with the information that the latter needs about such convection and refraction terms in the form of 'equivalent source' data... Because of this situation, a correct formulation can be obtained... only by extracting from the right-hand side source term all propagation-type terms and placing them on the left-hand side of the wave equation."

The situation would be quite different if the turbulent sources were not thought of as acoustic singularities embedded in the flow but if, instead, the sources were spatially extended with their fluctuations being coherent in the transverse direction over the whole of the shear layer. Under these assumptions it would not be a very logical procedure to consider sound emanating from source elements individually and the need for isolating 'true sources' from secondary refraction effects would be less obvious. The effect of the mean shear would in this case be primarily one on the source mechanism itself. Or as Crighton [15] put it: "Whether or not eq. (5.24) constitutes a significant improvement upon eq. (5.19) remains to be seen, as the identification of important processes which should be retained on the left is done entirely by assertion, and without any rational expansion procedure in mind which would enable generation and propagation effects to be distinguished."

The price which must be paid for including the convection and refraction effects in the wave operator part of the convected equation is a great increase in the complexity of the solutions when compared to the Lighthill-Curle source integrals eq. (4.8) based on the almost trivial Kirchhoff solution to the ordinary wave equation.

5.5 Solutions to Lilley's equation

It was shown by Lilley [17] that equations of the type derived in par. 5.4 can be used to describe the hydrodynamic instability phenomena which are characteristic of transversely sheared flow, be it laminar or turbulent. The large-scale structure of the turbulence in such shear layers are believed to be the result of the growth of local instabilities associated with the mean motion and the mean temperature field. The equation defining this instability is the Orr-Sommerfeld equation and the instabilities correspond to the eigenvalues of this equation. It can be shown that the 'most unstable modes' contribute the major proportion of energy to the mean square and mean product terms within the turbulence.

Yet, this ability of a certain class of differential equations to describe, at least in principle, the cause and the effect of aerodynamically generated noise at the same time, has not led, up till now, to a theoretical solution of the problem. Determination of the source terms in any of the 'true source' identification methods is still left to experiment or speculation.

The ability of Lilley's wave operator to describe, on the other hand, sound convection and refraction effects has been successfully tested by several authors by solving an equation of the following or a similar form

$$\frac{\partial^3 r'}{\partial t^3} - \frac{\partial}{\partial t} \frac{\partial}{\partial x_i} (a^2 \frac{\partial r'}{\partial x_i}) + 2 \frac{\partial \bar{c}_i}{\partial x_2} (a^2 \frac{\partial r'}{\partial x_2}) = - 2\gamma \frac{\partial \bar{c}_1}{\partial x_2} \frac{\partial^2 c_i' c_j'}{\partial x_1 \partial x_k} + \frac{\partial}{\partial t} \frac{\partial^2 c_i' c_j'}{\partial x_1 \partial x_j} \quad (5.26)$$

In eq. (5.26), which is linear in the fluctuating pressure,

$$r = \ln(p/p_0) = \ln(1 + p'/p_0) \approx p'/p_0 = r' \quad (5.27)$$

all the many source terms feasible have been dropped except for those representing non-linear interactions in the solenoidal (incompressible) part of the turbulent velocity field:

$$\frac{\partial c_i}{\partial x_i} = 0; \quad \frac{\partial c_i'}{\partial x_j} \frac{\partial c_j'}{\partial x_i} = \frac{\partial^2 c_i' c_j'}{\partial x_i \partial x_j}; \quad c_k' \frac{\partial c_i'}{\partial x_k} = \frac{\partial c_i' c_k'}{\partial x_k} \quad (5.28)$$

Due to this approximation in the source terms eq. (5.26) is more restrictive than even the linearized eq. (4.15) in Lilley's [17] original report. Its specific form is particularly attractive since it combines the merits of a convected wave equation with the simplicity of the Lighthill-type of source approximation,

$$T_{ij} \approx \rho_0 c_i' c_j' \quad (5.29)$$

Mani [20] recognized an additional advantage of eq. (5.26) in the apparent similarity of the 'shear-noise' and 'self-noise' terms, both being quadratic in the fluctuating velocities.

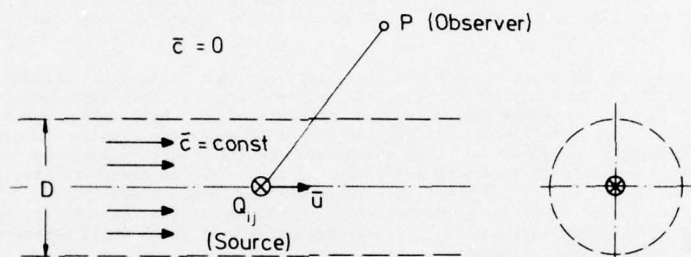
At this stage, it seems to have been almost inevitable that Lighthill's small-scale eddy model, too, had to be introduced, thus reducing the problem to a purely acoustic one. Mani [20] consequently considered a single point quadrupole embedded in and moving along the axis of an infinite cylindrical shear layer with an idealized plug-flow profile (Fig. 3). He introduced

$$c_i' c_j' = Q_{ij}^0 \delta(y) \delta(z) \delta(x - \bar{u}t) \exp(i\omega t) \quad (5.30)$$

with Q_{ij}^0 constant into the 'self-noise' term, disregarding the 'shear-noise' term of eq. (5.26).

Balsa [21] extended Mani's analysis for an arbitrary radial velocity profile $\bar{c}(R)$. He derived yet another convection factor for a quadrupole on the axis in addition to that of par. 5.1. Balsa also determined a second weighting function which does not depend on the order of the acoustic singularity (quadrupole, dipole etc.). The latter is given in the form of a 'refraction integral' over $\bar{c}(R)$.

Fig. 3: Mani's [20] model for studying the refraction of sound from an acoustic singularity (Q_{ij}) embedded in a plug flow.



Finally, Tester and Morfey [22] considered a quadrupole type of ring source concentrated at a constant radius to investigate flow and non-uniform density effects on sound radiation from jets.

All of these applications of Lilley's wave operator seem to have improved our ability to interpret far-field noise directional characteristics of, in particular, hot jets. This progress, however, does not imply an improved model of the 'true source' sound generation process itself.

6. MODELS OF TURBULENT SOURCE MECHANISMS

6.1 The various concepts of stationary or moving turbulent sources

In the two preceding chapters 4 and 5 we have presented different mathematical procedures common in aerodynamic noise theory. They differ, first of all, in the complexity of the governing differential equations and in their corresponding integrals if these are available, at all. Second, one may discern different concepts by which the various approaches introduce equivalent sources. For free (unbounded) turbulence generating sound these source concepts may be characterized as follows.

Concept 1: The medium is homogeneous.
The mean flow field acts only on the source mechanism.
The observer is at rest.
The equivalent sources are at rest.

This concept is typical of acoustic analogy theories. The source distribution is prescribed (or measured) in the observer's system of coordinates. Linear turbulence/mean-flow interactions are taken as equivalent source mechanisms which may, in cases, even dominate the non-linear turbulence/turbulence interactions.

Concept 2: The medium is homogeneous.
The mean flow field only acts on the source mechanism.
The observer is at rest.
The equivalent sources move uniformly.

This concept tries to account for Doppler amplification due to source convection. Sources are prescribed in a system moving with the source convection speed where such a quantity can be sensibly defined.

Concept 3: The medium is inhomogeneous in density or temperature.
The mean flow field acts mainly on the sound propagation process.
The observer is at rest and outside the flow.
The equivalent sources may or may not move.

This concept accounts for sound convection and refraction by mean-flow and other inhomogeneities. The 'true sources' in this case have to be prescribed by the turbulent generation process in distinction from any propagation effects within the source region. Linear turbulence/mean flow interactions are not accepted as a relevant source mechanism.

Concept 4: The medium is homogeneous.
The mean flow is unidirectional and uniform.
The observer is at rest, but inside the flow.
The equivalent sources are at rest.

This concept is due to Goldstein [3] and was particularly meant to apply to the noise generated by fans and compressors embedded in an infinite straight duct containing a uniform flow. It starts from the Lighthill equation written in coordinates x_i moving with the mean flow,

$$\frac{\partial^2 \rho'}{\partial t^2} - a_0^2 \frac{\partial^2 \rho'}{\partial x_i^2} = \frac{\partial^2 T_{ij}'}{\partial x_i \partial x_j} \quad (6.1)$$

The stress tensor T_{ij}' is expressed in terms of the velocities c_i' relative to the mean flow,

$$c_i' = c_i - \delta_{ij} \bar{c}_j \quad (6.2)$$

By transforming into the fixed (x_i) system Goldstein found the following wave equation to be valid,

$$\frac{\partial^2 \rho'}{\partial t^2} - a_0^2 \frac{\partial^2 \rho'}{\partial x_i^2} = \frac{\partial^2 T_{ij}'}{\partial x_i \partial x_j}; \quad \frac{\partial}{\partial t} = \frac{\partial}{\partial t} + \bar{c}_j \frac{\partial}{\partial x_j} \quad (6.3)$$

Eq. (6.3) differs from a 'convected wave equation' earlier derived by Ribner [10] only in the fact that T_{ij}' is still in terms of the moving frame velocity fluctuations c_i' .

None of these four different concepts is principally restricted to a particular turbulent source structure, though most practical applications of these concepts were limited to the consideration of acoustic singularities as equivalent to a small-scale turbulent eddy model.

The simplicity and beauty of the original Lighthill concept 1 lies in its universal applicability and flexibility concerning the specific character of the mean flow and turbulence structures. It simply requires the measurement of mean and fluctuating quantities (including their space-time covariance) throughout the flow region. But in order to reduce the amount of experimental data required and to facilitate the mathematical procedure by which the far-field is to be calculated from the near-field data, different expansion schemes have been applied to the equivalent turbulent source quantity which will briefly be discussed in paragraphs 6.2 and 6.4.

6.2 Lighthill's multi-pole source expansion

The inhomogeneous wave equation (4.5) may be written in the following form,

$$\frac{1}{a_0^2} \frac{\partial^2 p}{\partial t^2} - \frac{\partial^2 p}{\partial x_i^2} = \frac{\partial M}{\partial t} - \frac{\partial F_i}{\partial x_i} + \frac{\partial^2 T_{ij}}{\partial x_i \partial x_j} = q \quad (6.4)$$

The corresponding source integrals, in the absence of any bounding surfaces,

$$(p - p_0) 4\pi = \int_V \frac{1}{r} \left[\frac{\partial M}{\partial t} \right] dV - \int_V \frac{1}{r} \left[\frac{\partial F_i}{\partial x_i} \right] dV + \int_V \frac{1}{r} \left[\frac{\partial^2 T_{ij}}{\partial x_i \partial x_j} \right] dV \quad (6.5)$$

exhibit three contributions to the radiated pressure $p - p_0$ which differ in their mathematical structure. From these it is possible to draw a very formal analogy of the sound generated aerodynamically to sound fields originating from ordinary acoustic point sources like monopoles, dipoles and quadrupoles. The distinction of three types of simple sources corresponds to three different ways in which one can cause kinetic energy to be converted into the acoustic energy of fluctuating longitudinal motions in a compressible medium:

1. By forcing the mass in a fixed region of space to fluctuate as with a loudspeaker diaphragm embedded in a very large baffle.
2. By forcing the momentum in a fixed region of space to fluctuate or, which is the same thing, forcing the rates of mass flux across fixed surfaces to vary; both these occur when a perfectly solid object vibrates without volume changes.
3. By forcing the rate of momentum flux across a fixed surface to vary. This is the typical feature when sound is generated by fluctuating shearing motions in a turbulent fluid flow.

This, after Lighthill, is a linear sequence of methods of energy conversion in that each of the described mechanisms prove less efficient than the preceding one. The individual character of the three types of source mainly involved in aerodynamic noise was described in detail in paragraphs I, 5.1 to I, 5.3 of ref. [1] by considering the acoustic equivalent of a volume element of $\partial M / \partial t$, $\partial F_i / \partial x_i$ and $\partial^2 T_{ij} / \partial x_i \partial x_j$, respectively.

It is here pointed out that the specific directivity patterns and the acoustic efficiencies of the individual components of this multi-pole expansion could only be derived for an element of, in most cases, an extended turbulent source field. Conclusions for the source field as a whole are valid only when the latter

may be modelled by a large number of such source elements which all radiate independently. This brings us to what may be called the 'eddy' model in aerodynamic noise theories.

6.3 The idealized model of small-scale isotropic turbulence

The only really straightforward theoretical model that provides a complete set of conditions by means of which the whole problem of sound generation can be solved analytically, is the model of homogeneous and isotropic turbulence in an incompressible and inviscid fluid. This was treated by Proudman [24] and represents one of the earliest applications of Lighthill's theory.

The implications and certain shortcomings of a more or less isotropic eddy model were discussed in detail in chapter II, 6 of ref. [17]. The definition of 'correlation volumes' V_c , the question of the 'acoustical compactness' of the eddy and the derivation of an acoustic intensity from 'unit volume of turbulence' were all reviewed with respect to dimensional analyses common in aerodynamic noise theory.

We recall here that if this kind of a turbulence model were strictly valid we would not need to evaluate double integrals over complicated source correlation functions in order to obtain the far-field sound intensities I_M , I_D or I_Q as due to a monopole, dipole or quadrupole distribution, respectively,

$$I_M = \frac{1}{16\pi^2 \rho_0 a_0^2} \frac{1}{|x_i|^2} \int_V \int_V \overline{\left[\frac{\partial M}{\partial t} \right]_t^+ \left[\frac{\partial M}{\partial t} \right]_t^+} dv dv' \quad (6.6)$$

$$I_D = \frac{1}{16\pi^2 \rho_0 a_0^3} \frac{x_i x_j}{|x_i|^4} \int_V \int_V \overline{\left[\frac{\partial F_i}{\partial t} \right]_t^+ \left[\frac{\partial F_j}{\partial t} \right]_t^+} dv dv' \quad (6.7)$$

$$I_Q = \frac{1}{16\pi^2 \rho_0 a_0^5} \frac{x_i x_j x_k x_l}{|x_i|^6} \int_V \int_V \overline{\left[\frac{\partial^2 T_{ij}}{\partial t^2} \right]_t^+ \left[\frac{\partial^2 T_{kl}}{\partial t^2} \right]_t^+} dv dv' \quad (6.8)$$

where t denotes differences in retarded times at the two source points.

Instead, we would derive the corresponding intensities per unit volume,

$$J_M = \frac{1}{16\pi^2 \rho_0 a_0^2} \frac{1}{|x_i|^2} \overline{\left(\frac{\partial M}{\partial t} \right)^2} V_c \quad (6.9)$$

$$J_D = \frac{1}{16\pi^2 \rho_0 a_0^3} \frac{x_i x_j}{|x_i|^4} \overline{\frac{\partial F_i}{\partial t} \frac{\partial F_j}{\partial t}} V_c \quad (6.10)$$

$$J_Q = \frac{1}{16\pi^2 \rho_0 a_0^5} \frac{x_i x_j x_k x_l}{|x_i|^6} \overline{\frac{\partial^2 T_{ij}}{\partial t^2} \frac{\partial^2 T_{kl}}{\partial t^2}} V_c \quad (6.11)$$

and simply multiply these by the number of correlation volumes into which the whole turbulent source region was subdivided.

For a turbulent jet, for instance, the number of independent eddies was estimated by Siddon [23] to lie around 2.500. For such very small correlation volumes inhomogeneities of the medium and the flow would not so much influence the source mechanism itself but the propagation of the sound emitted by the eddy. This situation surely calls for a wave equation which can properly describe the sound refraction of an acoustic singularity embedded in a transversely sheared flow.

It is within the frame-work of this very special turbulence model that Lilley's [17] and Mani's [20] concepts indeed provide a necessary refinement of Ribner's [10] earlier rough estimates of convection and refraction effects on jet noise.

6.4 Michalke's multi-mode expansion for the noise of cylindrical flows

Lighthill's multi-pole analysis, being confined to the characteristics of small source elements only, did not require the introduction of coordinates which were suitably adjusted to the specific geometry of the specific flow under consideration. But if one wants to really evaluate a source integral, say,

$$p - p_0 = \frac{1}{4\pi} \int_V \frac{1}{r} [q] dv \quad (6.12)$$

for a prescribed source distribution q one finds it more convenient to introduce adjusted source coordinates. For a circular jet, e.g., Michalke [25] writes the radiated pressure $p' = p - p_0$ at the observer P in terms of spherical coordinates $(\bar{r}, \theta, \varphi)$. The source point Q , on the other hand, is denoted by cylindrical

coordinates (x, r, φ') where the x -axis coincides with the jet axis and φ' is the azimuth angle at the circumference (Fig. 4). In the source integral corresponding to eq. (6.12),

$$p'(\vec{r}, \theta, \varphi, t) = \frac{1}{4\pi} \int_V \frac{1}{r_0} q(x, r, \varphi', t - \frac{r_0}{a_0}) dV \quad (6.13)$$

the retarded time is written down explicitly with r_0 denoting the distance between P and Q.

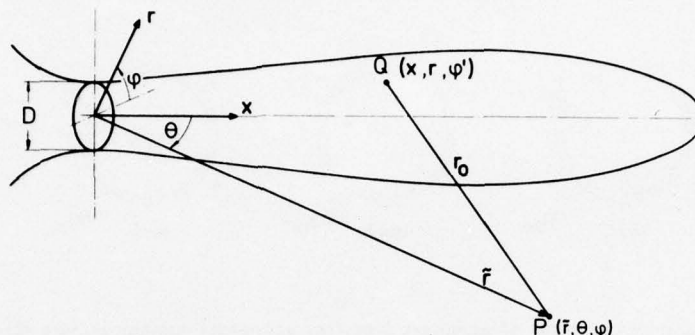


Fig. 4: Observer (P) and source (Q) coordinates for treating noise from a cylindrical flow.

The reason for introducing cylindrical instead of Cartesian coordinates to describe the source function q is that one may easily perform a Fourier decomposition of q into its azimuthal modes, q_m ,

$$q(x, r, \varphi', t) = \sum_{m=0}^{\infty} q_m(x, r, t) \exp(im\varphi') \quad (6.14)$$

The pressure p' may be similarly expanded,

$$p'(\vec{r}, \theta, \varphi, t) = \sum_{m=0}^{\infty} p_m(\vec{r}, \theta, t) \exp(im\varphi) \quad (6.15)$$

Finally q_m and p_m , which are random functions in time, may be Fourier transformed with respect to t ,

$$\int_{-\infty}^{+\infty} q_m(x, r, t) \exp(i\omega t) dt = q_{m\omega}(x, r) \quad (6.16)$$

$$\int_{-\infty}^{+\infty} p_m(\vec{r}, \theta, t) \exp(i\omega t) dt = p_{m\omega}(\vec{r}, \theta) \quad (6.17)$$

With the aid of the source integral (6.13) we may thus relate azimuthal frequency components, $p_{m\omega}$, of the radiated pressure to the corresponding azimuthal frequency components, $q_{m\omega}$, of the source fluctuations. This is shown schematically in Fig. 5 for the first three modes ($m = 0, 1, 2$) of a ring source element. The plus and minus signs indicate the instantaneous phase distribution of the different modes.

So far, this expansion scheme has only made use of a natural periodicity inherent in the φ -coordinate which repeats itself every 2π . It would apply to a source distribution which is dominated by a strong axisymmetric mode ($m = 0$) in the same way as it would apply to a source whose energy is evenly distributed over an infinite number of modes. In fact, the latter case would be equivalent to a small-scale eddy pattern at the circumference.

But if no specific turbulence model is introduced, all one can say at this stage is that a higher-order mode is most likely a less efficient sound emitter than the next lower one due to cancellation effects in the noise emanating from anti-phase source elements. In this respect, the present expansion scheme bears some faint similarity with Lighthill's multi-pole expansion.

It should be clear, however, that our present expansion scheme is particularly suitable to cylindrical flow like a jet which is known to perform strong random ring-vortex ($m = 0$) and fishtail wiggling ($m = 1$) type of motions, Michalke [25] also pointed out that on the jet axis ($r = 0$) all except the $m = 0$ mode must be zero, be it in the source region or in the far-field. Yet, the real benefits of treating turbulence

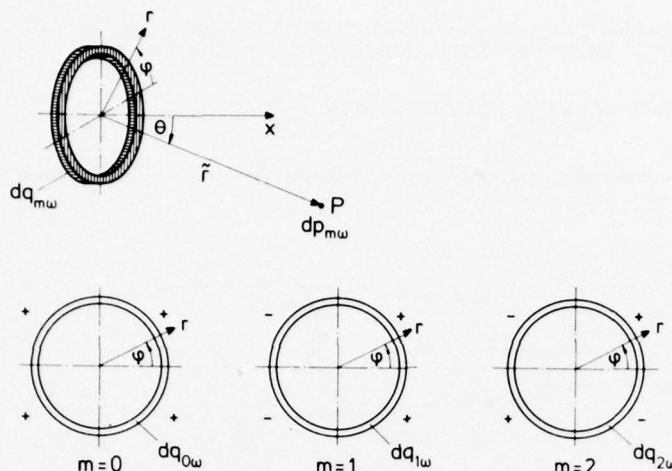


Fig. 5: Illustration of azimuthal frequency components of a ring source element dq .

and noise of a circular jet in terms of azimuthal frequency components becomes evident when a realistic model of the turbulent source fluctuations is deduced from a complete set of turbulence measurements and introduced into a conclusive jet noise theory.

The first step in this direction was done by Michalke and Fuchs [13] on the basis of eq. (4.25) of these lecture notes.

6.5 The large-scale coherent turbulence model in jet noise prediction

Our understanding of how noise is generated by the turbulent mixing of a round jet with the surrounding medium has been modified since orderly structures have been identified by several techniques. The large-scale phenomena show up most clearly in the fluctuating pressure field induced by the mixing process. The idea of large-scale coherent sound source patterns inside turbulent jets is now supported by a growing number of researchers as may be inferred from published accounts of the 1970 Symposium on Aerodynamic Noise (University of Loughborough) [26], the 1973 AGARD Meeting on Noise Mechanisms (Brussels) [27] and the 1974 Colloquium on Coherent Structures in Turbulence (University of Southampton) [28].

It is now felt that, underlying the random and disordered motion in the mixing zone of a jet, an orderly structure of turbulence exists whose phase variations, though random in time, show a remarkably strong coherence spatially over as much as 5 to 10 jet diameters D in the axial and several jet diameters in the radial direction. These phenomena, by which the jet as a whole appears as a coherent source, are particularly clear in the relevant range of Strouhal numbers

$$St = \frac{fD}{U_0} = 0.1 - 2.0 \quad (6.18)$$

in the lower-order ($m = 0, 1, 2, 3$) azimuthal constituents of the jet pressure field. They can be shown to occur in a broad range of jet exit Mach numbers,

$$M = \frac{U_0}{a_0} = 0.1 - 0.8 \quad (6.19)$$

and have been studied in different model jet facilities for Reynolds numbers up to

$$Re = \frac{U_0 D}{\nu} = 10^4 - 10^6 \quad (6.20)$$

Recent experiments at the ONERA and the DFVLR seem to indicate that in the near-field of real jet engines, too, these structures may be identified.

The theory favoured by the joint DFVLR-TUB group in Berlin⁵ essentially based on Lighthill's inhomogeneous wave equation approach and, in its present state of development, concentrates on the mean flow-turbulence interaction terms which are generally accepted as the dominant contributors to subsonic jet noise even in their much more restricted form as treated, among others, by Seiner and Reethof [29]. Our analysis will be further extended to also account for gradients in the temperature field. It may be taken as an advantage of the present theoretical approach that the actual pressure source function W_{p1p2} will be the same in the extended form of the theory.

A possible closure of the jet noise problem thus requires the measurement of the cross-spectral density function W_{p1p2} of the turbulent pressure p throughout the jet source region.

If this can be done with the necessary accuracy, it is possible to evaluate the source integral quantitatively with no dimensional arguments or matching factors being needed. The result of our combined experimental and theoretical effort can then be compared with far-field noise measurements in terms of spectra and directivity.

In order to characterize our prediction scheme, we write the source integral of ref. [13] in a compact form similar to that used in refs. [30] and [31].

$$W_{MT}(\bar{R}, \theta) = \frac{1}{\bar{R}^2} \sum_{m=0}^{\infty} \int_V d\bar{V}_{a1} \int_V d\bar{V}_{a2} \bar{W}_{12,m}(X_1, X_2, R_1, R_2) \bar{F}_{r,m}(\sigma) \bar{F}_x(\tau) \quad (6.21)$$

where the far-field power spectral density of the noise due to mean-flow/turbulence interactions, W_{MT} , was expanded into a series of azimuthal constituents with the following abbreviations being used

$\bar{R} = \bar{r}/D$	distance of far-field point (normalized)
$X = x/D$; $R = r/D$	normalized source coordinates
$d\bar{V} = 2\pi R dR dX$	annular volume element of source region
$\sigma^a = 2\pi St M R \sin\theta$	modified radial source coordinate
$\tau = 2\pi St M (X_2 - X_1) \cos\theta$	modified axial source coordinate

The integral (6.21) involves the cross spectral density function of the jet pressure field. In distinction from other pressure source models discussed in par. 4.3, however, this primary turbulent source function is weighted by two functions whose arguments depend on the Helmholtz number,

$$He = St M = D/\lambda$$

indicating that sound radiation from an extended source like a jet ought to be a function of not only the purely aerodynamic source parameters but also of the dimensions of the source in relation to the acoustic wave-length λ .

It is only logical when, apart from the trivial "decay function" $1/\bar{R}^2$, the source integral (6.21) incorporates additional weighting functions $\bar{F}_{r,m}(\sigma)$ since the present theory was especially constructed to deal with large-scale sources rather than small eddies.

The real and the imaginary parts of the function \bar{F}_x ,

$$\bar{F}_x = \exp(-it) \quad (6.22)$$

may take positive as well as negative values depending on the axial displacement times $\cos\theta$ in relation to the acoustic wave-length. Hence we have termed \bar{F}_x 'axial interference function'.

The other weighting function is

$$\bar{F}_{r,m} = \frac{1}{4} St^2 M^4 \hat{Z}_{m,1} Z_{m,2} \quad (6.23)$$

where \hat{Z}_m denotes the complex conjugate value of Z_m ,

$$Z_m = (-i)^m \pi \{ 2A_0 J_m(\sigma) + i A_1 [J_{m-1}(\sigma) - J_{m+1}(\sigma)] - A_2 [J_{m-2}(\sigma) + J_{m+2}(\sigma)] \} \quad (6.24)$$

with

$$\begin{aligned} A_0 &= \frac{1}{(1 - UM \cos \theta)^3} \left[2 \cos^2 \theta \frac{\partial U}{\partial X} + \sin^2 \theta \left(\frac{\partial V}{\partial R} + \frac{V}{R} \right) \right] - i 2\pi He \cos \theta \frac{(2 - UM \cos \theta)}{(1 - UM \cos \theta)^2} U \\ A_1 &= \frac{\sin 2\theta}{(1 - UM \cos \theta)^3} \left[\frac{\partial U}{\partial R} + \frac{\partial V}{\partial X} \right] - i 2\pi He \sin \theta \frac{(2 - UM \cos \theta)}{(1 - UM \cos \theta)^2} V \\ A_2 &= \frac{\sin^2 \theta}{(1 - UM \cos \theta)^3} \left[\frac{\partial V}{\partial R} - \frac{V}{R} \right] \end{aligned} \quad (6.25)$$

and $U = \bar{u}/U_0$, $V = \bar{v}/U_0$ as the local mean flow velocities.

The way in which the Bessel functions J_m act upon the source integral (6.21) for different values of the radial source coordinate r times $\sin\theta$ in relation to suggests to term $\bar{F}_{r,m}$ 'radial interference function'.

We presume that our experimental program will in due course provide us with a sufficient body of data concerning the cross spectral density of the pressure field, its magnitude expanded into several lower-order azimuthal constituents $|W_{12,m}|$ and their corresponding phase characteristics, which are given as a function of Strouhal number. As was already alluded to in par. 4.3 e), the weighting function $\bar{F}_{r,m}$ limits in a natural way the spatial extent of the region over which the pressure source function is to be integrated.

The spectrum and directivity of the far-field noise will, according to eq. (6.21) depend on the following flow properties

- the mean velocity field and its gradients,
- the intensity of the different azimuthal frequency components of the pressure field,
- the spatial coherence and phase distribution of the latter in both axial and radial directions.

The presently available experimental results indicate that a relatively simple model for $W_{12,m}$ with emphasis on the $m = 0$ and 1 modes and with almost complete coherence in planes normal to the jet may be used to evaluate the integral (6.21).

6.6 Powell's vortex model of aerodynamic noise

The pressure source models discussed in paragraphs 6.5 and 4.3 represent typical examples of a concept which considers the turbulent flow field as a continuous distribution of equivalent sound sources. Basically the same concept underlies Lighthill's eddy model, though in the latter the characteristic scales of the sources are considered extremely small compared to the dimensions of the flow.

By a concept common in hydrodynamics, one may regard certain incompressible flow fields as being induced by relatively simple vortex motions. Given the corresponding vorticity distribution, one may derive from it such secondary field quantities as pressure and velocity at any arbitrary point in the flow. This concept being applicable to turbulent flow fields, too, Powell [32] proposed a theory of vortex sound. According to this model, the vorticity within a compact eddy in a weakly compressible medium is identified as the basic source element in that it is considered to induce both the hydrodynamic turbulent near-field and the acoustic far-field.

This concept is appealing in view of, e.g., the formation and convection of vortices in plane and cylindrical jets and wakes. Powell showed that changes in circulation or area of a vortex ring gives rise to a dipole sound field, the former being illustrated by oscillating flow about a fixed sphere, and the latter by a simple model for the aeolian tone attributable to the stretching of vortex rings.

In an acoustic analogy approach Powell's concept may be straight forwardly formulated in terms of the wave equation (4.5) for an inviscid, quasi-incompressible, isentropic source term with $m = 0$ and $f_i = 0$:

$$\frac{1}{a_0^2} \frac{\partial^2 p}{\partial t^2} - \nabla^2 p = \rho_0 \nabla \cdot (\bar{\omega} \times \bar{c}) + \rho_0 \nabla^2 (c^2/2) \quad (6.26)$$

In the derivation of eq. (6.26) from (4.5) use has been made of the vector identity

$$c_i \frac{\partial c_j}{\partial x_i} = (\bar{c} \cdot \nabla) \bar{c} = (\nabla \times \bar{c}) \times \bar{c} + \nabla (c^2/2) \quad (6.27)$$

which for a solenoidal velocity field ($\partial c_i / \partial x_i = \nabla \cdot \bar{c} = 0$) and with $\bar{\omega} = \nabla \times \bar{c}$ denoting the vorticity vector may also be written as

$$\frac{\partial^2 c_i c_j}{\partial x_i \partial x_j} = \nabla \cdot (\bar{c} \cdot \nabla) \bar{c} = \nabla \cdot (\bar{\omega} \times \bar{c}) + \nabla^2 (c^2/2) \quad (6.28)$$

With regard to the second term on the right side of eq. (6.26) Powell [32] argues that the only mechanism present that could account for a change of the kinetic energy $\rho_0 c^2/2$, in a free inviscid flow is the production of acoustic energy itself. The contribution from this term is 'of the same functional form' in terms of a dimensional analysis as the vorticity term in eq. (6.26), but it is factored by a very small coefficient [of order M^5]. Hence Powell found it reasonable to drop the kinetic-energy term.

Howe [33] in his par. 2 was able to show that, for the rather special case of an isolated, acoustically compact vortical region (i.e. a turbulent eddy) the second term on the right side of eq. (6.26) may be omitted for small Mach numbers. Howe, at the same time, derived a more general wave equation, the source terms of which are all functions of either the vorticity or entropy fluctuations only. Howe's own 'reformulation of the acoustic analogy' will be cited here as the latest basic development of general interest in aero-dynamic noise theory.

It may be noted at the end of this section that an integral over Powell's vorticity source term has been evaluated by Hardin [34] for an axisymmetric train of toroidal vortices as an over-simplified model of the orderly structures in circular jets. Hardin concludes from his analysis that 'the noise production occurs mainly close to the jet exit and is primarily due to changes in the toroidal radii. It should be mentioned here that Laufer, Kaplan and Chu [35] reckon the pairing process of vortices, as they coalesce further downstream, to be responsible for the noise from large-scale turbulent motion in jets.

6.7 Howe's vorticity and entropy-gradient model

The effect of nonuniform combustion processes on jet engine noise and the issue of 'excess jet noise' led Howe [33] to reformulate and generalize Powell's [32] theory of vortex sound.

We have learnt from the preceding paragraphs that aerodynamic noise theories are usually based first, on some kind of a wave operator which describes the propagation of disturbances and which forms the left-hand side of a wave equation and, second, a number of source terms which describe the generation of these disturbances and which form the right-hand side of the wave equation. Concerning sound propagation in an arbitrary nonuniform flow, we have seen in par. 3.1 that there is no easy way of deriving a 'convected wave equation' in terms of the perturbation pressure, density or velocity alone. Only for the special case of a unidirectional transversely sheared flow was it possible to derive a relatively simple differential operator eq. (3.14) which formed the basis for Lilley's [17] theory.

Howe [33], first of all, managed to derive a differential wave operator which is of second order only and which very closely resembles that derived in par. (3.3) for a uniform flow and, yet, is valid under more general conditions. For a compressible, irrotational velocity field,

$$\bar{\omega} = \nabla \times \bar{c} = 0 \quad (6.29)$$

Howe [33] introduced a velocity potential ϕ ,

$$\bar{c} = \nabla \phi = \partial \phi / \partial x_i \hat{x}_i; \quad \phi(x_i, t) = \phi_0(x_i) + \phi'(x_i, t) \quad (6.30)$$

The continuity equation (2.2) (with $m = 0$) may then be written as

$$\frac{1}{\rho} \frac{\partial \rho}{\partial t} + \frac{\partial^2 \phi}{\partial x_i^2} = 0; \quad \frac{D}{Dt} = \frac{\partial}{\partial t} + \frac{\partial \phi}{\partial x_i} \frac{\partial}{\partial x_i} \quad (6.31)$$

The momentum equation (2.4) (with $f_i = 0$) for an inviscid ($\tau_{ij} = 0$) fluid may be reduced by using eqs. (6.27)

and (6.29) to yield

$$\frac{\partial^2 \theta}{\partial x_i \partial t} + \frac{\partial(c^2/2)}{\partial x_i} + \frac{1}{\rho} \frac{\partial p}{\partial x_i} = 0 \quad (6.32)$$

If, finally, isentropy is assumed in eq. (2.6),

$$d\rho = \frac{1}{a^2} dp; a = a_0 = \text{const} \quad (6.33)$$

we may write down an integral of eq. (6.32)

$$\frac{\partial \theta}{\partial t} + \frac{1}{2} \left(\frac{\partial \theta}{\partial x_i} \right)^2 + a_0^2 \int \frac{dp}{\rho} = \text{const} \quad (6.34)$$

Next we take D/Dt of eq. (6.34),

$$\frac{D}{Dt} \left\{ \frac{\partial \theta}{\partial t} + \frac{1}{2} \left(\frac{\partial \theta}{\partial x_i} \right)^2 \right\} + \frac{a_0^2}{\rho} \frac{Dp}{Dt} = 0,$$

and subtract from it a_0^2 times eq. (6.31),

$$\left(\frac{\partial}{\partial t} + \frac{\partial \theta}{\partial x_j} \frac{\partial}{\partial x_j} \right) \left\{ \frac{\partial \theta}{\partial t} + \frac{1}{2} \left(\frac{\partial \theta}{\partial x_i} \right)^2 \right\} - a_0^2 \frac{\partial^2 \theta}{\partial x_i^2} = 0. \quad (6.35)$$

The first term of eq. (6.35) may be given the following form:

$$\frac{\partial^2 \theta}{\partial t^2} + 2 \frac{\partial \theta}{\partial x_i} \frac{\partial^2 \theta}{\partial x_i \partial t} + \frac{\partial \theta}{\partial x_i} \frac{\partial \theta}{\partial x_j} \frac{\partial^2 \theta}{\partial x_i \partial x_j}$$

the time derivative $\partial/\partial t$ of which is

$$\begin{aligned} & \frac{\partial^3 \theta}{\partial t^3} + 2 \frac{\partial \theta}{\partial x_i} \frac{\partial^3 \theta}{\partial x_i \partial t^2} + 2 \frac{\partial^2 \theta}{\partial x_i \partial t} \frac{\partial^2 \theta}{\partial x_i \partial t} + \frac{\partial \theta}{\partial x_i} \left(\frac{\partial \theta}{\partial x_j} \frac{\partial^3 \theta}{\partial x_i \partial x_j \partial t} + \frac{\partial^2 \theta}{\partial x_j \partial t} \frac{\partial^2 \theta}{\partial x_i \partial x_j} \right) + \frac{\partial \theta}{\partial x_j} \frac{\partial^2 \theta}{\partial x_i \partial x_j} \frac{\partial^2 \theta}{\partial x_i \partial t} \\ & = \left\{ \frac{\partial^2}{\partial t^2} + 2 c_i \frac{\partial}{\partial x_i} \frac{\partial}{\partial t} + 2 \frac{\partial c_i}{\partial t} \frac{\partial}{\partial x_i} + c_i c_j \frac{\partial^2}{\partial x_i \partial x_j} + c_i \frac{\partial c_j}{\partial x_i} \frac{\partial}{\partial x_j} + c_j \frac{\partial c_i}{\partial x_j} \frac{\partial}{\partial x_i} \right\} \frac{\partial \theta}{\partial t} \end{aligned} \quad (6.36)$$

Hence with the aid of identity (5.14) and

$$\frac{\partial c_i}{\partial t} \frac{\partial}{\partial x_i} + c_j \frac{\partial c_i}{\partial x_j} \frac{\partial}{\partial x_i} = \frac{D c_i}{Dt} \frac{\partial}{\partial x_i} \quad (6.37)$$

we may rewrite eq. (6.36) in terms of the time derivative of the velocity potential, $\dot{\theta} = \partial \theta / \partial t$,

$$\left\{ \frac{D^2}{Dt^2} + \frac{D c_i}{Dt} \frac{\partial}{\partial x_i} - a_0^2 \frac{\partial^2}{\partial x_i^2} \right\} \dot{\theta} = 0 \quad (6.38)$$

Eq. (6.38) constitutes a nonlinear equation describing the propagation of perturbations $\dot{\theta}$, through a compressible medium which is in an arbitrary, but irrotational, mean motion specified by $\theta_0(x_i)$. In the acoustic approximation eq. (6.38) may be linearized with respect to $\dot{\theta}' = \partial \dot{\theta} / \partial t$ by neglecting fluctuations in the propagation operator. According to eqs. (6.36) and (6.37) we approximate

$$\frac{D^2}{Dt^2} \approx \frac{\partial^2}{\partial t^2} + 2 \bar{c}_i \frac{\partial^2}{\partial x_i \partial t} + \bar{c}_i \bar{c}_j \frac{\partial^2}{\partial x_i \partial x_j} + \bar{c}_i \frac{\partial \bar{c}_j}{\partial x_i} \frac{\partial}{\partial x_j} \quad (6.39)$$

$$\frac{D c_i}{Dt} \frac{\partial}{\partial x_i} \approx \bar{c}_j \frac{\partial \bar{c}_i}{\partial x_j} \frac{\partial}{\partial x_i}; \quad \bar{c}_i = \frac{\partial \theta_0}{\partial x_i} \quad (6.40)$$

Howe [33] reasoned that the last terms of eqs. (6.39) and (6.40) may be dropped if $\bar{c}^2 \ll a_0^2$ and that, in this particular case, eq. (6.38) may be written in exactly the form of the classical convected wave equation (3.17) for sound propagation in a uniform flow:

$$\left\{ \frac{D^2}{Dt^2} - a_0^2 \frac{\partial^2}{\partial x_i^2} \right\} \dot{\theta} = 0 \quad (6.41)$$

Having thus demonstrated for the first time that $\dot{\theta}$ is the most convenient ('natural') variable for treating sound propagation in nonuniform flows with

$$\dot{\theta} = \text{const} + \frac{1}{2} c^2 + \int \frac{dp}{\rho} \quad (6.42)$$

(compare eq. (6.34)), Howe [33] generalized this variable by adding a term representing entropy inhomogeneities:

$$B(x_i, t) = \int \frac{dp}{\rho} + \int T ds + \frac{1}{2} c^2 = w + \frac{1}{2} c^2 \quad (6.43)$$

The new variable B represents the sum of the specific enthalpy (or heat function) w, with

$$dw = \frac{dp}{\rho} + T ds \quad (6.44)$$

and the specific kinetic energy. B may thus be termed 'specific stagnation enthalpy'.

In his new approach to aerodynamic noise problems Howe always neglects effects of viscous dissipation,

entropy variations being entirely due to heat conduction. Therefore with the aid of eqs. (6.27) and (6.44) the momentum eq. (2.4) with $f_i = 0$ reads

$$\frac{\partial c_i}{\partial t} + \frac{\partial B}{\partial x_i} = -\bar{\omega} \times \bar{c} + T \frac{\partial s}{\partial x_i} \quad (6.45)$$

The continuity eq. (2.2) with $m = 0$ and eq. (2.7) may be written as

$$\frac{1}{a^2} \frac{Dp}{Dt} + \frac{\partial c_i}{\partial x_i} = \frac{1}{c_p} \frac{Ds}{Dt} \quad (6.46)$$

Taking the divergence of eq. (6.45) and the partial time derivative of eq. (6.46) enables the elimination of the velocity term,

$$\frac{\partial}{\partial t} \left(\frac{1}{a^2} \frac{Dp}{Dt} \right) - \frac{\partial^2 B}{\partial x_i^2} = \text{div} (\bar{\omega} \times \bar{c} - T \text{grad } s) + \frac{\partial}{\partial t} \left(\frac{1}{c_p} \frac{Ds}{Dt} \right) \quad (6.47)$$

In a procedure similar to that of Lighthill in his analogy theory, Howe adds terms on both sides of eq. (6.47) in such a way that the left-hand side resembles that of eq. (6.38):

$$\left\{ \frac{1}{a^2} \frac{D^2}{Dt^2} + \frac{1}{a^2} \frac{Dc_i}{Dt} \frac{\partial}{\partial x_i} - \frac{\partial^2}{\partial x_i^2} \right\} B = \text{div} (\bar{\omega} \times \bar{c} - T \text{grad } s) + \frac{\partial}{\partial t} \left(\frac{1}{c_p} \frac{Ds}{Dt} \right) + \left\{ \frac{1}{a^2} \frac{D^2 B}{Dt^2} + \frac{1}{a^2} \frac{Dc_i}{Dt} \frac{\partial B}{\partial x_i} - \frac{\partial}{\partial t} \left(\frac{1}{a^2} \frac{Dp}{Dt} \right) \right\} \quad (6.48)$$

Replacing $\partial B / \partial x_i$ on the right-hand side of eq. (6.48) with the aid of eq. (6.45) finally yields

$$\left\{ \frac{1}{a^2} \frac{D^2}{Dt^2} + \frac{1}{a^2} \frac{Dc_i}{Dt} \frac{\partial}{\partial x_i} - \frac{\partial^2}{\partial x_i^2} \right\} B = \text{div} (\bar{\omega} \times \bar{c} - T \text{grad } s) - \frac{1}{a^2} \frac{Dc_i}{Dt} (\bar{\omega} \times \bar{c} - T \text{grad } s) + \frac{\partial}{\partial t} \left(\frac{1}{c_p} \frac{Ds}{Dt} \right) + \frac{1}{a^2} \frac{D^2 B}{Dt^2} - \frac{1}{a^2} \frac{Dc_i}{Dt} \frac{\partial c_i}{\partial t} - \frac{\partial}{\partial t} \left(\frac{1}{a^2} \frac{Dp}{Dt} \right) \quad (6.49)$$

In a procedure which Howe [33] did not describe very well in his paper he was able to prove that an equivalent form of eq. (6.49) is the following

$$\left\{ \frac{D}{Dt} \left(\frac{1}{a^2} \frac{D}{Dt} \right) + \frac{1}{a^2} \frac{Dc_i}{Dt} \frac{\partial}{\partial x_i} - \frac{\partial^2}{\partial x_i^2} \right\} B = \text{div} (\bar{\omega} \times \bar{c} - T \text{grad } s) - \frac{1}{a^2} \frac{Dc_i}{Dt} (\bar{\omega} \times \bar{c} - T \text{grad } s) + \frac{D}{Dt} \left(\frac{T}{a^2} \frac{Ds}{Dt} \right) + \frac{\partial}{\partial t} \left(\frac{1}{c_p} \frac{Ds}{Dt} \right) \quad (6.50)$$

This second-order differential equation has several advantages over the higher-order 'shear refraction equation' discussed in par. 5.4. Whether it will initiate a new generation of aerodynamic noise theories remains to be seen.

We conclude this review on the present state of the art in aerodynamic noise theory with Howe's own interpretation of eq. (6.50):

"At points of the flow exterior to vorticity and entropy inhomogeneities, the terms on the right of eq. (6.50) vanish identically, and the irrotational perturbation flow equation (6.38) is obtained, but with account taken of the variations in the sound speed. The linearized form of that equation describes the propagation of small acoustic disturbances in the mean irrotational flow. The Lighthill acoustic analogy is based on just such an identification of part of the general Navier-Stokes equation with the wave operator in space devoid of vorticity and entropy fluctuations. It is natural therefore to pursue such an analogy in the present case. The terms on the right-hand sides of eq. (6.50) then assume the roles of inhomogeneous acoustic source terms, but they have the distinctive property of being confined solely to regions of the flow where the vorticity and entropy-gradient vectors are non-vanishing. When the characteristic Mach number is sufficiently small and the flow is isentropic, the second term on the right of (6.50) may be neglected and, in the absence of a mean flow that equation then reduces essentially to Powell's result embodied in (6.26)."

Howe [33] already applied his equation to a few simple examples of a vortex filament or a compact turbulent eddy moving in a flow with specified solid boundaries (e.g., a plate or a duct). The method adopted seems particularly suitable for treating sound scattering problems when the acoustic sources are already known in detail. It may be noted, however, that both the vorticity and entropy fluctuations are less convenient quantities when dealing with problems of aerodynamic noise generation where the turbulent sources cannot be assumed known but have to be measured like for instance, in the case of jet mixing noise.

7. FINAL REMARKS

Considerable efforts have already been expended in aerodynamic noise theory to develop the analytical tools for calculating the sound radiation and propagation from turbulent sources. While the cause (the turbulence) and the effect (the noise) may both be described by basically the same differential equations of fluid dynamics (par. 2), the various approaches to the problem differ in the way they manipulate these equations in order to isolate those terms or effects which are responsible for the noise generation process as distinct from the propagation mechanisms (par. 4 and 5). This theoretical source identification procedure is often guided by the (linearized) differential equations known from the acoustics of homogeneous or inhomogeneous moving media (par. 3).

Attempts to substantiate the respective source terms by either theory or experiment are very scarce. It may be recalled, however, that a real closure of an aerodynamic noise problem would require a comprehensive analytical model of the turbulent sources, the calculation of the sound field from these sources and finally a comparison of these predictions with measured far-field intensities, spectra and directivities. So far, the research activities have far too often been confined to just one of the four major problem areas into which aerodynamic noise may be subdivided,

- studies into the structure of turbulence in real flows,
- manipulations of basic fluid dynamics equations,
- solutions to wave equations of one kind or another for fictitious acoustic point sources.
- studies of the radiated far-field characteristics.

For instance, very sophisticated conditional sampling techniques have been developed to study in every detail certain events in a turbulent flow like the occurrence of spikes in a turbulent signal or the passage of large vortices which may or may not be important with respect to the sound emission. The coherent structures observed in turbulent shear layers (par. 6) is another example which calls for a rigorous treatment in an aerodynamic noise theory which need not be restricted to jet noise only. It would certainly be superior to a calculation which deals with imaginary acoustic singularities convected in a specific mean-flow environment.

In the present situation which is unsatisfactory with respect to the turbulence models employed, some experimentalists have devised diagnostic tools to trace and analyse the aerodynamic source fluctuations from measuring positions far remote from the flow:

- directional microphones or microphone array arrangements,
- ellipsoidal or parabolic acoustic mirrors,
- infra-red radiation receptors,
- laser-beam absorption or scattering methods.

Others have designed special 'causality correlation' techniques to enable a direct comparison of the cause and the effect in aerodynamic noise: A high statistical coherence of the flow signal (e.g., pressure or velocity measured with an inserted probe) with the radiated acoustic pressure indicates that the flow signal is closely related to the aerodynamic source fluctuation.

Since aerodynamic noise theory, to date, is so far from being conclusive in itself and should not be thought of as a matter of pure mathematics, it may be necessary to take into account all these experimental procedures when new research activities are to be defined. This review of the basic theoretical concepts should thus be seen in close connection with the other papers of this series dealing with more specified aerodynamic noise problems like jet efflux noise, excess noise, fan noise, air frame self-noise and interaction noise, and also with a variety of experimental noise source location and identification techniques.

The possible final conclusions from such an overview of the present state of the art in aerodynamic noise (both theory and experiment) could probably be stimulated by Ffowcs-Williams' / 27 / evaluation report on the AGARD Specialist's Meeting on 'Noise Mechanisms' (Brussels, 1973) to which the present AGARD Lecture Series on 'Aerodynamic Noise' was intended to be a follow-up. The concepts and treatments then proposed have now been further developed and may be subjected to appraisal in the light of three years' extra experience.

REFERENCES

- [1] Fuchs, H.V.; Michalke A.: "Introduction to aerodynamic noise theory."
In Progress in Aerospace Sci., D. Küchemann, Ed.
(Pergamon, Oxford, 1973) Vol. 14, Chap. 5, pp. 227-297.
- [2] Blokhintsev, D.I.: "Acoustics of a nonhomogeneous moving medium", Leningrad (1946), Translation:
NACA TM 1399 (1956).
- [3] Goldstein, M.E.: "Aeroacoustics", NASA SP-346 (1974). See also: J. Sound Vibr. 30 (1973), pp 79-84.
- [4] Fuchs, H.V.: "Fluctuations in a uniform moving medium originating from convected sources", Univ.
Southampton, ISVR Memo. 280 (1969).
- [5] Oestreicher, H.L.: "Field of a spatially extended moving sound source", JASA Vol. 29, 11 (1957),
1223-1232.
- [6] Morfey, C.L.; Tanna, H.K.: "Sound radiation from a point force in circular motion", Journ. Sound
Vibr. 15 (1971), pp. 325-351.
- [7] Lighthill, M.J.: "On sound generated aerodynamically. I General theory", Proc. Roy. Soc. London A,
211 (1952), 564-587.
- [8] Curle, N.: "The influence of solid boundaries upon aerodynamic sound", Proc. Roy. Soc. London, Ser.
A Vol. 231 (1955), 505-513.
- [9] Meecham, W. C.; Ford, G.W.: "Acoustic radiation from isotropic turbulence", J. Acoust. Soc. Amer.
30 (1958), 318-322.
- [10] Ribner, H.S.: "The generation of sound by turbulent jets", Adv. Appl. Mech. 8 (1964), Academic Press,
103-182.
- [11] Lighthill, M.J.: "Jet noise", AIAA Journal 1 (1963), 1507-1517.

- [12] Lighthill, M.J.: "On sound generated aerodynamically. II Turbulence as a source of sound", Proc. Roy. Soc. London A, 222 (1954), 1 - 32.
- [13] Michalke, A.; Fuchs, H.V.: "On turbulence and noise of an axisymmetric shear flow", J. Fluid Mech. 70 (1975), 179-205.
- [14] Ffowcs Williams, J.E.: "The noise from turbulence convected at high speed", Phil. Trans. A 255 (1963), pp. 469-503.
- [15] Crighton, D.G.: "Basic principles of aerodynamic noise generation", Prog. Aerospace Sci. 16,1 (1975), pp. 31-96.
- [16] Phillips, O.M.: "On the generation of sound by supersonic turbulent shear layers", J. Fluid Mech. 9 (1960), 1-28.
- [17] Lilley, G.M.: "Generation of sound in a mixing region", AFAPL-TR-72-53 Vol. IV (1972), 2-97.
- [18] Doak, P.E.: "Analysis of internally generated sound in continuous materials: II. A critical review of the conceptual adequacy and physical scope of existing theories of aerodynamic noise, with special reference to supersonic jet noise", J. Sound & Vib. 25 (1972), 263-335.
- [19] Pao, S.P.: "Aerodynamic noise emission from turbulent shear layers", J. Fluid Mech. 59 (1973), 451-479.
- [20] Mani, R.: "The influence of jet flow on jet noise", J. Fluid Mech. 73 (1976), pp. 753-793.
- [21] Balsa, T.F.: "The far-field of high frequency convected singularities in sheared flows, with an application to jet-noise prediction", J. Fluid Mech. 74 (1976), pp. 193-208.
- [22] Tester, B.J.; Morfey, C.L.: "Developments in jet noise modeling. Theoretical predictions and comparisons with measured data", AIAA Paper 75-477 (1975).
- [23] Siddon, T.E.: "Noise source diagnostics using causality correlations", AGARD-CP-131 (1974), Paper 7.
- [24] Proudman, I.: "The generation of noise by isotropic turbulence", Proc. Roy. Soc. A 214 (1952), 119-132.
- [25] Michalke, A.: "An expansion scheme for the noise from circular jets", Z. Flugwiss. 20 (1972), 229-237.
- [26] Fisher, M.J.; Lowson, M.V.: "Aerodynamic noise", J. Fluid Mech. 48 (1971), 593-603.
- [27] Ffowcs Williams, J.E.: "Technical evaluation report on Fluid Dynamics Panel Specialists Meeting on Noise Mechanisms", AGARD-AR-66 (1974).
- [28] Davies, P.O.A.L.; Yule, A.J.: "Coherent structures in turbulence", J. Fluid Mech. 69 (1975), 513-537.
- [29] Seiner, J.M.; Reethof, G.: "On the distribution of source coherency in subsonic jets", AIAA Paper No. 74-4 (1974).
- [30] Armstrong, R.R.; Fuchs, H.V.; Michalke, A.: "Coherent structures in jet turbulence and noise", AIAA-Paper 76-490 (1976).
- [31] Armstrong, R.R.; Fuchs, H.V.; Michalke, A.; Michel, U.: "Influence of Mach number on pressure fluctuations relevant to jet noise", Proc. Noise Control Conf., Warsaw 1976.
- [32] Powell, A.: "Theory of vortex sound", JASA 36 (1964), 177-195.
- [33] Howe, M.S.: "Contributions to the theory of aerodynamic sound, with application to excess jet noise and the theory of the flute", J. Fluid Mech. 71 (4) (1975), pp. 625-673.
- [34] Hardin, J.C.: "Analysis of noise produced by an orderly structure of turbulent jets", NASA TN D-7242 (1973).
- [35] Laufer, J.; Kaplan, R.E.; Chu, W.T.: "On the generation of jet noise", AGARD-CP-131 (1974), Paper 21.

JET NOISE

by

M.J. Fisher and C.L. Morfey

Institute of Sound and Vibration Research
University of Southampton, England

1. INTRODUCTION

In recent years the term "jet noise" has come to mean many different things to different people. To the layman it conveys the impression of the total noise emanating from an aircraft exhaust system. However studies have shown that this "total noise" is composed of several components which should, whenever possible, be considered separately. The most fundamental of these, and certainly the component which is in principle the most difficult to eliminate, is that due to the turbulent mixing of the jet exhaust with the ambient fluid downstream of the nozzle exit plane. We term the resulting sound "jet mixing noise." In incorrectly expanded jet exhaust flows, the presence of the resulting shock waves leads to a further source of noise which we shall term "shock associated noise." In general this source gives rise to two components, one a set of discrete tones, often referred to as "screech", together with more broad band radiation which we shall term "broad band shock-associated noise."

These sources are, to the best of our knowledge, the only significant contributors to the "total noise" which exist downstream of the nozzle exit plane. However, the advent, in particular, of high-bypass ratio, relatively low jet efflux velocity engines has brought to attention additional sources of noise. These are variously referred to as "excess" noise, "tailpipe" noise or "core" noise. Historically the term "excess noise" was coined to account for measurements of total noise which were in excess of that anticipated from available predictions of the downstream noise sources introduced above. The precise origin and dependences of this noise component remain to be established. As the second name implies they are apparently associated with the engine tailpipe and appear to a far field observer as a source located at the nozzle exit plane. However, the question still remains to some extent whether this noise is generated within the engine (i.e. combustion, flow over obstructions etc.) and subsequently travels down the tailpipe in the form of acoustic energy to be radiated from the nozzle exit, or whether it originates as the result of interaction between vorticity and the nozzle termination. Current evidence, in particular the relative effectiveness of acoustic tailpipe liners, would appear to identify the former as dominant in practice.

In the following sections we shall review each of the noise components in turn, and attempt to outline the extent to which current fundamental understanding will stand the test of prediction. We shall not consider purely empirical prediction methods, which may in some cases be more satisfactory in practice at the present time.

2. JET MIXING NOISE

The source of jet noise which has historically received the majority of attention, both theoretically and experimentally, is the jet mixing noise component. Theoretical work due to Lighthill [1], [2] showed how this noise could be generated in a freely exhausting jet flow as a result of the fluctuating Reynolds shear stress. These concepts have dominated the study of jet noise for the past twenty-five years and offer a strong foundation for both the study and prediction of jet mixing noise. A basic attraction of the Lighthill formulation is undoubtedly the relative simplicity with which an expression for the strength of the contributing "noise sources" is obtained. It is equally true however that proper evaluation of that expression from available fluid mechanics (i.e. turbulence) data is by no means straightforward. Certainly very useful predictions do emerge fairly readily, notably that the noise output should vary as the eighth power of the jet efflux velocity. However, in 1971 Lush [3] published a series of carefully conducted jet noise measurements which high-lighted certain significant and systematic discrepancies between measurement and the predictions available from the Lighthill formulation. These observations have since been amply confirmed by independent measurements, among which we would note in particular those of Tanna [4] which cover arguably the largest envelope of test conditions available in a single systematic study of jet mixing noise.

It is to be emphasised, however, that the now established existence of such discrepancies does not represent errors in the basic Lighthill theory per se. It is the knowledge of the quantities required for evaluation of the source term which is inadequate. A portion of that source term represents as equivalent acoustic sources the processes of refraction and scattering of acoustic radiation by the jet flow. This, together with the nature of the discrepancies reported by Lush (loc cit) led Lilley [5] to undertake a reformulation of the governing equations in a manner which separates more explicitly the generation of acoustic energy and its subsequent transmission through the jet flow field. This work has led in the past few years to a new area of jet noise study termed "flow-acoustic interaction" as represented for example in the papers of Mani [6], Tester and Morfey [7] and Howe [8].

In the following sections we begin by outlining the predictions available from the original Lighthill formulation and indicate where discrepancies are experienced. The flow acoustic interaction studies offer a potential for reducing such anomalies, but at present they must be regarded as on-going work. We shall therefore in these notes restrict ourselves to a description of the general principles and physical phenomena involved, and will discuss only the general implications of this type of work.

2.1 The Lighthill Formula

The essence of the Lighthill theory of aerodynamic noise is the formulation of an acoustic analogy in

which the complicated process of sound generation by turbulence is modelled in terms of an equivalent set of acoustic sources embedded in an otherwise uniform medium at rest. By a simple re-arrangement of the equations of fluid motion (see the Appendix) it was shown that noise production in free unbounded turbulent flows was equivalent to an array of quadrupole sources of strength per unit volume.

$$T_{ij} = \rho U_i U_j + (p - a_0^2 \rho) \delta_{ij} - ij$$

For an observer at a large distance from the source region, the resulting acoustic pressure field is (see Appendix Eq.(14))

$$p(\vec{x}, t) - p_0 = \frac{1}{4\pi a_0^2 r} \int_V \frac{\partial^2 T_{rr}}{\partial t^2} (\vec{y}, t - r/a_0) dV(\vec{y}) \quad (1)$$

where

$$T_{rr} = \rho U_r^2 + (p - a_0^2 \rho)$$

and U_r is the fluid velocity in the direction of the observer. As is usual, the viscous stress tensor σ_{ij} is neglected. This result shows that the radiation amplitude is proportional to the sum of elementary source strengths over the flow region, while the appearance of retarded times, $t - r/a_0$, emphasises that in general phase differences must be accounted for during the integration process.

The latter may however be neglected for compact source regions, that is whenever the acoustic wavelength is long compared to the extent of the source region over which significantly correlated source fluctuations exist. A scaling law for the radiated intensity is then derived in [1] with the aid of the following additional assumptions.

- (a) Pressure and density are isentropically related (i.e. $p' - a_0^2 \rho' = 0$)
(This is not appropriate for hot jet, however)
- (b) $\rho U_r^2 \sim \rho_s U_J^2$ where ρ_s is a density appropriate to the most intense source region and fluctuating velocities U_r' are assumed to scale in proportion to the jet efflux velocity U_J ;
- (c) $\frac{\partial^2}{\partial t^2} \sim \omega^2 \sim \left(\frac{U_J}{D}\right)^2$

The second time derivative is assumed equivalent to a frequency squared weighting, while typical frequencies are assumed proportional to jet velocity and inversely proportional to a typical flow scale which varies as jet diameter (D).

- (d) $dV(\vec{y}) \sim D^3$.

Combining these assumptions in (1) we anticipate far field intensity to vary dimensionally as

$$I(r, \theta) \sim \frac{\rho_s^2 U_J^8 D^2}{\rho_0 a_0^5 r^2} \quad (2)$$

Of particular significance is the observation that the intensity varies in proportion to the eighth power of jet efflux velocity, implying a 24dB noise increase for each doubling of velocity.

The compact source restriction appropriate to (2) is however valid only for jet velocities which are small compared to the speed of sound, a situation seldom experienced in aero-engine applications. Lighthill argued that this restriction could be eased if the estimates of T_{rr} were based on a set of sources convecting at speed appropriate to the convection velocity of the most intense turbulence. With such a re-formulation Eq.(2) above becomes

$$I(r, \theta) \sim \frac{\rho_s^2 U_J^8 D^2}{\rho_0 a_0^5 r^2} (1 - M_c \cos \theta)^{-5} \quad (3)$$

where M_c is normally taken to be of order $\frac{0.7 U_J}{a_0}$. Note that (3) reduces to (2) as the jet Mach number tends to zero.

For $\theta = 90^\circ$ therefore the dimensional variation remains unaltered, but at angles closer to the jet axis, $\theta < 90^\circ$, augmentation in accordance with five powers of the Doppler factor, $(1 - M_c \cos \theta)$, is anticipated reflecting the enhanced efficiency of the convecting quadrupole and sources for radiation directions close to their direction of motion.

Eq.(3) thus represents the anticipated scaling of overall intensity as a function of jet velocity, angle of observation etc. It was however the extension by Lush [3] of this type of scaling argument to the anticipated variation of intensity in proportional frequency bands, 1/3 octave for example, which conclusively demonstrated the limitations of the Lighthill approach for prediction purposes (see following section). Lush argued that the intensity in proportional frequency bands, centre frequency f , should vary at a given angle θ in accordance with

$$I(f, r, \theta) \sim \frac{\rho_s^2 U_J^8 D^2}{\rho_0 a_0^5 r^2} (1 - M_c \cos \theta)^{-5} F\left(\frac{fD}{U} (1 - M_c \cos \theta)\right). \quad (4)$$

The variation is identical to that for overall intensity except for the addition of the spectrum

function $F(\frac{fD}{U}(1-M_c \cos \theta))$. The appearance of the Doppler factor emphasises again that the equivalent sources are assumed to be in motion, the factor $f(1-M_c \cos \theta)$ ensuring that the same source frequency is considered irrespective of the angle from which it is observed.

We close this section with the reminder that a jet velocities such that $M_c \cos \theta$ can approach unity, the more complete Doppler factor

$$\{(1-M_c \cos \theta)^2 + (\alpha^2 \sin^2 \theta + \beta^2 \cos^2 \theta) M_c^2\}^{\frac{1}{2}}$$

should be employed [9].

2.2 Comparison with experiment

In this section we shall explore the degree of agreement between the predictions of Eq.(3) and (4) and jet noise measurements, utilizing the results of [4] in view of the large range of parameters available therein. We shall also restrict ourselves initially to isothermal jet flows, that is flows where the jet static temperature at nozzle exit is equal to the ambient temperature.

The comparison between (3) and experimental observation is shown in Fig.1, for four angles of observation. At 90° to the jet axis, very acceptable agreement is observed. However at angles less than 90° the predicted convective amplification clearly overestimates the measured levels, while in the forward arc, $\theta > 90^\circ$, the converse applies; that is the anticipated convective attenuation is not observed. The influence of these discrepancies on the directivity of the overall sound is shown in Fig.2, where it is clear that the dimensional reasoning, Eq.(3), significantly overestimates the degree of directionality observed in practice.

The origin of these differences becomes clearer when data and prediction are compared on a spectral basis as suggested in Eq.(4). Figs. 3a) through d) show comparisons of the predicted and measured directivities for four values of the reduced frequency.

$$\frac{fD}{U} (1-M_c \cos \theta) = \frac{f}{s} \frac{D}{U}$$

equal to 0.1, 0.3, 1.0 and 3.0 respectively. We note that constant values of $\frac{f}{s} \frac{D}{U}$ are required to keep the spectrum function $F(\cdot)$ constant as dictated by (4), with the result that the observed frequency increases with decreasing angle of observation. Inspection of Fig.3 indicates the following.

- At the lowest Strouhal number, reasonable agreement is obtained except at angles close to the jet axis, where measurement significantly exceeds prediction. Also demonstrated in Fig.3a) is the change of prediction involved by assuming that the source is ten diameters downstream of the nozzle exit plane and allowing for the increase of observation angle relative to the source thus incurred. For the present measurement arrangement, $r/D = 72$, the correction is relatively small, but does offer some improvement in the comparison. The influence of such a correction is particularly significant where experimental limitations impose the use of small r/D values.
- The remaining comparisons, Figs.3b), c), and d) all exhibit the same general feature that the predicted degree of directivity exceeds that observed experimentally, the magnitude of the discrepancy becoming progressively larger as the reduced frequency is increased. We can summarize these observations as follows.

For the majority of frequencies the theory of freely convecting quadrupole sources overestimates the observed directivity, the magnitude of the discrepancies increasing as

- The frequency is increased
- The jet efflux velocity is increased
- The angle of observation is decreased

We shall return to offer some degree of explanation for these observations in Section 2.4 below.

2.3 Effect of temperature on jet mixing noise

In the review of jet mixing noise above we have avoided, as does the Lighthill theory, the question of the effect of jet temperature on the radiated noise field. Early considerations appear to have concentrated on the idea that the principal effect of the elevated temperatures used in practice would be to reduce noise, as a result of the decrease of density in the source region in the Lighthill stress tensor $T_{ij} = \rho U_i U_j$. However carefully controlled experiments at the N.G.T.E. in England and by SNECMA in France showed that such a picture was too simple. Those results [10], subsequently confirmed by others [11], [12] show that at low jet efflux velocities, increased temperature increases the noise radiation, while at higher velocities the converse is true as shown in Fig.4. Hoch et al [10] chose to characterise this variation empirically by the parameter $\frac{\rho_j}{\rho_0} \omega$ where ω varies from -0.75 at a velocity of 500 ft/s to a value approaching +2 at 1500 ft/s.

It appears to have been Lush [11] who first attempted to provide a rational explanation for these observations. Concentrating on the $\theta=90^\circ$ observation position to avoid the problems of convective amplification outlined above, he argued that for heated flows one can no longer neglect the second term, $(p-a_0^2 \rho)$, of the Lighthill stress tensor as was done above for isothermal jet flows. He chose in fact to divide the density fluctuations into a portion which were isentropically related to pressure, the remainder being attributed to entropy fluctuations; for a perfect gas this leads to the approximation

$$T_{ij} = \rho_s U_i U_j + p' \left(1 - \frac{a_0^2}{a^2}\right) + \frac{\rho_s a_0^2}{C} S'$$

The superscript ' is used here to denote a fluctuation of the quantity involved relative to its time-

averaged mean value, these being the quantities of significance in view of the fact that the far field acoustic pressure is proportional to the second time derivative of T_{ij} , Eq.(1).

Scaling the entropy fluctuation S' in proportion to the entropy difference across the jet shear layer (i.e. $S' \sim S_J - S_0 = C_p \log_e \left(\frac{T_J}{T_0} \right)$) leads to a dimensional form for the far field intensity contributed by the first and third terms above, of the form

$$I \sim \frac{\rho_s^2 U_J^8 D^2}{\rho_0^2 a_0^5 r^2} + K \frac{\rho_s^2 U_J^4 D^2}{\rho_0^2 a_0^3 r^2} \left(\log_e \frac{T_J}{T_0} \right)^2 \quad (5)$$

where K is an unknown constant and the implicit assumption is made that the Reynolds shear stress and entropy source terms are uncorrelated. This expression does appear of the correct form to explain the phenomena observed in Fig.4. At high velocities, where the additional U_J^4 term resulting from the entropy fluctuations will be least important, we obtain the observed reduction in noise with increasing temperature as a result of the diminishing value of the source region density ρ_s . Conversely at low enough velocity the additional U_J^4 term will dominate, causing the intensity to increase with increasing temperature. In terms of the data then available Lush [11] was able to demonstrate a quite convincing agreement between the predictions of Eq.(5) and measured data.

These ideas were subsequently re-examined by Tanna et al [12] utilizing data for a significantly larger range of temperature and velocity than that available to Lush. This work suggested that for an extensive range of temperature Lush's scaling of source temperature (and hence density) as the geometric mean of the jet efflux and ambient temperature (i.e. $\sqrt{T_s} = \sqrt{T_J T_0}$) was not adequate, and a better estimate was

$$T_s = 0.7(T_J - T_0) + T_0$$

commensurate with knowledge of the probable temperatures existing in the most intensely turbulent region of the jet shear layer.

With the range of variables available in this latter work it was also possible to estimate spectra associated with the Reynolds shear stress and entropy sources separately, by assuming that at high velocities the former dominated while at low velocity and high temperature the entropy term was the sole contributor. The spectra so derived were then combined into a prediction scheme, based on (5), to calculate spectra at intermediate values of temperature and velocity where both sources were appreciable contributors. This revealed the strong probability that the two sources were not uncorrelated as previously supposed but were in fact strongly correlated. This observation is not really surprising when it is remembered that both the Reynolds shear stress and entropy fluctuations are created by the same turbulent mixing process. The relative success of the work of [12] is demonstrated in Fig.5 where the predictions of overall sound pressure level, obtained by integrating the predicted spectra, are compared with the values measured. Comparison of individual spectra showed agreement within 1-2 dB over an extensive range of parameters.

In spite of these reassuring results Morfey [13] was in the meanwhile questioning the correctness of the U_J^4 scaling for the entropy term proposed by Lush. The essence of this argument was that in the absence of processes associated with heat conduction and viscosity, normally neglected at Reynolds numbers appropriate to jet noise studies, entropy must be conserved in a frame of reference following a fluid particle (i.e. $Ds = 0$), where $\frac{D}{Dt}$ denotes a total derivative.

It thus follows, since

$$\frac{Ds}{Dt} = \frac{\partial s}{\partial t} + v_i \frac{\partial s}{\partial x_i},$$

that the second time derivative required to scale the Lighthill stress tensor is

$$\frac{\partial^2 s'}{\partial t^2} = - \frac{\partial}{\partial t} \left(v_i \frac{\partial s'}{\partial x_i} \right) = - \frac{\partial}{\partial t} \frac{\partial}{\partial x_i} (v_i s') + \frac{\partial}{\partial t} \left(s' \frac{\partial v_i}{\partial x_i} \right)$$

which following normal scaling law procedure will yield a modified version of (5) of the form

$$I \sim \frac{\rho_s^2 U_J^8 D^2}{\rho_0^2 a_0^5 r^2} + K \frac{\rho_s^2 U_J^6 D^2}{\rho_0^2 a_0^3 r^2} \left(\log_e \frac{T_J}{T_0} \right)^2 \quad (6)$$

We see that while the same temperature dependences are anticipated the additional term now varies as the sixth as opposed to fourth power of velocity.

From the experimental point of view, the difficulty of deciding which of the scaling laws, (5) or (6), provides the better fit to measurements arises from a re-analysis of Tanna's data [4] by Szewczyk (ISVR unpublished work) that a combination of V_J^6 and U_J^8 terms uncorrelated gives a slightly better fit than the originally proposed V_J^4 and V_J^8 terms with positive correlation.

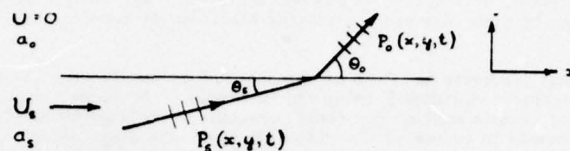
In addition, the form of the temperature dependence shown for the entropy term in (5) or (6) should not be regarded as final for similar reasons, although there is reasonable agreement between the measured and predicted trends based on low velocity data.

2.4 Acoustic-mean flow interaction

We have already demonstrated in Section 2.2 the type of discrepancy which exists between predictions based on the Lighthill acoustic analogy of freely convecting quadrupoles, and experimental data. In this

section we introduce the concepts involved in the flow/acoustic interaction studies, which appear to offer the potential of reducing such differences.

We begin with the very simple two-dimensional situation, shown below, in which a disturbance $P(x, y, t)$ is approaching an interface which divides fluid of velocity U_s and sound speed a_s from an ambient medium with sound speed a_0 .



That disturbance approaches the boundary in the form of waves whose normal makes an angle θ_s with the interface, is then refracted to emerge at angle θ_o into the ambient fluid.

We may write descriptions of these disturbances in the form

$$P_s(x, y, t) = A_s \exp[j(\omega t - k_s x \cos \theta_s - k_s y \sin \theta_s)]$$

$$P_o(x, y, t) = A_o \exp[j(\omega t - k_o x \cos \theta_o - k_o y \sin \theta_o)]$$

in the flow and ambient regions respectively, although it must be clearly understood the descriptions are appropriate to a space-fixed observer in both cases.

Matching the x component wave numbers across the boundary,

$$\text{i.e. } k_s \cos \theta_s = k_o \cos \theta_o$$

and application of Snell's law of refraction, i.e.

(which amounts to matching axial phase speeds across the interface) is sufficient to yield an expression for $k_s \sin \theta_s$, which as the defining equations above demonstrate, describes propagation in the y direction within the flow region. It is

$$k_y \equiv k_s \sin \theta_s = \frac{\omega}{a_o} \left[(1 - M \cos \theta_o)^2 \left(\frac{a_s}{a_o} \right)^{-2} - \cos^2 \theta_o \right]^{1/2},$$

where $M = \frac{U_s}{a_o}$.

Of particular relevance to our present considerations is the fact that K_y may be either real or imaginary, depending on the sign of the term in the square brackets. It is in fact imaginary for all values of the emergence angle θ_o less than some critical value θ_c , where *

$$\cos \theta_c = \frac{1}{\frac{a_s}{a_o} + M}.$$

The physical significance of θ_c is that it corresponds to the angle of emergence of a sound wave travelling in the flow region in a direction parallel to the x axis, as can be seen by putting $\theta_s = 0$ in the Snell's law relation above. Thus all genuine sound waves in the flow field, that is waves whose phase speed relative to the moving fluid is a_s , must emerge at angles greater than θ_c . For this reason the angular range $0 < \theta_o < \theta_c$ is commonly referred to as the cone of silence, since sound waves in the flow cannot penetrate into that angular range. Consideration of the value of θ_c , even for the relatively modest flow conditions $\frac{a_s}{a_o} = M = 1$, indicates that it will be of order 60° . We thus obtain the apparently contradictory result that in many practical cases the angle of peak noise radiation from jet flows, circa 45° , is contained within the cone of silence. It is necessary therefore to consider the nature of disturbances, within the flow region, which can emerge into the cone of silence.

For cases in which K_y is imaginary, i.e. $\theta_o < \theta_c$, the defining equation for disturbances in the flow region becomes

* We note also a maximum value of θ_o for which K_y is real, but shall not consider this further here, i.e. forward arc cone of silence.

$$P_s(x, y, t) = A_s \exp[j(\omega t - k_0 x \cos \theta_0)] \exp[-|K_y| y],$$

$$|K_y| \equiv \frac{\omega}{a_0} |\cos^2 \theta_0 - (1 - M \cos \theta_0)^2 \left(\frac{a_s}{a_0}\right)^{-2}|^{\frac{1}{2}}.$$

It appears therefore that a disturbance originating a distance \bar{y} below the interface, which subsequently radiates into the cone of silence, will suffer an exponential decay, $\exp[-|K_y| \bar{y}]$ prior to its arrival at that interface. The analogy between this process and the behaviour of cut-off duct modes is of course obvious.

Some idea of the physical processes involved can be obtained by considering the wave number/frequency decomposition of a source located a distance \bar{y} below the interface. It is well known that for such a source located in an infinite uniform medium only those portions of the wave number/frequency spectrum, $S(k, \omega)$, having axial phase speeds in excess of the effective sound speed can contribute to the far field radiation. Further the radiation angle to which a particular value of $S(k, \omega)$ contributes is that for which its phase speed, resolved in that direction, is equal to the appropriate speed of sound. In similar vein we can identify the wave number components which radiate outside and inside the cone of silence respectively. Those for which the axial phase speed is greater than $(a_s + U_s)$ can generate an acoustic field in the moving stream which would radiate to the boundary even in the limit that the distance $\bar{y} \rightarrow \infty$. However on arrival at that boundary the minimum phase speed of this set is $(a_s + U_s)$ so that in radiating into the ambient fluid the minimum angle of emergence is given by

$$(a_s + U_s) \cos \theta_{\min} = a_0$$

which again defines the cone of silence angle. We see therefore that those wave number components, whose axial phase speeds are supersonic relative to the moving fluid, all yield radiation outside the cone of silence.

However, let us now consider a further subset of wave number/frequency components whose axial phase speeds, U_x , are in the range

$$a_0 \leq U_x < (U_s + a_s).$$

That is, they are subsonic relative to the moving fluid, but supersonic relative to the ambient fluid. They cannot therefore produce an acoustic field in the normal sense within the moving fluid. In fact a destructive interference occurs leading to the exponential decay specified above. However, if $|K_y| \bar{y}$ is not too large some residual of these disturbances arrives at the interface. Their axial phase speed is now supersonic relative to the ambient medium so that, in essence, the boundary can be regarded as a new source which can radiate an acoustic field to fill the angular range between the flow axis and the cone of silence angle. The amplitude of the acoustic field in this region will of course now depend, among other things, on the severity of the exponential decay and hence on the distance of the source region from the flow boundary, \bar{y} . We see therefore that the behaviour of source fluctuations which radiate inside and outside the cone of silence respectively is likely to be rather different, and it is useful to use the cone of silence angle as a boundary for future discussion.

- a) Radiation outside the cone of silence ($\theta_0 > \theta_c$) - The early comparisons due to Lush [3], with their relatively limited range of variables, suggested that outside the cone of silence angle the predictions based on the Lighthill acoustic analogy were reasonably acceptable. However, the extended range due to Tanna [4] does, as we have seen in Figs. 3b), c) and d), suggest that even at relatively large angles to the jet axis the measured directivity is less than that predicted by the five powers of Doppler factor

The work of [7] indicates that there are two principal physical mechanisms associated with flow shrouding of a source, which account for such differences. * The first is demonstrated in Fig. 6a) where rays emanating from a stationary source embedded in the moving fluid are traced across the interface using the Snell's law relationship. It is clear that a "packing" of rays occurs as one proceeds from the $\theta_0 = 90^\circ$ position towards the cone of silence angle. Thus even if the acoustic energy flux per unit area, i.e. the intensity, were independent of angle in the flow region it would be non-uniform in the ambient region as a result of this ray focussing phenomenon. In fact as [7] shows for an axisymmetric situation since acoustic energy radiated in the angular range $\theta_s \pm \theta_s + d\theta_s$ must appear in the angular range θ_0 to $\theta_0 + d\theta_0$, the areas on a sphere of radius R through which this energy passes are

$$2\pi R^2 \sin \theta_0 d\theta_0 \quad \text{and} \quad 2\pi R^2 \sin \theta_s d\theta_s$$

with and without refraction respectively.

Thus the relative intensities are in the ratio

$$\frac{I(\theta_0)}{I_s(\theta_s)} = \frac{\sin \theta_s d\theta_s}{\sin \theta_0 d\theta_0} = \frac{d(\cos \theta_s)}{d(\cos \theta_0)}.$$

* In these notes we take a relatively simplified view. The reader should consult [7] for a more rigorous account.

Use of Snell's law to determine the ratio $\frac{d(\cos\theta_s)}{d(\cos\theta_o)}$ then yields

$$\frac{I(\theta_o)}{I(\theta_s)} = \frac{a_s}{a_o} (1 - M \cos\theta_o)^{-2}.$$

Finally let us consider how the intensity measured in the flow $I_s(\theta_s)$ might vary in terms of a simple source model. In view of Eq.(3) and (4), in which all directional effects are attributed to source motion we shall consider a source which, if placed at rest in a uniform stationary medium, yields a uniform pressure field. If that source is now embedded in a uniform flow and allowed to convect with the flow, as shown schematically in Fig. 6b), the pressure observed by an observer also moving with the fluid will be independent of emission angle θ_s . However as shown in [14], the fact of fluid motion renders the intensity measured by a stationary observer in the fluid non uniform, its angular dependence being of the form

$$I_s(\theta_s) \propto (1 + \frac{U}{a_s} \cos\theta_s)^2$$

which using Snell's law becomes

$$I_s(\theta_s) \propto \frac{1}{(1 - M \cos\theta_o)^2}.$$

Thus combining this variation of $I(\theta_s)$ with the ray focussing effect discussed above we find the directivity is given by

$$\frac{I(\theta_o)}{I(\theta_o=90^\circ)} = (1 - M \cos\theta_o)^{-4}.$$

We observe therefore that a source which is basically omni-directional will exhibit a directivity of $(1 - M \cos\theta_o)^{-4}$ when immersed in and convecting with a fluid of velocity U . This result however applies, as the model outlined above implies, to a single isolated source. In jet noise on the other hand we have a volume distribution of sources, which results in the fourth power dependence above being reduced to a third power.

The reason is shown schematically in Fig. 6c). We consider a space fixed portion of the source region AB and assume that at time t a convecting source (i.e. eddy), also of length AB, is coincident with it. At this instant, furthermore an acoustic signal is emitted from A. The acoustic signal from the space fixed point B must therefore be emitted at the later time $\left(\frac{t + L \cos\theta_o}{a_o}\right)$ if it is to reach the observer simultaneously. However at this time the "eddy" had been convected to the position indicated by A'B', where $BB' = \frac{UL \cos\theta_o}{a_o}$. Thus the 'volume' of the convecting source which contributes sound in the space fixed 'volume' AB is proportional to $L(1 - M \cos\theta_s)$. This must be allowed for in integrating over a fixed volume of turbulence, so that for a volume distribution of sources the directivity becomes

$$\frac{I(\theta_o)}{I(\theta_o=90^\circ)} = \frac{1 - M \cos\theta_o}{(1 - M \cos\theta_o)^4} = (1 - M \cos\theta_o)^{-3}.$$

This predicted directivity has been compared with experimental data by Tanna [4] as shown in Figs. 3c) and d), and for the majority of the results exhibits very acceptable agreement for angles of observation outside the cone of silence.

- b) Inside the Cone of Silence ($\theta_o < \theta_c$) - While the directivity obtained with due allowance for flow shrouding and refraction shows reasonable agreement with experiment outside the cone of silence, it clearly overestimates the measured levels inside the cone of silence, a fact which we might attribute to the exponential decay mechanism outlined above.

Fisher and Szewczyk [15] have conducted an order of magnitude feasibility study of this possibility. In that work they equated the difference between the levels predicted on the basis of a freely convected quadrupole model and those measured, to the reduction of amplitude anticipated for a source a distance \bar{y} below a flow boundary, i.e.

$$\Delta(\text{dB}) = 20 \log_{10} \left| e^{-|K_y| \bar{y}} \right| \quad (\theta_o < \theta_c)$$

which using the expression for $|K_y|$ derived above becomes

$$\Delta(\text{dB}) = 55 \frac{\bar{y}}{a_o} \left| \cos^2\theta_o - (1 - M \cos\theta_o)^2 \left(\frac{a_s}{a_o} \right)^{-2} \right|^{\frac{1}{2}}.$$

Using experimental data they were then able to calculate values of \bar{y} necessary to account for derived values of the theoretical/experimental discrepancy, $\Delta(\text{dB})$. A typical set of results are shown in Fig. 7 for the range of jet efflux conditions and angle of observation indicated thereon. The major importance of these results is that they show that the values required are indeed of an acceptable order of magnitude. We also note that, although the theoretical/experimental differences increase with increasing frequency, the values of \bar{y}/p decrease, commensurate with the idea that higher frequencies are produced closer to the nozzle where the shear layer is thinner. Thus it does appear that the exponential decay mechanism is at least of the correct order of magnitude to account for the

differences between theory and experiment.

More recently detailed numerical solutions of the Lilley equation have been undertaken by Tester [7], based on a model of a ring source located in the jet flow at the radial station for a given source frequency (based on source location data) the agreement between measured and calculated directivities is as shown in Fig.8.

However extension of these calculations to higher velocities indicates that the calculated levels, at angles well within the cone of silence, progressively underestimate those measured. The reasons are not currently entirely clear, but two strong possibilities do exist. First, the model of a ring source at one radial location may be too simple when the exponential decay process yields large attenuations of perhaps 30 - 40 dB. In such a situation relatively weak sources in the outer portions of the shear layer, which are less effectively attenuated, may become significant and set a lower limit on the measured levels. Secondly, turbulent scattering of acoustic energy into the cone of silence is a possibility which justifies future attention.

In summary, while future work is clearly required to improve our understanding of flow/acoustic interaction processes, particularly with a view to application of this work to detailed jet noise prediction, it does appear that such studies offer considerable potential in providing a rational explanation for many of the observed features of jet noise radiation.

- c) **Suppressor Operation** - In this final section on the topic of flow/acoustic interaction we shall explore the possible role of these phenomena in the operation of jet noise suppression devices. A number of current jet noise suppressors appear to operate either by causing the jet flow to spread more rapidly than that for the datum conical nozzle (i.e. fish tailing jets [16]), or by surrounding certain noise producing regions with flow (i.e. multi-tube or chuted nozzles).

Fisher [15] suggests that a rational explanation for the observed characteristics of these suppressors is possible if one assumes that the principal role of the mean flow modification is to increase the depth of flow separating the noise producing region from the ambient atmosphere (i.e. on increase of the effective depth \bar{y}). This differs from more conventional explanations, based on the Lighthill analogy, in which attenuations are attributed to factors such as reduced shear, reduced source volumes etc. However the latter do not adequately explain two commonly observed features of suppressor nozzles. First the lack of benefit obtained at large angles to the jet axis, and more particularly the increased attenuation, relative to a datum conical nozzle, observed as the jet velocity is progressively increased. Let us therefore explore the way in which flow/acoustic interaction may account for such observations.

To this end we assume that the only modification created by the introduction of the suppressor flow is to increase the effective depth from \bar{y}_c for the datum circular nozzle to \bar{y}_s for the suppressor nozzle, the character of the main noise producing region remaining otherwise unmodified.

Thus, for observation angles outside the cone of silence, where the depth of flow separating the source from the boundary has no effect, no attenuation is anticipated. However on entering the cone of silence the increasing effective depth created by the suppressor flow will yield a larger exponential decay, to given an attenuation relative to the conical nozzle of

$$A(\text{dB}) = \frac{55f(\bar{y}_s - \bar{y}_c)}{a_0} \left| \cos^2 \theta_0 - (1 - M \cos \theta_0)^2 \left(\frac{a_s}{a_0} \right)^{-2} \right|^{\frac{1}{2}}.$$

For interpretative purposes it is useful to write this expression in the expanded form

$$A(\text{dB}) = \frac{55fD}{V_J} \frac{(y_s - y_c)}{D} \frac{V_J}{a_0} \left| \cos^2 \theta_0 - (1 - M \cos \theta_0)^2 \left(\frac{a_s}{a_0} \right)^{-2} \right|^{\frac{1}{2}}$$

and to assume on the basis of the data in Fig.7 that both \bar{y}_s/D and \bar{y}_c/D are constant for a given value of Strouhal number fD/V_J .

The characteristics of the observed attenuation are then expected to be as follows:

- Attenuation will occur as one enters the cone of silence and will progressively increase with further reduction of observation angle, as a result of the increase of value of the $\left| \cos^2 \theta_0 - (1 - M \cos \theta_0)^2 \left(\frac{a_s}{a_0} \right)^{-2} \right|^{\frac{1}{2}}$ term above.
- An increase of jet efflux velocity will increase the angular range over which attenuations are observed, as a result of the increased cone of silence angle.
- An increase of jet efflux velocity will increase the magnitude of the attenuations, as a result of V_J/a_0 term in the expression below.

Some confirmation for these ideas is presented in Fig.9, which shows a comparison of measured field shapes for a circular nozzle and rapidly spreading fish-tailed jet. Outside the cone of silence angle the levels are quite similar, but once one enters the cone of silence the fish-tailed jet shows increasing benefits, whose characteristics are qualitatively in agreement with the suggestion above.

3. SHOCK ASSOCIATED NOISE

As the pressure ratio of a convergent nozzle exceeds a certain critical value (1.89 for air with $\gamma = 1.4$), a series of shock cells, sometimes also termed shock diamonds, are observed to form in the jet exhaust flow. Further increase of pressure serves to extend the length and spacing of the successive cells. The spacing is given approximately by

$$L = 1.25 \beta D.$$

$\beta \equiv \sqrt{M_j^2 - 1}$ and M_j is the fully expanded jet Mach number, a function of pressure ratio alone.

The presence of these shock cells is known to give rise to two types of noise. The first, described by Powell [17], is a discrete tone radiation often termed screech. As discussed below it appears to owe its origin to a feedback mechanism between the shocks and nozzle lip. The second component, termed broad band shock associated noise, has been investigated in some detail by Harper-Bourne [18]. That work shows that the noise arises as a result of turbulent eddies interacting with the shock cell structure to form an array of partially correlated sources.

3.1 Discrete tone radiation (Screech)

The mechanism giving rise to screech is, in principle, straightforward. We consider a disturbance (i.e. an eddy) leaving the nozzle lip at time $t = 0$. It therefore arrives at the end of the first shock cell at time $t_1 = \frac{L}{V_c}$ where V_c is the eddy convection velocity. Here it interacts with the shock wave, generating an acoustic wave which travels upstream in the ambient air surrounding the jet to re-disturb the nozzle exit flow. This in turn creates a new eddy which travels away downstream and hence the process repeats to create a feedback loop. The cycle time for the process is therefore the sum of the eddy convection time $\frac{L}{V_c}$ and the time taken for the sound wave to travel from the shock to the nozzle $\frac{L}{a_0}$.

The frequency is the reciprocal of the 'cycle' time and is therefore

$$f_s = \frac{V_c}{L(1 + M_c)}.$$

Ample evidence does exist to confirm that discrete frequency radiation from shock containing flows does occur at this frequency and its harmonics.

By contrast, one can be far less categorical regarding the parameters which control the amplitude of these tones. Common experience indicates they are often important contributors on cold model jets, but seldom occur significantly on aero-engine configurations, although some minor structural damage to a V.C. 10 tailplane, attributable to screech, has been reported by Hay [19].

Experience on cold model jets at the ISVR indicates that for a normal nozzle configuration screech tone amplitudes are frequently non-stationary, varying by a factor of five while the jet is operated at ostensibly constant conditions. This phenomenon can be eliminated with the provision of a large reflector plate in the nozzle exit plane. The tone amplitudes are both stabilized and increased. Stable tones, but at a much lower level, are also obtained if the reflector plate is covered with a layer of acoustic foam. It was also found that the addition of a small projection on the nozzle lip, with this latter configuration, was effective in eliminating the tones at least to the extent where they were not detectable on 6% bandwidth spectral analysis.

From this experience it is concluded that the amplitude of screech tones is very dependent both on the presence of acoustically reflecting surfaces in the vicinity of the nozzle exit plane and on the state of the nozzle flow.

3.2 Broad band shock associated noise

The character and dependences of this second component of shock cell noise have been investigated in considerable detail by Harper-Bourne [18], using the configuration outlined above to eliminate screech tones.

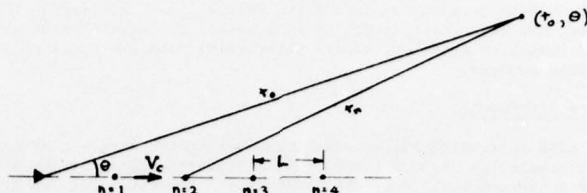
The variation of the overall sound pressure level for an unheated jet as a function of jet velocity is shown in Fig.10a) for three angles of observation. It is clear that once the nozzle chokes ($M_j = 1$) the OASPL's at 90° and 143° rise extremely rapidly and the field becomes virtually omni-directional. A more informative manner of plotting the data for $M_j > 1$ is shown in Fig.10b). Also shown there is a linear extrapolation of the mixing noise data from Fig.10a). It is apparent that once the shock noise dominates, the OASPL varies as β^4 over the majority of the pressure ratio range. This in turn suggests that the source amplitude varies as β^2 , which use of the Rankine Hugoniot relations shows is in direct proportion to the pressure jump across the shock wave. Harper-Bourne furthermore was able to confirm using a crossed beam Schlieren system, that this was indeed the variation of fluctuation amplitude observed at the shock cell ends. Finally shown in Fig.10c) is the variation of OASPL as a function of pressure ratio (i.e. β) for a range of jet efflux temperatures, together with estimates of the mixing noise contribution at the two extremes of temperature considered. We note that the mixing noise contribution is larger at the higher temperature as a result of the higher associated jet efflux velocity at a fixed pressure ratio. However again once the shock cell noise dominates, a β^4 dependence is observed at levels which are independent of jet temperature.

Thus with respect to the variation of overall intensity of broad band shock associated noise we conclude

- It is independent of observation angle
- It is independent of jet temperature and hence jet efflux velocity, being solely a function of pressure ratio in accordance with the empirical relationship

$$\text{OASPL (dB)} = 158.5 + 10 \log_{10} \left| \left(\frac{D}{R} \right)^2 \beta^4 \right|.$$

The spectral character of shock associated noise is demonstrated in Fig.11, where the spectrum of noise from a convergent under-expanded nozzle is compared with that from a convergent-divergent, shock free nozzle, both of which were operated at the same pressure ratio and temperature. This shock associated noise component is clearly reasonably broad band, but exhibits a distinct spectral peak. This peak arises due to interference between radiation from the various shock cells as shown schematically below.



We suppose that an eddy convecting down the shock cell array causes each to emit a signal whose relative phase is set by the eddy convection time. Hence, considering for simplicity a narrow band of frequencies the source fluctuation at the n th source is of the form

$$A_n(\omega) \cos \omega \left(t - \frac{nL}{V_c} \right).$$

We can next sum the contribution from all such sources, with due allowance for retarded time. The signal received by a far-field observer at distance r_o and angle θ is therefore

$$\begin{aligned} p(r, \theta, t + r_o/a_o) &= \frac{1}{r_o} \sum_n A_n(\omega) \cos \omega \left(t - \frac{nL}{V_c} + \frac{nL \cos \theta}{a_o} \right) \\ &= \frac{1}{r_o} \sum_n A_n(\omega) \cos \left(\omega t - \frac{nL}{V_c} (1 - M_c \cos \theta) \right) \end{aligned}$$

where $M_c \equiv \frac{V_c}{a_o}$.

The mean square pressure at frequency ω is therefore

$$\overline{p^2(r, \theta, \omega)} = \frac{1}{r_o^2} \sum_n \sum_m A_n(\omega) A_m(\omega) \cos \left| \frac{(n-m)\omega L (1 - M_c \cos \theta)}{V_c} \right|.$$

We note that the summation above is made up of two distinct types of term. First, those for which $n = m$ represent the sum of contributions from each shock cell acting alone. This is the mean square pressure which would be obtained if the sources were statistically independent or uncorrelated. However since the sources are driven by the same eddy, some degree of correlation is anticipated and is represented by the remaining terms for which $n \neq m$. We note also that these remaining terms will yield a maximum contribution whenever the argument of the cosine is either zero or an integer multiple of 2π . The former condition corresponds to the Mach angle, $M_c \cos \theta = 1$, but we shall not consider this further as experience suggests that jet mixing noise is normally the major contributor at this angle. The second condition however implies that we should expect a peak shock cell noise contribution at frequencies given by

$$f_p = \frac{V_c}{L(1 - M_c \cos \theta)}.$$

That is for an observation angle of $\theta = 90^\circ$ the peak frequency is $\frac{V_c}{L}$ and then varies in the manner of an apparent Doppler shift at other angles. A comparison between this prediction and experiment has been included in Fig. 11. We also note finally that for $\theta = 180^\circ$,

$$f_p = \frac{V_c}{L(1 + M_c)},$$

which is identical to the screech frequency discussed previously. It appears therefore that at the screech frequency the shock associated noise from an array of shocks will all combine constructively to yield the strong forward radiation needed to maintain the feedback loop.

For more complete details of the prediction of shock associated noise the reader is referred to [18]. We note however an important typographical error in that work: Eq. (27) should read:-

$$G_p(r_o, \theta, \omega) = G_o(r_o, \omega) \left| 1 + \sum_{i=1}^{N-1} \frac{2}{N} C_i(\omega) \sum_{s=0}^{N-(i+1)} \cos \left| \frac{\omega L}{V_c} (1 - M_c \cos \theta) (1 - \mu_{si}) \right| \right|.$$

4. THE STATIC TO FLIGHT DILEMMA

A set of notes on jet noise would be incomplete at the present time without some brief mention of recent work on static to flight effects. The majority of our knowledge on jet noise is clearly derived from static tests, but normally the practical requirement is to predict the noise field generated when the nozzle is in forward motion at speeds up to 250 knots ($M_A = .37$). Early estimates of the differences due to forward motion appear to have centred on the idea that the principal effect of flight would be to reduce the velocity difference between the jet efflux and the ambient fluid from U_j statically to $(U_j - U_A)$ in flight. (U_A = aircraft forward speed). Assuming that both turbulence intensity and the time scales of the turbulence

scale on this velocity difference then a static to flight noise reduction of

$$\Delta(\text{dB}) = 10 \log_{10} \left(\frac{U_J - U_A}{U_J} \right)^8$$

might be expected.

However a considerable volume of flight testing now shows such a prediction to be grossly over-optimistic. A recent comprehensive survey has recently been presented by Bushell [20], who chose to empiricise the static to flight difference in the form

$$\Delta(\text{dB}) = 10 \log_{10} \left| \left(\frac{U_J - U_A}{U_J} \right)^m (1 + M_A \cos \theta) \right|$$

The variation of the empirical exponent m with angle of observation for a wide range of aircraft types is shown in Fig. 2. It is clear that m is a strong function of angle, reducing from about 5.5 at small angles to zero at $\theta = 90^\circ$ and then going negative, implying that for the forward arc the noise actually increases in going from static to flight.

These and other difficulties associated with accurate estimation of the flight performance of various types of jet noise suppressor nozzles have led to a search for methods of simulating forward motion to avoid the expensive process of bringing these nozzles to a flight standard. Two principal methods of simulation are currently in vogue, namely the use of anechoically treated wind tunnels [21] and the use of large area ratio co-axial jet configurations. In both cases the principle is to submerge the jet under test in a large co-flowing stream.

The results from such simulations appear in general to be internally consistent and demonstrate a fairly uniform reduction of noise irrespective of angle of observation as indicated in Fig. 12. Clearly the results are quite significantly different. For example the wind tunnel results would imply that for a jet velocity of 1,000 ft/s and a flight speed of 200 ft/s (or 125 knots) a noise reduction at $\theta = 90^\circ$ of order 5 dB might be expected, while actual flight experience would suggest no change.

The reason is the possibility that tailpipe noise, present on aero engines but not on the model simulation, is not reduced by forward speed and may even be amplified in the forward arc as a result of forward motion. Thus the anticipated jet mixing noise reduction is severely reduced by an underlying content of tailpipe noise which is not apparent on the static test, but becomes more so in the flight environment.

It is clear however that an improved understanding of static to flight behaviour is required before one can ascertain whether the noise reductions implied by the wind tunnel simulations can be realised in the practical situation.

REFERENCES

- [1] M.J. LIDTHILL 1952 Proc. Roy. Soc. A. Vol. 211, 564-587. On Sound Generated Aerodynamically - I - General Theory.
- [2] M.J. LIDTHILL 1954 Proc. Roy. Soc. A. Vol. 222, 1-32. On Sound Generated Aerodynamically - II - Turbulence as a Source of Sound.
- [3] P.A. LUSH 1971 J. Fluid Mech. Vol. 46, 477-500. Measurements of subsonic jet noise and comparison with theory.
- [4] H.K. TANNA 1976 Journal Sound and Vibration in Press Summer 1976. An Experimental Study of Jet Noise: Part I, Turbulent Mixing Noise.
- [5] G.M. LILLEY, P.J. MORRIS and B.J. TESTER 1973 A.I.A.A. Paper No. 73-987. On the Theory of Jet Noise and its Applications.
- [6] R. MANI 1972 Journal of Sound and Vibration Vol. 25, 337-347. A Moving Source Problem Relevant to Jet Noise.
- [7] B.J. TESTER, C.L. MORFEY 1976 Journal Sound and Vibration. Vol. 46. Development in Jet Noise Modelling and Theoretical Predictions and Comparisons with Measured Data.
- [8] M.S. HOWE 1975 Journal Sound and Vibration. Vol. 43, 77-86. An Application of Energy Conservation to the Solution of Radiation Problems Involving Uniformly Convected Source Distributions.
- [9] J.E. FLOWCS WILLIAMS 1963 Phil. Trans. Roy. Soc. A 255, 469-503. The Noise from Turbulence convected at High Speeds.
- [10] R.G. HOCH et al 1973 Journal Sound and Vibration. Vol. 28, 649-668. Studies of the Influence of Density on Jet Noise.
- [11] P.A. LUSH, M.J. FISHER, K. AHUJA 1973 Proc. British Acoustical Society, Spring Meeting (April 1973) Noise from Hot Jets. see also M.J. FISHER, P.A. LUSH, M. HARPER-BOURNE 1973 Journal Sound and Vibration Vol. 28, 563-585 Jet Noise.
- [12] H.K. TANNA, P.D. DEAN, M.J. FISHER 1975 Journal Sound and Vibration Vol. 39, 429-460. The Influence of Temperature on Shock free Supersonic Jet Noise.
- [13] C.L. MORFEY 1973 Journal Sound and Vibration Vol. 31, 391-397. Amplification of Aerodynamic Noise by Convected Flow Inhomogeneities.
- [14] D.I. BLOKHINTSEV 1946 English Translation NACA-TM-1399 (1956) Acoustics of a Non-Homogeneous Moving Medium.
- [15] M.J. FISHER, V.M. SZEWCZYK 1974 A.R.C. Paper No. 35, 212-N897. Flow-Acoustic Interaction Effects in Jet Noise.
- [16] R. HOCH, R. HAWKINS 1973 AGARD Conference Pre-print No. 131 on Noise Mechanisms. Recent Studies into Concorde Noise Reduction.

- [17] A. POWELL 1953 Proc.Phys.Soc.B. Vol.66, 1029-1056. On the Mechanism of Choked Jet Noise.
 [18] M. HARPER-BOURNE, M.J. FISHER 1973. AGARD Conference Pre-print No.131 on Noise Mechanisms. The Noise from Shock Waves in Supersonic Jets.
 [19] J.A. HAY, E.G. ROSE 1970 Journal Sound and Vibration Vol.11, 411-420. In Flight Shock Cell Noise.
 [20] K.W. BUSHELL 1975 A.I.A.A. Paper No. 75-461. Measurement and Prediction of Jet Noise in Flight.
 [21] B.J. COCKING, W.D. BRYCE 1975 A.I.A.A. Paper No.75-462. Subsonic Jet Noise in Flight Based on Some Recent Wind Tunnel Tests.

APPENDIX A

LIGHTHILL'S ACOUSTIC ANALOGY

The problem of noise produced by a free turbulent flow in the absence of mass injection and externally applied forces was developed by Lighthill by combining the equations describing the conservation of mass and momentum.

They are respectively

$$\frac{\partial \rho}{\partial t} + \frac{\partial}{\partial x_i} (\rho v_i) = 0 \quad (1)$$

$$\frac{\partial}{\partial t} (\rho v_i) + \frac{\partial}{\partial x_j} (\rho v_i v_j) + \frac{\partial p}{\partial x_i} - \frac{\partial \sigma_{ij}}{\partial x_j} = 0 \quad (2)$$

where σ_{ij} is the viscous stress tensor.

The equations are written in tensor notation, implying that summation over the values of i and j equal to 1, 2, 3 is required. For example, Eq.(1) written out in full is

$$\frac{\partial \rho}{\partial t} + \frac{\partial}{\partial x_1} (\rho v_1) + \frac{\partial}{\partial x_2} (\rho v_2) + \frac{\partial}{\partial x_3} (\rho v_3) = 0$$

where x_1, x_2, x_3 are three orthogonal co-ordinates and v_1, v_2, v_3 the velocity components in these directions.

A wave equation may now be developed by differentiating (1) wrt time and (2) wrt the space co-ordinate x_i . Subtraction of the two resulting equations eliminates ρv_i to yield

$$\frac{\partial^2 \rho}{\partial t^2} - \frac{\partial^2}{\partial x_i \partial x_j} (\rho v_i v_j) - \frac{\partial^2 p}{\partial x_i^2} + \frac{\partial^2 \sigma_{ij}}{\partial x_i \partial x_j} = 0 \quad (3)$$

We now subtract $a_0^2 \frac{\partial^2 \rho}{\partial x_i^2}$ from both sides of this equation to form a wave equation for density as follows,

$$\frac{\partial^2 \rho}{\partial t^2} - a_0^2 \frac{\partial^2 \rho}{\partial x_i^2} = \frac{\partial^2}{\partial x_i \partial x_j} [\rho v_i v_j + (p - a_0^2 \rho) \delta_{ij} - \sigma_{ij}] \quad (4)$$

where $\delta_{ij} = 1 \quad i = j$
 $= 0 \quad i \neq j.$

The term in square brackets on the rhs of (4) is traditionally denoted by T_{ij} and is called the Lighthill stress tensor. If T_{ij} is equal to zero then (4) reduced to the form of a wave equation showing that the density fluctuations are then propagated in the manner of sound waves. In fact, outside the flow region T_{ij} will be zero, at least to the accuracy of linear acoustic theory. The only contribution to velocity fluctuations are variations of acoustic particle velocity. However, second order products of particle velocity like $v_i v_j$ are negligible for linear acoustic waves. The term $p - a_0^2 \rho$ is similarly zero in a sound field or for that matter for an isentropic process. This leaves only the viscous term which is known to attenuate sound waves over relatively large distances, but is negligible for many practical purposes. Thus outside the flow the density fluctuations are predicted to propagate like sound waves, and the rhs may be regarded as a source term.

$$\frac{\partial^2 \rho}{\partial t^2} - a_0^2 \frac{\partial^2 \rho}{\partial x_i^2} = \frac{\partial^2 T_{ij}}{\partial x_i \partial x_j} \quad (5)$$

If it is assumed that T_{ij} is known then the solution of (5) is

$$\rho(\underline{x}, t) - \rho_0 = \frac{1}{4\pi a_0^2} \int_V \frac{\partial^2}{\partial y_i \partial y_j} T_{ij}(\underline{y}, t - \frac{|\underline{x} - \underline{y}|}{a_0}) \frac{dV(\underline{y})}{|\underline{x} - \underline{y}|} \quad (6)$$

where $\rho(\underline{x}, t)$ is the density observed at position \underline{x} and time t outside the source region.

The interpretation of this result is that the density fluctuations observed outside the flow region are those which would be produced by an array of sources of strength $\partial^2 T_{ij} / \partial y_i \partial y_j$ per unit volume distri-

buted over regions occupied by the flow, and evaluated at the correct retarded time. These sources are termed acoustically equivalent meaning that this set of sources would produce precisely the acoustic radiation due to the flow. However, it is important to realise that these sources are used to replace the flow in a medium at rest. For the acoustic problem the flow no longer exists; only the array of equivalent sources.

The nature of these 'sources' is also of interest. Reference to Eq.(4) indicates that the rhs is composed of the actual stresses on the fluid due to pressure and viscous forces, the apparent or Reynolds stress (i.e. the $\rho u_i u_j$ term) less the stress which would be created by the density perturbation contained in the $a_0^2 \rho$ term. It is argued therefore that the source strength $\partial^2 T_{ij} / \partial x_i \partial x_j$ is composed of the difference between the effective stresses on the fluid and those imposed by the density field and it is this residual stress which is the forcing function for the radiated density field.

Finally, it is to be emphasised that Eq.(9) is exact, no approximations being involved in its derivation. Thus were the second space derivatives of T_{ij} at the appropriate retarded times $(t - |x - y|/a_0)$ known accurately the density and hence sound field could be precisely specified. It is, in fact, finding approximate methods of estimating the rhs of (6) where the results obtained are not too dependent on those approximations which offer the major challenge to the theoretician.

THE Lighthill FORMULAE

In this section we present a number of techniques which have been proposed for providing reasonable estimates of the noise radiated by jet flows. As one example of the problems involved, however, it is tempting in view of Eq.(6) to assume first that the observer at x is sufficiently far from the source that $|x - y|$ can be replaced by $|x|$ in the denominator and secondly that the source is small compared to the acoustic wavelength so that retarded times can be neglected for such a compact source. Eq.(6) reduces to

$$\rho(x, t) - \rho_0 = \frac{1}{4\pi a_0^2 |x|} \int \frac{\partial^2 T_{ij}}{\partial y_i \partial y_j} (y, t - \frac{|x|}{a_0}) dV(y),$$

Gauss' theorem, however, tells us that any volume integral of the divergence of a function may be replaced by a surface integral of that function over any chosen closed surface. Thus the integral becomes

$$\int_S \frac{\partial T_{ij}}{\partial y_j} (t - \frac{|x|}{a_0}) dS_i$$

We now merely have to choose the surface outside the flow where T_{ij} is zero to obtain the result that the source strength is zero. Clearly, the approximations made are too crude and in fact our major mistake was that of neglecting the retarded times. This, of course, tells us immediately that the equivalent sources of (6) are not monopole, but of some higher order. Our approximation above resulted in precisely the anomaly which occurs when radiation from any multipole is estimated with neglect of retarded times; complete cancellation occurs. It appears, therefore, that progress is unlikely to be made by attempting approximate estimates of the simple source strengths of Eq.(6). Rather we should attempt to reformulate the problem in terms of a multipole source strength where the cancellation between the component source strengths will tend to take care of itself.

For convenience we rewrite (6) in the form

$$\rho(x, t) - \rho_0 = \frac{1}{4\pi a_0^2} \int_V \frac{1}{r} \frac{\partial^2}{\partial y_i \partial y_j} T_{ij}(y, t - \frac{r}{a_0}) dV(y) \quad (7)$$

where $r \equiv |x - y|$ is the distance from the elemental sources to the observer.

Using Gauss' theorem

$$\int_V \frac{\partial}{\partial y_i} \left[\frac{1}{r} \frac{\partial T_{ij}}{\partial y_j} \right] dV = \int_S \frac{1}{r} \frac{\partial T_{ij}}{\partial y_j} dS_i = 0 \quad (8)$$

as argued above.

Expanding the L.H.S. of (8) we find therefore

$$\frac{1}{r} \frac{\partial^2 T_{ij}}{\partial y_i \partial y_j} = - \frac{\partial T_{ij}}{\partial y_j} \frac{1}{y_i} \left(\frac{1}{r} \right) \quad (9)$$

Now $r^2 = (x_i - y_i)^2$ and on differentiating with respect to x_i and y_i in turn, we obtain

$$r \frac{\partial r}{\partial x_i} = (x_i - y_i)$$

$$r \frac{\partial r}{\partial y_i} = -(x_i - y_i)$$

thence

$$\frac{\partial r}{\partial x_i} = - \frac{\partial r}{\partial y_i} \quad (9a)$$

therefore $\frac{\partial}{\partial y_i} \frac{1}{r} = -\frac{1}{r^2} \frac{\partial r}{\partial y_i} = \frac{1}{r^2} \frac{\partial r}{\partial x_i} = -\frac{\partial}{\partial x_i} \left(\frac{1}{r} \right)$ by (9a).

Hence (9) becomes

$$\frac{1}{r} \frac{\partial^2 T_{ij}}{\partial y_i \partial y_j} = \frac{\partial}{\partial x_i} \frac{1}{r} \frac{\partial T_{ij}}{\partial y_j}$$

Hence re-substituting in (7)

$$\rho(x, t) - \rho_0 = \frac{1}{4\pi a_0^2} \int_V \frac{1}{r} \frac{\partial T_{ij}}{\partial y_j} (y, t - \frac{r}{a_0}) dV(y)$$

We may now repeat this procedure for the remaining integral to obtain

$$\rho(x, t) - \rho_0 = \frac{1}{4\pi a_0^2} \frac{\partial}{\partial x_i} \int_V \frac{1}{r} T_{ij} (y, t - \frac{r}{a_0}) dV(y) \quad (10)$$

The reader should not be misled by the rather deceptive similarity between Eqs. (7) and (10). In the former, the equivalent sources are monopoles of strength proportional to a second space derivative of T_{ij} . Thus these derivatives must be estimated at appropriate retarded times before integration. In (10) the source is quadrupole as indicated by the double derivative, but the whole flow is now acoustically equivalent to a single quadrupole of total strength given by the integral in (10). Thus we are now attempting to scale a total source strength not the strengths of various and largely cancelling individual contributors.

Equation (10) gives the radiation field at all distances from the source region, however, we are primarily concerned with the far field radiation. Thus we may neglect terms which decay faster than $1/r$: In effect, the space derivatives need only be applied to T_{ij} , i.e.

$$\frac{\partial}{\partial x_j} \{T_{ij}(y, t - \frac{r}{a_0})\} = T_{ij}'(y, t - \frac{r}{a_0}) (-\frac{1}{a_0} \frac{\partial r}{\partial x_j})$$

Now $\frac{\partial r}{\partial x_j} = \frac{x_j - y_j}{r}$ by (9a) and the derivative of T_{ij} with respect to $t - r/a_0$ is equal to $\partial T_{ij} / \partial t$.

$$\text{Thus} \quad \frac{\partial}{\partial x_i} \{T_{ij}(y, t - \frac{r}{a_0})\} = -\frac{(x_i - y_i)}{r} \frac{1}{a_0} \frac{\partial T_{ij}}{\partial t} (y, t - \frac{r}{a_0})$$

Therefore the far field radiation is given by,

$$\rho(x, t) - \rho_0 = \frac{1}{4\pi a_0^4} \int_V \frac{(x_i - y_i)(x_j - y_j)}{r^3} \frac{\partial^2 T_{ij}}{\partial t^2} (y, t - \frac{r}{a_0}) dV(y) \quad (11)$$

If we now make the further assumption that the source region is small compared with the distance to the observer, i.e. $|x| \gg |y|$ then (11) may be rewritten

$$\rho(x, t) - \rho_0 = \frac{1}{4\pi a_0^4} \frac{x_i x_j}{r^3} \int_V \frac{\partial^2 T_{ij}}{\partial t^2} (y, t - \frac{r}{a_0}) dV(y) \quad (12)$$

This result may be rewritten in a more physically meaningful form by combining the direction cosines $x_i x_j / r$ with T_{ij} to form a scalar source strength. If the viscous part of T_{ij} is neglected, the source strength becomes,

$$\frac{u_i x_i}{r} \frac{u_j x_j}{r} + (p - a_0^2 \rho) \delta_{ij} \frac{x_i x_j}{r^2}$$

Now $u_i x_i / r$ is simply the resolved part of the velocity in the direction of the observer, which we denote by u_r and $\delta_{ij} x_i x_j / r^2 = 1$. Thus the quadrupole source strength may be written,

$$T_{rr} = \rho u_r^2 + p - a_0^2 \rho \quad (13)$$

Since in the sound field $p - p_0 = a_0^2 (\rho - \rho_0)$, the far field pressure amplitude is given finally by,

$$p(x, t) - p_0 = \frac{1}{4\pi a_0^2 r} \int_V \frac{\partial^2 T_{rr}}{\partial t^2} (y, t - \frac{r}{a_0}) dV(y) \quad (14)$$

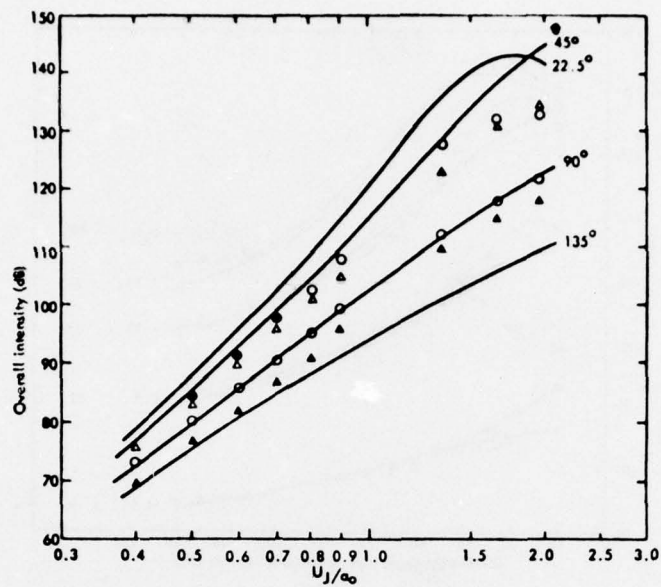


Fig.1 Velocity dependence of overall intensity: $T_j/T_0 = 1$. — freely convecting quadrupole theory
 θ : \triangle 135° ; \circ 90° ; \triangle 45° ; \bullet 22.5°

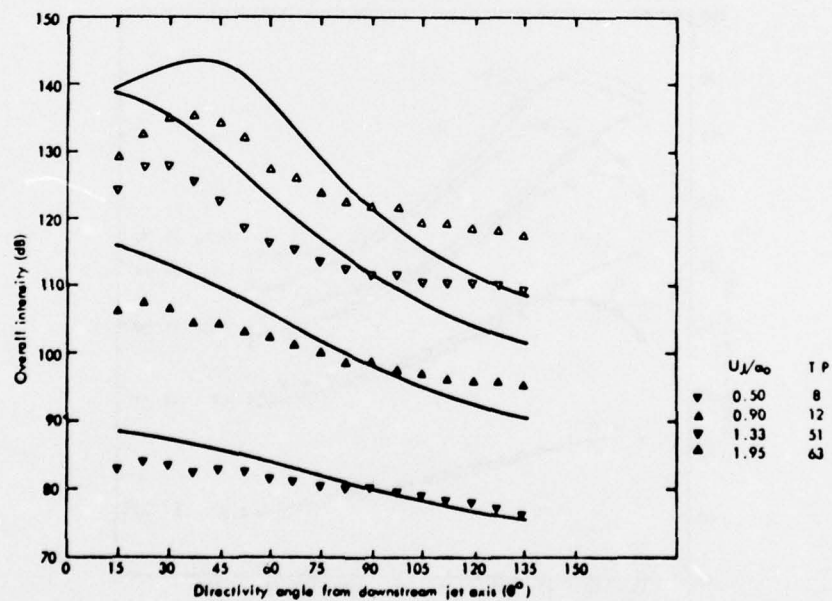


Fig.2 Directivity of overall intensity: $T_j/T_0 = 1$. — freely convecting quadrupole theory

BEST AVAILABLE COPY

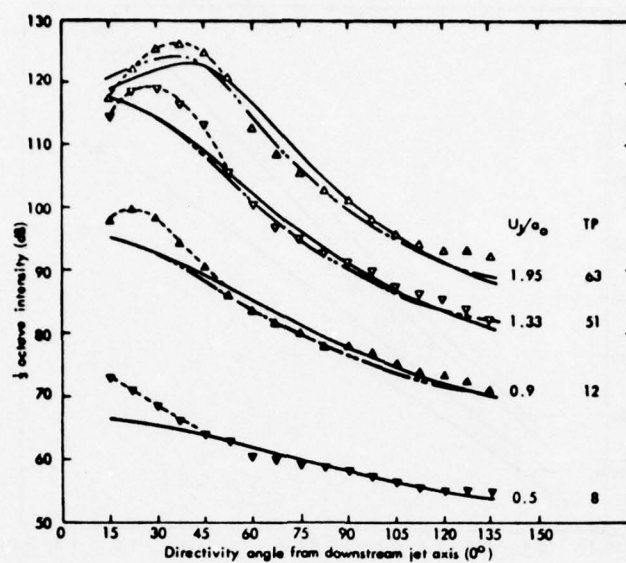


Fig.3(a) Directivity of $\frac{1}{3}$ octave intensity at $f_s D/U_j = 0.1$; $T_j/T_0 = 1$. — freely convecting quadrupole theory; --- same theory with modified θ (source at $X/D = 10$); experiment

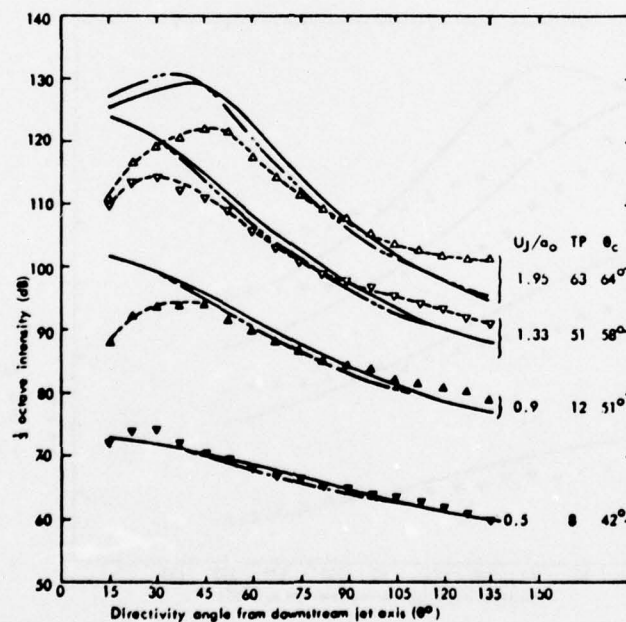


Fig.3(b) Directivity of $\frac{1}{3}$ octave intensity at $f_s D/U_j = 0.3$; $T_j/T_0 = 1$. — freely convecting quadrupole theory; --- same theory with modified θ (source at $X/D = 10$); experiment

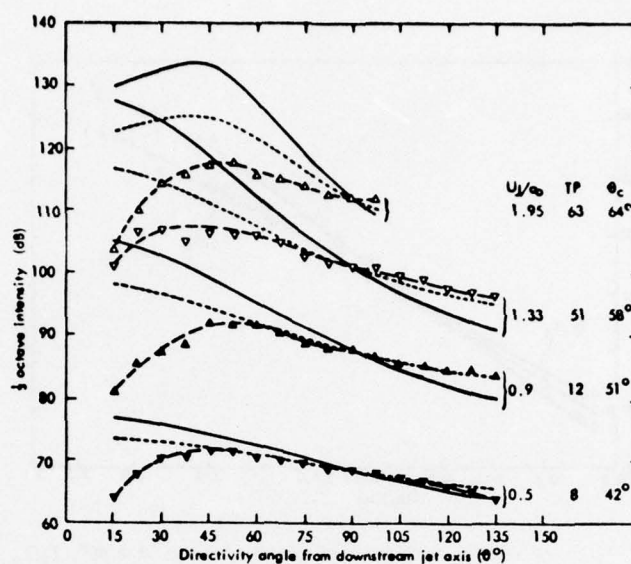


Fig.3(c) Directivity of $\frac{1}{3}$ octave intensity at $f_s D/U_J = 1.0$; $T_J/T_0 = 1$. (a) — freely convecting quadrupole theory (5 powers of doppler factor); (b) ----- 3 powers of doppler factor; --- experiment

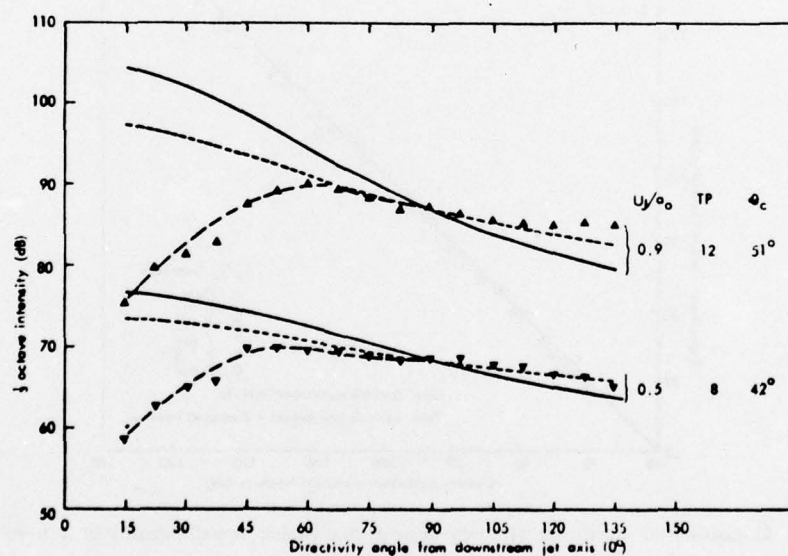


Fig.3(d) Directivity of $\frac{1}{3}$ octave intensity at $f_s D/U_J = 3.0$; $T_J/T_0 = 1$. (a) — freely convecting quadrupole theory (5 powers of doppler factor); (b) ----- 3 powers of doppler factor; --- experiment

BEST AVAILABLE COPY

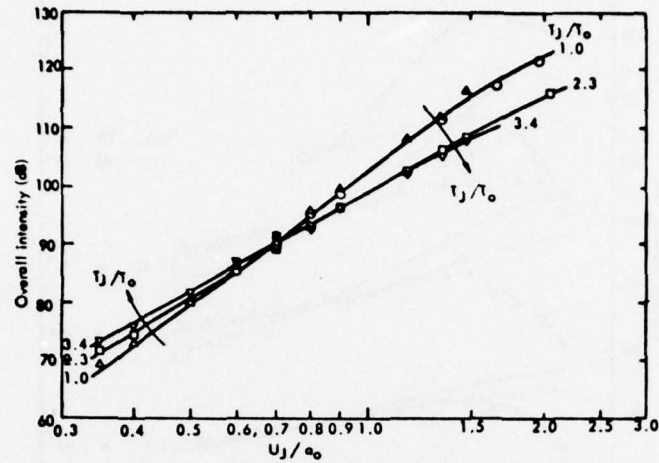


Fig.4 Effect of T_j/T_0 on velocity dependence of overall intensity: $\theta = 90^\circ$, T_j/T_0 (nominal):
 \triangle cold; \circ 1.0; \square 2.3; ∇ 3.4

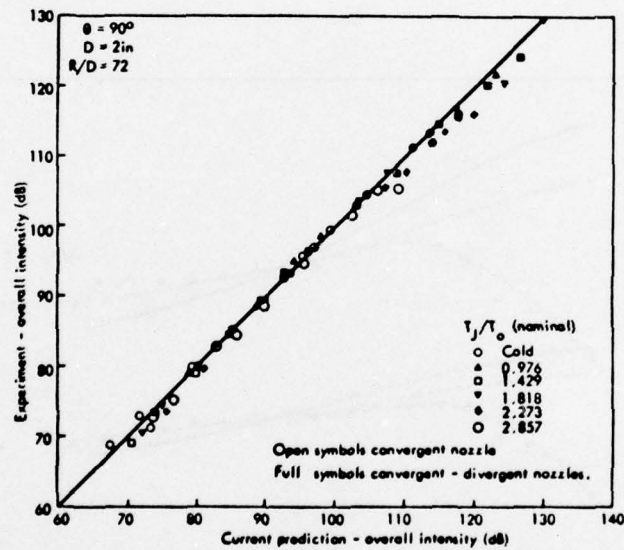


Fig.5 Comparison of experiment with current prediction model: overall intensity at $\theta = 90^\circ$

BEST AVAILABLE COPY

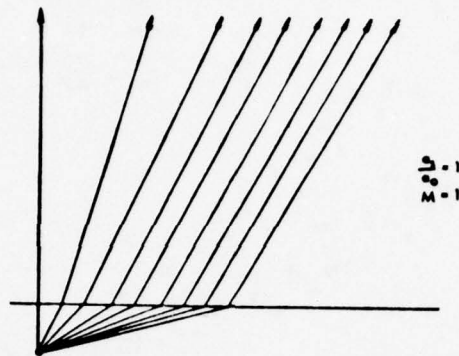


Fig.6(a) Demonstrating ray focussing

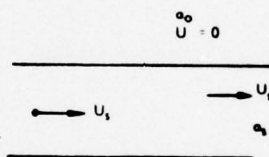


Fig.6(b) A shrouded and convecting source

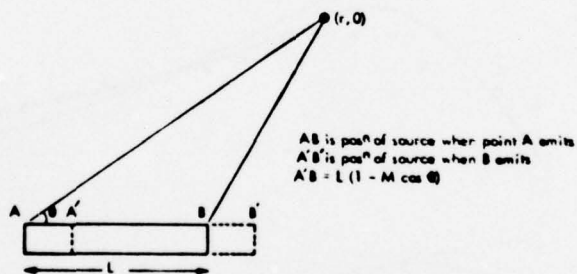


Fig.6(c) The contribution of a convecting source distribution

BEST AVAILABLE COPY

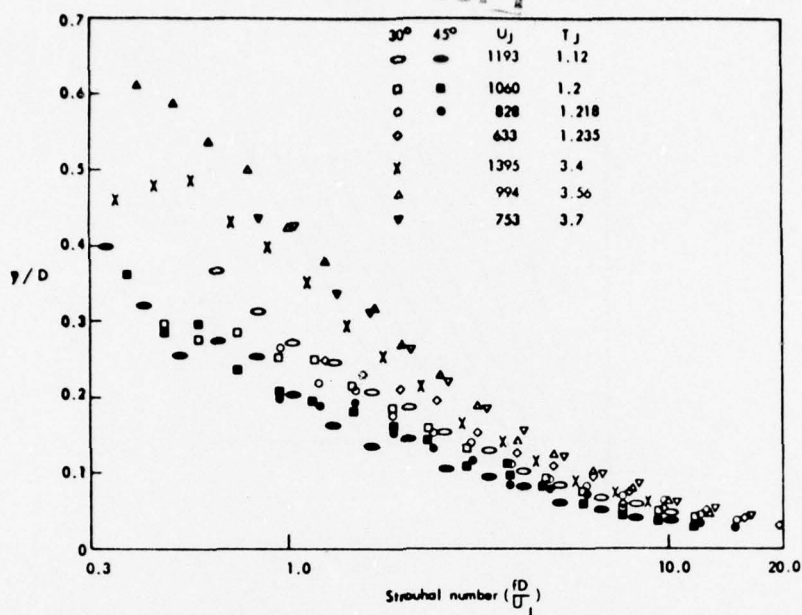


Fig.7 Effective source depth as a function of Strouhal number for a circular nozzle

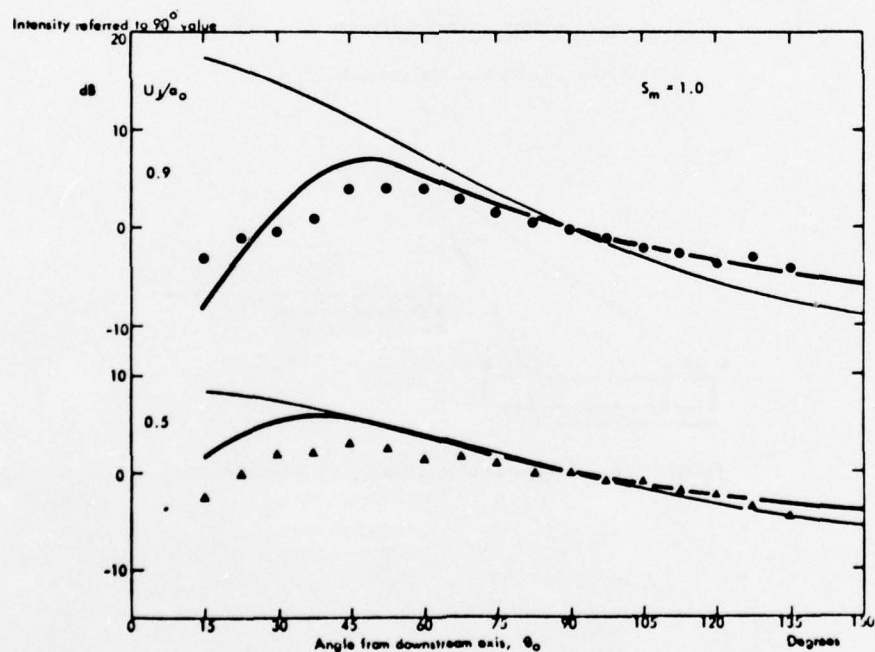


Fig.8 Directivity of isothermal jet noise: comparison of the theoretical models with $\frac{1}{3}$ -octave data, for $S_m = 1.0$.
 Code: Δ, \bullet Lockheed Georgia measurements; $— (D_m(\theta)/D_m(90^\circ))^{-5}$ where D_m is the modified doppler factor with $U_c = .67U_j$ and $\alpha = 0.3$; $—$ calculation from Reference 7

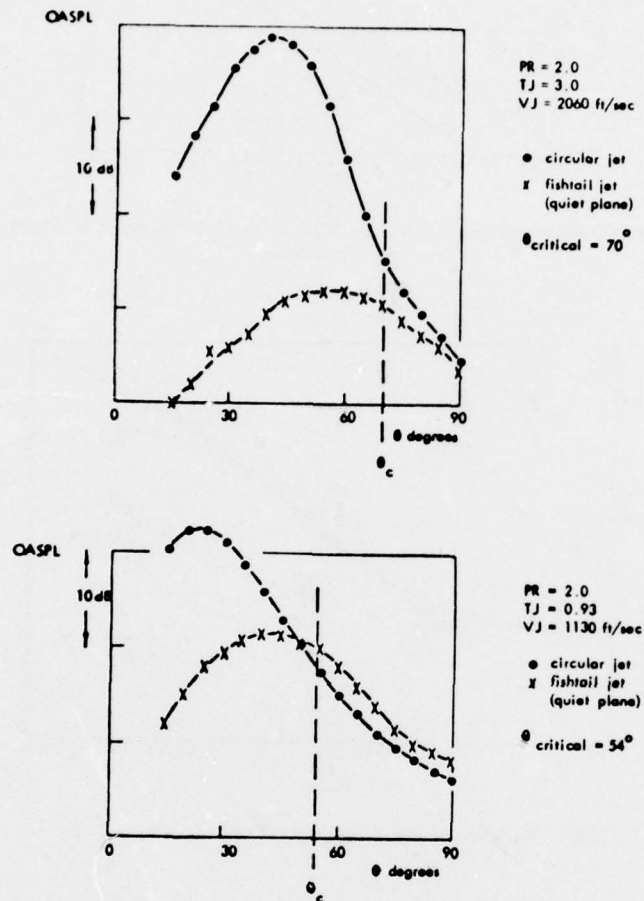


Fig.9 Comparative field shapes for circular and fishtail jets

BEST AVAILABLE COPY

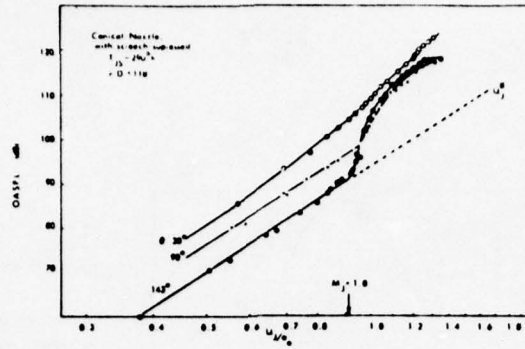


Fig. 10(a) Velocity dependence of overall intensity of jet noise at several angles to the jet showing shock associated noise

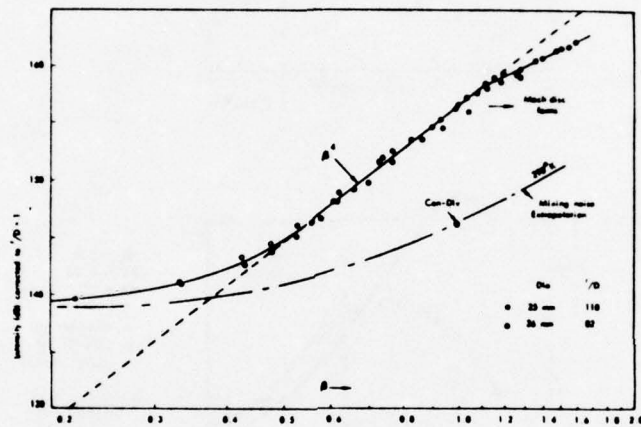


Fig. 10(b) Variation of overall intensity at 90° to jet with $\sqrt{M^2 - 1}$

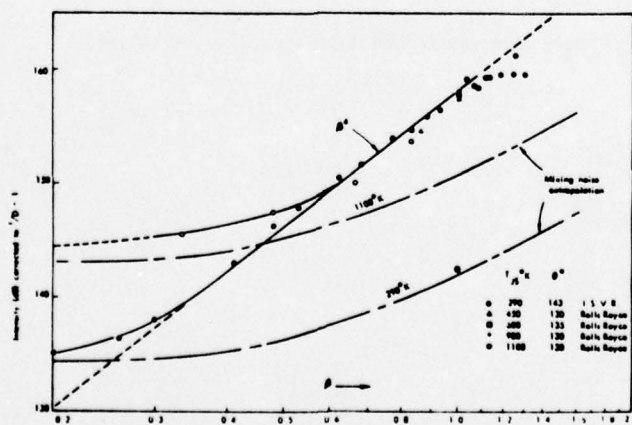


Fig. 10(c) Variation of overall intensity in forward arc with $\sqrt{M^2 - 1}$ for a range of temperatures from cold to 1100°K

BEST AVAILABLE COPY

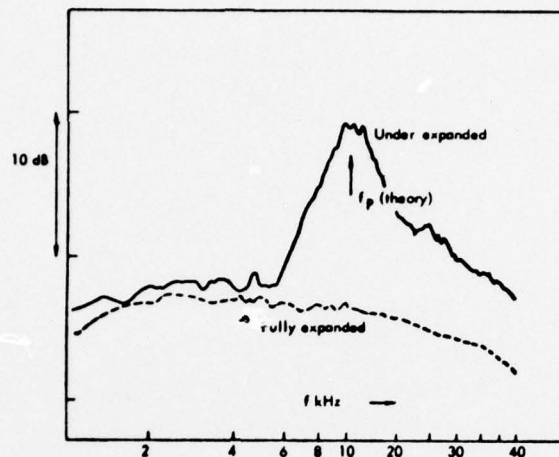


Fig.11 Comparison of supersonic jet noise spectra for a fully expanded and under expanded flow ($\theta = 90^\circ$, $\beta = 1.0$)

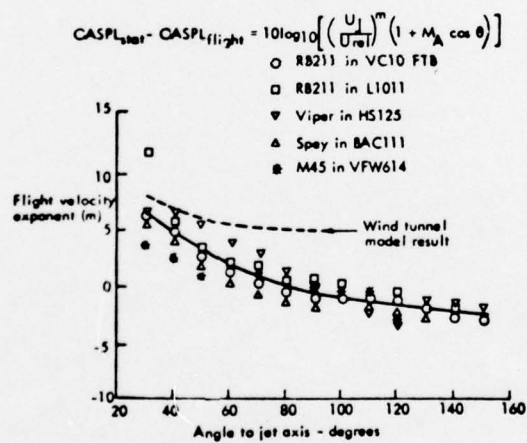


Fig.12 Comparison of flight velocity exponents

GAS TURBINE ENGINE EXHAUST NOISE

by

Dr Kenneth W. Bushell
Noise Project Engineer
Rolls-Royce (1971) Limited, Derby, England

SUMMARY

This lecture aims to review the sources of noise which emanate from the exhaust of a gas turbine engine. The most important of these are considered to be associated with the combustion system, the turbine, the exhaust system, obstructions, turbulence/noise interaction with the jet structure. Also considered is the jet mixing noise due to single and coaxial streams. Wherever possible prediction methods for these sources are given and reviewed. Reflections from the ground are also reviewed because of the influence these can have in the lower frequency part of the spectrum.

Finally, the effects of flight or forward speed on these noise sources is considered.

1. INTRODUCTION

The title given to this lecture implies a very wide scope since any noise emanating from the exhaust nozzle of a gas turbine engine may be called exhaust noise. Also the noise created external to the nozzles by the gas stream which exhausts from the engine may be similarly named. It is the intent of this lecture to discuss the sources of noise which, in the published literature, have been variously called, 'excess noise', 'tailpipe noise', 'core noise', 'combustor noise' etc., that is, all sources which propagate rearwards other than that from the fan or compressor which is dealt with in Dr. Lowrie's lecture in this series. These sources are illustrated in Fig.1, which also indicates their directivities in a simplified manner.

Noise associated with the turbine is difficult to categorise because often there is a fairly arbitrary division between the noise created by flow through the turbine blading and that created by the interaction of upstream turbulence or temperature fluctuations with the turbine. Usually this division is made on a basis of frequency, with high frequency noise being called turbine noise, and the low or mid frequency noise being given any of the aforementioned alternative names.

In this lecture some aspects of turbine noise will be discussed as part of the total exhaust noise. The subject of turbine noise is however, rather like fan noise, sufficient for a separate lecture and thus cannot be covered exhaustively in the present one.

The topic of jet noise will also be covered, following on from Dr. Fisher's lecture on fundamental aspects to discuss practical prediction methods which are currently widely employed in industry, these being largely of an empirical nature, for both single stream jets and co-flowing or coaxial streams.

Also, because of its importance to the interpretation of engine noise data the influence of reflections from the ground plane on noise measurements will be briefly mentioned. This topic, however, belongs more strictly to the general topic of noise propagation and measurement.

Since predictions of the jet noise are used in the diagnosis of other exhaust noise sources these are reviewed first. The known characteristics of the other constituents of exhaust noise are then reviewed moving systematically through the engine from the combustion chamber to the exhaust. Finally the effect of forward speed, or aircraft flight on exhaust noise is discussed.

2. JET MIXING NOISE2.1 Single Streams

The fundamentals of jet mixing noise and its basic characteristics have been described by Dr. Fisher in the previous lecture. The major parameters controlling its generation are:-

V_J the exhaust velocity,
 A_J the exhaust nozzle area,
 T_J the exhaust total temperature,
(or ρ_J the exhaust gas density),

together with another important factor:-

r the measurement distance.

The shape of the nozzle may be important also, whether it is round, rectangular, or corrugated for example. Nozzle shapes other than round, i.e. chuted or corrugated are usually employed as jet noise suppressors, thus only the basic round conical nozzle will be considered here.

Over a period of many years, measured jet noise data both for engines and model nozzles have been correlated against the above parameters and the resultant curves published, sometimes with sufficient detail to provide a complete jet noise prediction scheme. See for example, in date order References 1 to 8.

The earlier prediction methods prior to about 1970 were mainly concerned with high velocity jets and the low velocity data was often suspect due to contamination by sources of noise other than jet mixing noise such as combustion noise or engine internal noise. The recent upsurge in jet noise research has overcome these problems and demonstrated that jet mixing noise free of contamination by other sources can be measured down to velocities as low as 300 ft/sec. (4,9,10,11)⁺. A literature survey reveals however that this is merely a 'rediscovery' of results obtained many years previously (12). The more recent data has the advantage however of being more readily available, more fully reported, and demonstrably free of contamination and of reflection effects due to the presence of the ground beneath the rig since these data have been obtained in anechoic conditions.

In particular, the recent research has fully explored the effects of temperature by carefully designed experiments, the results obtained by research groups in Britain, France and the U.S.A. being in excellent agreement (References 11, 13, 14 15). Fig.2 shows a set of data plotted as overall sound pressure level (OASPL) against velocity for a range of jet temperatures (from Reference 11). This shows a progressive increase in noise with temperature, which becomes greater the lower the velocity. At high velocities this trend is reversed. (11,14).

A simple form of data correlation has been found to collapse these effects of temperature using the jet density in the form:-

$$\text{OASPL} = 10 \log_{10} \left(\frac{\rho_J}{\rho_{\text{ISA}}} \right)^{\omega}$$

where ω is a function of jet velocity.

The data of Fig.2 when normalised is shown in Fig.3. The complete correlation for jet noise is:

$$\text{OASPL} = \text{function of} \left(\frac{V_J}{a_o} \right) + 10 \log_{10} \left(\frac{\rho_J}{\rho_o} \right)^{\omega} + 10 \log_{10} \left(\frac{A_J}{r^2} \right) + 20 \log_{10} \left(\frac{p_o}{p_{\text{ISA}}} \right)$$

and ω is a function of $\left(\frac{V_J}{a_o} \right)$

where V_J, ρ_J, A_J , are as defined earlier.

a_o is ambient speed of sound

ρ_o is atmospheric density

Fig.4 shows a generalised chart with the normalised overall sound pressure level as a function of velocity and angle and together with Fig.5, which gives the variation of ω with $\frac{V_J}{a_o}$, these are sufficient for a prediction of OASPL for a single stream jet. This prediction will be for free field conditions and for a loss free atmosphere (i.e. will be devoid of any effects of atmospheric absorption etc.).

These two figures are the latest available data from the Society of Automotive Engineers (SAE) - A21 Jet Noise Subcommittee which is an internationally based group that has been working since 1972 (see Reference 5 and 8) to produce an internationally acceptable jet noise prediction scheme. This subcommittee has representatives from almost all major organisations engaged in noise research including Boeing, Douglas, General Electric, Lockheed, NASA, NGTE, Pratt and Whitney, and Rolls-Royce, who have contributed basic data from their research programmes, much of which is as yet unpublished but undoubtedly represents the best data available at this time.

Fig.6 shows an example of the level of agreement obtained by compiling data from such a wide range of organisations. It is not exhaustive but gives an appreciation of the scatter which is experienced even with 'good' facilities and measurement techniques. It will be noted that the 'scatter' of data collected from many different rigs is greater than that from each individual rig (reference Fig.3).

The spectrum shape is more difficult to predict because simple correlations based upon Strouhal number $\frac{fD_J}{V_J}$, (D_J = nozzle diameter) are not sufficient to collapse the measured spectra at all angles and temperatures. Fig.7 shows the effect of temperature on spectral collapse and Fig.8

+ Numbers in parenthesis indicate references.

shows the change in spectrum shape with angle for a constant temperature. Full spectral data for prediction purposes is given in Ref.8. Improvements in the quality of the data correlation and hence accuracy of prediction are continuing and the work of the SAE committee will be published as SAE Aerospace Recommended Practice (ARP) 876 and updated as necessary.

Recently, concerted efforts have been made by NASA to produce prediction methods for each engine component (16,17). The work is coordinated by the Office of Aircraft Noise Prediction, which is contracted to ANOP - Hence reference to the ANOP method is common. The method for jet mixing noise has been published (7). Although presented in a different way, the OASPL's obtained from this method are not significantly different from those given by the SAE proposed method, and in fact the ANOP method uses a very similar scheme for temperature normalisation. This method was also reviewed in the previous AGARD lecture given in 1975 by John Tyler (18).

2.2 Coaxial Streams

Many modern engines have relatively high bypass ratios with the fan jet and the turbine or core jet exhausting through separate coaxial nozzles. Various configurations exist which are often referred to as short, medium, or long cowl engines (Fig.9). The axial position of the two exhaust nozzles might be thought to assert a primary influence on the noise from the total jet system but experimental data from models shows this to be only a secondary effect. The primary variables are found to be:-

$$\text{Area Ratio, (AR)} = \frac{\text{Area of bypass nozzle}}{\text{Area of core nozzle}}$$

$$\text{Velocity Ratio, (VR)} = \frac{\text{Velocity of bypass jet}}{\text{Velocity of core jet}}$$

The coaxial effect is also a strong function of frequency.

Fig.10 illustrates the effect of velocity ratio and area ratio on the OASPL, and Fig.11 shows the effect of velocity ratio on the spectrum shape at a fixed area ratio. These results are taken from the work of Cocking at NGTE (19) which constitutes the most thorough investigation of coaxial jet noise yet published. One important feature of this research is that in addition to cold flows, core temperatures representative of those in engines were also used. Although the qualitative characteristics of the noise of coaxial streams with a cold core are similar to those for a hot core, the absolute magnitude of the effects are temperature dependent, although no systematic variation with temperature has yet been determined. For practical predictions, a representative core stream temperature of 700°K is used. The effect of temperature is discussed by Cocking in Reference 19 and further cold data has been published in References 13, 20 and 21.

The other variable important in jet noise is the angle, of noise radiation or the 'directivity'. The noise directivity of coaxial jets follows the basic directivity of the core jet alone, the coaxial effect varies only slightly with angle, the main variation occurring very close to the jet axis (19).

The proposed SAE coaxial jet method based upon the NGTE data is presently under review by Jet Noise Subcommittee (8) and will be published as part of ARP 876 after comparison with other data available to that subcommittee. NASA have also published a method (7) but this is based on data with a cold core flow and is not considered as representative as that based on the NGTE data.

2.3 Shock Cell Noise

The other component of jet noise is that experienced at supersonic exhaust velocities when shock waves are present in the exhaust. The mechanism of this source is well understood and is described in the previous lecture by Dr. Fisher - A numerical prediction procedure has been developed from the work of Dr. Fisher and Harper-Bourne (22) and is currently under review by the SAE Jet Noise subcommittee (8).

3. GROUND REFLECTION EFFECTS

These have been extensively covered in the literature (23,24) and thus are reviewed very briefly. A typical geometric set up for a full scale engine test is shown in Fig.12. This shows two ray paths from source to receiver, the path length difference being Δr . For wave cancellation this path difference is related to the wavelength of the sound by

$$\Delta r = \frac{n\lambda}{2} \quad \text{where } n = 1, 3, 5, 7 \text{ etc.}$$

For value of n of 2,4,6 etc. the signals are in phase and augment.

The effects on engine measurements are large as illustrated in Fig.13.

The as measured noise shows large peaks at around 200 Hz and 1000 Hz which could be interpreted as two separate sources, which clearly is incorrect as seen when the true free field is obtained. Fig.13 in fact shows a small over correction at the two cancellation frequencies due to the application of the theoretical correction.

Fig.14 shows a normalised correction spectrum showing the theoretical correction for a point source over a perfectly reflecting surface compared to free field and that obtained for a real engine source size to height ratio D/h_m of 0.2, 0.3, 0.4 where D is the nozzle diameter and h_m is the height of the engine above the ground.

4. ENGINE EXHAUST NOISE

Examples of measured total engine exhaust noise for a low bypass ratio engine (the Spey 512) are given in Fig.15 at a relatively high thrust setting and in Fig.16 at a very low approach thrust setting. At the high power good agreement with the jet prediction is shown, whereas at low power there is considerable excess of measured noise above the jet prediction based on clean model rig data (8), which originally led to the term 'excess' noise.

A narrow band analysis reveals further details of the character of this noise. Fig.17 shows the existence of compressor discrete tones, turbine discrete tones whose origin is known together with considerable amounts of broad band noise whose origin cannot immediately be determined.

Experiments have been conducted with extensive acoustic treatment in the tailpipe of this engine. Figs.16 and 17 shows that considerable reduction of the far field noise is obtained, the most likely reason being that the additional noise originates from within the engine and the acoustic liner attenuates this during its propagation through the tailpipe.

There are other possible explanations but this experiment clearly indicates that the additional noise mechanisms originate within the engine and can be affected by internal modifications to the engine.

An example of the exhaust noise from a high bypass ratio engine at approach power is shown in Fig.19. Here the additional mid frequency noise has a distinctive peaked character centred on 400 Hz. The effect of changing the core nozzle size is shown in Fig.18. With increasing nozzle size and reducing jet velocity the very low frequency part of the spectrum reduces but the mid frequency peak remains constant, indicating its lack of dependence on jet velocity. Experiments with tailpipe liners has shown that this peak may be virtually eliminated by such liners, again indicating the existence of internal sources.

Other examples are appearing in the literature showing that similar effects have been observed on a wide range of engine types and manufacture (see references 4, 5, 25, 26, 27, 28).

The causes of this additional noise may be many and to date no single cause has been determined. Research on full scale engines and component rigs has however identified a wide range of possible contributing sources (see Fig.19). The major ones to be discussed here, proceeding through the engine are:-

1. Combustion noise.
2. Interaction of combustion products with the turbine.
3. Turbine noise.
4. Interaction of turbine exhaust flow with struts and obstructions.
5. Interaction of upstream noise and unsteady flow with the nozzle and the jet structure.

The problem facing the engine manufacturer is to be able to identify which particular mechanisms are responsible for the major noise nuisance in his particular engine.

This becomes particularly important in estimating the noise of project engines which exist only as drawings and/or performance models.

The advances in engine noise reduction brought about by the reduction in jet noise in going to high bypass ratio and by the use of extensive acoustic linings to attenuate fan noise has revealed these exhaust noise sources as a potential block on any further noise reduction. As a result, major research programmes are underway in many prominent establishments and aerospace companies, and new reports and papers on this topic are continuously appearing in the literature. Thus, this lecture has to be a state of the art review rather than a presentation of fixed and well tried technology, but it is hoped, it will give a good foundation on which the serious researcher may build.

4.1 Combustion Noise

It has long been felt that because of the enormous heat release that occurs in a gas turbine combustion chamber, and because it is designed to be a turbulent process with recirculation and violent mixing processes that it is an inherently noisy process and could, indeed perhaps should, be one of the major noise producers in an engine. At the time of writing, it is the author's opinion that there has as yet been no indisputable demonstration that broadband noise produced in the combustion system contributes directly to the far field exhaust noise. The qualification of 'broadband' noise is used because there are a considerable number of instances where discrete frequency noises (combustor 'howl' or 'rumble') heard in the far field can be traced to combustor instabilities and can often be cured by small changes to the combustor geometry. These are generally of very low frequency and manage to propagate through the turbine and nozzle with little difficulty.

There is ample evidence that a combustion system operating in isolation from the turbine creates high noise levels. Fig.20 shows an example of a full scale annular combustor tested by the General Electric Co. (29 and 30). A large diffuser or horn is used downstream of the combustor to reduce jet exhaust velocity and to improve the impedance match for the sound propagation. (Actually tests conducted with and without the horn do not show any consistent effect). The noise resulting from this is shown in Fig.21 for cold and hot flow. Without detailed data on the jet flow it is difficult to decide how much combustion noise and how much jet noise is present. However in an

associated experiment a 12" deep resonator suppressor was added downstream of the combustor. This gave considerable reductions in noise over a wide frequency range as shown in Fig.22 indicating that there is considerable direct noise from the chamber, in a frequency range which can easily be confused with jet noise in the complete engine.

Fig.23 shows a further example from a recent paper from The Boeing Company (31) which shows very similar results from a single combustion chamber in a pipe. Here also, deep acoustic liners were tested and these again show noise reduction over a wide frequency range.

At Rolls-Royce, research on combustor and combustor-turbine interaction is being carried out using the components of a Viper turbojet engine. The rig is illustrated in Fig.24 showing builds of the annular chamber both with and without the turbine.

The results for the combustor alone are shown in Fig.25. A prediction is shown for the jet noise created by the exhaust flow (using methods described in Section 2.1 above) indicating the additional noise contributed by the combustor. A discrete frequency source is indicated in this result in addition to the broadband noise, an example of combustor 'howl' referred to above. As the temperature is increased large increases in low frequency noise occur but the high frequency actually reduces. This experiment was performed at a constant corrected mass flow $\frac{M\sqrt{T}}{P}$ thus as T increases, the absolute

mass flow (M) reduces. It has been deduced from this behaviour observed over a wide range of tests that the high frequency noise is caused by the presence of the combustion chamber as a turbulence producer and is a function of the mass flow or velocity through it. It has been reported (39) that similar results have been observed in other noise experiments involving isolated combustion chambers.

The noise made by running the Viper combustor and turbine together is given in Fig.26. Although not shown here the effect of increasing the temperature was to increase the low frequency noise as observed with the combustor running alone. A comparison between the two sets of data is given in Fig.26 at the same corrected mass flow and combustor temperature rise. It is seen that the low frequency noise agrees well and might indicate that in the complete engine the low frequency is due directly to the combustion noise. It should be mentioned that no correction has been applied for the increased pressure in the combustor when running with the turbine, nor for attenuation of noise through the turbine. These effects are difficult to estimate but occur in opposite sense and may cancel each other to a large extent. The high frequency noise is attributable to the turbine, but there remains a large region of mid frequency noise whose source cannot immediately be identified. Possibilities for this are combustor-turbine interaction noise, or noise generated in the tailpipe by flow interaction with the exhaust strut.

The directivity of combustion noise is very similar to that of jet noise, peaking close to the jet axis (29, 30, 31).

The theory of combustion noise is still at an early stage although considerable effort has recently been carried out on the noise mechanisms due to laminar and turbulent premixed flames and to diffusion flames. The theory is not yet sufficiently well developed to be of immediate use to the gas turbine noise engineer since in general a detailed knowledge of the turbulent flow field is required to expedite the calculation and for real combustors this is not usually known. Thus the main outcome of the theoretical treatment is in the form of scaling laws.

A multitude of scaling laws may be found in the literature for simple flames, complete combustors, and for total exhaust noise on the assumption that this is entirely due to the combustor. The various theories and resultant scaling laws have been reviewed in recent papers (32, 33, 34).

It is sufficient to state here that, so far, no single theoretical or empirical function has been determined which draws together the results of combustors operating alone and within engines in a satisfactory manner. The most important requirement is an exhaust noise correlation and prediction scheme for the complete engine and a tentative procedure will be given later (Section 5).

4.2 Combustor - Turbine Interaction Noise

This source is now often referred to as 'indirect' combustion noise and arises from the propagation of temperature fluctuations from the combustion chamber through the turbine static and rotating blade rows. The interactions of these temperature fluctuations, which are convected by the flow, with the large pressure and velocity changes which occur in the turbine give rise to pressure waves which are transmitted through the exhaust system and radiate as noise. The theoretical model for this mechanism has been developed and published by Cumpsty and Marble (35, 36).

Pickett has also published a similar theory for the mechanism (37, 38). The main difference between the two methods is that the Cumpsty and Marble method allows for the detailed effects of wave reflection and transmission through each blade row, whereas that of Pickett ignores any interaction and for a multi-row machine simply sums the individual contributions from each row.

The formulation of both methods is such that the effects of fluctuations in velocity and pressure can also be dealt with, indeed in the case of the method of Cumpsty and Marble, this becomes necessary when more than one stage is considered because each blade row produces pressure and vorticity waves which in turn are affected by the other rows.

In order to calculate the acoustic power and spectrum output from an engine the input temperature fluctuation amplitude and spectrum are required. Pickett gives such information measured in a JT3D engine which indicates that values of the standard deviation of the temperature fluctuations expressed as a proportion of absolute temperature (σ/T) around 0.01 to 0.02 appear typical. However, these measured results appear to be open to interpretation, particularly in respect of the spectrum shape of the temperature fluctuation.

Cumpsty in Reference 36 shows calculations of acoustic power for a number of engines and compares them with the measured total exhaust noise. The two examples for the Spey and JT8D shown in Fig.27 and 28 indicate that the calculated results give reasonable agreement with the level and the trend of excess exhaust noise with engine condition, in this case indicated by the jet velocity.

Pickett in Reference 38 shows a similar calculation for the JT3D with, if anything, rather less acceptable agreement although the trend with engine power condition is again well established.

Although the acoustic spectrum can, to a certain extent be 'manipulated', the response of the turbine appears to be a maximum around a frequency of about 400 Hz which is close to the peak frequency commonly associated with the exhaust or core noise. Fig.29 taken from Reference 38 shows the predicted spectrum shape compared with measured data. In this comparison the absolute level of the prediction has been adjusted for a 'best fit'.

There are clear indications from these analyses that this 'indirect' combustion mechanism has many of the characteristics required to explain a significant proportion of the exhaust noise. No doubt future noise experimentation will address the problem of resolving the contribution from this source as distinct from direct combustor noise. However, since the direct combustor noise will be modified by its passage through the turbine, it may prove impossible to separate the two mechanisms completely.

4.3 Turbine Noise

Although the existence of turbine noise in the total engine noise signature was identified some considerable time ago (39), very little information has been published on the subject, mainly due to the available data being considered proprietary to each engine manufacturer. More recently some review papers and research results have been published as a result of the importance of the source becoming more widely recognised and reflecting the additional research activity in this field which has resulted (25, 26, 28, 30, 40, 41, 42).

Some of the essential features of turbine noise are indicated in the engine measurement on a Conway engine shown in Fig.30. These are the presence of discrete tones originating from each rotating blade row, sum and difference frequency tones and broadband noise. The sum and difference tones appear with multi-stage turbines producing tones at frequencies equal to $n_1 f_1 \pm n_2 f_2 \pm n_x f_x$ where f_1 to f_x are the fundamental frequencies of the individual stages and n_1 to n_x are integers where $n = 1$ is the fundamental. Also shown on this figure is the 'haystacking' of tones which is a broadening of the base of a tone due primarily to propagation of that tone through the turbulent exhaust jet.

Taking these features in turn and looking first at discrete tone noise, the mechanism of this source is reasonably well understood. It may arise from interaction with upstream turbulent flow, in which case it is usually referred to as a 'distortion' tone and is generated just as in the case of a fan (see Dr. Lowrie's lecture in the series for further details). The major source of tone noise in a turbine is due however to the interaction of stator wakes with the rotor, or rotor wakes with a downstream stator hence the name 'interaction' tones. Since rotor - stator axial gaps tend to be small (typically 0.4 of the blade chord or less) this source usually dominates and in some instances can be the dominant source in the total engine. Increasing rotor-stator gaps is a simple way of reducing tone noise but leads to long engines. An alternative approach as in the case of fans is to employ the correct ratio of stators to rotors to obtain acoustic 'cut-off' of the interaction tone. This again is described by Dr. Lowrie in connection with fans. The general theory of tone propagation and cut off is dealt with in detail by Tyler and Sofrin (43).

For rotor-stator spacing, various rules have been obtained by experiment and the change of tone noise with spacing tends to be within the range $10 \log (g/c)$ to $20 \log (g/c)$ where g is the axial gap and c is the upstream chord, i.e. a change of 3 to 6 dB for each doubling of the gap/chord ratio (39, 41).

The Spectral broadening of the tones referred to as 'haystacking' is a very interesting phenomenon and has attracted considerable attention (26, 28, 30, 40, 41, 42, 44). Fig.31 illustrates some of the variations which have been observed. Clearly this variability makes the determination of tone level rather difficult because it is no longer clear how much of the broadband energy to integrate into a representative tone level. The effect has been shown to be related to a number of things, for example the outlet swirl angle of the turbine which in turn was related to high levels of low frequency exhaust noise most probably caused by separation of the flow around the outlet struts (4, 40). The broadening has also been shown, in other experiments to be caused by propagation through the turbulent jet exhaust flow into the far field. In particular in a high bypass ratio engine, the effect is influenced markedly by the relative positions of the bypass and core jet nozzles (41, 42) as shown in Fig.32.

Another interesting feature of this 'haystacking' is illustrated in Fig.33. This is an asymmetric skewing of the tone with angle of the measurement, the sideband peak changing from one side of the blade passing frequency tone to the other. Similar effects have been observed in experiments where a discrete tone from a loudspeaker has been radiated through a nozzle shear layer (28, 44).

Turbine broadband noise is less well understood and is often difficult to identify precisely due to the presence of a multitude of discrete tones, particularly when these tones are 'haystacked'. It is generally considered to be of a high frequency, which may be demonstrated by cold flow model data (39) but when installed in the complete engine in the presence of other broadband sources, say from the combustor, it is extremely difficult to separate out precisely the broadband noise due only to the turbine. There is however no doubt that high frequency broadband noise sources from the turbine do exist, although the latest available review papers on turbine noise (41, 42) do not

consider this source in its own right and tend to leave the impression that the only high frequency broadband turbine source is the 'haystack' around the tone. The effects of core engine acoustic liners tested in a high bypass ratio engine have indicated the presence of significant high frequency broadband as well as tone noise. As with fans, it is thought that the main broadband sources are due to the regions of high aero-dynamic loss in the blading. Other sources may be due to the interaction with upstream turbulence, either from the combustor or from the wakes of other blade or vane rows.

The prediction of turbine noise is not well developed, and it is not possible to give here an up to date method which is considered satisfactory. Methods involving varying amounts of finesse or complication have been published (30, 39, 41) but as mentioned earlier, since turbine noise data is often considered proprietary, the latest most definitive prediction techniques developed by the industry are not yet published. A comparison and critique of the existing methods is given in Reference 42.

4.4 Strut and Obstruction Noise

Most engine exhaust systems have a system of struts which support the final shaft bearing and centre core or bullet. Sometimes these struts are also designed to remove residual swirl from the turbine exhaust flow. In general they are designed for minimum aerodynamic loss and low incidence at the engine design condition. At low power conditions, the flow incidence can be significantly different, possibly enough to cause flow separation around the struts. There is evidence to show that if separation does occur, very large increases in noise can result. An example of this for the model turbine shown in Fig.34 was published in Reference 4 and the experimental results are shown in Fig.35. The changes in noise in this instance could be related to the flow incidence angle onto the strut (Fig.36).

Bryce and Stevens (45) have published the results of a very thorough investigation of strut noise in a cold model of a turbojet exhaust system. Their model is illustrated in Fig.37 and typical results are given in Fig.38 showing the effect of increasing the swirl angle at fixed values of the exhaust jet velocity. The datum jet line on this figure is the noise of the model completely empty of centrebody, struts etc. In the test series it was also established that neither the swirler vanes, nor the centrebody were in themselves significant noise producers, leaving the struts and possibly nozzle based sources as the primary sources. Also the use of acoustic liners in the jet pipe confirmed that the noise above 1.25 kHz was internally generated, and correlation techniques produced evidence which strongly indicated that the noise at frequencies below 1.25 kHz was also generated internally. Bryce and Stevens concluded that the distinct change of spectrum shape at around 1.25 kHz was due to duct propagation and cut off effects. They found they could correlate the noise of the strut system against strut velocity and inlet swirl angle. Both inlet and outlet strut velocities were tried, the outlet being considered the most suitable. The correlations are shown in Figs.39 and 40.

Thus, in certain circumstances it seems clear the exhaust struts in an engine could be powerful noise generators although so far as the author is aware, they have not been positively identified as the major exhaust noise source in any current engines.

The work published so far specifically on a cascade of struts has not involved systematically varying the upstream turbulence. This is primarily because such experiments are difficult to conduct, most systems which generate turbulence also generate noise and thus it becomes difficult to separate the effects. Attempts have been made using single obstructions in a pipe with and without turbulent inflow (46) which showed that the noise of the obstruction alone was generally the most dominant source, the effect of additional upstream turbulence (created in this experiment by auxiliary jets) made little difference (Fig.41) if anything, the noise tended to reduce, probably because the turbulence destroyed the regular vortex shedding. Fig.41 clearly shows a reduction in the discrete frequencies. Results of further experiments on obstruction noise may be found in References 30, 46, 47, 48, 49.

There are usually no major obstructions in an engine exhaust unit other than the tailbearing struts, although notable exceptions do exist such as reheat flame stabilising gutters in supersonic turbojet engines. Also, from time to time, instrumentation rakes are mounted in the jet pipe and these have been known to create high noise levels. There are frequently obstructions in the form of aerofoil shaped support struts or service ducts in the bypass ducts of some engines. As a result, additional noise sources may be created, which can lead if not to a community noise problem, can certainly invalidate the results of definitive or diagnostic noise tests if not located and suppressed.

4.5 Exhaust Turbulence and Nozzle Based Sources

The possibility of the existence of strong nozzle based sources resulting from unsteady flow exhausting from a jet engine has been recognised for a long time (50). The simple approach to this is to postulate the existence of monopole sources due to unsteady mass discharge from the nozzle, and dipole sources resulting from the unsteady forces exerted on the walls of the nozzle. These sources are often referred to as 'lip noise'. The problem really arises in trying to distinguish these sources from those which are generated upstream of the nozzle and radiate from the nozzle exit, since these too can be represented theoretically by a combination of monopoles and dipoles placed at the nozzle exit. A number of experiments have been conducted with the object of identifying these sources but it has not yet proved possible to be certain that the process used to generate the turbulence is not the source of noise created rather than any additional mechanism caused by the resultant turbulence interacting with the nozzle (26, 46).

There is no shortage of theoretical studies which describe a wide range of possible mechanisms of exhaust noise which involve the transmission of turbulent flow through the nozzle and interaction

with the jet (50, 51, 52, 53). Further definitive experimentation is necessary to demonstrate the unambiguous existence of these nozzle based sources.

Recent experimentation has, however, revealed another extremely interesting and important mechanism involving the interaction of upstream noise and the jet structure. These experiments (27, 54, 55, 56), show that when a discrete frequency noise is introduced upstream of a nozzle operating at subsonic jet velocities, the jet noise may be amplified by up to 6dB over a wide frequency range and at all angles (55). In other words, the whole jet noise radiation is increased. In the initial experiments using plane wave excitation the amplitudes needed were high, completely dominating the radiated far field, and unrepresentative of real engine situations. However, later experiments using higher order modes which are still below the pipe cut-off have shown that considerable amplification can be obtained with discrete tone excitations which, in terms of the far field level, are more typical of real engines as shown in Fig.42, which is taken from Reference 55. Independent work at Rolls-Royce (56) has confirmed these results as indicated by the result shown in Fig.43. Preliminary experiments also indicate that these amplification effects may be obtained with broadband excitation or turbulence although with broadband sources it is clearly much more difficult to be sure of distinguishing the individual effects. The important result from these experiments is that the whole jet noise radiation is amplified, there being no particular spectral or radiation characteristics which enable the amplified source to be distinguished from the unamplified source. This could explain why considerable noise variations have been obtained from model jet rigs which are nominally free of upstream noise or other disturbances. It could also constitute a major source of 'excess' exhaust noise, which is of course intimately associated with the other sources present such as fan, turbine and combustion noise.

Clearly these recent experiments have opened a new era in the study of exhaust noise.

5. PREDICTION OF OVERALL EXHAUST NOISE

It is abundantly clear from the preceding section that our knowledge of exhaust noise mechanisms is far from complete, and that no single mechanism has been found to account for all the observed exhaust noise effects. More likely, there will be a few dominant mechanisms and each engine will have its own characteristic 'mix' of these. Thus to think in terms of a generalised prediction method is perhaps being rather optimistic. During the development of our knowledge of exhaust noise, various prediction procedures have been proposed, the earliest being based on jet exhaust velocity (4, 5). More recently, the combustor has been considered as the major contributor and a host of methods have been published. These have been conveniently reviewed in two recent papers (32, 34) and for a full history the reader is referred to these. These methods are invariably empirical using a combination of flow parameters relevant to the combustor and the turbine such as combustor temperature rise, mass flow, combustor discharge velocity, fuel air ratio etc.

It may well transpire that these methods are attempting to describe empirically the noise described as 'indirect' combustion noise in Section 4.2. This 'indirect' combustion noise of course can be calculated provided the fluctuations in combustor exit temperature are known. Clearly this information will only be known in some very specific instances for engines that already exist. For new engine projects, some empiricism is therefore necessary.

The latest 'generalised' method available is one recently submitted by the General Electric Co. to the SAE A21 Jet Noise Subcommittee for evaluation (57). This method predicts the mid frequency (~ 400 Hz) noise source for a range of turbojets, turbofans and turboshaft engines and is based on work previously published (29, 30, 34) for combustor noise together with a parameter which describes the different amounts of turbine work extracted in these different types of engines. Additional data from Rolls-Royce engines has been shown to agree well with the method as shown in Fig.44.

To use the method, the peak $\frac{1}{3}$ octave SPL is obtained from Fig.44 where

OAPWL = overall sound power level (watts re 10^{-13})

\dot{W} = mass flow in lb/sec.

T = total temperature in $^{\circ}\text{Rankine}$

ρ = density

Station 0 = ambient

3 = combustor inlet

4 = combustor exit

5 = low pressure turbine exit

and $\Delta T = T_4 - T_5$ at the engine design condition

The spectrum shape and directivity are empirical in nature. The recommended spectrum shape is given in Fig.45, and the directivity in Fig.46.

The SPL = PWL - 20 log R + DI - AA - 9.3

where R is the radius in feet

DI is the directivity index (Fig.46)

AA is the air attenuation.

This method appears to correlate satisfactorily the OAPWL from a wide range of engines. The scatter of spectral data and directivity is much larger (see Reference 57) and will hopefully be further refined before publication as an SAE recommended method. In its present form however, it is probably the best method which is generally available at this time.

6. IN FLIGHT EFFECTS ON JET AND CORE NOISE

Dr. Fisher in the previous lecture has introduced the static to flight dilemma that has recently become evident from comparisons of real aircraft flyover data with data obtained from model jets tested under forward speed conditions in wind tunnels or large area ratio coaxial jet rigs.

The discrepancy between these sets of data is illustrated by typical static and flight field shapes of the OASPL from a pure turbojet engine, the Viper shown in Fig.47 and a low bypass ratio engine, the Spey 512 in Fig.48. These show that although near to the jet axis a large reduction is obtained in going from static to flight, there is virtually no change around the 90° angle and an increase in absolute noise level in the forward arc (58). The results from simple models tested in a wind tunnel (59) are shown in Fig.49 and in a coaxial rig (60) in Fig.50. In the model experiments there is a clear reduction with forward speed at 90° and in both data sets, and where data is available, a reduction is also shown in the forward arc. The field shapes shown in Fig.50 from the coaxial rig require a small correction due to the passage of the sound through the shear layer; but after correction there is still a reduction in the forward arc noise, in contradiction to the full scale flight data.

A useful way of summarising this behaviour is to establish a flight velocity index (m) as a function of angle according to:-

$$OASPL_{static} - OASPL_{flight} = 10 \log_{10} \left[\left(\frac{V_j}{V_{rel}} \right)^m (1 - M_a \cos \theta) \right]$$

where V_j = jet velocity

V_{rel} = $V_j - V_{Aircraft}$

M_a = Aircraft Mach No.

θ = Angle to intake axis

The aircraft data from (58) and model data from (59) are shown in Fig.51.

Since the publication of references 59 and 60 other work has confirmed the results for models (61, 62). It has been established that the index m from the model tests is a function of the area ratio of the coaxial rig used to simulate flight, the ultimate being a large wind tunnel with the measuring microphone installed actually in the tunnel stream (Fig.52).

Further more definitive aircraft data has also become available, for example for the Viper engine in the Provost aircraft and flown at two forward speeds, Fig.53. These results confirm the increase of noise in the forward arc and show a small reduction at 90° .

Data obtained on the Bertin Aerotraine which is a land based moving vehicle propelled by a turbojet engine (61) shows very similar results to those obtained in flight except that for subsonic jet velocities there was no measurable increase in the forward arc. For supersonic jet velocities with a conical nozzle there was significant amplification in the forward arc, it being clearly associated with the presence of shock cell noise at these angles. An excellent description of the Bertin Aerotraine, its method of operation and the results obtained with it are to be found in references 63 and 64.

The conclusions of reference 63 are that the observed discrepancy between models and full scale data may be due to five main phenomena, likely to be strongly coupled. These are:-

- (a) the radiation of nozzle-based sources induced by internal or external aerodynamic perturbations of the nozzle flow that might compete with jet mixing in the forward arc,
- (b) The jet coherent structures that might radiate sound in the forward arc and/or impede in one way or another the relative velocity effect,
- (c) the parametric amplification of jet noise by initial flow turbulence and internal noise that makes jet mixing sound noisier than it should according to model jet noise predictions,
- (d) the noise induced by residual swirl and that radiated by the initial flow turbulence that unreported aerodynamic measurements have shown to be very high on a jet engine and that probably alters the jet mixing process,
- (e) the ingestion of external turbulence that should also affect the jet mixing process.

•

10

10

1

1

- Handwritten text, likely a signature or name, written vertically.

8. SAE A21 Committee Proposed ARP 876
Gas Turbine Jet Exhaust Noise
(a) Prediction July 1975
 (Circulated to SAE Committee Members)
 Revised:-
(b) Coaxial jet added Nov. 1975
(c) Later revision July 1976

9. P.A. Lush Measurements of Subsonic Jet Noise and Comparison with Theory
J. Fluid Mech. 46 477-500 (1971)

10. K.K. Ahuja An Experimental Study of Subsonic Jet Noise and Comparison with
K.W. Bushell Theory
J. Sound and Vibration (1973) 30 (3) 317-341

11. B.J. Cocking The Effect of Temperature on Subsonic Jet Noise
ARC R & M 3771 1975
(Supersedes NGTE R 331 1974)

12. A. Powell A Schlieren Study of Small Scale Air Jets and some Noise
Measurements on Two-inch Diameter Air Jets
ARC Paper 14726 (1951)

13. C.D. Simcox A Status Report on Jet Noise Suppression as seen by an aircraft
W.C. Swan manufacturer
AIAA Paper 73-816 Aug.1973

14. R.G. Hoch Studies of the Influence of Density on Jet Noise
J.P. Duponchel J. Sound and Vibration Vol.28 No.4 1973
B.J. Cocking
W.D. Bryce

15. H.K. Tanna Effect of Temperature on Supersonic Jet Noise
M.J. Fisher AIAA Paper 73-991 Oct.1973
P.D. Dean

16. J.P. Raney New Computer System for Aircraft Noise Prediction
W.E. Zorumski Inter Noise 74 Proceeding p183-186

17. J.P. Raney An overview of NASA's Aircraft Noise Prediction Program
AIAA 75-536 March 1975

18. J.M. Tyler Jet Engine Noise and its Control AGARD Lecture Series 77
'Aircraft Noise Generation, Emission and Reduction'
June 1975

19. B.J. Cocking An Experimental Study of Coaxial Jet Noise
NGTE Report R 333 1974

20. G.W. Bielak Coaxial Flow Jet Noise
Boeing/Aeritalia Document D6E-10041-1 April 1971

21. W.A. Olsen Jet Noise from Coaxial Nozzles over a wide range of Geometric
R. Friedman and Flow Parameters
AIAA Paper 74-43 Jan.1974

22. M. Harper-Bourne The Noise from Shock Waves in Supersonic Jets
M.J. Fisher AGARD Conf. Proc. CP-131
'Noise Mechanisms' Sept.1973

23. - Acoustic Effects Produced by a Reflecting Plane
SAE AIR 1327 Jan.1976

24. W.L. Howes Ground Reflection of Jet Noise
NASA Tech. Report R 35, 1959

25. R.G. Hoch Recent Studies into Concorde Noise Reduction
R. Hawkins AGARD CP - 131 - 'Noise Mechanisms' Sept.1973

26. D.C. Matthews Progress in Core Engine and Turbine Noise Technology
A.A. Peracchio AIAA Paper 74-948 Aug.1974

27. R.P. Gerend
H.P. Kumasaka
J.P. Roundhill
Core Engine Noise
AIAA Paper 73-1027 Oct.1973
28. R.G. Hoch
P. Thomas
E. Weiss
An Experimental Investigation of the Core Engine Noise of a Turbofan Engine
AIAA Paper 75-526 March 1975
29. S.B. Kazin
J.J. Emmerling
Low Frequency Core Engine Noise
ASME Paper 74-WA/Aero 2 Nov.1974
30.
Core Engine Noise Control Program. Final Report
FAA-RD-74-125 Aug.1974
31. R.P. Gerend
B.N. Shivashankara
Compact Combustion Noise Suppressor
AIAA Paper 76-42 Jan.1976
32. R.G. Huff
B.J. Clark
R.G. Dorsch
Interim Prediction Method for Low Frequency Core Engine Noise
NASA TMX-71627 Nov.1974
33. W.C. Strahle
A Review of Combustion Generated Noise
AIAA Paper 73-1023 Oct.1973
34. R.E. Motsinger
J.J. Emmerling
Review of Theory and Methods for Combustion Noise Prediction
AIAA Paper 75-541 March 1975
35. N.A. Cumpsty
F.E. Marble
The Generation of Noise by the Fluctuations of Gas Temperature into a Turbine
Cambridge University Engineering Department Report CUED/A Turbo/TR57 1974
36. N.A. Cumpsty
Excess Noise from Gas Turbine Exhausts
ASME Paper 75-GT-61 March 1975
37. G.F. Pickett
Turbine Noise due to Turbulence and Temperature Fluctuations
Pres. at 8th Int. Congress on Acoustics London July 1974
38. G.F. Pickett
Core Engine Noise due to Temperature Fluctuations Convecting through Turbine Blade Rows
AIAA Paper 75-528 March 1975
39. M.J.T. Smith
K.W. Bushell
Turbine Noise - Its Significance in the Civil Aircraft Noise Problem
ASME Paper 69-WA/GT-12 Nov.1969
40. J.S. Fletcher
P.H. Smith
The Noise Behaviour of Aero Engine Turbine Tones
AIAA Paper 75-466 March 1975
41. S.B. Kazin
R.K. Matta
Turbine Noise Generation, Reduction and Prediction
AIAA Paper 75-449 March 1975
42. D.C. Mathews
R T. Nagel
J.D. Kester
Review of Theory and Methods for Turbine Noise Prediction
AIAA Paper 75-540 March 1975
43. J.M. Tyler
T.G. Sofrin
Axial Flow Compressor Noise Studies
SAE Transactions Vol.73 309-332 1962
44. S.M. Candel
M. Jullian
A. Julienne
Shielding and Scattering by a Jet Flow
AIAA Paper 76-545 July 1976
45. W.D. Bryce
R.C.K. Stevens
An investigation of the noise from a scale model of an Engine Exhaust System
AIAA Paper 75-459 - March 1975

46. K.K. Ahiya
An Experimental Study of Subsonic Jet Noise with particular reference to the Effects of Upstream Disturbances
M. Phil Thesis University of London June 1972
47. C.G. Gordon
G. Maidanik
Influence of Upstream Flow Discontinuities on the Acoustic Power Radiated by a Model Air Jet
NASA CR-679 Jan.1967
48. H.H. Heller
S.E. Widnall
C.G. Gordon
Correlation of Fluctuating Forces with the Sound Radiation from Rigid Flow Spoilers
NASA CR-1340 1969
49. T.M. Tower
et al
Noise Generation by Cylindrical Spoilers Immersed in an Air Duct
Aero and Mech. Sciences Report 1092 Princeton Univ. NJ
50. J.E. Ffowcs-Williams
C.G. Gordon
Noise of Highly Turbulent Jets at Low Exhaust Speeds
AIAA Journal Vol.3 No.4 April 1965
51. J.E. Ffowcs-Williams
et al
Papers on Novel Aerodynamic Noise Source Mechanisms at Low Jet Speeds
ARC Current Paper 1195 1972
52. D.G. Crighton
Mechanisms of Excess Jet Noise
AGARD Conf. Proc. 131 1973
53. J.R. Jacques
The Acoustic Response of a Nozzle Flow to an Externally Applied Low Frequency Pressure Field
J. Sound and Vibration 41 Pt.1 1975
54. D. Bechert
E. Pfizenmaier
On the Amplification of Broadband Jet Noise by a Pure Tone Excitation
J. Sound and Vibration (1975) 43 (3) 581-587
55. D. Bechert
E. Pfizenmaier
On the Amplification of Broadband Jet Noise by a Pure Tone Excitation
AIAA Paper 76-489 July 1976
56. C.J. Moore
Unpublished work at Rolls-Royce (to be published)
57. R. Matta
Core Noise Prediction Communication to SAE A-21 Jet Noise Subcommittee May 1976
See also:-
Core Engine Noise Control Program
Final Reports Vol.III Supplement I
FAA RD-74-125, III-I March 1976
58. K.W. Bushell
Measurement and Prediction of Jet Noise in Flight
AIAA Paper 75-461 March 1975
59. B.J. Cocking
W.D. Bryce
Subsonic Jet Noise in Flight Based on some Recent Wind Tunnel Results
AIAA Paper 75-462 March 1975
60. U. von Glahn
D. Groesbeck
J. Goodykoontz
Velocity Decay and Acoustic Characteristics of various Nozzle Geometries in Forward Flight
AIAA Paper 73-629 July 1973
61. A.B. Packman
K.W. Ng
R.W. Paterson
Effect of Simulated Forward Speed on Subsonic Jet Exhaust Noise
AIAA Paper 75-869 1975
62. H. Plumblee
H.K. Tanna
In flight Simulation Experiments on Jet Noise with particular reference to the correspondence between Acoustic and Turbulence Measurements
Workshop on the Effects of Forward Velocity on Jet Noise
NASA Langley Research Centre, Hampton January 1976
63. P. Drevet
J.P. Duponchel
J.R. Jacques
Effect of Flight on the Noise from a convergent Nozzle as observed on the Bertin Aerotrain
AIAA Paper 76-557 July 1976

64. R. Hoch
M. Berthelot Use of the Bertin Aerotraine for the Investigation of Flight
Effects on Aircraft Engine Exhaust Noise
AIAA Paper 76-534 July 1976
65. - DC 9 Flight Demonstration Program with Refanned JT8D
Engines
Final Report NASA CR-134860 July 1975
66. J.R. Stone On the Effects of Flight on Jet Engine Exhaust Noise
NASA TMX-71819 Nov.1975

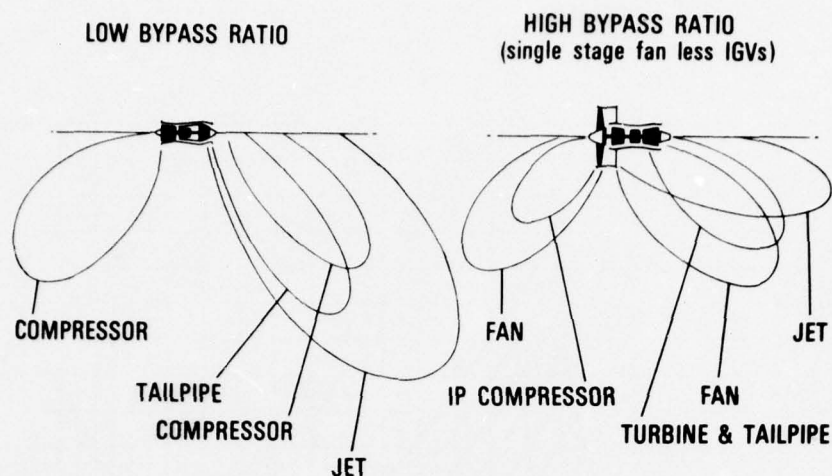


Fig.1 Component Noise Sources of Low and High Bypass Ratio Engines

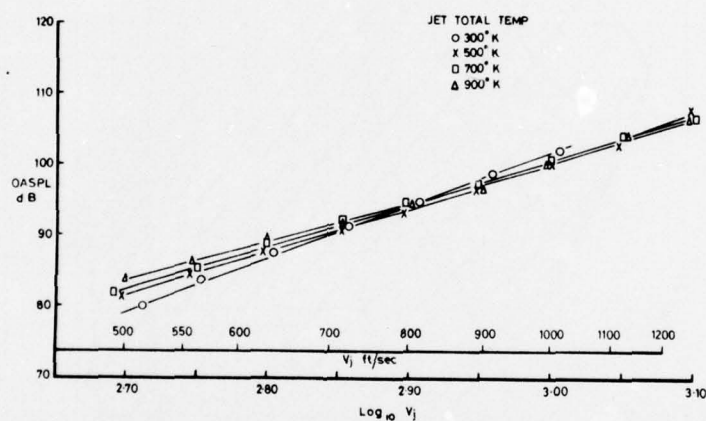


Fig.2 Effect of Temperature on Jet Noise at 90° to Axis
(from Ref 11)

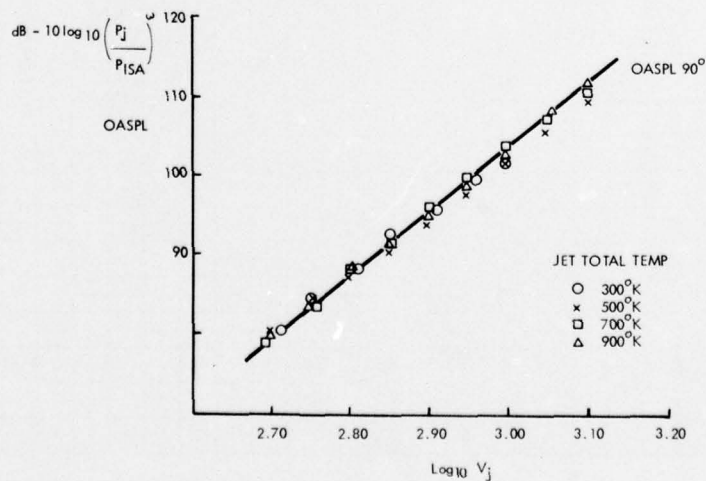


Fig.3 Jet Noise Normalised for Jet Density
(from Ref 11)

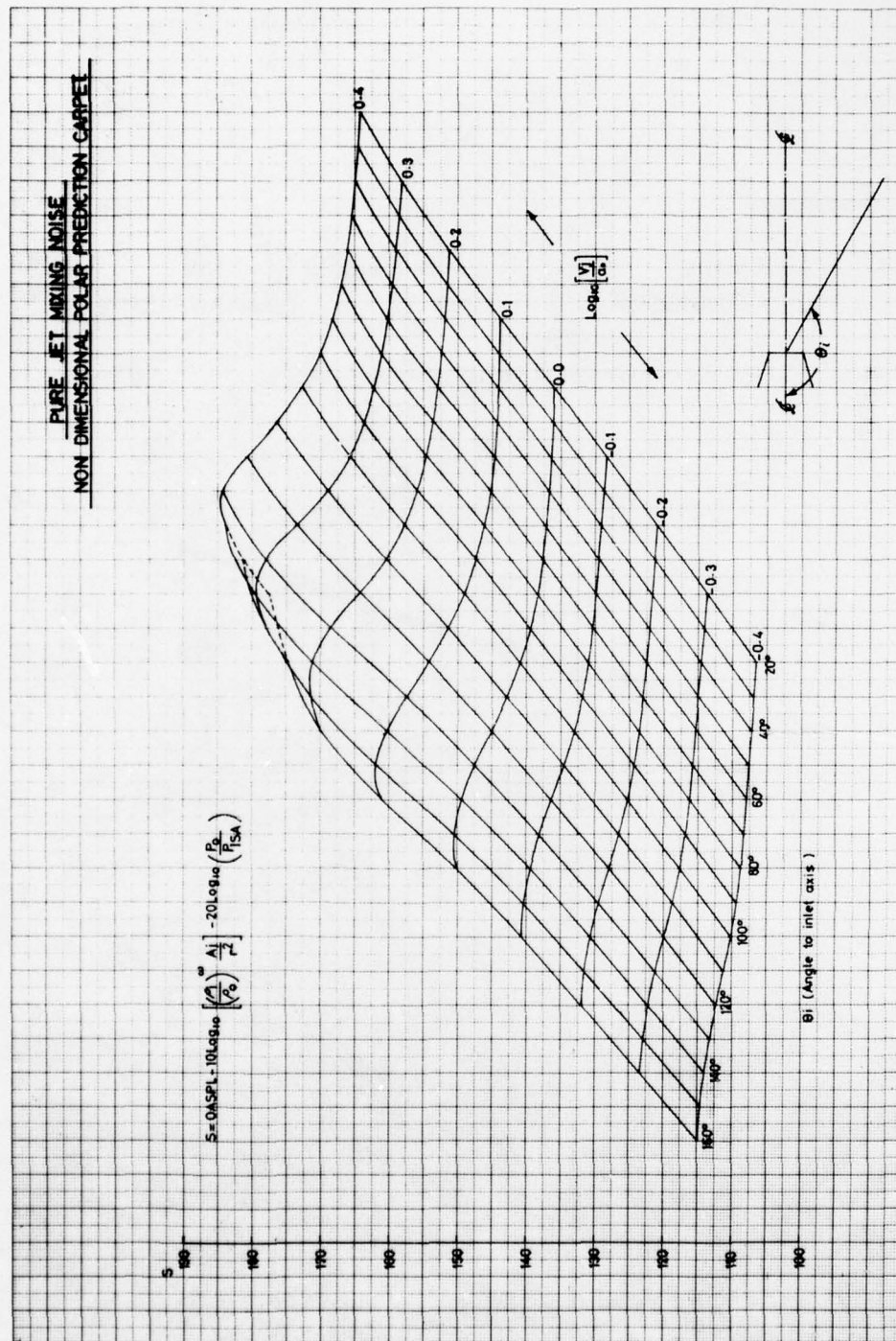


Fig. 4
Pure Jet Mixing Noise - Non-Dimensional Carpet
SAE Proposed Method (from Ref 8)

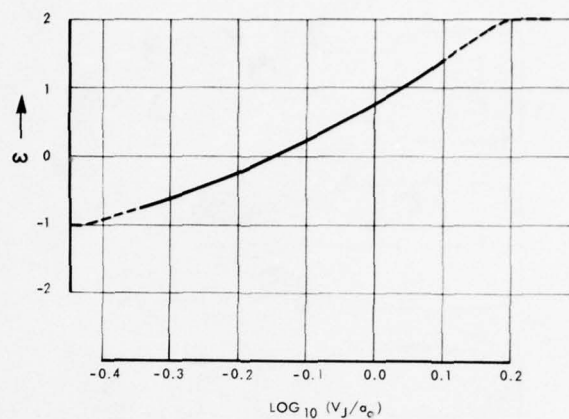


Fig.5 Variable Density Index as a function of Jet Velocity
(from Ref 8)

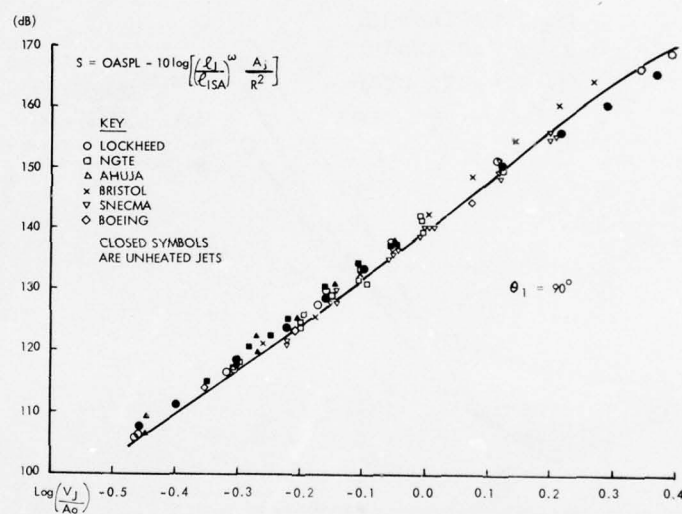


Fig.6 Comparison of Jet Noise data used to compile
SAE Prediction Procedure

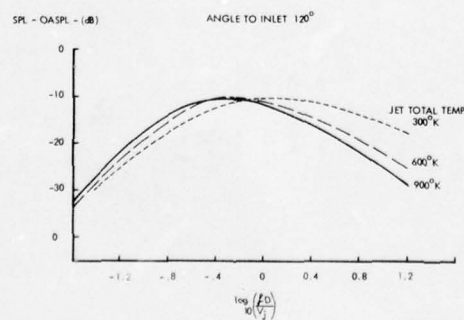


Fig.7 Effect of Temperature on Jet
Noise Spectra
(from Ref.8)

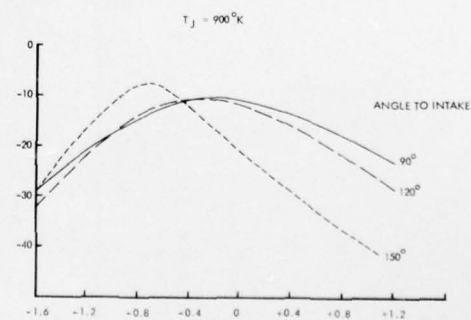


Fig.8 Effect of Angle on Hot
Jet Noise Spectra
(from Ref.8)

Fig.9

Variations in Coaxial
Jet Configurations
in Modern Engines

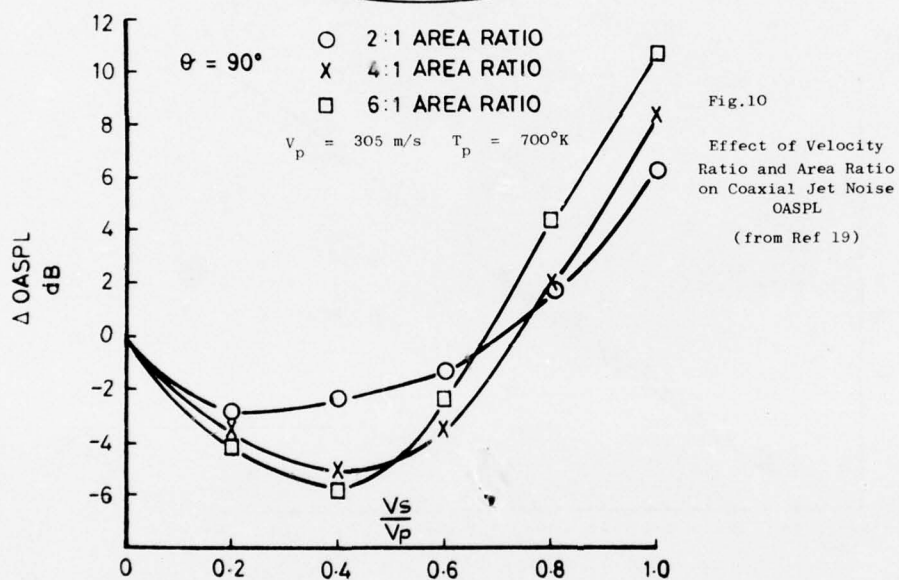
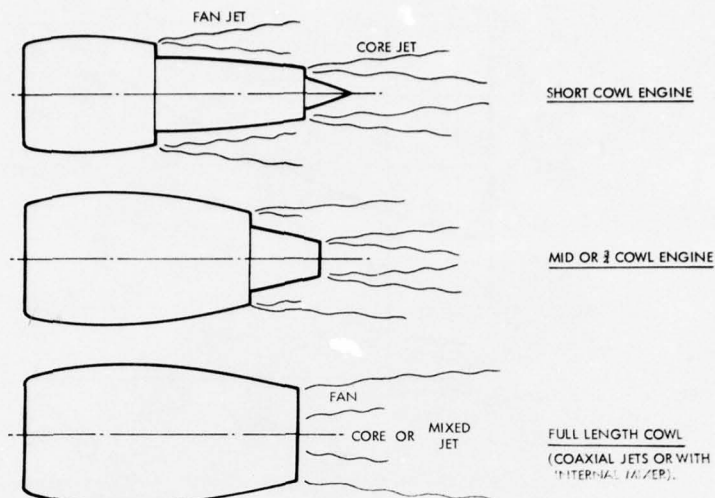
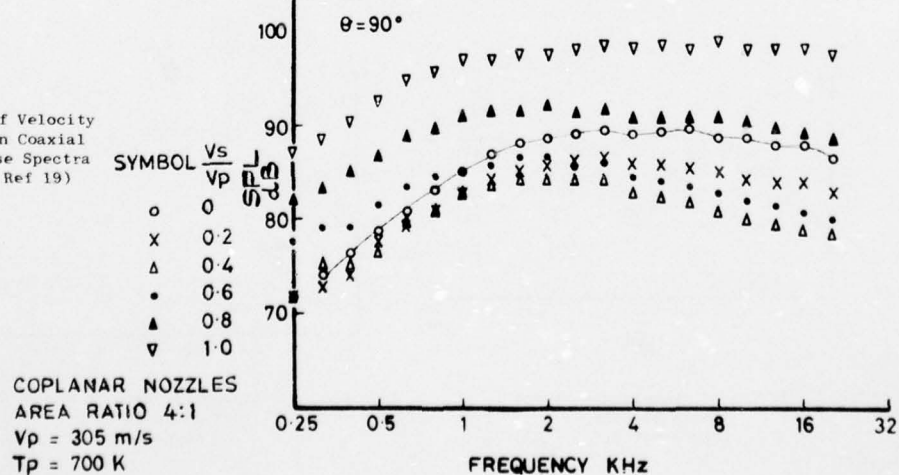


Fig.11

Effect of Velocity
Ratio on Coaxial
Jet Noise Spectra
(from Ref 19)



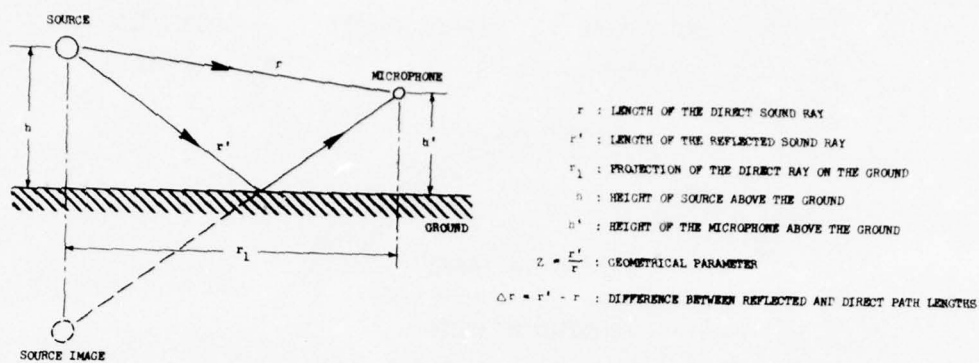


Fig.12

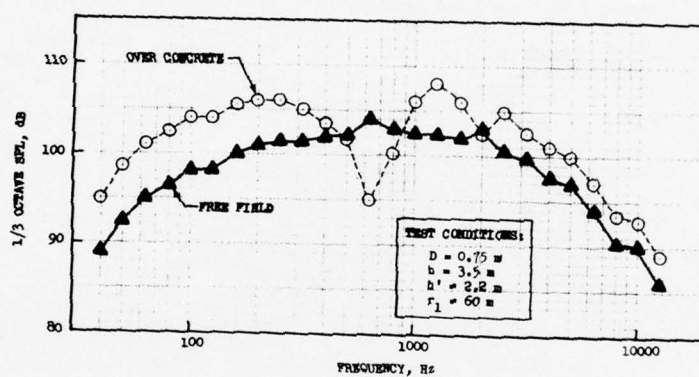
 Geometry of Source
 Receiver and Reflecting Surface
 (from Ref 23)


Fig.13

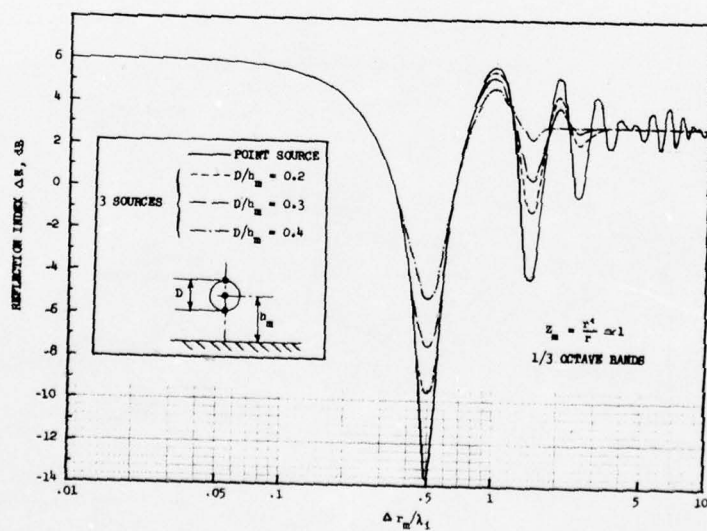
 Engine Measurement over Concrete
 Corrected to Free Field
 (from Ref 23)


Fig.14

 Theoretical Ground Reflection
 Index for Perfect Reflecting Surface
 (from Ref 23)

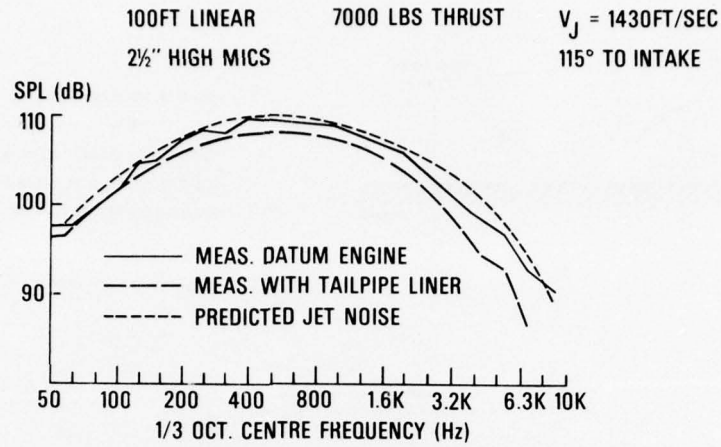


Fig.15

Example of Rolls-Royce Spey Rear Arc Noise at High Thrust showing effect of Tailpipe Liner and Comparison with predicted Jet Noise

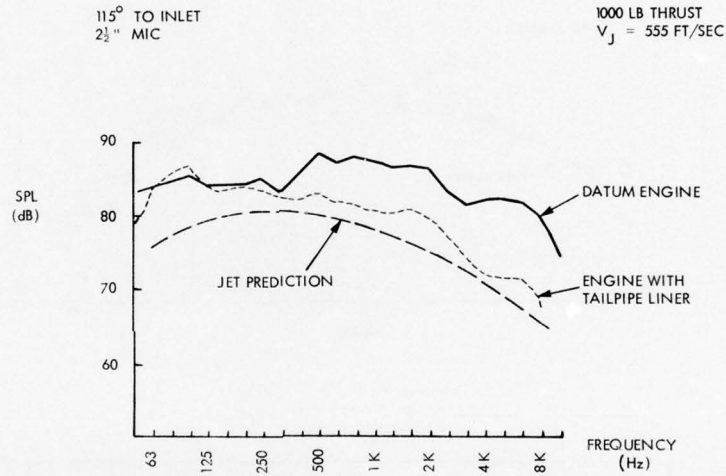


Fig.16

As Fig.15 but at very low thrust

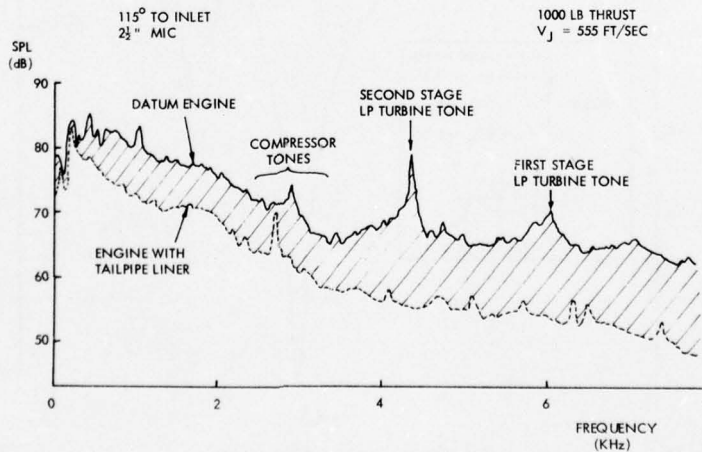


Fig.17

Narrow Band Analysis of Rolls-Royce Spey Rear Arc Noise showing Component Sources and Effect of Tailpipe Liner

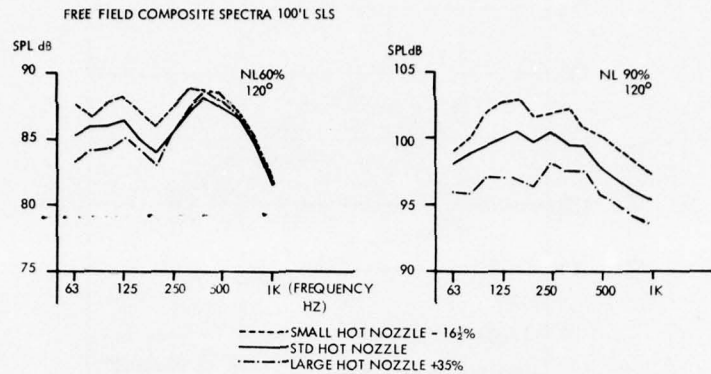


Fig.18 Effect of Core Nozzle size on Exhaust Noise of Rolls-Royce RB 211 High Bypass Ratio Engine

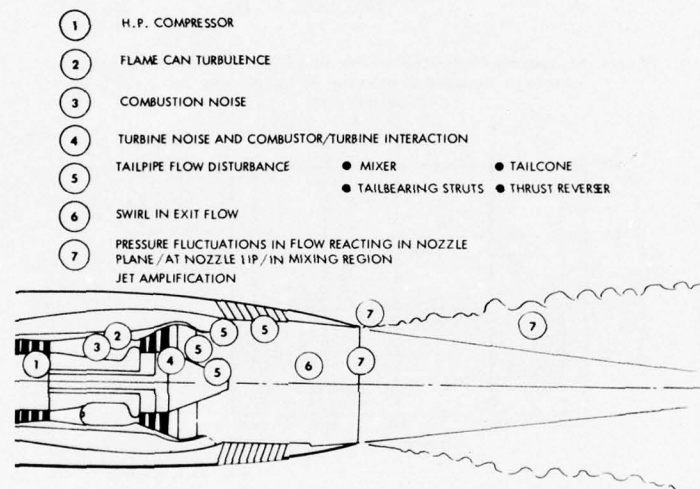


Fig.19 Some possible Tailpipe Noise Sources

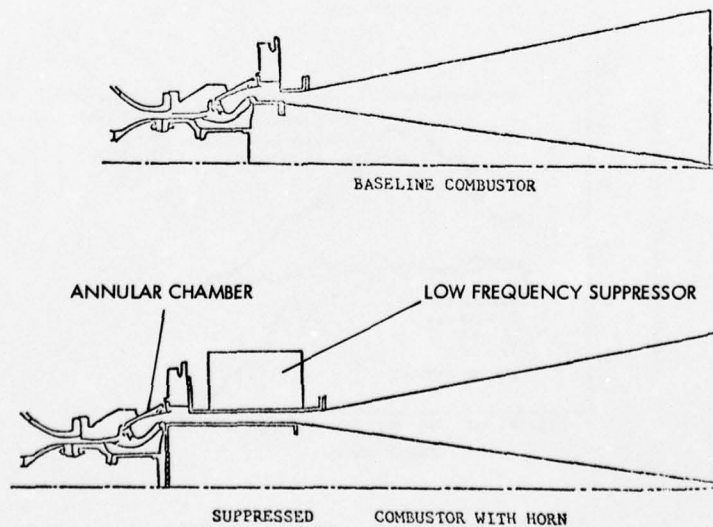


Fig.20 Full Scale General Electric Annular Combustion System tested in isolation (from Ref.30)

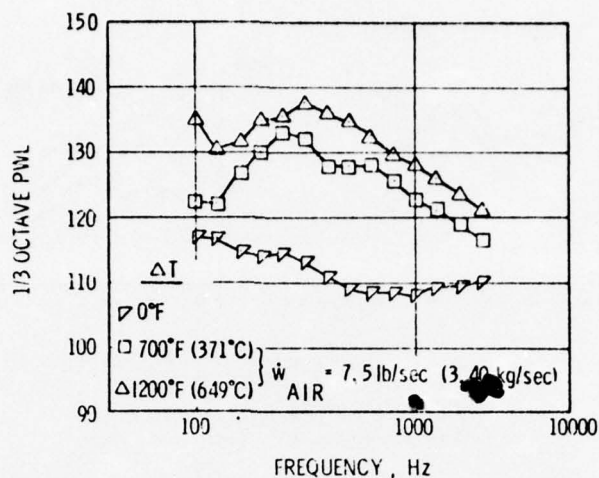


Fig.21 Effect of Temperature Rise on Noise of the Fullscale General Electric Annular Combustor shown in Fig.20 (from Ref.29)

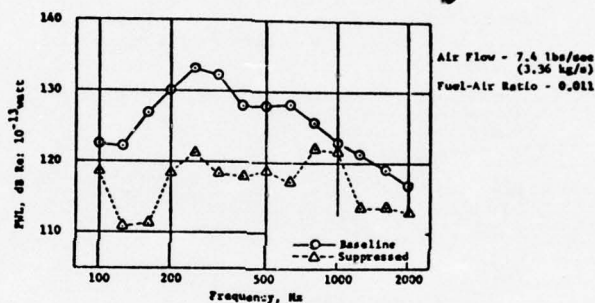


Fig.22 Effect of Deep Resonator Suppressor on the Combustor of Fig.20 (from Ref.30)

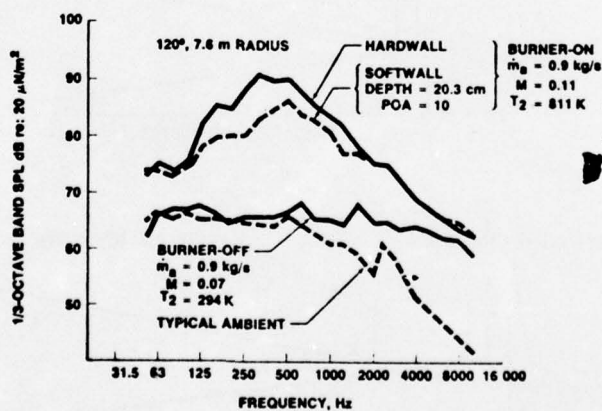


Fig.23 Combustor Noise from a Single Can Combustor and the effect of Noise Suppressor (from Ref.31)

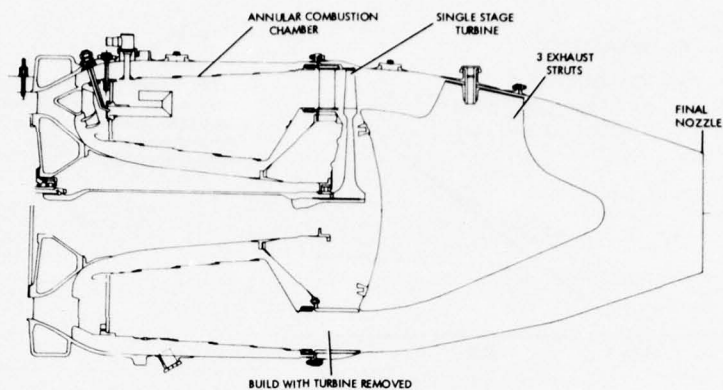


Fig. 24 Rolls-Royce Viper Annular Combustion Rig - with and without Turbine

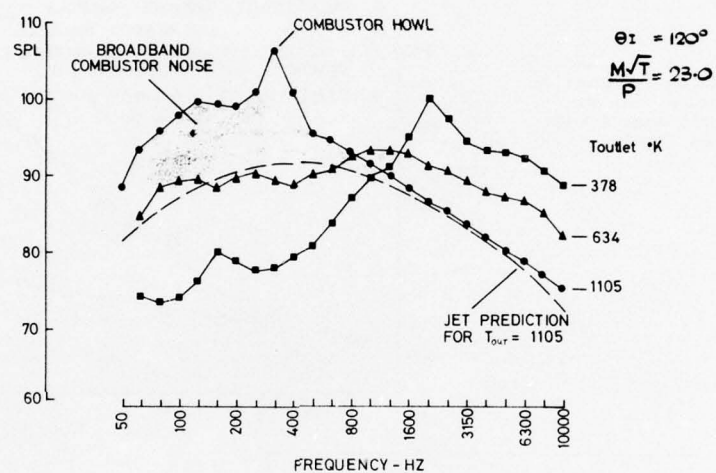


Fig. 25 Effect of Temperature Rise on Rolls-Royce Viper Combustion Noise (No Turbine)

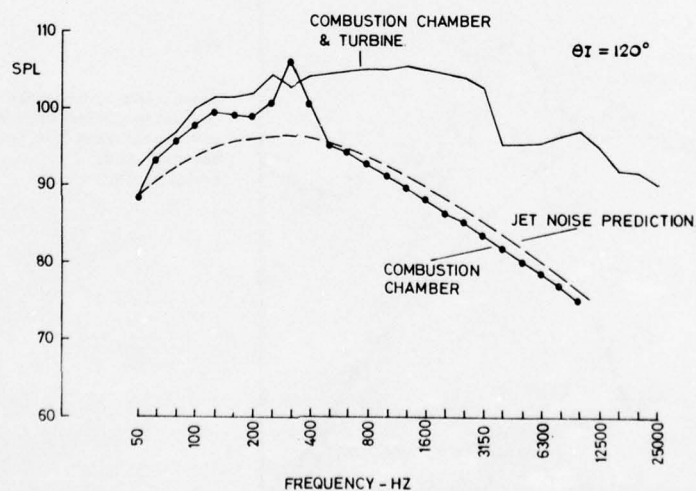


Fig. 26 Influence of Combustion Noise on Total Viper Exhaust Noise (with Turbine and Exhaust Unit)

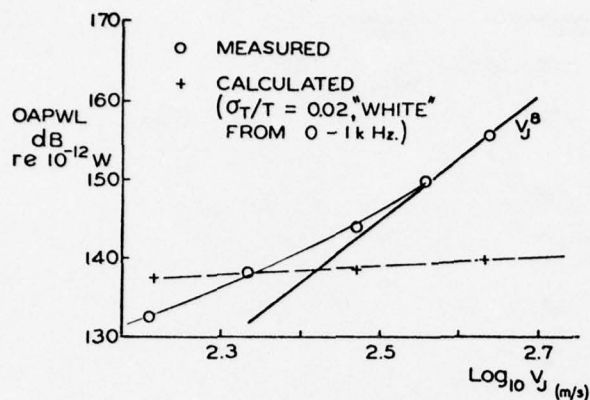


Fig. 27

Predicted "Indirect" Combustion Noise and measured Rear Arc overall Acoustic Power for the Rolls-Royce Spey 512.
(From Ref. 36)

Fig. 28

Predicted "Indirect" Combustion Noise and measured Rear Arc overall Acoustic Power for the Pratt & Whitney JT8D-9.
(From Ref. 36)

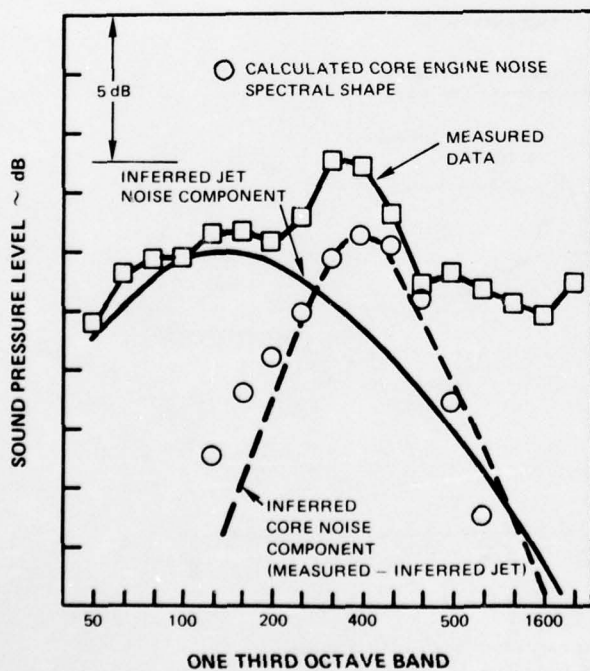
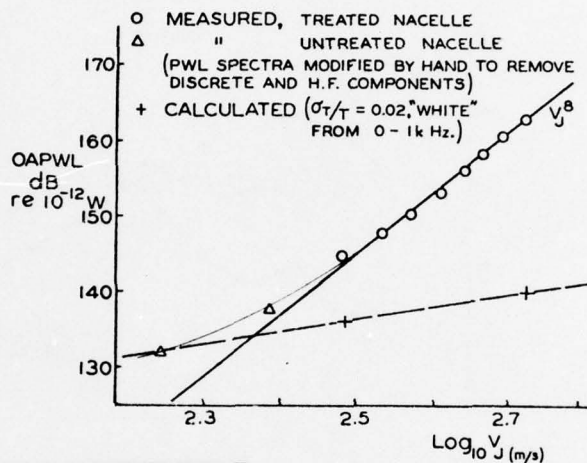


Fig. 29

Comparison of predicted "Indirect" Combustion Noise Spectrum shape and measurement for the Pratt & Whitney JT3D.
(From Ref. 38)

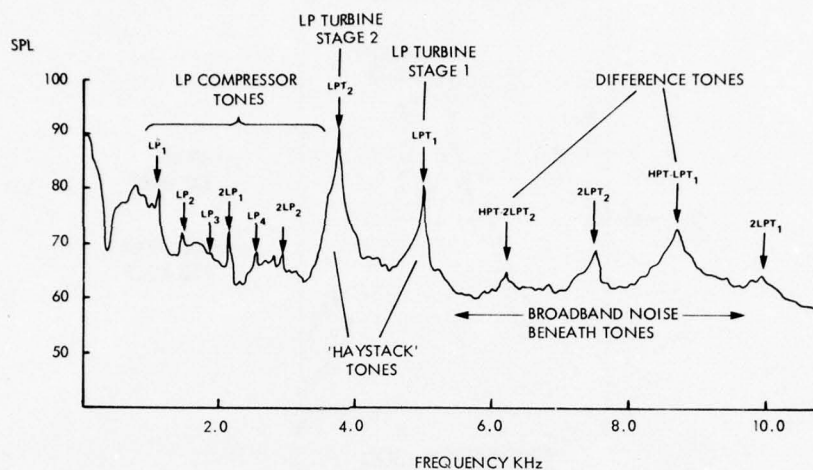


Fig.30

General characteristics of Turbine Noise
Demonstrated by Narrow Band Analysis of
the Rolls-Royce Conway Rear Arc Noise

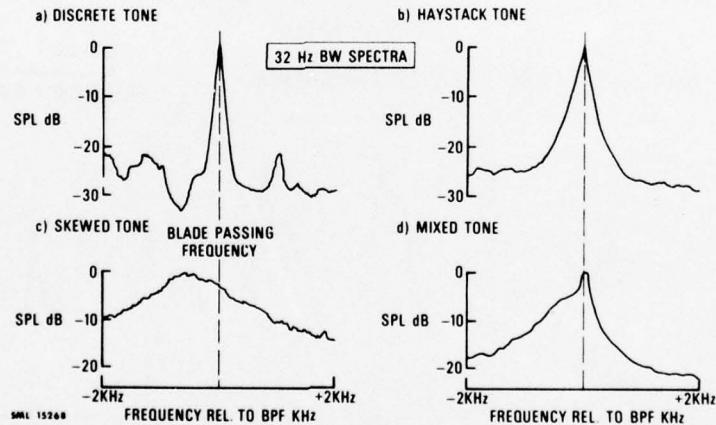


Fig.31

Illustrations of Typical Turbine
Tone Types
(From Ref.40)

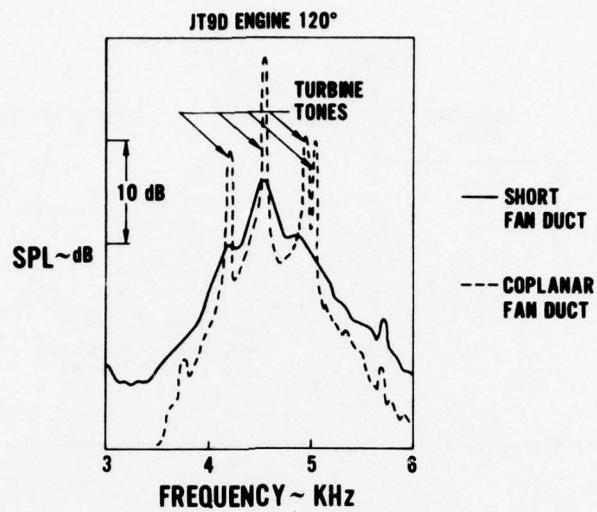


Fig.32

Effects of Fan Duct Configuration
on Turbine Noise
(From Ref.26)

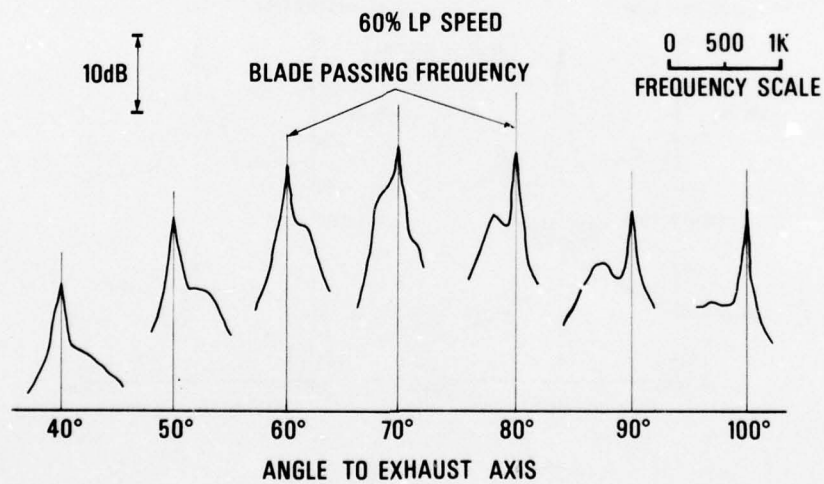


Fig.33

Demonstration of Turbine Tone Skewing
from the Rolls-Royce Conway
(From Ref. 40)

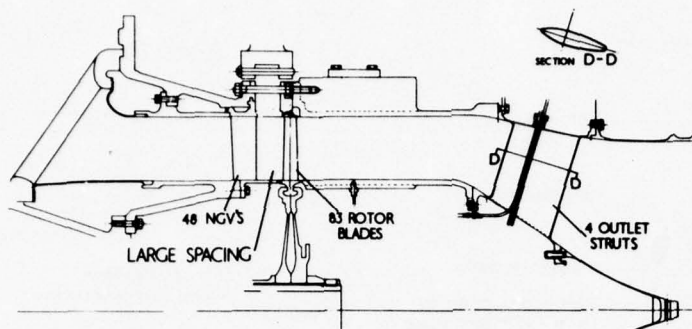
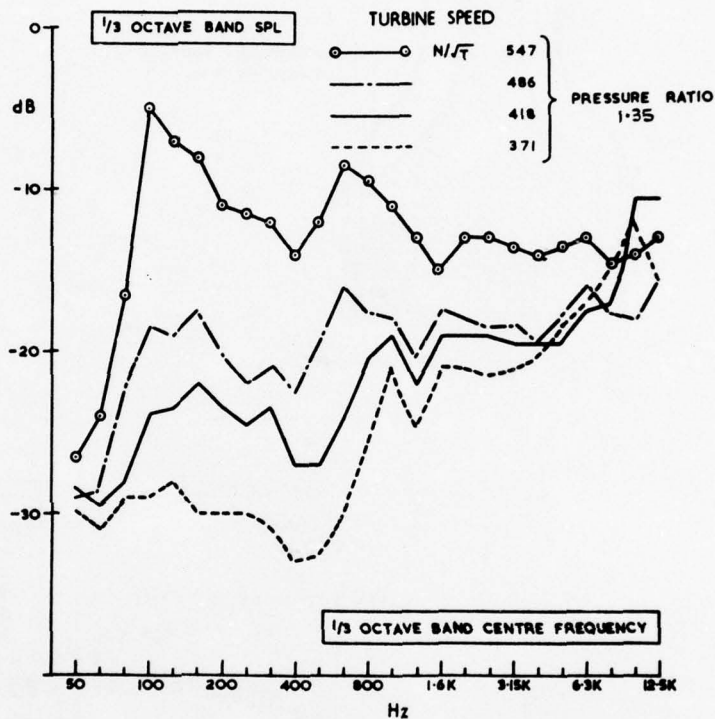


Fig. 34

General Arrangement of
Rolls-Royce Cold Flow
Research Turbine

Fig. 35

Change of Exhaust Noise
with Turbine Speed from
Turbine shown in Fig. 34.



CONSTANT PRESSURE
RATIO PR = 1.35

VARYING N/\sqrt{T}

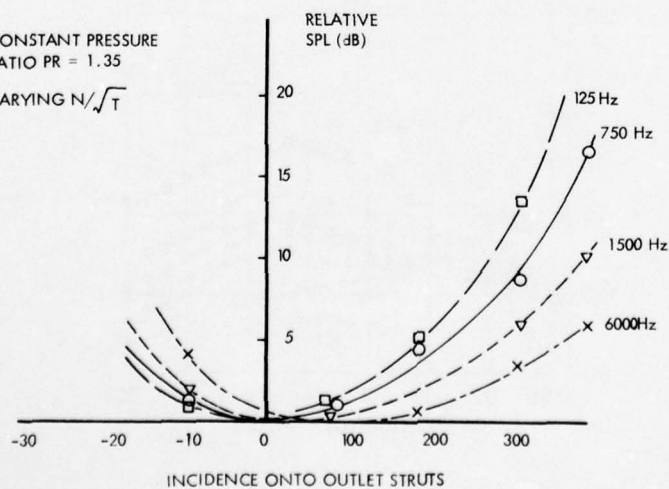


Fig. 36

Correlation of Noise and
Strut Incidence on the
Turbine shown in Fig. 34.

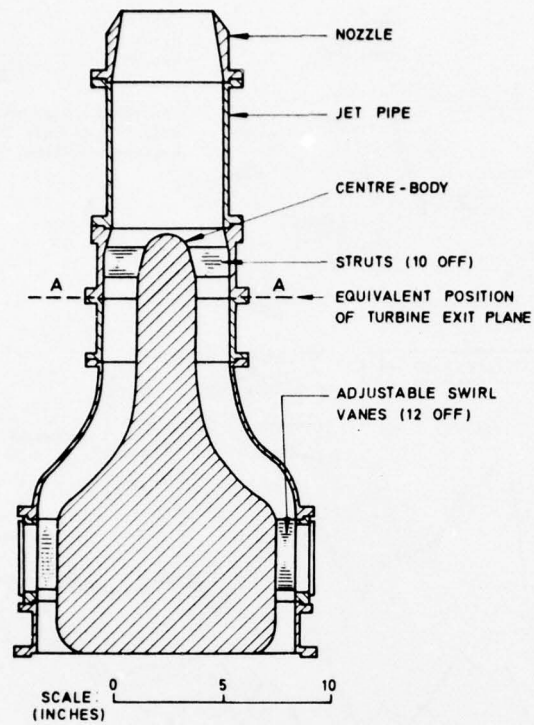
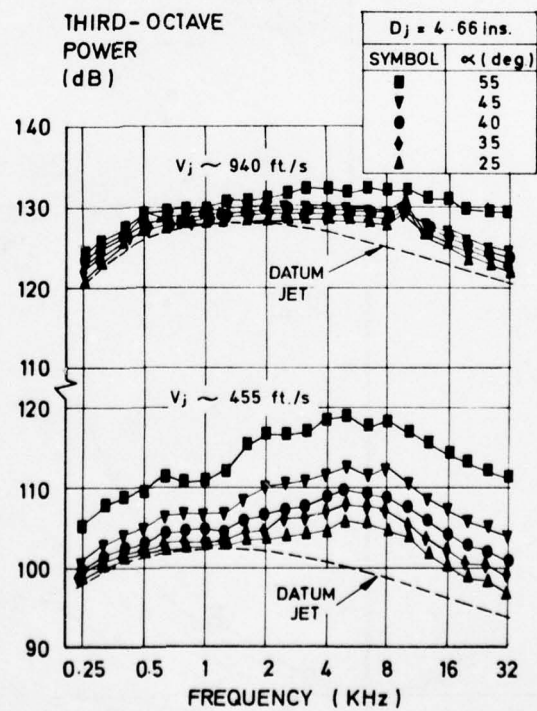


Fig. 37

NGTE Model Exhaust System
for Strut Noise Investigation
(From Ref. 45)

Fig. 38

Effect of Swirl on Strut
Noise Power Spectra
(From Ref. 45)



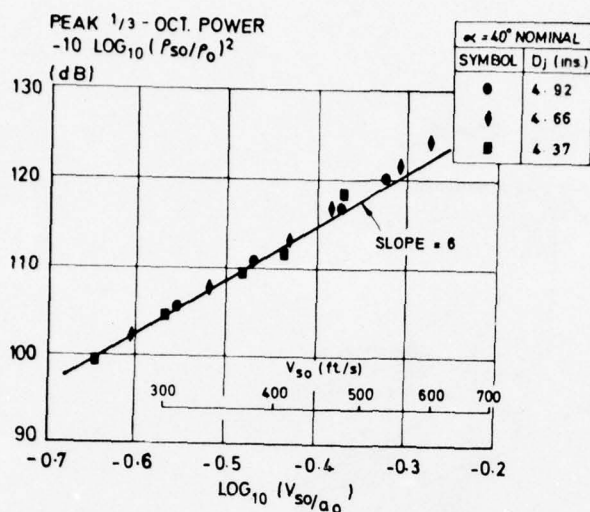


Fig.39

Correlation of Peak Strut Noise with Strut Outlet Velocity.
 (From Ref.45)

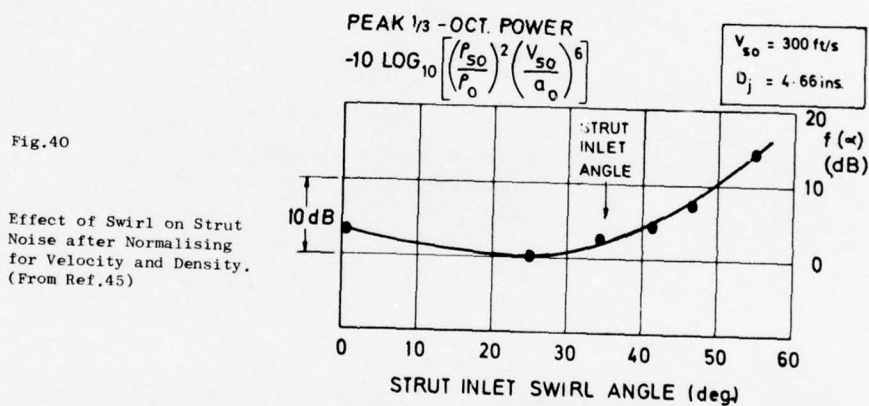


Fig.40

Effect of Swirl on Strut Noise after Normalising for Velocity and Density.
 (From Ref.45)

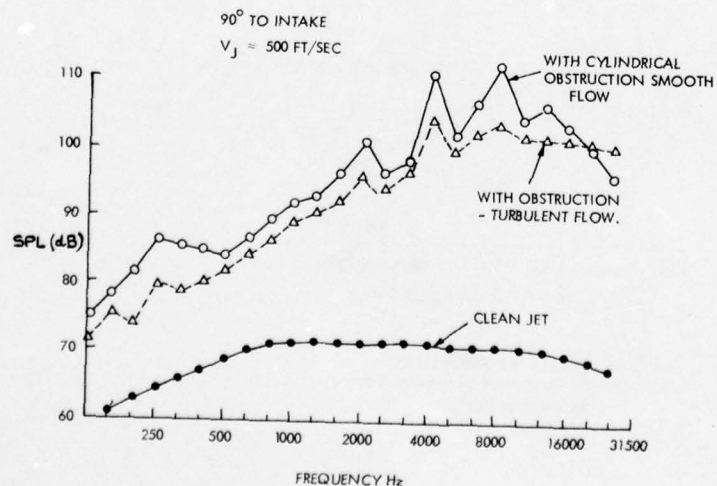


Fig.41

Example of Noise from Cylindrical Obstruction showing effect of upstream turbulence.
 (From Ref.46)

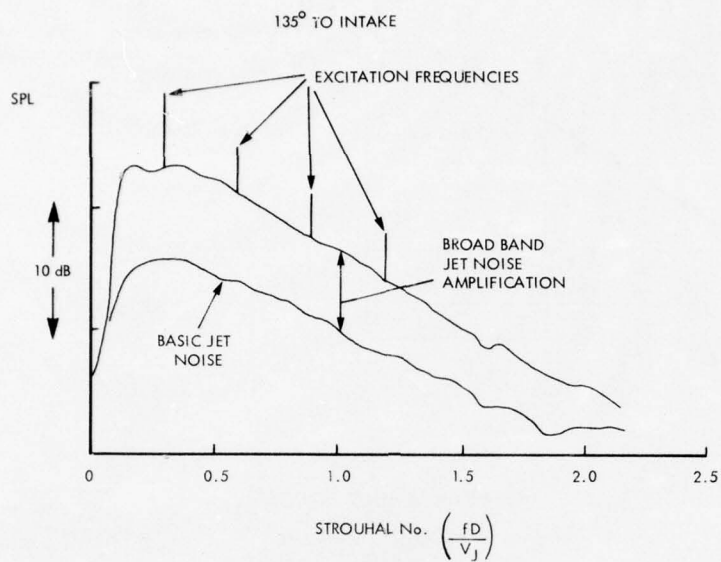


Fig.42

Amplification of Jet Noise by Upstream
Discrete Tone
(From Ref.55)

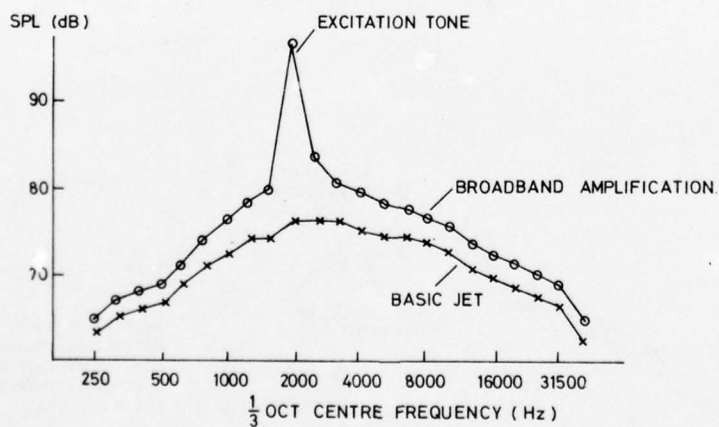


Fig.43

Further Example of Amplification
Jet Noise by Upstream Discrete Tone
(From Ref.56)

AD-A037 334

ADVISORY GROUP FOR AEROSPACE RESEARCH AND DEVELOPMENT--ETC F/G 20/1
AERODYNAMIC NOISE.(U)
JAN 77

UNCLASSIFIED

AGARD-LS-80

NL

2 of 4
AD
A037334



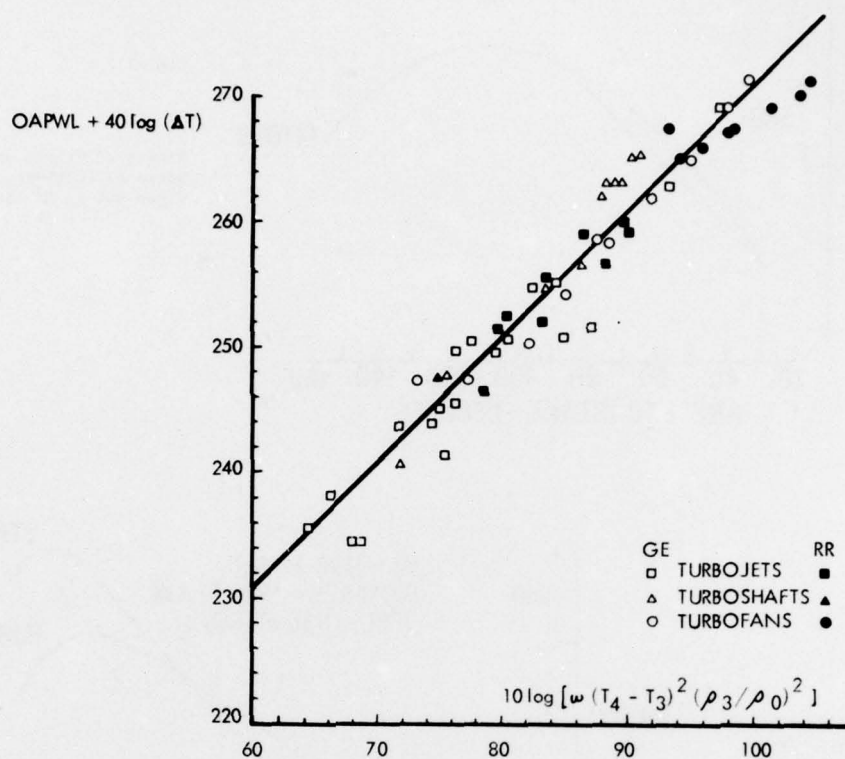


Fig.44

Correlation for Core Noise Power Level
(From Ref.57)

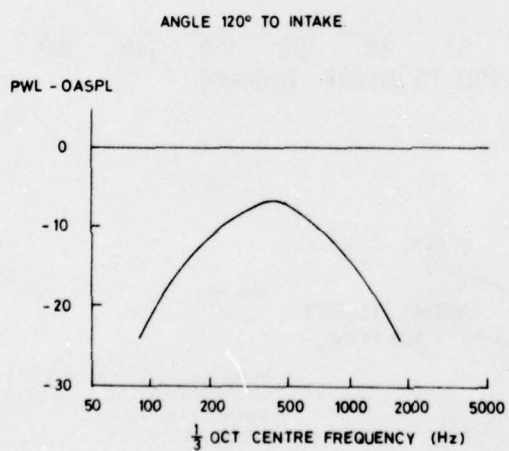


Fig.45

Core Noise Spectrum
(From Ref.57)

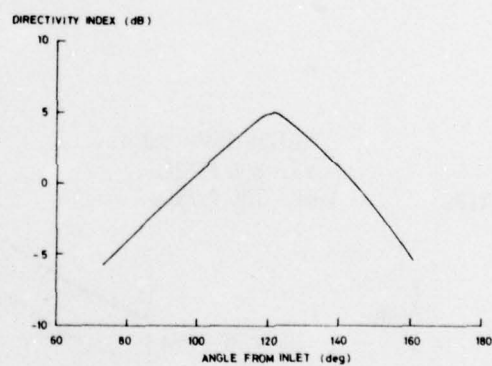


Fig.46

Core Noise Directivity
(From Ref.57)

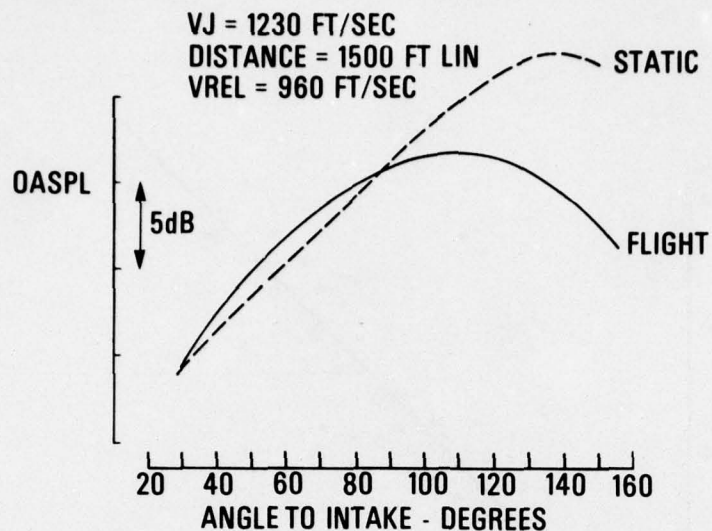


Fig.47

Effect of Flight on the
Noise of Rolls-Royce
Viper 601 in HS 125.

Fig.48

Effect of Flight on the
Noise of Rolls-Royce
Spey 512 in BAC 111.

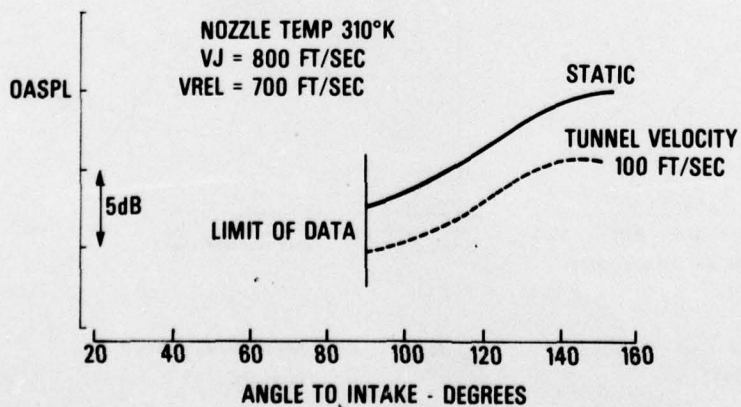
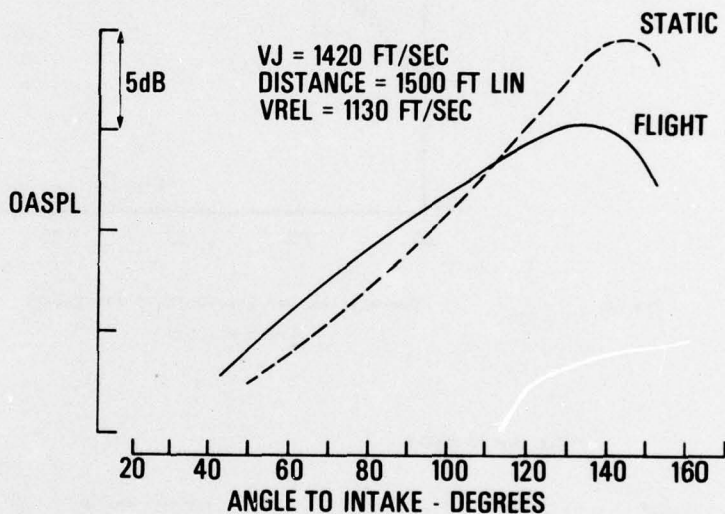


Fig.49

Model Conical Nozzle Static
to Flight Effect from Wind
Tunnel Simulation
(From Ref.59)

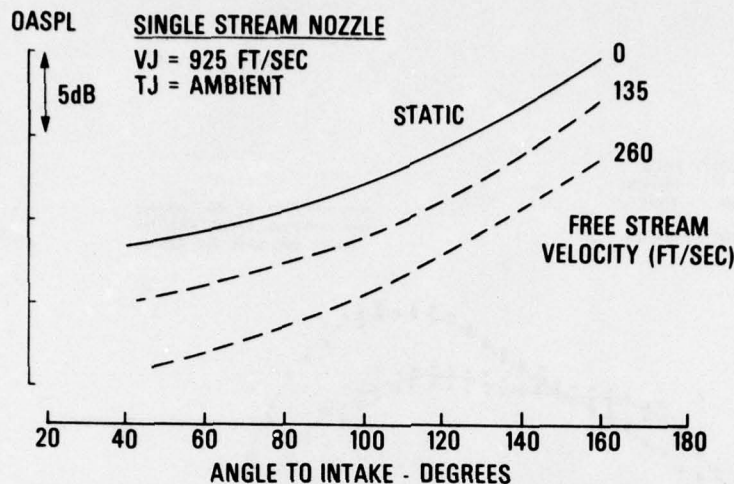
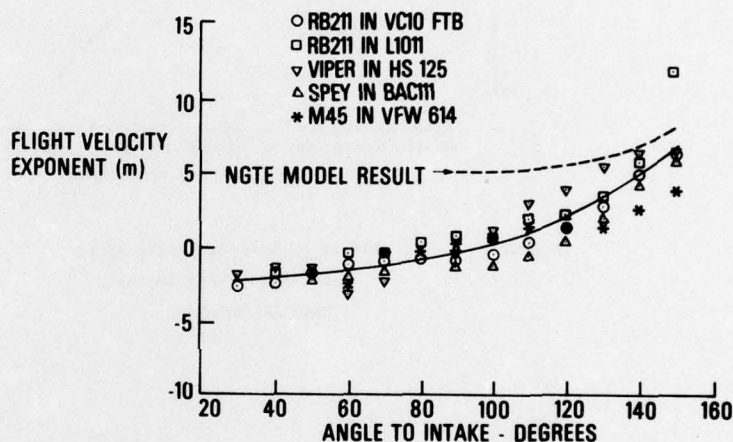


Fig.50

Model Flight Simulation
 using Coaxial Jet
 (From Ref.60)

Fig.51

Full Scale Engine
 Flight Velocity Exponent



- ◇ NGTE CO-AXIAL RIG
 - x VON GLAHN ET AL
 - PACKMAN ET AL
 - 24ft TUNNEL, MICROPHONE IN STREAM
- } MICROPHONES
OUTSIDE
STREAM

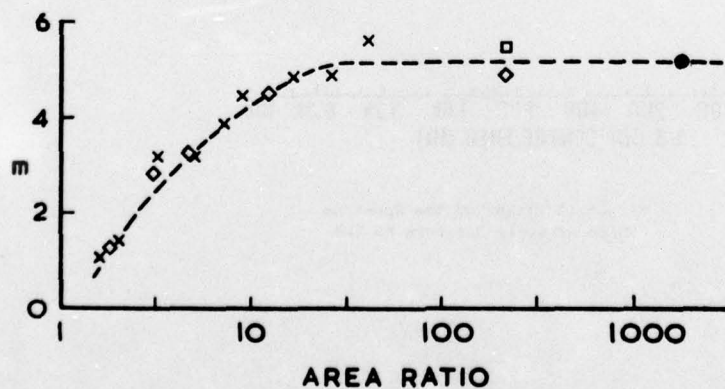


Fig.52

Effect of Secondary Flow
 Area Ratio on Flight
 Velocity Exponent for
 Model Simulation.

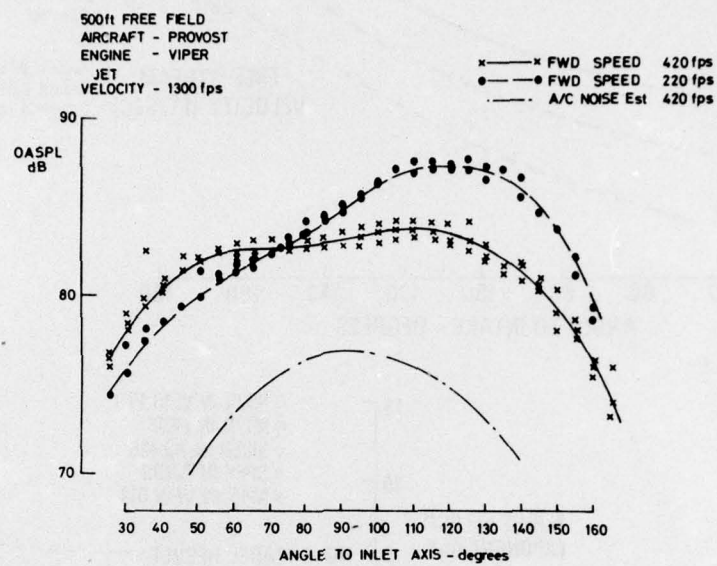


Fig. 53
Effect of Varying Flight Speed
on Noise of Viper in the
BAC Jet Provost

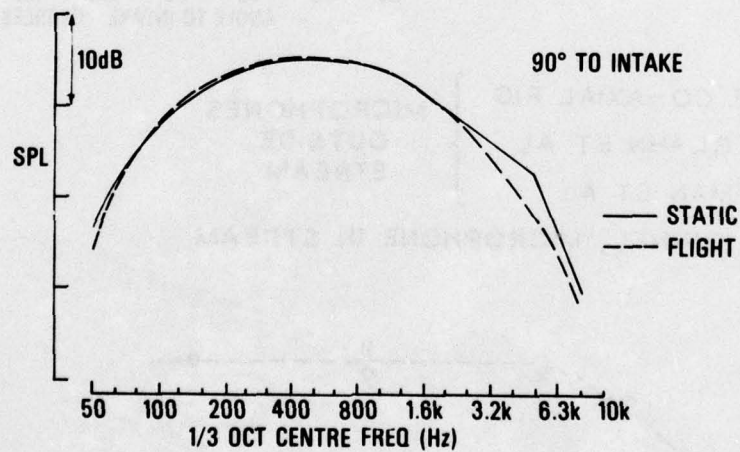


Fig. 54
Effect of Flight on the Spectrum
Shape of Viper Noise in HS 125

COMPARISON OF FLIGHT AND STATIC OASPLs

DC-9-31/JT8D-109 JET AND CORE NOISE

$V_J = 1310$ FT/SEC $V_R = 1013$ FT/SEC

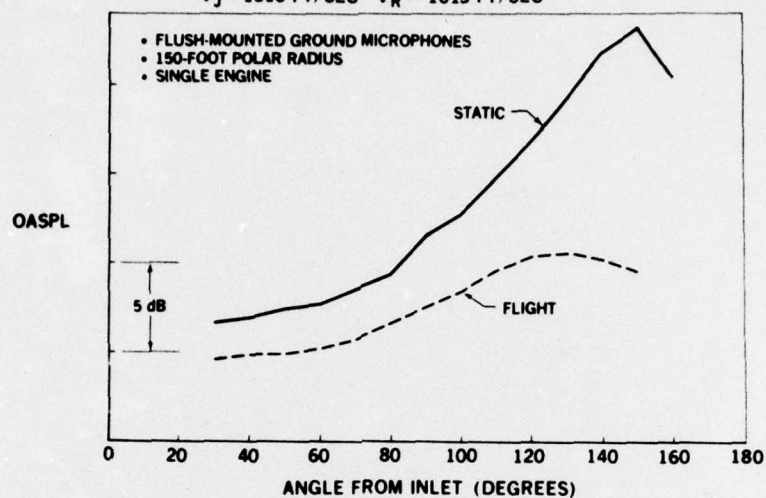


Fig.55

Effect of Flight on Noise of JT8D Refan
in Douglas DC 9
(From Ref.65)

STATIC TO FLIGHT JET NOISE REDUCTION

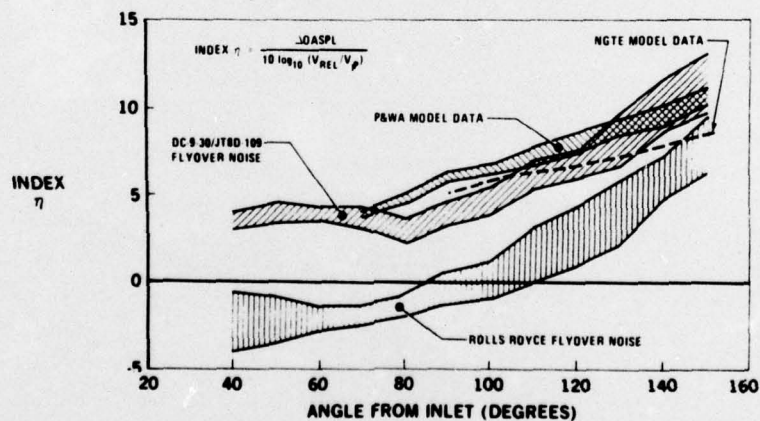


Fig.56

Flight Velocity Exponent for JT8D Refan
Jet Noise Component compared with previous
fullscale and Model Data
(From Ref.65)

FAN NOISE

by

B. W. LOWRIE

Head of Noise Research-Aero Division
Rolls-Royce (1971) Ltd, Derby, England

SUMMARY

The nature of aero engine fan generated noise is described in terms of both spectral and radiative properties both statically and, where possible, in flight. Basic concepts and theoretical approaches are considered, including dimensional analysis, and thus features of the sources deduced.

It is found that fans produce both tonal and random noise. While the sources of the tonal noise are several they can be defined quite specifically, and consist in the main of regular lift fluctuations created on individual blades by inflowing distortions. For the exceptional case of supersonic relative velocity the tonal noise is dominated by the steady pressure field relative to the blade row becoming at high supersonic speeds, a shockwave-expansion pattern. The significant sources of broad band noise are less well defined but could be produced equally well by self-excited phenomena on blade rows as by fluctuations in the inflowing airstream.

1. INTRODUCTION

Until the advent of high bypass ratio aero engines in the 1960's there was little experience of the nature of the noise generated by large, high-speed, single-stage fans. However, the noise of multistage axial compressors such as those in low bypass ratio engines and in pure jet engines, provided valuable data and warnings of the problems. Thus, the first commercial high bypass ratio engines were designed mindful of the noise that the fan would produce, and had features specifically to reduce the noise generated by that component.

The first generation commercial jet airliner had a noise signature dominated by jet mixing noise and it was only at the lower engine ratings (on approach to land typically) that the multistage compressor noise was of any consequence. Indeed, it was reported (Ref. 1) that these early jet airliners were 10 to 20dB noisier at approach than their turbo-propeller equivalents and the noise at ground level was comparable with the jet noise during take-off.

The lack of experience of single stage fan noise did not mean, therefore, that no attempts were made to theoretically model the generating mechanisms. On the contrary, ideas and theoretical treatments were developed by the early 1960's, for example Refs. 2 and 3. Thus, the growing experience of single-stage fan noise during the 1960's and up to the present has had the not inconsiderable advantage of a useful theoretical framework on which to build.

The early multi-stage data plus some single stage experiments and the developing theoretical ideas had, by the mid 1960's produced concrete ideas and concepts and Ref. 4 contains a representative statement of the understanding that was used for design of the high bypass ratio engine fans now in service. Since the mid 1960's there has been a rapid development in both experience and theoretical modelling of aero engine fan noise. Today, although ingenious and very highly developed theories are available, these have largely been used as guidance for experiments and, as with most fields of engineering, it is the experimental data and its interpretation which provides for the essential prediction and control of aero engine fan noise radiation.

2. PRELIMINARY OBSERVATIONS ON FAN NOISE

The farfield acoustic signal produced by any source mechanism is usually adequately described by a combination of its spectral and radiative properties. That is, the observer's response is due to the spectral character of the acoustic field in his immediate locality. Further, for aircraft noise, the most commonly used unit is the Perceived Noise decibel (PNdB), and this unit is defined in terms of the level of the acoustic signal in each of the preferred third octave bands over the audible range. Thus, it is tempting to measure fan noise by the 1/3 octave levels observed as a function of distance and angle relative to the turbomachine axis. However, it has been found that such representation masks many important and informative features of the acoustic signal, and in describing the spectral character use is made of narrowband (constant bandwidth) analysis.

Figure 1 shows a typical narrowband analysis of the acoustic signal produced by a single stage fan running at subsonic tip speed observed at 60° to its intake axis. The features which are prevalent are the tones at blade passing frequency and its harmonics and the base level of broadband random noise. Figure 2 illustrates a typical spectrum that is observed in the forward arc of a

ducted fan running at supersonic relative speeds. Here, the dominant features are tones at all multiples of the shaft rotational frequency and surprisingly, perhaps, the blade passing frequency is not at all predominant. Thus, first observations of fan noise show some expected, and at least one surprising feature.

On the face of it a strong tone at blade passing frequency (and harmonics) accompanied by a significant level of random noise is not surprising. However, the emergence of all the engine order tones at supersonic fan tip speeds is. To understand these observations a resume of relevant acoustic theories is necessary.

2.1 Duct Acoustic Theory

Although there are alternative theoretical approaches to the propagation and radiation of aero engine fan noise it has been found that the most useful concepts arise from the work of Tyler and Sofrin (Ref.2). The acoustic analysis there is limited to waves in ducts with no flow, however further developments have shown (Ref.5) that the essential features are representative.

Following the techniques in Ref.2 the behaviour of acoustic waves in a cylindrical duct can be described by solutions to the acoustic wave equation, which, in cylindrical co-ordinates can be written

$$\frac{1}{c^2} \cdot \frac{\partial^2 h}{\partial t^2} - \frac{1}{r} \frac{\partial}{\partial r} \left(r \frac{\partial h}{\partial r} \right) - \frac{1}{r^2} \cdot \frac{\partial^2 h}{\partial \theta^2} - \frac{\partial^2 h}{\partial x^2} = 0 \quad (1)$$

Assume a solution of the form $p = R(r) \cdot \Theta(\theta) \cdot X(x) e^{i\omega t}$

Substituting and dividing by $-p$ we get

$$\left(\frac{\omega}{c}\right)^2 + \frac{1}{R} \frac{\partial^2 R}{\partial r^2} + \frac{1}{R \cdot r} \cdot \frac{\partial R}{\partial r} + \frac{1}{r^2} \cdot \Theta \cdot \frac{\partial^2 \Theta}{\partial \theta^2} + \frac{1}{X} \frac{\partial^2 X}{\partial x^2} = 0 \quad (2)$$

$$\text{Rearranging } \frac{1}{X} \cdot \frac{\partial^2 X}{\partial x^2} = -\left(\frac{\omega}{c}\right)^2 - \frac{1}{R} \frac{\partial^2 R}{\partial r^2} = \frac{1}{R \cdot r} \cdot \frac{\partial R}{\partial r} - \frac{1}{r^2} \cdot \Theta \cdot \frac{\partial^2 \Theta}{\partial \theta^2} \\ = -k_x^2 \quad (\text{independent of } x)$$

$$\therefore \frac{\partial^2 X}{\partial x^2} + k_x^2 X = 0$$

$$\text{The solution is } X(x) = A e^{-ik_x x} + B e^{ik_x x} \quad (3)$$

$$\text{Similarly } \frac{1}{r} \cdot \Theta \cdot \frac{\partial^2 \Theta}{\partial \theta^2} = -k_\theta^2 \quad (\text{independent of } \theta)$$

$$\text{and has the solution } \Theta(\theta) = C e^{-ik_\theta r \theta} + D e^{ik_\theta r \theta}$$

$$\text{or more conveniently } \Theta(\theta) = E \cos(k_\theta \cdot r \theta + \phi)$$

where ϕ is an arbitrary phase angle.

In a real circular duct for the solution to be instantaneously true for all θ , this function must repeat exactly for each 2π in θ

$$\text{i.e. } \Theta(\theta) = \Theta(\theta + 2\pi)$$

$$\therefore k_\theta \cdot r \text{ must be an integer.} = m \text{ say}$$

$$\text{i.e. } \Theta(\theta) = E \cos(m\theta + \phi) \text{ where } m = \text{Integer.} = k_\theta r$$

$$\text{Thus we can write } \Theta(\theta) = C e^{-im\theta} + D e^{im\theta} \quad (4)$$

$$\text{Finally } \frac{1}{R} \cdot \frac{\partial^2 R}{\partial r^2} + \frac{1}{r \cdot R} \cdot \frac{\partial R}{\partial r} + \frac{1}{r^2} \cdot \Theta \cdot \frac{\partial^2 \Theta}{\partial \theta^2} = -k_r^2 \quad (\text{independent of } r)$$

$$\text{Now } \frac{1}{r^2} \cdot \Theta \cdot \frac{\partial^2 \Theta}{\partial \theta^2} = -k_\theta^2 = -\frac{m^2}{r^2}$$

$$\text{Thus } \frac{1}{R} \cdot \frac{\partial^2 R}{\partial r^2} + \frac{1}{r \cdot R} \cdot \frac{\partial R}{\partial r} + k_r^2 - \frac{m^2}{r^2} = 0$$

$$\text{Make the substitution } y = k_r \cdot r \text{ and } \frac{\partial}{\partial r} = k_r \cdot \frac{\partial}{\partial y}$$

and the equation becomes multiplying by R/k_r^2

$$\frac{\partial^2 R}{\partial y^2} + \frac{1}{y} \cdot \frac{\partial R}{\partial y} + \left(1 - \frac{m^2}{y^2}\right) \cdot R = 0$$

which is a Bessel Equation of order m and has the solution

$$R = G J_m(y) = G J_m(k_r \cdot r) \quad (5)$$

Since we are concerned with the solution in a circular duct where the real solution must be finite everywhere, the alternative Newman-Bessel function $Y_m(y)$ is not considered since it has an infinite value on the axis. It is however necessary for a complete solution in an annular duct.

Thus grouping the whole solution together and combining all the arbitrary constants into one we get

$$p = A \cdot J_m(k_r r) e^{im\theta} e^{ik_x x} e^{i\omega t}$$

$$= A \cdot J_m(K_r r) e^{i(m\theta + k_x x + \omega t)}$$

and equation (2) becomes replacing w/c by k^2 & $\frac{1}{x} \cdot \frac{\partial^2 x}{\partial x^2}$ by k_x^2 etc:

$$k^2 - k_r^2 - k_x^2 = 0$$

note that for this to represent all possible solutions both k_x & m can be positive or negative.

It is convenient at this stage for reasons which will become clear in section 2.1.1 to define the solution in terms of the particular values of kr which are admissible. For any particular circumferential mode order (defined by m) there will be a set of values of k_r each one of which is specified by the radial order parameter μ . The wavenumber K_r is therefore written conveniently in the subscripted form $k_{r\mu}$, and likewise the amplitude. The possible solutions to the equation are now:-

$$p_{\mu\mu}(r, \theta, x, t) = A_{\mu\mu} J_m(K_{r\mu} r) \exp^{i(m\theta + k_x x + \omega t)}$$

$$\text{where } k_x^2 = (w/c)^2 - K_{r\mu}^2$$

and the acoustic pressure field in a circular duct can be represented by the total sum of these independent modes.

where

- m = number of circumferential wavelengths of the mode.
- μ = number of radial zeros or nodes
- $A_{\mu\mu}$ = amplitude of the m, μ mode.
- $K_{r\mu}$ = radial wave number of the mode.
- K_x = axial wave number of the mode.
- ω = circular frequency
- X = distance along duct in axial direction.

Ignoring for the moment the perhaps unfamiliar, and therefore, uninformative Bessel function $J_m(K_{r\mu} r)$ the remainder of the expression describes a wave which has m wavelengths around the circumference of the duct and a wavelength $2\pi/K_x$ in the axial direction (assuming K_x real) with a circumferential frequency of ω . For K_x imaginary, the mode does not have a constant amplitude as x varies but rather increases or decreases exponentially. This latter occurs for a given mode (therefore fixed $K_{r\mu}$) at frequencies below a critical $\omega^* = c K_{r\mu}$. This change in axial behaviour of the mode is obviously of great interest, since if a pressure pattern produced by a fan in a duct is at a frequency below the critical frequency then in a real case it will decay along the duct and will emerge at a lower level than if it propagated at constant amplitude. Clearly, the important features are the conditions under which $K_{r\mu}$ is high (and so is the critical frequency) and the rate of decay that can be achieved.

2.1.1 Properties of Bessel Functions

In order to understand physically the mathematical conditions described above some knowledge of Bessel functions is necessary. These are fully described in text books on the subject but the relevant features are summarised here.

Bessel functions of the first kind (J) can be described as sinuous curves, symmetrical or anti-symmetric, about zero argument for even and odd orders (m) respectively, which vary about a zero mean with peak amplitudes (positive and negative) which reduce with increasing argument. Only the zeroth order Bessel function has a finite amplitude ($=1$) at the origin and only the first order has other than zero slope at the origin. These features are illustrated in Fig.3.

The only solutions to the mode equation above, which are admissible, are those where the radial pressure profile matches the duct wall boundary condition. This can be interpreted in the case of an acoustically hard wall as a pressure minimum or maximum. Thus, the only admissible values for $K_{r\mu}$ are those for which $(K_{r\mu} r)$ equals the argument of the m th order Bessel function at a turning point. Clearly for a given circumferential order (m) we are interested in the lowest value of $K_{r\mu}$ ($K_{r\mu 0}$). Since, if the frequency is lower than the critical value for the lowest radial order, it will be so for all radial orders of that circumferential order. This means we need only consider the argument of the first maximum of the Bessel function and conveniently, except for the J_0 mode, this occurs near $(m+1)$. See Fig.4.

2.1.2 Critical Frequencies in Ducts

Following this approach we find that the critical frequency

$$w^*m = C \cdot K_{mu} \quad (K_x^* \approx 0)$$

$$\approx \frac{C(m+1)}{r}$$

The critical circumferential tip speed of the pattern

$$U_t^* = \frac{w^* \times 2 \pi r}{2 \pi \cdot m} \\ = \frac{C(m+1) 2 \pi r}{2 \pi r \cdot m}$$

$$\text{i.e. } U_t^* = \left(\frac{m+1}{m} \right) \cdot C$$

For large m this is sonic tip rotational speed!

For all non-zero circumferential orders U_t^* is greater than sonic, thus apparently any pressure pattern created in a duct must rotate at supersonic conditions before it can propagate acoustically.

2.1.3 Decay of Subcritical Pressure Field

The decay of the pressure field under subcritical conditions is described by the term $\exp. -ikx$ where K_x is imaginary.

$$K_x = i \sqrt{k_m^2 - (w/c)^2} = \frac{i}{c} \sqrt{w^{*2} - w^2} = \frac{i w^*}{c} \sqrt{1 - \frac{w}{w^*}}$$

$$\text{rate of amplitude decay} = \exp. \left[-x \cdot \frac{w^*}{c} \sqrt{1 - \left(\frac{w}{w^*} \right)^2} \right]$$

$$\text{Decay in SPL} = \frac{20}{\log_e 10} \cdot \frac{w^*}{c} \sqrt{1 - \left(\frac{w}{w^*} \right)^2} / \text{unit length}$$

$$\text{or since } \frac{w^*}{c} = K_{mu} \approx \frac{m+1}{r}$$

$$\text{SPL decay} \approx 8.7 (m+1) \cdot \sqrt{1 - \left(\frac{w}{w^*} \right)^2} / \text{duct radius}$$

Even for a first order mode ($m = 1$) when w is 90% of critical, the decay rate is approximately 7.6dB/radius. Obviously, higher order modes would decay even more rapidly, in fact at such a rapid decay rate that within a reasonable duct length pressure patterns significantly below the critical frequency can be assumed not to propagate at all and are termed "cut-off".

A very good demonstration of this decay was shown by Moore (Ref.6) and reproduced here in Fig.5. Each of the components of the pressure field bound to a four-bladed rotor are shown to decay precisely at the rate predicted. Incidentally, it will be noted that the highest two harmonics are found to reach a bottom limit of sound pressure level and hence a level at which propagation from some different mechanism is occurring.

In the case of a fan rotating in a duct there is always a pressure field generated by the steady flow pattern around the blades which rotates with them. This analysis and Moore's experiments show that such a pressure field at subsonic fan tip speeds would not be expected to propagate to the duct end or radiate to the far field.

2.2 Interaction Tones

As shown earlier, (Fig.1) blade passing tones and harmonics do, in fact, radiate and therefore the source of these tones must be a pressure pattern which is rotating in the duct at a supersonic relative speed, even though the fan itself is subsonic.

2.2.1 Generation of Interaction Tones

Tyler and Sofrin, in their classical paper, (Ref.2) explain this as due to an interaction between the steady rotor flow field and the steady flow field around an adjacent stator blade row or system. Essentially, if the numbers of rotor and stator blades are unequal the flow fields can produce a "pattern of events" which rotates faster than the rotor and can thus move supersonically even with a subsonic fan.

This phenomenon is illustrated in Fig.6 by the pattern of events (in this case, simply rotor-stator coincidence) which occurs during a 90° rotation of a four-bladed rotor adjacent to three stator blades. The coincidence is seen to rotate one full revolution in the same direction.

In fact, if the number of rotor blades is B and stator blades is V , a pattern occurring at n times blade passing frequency can be formed of m circumferential wavelengths

where $m = nB \pm kV$ (k is any integer)

and will rotate at $\frac{nB}{m} = \frac{nB}{nB \pm kV}$ times the rotor speed.

In the case quoted $n = 1$, $k = -1$

and therefore, $m = 1$

and the speed = $\frac{4}{4 - 3} = 4$ times rotor speed.

2.2.2 Radiation of Interaction Tones

In addition to developing the theory and mechanisms by which interaction tones are generated and propagate in circular (and also in annular) ducts, Tyler and Sofrin arrive at a method of predicting the radiative behaviour of these acoustic phenomena.

The theoretical model used is simplified somewhat from the real case and assumes that a given "spiral mode" propagating in a duct can be simply regarded as a rotating pressure pattern at its termination. In calculating the radiation it is assumed that the duct terminates in an infinite baffle and that all the energy is radiated. Typical calculated radiation patterns have highly directional "lobes" and for a given mode one particular lobe tends to dominate. Further, the direction of this dominant lobe is a very strong, almost unique, function of the "cut-on" ratio (actual to critical frequency), this is illustrated in Figs.9 and 10. A mode which is at a frequency (or speed of rotation) only slightly above cut-off ("cut-on" ratio little greater than 1) radiates primarily at high angles to the duct axis, i.e. some 60° to 70° . While a mode which is at a high frequency or cut-on ratio radiates predominantly close to the axis. Only the various radial orders of the zeroth circumferential order ($m = 0$) modes actually radiate along the axis.

The radiation of Fan tones has been further examined by other authors, notably Lowson (Ref.10) and Lansing (Ref.11). Although quite different mathematical assumptions are used in each case the general trends and much of the detail predicted by Tyler and Sofrin is found to be correct, the largest errors being due to the infinite baffle assumption. But, as shown by Lansing, these errors are only at large angles to the axis approaching 90° where the radiation is weak in any case.

The radiation theory of Tyler and Sofrin, discussed above, generally describes the forward radiation through a fan intake and should, in principle, describe the radiation in the rearward arc. However, a feature of the conditions of rearward arc radiation is the high speed jet which issues from the fan nozzle of a bypass engine through which the tone is propagating. This is found to have two significant effects:

- (i) The radiation is re-directed by the shear layer (Snell's law) refraction away from the axis, and
- (ii) The high degree of turbulence normally present in this mixing layer between the fan jet and the ambient air scatters the acoustic wave patterns sufficiently to obliterate the highly directional lobes of radiation and instead produce a more diffuse field shape. This is illustrated in Fig.16.

2.3 Tones at Supersonic Fan Speeds

The dominant fan blade passing tones and harmonics which are observed at subsonic fan speeds can be satisfactorily explained as described. However, the same concepts suggest that supersonically the fan blade pressure field ought to propagate and thus, even without interactions, the acoustic signal would still be expected to be dominated by blade passing frequency and its harmonics. Figure 2 illustrates that this is not so and some further explanation is necessary.

2.3.1 Origins of Shaft Order Tones

When the relative flow onto a fan rotor is supersonic, the flow field immediately upstream of the fan is made up of shock waves and expansions, see Fig.7. Such a system has a degradation of energy built-in and is as a consequence, non-linear in behaviour. That is the flow passes through the system of shocks in an irreversible manner. This requires a new approach and has been adequately investigated by several authors, Ref.7 for instance. It is found that any slight variations from average in the shock strengths or positions produced by individual blades, result in sufficient variation in propagation speed of the individual shocks away from the plane of the fan rotor for the pressure pattern to become uneven. This occurs to the extent of not producing the same repetition for each blade, see Fig.8. Such a pattern which repeats with each revolution of the fan would, therefore, contain all the harmonics of fan rotational speed rather than blade passing frequency, in line with the observations in Fig.2.

2.3.2 Radiation of Shaft Order Tones

Once the generation of the shaft order tones ("Multiple Pure Tones" or "Buzz-Saw" noise) has occurred they are propagated as spiral waves in the duct upstream of the fan and thus the radiation process is exactly the same as for the spiralling acoustic modes described in Section 2.3.2 above.

Over the normal range of operation of today's bypass engine fans, i.e. upto tip relative Mach numbers of around 1.5, the "cut-off" ratios of the various engine order tones, all of which spin at the same speed as the rotor, are obviously low. Indeed the low engine orders can be cut off. This component of noise, therefore, radiates at large angles to the intake axis, in the range 40° - 70° typically.

2.4 Other Components of Fan Noise

The sources of the dominant tones in the acoustic field of an aero engine fan have been described in qualitative terms but little has been said of the source of the remaining broad band noise component or the sometimes observed tones from a subsonic fan at low level at multiples of shaft rotational speed, see Fig.1. The latter can simply be explained (Ref.8) as being caused by the same interaction mechanisms as the dominant tones and are due to the blades not being absolutely identical. Their amplitude is generally much lower than the dominant tones (20dB lower typically) and can usually be ignored.

2.4.1 Broad Band Fan Noise

The broad band noise, on the other hand, is spread over a wide band of frequencies, and is, therefore, of similar importance to the blade passing tones.

The non-ordered nature of broad band noise suggests that the sources will be found in the random flow processes which occur in most turbomachinery. These include turbulent boundary layers, turbulent wakes, regions of separation and the interaction of such random flows with adjacent solid surfaces. The investigation of such mechanisms must, by their nature, be largely empirical, although theoretical treatments such as Ffowcs-Williams and Hawkings (Ref.9) draw attention to the many possible mechanisms. Essentially, in fluctuating flows of low Mach numbers the most efficient sources are monopole types which imply fluctuations in mass. In the usual absence of such highly efficient sources (steady flow) the next most efficient type becomes prominent, i.e. dipole type which imply fluctuations in momentum or applied force. Again, in the absence of dipole-type, quadrupole type sources usually associated with fluctuating stresses become important, and so on. Thus, although it is apparently impossible to eliminate broad band noise sources from fluid flow machines, the generation can be controlled by eliminating or reducing the more acoustically efficient processes. Since this usually is consistent with good aerodynamic performance the problem of control reduces to understanding the base level due to turbulent boundary layers and wakes which are present, and keeping that to a minimum.

2.4.2 Broad Band Noise Radiation

Because of the sources of broad band noise are random, the radiative properties, in particular the directionality is also random. This might suggest that the energy should be uniformly radiated in all directions. However, because the initial propagation of the noise must be along the circular duct which contains the fan, some "focussing" of the sound occurs.

The simple way of viewing this focussing is to represent the propagation of the random noise in a circular duct as the sum of a large number of randomly-phased spiral waves of all possible modes. This is analogous to representing the broad band signal observed in the far-field as the sum of a large number of sinusoidal signals such as is implied by narrowband spectral analysis. Further, the simple assumption is made that all the modes have equal amplitude in the duct. From Fig.10 the rate of change of radiation angle with cut-on ratio is high at low cut-on ratios (high angle radiation) and falls rapidly as the cut-on ratio increases. This suggests that radiation will tend to concentrate near to the axis since there should be only a few modes with low cut-on ratios which radiate at high angles. Indeed, this supposition holds qualitatively and Fig.11 shows the inlet radiation field shape of typical fan broad band noise and clearly illustrates the focussing of the broad band noise into a sector around the axis with a fall-off at angles above 40° to the axis.

In the rearward arc, the comments made with respect to interaction tones hold and the broad band noise radiates primarily at high angles to the exit axis.

2.5 Dimensional Analysis of Fan Noise

In order to simplify the assessment of the parameters which are significant to the generation of noise of fans or any turbomachine, the well-known technique of dimensional analysis can be used to some advantage. Briefly, the parameters thought to be important need only be considered as non-dimensional groups to examine their effect and this reduces the number of independent parameters that are considered.

The dependent parameter we wish to describe is the acoustic intensity I in a given frequency range $f - \Delta f$ to $f + \Delta f$ at a point in space located by the polar co-ordinates R (radius) and θ (angle with respect to the turbomachine axis).

The other independent (causing) variables are the representative gas properties, ρ , p , a , μ both at source and at observation points; the fan dia. D , plus as many non-dimensional length ratios as are needed (including g/c); speed N and, from aerodynamic experience, one other non-dimensional parameter representing the operating condition (pressure ratio, PR , for example).

So we have :-

$$I = f(f, \Delta f, R, \theta, \rho, p, a, \mu, p_o, p, a_o, \mu_o, D, N, PR, \text{plus geometric ratios}).$$

Of these parameters, $f, \Delta f, R, \rho, p, a, \mu, p_o, p, a_o, \mu_o, D$ and N are dimensional in terms of the basic dimensions of mass, length and time (M, L and T) and these plus I can be related by $(14 - 3) = 11$ non-dimensional groups according to the "Buckingham π Theorem."

Parameter Dimension	I	f	Δf	R	ρ & ρ_o	p & p_o	a & a_o	μ & μ_o	D	N
M	1				1	1		1		
L	0			1	-3	-1	1	-1	1	
T	-3	-1	-1			-2	-1	-1		-1

Making use of some known relationships and inspection, the 11 independent, non-dimensional groups chosen are :-

$$\frac{I}{\rho_o a_o^2}, \frac{\Delta f}{f}, \frac{f}{N}, \frac{R}{D}, \frac{p}{\rho_o}, \frac{p}{p_o}, \frac{a}{a_o}, \frac{\mu}{\mu_o}, \frac{aD}{\mu}, \frac{ND}{a}, \frac{p}{\rho a^2}$$

The group involving I is simply a statement of the acoustic effect, in a dynamically similar environment, of altering the environmental conditions.

The ratios $p/\rho_o, p/p_o$ etc. are simply ratios of the gas properties where the acoustic signal is generated to that where it is observed. Provided these ratios do not depart too far from unity, and in fans they are generally in the range 1 to 1.5, then the only significant effect is a rematching of the pressure and velocity components of the acoustic wave to transmit the same energy. It is assumed that all the acoustic energy generated must radiate. Thus these terms can be explicitly accounted for by the relation $I \propto p/\rho_o$, and this is done by forming the group $\frac{I}{\rho_o^2}$ instead of $\frac{I}{\rho_o a_o^2}$ and then eliminating $p/\rho_o, p/p_o$ etc. from further consideration.

The terms $\frac{\Delta f}{f}$, and $\frac{f}{N}$ simply express how frequency bandwidths and absolute frequencies should scale with changes in speed for dynamic similarity. Alternatively $\frac{f}{N}$ might be replaced by $\frac{fD}{a}$ i.e. a Strouhal number.

R and the co-ordinate θ define the point of measurement in non-dimensional terms. If the noise is being determined in the acoustic farfield for the source then by definition IR^2 must be constant and thus the functional relationship between $\frac{I}{\rho_o^2}$ and R is made explicit.

Since it is usually found that Reynold's number, $\frac{f a D}{\mu}$ can be ignored to a first order in fluid flow problems we make that assumption here, and finally $\frac{p}{\rho a^2}$ is, in fact γ the ratio of specific heats which we can assume constant since we usually have air as the gas.

Thus, taking account of all these assumptions we can write the observed farfield acoustic intensity from a fan as:

$$I(R, \theta) = \frac{p^2}{\rho a} \cdot \frac{D^2}{R^2} \cdot g\left(\theta, \frac{\Delta f}{f}, \frac{f}{N}, \frac{ND}{a}, P.R.\right)$$

Assuming:

- (i) We are comparing geometrically similar systems.
- (ii) The observation is in the farfield acoustically, and
- (iii) Reynolds number is not an important parameter.

Normally the observation is in SPL:

$$\therefore \text{SPL} = 10 \log_{10} \left[\frac{p^2}{\rho_{\text{ref}}^2} \cdot \frac{p_o a_o}{\rho a} \cdot \frac{D^2}{R^2} \cdot g\left(\theta, \frac{\Delta f}{f}, \frac{f}{N}, \frac{ND}{a}, P.R.\right) \right]$$

In carrying out experiments we, therefore, only need to examine the variation of SPL with the four parameters $\theta, f/N, ND/a$ and $P.R.$. The bandwidth ratio $\frac{\Delta f}{f}$ can again be explicitly dealt with provided the analysis successfully separates discrete f tones (SPL independent of $\frac{\Delta f}{f}$) and random noise (SPL correction = $10 \log_{10} \frac{\Delta f}{f}$).

In comparing one fan with another, for tones or broad band noise separately, the effects of any geometric changes can be isolated by comparing at the same $\theta, f/N, ND/a$ and $P.R.$, or since $P.R.$ was chosen arbitrarily as a second parameter representing the operating condition, a search may be made for an alternative aerodynamic parameter which might render SPL independent of all geometric ratios. As shown in Section 4, fan broad band noise is reasonably correlated by using air incidence onto the rotor blade as this parameter.

3. 3. TONE GENERATION BY SUBSONIC FANS

In Sections 2.1 and 2.2 the basic ideas were discussed of how fans running at subsonic tip speeds generate tones at blade passing frequency and harmonics by interaction processes. For simplicity the discussion assumed that the only interactions of concern were those between rotor blade rows and stator blade rows. Simple consideration shows that although a moving blade row must be involved, it could interact with a stationary or other moving blade row to produce generating processes providing only that there is relative motion. Similarly, since the blade row can consist of only 1 blade, any struts or other stationary obstacles to the unsteady pressure field of the rotor could be the cause of propagating tones being generated. What is perhaps not quite so obvious is that while the significant part of the flow field of the rotor which interacts with the stators could be the wakes, conversely any wakes or distortions in the inlet rotor flow could interact with the rotor and produce propagating tones again at rotor blade passing frequency and its harmonics. While it is easy to see that tone noise generated by rotor wakes contacting a stator blade row must be of and harmonics because that is the excitation contained in the wakes, the reasons why similar frequencies should be observed when a rotor rotates in a wake system generated by the inlet may not be so obvious.

Although rigorous mathematical proofs are available, simple physical arguments are used here in preference. The process of the rotor blades passing through a succession of wakes can be viewed in different frames of reference, the most obvious being either stationary or moving with the rotor. Obviously, by analogy with the stator blade interaction, if the latter frame of reference is used the flow field fluctuations around the rotor contain only the excitation frequencies of the wake system as seen by the rotor. However, a stationary observer is not in that frame of reference. In the stationary frame of reference the wakes are fixed and the rotor blades pass through them. This interaction can be viewed as a series of stationary positions (the wakes) each of which is excited by the rotor blades at, therefore, blade passing frequency and its harmonics. It should be emphasised that these two concepts are in no way incompatible, and this is a case where varying the frame of reference of observation varies the frequency; another is the wellknown Doppler effect on the frequency of any moving source of sound.

3.1 Sources of Tones in Subsonic Aero Engine Fans

As well as the more obvious interactions between moving and stationary blade rows, the preceding discussion has illustrated other possible sources. Thus, it is important to establish by direct experiment which are the important sources on typical aero engine fans.

Experiments carried out with a fan rotor in the duct and no OGV's showed that a significant level of tone was generated due, apparently, to the rotor alone. This tone level is unsteady and on average has a field shape of little character, as shown in Fig.12.

3.1.1 Rotor-Distortion Interaction Tones

This rotor-alone tone level is due to interactions between the rotor blades and unsteady aerodynamic distortions in the intake. The cause of this phenomenon is primarily free atmospheric motions being distorted into long correlated sausages by the sink flow into the fan intake, although secondary effects due to the wall boundary layer are also involved as is demonstrated in Fig.13. In that figure, reproduced from Ref.12, the effects of a gauze screen to reduce the turbulence, and a suction slot, with and without suction to remove the boundary layer alone, and in combination, show this. The importance of these effects derive from the fact that this tone source reduces to insignificant levels in-flight as has been shown several times, Refs.12 and 13 for instance. The observations in Fig.13 illustrate well that at tip Mach numbers of around 0.7 the annulus boundary layer has a dominant effect while at around tip Mach numbers of 1.00, the presence or absence of the annulus boundary layer is of little consequence. Similarly at sonic tip speeds the gauze (turbulence reducing) screen has a dominant effect on the tone level, but has little effect at the lower Mach numbers. From these types of observations it has been deduced that large scale atmospheric motions become largish scale circulatory motions in the fan intake flow, represented entirely by streamwise vorticity. (Cross-stream vorticity is virtually eliminated by the sinkflow). The magnitude of the fluctuating velocities are large and the scale is large, of the order 0.2-0.3 intake diameters with a long persistence lasting sometimes several seconds. These fluctuations can directly interact with the fan and produce tones at near sonic tip speeds, (V small, see Section 2.2.1). By initiating distortion development of the turbulent boundary layer on the annulus wall these atmospheric disturbances create smaller cross-stream scale wakes (of order 2-5% of fan dia.) which have the same persistence and can, therefore, produce tone generation at lower Mach numbers ($V \rightarrow B$, Section 2.2.1). The scale of the distortions will scale to fan intake size. Thus, the acoustic behaviour which is governed by the scale will not vary with physical size. Figure 14 shows a typical summary graph of static fan tone level due to atmospheric distortion. Whilst it would be ideal if this data could be regarded as unique, it must be admitted that these tone levels are found to alter significantly from day to day on a test site and no doubt can vary enormously from one test site to another due to prevailing weather conditions. The levels can be further increased by distortions due to the wakes of obstructions present around open test sites.

The presence of distortion-interaction tones, on static tests only, obviously makes such tests unrepresentative of flight and has been a major reason why experimental progress on rotor-stator interaction tones has been slow, even though the theoretical concepts are very clear. For this reason attempts are being made currently to "condition" the air entering a model fan intake to make its degree of atmospheric distortion representative of flight.

So we have :-

$$I = f(f, \Delta f, R, \theta, \rho, p, a, \mu, \rho_o, p_o, a_o, \mu_o, D, N, PR, \text{ plus geometric ratios}).$$

Of these parameters, $f, \Delta f, R, \rho, p, a, \mu, \rho_o, p_o, a_o, \mu_o, D$ and N are dimensional in terms of the basic dimensions of mass, length and time (M, L and T) and these plus I can be related by $(14 - 3) = 11$ non-dimensional groups according to the "Buckingham π Theorem."

Parameter Dimension	I	f	Δf	R	$\frac{\rho}{\rho_o}$	$\frac{p}{p_o}$	$\frac{a}{a_o}$	$\frac{\mu}{\mu_o}$	D	N
M	1				1	1		1		
L	0			1	-3	-1	1	-1	1	
T	-3	-1	-1			-2	-1	-1		-1

Making use of some known relationships and inspection, the 11 independent, non-dimensional groups chosen are :-

$$\frac{I \rho_o a_o}{p_o^2}, \frac{\Delta f}{f}, \frac{f}{N}, \frac{R}{D}, \frac{\rho}{\rho_o}, \frac{p}{p_o}, \frac{a}{a_o}, \frac{\mu}{\mu_o}, \frac{aD}{\mu}, \frac{ND}{a}, \frac{p}{\rho a^2}$$

The group involving I is simply a statement of the acoustic effect, in a dynamically similar environment, of altering the environmental conditions.

The ratios $\rho/\rho_o, p/p_o$ etc. are simply ratios of the gas properties where the acoustic signal is generated to that where it is observed. Provided these ratios do not depart too far from unity, and in fans they are generally in the range 1 to 1.5, then the only significant effect is a rematching of the pressure and velocity components of the acoustic wave to transmit the same energy. It is assumed that all the acoustic energy generated must radiate. Thus these terms can be explicitly accounted for by the relation $I \propto p/\rho c$, and this is done by forming the group $\frac{I \rho c}{p^2}$ instead of $\frac{I \rho_o a_o}{p_o^2}$ and then eliminating $\rho/\rho_o, p/p_o$ etc. from further consideration.

The terms $\frac{\Delta f}{f}$, and $\frac{f}{N}$ simply express how frequency bandwidths and absolute frequencies should scale $\frac{f}{a}$ with changes in speed for dynamic similarity. Alternatively $\frac{f}{N}$ might be replaced by $\frac{fD}{a}$ i.e. a Strouhal number.

$\frac{R}{D}$ and the co-ordinate θ define the point of measurement in non-dimensional terms. If the D noise is being determined in the acoustic farfield for the source then by definition IR^2 must be constant and thus the functional relationship between $\frac{I \rho a}{p^2}$ and $\frac{R}{D}$ is made explicit.

Since it is usually found that Reynold's number, $\frac{f a D}{\mu}$ can be ignored to a first order in fluid flow problems we make that assumption here, and finally $\frac{p}{\rho a^2}$ is, in fact γ the ratio of specific heats which we can assume constant since we usually have air as the gas.

Thus, taking account of all these assumptions we can write the observed farfield acoustic intensity from a fan as:

$$I(R, \theta) = \frac{p^2}{\rho a} \cdot \frac{D^2}{R^2} \cdot g \left(\theta, \frac{\Delta f}{f}, \frac{f}{N}, \frac{ND}{a}, P.R. \right)$$

Assuming:

- (i) We are comparing geometrically similar systems.
- (ii) The observation is in the farfield acoustically, and
- (iii) Reynolds number is not an important parameter.

Normally the observation is in SPL:

$$\therefore \text{SPL} = 10 \log_{10} \left[\frac{p^2}{p_{\text{ref}}^2} \cdot \frac{\rho_o a_o}{\rho a} \cdot \frac{D^2}{R^2} g \left(\theta, \frac{\Delta f}{f}, \frac{f}{N}, \frac{ND}{a}, P.R. \right) \right]$$

In carrying out experiments we, therefore, only need to examine the variation of SPL with the four parameters $\theta, f/N, ND/a$ and PR . The bandwidth ratio $\frac{\Delta f}{f}$ can again be explicitly dealt with provided the analysis successfully separates discrete $\frac{\Delta f}{f}$ tones (SPL independent of $\frac{\Delta f}{f}$) and random noise (SPL correction = $10 \log_{10} \frac{\Delta f}{f}$).

In comparing one fan with another, for tones or broad band noise separately, the effects of any geometric changes can be isolated by comparing at the same $\theta, f/N, ND/a$ and $P.R.$, or since PR was chosen arbitrarily as a second parameter representing the operating condition, a search may be made for an alternative aerodynamic parameter which might render SPL independent of all geometric ratios. As shown in Section 4, fan broad band noise is reasonably correlated by using air incidence onto the rotor blade as this parameter.

3.1.2 Rotor-Stator-Interaction Tones

Despite the confusing phenomenon of rotor-distortion interaction tones being present on all static tests of model and full scale aero engine fans, considerable progress has been made to establish experimentally the occurrence of these tones and some of the controlling parameters. The earliest attempt, known to the author, to attempt to calculate the levels of such interaction tones is that in Ref.3. The estimates were of acoustic power level of the tones so generated and relied heavily on the work of Kemp and Sears, Refs. 14 and 15, and treated the blades as acoustically compact dipoles. This relatively simple approach produced apparently good agreement and it is interesting that although many more sophisticated methods have been developed since, the main assumptions have been retained. The analysis of Ref.3 takes no account of the effect of the duct on the propagation and radiative properties of the interaction tones but does highlight one aspect which is still as significant as ever and that is the effect of the physical spacing between the inter-acting blade rows.

3.1.2.1 Effect of Rotor-Guide Vane Spacing

Hetherington (Ref.3) found that when the blade rows are very close the interaction is dominated by the potential field of the rotor exciting the stators, while at greater distances the velocity wake deficit was the dominant cause. This is due to the rapid decay with distance of the potential pressure (or velocity) field as typically calculated in section 2.1.3 and the less rapid decay of the "velocity wake". At the spacings now prevalent between fan and OGV's on a high bypass ratio engine ($g/c > 1$) the wake deficit is universally found to be the dominant cause of stator excitation and the rules which exist today are compatible with, and sometimes rely completely on, this assumption. Silverstein et al, Ref.16, found that wakes of isolated aerofoils decay at the rate $\propto 1/g$ where g is the distance downstream from the trailing edge of the aerofoil, thus giving a spacing effect of $-20 \log_{10} (g)$ or, more conventionally, since (g/c) (c is rotor blade chord) is the normalised gap the effect is normally $-20 \log_{10} (g/c)$. It is questionable whether isolated aerofoil wake data is even relevant in the rotating blade row situation where not only conditions vary radially but radial pressure gradients and thus radial wake migrations occur. In fact, the real wake flow downstream of a rotor is so complicated that rules derived as above can only be a rough guide. The data presented in Ref.17 shows approximately 6dB reduction in tone power in going from $g/c = 2$ to 4. The rate is surprisingly not maintained at small g/c 's and from 2 to 0.5 a further increase of only 5dB is observed. Obviously, freely available data is sparse on this subject probably for commercial reasons but an average rate of 4dB/doubling or $13 \log_{10} (g/c)$ represents the data quoted. Note this is slightly different from that suggested by Silverstein's wake data!.

3.1.2.2 Tone Propagation Through Blade Rows

An aspect of interaction tone noise noted frequently is the difference in power level propagated out through the inlet (forward arc) from that radiated from the downstream nozzle (rearward arc). Since the source of interaction tones is at the stators it has been suggested that this effect is due to the transmission and reflection properties of the relatively high Mach number flow through the rotor blade row, redirecting upstream propagating spiral waves back downstream and thus enhancing the rearward arc tone level at the expense of the forward arc. This phenomenon has been examined by Philpott, Ref.18, who concluded that of the blade row acoustic transmission theories available, the simplest is due to Amiet, Ref.19. Philpott adapted this using strip theory and a radial distribution of source strength $\propto M$, and accounted for the results from several fans. A typical estimate from this approach applied to the 2nd harmonic * of blade passing frequency is illustrated in Fig.15.

3.1.2.4 Source Strengths of Rotor-Stator-Interactions

Although theoretical treatments are available to calculate the stator blade row response to wakes they are of little value when the details of the real wakes with which we are concerned are largely unknown. The theories do suggest that the strength of the response of the stator row can be varied significantly by altering the orientation of the propagating wave fronts relative to the chord lines of the individual stator blades. This can be achieved by altering the ratios of blade/vane numbers within the "cut-on" regime. However, no definitive experiments which demonstrate benefits of this effect clearly and unequivocally are available.

The data in Ref.17 for a 52 inch diameter fan shows higher powers of fan interaction tone noise in the forward arc at fan blade tip Machs nearly sonic. This suggests that if rotor blockage effects are at all important, a significantly higher level of tone must be initially propagated upstream rather than downstream giving some credence to preferential wave front orientation. Quantitative experimental data on this effect is not available.

The behaviour of the wakes is largely an unknown quantity over the range of operating conditions of fans. In consequence no reliable "a-priori" prediction can be made of fan interaction tone levels.

Probably for commercial reasons again, data on absolute levels of rotor-stator interaction tones is sparse but in Ref.17 some data is given showing that the interaction tone power level is initially negligible and rises rapidly through "cut-off" speed to produce a near constant power level at higher speeds. At the usual blade-vane spacing of $g/c = 2$ this constant level was found to be $\approx 132 \text{ dB re } 10^{-12} \text{ watts}$ for a 52 inch diameter fan, see Fig.20.

* Throughout this lecture 2nd Harmonic is used to denote twice the fundamental frequency.

3.1.2.5 Sum and Difference Tones

Noise measurements of multistage compressors and fans with small substages have shown, see Fig.21, that frequencies representing the blade passing of each row are observed plus sums and differences of those frequencies. This can occur due to any one of a variety of interaction processes involving the moving and stationary blade rows.

A possible cause of this phenomena can be explained physically by considering a propagating interaction of the downstream rotor row with the preceding stator wakes. The observed frequency would be the downstream rotor blade passing frequency. Now suppose that the flow around the stators is excited (modulated) by the flow from the upstream rotor, then the stator wakes, and therefore the amplitude of the downstream rotor interaction tone, will be modulated at the upstream rotor blade passing frequency. Spectral analysis of such an acoustic signal will show the downstream rotor blade frequency plus and minus the upstream rotor blade frequency.

It is important to realise that this is only one of several plausible hypotheses for the cause and in due course no doubt experiments will define the important mechanisms.

4. BROAD BAND NOISE OF FANS

The random nature of broad band noise has made it more difficult initially to define the sources. However, it has been found, not unexpectedly, that the level of broad band noise produced by a fan rises with speed and with aerodynamic loading (throttling). In Ref.17 with limited data these general observations on a family of three fans were correlated using fan tip Mach number and the aerodynamic D-factor to represent the loading. (Two parameters, as found necessary in Section 2.5).

Recently, more comprehensive data from a wide variety of aero engine fan designs has been examined, Ref.20, and concluded that a better correlation is produced by taking rotor relative Mach number and tip incidence as the primary parameters. It is also found that the dominant noise source is self-excited noise of the rotor and any stator based sources are usually not significant. This, incidentally, is the form of prediction in Ref.4 of ten years earlier but this later finding is based on more representative experimental data.

In common with interaction tones (but apparently not with rotor-distortion tones), rotor blockage has a profound effect on the distribution of broad band noise radiated forward and rearward respectively. It is not convenient to treat broad band noise by the same techniques as are successful with discrete tones and the rotor blockage effect is observed on a purely empirical basis. The ratio forward to rearward acoustic power is found to be $(1 - M^8):(1 + M^8)$. This ratio is combined with an assumed source strength which varies radially in proportion to M^6 .

The resulting correlations found in Ref.20 are shown in Figs.17 and 18. The SPL's assessed there are the level of the peak $\frac{1}{3}$ rd octave band which occurs at 30° in the forward arc and around 110° in the rearward arc. The levels in other $\frac{1}{3}$ rd octave bands can be assessed by using Fig.19.

Although there is no pretence in Ref.20 that dimensional analysis was used to any great degree in the detailed studies the final form of the correlations can be related very closely to the form suggested by the analysis in Section 2.5. Namely, that:

- (i) Two parameters representing the aerodynamic conditions are necessary.
- (ii) The peak frequency scales with speed (actually blade passing frequency).

The scatter of results still evident in Figs.17 and 18 is attributed by the authors of Ref.20 to other design parameters of the fans. This is clearly consistent with any one of the unspecified geometric parameters which the dimensional analysis includes. More importantly, the analysis of Section 2.5 concludes that the SPL should strictly be normalised by $-10 \log_{10} \left(\frac{2^2 \rho a^2}{P_a} \left(\frac{P}{P_a} \right)^2 \right)$, not just $-10 \log_{10} \left(\frac{P}{P_a} \right)^2$, and it may be that in comparing fans of different pressure ratios the extra terms could be significant and may account for some of the scatter. The consistency of the observed broad band noise levels and the M^6 law suggests that dipole-type sources are dominating and that these sources are due to turbulence interacting with hard surfaces. The strong rotor blockage effects clearly shown in the broad band noise data are good evidence that the sources are in the downstream region of the rotor flow, but apparently for the results shown are associated with the rotor blades and not the exit guide vanes.

5. MULTIPLE PURE TONE OR "BUZZ-SAW" NOISE

The nature of the shock and expansion flow field existing upstream of fan running at supersonic tip speeds can be treated using two-dimensional theory to determine the propagation of an initially slightly uneven shock pattern. This "ordered" or deterministic approach while helpful in explaining the phenomenon is not easily applicable since it requires a determination or assumption of the initial variability in the individual shock strengths. Since the blades are usually designed to have identical shapes, this variability is deliberately small. In fact, it is better to allow for this variability by some statistical representation and calculate the typical development. This approach has been investigated at length in Ref.17 and it appears that

while fan blades with concave leading (suction) surfaces should produce on average less surviving (uncombined) shocks at the intake face, they will produce more noise than a fan with convex leading surfaces. The absolute level is dependent on the variability of the initial shocks and is better obtained empirically.

Figure 22, from Ref.17, shows the variations of normalised sound power with rotor tip Mach number from two large scale fans. The directivity of this sound power can be predicted as indicated in Section 2.3.2 and this is shown in Fig.23 where the computed directivity is plotted as a function of cut-off ratio. The latter can be calculated for any engine order, by recalling that all engine orders rotate at shaft speed. Note that engine orders which are "cut-off" are observed not to radiate efficiently.

The spectrum of "buzz-saw" noise is naturally random but usually is dominated by a pronounced peak in SPL at engine orders near half-blade passing frequency.

6. CONCLUDING REMARKS

This lecture has attempted to describe the current state of general knowledge of the mechanisms and control of Aero Engine Fan Noise. The limited understanding of some features is obvious and there are obviously ongoing investigations which will render outdated some of the statements here. It is worth, by way of a very brief statement of understanding as seen by the author, summarising the state of the art.

6.1 Subsonic Tone Noise Situation

The theory and mechanisms of tone noise generated by fans at subsonic speeds are reasonably well understood and control by "cut-off" is widely applied. Control by wave orientation (also due to blade/vane numbers) is probably not widely understood, nor is it experimentally proven. No practical means of reducing this source by reducing the stator response has been suggested or demonstrated, but some promise lies in controlling rotor wakes as a means of reducing this source of noise.

Means are actively being developed to eliminate the distortion-interaction tones on static tests which mask the interaction tones that are important in-flight.

6.2 Broad Band Noise

Good empirical correlations are tending to indicate that some sort of base level of broad band noise generation has been reached which is possibly dipole in nature. The precise source is not obvious, however, although the evidence suggests it is the flow in the region of the rotor tip since it correlates on tip relative Mach number and incidence.

6.3 Multiple Pure Tone Noise

Here, the mechanism is understood and can be calculated given sufficient rotor blading details. The source is related closely to the manufacturing tolerances of the fan blades and probably can be controlled only little at source. Conveniently, acoustic linings are particularly effective in reducing this source in practice.

It has not been the intention to carry out a complete review here of the literature on fan noise, nor to present all the theory which might be relevant, but simply to present that theory that can be usefully applied today. For the former purposes the review paper by Morfey, Ref.21, surveys the field well and lists as references most of the relevant papers.

REFERENCES

1. Lloyd P. "Some Aspects of Engine Noise".
Journal of R.Ae.Soc. Vol. 63 p541-548, 1959.
2. Tyler J.M. and Sofrin T.G. "Axial Compressor Noise Studies".
SAE Trans. Vol. 70 1962 p309-332.
3. Hetherington R. "Compressor Noise Generated by Fluctuating Lift
Resulting From Rotor Stator Interaction".
AIAA Journal Vol.1 No.2 1963, p473-474.
4. Smith M.J.T. and House M.E. "Internally Generated Noise From Gas Turbine
Engines. Measurement and Prediction".
ASME Journal of Engineering For Power, Vol.89
1967 p.177-190.
5. Sofrin T.G. and McCann J.C. "Pratt and Whitney Experience in Compressor Noise
Reduction".
Paper presented at 72nd Meeting of the Acoustical
Society of America, 1966.
6. Moore C.J. "In Duct Investigation of Subsonic Fan "Rotor Alone"
Noise.
J. Acoust. Soc.of America, Vol.51 (pt.1) 1972,
p1471-1481.
7. Sofrin T.G. and Pickett G.F. "Multiple Pure Tone Noise Generated by Fans at
Supersonic Tip Speeds".
Int.Symp.Fluid Mech.and Des. of Turbomachinery Penn.
State University 1970. NASA SP 304, ptII.
8. Mather J.S.B. "New Observations on Tone Generation in Fans".
Savidge J. and Fisher M.J. Journal of Sound & Vibration, Vol. 16 p407-418,
1971.
9. Ffowcs-Williams J.E. "Sound Generation by Turbulence and Surfaces in
and Arbitrary Motion".
Hawkings D.L. Phil.Trans.of Roy.Soc. (London)A264, 321-342, 1969.
10. Lowson M.V. "Theoretical Analysis of Compressor Noise".
Journal of Acoustic Soc. of American Vol. 47 No.1
(pt.2) p371-385.
11. Lansing L. "Exact Solution For Radiation of Sound From a Semi-
Infinite Circular Duct With Application to Fan and
Compressor Noise".
Proc. of Symp. at NASA Ames, NASA SP228.
12. Lowrie B.W. "Simulation of Flight Effects on Aero Engine Fan Noise".
AIAA 2nd Aero-Acoustics Specialists Conference,
1975 AIAA Paper 75-463.
13. Merriman J.E. and Good R.C. "The effect of Forward Motion on Fan Noise"
AIAA paper 75-464, March 1975.
14. Kemp N.H. and Sears W.R. "Aerodynamic Interference Between Moving Blade Rows".
Journal of Aeronautical Sciences, Vol.20, No.9 1953
p585-597.
15. Kemp N.H. and Sears W.R. "Unsteady Forces Due to Viscous Wakes in Turbomachines".
Journal of the Aeronautical Sciences, Vol.22 No.7 1955
p478-483.
16. Silverstein A., Katgoff S and Bullivant W.K. "Downwash and Wake Behind Plain and Flapped Aerofoils".
NASA Report 651, 1939.

17. Burdsall E.A. and Urban R.H. "Fan-Compressor Noise: Prediction, Research, and Reduction Studies". USA, DOT/FAA Report FAA-RD-71-73, February 1971.
18. Philpott M.G. "The Role of Rotor Blockage in the Propagation of Fan Noise Interaction Tones". AIAA Paper 75-447, March 1975 .
19. Amiet R.K. "Transmission and Reflection of Sound by Two Blade Rows". Journal of Sound and Vibration 34(3), 1974 p399-412.
20. Ginder R.B. and Newby D.R. "A Study of Factors Affecting the Broadband Noise of High Speed Fans". AIAA Paper 76-567, July 1976.
21. Morfey C.L. "Rotating Blades and Aerodynamic Sound". Journal of Sound and Vibration 1973 28(3) p587-617.

SPECTRA FROM A SMALL MODEL FAN WITH
OUTLET GUIDE VANES, 60° TO INTAKE AXIS.
TIP RELATIVE MACH NUMBER 0.72

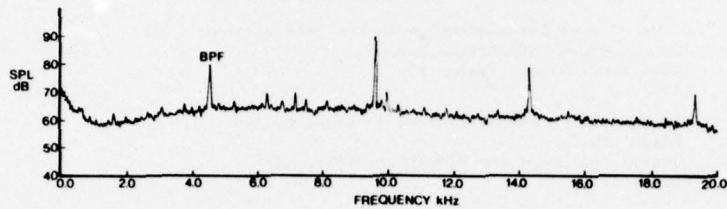


Fig. 1

Typical Buzz Saw Spectrum

60° TO INTAKE AXIS 1350 F.P.S. TIP SPEED

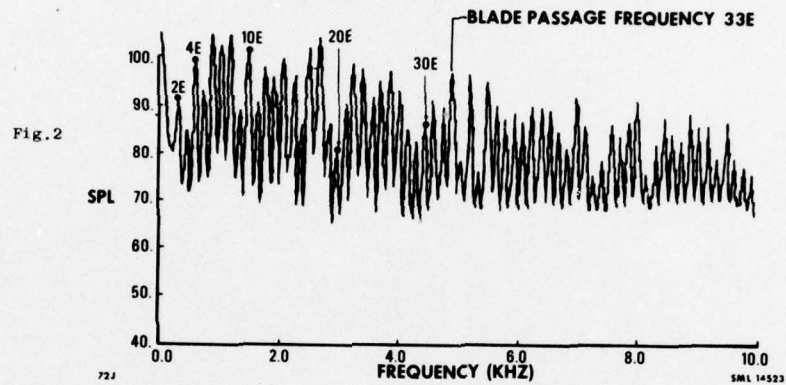


Fig. 2

GRAPHS OF THE BESSEL FUNCTIONS
OF ORDER $m = 0, 1, 2$

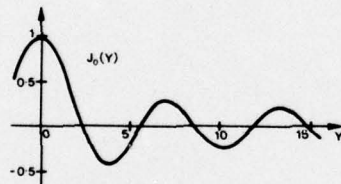
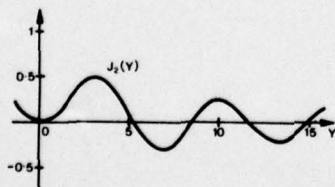
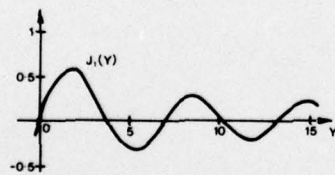


Fig. 3



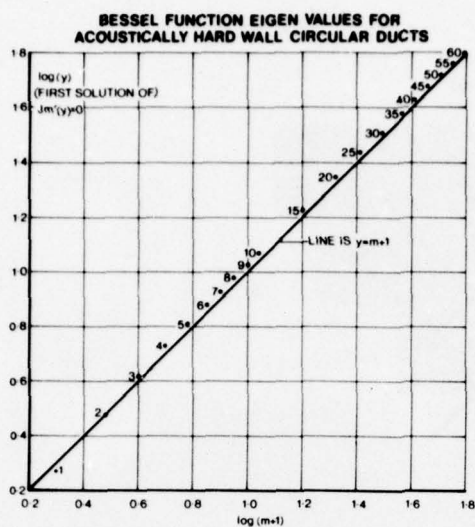


Fig. 4

AXIAL VARIATION OF SEVERAL HARMONICS OF THE FAN BLADE-PASSING FREQUENCY, OBTAINED FROM FOURIER ANALYSIS OF AVERAGED WAVEFORMS AT VARIOUS AXIAL POSITIONS. BROKEN LINES SHOW THEORETICAL DECAY RATES.

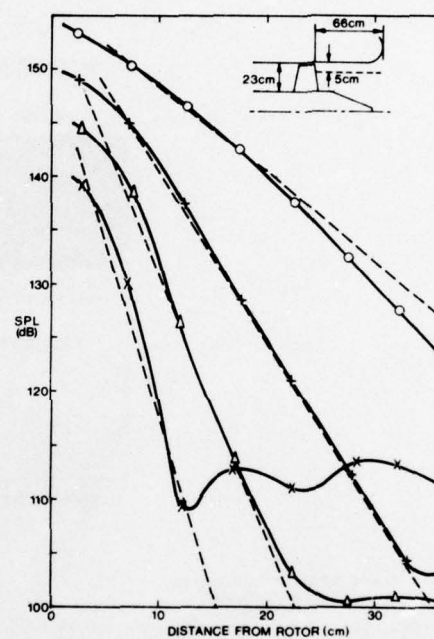


Fig. 5

ILLUSTRATION OF ROTOR STATOR INTERACTIONS

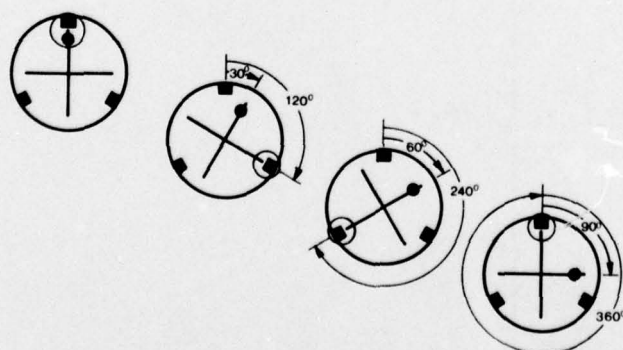


Fig. 6

SHOCK WAVE PATTERN FROM AN ACTUAL FAN

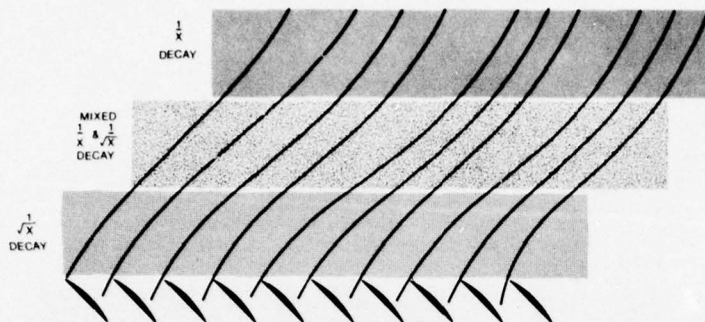


Fig. 7

WAVEFORMS AND SPECTRA IN COMBINATION
TONE DEVELOPMENT

PRESSURE SIGNATURE

PRESSURE SIGNATURE

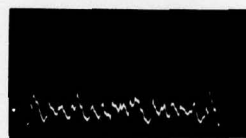
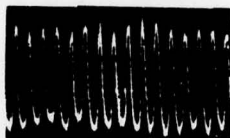
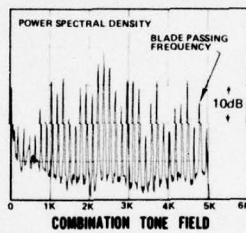
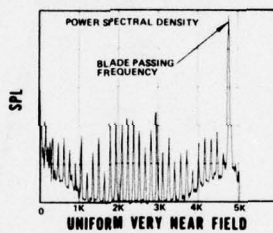


Fig. 8



UNIFORM VERY NEAR FIELD

COMBINATION TONE FIELD

COMPUTED RADIATION PATTERNS
FOR CYLINDRICAL DUCT

m=1, p=0 MODE

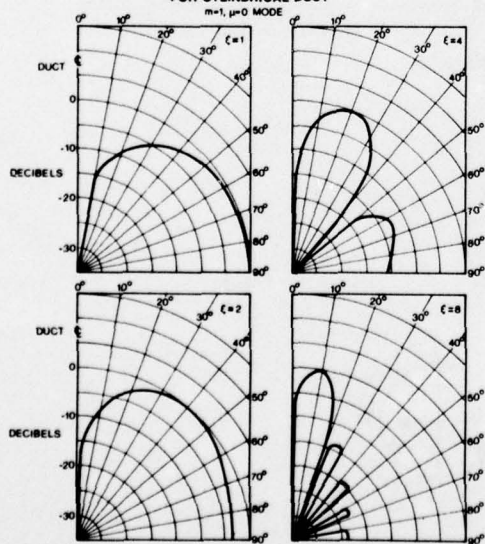


Fig. 9

THE VARIATION OF THE PRINCIPLE LOBE RADIATION ANGLE
WITH MODE CUT-ON RATIO

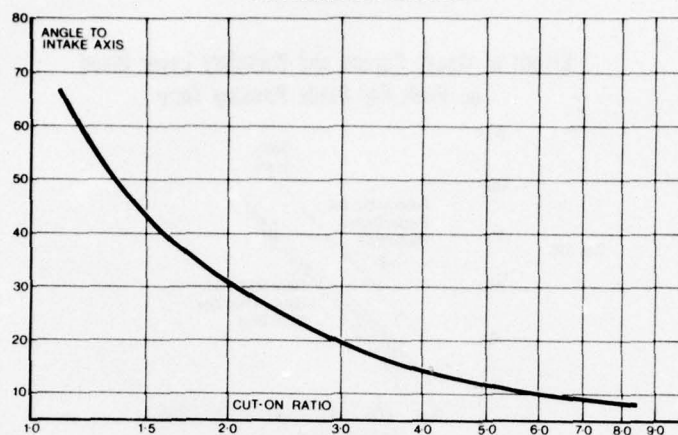


Fig.10

FAN BROADBAND NOISE
POLAR FIELD SHAPE

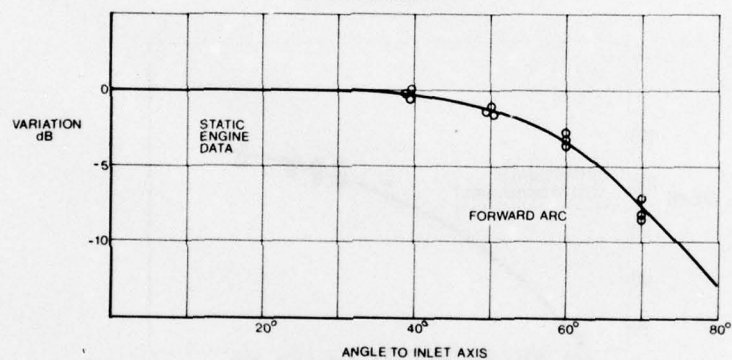


Fig.11

POLAR FIELD SHAPE OF B.P.F. FUNDAMENTAL TONE FROM SMALL MODEL FAN.
TIP RELATIVE MACH. NUMBER 0.72

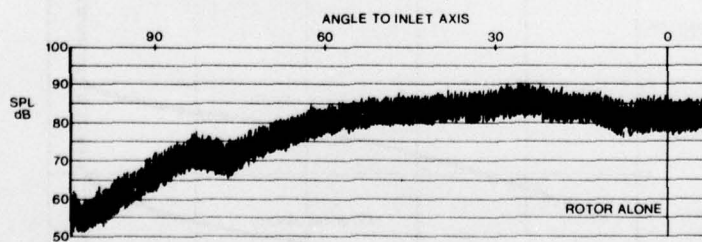


Fig.12

Effect of Gauze Screen and Boundary Layer Bleed on Peak Fan Blade Passing Tone

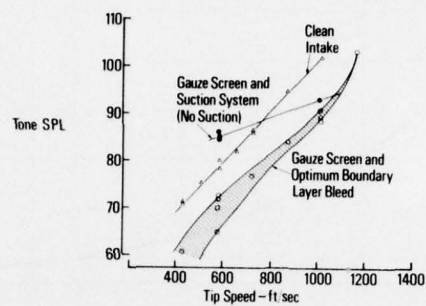


Fig. 13

Blade Passing Tone Level of 20 Inch Fan

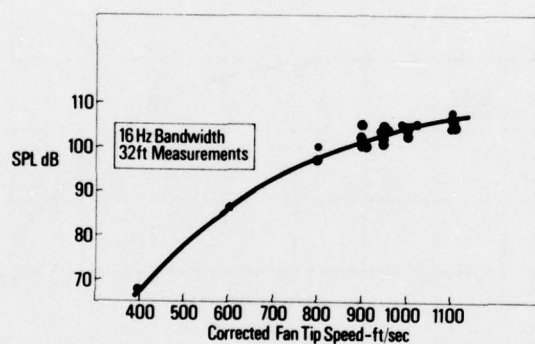


Fig. 14

EFFECT OF VARYING BLADE NUMBERS 2nd B.P.F.

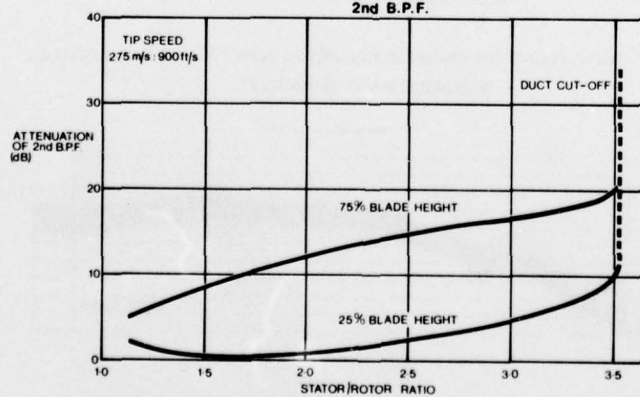


Fig. 15

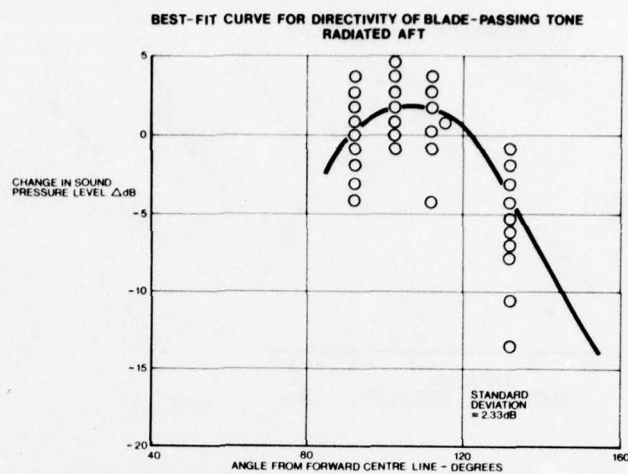


Fig. 16

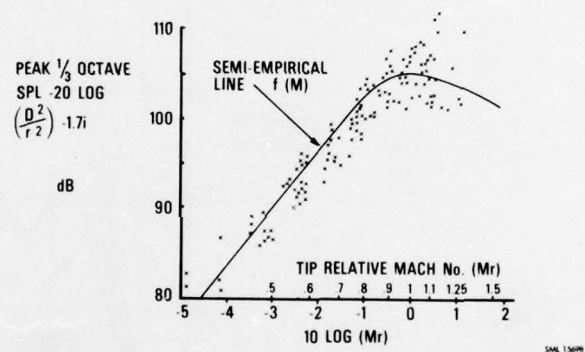
Forward Arc Correlation

Fig. 17

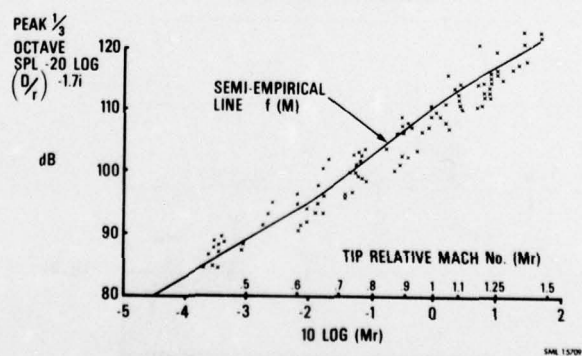
Rear Arc Correlation

Fig. 18

Fan Broadband Noise Spectra

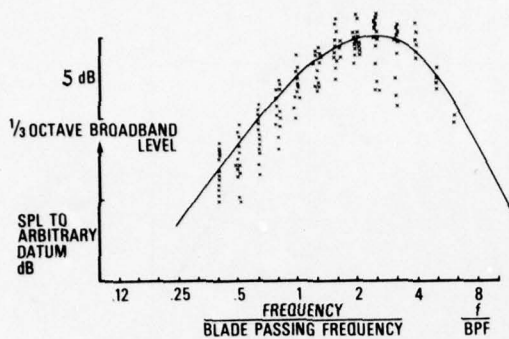


Fig. 19

EFFECT OF ROTOR-STATOR SPACING ON AFT RADIATED BLADE-PASSING FREQUENCY POWER LEVEL

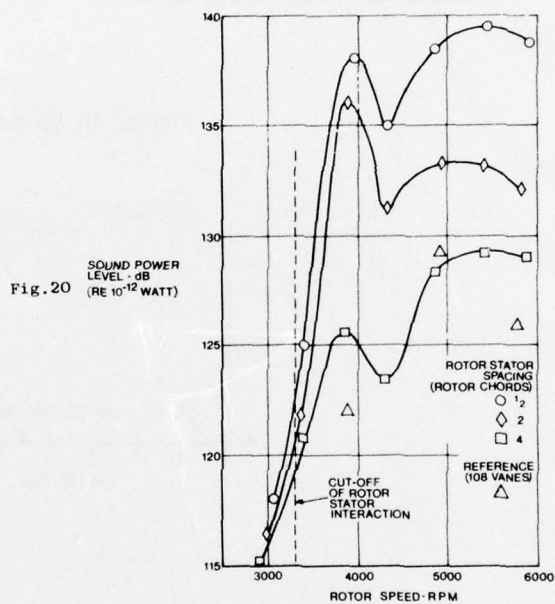


Fig. 20

NARROW BAND ANALYSIS OF CF6 NOISE IN THE AFT QUADRANT-APPROACH POWER

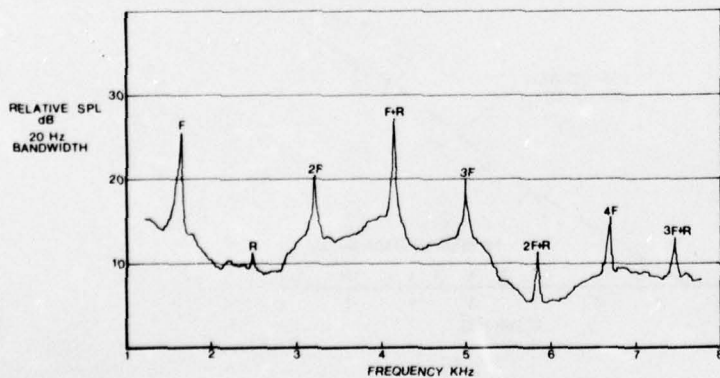


Fig. 21

OVERALL COMBINATION TONE SOUND POWER NORMALIZATION

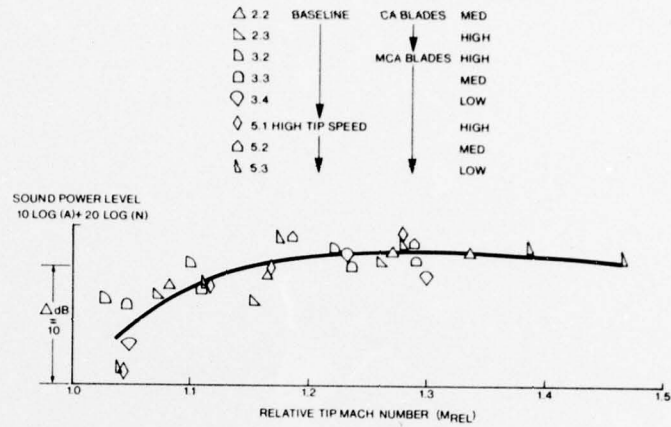


Fig. 22

COMBINATION TONE DIRECTIVITY INDEX

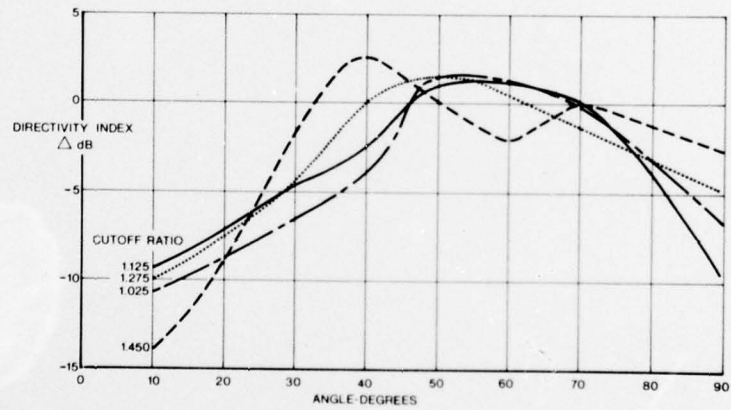


Fig. 23

AIRFRAME SELF-NOISE — FOUR YEARS OF RESEARCH

Jay C. Hardin
 NASA Langley Research Center
 Hampton, Virginia 23665, U.S.A.

SUMMARY

This paper presents a critical assessment of the state of the art in airframe self-noise. Full-scale data on the intensity, spectra, and directivity of this noise source are evaluated in the light of the comprehensive theory developed by Ffowcs-Williams and Hawkings. Vibration of panels on the aircraft is identified as a possible additional source of airframe noise. The present understanding and methods for prediction of other component sources — airfoils, struts, and cavities — are discussed and areas for further research as well as potential methods for airframe noise reduction are identified. Finally, the various experimental methods which have been developed for airframe noise research are discussed and sample results are presented.

INTRODUCTION

The importance of airframe self-noise as the "ultimate noise barrier" to the reduction of noise levels produced by future commercial aircraft was recognized just 4 years ago as a result of NASA-sponsored research on the Advanced Technology Transport.¹ This work included preliminary calculations, based upon sailplane data, which indicated that the nonpropulsive noise produced by a large subsonic aircraft on landing approach lay only approximately 10 EPNdB below the FAR-36 certification levels. The surprisingly high intensity of this hitherto neglected noise source could, if verified, impose a troublesome lower bound on aircraft noise reduction. Thus, significant research efforts toward experimental evaluation of the magnitude and characteristics of airframe self-noise were stimulated.

Verification of the existence of these high levels involved ground measurements of noise produced by large aircraft during landing approach flyovers. Such measurements are difficult to make and interpret since, for safety reasons, such aircraft usually cannot be flown without power (deadstick). Thus, there is the necessity for some method of separating the airframe or nonpropulsive noise from the engine noise, as well as for accurate determination of the aircraft position and velocity for correlation with noise data. Nevertheless, the work was pursued with the result that the predicted levels were generally confirmed. For example, The Boeing Company has cited measured airframe noise levels for the 727 and 747 aircraft² approximately 8 EPNdB below FAR-36 standards.

The significance of this lower bound set by airframe noise lay in its impact on future noise regulations. Since it would be counterproductive to require engine noise levels much below those of nonpropulsive sources, the potential for further overall aircraft noise reductions is limited unless nonpropulsive noise generation can be controlled.

For this purpose, airframe self-noise research was begun, with the goals of understanding the generation and propagation of aircraft nonpropulsive noise as well as its reduction at the source. The first such attempts were empirical in nature, involving correlations of airframe noise measurements with gross aircraft parameters such as weight, velocity, and aspect ratio.³ Such studies led to useful prediction schemes but did little to identify and rank order the sources of the noise. Gradually, however, some understanding of the actual sources and their relative importance began to emerge. For the "clean" (cruise configured) aircraft, it is now generally conceded that the primary sources are associated with the interactions of the wake of the wing with the wing itself, while for the "dirty" (landing configured) aircraft, noise generated by the flaps and the landing gear/wheel well combination becomes dominant. Attempts are now being made to study these individual component sources in isolation in order to better characterize the physical mechanisms involved.

This paper contains a critical assessment of the present understanding of airframe self-noise in order to identify potential methods of noise reduction as well as to highlight areas where further research is needed. A review of full-scale data on the magnitude, spectra, and directivity of this type of aircraft noise is presented, followed by a discussion of theory in an attempt to establish a theoretical framework which can explain the observations. Analytical models for noise generation by the individual component sources are reviewed, and the various measurement techniques now being employed in airframe noise research are evaluated.

AN OVERVIEW OF AIRFRAME NOISE

There are many potential sources of airframe noise on an aircraft, as shown schematically in Figure 1. Each of these sources is believed to have its own characteristic amplitude, spectrum, and directivity. If one measures the overall airframe noise produced by an aircraft, one sees the resultant produced by the summation of these individual sources. While this may be confusing from the standpoint of defining and evaluating mechanisms, it is, nevertheless, the noise field of ultimate interest. Thus, it may be useful to review available overall airframe noise measurements.

A table listing 65 data points published prior to 1975 has been compiled by Hardin et al.⁴ However, many of these early data were obtained using less than optimum measurement and analysis techniques. Microphones were often pole mounted in order to compare results with certification levels, determination

of the aircraft position and velocity was crude, and only minimal efforts to remove the effects of residual engine noise were made. Recently, however, two studies which attempt to overcome these objections were published.

The first of these studies⁵ presented measurements of Aerocommander, Jetstar, CV-990, and B-747 aircraft. The microphones were mounted flush with the ground to remove spectral distortion produced by reflection and radar was employed to track the aircraft as it flew a nearly constant airspeed glide slope over the microphone array. Some data obtained in this study for the clean configurations are listed in Table 1 and are plotted in Figure 2. The data in Figure 2 were normalized to an altitude of 152 meters by assuming an inverse square dependence on distance but were not corrected for pressure doubling effects due to the flush mounting of the microphones. Data from Reference 5 on the Aerocommander are not included as this aircraft is propeller driven and exhibited significantly higher normalized sound levels which the authors attributed to noise generation by the feathered propellers.

Also presented in Table 1 and Figure 2 are clean configuration data on the HS125, BAC111, and VC10 obtained by Fethney.⁶ This study employed flush-mounted microphones and a kine-theodolite system for precise position tracking, repeat flights to reduce statistical variability in the data, and extensive efforts to determine and remove residual engine noise from the data. These data on the figure are also normalized to an altitude of 152 meters and are not corrected for ground augmentation. Reference 6 also contained data on the HP115, a delta-winged research aircraft, which is not included herein due to the fact that it had nonretractable landing gear.

The data presented in Figure 2 indicate the airframe noise level directly beneath the various clean configured aircraft flying at an altitude of 152 meters as a function of airspeed. Also shown on the figure is a line indicating the expected behavior if these levels exhibited fifth-power dependence on velocity. By noting the sets of data points for individual aircraft, it can be seen that the velocity dependence is approximately the fifth power. This is a lower velocity dependence than would be observed for a dipole source.

The airframe noise levels generated in the landing configuration are believed to be more dependent upon the detailed design of the aircraft than those of the cruise configuration. Several additional components such as leading-edge slats, trailing-edge flaps, landing gear, and wheel wells are deployed during landing whose relative contributions to the overall noise may vary considerably from aircraft to aircraft. Further, these sources are not necessarily independent, but may interact with each other due to changes in the total flow field. Although it is difficult to directly measure the effects of the individual components on the airframe noise, Fethney⁶ made some estimates based upon measurements for the VC10. The data shown in Figure 3 for comparison are decibel increases over the clean configuration overall sound pressure level as produced by several different flight conditions. The total change in airframe noise level from the cruise to approach configurations for this aircraft was 11 dB. Either flap deployment or landing gear deployment with open wheel well is estimated to account for about 9 dB individually. Note that the difference in noise level between open and shut undercarriage doors is estimated to be about 4 dB. This seems to indicate that substantial noise may be generated by large open cavities which suggests a method for noise reduction on those aircraft whose undercarriage doors normally remain open after gear deployment.

Based upon early measurements, Healy⁷ suggested that airframe noise directly below an aircraft produced a "haystack" type spectrum which peaked at a constant Strouhal number based on airspeed and a characteristic wing thickness. More recent measurements indicate a much more complex spectrum. Figure 4 displays the peak one-third-octave band spectra normalized to equal overall sound pressure levels (OASPL) for the clean configured Jetstar, CV-990, and 747 aircraft as measured by Putnam et al.⁵ Although such measurements are complicated due to the fact that the moving source produces a nonstationary signal, third-octave analyses are generally reliable as long as short averaging times are employed. Note that the spectra exhibit two peaks, a lower one in the vicinity of 200 Hz, which corresponds roughly to the frequency predicted by Healy's Strouhal relation, and a higher one near 1250 Hz. However, Putnam et al. stated the surprising result that the shape of these spectra and the position of the peaks showed no consistent change with airspeed. Spectra for the HS125 and BAC111 obtained by Fethney⁶ display the same shape and peak location.

The change in spectrum shape for the VC10 in going from the clean to dirty configurations is illustrated by the data of Figure 5. The characteristic double peaked clean spectrum is not discernible for this aircraft. The major difference in the dirty configuration spectrum is a broadband increase in level, particularly at the low-frequency end. Figure 6 shows a narrow-band analysis of the low-frequency portion of spectra, similar to those of Figure 5, obtained under somewhat different flight conditions. Note the appearance of narrow peaks in both the clean and dirty configurations.

The directivity of airframe noise has only recently begun to be explored and only a modest amount of data exist in the open literature. Figures 7 and 8 depict spectra directly below and to the side, respectively, of the HP115 aircraft in the cruise configuration. (Note that this aircraft has a non-retractable landing gear.) Although this is a delta-wing craft, it exhibits essentially the same spectral shape below as that observed by Putnam et al.⁵ for more conventional configurations. To the side, however, the higher frequency peak shifts from about 1 kHz to 2 kHz. This behavior indicates that different noise sources may dominate at different angles with respect to the aircraft.

Figure 9 portrays the reductions in measured overall noise levels (over those directly below the aircraft) with sideline distance for the four aircraft tested by Fethney.⁶ These data are compared with predicted reductions based upon considering the total aircraft either as a point monopole (solid curve) or as a point dipole (dashed curve) oriented in the lift direction. The fact that the data cluster about the solid curve indicates a monopole-like fall off to the side. Similar behavior has been observed by Lasagna and Putnam⁸ for the Jetstar aircraft in the landing configuration. This result is important in its implications for the source type dominant in airframe noise as well as for the airframe noise "footprint."

Figure 10 shows airframe noise measurements in the flyover plane for a clean configured Douglas DC-10 aircraft.⁹ The data have been corrected for an inverse square falloff with distance and are plotted as a

function of λ , the angle of the approaching aircraft with respect to the horizontal. (Before normalizing, the airframe noise peaked slightly before the aircraft was directly overhead.)

The above measured data are compared with calculated values of the sum of two dipoles oriented, respectively, in the lift and drag directions. Note that the main directivity features of the measurements are supported by the calculations. The best agreement between the measured data and this theoretical approach is obtained when the dipoles are negatively correlated.

A THEORETICAL BASIS FOR AIRFRAME NOISE

The most inclusive theoretical basis for the study of sound production by the airframe is that developed by Ffowcs-Williams and Hawkins¹⁰ who extended the Lighthill-Curle¹¹⁻¹³ theory of aerodynamic sound generation to include arbitrary convection motion. For this case, the wave equation governing the generation and propagation of sound admits the general solution

$$4\pi a^2 (\phi(\vec{x}, t) - \rho_0) = \frac{\partial^2}{\partial x_i \partial x_j} \int_V \left[\frac{T_{ij} J}{r |1 - M_r|} \right] d\vec{r} - \frac{\partial}{\partial x_i} \int_S \left[\frac{P_{ij} n_j A}{r |1 - M_r|} \right] dS(\vec{r}) + \frac{\partial}{\partial t} \int_S \left[\frac{\rho_0 v_n}{r |1 - M_r|} \right] dS(\vec{r}) \quad (1)$$

This solution implies that the sound sources may be represented by a quadrupole distribution related to the Lighthill stress tensor T_{ij} within the volume of turbulence, a surface distribution of dipoles dependent upon the compressive stress tensor P_{ij} and a surface distribution of monopoles produced by the normal velocity of the surface v_n . Ffowcs-Williams and Hawkins¹⁰ further showed that, for the case of a rigid surface, the monopole distribution degenerates into a distribution of dipoles and quadrupoles throughout the volume contained within the surface.

In the majority of airframe noise research to date, the aircraft has been assumed to be rigid. Application of this assumption in the above theory implies that airframe noise consists of a distribution of dipoles and quadrupoles. Further, at the low Mach numbers of interest (approximately 0.3 for landing approach), the quadrupole distribution has been neglected. Thus, airframe noise sources have been considered as dipole in nature. These dipole sources have also been assumed to be compact and, often, replaced by equivalent point dipoles acting at the center of the distribution.

Several aspects of experimental data regarding airframe noise are difficult, if not impossible, to explain in terms of such a theory.

First, the velocity dependence of airframe noise has consistently been found to be less than the sixth power which would be expected of an aerodynamic dipole. This result has led to considerable interest in the theories of Ffowcs-Williams and Hall¹⁴ and Powell.¹⁵ They considered the radiation from a volume of turbulence near the edge of a rigid halfplane and found that the sound production of quadrupoles with axes in a plane normal to the edge was enhanced such that the far-field sound intensity varied as the fifth power of the typical fluid velocity. However, there was no enhancement of quadrupoles with axes parallel to the edge.

Second, the definite monopole-like sideline directivity of airframe noise, which has been observed by independent research groups, is hard to understand on the basis of a purely dipole theory. Certainly, it is possible for three mutually perpendicular dipoles to masquerade as a monopole. However, this requires them to be statistically independent and of equal amplitude. While it is not hard to imagine the overall fluctuating lift and drag forces on an aircraft to be the same order of magnitude, a fluctuating side force of equal strength is more difficult to visualize. About the only place where such a force could exist in the clean configuration is on the vertical tail. However, since it is much smaller in area than the wing surface, much higher fluctuating pressures on its surface would be required.

Finally, the source of the high-frequency peak in the airframe noise spectrum (see Fig. 4) is puzzling. This peak, which was observed by both Putnam et al.⁵ and Fethney,⁶ is higher in frequency than that expected from known wing noise mechanisms and seems to be relatively insensitive to airspeed. Since the frequency of an aeroacoustic source ordinarily scales on airspeed, the presence of this peak suggests the possibility of radiation from fundamental vibratory modes of the aircraft structure. Although such vibration has not previously been considered as a source of airframe noise, just such a spectral peak has been observed by Davies¹⁶ who investigated sound produced by turbulent boundary-layer excited panels. Shown in Figure 11 is the one-third-octave band spectrum of acoustic power radiated by a 0.28-meter by 0.33-meter steel panel of 0.08 mm thickness which was mounted in the side of a low-turbulence wind tunnel. Davies found that the frequency of this peak was reasonably independent of flow speed.

A similar spectrum has also been observed by Maestrello¹⁷ who reported interior measurements in an unupholstered Boeing 720 aircraft. Shown in Figure 12 are spectra of panel acceleration as well as sound pressure level close to the panel for the aircraft in flight at a Mach number of 0.87 and an altitude of 7700 meters. Also shown are the changes in these spectra with cabin pressure. Maestrello notes that the sound pressure level varies as the fifth power of velocity. He further observes that most sound radiation comes from the edges of the panels and demonstrates methods for noise reduction by stiffening the panel boundaries. If panel vibration is truly responsible for the high-frequency peak observed in airframe noise radiation, Maestrello's techniques offer a direct method of noise reduction.

The above phenomena emphasize the necessity of a closer look at the assumptions employed in the theory of airframe noise. While it is wise to recall that there are many absolutely equivalent formulations of aeroacoustic sources, the enhancement of quadrupole sources in the vicinity of an edge as predicted by Ffowcs-Williams and Hall¹⁴ and Powell¹⁵ suggests that quadrupole terms in any theoretical formulation should not be dismissed lightly. Further, the evidence cited previously which indicates that vibration may be a source of airframe noise brings into question the assumption of rigidity. If the surface vibrates, the monopole source term in Equation (1) may dominate which would explain the monopole-like sideline directivity that has been observed. Of course, there is still no mass addition to the flow but, due to

the size of the body, each point on the surface may be acting as a baffled piston unable to effectively interfere with its mate of opposite phase elsewhere. The large size of the body also sheds doubt on the assumption of compactness. The spatial extent of the source region is of the order of the span of the aircraft while a typical frequency of interest has a wavelength of 0.5 meter. It is possible to take into account the correlation length of the source distribution and replace each correlated region by a point source as suggested in Reference 18. However, even the correlation length may be of the order of, or larger than, the wavelength. Thus, the assumption of compact sources cannot be rigorously justified. Further, this "component source technique" neglects diffraction of the sources by the fuselage which may be important in airframe noise and could be partially responsible for the observed directivity pattern.

COMPONENT SOURCES OF AIRFRAME NOISE

As noted earlier in this paper, airframe noise is the resultant of many different noise generating mechanisms. Thus, in order to render the research problem more manageable, it is prudent to identify and evaluate these individual sources.

The work of Curle,¹³ who extended Lighthill's^{11,12} theory to include the case where rigid bodies are present within the field of interest, showed that the sound generation in the presence of a body could be expressed by a distribution of dipoles over its surface in addition to the usual volume integral. The strength of these dipoles is related to the fluctuating pressure experienced by the surface. This theory is exact and highly useful for computational purposes. However, it has led to a certain amount of confusion about the roles of surfaces in sound generation. Actually, a rigid surface can produce no sound, as can be seen by noting that the acoustic energy flux must approach zero close to a rigid surface.¹⁹ Thus, the true sources of sound are disturbances within the flow field itself and the surface can act only in changing the strengths of these volume sources and in reflecting and diffracting the sound they produce. The fact that the flow disturbances generate the fluctuating pressures on the surface is responsible for the alternate description of the sound production. The importance of this result is that it emphasizes the vital role played by the local flow field about the airframe components. Little is known about such flows.

The many different noise generating mechanisms which comprise airframe noise can be crudely classed in terms of three simple models, that is, noise generation by cylinders, streamlined bodies, and cavities. Although the geometry of real aircraft may differ substantially from the models which have been analytically and experimentally studied, it is assumed that the basic noise generation mechanisms remain valid. As a comprehensive review of the literature has been attempted by Hardin et al.,⁴ only the best present understanding of these mechanisms will be discussed.

Cylinders

Perhaps the simplest and best understood of all examples of sound generation by flow/surface interaction is that of a cylinder in a flow. Fortunately, this is also a useful example as the entire undercarriages of aircraft are constructed essentially of cylinders of various lengths and orientations. As the flow attempts to negotiate the cylindrical contour, it separates from the surface creating a turbulent wake. This wake is highly vortical which results in a solenoidal velocity field that induces fluctuating forces on the cylinder in the streamwise and normal directions. The situation is shown schematically in Figure 13.

The exact nature of the wake and, thus, the sound produced is highly dependent upon the Reynolds number ($Re = Ud/\nu$, where U is the flow speed and d is the cylinder diameter) of the flow. Typical Reynolds numbers for aircraft undercarriage components during landing approach are in the range 10^5 to 10^6 . In this range, the classical periodic Von Karman vortex street breaks down and the wake becomes random. The most relevant work in this area is that by Fung²⁰ who studied the fluctuating lift and drag forces on cylinders for the range $3 \times 10^5 < Re < 1.4 \times 10^6$. He found the root-mean-square fluctuating lift and drag coefficients to be 0.13 and 0.04, respectively, that is

$$C_L = \sqrt{\frac{\overline{F_N^2}}{qA_P}} = 0.13 \quad (2)$$

and

$$C_D = \sqrt{\frac{\overline{F_D^2}}{qA_P}} = 0.04$$

where the overbar indicates a time average, $q = 1/2 \rho_0 U^2$ is the dynamic pressure and $A_P = \ell d$ is the projected area where ℓ and d are the length and diameter of the cylinder, respectively. Unfortunately, the correlation of these lift and drag forces was not measured. The manner in which they are correlated could have a significant effect on the noise produced.

In the case of a cylindrical component of an aircraft, if it is assumed that wavelengths of the sound produced are large compared with the dimensions of the cylinder, retarded time differences in the source region may be neglected and the sound calculated as if from a moving point dipole through the theory of Lowson.²¹ Further, in the absence of any information on the correlation of fluctuating lift and drag and noting that the RMS drag is only a third of the lift, the drag contribution will be neglected entirely. Thus, assuming the aircraft to be flying at the constant airspeed U , the acoustic pressure at the observer location x is given by

$$p(\vec{x}, t + \frac{r}{a}) = \frac{\cos \beta}{4\pi(1 - M_r)^2 ar} \frac{dF_N(t)}{dt} \quad (3)$$

where β is the angle between the force and the observer direction and $M_r = M \cos \theta$ where $M = U/a$ and θ is the angle between the flight path and the observer direction. Thus, taking the aircraft to be far enough from the observer that changes in β , θ , and r are negligible over the time for which the fluctuating force is correlated, the spectrum of acoustic pressure at the observer location is related to the spectrum of the fluctuating lift through

$$S_a(\vec{x}, \omega) = \frac{\cos^2 \beta}{16\pi^2(1 - M_r)^4 a^2 r^2} \omega^2 S_N(\omega) \quad (4)$$

Measurements of the spectrum of the fluctuating lift on a circular cylinder in the appropriate Reynolds number range have also been obtained by Fung.²⁰ Figure 14 presents Fung's data on the normalized power spectrum of lift fluctuations at a Reynolds number of 5.7×10^5 in comparison with the analytical relation

$$S_N(\omega) = \frac{2 F_N^2 d}{\pi U} \sqrt{\frac{\alpha}{\pi}} \left(\frac{\omega d}{2\pi U} \right)^2 e^{-\alpha \left(\frac{\omega d}{2\pi U} \right)^2} \quad (5)$$

where α is a nondimensional parameter taken as 6.94×10^1 . This spectrum is defined such that the total power is obtained by integrating over only nonnegative frequencies.

Since Fung found that the normalized spectra at other Reynolds numbers in the range of interest were not appreciably different, Equation (5) may be employed in Equation (4) to calculate the mean-square acoustic pressure at the observer location, that is

$$\overline{p^2(\vec{x})} = \int_0^\infty S_a(\vec{x}, \omega) d\omega = \frac{3}{8} \frac{F_N^2 M^2 \cos^2 \beta}{(1 - M_r)^4 r^2 d^2 \alpha} \quad (6)$$

with the resulting overall sound pressure level

$$\text{OASPL}(r, \beta, \theta) = 10 \log_{10} \left(\frac{\overline{p^2(\vec{x})}}{p_0^2} \right) \quad (7)$$

where p_0 is a reference pressure usually taken as $2 \times 10^{-5} \text{ N/m}^2$. Equations (4) and (7) may be employed to estimate the spectra and overall sound-pressure levels produced by moving cylinders.

Streamlined Bodies

The most fundamental (in the sense of being omnipresent) component source of airframe noise is produced by the flow over the streamlined surfaces of the aircraft. Taking such surfaces to be rigid (i.e., neglecting any radiation due to panel vibration which was indicated as a possible source earlier in the paper), a dipolelike sound generation may still be observed which can be related to the fluctuating forces experienced by the surface. There are three mechanisms²² by which such forces may be developed: the pressure field arising in the turbulent boundary layer over the surface, force fluctuations induced by vorticity shed from the surface, and the action of any turbulence present in the incident stream. However, these phenomena are not equally efficient in noise generation and, of course, their relative contributions vary with the characteristics of the flow field in which the surface is placed.

Boundary-Layer Turbulence. The question of sound generation by boundary-layer turbulence has been effectively resolved by Powell²³ who used the "reflection principle" to show that the major surface dipoles vanish on an infinite, flat, rigid surface leaving only the viscous dipoles with axes lying in the surface itself. Since such viscous stresses can only become significant at Reynolds numbers much smaller than those developed on commercial aircraft, direct radiation from the turbulent boundary layer is a much less efficient source of direct radiation than others present even for moderately curved surfaces (as long as no separation occurs). This result remains valid for finite surfaces when the surface is larger than the sound wavelength — which is usually the case in airframe noise — except near the edges. This "edge noise" source will be discussed below.

In reference to the panel vibration source proposed earlier in this paper, it might be mentioned that Laufer et al.²⁴ have considered the case where the surface is flexible and able to respond to the boundary-layer excitation. They remark that for surfaces of limited extent, wall motion becomes equivalent to a simple source system of high acoustic efficiency and can quickly become the most important feature of the practical boundary-layer-noise problem. Thus, it appears that the boundary-layer pressure fluctuations are not major sources of noise, but the aircraft surface may generate sound through vibration and may reflect sound produced by other sources. Both of these roles require further research for better understanding.

Wake Vorticity. Sound generation by force fluctuations induced by vorticity shed from the surface is probably the primary cause for the experimentally observed fact that aerodynamic surfaces radiate predominantly from slender strips along their edges. At the edge of an aerodynamic surface, the flow must separate shedding vorticity into a wake. This vorticity will induce fluctuating surface pressures which fall off with distance from the vortex. Thus, the largest pressures will occur close to the edge. In addition, noncancellation of boundary-layer fluctuations also occurs in this region. Which of these

effects is dominant is not known at this time, although wake induced pressures normally should be more intense. However, both point to "edge noise" as a primary source of airframe sound generation.

The present understanding of this source is well depicted by Figure 15 which is taken from a report by Siddon.²⁵ Siddon suggests that alternate vortex shedding, with a fairly narrow band of preferred frequencies, leads to a time-dependent relaxation of the Kutta condition at the trailing edge. The "stagnation streamline" switches cyclically from the upper to the lower surface, thus inducing a fluctuating force concentration near the edge. Note that this is exactly the same mechanism responsible for the production of strut noise as discussed earlier.

There has been extensive work on the prediction of this edge noise source and numerous, sometimes conflicting, theories have been produced.⁴ Again, the generation process is highly dependent upon Reynolds number. Much recent work^{26,27} has dealt with the intense tones which can be produced by isolated airfoils with laminar boundary layers. However, such tones require Reynolds numbers based on airfoil chord length of less than about 2×10^6 while commercial aircraft ordinarily exhibit Reynolds numbers of many millions. At these higher Reynolds numbers, a transition similar to the collapse of the classical Von Karman street behind a cylinder apparently occurs and a more broadband radiation results.

Fink²⁸ has experimentally evaluated the various theories for trailing-edge noise generation. He concludes that the best present theories are those by Ffowcs-Williams and Hall¹⁴ and Powell.¹⁵ The first of these papers considers the scattering of sound generation by Lighthill type quadrupoles due to the presence of a half plane in the flow. The results show that sound output of quadrupoles associated with fluid motion in a plane normal to the edge is increased by a factor $(Kr_0)^{-3}$ where $K = \omega/a$ is the acoustic wave number and r_0 is the distance of the center of the eddy from the edge. There is no enhancement of sound from longitudinal quadrupoles with axes parallel to the edge. According to this theory, the mean-square pressure produced by a single eddy near the trailing edge is

$$\overline{p^2}(r, \theta, \phi) = \frac{\rho_o^2 U^5 \gamma^2 V_o^2 \sin \phi \sin^2 \theta_o \cos^2 \frac{\theta}{2}}{\pi^2 a \delta r_o^3 r^2} \quad (8)$$

where γ is the turbulent intensity, V_o is the eddy volume, δ is the streamwise correlation length of the eddy, θ is the angle between the streamwise and observer directions, θ_o is the angle that the mean flow makes with the trailing edge and ϕ is the angle between the trailing edge and observer directions. This expression can then be summed at the observer location over all the (independent) eddies near the trailing edge. Note that this theory implies a dependence on the fifth power of velocity and the turbulence intensity squared. It also gives rise to a directivity pattern in a plane normal to the edge dependent upon $\cos^2 \theta/2$. This directivity pattern, which Hayden²⁹ has associated with a "baffled dipole," is shown in Figure 16. Finally, the theory predicts that a "swept" trailing edge (relative to the mean flow direction) would produce less noise due to the $\sin^2 \theta_o$ dependence.

It should be noted here that summation of Equation (8) over all eddies to produce the total mean-square pressure at an observer location must be approached with extreme caution. The primary trailing-edge source on an aircraft is the wing. Thus, the source dimension is of the order of the span. Since airframe noise is typically of interest at distances of only a few spans from the aircraft, the geometric far field of the source distribution has not been reached and a simple summation employing average values of distances and angles could be in considerable error. For this case, a "stripwise" summation as suggested by Hayden et al.¹⁸ is undoubtedly superior. Further, the fact that these sources are in motion should, of course, be taken into account.

The variables which appear in Equation (8) are fairly straightforward to obtain with the exception of those which characterize the eddy. Clark³⁰ has made measurements in the wake behind an airfoil placed in the potential core of a low-turbulence jet. These measurements suggest that the controlling parameter in the eddy size is actually the width of the wake, Δ , and that the number of eddies across a span b should be $\approx b/\Delta$. The eddies are apparently ellipsoidal with $\delta \approx 3/2 \Delta$ and $V_o \approx 3/4 \Delta^3$. Thus, if the eddy distance r_o is taken as $3/2 \Delta$, Equation (9) becomes

$$\overline{p^2}(r, \theta, \phi) = \frac{\rho_o^2 U^5 \gamma^2 \Delta^2 \sin \phi \sin^2 \theta_o \cos^2 \frac{\theta}{2}}{9\pi^2 a r^2} \quad (9)$$

This relation indicates that sound generation by an aerodynamic surface is highly dependent upon the width of its wake. The drag of the body is also related to the wake width, a result which has led Revell³¹ to attempt to predict airframe noise from steady-state drag.

Unfortunately, very few measurements of the amplitude and spectra of this trailing-edge source exist due to the difficulty in making the required measurements in present-day flow facilities. Some data at very small scale were obtained by Clark.³⁰ These have been employed by Clark et al.³² in a recent attempt to develop an expression for the power spectrum of sound radiation by isolated airfoils. Their theory, however, requires a knowledge of the spectra of wake velocity components. It can be noted that this study also showed a low (-0.2) power dependence of the eddy correlation lengths on Reynolds number.

In the absence of precise information, practical estimation of the frequency content of trailing-edge noise might well employ the nondimensional spectrum obtained by Healy.⁷ This spectrum, shown in Figure 17, is a composite of spectra measured directly below several small aircraft with peculiarities removed. As the aircraft were all in the "clean" or cruise configuration, the primary source of noise directly below the craft should have been trailing-edge noise. For the peak frequency, Healy suggests

$$f_{\max} = 1.3 \frac{U}{t_w} \quad (10)$$

where t_w is a representative wing thickness. At positions other than directly below the aircraft, this relation should be modified to account for the Doppler shift, that is,

$$f_{\max} = \frac{1.3U}{t_w(1-M_t)} \quad (11)$$

Inflow Turbulence. The final mechanism by which fluctuating forces may be developed on an aerodynamic surface is through the action of incoming turbulence. Although atmospheric turbulence is ordinarily of too large scale and too low intensity to be important in this regard, airframe components, such as flaps, which lie in the wake of other portions of the aircraft may generate noise through this mechanism.

Although several different approaches to the analysis of this noise source have been devised,⁴ it is useful to observe that, since Ffowcs-Williams and Hall's¹⁴ work is purely concerned with scattering of sound near an edge, it is equally applicable to this case as well. In other words, their theory makes no distinction between incoming turbulence impinging on a leading edge and turbulence being shed from a trailing edge. Thus, Equation (9) can be employed to calculate the level and directivity of this leading-edge source as well. The same concerns about source distribution apply, with the only change being, perhaps, the characteristics of the eddies themselves.

When the observer is far enough away to be in the geometric far field of the entire leading-edge source (which probably is not the case for normal airframe noise measurements), an analysis of this problem has recently been formulated by Amiet.³³ This theory decomposes the incoming turbulence into Fourier components and then employs the Sears function to calculate the airfoil response. It yields an expression for the (one-sided) power spectral density of the radiated sound at a distance z directly above (or below) the airfoil as

$$S_a(0,0,z;\omega) = \frac{b}{\pi a} \left(\frac{2\mathcal{L}}{3\pi z} \right)^2 \gamma^2 (\rho_0 U)^2 \left[\frac{\Gamma(1/3)}{\Gamma(5/6)} \right]^2 \frac{\tilde{K}_x^2}{(1 + \tilde{K}_x^2)^{7/3}} \quad (12)$$

where the Von Karman spectrum has been used to describe the turbulence, b is the span of the airfoil, $\Gamma(\cdot)$ is the Gamma function, \mathcal{L} is the integral scale of the turbulence and

$$\tilde{K}_x = \frac{K_x \mathcal{L} \Gamma(1/3)}{\sqrt{\pi} \Gamma(5/6)}$$

where $K_x = \omega/U$. This relation holds as long as $MK_x b > 2$. The corresponding third-octave band sound pressure level is given by

$$\text{SPL} = 10 \log_{10} \left[\frac{\mathcal{L}^2 b}{2z^2} M^5 \gamma^2 \frac{\tilde{K}_x^3}{(1 + \tilde{K}_x^2)^{7/3}} \right] + 181.3 \quad (13)$$

Figure 18 shows a comparison of this relation with data on sound generation by an airfoil in an acoustic tunnel. A grid was placed in the tunnel in order to generate the incident turbulence.

Cavities

The final component source of airframe noise to be discussed in this section is sound generation by cavities in the surface of the aircraft. Recent data⁶ (see Fig. 3) indicate that one of the most intense sources of airframe noise on landing approach is produced by the wheel cavities of the aircraft since a significant increase in the broadband noise spectrum is observed when the wheel wells are opened. Although it is not yet clear whether this noise increase is due to the cavity itself or to a change in the flow field around the wing/flap system, considerable research into noise generation mechanisms of cavity flow has been stimulated.

The flow field within cavities has been of interest for several years due to fatigue and buffeting problems. Thus, extensive data on cavity flow fields have been obtained and methods for the reduction of internal pressure oscillations have been developed.³⁴ Unfortunately, however, few measurements of far-field sound generation by cavities exist due to the difficulty of making such measurements in present-day flow facilities.

The "basic" (this author's terminology) cavity noise mechanism is a fairly complex interaction between the shear layer over the cavity and the volume within it. The shear layer apparently has fundamental modes of instability which act as a forcing function to produce oscillation of the air within the cavity. A reasonably accurate expression for the frequencies of the shear layer instability modes in simple rectangular cavities has been developed by Rossiter,³⁵ that is,

$$f_m = \frac{U}{L} \frac{(m - 0.25)}{1/k_v + m} \quad m = 1, 2, \dots \quad (14)$$

where L is the length of the cavity in the flow direction and k_v is the ratio of eddy convection speed to the flow speed. However, the efficiency of this forcing function in producing sound depends upon how well it couples with the fundamental acoustic modes of the cavity. If the coupling is strong, very intense tones can be produced. These tones have been studied by Block and Heller.³⁶ Figure 19 displays a typical spectrum measured directly above the cavity in comparison with a spectrum of the fluctuating pressures inside the cavity for a length-to-depth ratio (L/D) of unity. The directivity of this noise source was determined to be nearly that of a monopole although small deviations do occur. On the basis

of this work, Bliss and Hayden³⁷ have developed a prediction relation for the mean-square pressure radiated by the cavity, that is,

$$\overline{p^2}(r) = [0.015(m - 1/4)q \frac{w}{r}]^2 \quad (15)$$

where q is the dynamic pressure and w is the width of the cavity. This equation assumes good coupling between the forcing frequency and the fundamental acoustic mode. Thus, predictions on the basis of this relation often tend to be high. Further, such coupling is usually only seen for the modes $m = 2, 3$, or 4 .

This "basic" cavity noise mechanism is primarily a low-frequency phenomenon, occurring for Strouhal numbers $St = fL/U$ less than about 2.5. Further, it is also critically dependent upon the cavity shape. Recent tests of a circular cavity conducted at NASA Langley produced much less noise radiation than a square cavity of side length equal to the diameter of the circular cavity. This is important as the cavities on real aircraft are much different in shape from the simple rectangular model.³⁷ Finally, of course, this tonal mechanism cannot be responsible for the observed broadband radiation of real aircraft cavities. Thus, it is necessary to consider other potential cavity noise mechanisms.

There are other possible sources of cavity noise. The shear layer shed from the leading edge of the cavity will induce fluctuating pressures on the edge resulting in an edge noise source as discussed previously. Further, the turbulence in the shear layer will impinge on the back wall of the cavity resulting in an incident turbulence source similar to that mentioned earlier. Thus, there is the potential for a "trailing-edge" source at the leading edge of the cavity and a "leading-edge" source at the trailing edge of the cavity. Both of these sources may be analyzed by the theories developed earlier and both will produce a more broadband noise. The analysis is simplified by the fact that these sources will appear compact.

An alternate theory, tailored to the case of the cavity, has recently been developed by Hardin and Mason³⁸ which allows the sound generation to be calculated on the basis of the vorticity present in the cavity flow. This theory identifies monopole, dipole, and quadrupole type sources inherent in the flow field over the cavity and has been applied in a two-dimensional model of cavity flow in order to better understand the broadband noise generation mechanisms. Figure 20 presents the spectrum of this noise source as calculated directly above a cavity with length-to-depth ratio of 2.0. Note that the broadband spectrum peaks near the Strouhal number of 4.0, which is considerably above the value of 2.5 below which tones are observed. Figure 21 displays the directivity of the sound in a plane parallel to the streamwise direction. Note that the peak intensity occurs slightly upstream of the cavity. This effect has also been observed in full-scale airframe noise tests.

EXPERIMENTAL RESEARCH TECHNIQUES

A common problem encountered in airframe noise research is the fact that the self-noise sources are not very intense compared either to propulsive noise sources or to background noise levels in typical test facilities. Overcoming this obstacle has required considerable innovation of new techniques and refinement of old ones.

Full-Scale Flight Testing

The first airframe noise testing was done utilizing full-scale aircraft. However, it is expensive, requires extensive instrumentation and can be dangerous. Ordinarily such tests must be accomplished with the aircraft's engines inoperative or at flight idle. Such operating conditions may not be possible with all aircraft. Furthermore, unless the engines are extremely quiet, it is necessary to look for a "window" between the low-frequency jet and ambient noise and the high-frequency compressor noise through which the airframe noise may be observed. Such windows do not exist for all aircraft.

There are numerous problems and subtleties connected with obtaining valid full-scale airframe noise measurements. The fact that the source is moving past a fixed observer makes the design of an optimum experiment difficult. Not surprisingly, the various groups which have attempted such measurements have utilized different approaches to the acquisition and analysis of the data. However, this makes comparison of data obtained in different tests a tenuous undertaking. Thus, one of the urgent needs in this field is some standardization of testing techniques. For this reason and at the risk of sounding didactic, this paper will discuss many of these problems and offer approaches to them.

The primary quantity of interest in airframe noise research is its impact on the community, or airframe noise "footprint." Thus, the objective of airframe noise testing should be to obtain the directivity of the total airframe noise produced by the aircraft. Since accurate positioning of an aircraft with respect to a microphone is difficult, and repeat flights are expensive, a good (practical) way to obtain such data is with an array of microphones in the shape of a tee. The flight path of the aircraft is along the cross of the tee. Of course, each microphone will measure a sound pressure time history which increases in intensity and then dies away as the aircraft flies past. However, by properly picking short segments of these records for analysis, such records can be employed to obtain the directivity of the airframe noise in the flyover plane as well as to increase the statistical reliability of the data. Similar analysis of the sideline microphones will allow the rest of the footprint to be obtained, although with increased variability.

One question which arises at this point is: How should the microphones be mounted? Early testing employed pole mounted mics as those are required for aircraft certification. However, this leads to ground induced cancellation which may occur in the frequency range of interest. Perhaps a better technique is to mount the microphones flush with a hard reflecting surface which produces a pressure doubling effect over the entire spectrum that is well understood and easily corrected. This technique has been employed in two recent studies^{5,6} with Fethney⁶ even cutting away the lower half of the microphone windscreen so that the mic would lie flat on the concrete runway.

A second question which arises is how the aircraft should be flown over the microphone array. As the aircraft's speed and distance from the observer are important parameters in airframe noise, ideally one would like to fly the aircraft at constant speed and altitude. However, to do so requires more than flight idle power, which increases the engine noise level, and risks introducing unwanted sources through aircraft acceleration as can be seen in the last term of Equation (1). Thus, it appears better to fly the aircraft at constant airspeed down a glide slope over the array. The pressure signals recorded by the microphones can later be corrected for the altitude variation utilizing an inverse square dependence of overall sound pressure level on observer distance as long as the observer was truly in the acoustic and geometric far fields of the aircraft.

The necessary corrections certainly require an accurate determination of the aircraft's position as a function of time. The best way of accomplishing this seems to be one of the radar tracking schemes which are usually available at suitable test sites. However, the problem is a little more complex. Typical aircraft of interest have spans and fuselage lengths of the order of 30 meters, while the altitude may be only 100 meters or so. Thus, there is a nonnegligible difference depending upon what reference point on the aircraft is used to determine the observer distance. One should like to use the "center of gravity" of the source distribution. However, this is not known. Thus, this author might suggest the center of gravity of the aircraft as being as reasonable as any other. Once a point is chosen, a simple way of measuring the correct distance is to mount a radar target reflector on the aircraft and then translate the data to the chosen point on the aircraft.

Another problem crops up when one tries to relate the aircraft position information to the measured pressure time histories. The signal arriving at the observer location at time t was transmitted by the source at the earlier time $t - r_e/a$ where r_e was the source-to-observer distance at the time of emission. These considerations lead to a complex relation between the known aircraft position at time t and the actual acoustic propagation distance which should be employed in correcting the pressure time histories.

A further consideration in such testing is the variability of the data. The statistical variability of any spectral analysis is inversely proportional to the product of the bandwidth and the analysis time. Thus, for fixed bandwidth, one should like for the analysis time to be as long as possible. However, in this case where both the source/observer distance and the directivity angle are changing with time, the process is nonstationary and too long an analysis time can lead to aberrations in the data. Thus, there must be a trade off between statistical variability and nonstationarity. This problem is not critical for third-octave analysis where analysis times of a few tenths of a second yield adequate estimates. However, for narrow-band analyses, severe problems arise. These may be overcome by averaging analyses of several microphones on a single flight or a few microphones on nominally identical repeat flights.

A final problem deals with calculation of overall sound pressure levels when the spectra are contaminated with engine noise. Some studies have merely calculated the OASPL value as if the engine noise were not there, others have integrated only up to some maximum frequency implying that all higher frequency power was engine noise while still others have attempted to subtract out the engine noise on the basis of static test data. Two problems with this last technique are that the static data are not measured at the same angles with respect to the aircraft as the airframe noise data and that no consideration of the known flight effects on jet noise has been given.

Model Testing

There are considerable incentives toward the use of models in airframe noise testing. Among these are the possibility of eliminating engine noise and reducing the cost and danger of testing of any changes prompted by the application of noise reduction techniques. However, certain disadvantages due to reduced source intensity and the necessity of developing scaling relations (particularly since airframe noise is known to be Reynolds number dependent) are introduced.

Remotely Piloted Vehicles. One such technique, involving the use of a remotely piloted vehicle (RPV) as the airframe noise source, has been investigated by Fratello and Shearin.³⁹ This testing is quite similar to that used in full-scale flight research. In preliminary work employing powered RPV's whose engines were stopped before crossing the microphone array, they were able to obtain a 10-dB signal-to-noise ratio in the clean configuration with an RPV whose wingspan was 1.5 m flying at an altitude of 3 m with a speed of 25 m/sec as shown in Figure 22.

The data acquisition and analysis procedures are more critical in this type of testing than in full-scale flight testing. The RPV must fly quite low over the array in order to produce a sufficient sound level at the microphone. Thus, the change in observer angle per unit time is large. However, acceptable methods for data collection have been devised. These utilize arrays of microphones and photodiodes as shown in Figure 23.

A more recent test program is employing an unpowered model of a Boeing 747 aircraft with a wingspan of approximately 2 m. Grit is glued onto the leading edges of the model surfaces to trip the boundary layer in an attempt to simulate full-scale Reynolds numbers. The model is dropped from a helicopter and allowed to seek its natural (known) glide slope until it is pulled up into nearly level flight over the microphone array. Figure 24 is a photo of the model mounted on the drop helicopter. A rather sophisticated control system for this RPV has been designed and installed.

Anechoic Flow Facilities. A second technique for whole model testing which has been investigated is the use of anechoic wind tunnels. Such testing is hampered by the fact that a tunnel produces its own surface interaction noise which is difficult to separate from the model noise. Thus, the tunnel must have a very low background noise level. Further, at present, the test section must be open such that the microphones may be placed outside the flow in order to avoid swamping the airframe noise signal by microphone wind noise. NASA Langley engineers have been successful in such testing at the NSRDC Quiet Flow Facility in Carderock, Maryland.⁴⁰ Figure 25 is a photo of a 0.03-scale model of a Boeing 747 aircraft mounted in this tunnel. This model was carefully constructed to properly represent insofar as possible full-scale

geometric and aerodynamic properties. Note that the mounting sting is airfoil shaped in order to minimize the generation of aeolian tones. These tests determined that model airframe noise can be geometrically scaled to that of the full-scale aircraft with the exception of cavity generated sound.⁴¹ The simple scaling relations for one-third-octave sound pressure levels and frequency are

$$SPL_F = SPL_M + 10 \log_{10} \left[(SF)^{-2} \left(\frac{U_F}{U_M} \right)^5 \left(\frac{r_M}{r_F} \right)^2 \right] \quad (16)$$

and

$$f_F = (SF) f_M \left(\frac{U_F}{U_M} \right) \quad (17)$$

where the subscripts F and M designate the full scale and model, respectively, and SF is the scale factor. Figure 26 shows a comparison of model and full-scale data for a 747 aircraft with leading-edge flaps deployed. The full-scale data were obtained by The Boeing Aircraft Company directly below the aircraft during flyover tests. This measurement position is geometrically similar to that employed in the model tests. When scaled by means of Equations (16) and (17), the model and full-scale data agreed within 3 dB. During the model tests, measurements of sideline noise levels with and without the vertical tail on the model were made. No difference in noise level could be observed.

Anechoic wind tunnels are also useful for testing of component sources of airframe noise. The data on airfoil sound generation shown in Figure 18 were obtained in the UTRC acoustic tunnel.³³ Another such tunnel⁴² exists at Bolt, Beranek and Newman, Inc., in Cambridge, Massachusetts. This tunnel was utilized to obtain the cavity noise data shown in Figure 19.

One of the problems with all types of testing in acoustic wind tunnels is the fact that the sound must propagate through the shear layer of the tunnel flow. It is known that propagation through such a shear layer can alter the directivity and reduce the high-frequency intensity of such sound. Although corrections for such changes are known for point sources at moderate frequencies,⁴³ those required for a distributed source such as an airframe model are still a matter for research.

A conceptually different, yet very similar, type of facility which is useful in airframe noise research is an anechoic chamber with quiet flow capability. Such facilities exist in many research organizations. A constraint for airframe noise testing, however, is that the flow must be large enough that a reasonable sized model may be tested. Such testing has been successfully accomplished in the chamber in the new Aircraft Noise Reduction Laboratory at NASA Langley Research Center. The air supply has a capability of 41 m³/sec which will allow a 52-m/sec velocity through a 1-m-diameter nozzle. Figure 27 is a photo of a recent experiment in this chamber to investigate cavity noise and the interaction of cavity/strut generated turbulence with downstream flaps. Figure 28 shows noise directivity patterns of the cavity alone in the plane normal to the flow for two different frequencies obtained during these tests in the facility of Figure 27. The flow speed was 119 m/sec and the cavity length and depth were 4 cm and 5 cm, respectively. Note that distinct lobes appear in the directivity pattern. Thus, the directivity pattern of the cavity tonal noise is not strictly monopole.

Moving Source Apparatus. A final type of facility which could be useful in airframe noise research is a moving source apparatus. This apparatus can be envisioned as some sort of tracked vehicle with a quiet propulsive system which would carry a model through an anechoic test section. Such an apparatus would accurately simulate an actual flyover in the sense that the model would move past a stationary observer and would eliminate some of the problems of anechoic wind-tunnel testing. However, development of a quiet propulsive system is a nontrivial undertaking. Although such devices have been discussed, the author knows of no instance of their actual use in airframe noise testing.

CONCLUDING REMARKS

This paper has presented a critical assessment of the state of the art in airframe self-noise. Full-scale data on the intensity, spectra, and directivity of this noise source were evaluated in the light of the comprehensive theory developed by Ffowcs-Williams and Hawkins. Vibration of panels on the aircraft was identified as a possible additional source of airframe noise. The present understanding and methods for prediction of other component sources — airfoils, struts, and cavities — were discussed and areas for further research as well as potential methods for airframe noise reduction were identified. Finally, the various experimental methods which have been developed for airframe noise research were discussed and sample results were presented.

REFERENCES

- ¹Gibson, J. S.: "The Ultimate Noise Barrier - Far Field Radiated Aerodynamic Noise," *Internoise 72 Proceedings*, M. J. Crocker, Ed., Inst. Noise Control Eng., pp. 332-337, 1972.
- ²Blumenthal, V. L., Streckenbach, H. M., and Tate, R. B.: "Aircraft Environmental Problems," *AIAA Paper No. 73-75*, Jan. 1973.
- ³Morgan, H. G., and Hardin, J. C.: "Airframe Noise - The Next Aircraft Noise Barrier," *Jour. of Aircraft*, Vol. 12, No. 7, pp. 622-624, July 1975.
- ⁴Hardin, J. C., Fratello, D. J., Hayden, R. E., Kadman, Y., and Africk, S.: "Prediction of Airframe Noise," *NASA TN D-7821*, Feb. 1975.

- ⁵Putnam, T. W., Lasagna, P. L., and White, K. C.: "Measurements and Analysis of Aircraft Airframe Noise," AIAA Paper No. 75-510, March 1975.
- ⁶Fethney, P.: "An Experimental Study of Airframe Self-Noise," RAE Tech. Memo, AERO 1623, Feb. 1975.
- ⁷Healy, G. J.: "Measurement and Analysis of Aircraft Far-Field Aerodynamic Noise," NASA CR-2377, Dec. 1974.
- ⁸Lasagna, P. L., and Putnam, T. W.: "Preliminary Measurements of Aircraft Aerodynamic Noise," AIAA Paper No. 74-572, June 1974.
- ⁹Pendley, R. E.: "Recent Advances in the Technology of Aircraft Noise Control," AIAA Paper No. 75-317, Feb. 1975.
- ¹⁰Ffowcs-Williams, J. E., and Hawkings, D. L.: "Sound Generation by Turbulence and Surfaces in Arbitrary Motion," Phil. Trans. Roy. Soc., Series A, No. 1151, Vol. 264, pp. 321-342, May 1969.
- ¹¹Lighthill, M. J.: "On Sound Generated Aerodynamically. Pt. I, General Theory," Proc. Roy. Soc., Vol. A 221, pp. 564-587, 1952.
- ¹²Lighthill, M. J.: "On Sound Generated Aerodynamically. Pt. II, Turbulence as a Source of Sound," Proc. Roy. Soc., Vol. A 222, pp. 1-32, 1954.
- ¹³Curle, N.: "The Influence of Solid Boundaries on Aerodynamic Sound," Proc. Roy. Soc., Vol. A 231, pp. 505-514, 1955.
- ¹⁴Ffowcs-Williams, J. E., and Hall, L. H.: "Aerodynamic Sound Generation by Turbulent Flow in the Vicinity of a Scattering Half Plane," J. Fluid Mech., Vol. 40, Pt. 4, pp. 657-670, 1970.
- ¹⁵Powell, A.: "On the Aerodynamic Noise of a Rigid Flat Plate Moving at Zero Incidence," JASA, Vol. 31, No. 12, pp. 1649-1653, 1959.
- ¹⁶Davies, H. G.: "Sound From Turbulent Boundary Layer Excited Panels," JASA, Vol. 49, No. 3, Pt. 2, pp. 878-889, 1971.
- ¹⁷Maestrello, L.: "Use of Turbulent Model to Calculate the Vibration and Radiation Responses of a Panel, With Practical Suggestions for Reducing Sound Level," J. Sound Vib., Vol. 5, pp. 407-448, 1967.
- ¹⁸Hayden, R. E., Kadman, Y., Bliss, D. B., and Africk, S. A.: "Diagnostic Calculations of Airframe Radiated Noise," AIAA Paper No. 75-485, 1975.
- ¹⁹Ribner, H. S.: "Aerodynamic Sound From Fluid Dilatations," AFOSR TN 3430, 1962.
- ²⁰Fung, Y. C.: "Fluctuating Lift and Drag Acting on a Cylinder in a Flow at Supercritical Reynolds Numbers," Jour. Aerospace Sciences, Vol. 27, No. 11, pp. 801-814, 1960.
- ²¹Lowson, M. V.: "The Sound Field for Singularities in Motion," Proc. Roy. Soc., Vol. 286, No. 1407, pp. 559-572, 1965.
- ²²Sharland, I. J.: "Sources of Noise in Axial Flow Fans," J. Sound Vib., Vol. 1, No. 3, pp. 302-322, 1964.
- ²³Powell, A.: "Aerodynamic Noise and the Plane Boundary," JASA, Vol. 32, No. 8, 1960.
- ²⁴Laufer, J., Ffowcs-Williams, J. E., and Childress, S.: "Mechanism of Noise Generation in the Turbulent Boundary Layer," AGARDograph 90, pp. 20-30, 1964.
- ²⁵Siddon, T. E.: "Noise Source Diagnostics Using Causality Correlations," AGARD-CP-131, Paper No. 7, 1973.
- ²⁶Patterson, R. W., Vogt, P. G., Fink, M. R., and Munch, C. L.: "Vortex Noise of Isolated Airfoils," AIAA Paper No. 72-656, 1972.
- ²⁷Tam, C. W.: "Discrete Tones of Isolated Airfoils," JASA, Vol. 55, No. 6, pp. 1173-1177, 1974.
- ²⁸Fink, M. R.: "Experimental Evaluation of Theories for Trailing Edge and Incident Fluctuation Noise," AIAA Jour., Vol. 13, No. 11, pp. 1472-1477, 1975.
- ²⁹Hayden, R. E.: "Noise From Interaction of Flow With Rigid Surfaces," NASA CR-2126, 1972.
- ³⁰Clark, L. T.: "The Radiation of Sound From an Airfoil Immersed in a Laminar Flow," Jour. of Eng. for Power, Vol. 93, Ser. A, pp. 366-376, 1971.
- ³¹Revell, J. D.: "Induced Drag Effect on Airframe Noise," AIAA Paper No. 75-487, 1975.
- ³²Clark, L. T., Chalupnik, J. D., and Hodder, B.: "Wake Related Sound Generation From Isolated Airfoils," JASA, Vol. 59, No. 1, 1976.
- ³³Amiet, R. K.: "Acoustic Radiation From an Airfoil in a Turbulent Stream," J. Sound Vib., Vol. 41, No. 4, pp. 407-420, 1975.

- ³⁴Heller, H. H., and Bliss, D. B.: "The Physical Mechanism of Flow Induced Pressure Fluctuations in Cavities and Concepts for Their Suppression," AIAA Paper No. 75-491, 1975.
- ³⁵Rossiter, J. E.: "Wind Tunnel Experiment on the Flow Over Rectangular Cavities at Subsonic and Transonic Speeds," R. and M., No. 3438, British A.R.C., 1964.
- ³⁶Block, P. J. W., and Heller, H.: "Measurements of Farfield Sound Generation From a Flow-Excited Cavity," NASA TM X-3292, 1975.
- ³⁷Bliss, D. B., and Hayden, R. E.: "Landing Gear and Cavity Noise Prediction," NASA CR-2714, 1976.
- ³⁸Hardin, J. C., and Mason, J. P.: "A Vortex Model of Cavity Flow," AIAA Paper No. 76-524, 1976.
- ³⁹Fratello, D. J., and Shearin, J. G.: "A Preliminary Investigation of Remotely Piloted Vehicles for Airframe Noise Research," AIAA Paper No. 75-512, 1975.
- ⁴⁰Shearin, J. G., and Block, P. J.: "Airframe Noise Measurements on a Transport Model in a Quiet Flow Tunnel," AIAA Paper No. 75-509, 1975.
- ⁴¹Shearin, J. G., Fratello, D. J., Bohn, A., and Burggraf, W.: "Model and Full Scale Large Transport Airframe Noise," AIAA Paper No. 76-550, 1976.
- ⁴²Kadman, Y., and Hayden, R. E.: "Design and Performance of High-Speed Free-Jet Acoustic Wind Tunnel," AIAA Paper No. 75-531, 1975.
- ⁴³Amiet, R. K.: "Correction of Open Jet Wind Tunnel Measurements for Shear Layer Refraction," AIAA Paper No. 75-532, 1975.

TABLE 1. CLEAN AIRFRAME NOISE DATA

Aircraft	U, m/sec	h, m	W, kg	b, m	OASPL
Jetstar	128.8	152.0	16682	16.6	84.6
Jetstar	154.5		16454		88.0
Jetstar	175.1		15909		90.5
Jetstar	182.8		15454		91.4
Jetstar	185.4		15136		91.6
CV-990	96.3	45.7	71364	36.5	85.0
CV-990	162.2		82273		94.1
747	133.9		228,182	59.4	95.3
747	114.3		227,727		92.5
HS125	74.1		6800	14.3	81.1
HS125	82.4				83.4
HS125	106				86.3
BAC111	90.6		30000	27.0	87.6
BAC111	111				90.2
BAC111	123				91.4
BAC111	133				92.9
VC10	82.9	182.9	90000	44.5	83.4
VC10	98.3				87.1
VC10	108				88.9

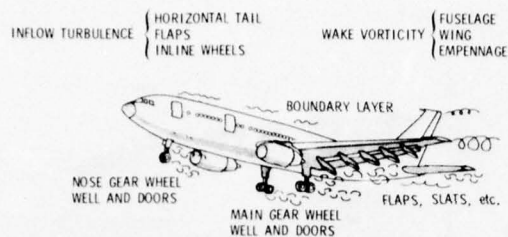


Figure 1. Schematic diagram illustrating potential sources of airframe noise.

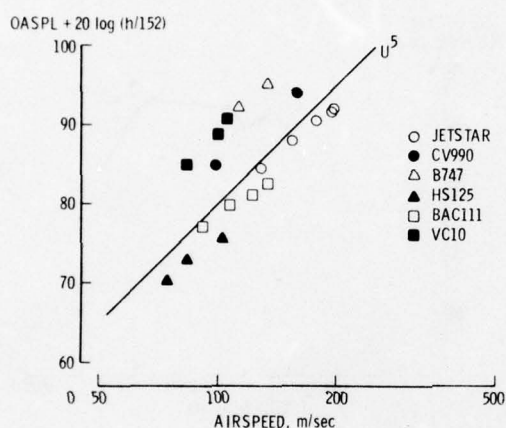


Figure 2. Clean airframe noise levels directly below aircraft normalized to an altitude of 152 m.

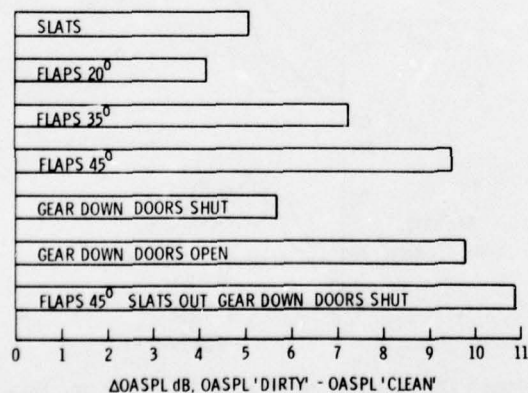


Figure 3. Estimated nonpropulsive noise increases due to changes from the cruise configuration for the VC10 airplane.

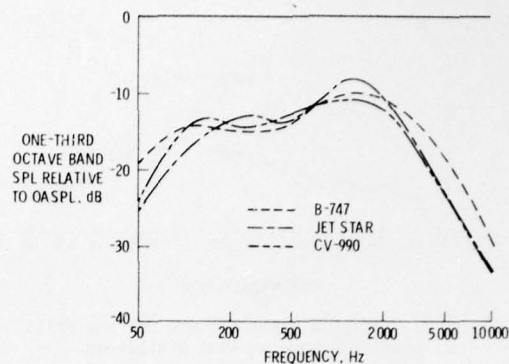


Figure 4. Clean configuration airframe noise spectra directly below aircraft normalized to equal overall sound pressure levels.

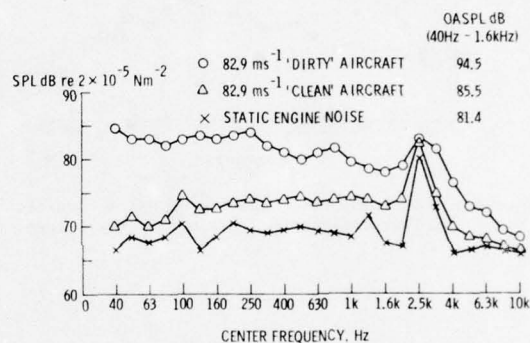


Figure 5. Comparison of one-third-octave band airframe noise spectra for dirty and clean configurations of VC10 aircraft flying overhead at 183 m altitude.

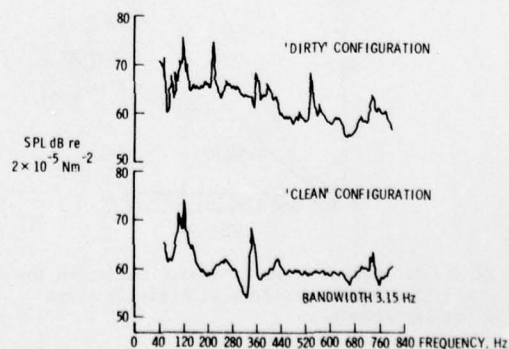


Figure 6. Comparison of narrow-band airframe noise spectra for VC10 aircraft in clean and dirty configurations at an airspeed of 104 m/sec and an altitude of 183 m.

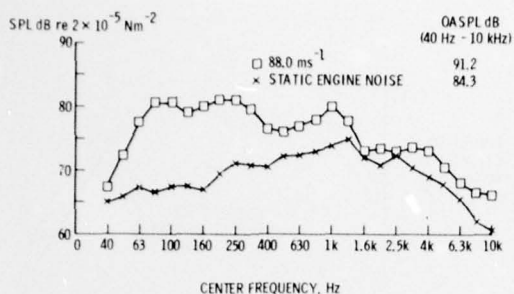


Figure 7. Airframe noise spectra for the HP115 aircraft overhead at 45.7 m altitude.

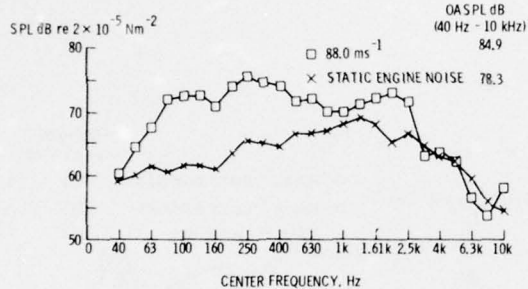


Figure 8. Airframe noise spectra of HP115 aircraft at a sideline distance of 76.2 m for an altitude of 45.7 m.

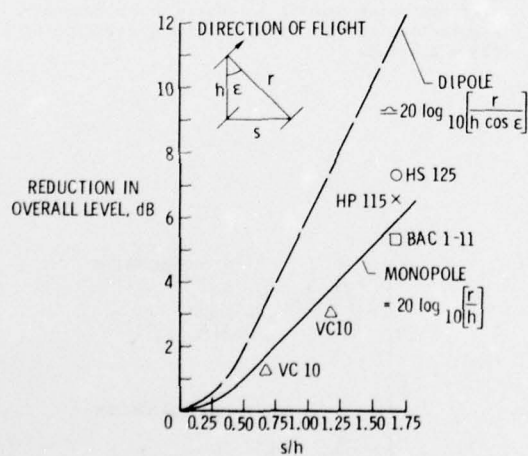


Figure 9. Measured and predicted reduction in sideline OASPLs for four aircraft in clean configurations.

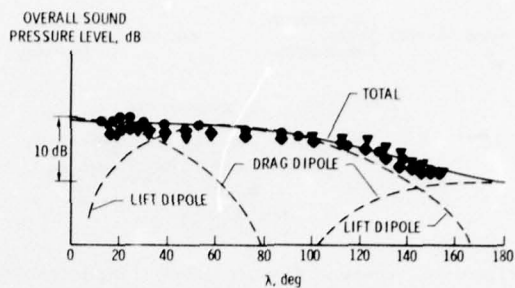


Figure 10. Directivity pattern of DC10 airframe noise in flyover plane compared to that calculated for dipoles oriented in the lift and drag directions.

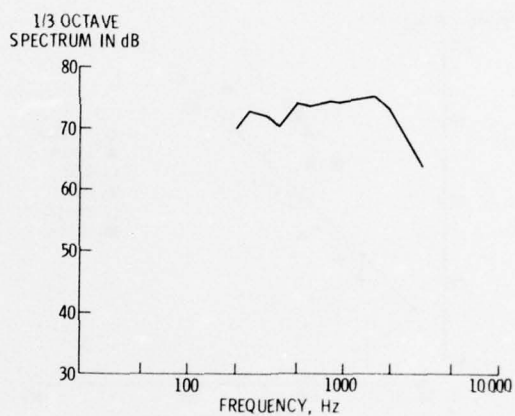


Figure 11. Spectrum of acoustic power radiated from 0.08 mm thick panel mounted in the side of a wind tunnel.

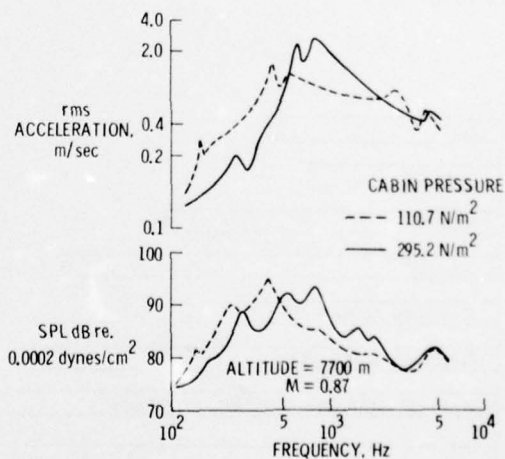


Figure 12. Radiated sound pressure levels and skin acceleration levels of B-720 airplane fuselage panel for two different values of cabin pressure.

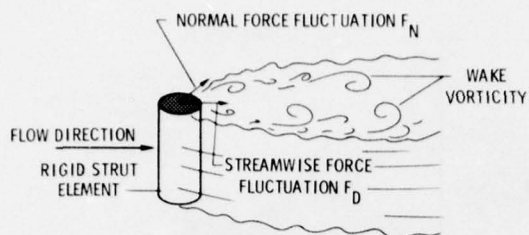


Figure 13. Schematic diagram of wake-generated forces on a cylindrical segment in an airstream.

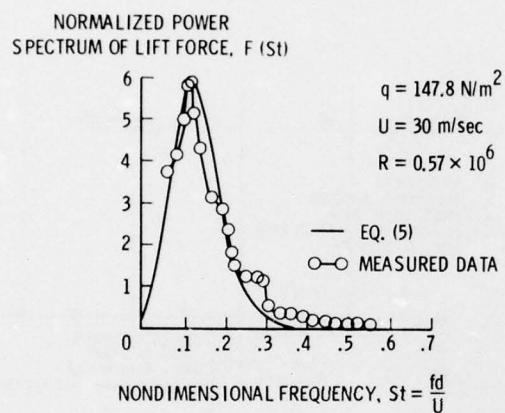


Figure 14. Normalized power spectrum for the lift force on a circular cylinder at a Reynolds number of 570,000.

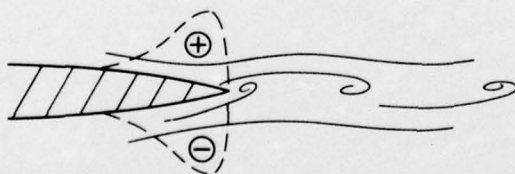


Figure 15. Schematic diagram of the flow field near a trailing edge and the wake-induced instantaneous pressure loading.

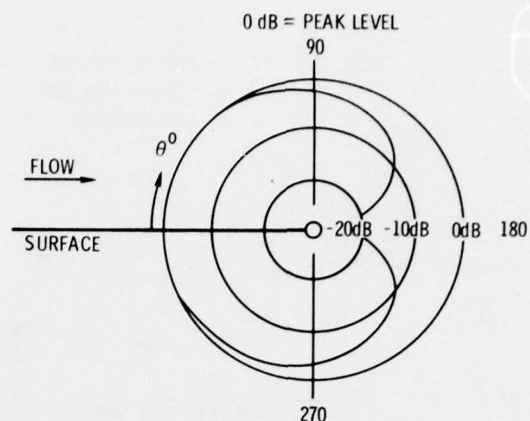


Figure 16. Directivity pattern of a baffled dipole due to flow off the edge of a finite surface.

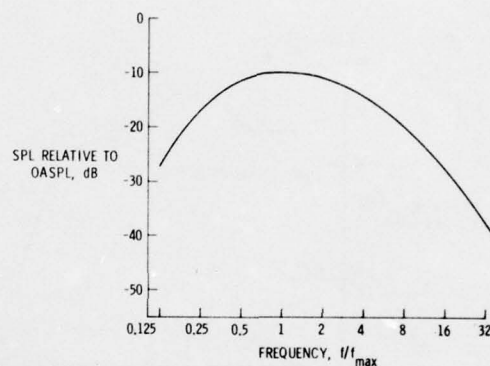


Figure 17. Nondimensional spectrum of trailing-edge noise directly below the edge.

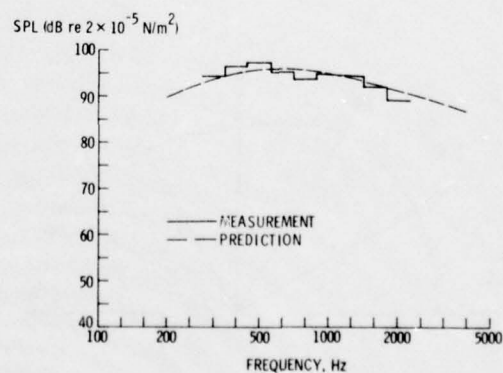


Figure 18. Comparison of measured and predicted noise spectra from an airfoil in incident turbulence for $M = 0.362$.

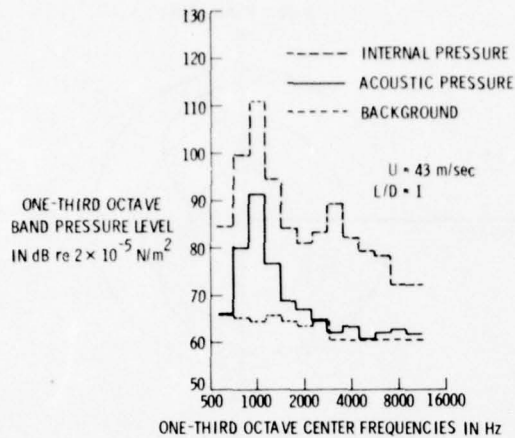


Figure 19. Comparison of the acoustic pressures radiated by a flow excited cavity with the fluctuating pressures within the cavity.

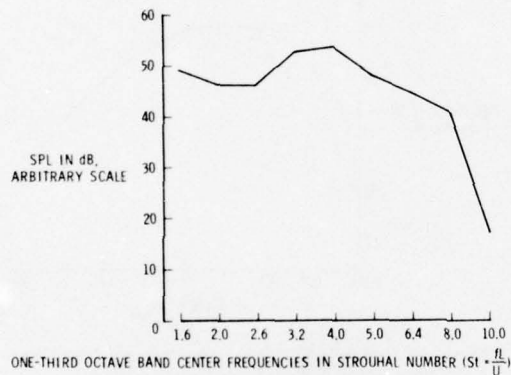


Figure 20. Broadband noise spectrum produced by a flow excited cavity for $L/D = 2.0$.

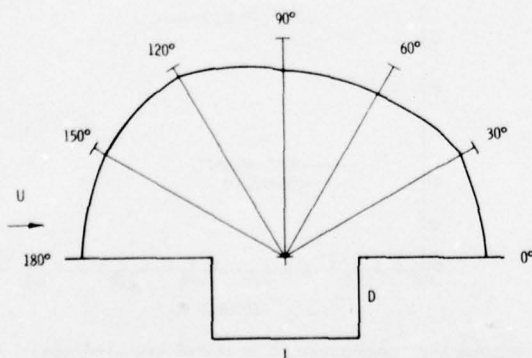


Figure 21. Calculated directivity pattern of broadband noise radiated from a flow excited cavity for $L/D = 2.0$.

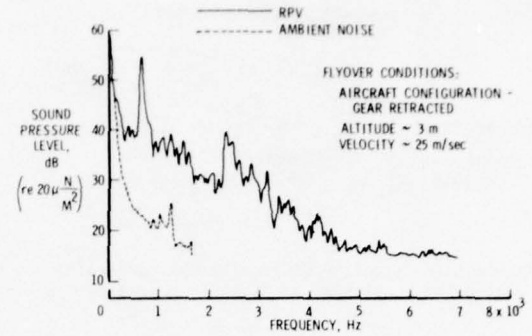


Figure 22. Sample airframe noise spectrum produced during an RPV flyover.

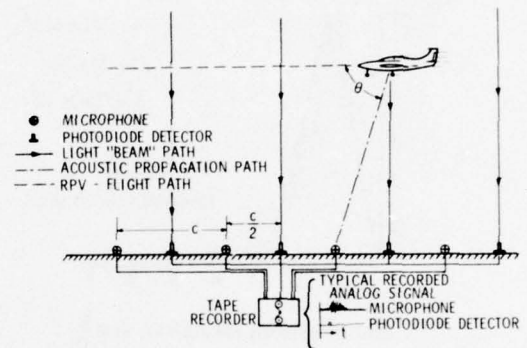


Figure 23. Schematic diagram of instrument array for RPV flyover noise measurements.



Figure 24. 0.03-scale model of Boeing 747 RPV mounted on drop helicopter.

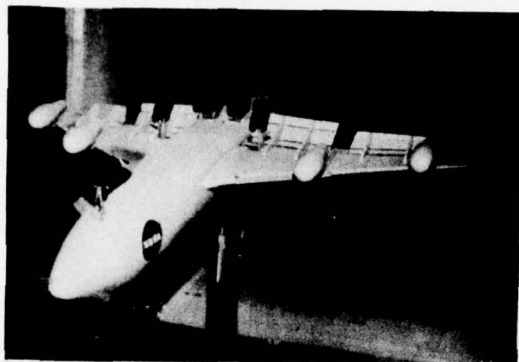


Figure 25. 0.03-scale model of Boeing 747 in NSRDC wind tunnel.

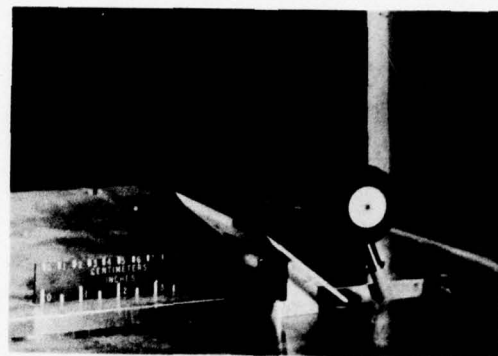


Figure 27. Cavity noise test apparatus in Langley open jet anechoic chamber.

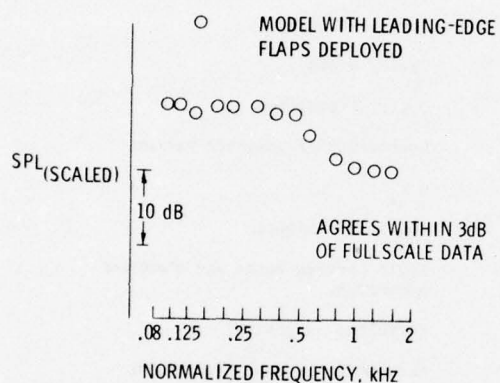


Figure 26. Comparison of model and full-scale airframe noise spectra of Boeing 747 for the leading-edge flap deployed condition.

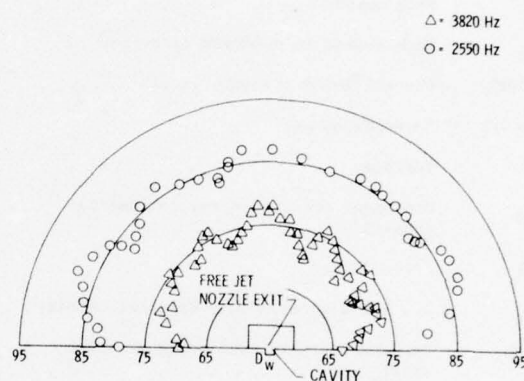


Figure 28. Directivity pattern of cavity radiated noise in plane normal to flow for $U = 119.36$ m/sec, $L = 4$ cm, and $D = 5$ cm.

SYMBOL LIST

A	Ratio of area elements	ℓ	Cylinder length
A_p	Projected area	m	Mode number
C_D	Fluctuating drag coefficient	n_j	Components of normal vector
C_L	Fluctuating lift coefficient	p	Acoustic pressure
D	Cavity depth	p_{ij}	Compressive stress tensor
EPNdB	Effective perceived noise level	p_o	Reference pressure
F_D	Streamwise force fluctuation	q	Dynamic pressure
F_N	Normal-force fluctuation	r	Observer distance
J	Jacobian of transformation	r_e	Observer distance at time of emission for moving source
K	Wave number	r_o	Distance of center of eddy from edge
K_x	Wave number in x-direction	s	Sideline distance
\tilde{K}_x	Nondimensional wave number in x-direction	t	Time
L	Cavity length	t_w	Wing thickness
M	Mach number	v_n	Normal velocity
M_r	Mach number in observer direction	w	Cavity width
OASPL	Overall sound pressure level	\vec{x}	Observer position
Re	Reynolds number	x_i	Components of position vector
S	Surface	z	$= x_3$
S_a	One-sided acoustic pressure spectral density	α	Spectral parameter
SF	Scale factor	β	Angle between force and observer directions
S_N	One-sided normal-force spectral density	γ	Turbulent intensity
SPL	One-third-octave band sound pressure level	δ	Streamwise correlation length
St	Strouhal number	ϵ	Observer angle
T_{ij}	Lighthill stress tensor	$\vec{\eta}$	Source position
U	Flow or aircraft speed	θ	Angle between flight path and observer directions
V	Volume	θ_o	Angle between mean flow and trailing-edge directions
V_o	Eddy volume	λ	Directivity angle in flyover plane
W	Aircraft weight	ν	Kinematic viscosity
a	Speed of sound	ρ	Far-field density
b	Wing span	ρ_o	Ambient density
c	Distance between microphones and diodes in RPV testing	ϕ	Angle between trailing edge and observer directions
d	Cylinder diameter	ω	Circular frequency
f	Frequency	Δ	Width of wake
f_m	Modal frequency	$\Delta OASPL$	Increment in overall sound pressure level
f_{max}	Frequency of spectral peak	$\Gamma(\cdot)$	Gamma function
h	Aircraft altitude	\mathcal{L}	Integral scale of turbulence
k_v	Ratio of eddy convection speed to flow speed		

Subscripts

F Full scale
M Model

Superscript

- Overbar - Time-average

AERO-ACOUSTIC MEASUREMENT AND ANALYSIS TECHNIQUES

Michael E. House

1. INTRODUCTION

So far the lectures in this series have concentrated on the fundamental theoretical work and the experimental evidence on aerodynamically generated noise from jet-effluxes, fans and complete airframes. In doing so, the lecturers have had naturally, to refer to some of the topics on measurement and analysis which are formally covered in this chapter. The reader is advised to refer back to the introductory lectures covering fundamental types of noise source and signal which will be encountered. In this chapter we discuss data collection, test environment, instrumentation, storage and display, signal analysis, and specialised measurement techniques

It should be noted at this juncture that in the treatment of these topics, the emphasis is on the use of the techniques and instruments in the capacity of a research, development or applications engineer; rather than as an expert in electronics and computer engineering.

2. GENERAL NOISE CHARACTERISTICS

2.1 Source Types

Figure 1 presents a summary of the main source characteristics for aerodynamically generated multi-poles (refer to the introductory lectures).

2.2 Spectral and Temporal Characteristics

Sound sources, in general can exhibit several distinct characteristics according to both the temporal pattern of overall amplitude and the shorter term time-dependency of sound pressure. The latter, of course, determines the frequency distribution or spectrum of noise. The time dependency of the overall sound level can be due to source strength changes or due to relative motion to the observer. We can arbitrarily classify the types of sound which we need to measure as follows:

- a) Continuous
- b) Transient
- c) Discrete
- d) Random

2.2.1 Continuous

Continuous noise or Stationary noise Signals are those whose level remains constant over a long time period. Usually it is sufficient to define the term 'level' as being the long term root mean square value of the sound pressure, but, when we have discussed some of the descriptors of signals in the later section 3.3 of these notes, it will be seen that a strict definition of stationarity requires other parameters also to remain constant with time.

2.2.2 Transient

In a transient sound, either a component of the total sound or the overall sound varies in level with time. The variation may be a growth in level, when a machine is started from rest; a decay, as when a loudspeaker is switched off in a reverberant or echo room; a steady rise to a peak followed by a steady fall, as with a vehicle drive-by or an aircraft fly-over; or a sharp impulsive noise, often with a very high level existing for only a very short time, such as with a pistol shot.

2.2.3 Discrete

A discrete tone noise source arises from a sound pressure wave-form pattern (in time) which is repetitive at some interval. Where the wave-form for one repetition takes the pattern of a harmonic (sine or cosine) function, then a single frequency discrete tone exists. If not, it is always possible to analyse the waveform into a number of sinusoidal wave-form components, whereupon the sound has multiple discrete tone form. An example of the former is the main note from a well struck tuning fork, and the latter the rich multi-tonal sound of a stringed instrument.

2.2.4 Random

Random sounds, in contrast to discrete sounds, have no repetition of wave-form over at least the longest period of time with which we have an interest. Individual time segments of the pressure wave-form have both differing amplitudes and pressure crossing time intervals. Thus, crudely, the signal may be thought of as having a multitude of possible discrete frequencies and with only a probability type of descriptor of their amplitudes. The result is a continuous frequency distribution when the sound is analysed.

2.2.5 Compound Characteristics

Of course, sounds may have characteristics compounded from certain of the above categories. For example, the transient fly-over noise from an aircraft may contain both random character noise from aerodynamic quadrupole sources in its jet exhaust and discrete tones arising from dipole sources from the blade in its propulsion fan. Impulse sounds can either be 'pure' with relatively simple pressure excursions, or can be more complex with a ringing decay in the form of an exponentially diminishing sine-wave. They may consist of a very sharp 'burst' of sound from a random process, as in a VTOL aircraft attitude control system.

Figure 2 summarises the wave-form, frequency spectrum and time history patterns of these main categories of sound.

3. INFORMATION THEORY

In this section we shall examine at a fairly elementary level, the 'information' contained in a record of the pressure waveform (or other parameter such as particle velocity wave-form). We refer to the continuous time pattern of the parameter whose fluctuations are being assessed and studied as the 'signal'.

Research and development into aerodynamically generated noise increasingly depends on a wide range of complex instrumentation, providing enormous quantities of such information. In order to interpret such information efficiently, the total data gathered in an experiment must be "boiled down" in such a way that we retain its essential meaning. The form of the reduced data must be chosen for each particular case to give the clearest understanding of the relationship between the measured property and other physical parameters of the system being examined.

3.1 Data Acquisition Rates

To illustrate the rate at which data can be gathered using currently available techniques, we note that an F.M. tape recorder system will acquire some 6×10^5 bits/sec and an oscilloscope and camera about 10^3 bits/sec. A bit is a binary digit, the unit used by data processing engineers to denote the simplest element of information, i.e. the presence or absence of an event or quantity. By contrast the simple meter plus pencil and paper technique has a capability of about 10 bits/sec. and a digital voltmeter plus print out system up to 10^3 bits/second.

Information theory concerns itself with the gathering, processing and display of quantities used to represent a physical property. Often the processing includes the conversion of an information record from a function of one variable to a function of another, and this is termed Signal Transformation.

3.2 Signal Information

A physical property of some process, machine or natural phenomenon can only be interpreted objectively by man in terms of something that he can see or count. For example, it is very difficult to judge the speed at which we travel in our motor cars unless we have a speedometer to look at and one well known way to assess the speed of a train is by counting the passing of telegraph poles in a given time interval. The engineer or scientist usually converts the physical property into an electrical voltage or mechanical displacement by means of a transducer and takes notes of the output of such a device either continuously or at intervals in time or space. We shall discuss either transformation in terms of voltage/time data, although the same techniques can be used for any record of one physical representation against another. We shall be mindful of the fact that, usually, our voltage signal will directly represent the sound pressure of the noise process we are measuring and analysing. We shall also for simplicity, restrict our attention to records which are dependent only on a single variable as shown in Figure 3.1. Such a record is often very useful but often contains either far too much information, or information in an inconvenient form for learning something of the system from which it was derived. The data can be in a number of forms:-

- a) Continuous function of time - Figure 3.1
- b) A discrete time sampled function which can be at any level - Figure 3.2
- c) A discrete quantity or step change function with continuous time - Figure 3.3
- or d) A discrete step function in both time and magnitude - Figure 3.4

These for example could correspond to:

- a) direct time record from a pressure transducer
- b) a cine frame record of a mercury manometer
- c) output from a wire wound potentiometer (with a narrow wiper)
- d) the readings of an automatic counting tachometer with digital display

3.2.2 Information Capacity

In principle, each type of information representation could house the same quantity of information. There is a certain time required for the signal to move from one level to another and for this to be identified, and clearly the more rapidly this can be achieved the more information can be gathered in a given time.

It was stated earlier that the presence or absence of some unit quantity constituted the simplest element of information. Increasing the number of levels or ranks of binary information can increase information capacity. An example is shown in Figure 3.5, where to represent any one of 8 signal levels A to H needs 3 bits e.g. $F = 1-0-1$. To represent this with a 4 level system would need 2 data gathering periods or 2 signal epochs, and in general the number of epochs (E) needed is equal to $\log_2 L$, where there are L signal levels.

A system of L levels which can change to a new level and be identified in T seconds has a capacity of $C = 1/T \log_2 (L)$ bits/second.

Similarly:

For the waveform of Figure 3.4 the number of levels L depends on the accuracy to which the numbers representing the physical quantity are stored. For fixed binary numbers contained in m storage locations with sampling at K per second $C = K \times m$. The waveform of 3.3 only gives information where there is a level change. If the changes occur, on the average, at intervals t_m then $C = 1/t_m \log_2 L$. Assuming that, for a continuous system such as Figure 3.1, the waveforms were m measured exactly; then in principle the information contained is limitless. However there is always some uncertainty imposed by random elements of the system being studied or by electronic noise.

It can be shown that for a continuous system that $C = k/2 \log_2 (1 + P/N)$ where P and N represent signal power level and noise power level respectively, the latter strictly speaking being of the Gaussian random type. Thus each type of representation of signal is capable of providing the same quantity of information by proper choice of time constant, signal-to-noise, and data storage.

The continuous waveform may be related to the sampled waveform (3.2) by assuming some upper limit to the rate of change or frequency content of the signal. It can be shown that to represent fully a signal with highest frequency component f_{\max} at least $2 f_{\max}$ samples per second must be acquired.

Thus $c = f_{\max} \log_2 (1 + P/N)$ and no matter what process is carried out on the acquired data, C is the maximum rate of retrieval of information. For example for a typical noise or vibration data system of signal to noise ratio 10^5 (50dB) and bandwidth 20kHz information is supplied at some 330,000 bits per second.

We now go on to describe and outline techniques used to extract the more useful information from this enormous flood of data.

3.3 Transformations

3.3.1 Conservative Transforms

Processes applied to signals in which the original form cannot be reconstructed are known as non-conservative. It is helpful however, first to discuss those which do permit the original signal to be conserved.

For discrete waveforms which repeat after an interval of time (or space) it is best to measure in terms of events per second (or per metre). We need to transform from a time (or distance) domain to a frequency domain.

3.3.1.1 Fourier Analysis - Any repetitive waveform may be divided into component sinusoidal waves of various frequencies by the well known Fourier Analysis. Sine waves are convenient because they have the same form on integration or differentiation and linear systems give sinusoid outputs for sinusoid inputs. Figure 4.1 shows a repeating voltage pulse and the first 3 Fourier components or harmonics. By retaining the phase relationship between each component, the original signal could obviously be reconstructed by summation of all the components.

The amplitudes A_n , B_n of each harmonic n can be determined from the expressions set out in Figure 4.1. These are seen to be of similar form where the original data is of the discrete sampled type as for the continuous waveform case. Theoretically we need an infinite set of harmonics but in practice lack of detail in the input signal sensibly limits the number. Physically the process of determining the coefficients can be regarded as masking of the time function by each component waveshape and averaging the masked result. This is easily seen for a unit pulse as shown in Figure 4.2. The amplitude and phase information can also be represented by a series of complex coefficients C_n in which case n can take negative values. In the vector representation shown on Figure 4.1, the negative values of n represent the complex conjugates, or mirror images in the real axis C_n^* , of the positive coefficients. Note that in complex notation, the forms of the time domain and frequency domain expressions are similar apart from a factor and the sign of the exponent.

3.3.1.2 Fourier Transforms - Where a function is not periodic we can still convert to the frequency domain by extending the period to infinity (effectively) thus making the fundamental frequency approach zero (f). To avoid C_n becoming also zero, we keep $n \times f$ finite by allowing the number of components n to become very large. We define a new frequency domain function by $V(f) = C_n/f$ whose relationships are set out on Figure 5, again for continuous and discrete functions. Notice again the same similarity of form in both time and frequency domain.

An example is shown in Figure 5.1 of the transform for a unit pulse of width δ . The frequency "spectrum" rapidly falls to a low value in the range zero to $1/\delta$ Hz, but hovers about the frequency axis asymptotically to infinity. In Figure 5.2 and 5.3 the effect of pulse width is illustrated (maintaining constant pulse area by increasing amplitude inversely). The effect is an inverse relationship between spectrum width and pulse width.

For a train of identical pulses at regular intervals (Figure 5.4); the frequency domain consists of a number of spectral lines at a frequency interval set by the repetition rate. The shape of the line spectrum envelope is controlled by the shape of each pulse and again there is an inverse width relationship between time and frequency domain. The discrete form of the pulse train example is shown in Figure 5.5. After frequency $Qf_0/2$ the envelope repeats in mirror image form and thus sets an upper frequency limit for a given sampling system. The length of signal record determines the spacing of the frequency lines and the number of samples taken determine the number of lines and therefore the frequency range. More samples give redundant information.

3.3.1.3 Other Conservative Transforms - These are mentioned briefly, but further reading should be sought for detailed accounts. There is no reason why sine wave components must be used for frequency analysis. Laplace Transforms use either exponentially decaying or increasing waves and are

used where expressions for the frequency domain would not otherwise converge, e.g. where the time function has a value at infinite time such as when a single voltage step is applied to a circuit.

The discrete information extension of Laplace transforms is termed a Z transform.

Walsh functions use square waves of various frequencies and can be used in place of Fourier analysis where the time domain signal has sharp regular changes. They have the advantage of requiring fewer harmonics to obtain full representation of the signal.

3.3.2 Non-Conservative Transforms

In achieving our aim to lose non-essential information it is often advantageous to be able to use several appropriate non-conservative transforms in conjunction with one another. Obviously tape recorded data or a digitally stored equivalent, enables many such processings to be attempted on the same time domain data until a satisfactory understanding of the physical system being studied is obtained. No real signal could be predicted with absolute confidence as it always contains some element of probability. Thus even sine waves in practice contain deterministic and probabilistic parts. The following techniques can, in the main, be applied to both types of signal.

3.3.2.1 Ensemble Averaging - This process is also known as cyclic averaging and signal education, and can be used to extract a signal known to be repetitive from within random signals or noise. A large number of time records of the signal are collected, each starting at the expected repetition frequency. This is achieved either by means of some triggering signal (on another tape channel) or by means of an accurate clock pulse in the sampling device. This is illustrated in Figure 6. Each record can be regarded as the sum of the repetitive or deterministic signal and the probabilistic component (6.1). Clearly, an ensemble average of the deterministic signal at each point in time from the triggering will be of identical form to each individual record (6.2). However, the probabilistic ensemble average will tend to zero for Gaussian noise (6.3) and after R averaging the signal to noise ratio will be effectively \sqrt{R} greater than initially. Figure 7 shows the graphical relationship between initial and final signal to noise (in decibels) and it can be seen that a signal originally buried in noise by 20 decibels becomes 20 decibels clear of the noise power after 10^4 averagings. Figure 8.1 shows the waveform of a signal in which a 0.8 volts peak to peak 500 Hz sine wave is immersed in noise of the order of 10 times this voltage range. The tone is clearly shown up when a 36 degrees of freedom Power Spectrum is calculated. Doubling the degrees of freedom indicates a slightly reduced 'noise' contribution to the sinusoidal component.

Figures 8.2 to 8.5 show the effect of progressively greater numbers of averagings of the waveform and the resulting progressive isolation of the 500 Hz component in the Fourier Transform of the averaged waveform. (The low frequency peaks should be ignored since they arise from slight amplitude fluctuations of the 500 Hz tone).

Education, which can be performed digitally or in analogue fashion, is clearly a useful tool in the interpretation of signals from rotating machinery.

3.3.2.2 Probability Functions - Sometimes the time at which a signal level was present is not important and we are merely interested to know how often a given level will occur. An example is in the analysis of strain data for possible overload. Here probability functions are helpful, sometimes termed amplitude domain representations.

The cumulative probability P_V of a signal at a level V can be obtained by summing all time intervals for which the signal is less than V and dividing by the total time T - see Figure 9.1. As V is raised, the value of P_V goes from zero to unity since all real signals have a finite range. For discrete samples signals we merely take the proportion of total samples below the specified levels of V .

The probability density function (P.D.F.) is more often useful and is in effect the differential or slope of the cumulative probability function. Clearly at high and low V the P.D.F. (symbol p_V) of zero and the total area under the curve must be the total or cumulative probability over the signal range and equals unity. The area between any two voltage values represents the probability that the signal is between them.

Examples of P_V and p_V are shown in Figure 9.2 for sinusoidal, random and other types of signal and these functions clearly enable the form of the time domain data to be distinguished. For a sinusoid the theoretically infinite value at the amplitude voltage becomes modified for real waves into the form indicated.

We can also examine the probability that one signal lies at one voltage whilst another signal lies at another voltage. A joint probability density function can thus be obtained for the two signals (Figure 9.3). Here the volume under the 3 dimensional surface is unity and the probability of the voltage lying between two values whilst the other lies between other values is given by the column enclosed by the voltage limit planes. For signals totally unrelated to each other the sections in each voltage plane are of identical form and equal to the individual P.D.F.'s. For more related signals the "plan view" becomes more and more ellipsoidal and eventually becomes a line bisecting the two voltage axes for completely correlated waveforms.

3.3.2.3 Overall Signal Parameters - The most common non-conservative parameters used to describe signals are single number values (for stationary signals whose average values remain time invariant). These can be obtained either from a further "boiling down" of the amplitude domain functions of 3.3.2.2 or found directly from the time domain.

a) Mean Value

Effectively the d.c. component. Obtained by time averaging the signal or from the difference in areas enclosed by the C.P. (Cumulative Probability) plot. Alternatively it is given by the 1st moment of area

of the P.D.F. about the $V = 0$ axis. Figure 10.1 illustrates this. Very highly damped electro-mechanical instruments display this value.

b) Mean Rectified Value

The cheaper dynamic signal meters indicate this value. The modulus of the signal is time averaged or alternatively the sum of the C.P. plot areas is taken (10.2). This parameter does not in itself have much physical significance except when known to be related to other parameters for simple waveforms.

c) Mean Square and R.M.S. Values

This is more useful as both positive and negative portions of the waveform are equally influential. Effectively the total energy of the signal is found by this means. The values can also be derived in terms of the probability functions as shown on Figure 10.3. Where a signal has a d.c. component, we can modify the mean square by operating on the difference value between signal and d.c.

The 2nd moment of the P.D.F. is thus a measure of the mean square value. For the total signal the 2nd moment is taken about the $V = 0$ axis and for the varying part about the $V = \text{mean value line}$. This is the same as the variance of the signal and thus the r.m.s. value and the standard deviation are equivalent.

Sometimes higher moments are useful and the 3rd order moment is used to examine skewness (or asymmetry of the probability distribution).

d) Peak Value

Peak value is of interest for example if it is required to avoid an overload in a system. For probabilistic parameters this is difficult when the P.D.F. has skirts which have a significant probability value at large signal voltages. In Figure 9.4 the area of the shaded portions represent the probability that the signal will exceed (positively or negatively) the value V_1 . An acceptable probability of failure can be chosen to define V_1 and hence monitored for overload risk. In electronic circuits we may choose to define V_1 on the basis of acceptable loss of signal energy due to overload.

e) Peak and Form Factors

These give a simple indication of signal type. The Peak Factor is defined as the ratio of peak value to r.m.s. value and is sometimes called the crest factor. A "broad" signal such as a square wave has a crest factor of unity, whilst a triangular or sawtooth wave gives a ratio of 1.732. Other values for various signals are given in Figure 9.5. It is useful to appreciate the typical crest factors for signals in order to avoid overload distortions when recording sound which has large peaky excursions.

The Form Factor is similar and is the ratio of r.m.s. to rectified mean values. Again this indicates the shape of the wave form giving a value of unity for a square wave and 1.14 for triangular waves.

3.3.2.4 Cross Correlation Functions - Just as one dimensional probability functions can be reduced to simple overall parameters, a joint probability density function can be reduced to a single factor by taking moments about both voltage axes. The result is the cross-correlation C_{AB} between the two waveforms. For the symmetrical type of joint probability plot, the value of C_{AB} will be zero indicating no relationship of one signal with the other. The cross-correlation can also be obtained from the time domain information by multiplying the signal values at each instant of time and averaging the result timewise. The expressions are shown in Figure 11.1.

All information about time and hence phase is lost in the averaging process. However, more information can be retained by delaying one signal with respect to the other and evaluating the cross-correlation for all values of delay time. The resultant function $C_{AB}(\tau)$ has a form which depends considerably on the two signals. If a random signal from a process is collected at points of the system which effectively delay one by a time τ_1 , with respect to the other, then the function $C_{AB}(\tau)$ will maximise at $\tau = \tau_1$, and will rapidly fall to zero for other values of τ .

Totally unrelated signals will give $C_{AB}(\tau)$ zero for all τ . Identical frequency sinusoidal signals will likewise peak up at τ_1 , but C_{AB} will also peak at intervals defined by the period of the sinusoidal components present (see Figure 11.3). If sinusoidal signals have superimposed noise, then the cross correlation will combine the characteristics of the components and we have another means of evaluating the true signal (11.4).

3.3.2.5 Auto-Correlation Function - This is simply the same as a cross correlation except that one signal is "crossed" with a delayed version of itself. In contrast to cross correlation the auto-correlation:-

- 1) is always maximum at zero delay ($\tau = 0$) as one would expect since a signal must have utmost correlation with itself;
- 2) at zero delay its value becomes the mean square value of the signal. (Thus for two signals, the cross correlation at zero delay is in effect a measure of the energy content of their related parts);
- 3) is symmetrical about $\tau = 0$, since, in this case, it does not matter which signal is delayed.

The auto-correlation is not a linear function and the sum of separate functions will not give the function for the total of their respective signals. Instead the summation involves cross correlation terms. An example of the auto-correlation of a random signal is shown in Figure 11.5. Other types, such as sine and mixed sine and noise have similar forms to their cross correlation apart from having the maximum at $\tau = 0$.

3.3.2.6 Correlation Function Coefficients - Sometimes cross correlation functions are normalised by means of the product of the r.m.s. values of each signal. Remembering that the r.m.s. is the auto correlation value at $\tau = 0$, the coefficient becomes:

$$R_{AB}(\tau) = \frac{C_{AB}(\tau)}{C_A(0)C_B(0)}$$

3.3.2.7 Power Spectra - Cross and auto-correlations are time domain averaged functions. In 3.3.1.2 we obtained frequency domain data by Fourier transformation. Fourier transformation of the auto-correlation function (using τ as a time variable) likewise yields frequency domain function which expresses the frequency distribution of the energy per unit bandwidth of the signal. This is termed the power spectral density and can be integrated for all frequencies to give the mean square value. It can be shown that the power spectrum can also be obtained by multiplying the Fourier transform of the signal by its conjugate and averaging over a number of samples. The expressions involved are set out in Figure 12.1. C_A is an even function producing a real function in the frequency domain. However the mathematical definition of f permits negative values, and for real frequencies the calculated power spectrum values must be doubled. Figure 12.2 shows an example of the power spectrum of a narrow band of random noise. Again the familiar inverse relationship between time and frequency domains holds and a wide band power spectrum results from an infinitesimally wide auto-correlation function.

For a pure tone the power spectrum theoretically consists of an infinitesimal width and infinite height. In practice at infinite delay the auto-correlation of all real signals must tend to zero and so the height of the line spectrum is limited to a finite value (12.3).

3.3.2.8 Cross Spectra - The Fourier transform of the cross correlation function gives the cross spectrum for two signals and indicates the power density at each frequency common to both signals and also gives the phase between them. This arises because the cross correlation function is not even and hence the frequency domain function is complex. The real component is termed the co-spectrum and the imaginary part the quad or quadrature spectrum. Alternatively an expression in argument and exponent form can be used as in Figure 12.4.

3.3.2.9 Coherence Function - More information can be obtained about a system by using the coherence function (12.5). Suppose we sample a signal A at input and B at output from a system whose frequency response function is $H(f)$ (Figure 12). The output at B may contain system noise as well as components arising from its treatment of input A. The cross spectrum between A and B measures the common part. The response is the ratio of this cross spectrum to the input spectrum, that is:

$$H(f) = \frac{S_{AB}(f)}{S_A(f)}$$

In the absence of noise the response would also be the square root of the ratio of the individual power spectra:

that is $H(f) = \sqrt{\frac{S_B(f)}{S_A(f)}}$ and therefore the ratio of these two denominations is unity for zero system noise. This ratio which is equivalent to:

$$\frac{S_A^2(f)}{S_A(f)S_B(f)}$$

is called the coherence function and is reduced to zero as more and more noise becomes included in B such that B and A become totally unrelated.

3.3.3 Function Relationships

Figure 13 summarises the relationships between the various non-conservative functions and values. Those marked with an asterisk can be used to separate signals from superimposed noise.

4. BASIC INSTRUMENTATION

For noise experiments, we need to make use of the basic instrumentation scheme depicted in Figure 14. Firstly the pressure signals from the experiment must be converted to an electrical (voltage) signal using a pressure-to-voltage transducer, which is termed a microphone when sound pressure fluctuations in air are being detected. It is unusual for the voltage signals from the transducer to be either strong enough, or to be in a suitable form simply to be passed directly to an instrument for determining the signal level. It has to be passed through some form of amplifier to increase its voltage as a faithful but magnified replica of the original signal without unacceptable distortion. We may wish to examine the frequency domain composition of the signal, and so some form of signal analyser may be coupled to the amplifier output. Finally it will be necessary to employ some type of display device in order that we may 'read' the values of the signal levels or spectral composition. When we measure the characteristics of a sound source in this manner, the instrumentation is said to be 'on-line', i.e. we measure the levels etc. at the very time that the experiment is in progress. Alternatively we may store the amplified signal in some form of store which can reproduce the original data-form at a later time for analysis metering and display.

4.1 Microphones

Microphones may be made either to respond to the acoustic pressure value or to the gradient of pressure. The latter are not of general merit for acoustic experimental work. Of the direct pressure types, the main categories in use are the moving coil, the condenser, the R.F. capacitor, the electret and the piezo-electric microphones.

There is no direct way of converting acoustic pressure into an electrical "copy" but a microphone diaphragm may be set in motion in sympathy with the incident acoustic pressure. The diaphragm movement may then be measured electronically. The main difference between microphone types lies in the method of detecting the diaphragm displacement.

4.1.1 Capacitor or Condenser Microphone

This type (Figure 15) generally gives the most accurate and consistent readings but is relatively expensive. It should be noted that since this microphone requires about 200 volts for its operation its use in potentially explosive environments (e.g. in an oil refinery) may be prohibited.

The metal diaphragm is placed close to, but insulated from, a metal backplate (Figure 15). The two parts thus form a capacitor which varies in value as the acoustic pressure displaces the diaphragm. A steady voltage is applied through a high resistance ($\approx 10^8$ ohms) to the capacitor, thus ensuring constancy of electrical charge. Thus the variable capacitance causes the voltage across it to vary ($V = Q/C$), as a "copy" of the acoustic pressure. Therefore, the voltage measured indicates the sound pressure. Sensitivity ranges from about 50mV per Pa for a 1" diameter diaphragm to 1mV per Pa for a $\frac{1}{4}$ " diameter.

Although this microphone is very good it has several sources of error which will be considered together in Section 4.1.7.

4.1.2 R. F. Capacitor Microphone

This is a type of condenser microphone which does not require the high polarisation voltage. Instead the capacitive effect of the microphone is used to modulate the frequency of a high frequency oscillator (typically 8MHz). Thus any sound wave incident on the diaphragm frequency modulates the carrier wave, (similar to V.H.F. FM radio). The carrier can then be modulated and the audiofrequencies extracted and amplified.

There are two major advantages of this type of microphone:

- a) Dust and particulate contamination of the diaphragm are reduced because it is no longer charged.
- b) The system may be operated at low voltages making it suitable for use in potentially explosive situations. Accuracy, reliability and sources of error are very much as for the conventional condenser microphone.

4.1.3 Electret Microphone

This is another derivative of the condenser microphone where the polarisation voltage is permanently "embedded" in the diaphragm. By making the diaphragm from a sandwich of ceramic polymers and plating the external surface with a metallic layer, the diaphragm can be induced to take up a permanent charge (Figure 16). This charge will remain stable throughout the life of the microphone. Operationally, the microphone behaves exactly as a normal condenser microphone, and a voltage output is produced proportional to the incident sound field. Such microphones are comparatively novel but initial problems matching the stability of a conventional condenser microphone have been largely overcome. They are also not now as expensive as they were and as an overall system they can be used with cheaper unspecialised pre-amplifiers and require no polarisation voltage supply.

4.1.4 Piezo-electric Microphone

Certain crystals behave like capacitors and develop charge and voltage across opposite faces when a force and strain is applied in another axis. In the piezo-electric microphone, a diaphragm is used to convert the acoustic pressure into a force (Figure 17). As in the capacitor microphone, a special amplifier must be used. Piezo-electric microphones are cheaper than the capacitor types but are easily damaged by elevated temperatures. The older types using Rochellesalt crystals were limited to 45°C maximum and the calibration was also temperature dependent. Older types were also damaged in high humidity conditions. Modern materials such as Barium Titanate permit operations up to 55°C and are only affected by humidity greater than 90%. Sensitivities are generally 25dB less than the equivalent area condenser microphone.

4.1.5 Low Frequency Microphones

Pressure equalisation effects and also cathode follower charge leakages mean that specially designed microphones must be used for signals where very low frequency components are expected, e.g. for sonic boom measurements. The microphone illustrated in Figure 18 is capable of measuring as low as 0.1Hz and has a sealed diaphragm in place of the usual equalisation ventilation hole. It is used with a special F.M. based (carrier) amplifier in place of the usual cathode following and power supply system.

4.1.6 Moving coil microphone

Attached to a diaphragm is a coil of fine wire which moves in a strong magnetic field when an acoustic pressure displaces the diaphragm. Thus the acoustic pressure generates a small voltage in the coil as the replica of the sound pressure and this is then amplified to a suitable level.

This type of microphone is quite robust, requires no cathode-follower for long cables but does not have the frequency range of the other types. This type of microphone is very useful for field work but is rarely used in contemporary aero-noise research. Care must be taken in strong magnetic fields (i.e. near transformers) to avoid erroneous or spurious signals.

4.1.7 Directional microphones

By using a long tube with slotted ports through which the sound field is sampled, a combined use of the interference principle and pressure gradients can lead to a highly directional microphone (Figure 19). For many relatively high frequency sources of aerodynamic sound, the acceptance cone angle for 6dB below peak levels can be as little as 30° either side of the axis, and hence the use of such a microphone might be considered in situations where unwanted reflections might occur from a rig or tunnel wall. On axis frequency response is maintained acceptably flat in the range 100 Hz to 20kHz.

4.1.8 Low Airflow-Self-Noise Microphones

Where microphones are to be used in modest airflows, of the order of 10 m/s or less, then simple foam ball wind shields are effective and give rise to negligible error due to its presence. For higher speed flows, special nose cones can be fitted which have been designed to create as little disturbance as possible which would give rise to flow boundary pressure fluctuations in the normal audio frequency test range (Figure 20). These cones impose a ± 2 to 3 dB change in high frequency response dependent

on the size of condenser mic and cone, and on the precise angle of sound wave incidence to the cone axis. Manufacturers data should be consulted for details in any given application. It is not possible to eliminate wind noise by these cones, but about 10dB improvement compared to a standard microphone and protection grid is obtained when the wind is along the axis of symmetry. As speed increases there will nevertheless become a limit where the self generated noise levels are unacceptably close to those to be measured from the test source. An approximate guide is that in a 160 km/hr airstream an overall level of just over 100 dB LIN is generated by the airflow, but high pass filtering at about 250 Hz would further improve the situation.

Using the same interference principle as for the long tube directional microphone, but optimised for the rejection of the convected turbulence pressures along the tube, a microphone has been developed which improves signal to noise ratio by up to 6dB. Acoustically originating waves in the airflow are not convected at the same speed as those due to the turbulence field and hence it is possible to arrange for these not to be rejected.

4.1.9 Sources of Error

The following sources of error may occur in all microphones:

- a) If the microphone or its stand is placed on a surface which is vibrating then the microphone diaphragm itself may vibrate relative to the microphone body and produce a spurious signal at the microphone output. Care must be taken to isolate microphones from vibrating components.
- b) In an airstream a microphone will generate turbulence whose pressure fluctuations produce unwanted diaphragm movements and hence output. Special wind shields are available as discussed in 4.1.8.
- c) Obviously very quiet sounds will produce very small output voltage from a microphone and although these small voltages may be amplified electronically to a workable magnitude a limit is reached where the microphone output becomes comparable to or less than, the inherent electronic noise generated by the amplifier. Thus, as sounds become weaker, a point is reached (generally at about 10 to 20 dB sound pressure level depending on microphone and amplifier), where the amplified output tends to become constant at the constant noise voltage of the amplifier. Manufacturer's data should be consulted when measuring "quiet" sounds.
- d) Very loud sounds produce large diaphragm displacements, with resulting non-linearity and distortion of the microphone output (in an extreme case the diaphragm could touch the backplate). Again the microphone manufacturer's data should be consulted as distortion is dependent both on the microphone and the amplifier (exercise caution above an S.P.L. of 120 dB.) Exposure to extreme noise levels, shocks due to dropping the microphone, or even careless clamping of the microphone body to a support may destroy the microphone or cause a serious loss in calibration.
- e) Due to the fact that the microphone diaphragm has mass and compliance and forms a damped resonant system at high frequency, the sensitivity of the microphone falls rapidly with increase of frequency above resonance. Ideally a microphone should measure pressure at a point, but since the diaphragm must be large enough to give sufficient sensitivity, the microphone measures the net pressure over the area of the diaphragm. Obviously this affects the response at frequencies where the acoustic wavelength becomes comparable with the diameter of the diaphragm. These effects, together with distortion of the sound field produced by the body of the microphone at short wavelength, result in a microphone response which is dependent on frequency, microphone shape and size and angle of sound wave arrival. A small microphone size is required for high frequency (short wavelength) measurements. The microphone response should be carefully studied if frequencies above 5kHz are to be measured. Typical response characteristics are shown in Figure 21. A microphone with a poor frequency response may give serious error when measuring close to the peak frequencies and it is therefore important to use high quality microphones for noise measurements and to point the microphone in the correct direction relative to the source of the sound. This is because types may be obtained to give the greatest possible response at either normal incidence, 90° to normal (grazing), or random (sound issuing simultaneously from all directions). Other microphones are designed to respond optimally in an enclosed "pressure" space environment as opposed to the normal free field situation.
- f) A small pressure equalizing channel must be provided between the cavity formed behind the microphone diaphragm and the outside atmosphere so that the diaphragm will not be distorted by changes in atmospheric pressure. Obviously the acoustic pressure tries to equalise as well and results in low sensitivity at low frequencies. By designing the channel carefully, equalisation is prevented at frequencies above a few Hertz, so that apart from keeping the channel clear the effect may be ignored except where special low frequency response is needed as in sonic boom over-pressure measurements.
- g) Elevated temperatures will cause loss of calibration or destroy microphones and hence must not exceed the manufacturer's quoted maximum, typically 150°C.
- h) The capacitor microphone requires amplification of its output and a steady voltage applied to the diaphragm to charge or polarise it. This means that an electrical circuit containing resistance etc., must be connected to the microphone and as the capacity and voltage of the microphone varies with sound pressure so electrical charge leaks through the external resistance causing the voltage to fall. An electronic circuit (called a cathode follower) keeps the leakage as small as possible, but some low frequency fall-off is inevitable. The low frequency signals vary slowly in time and so the leakage has longer to produce a loss of charge and voltage.

The effect of this leakage is shown in Figure 22. The low frequency response depends on the microphone cathode-follower (sometimes called a microphone amplifier). If measurements of low frequency sources are being conducted, follow the manufacturer's instructions and use the correct microphone and amplifier.

- i) A further action of the cathode-follower is to prevent the output cable of the microphone loading the microphone and producing a loss in sensitivity. Without the cathode-follower, all the microphone cable capacity would be connected directly to the microphone capacity so that a change in microphone capacity would produce a lower voltage change than that without the cable, i.e. the charge on the microphone can redistribute itself in the microphone and cable capacity. Since $V = \frac{Q}{C}$, and C is now larger, the resulting voltage will be less than for the microphone capacity alone.

Most microphones are calibrated for a given cathode-follower and connecting cable length.

The output cable from the cathode-follower is not critical due to the cathode-follower action. This is illustrated (Figure 23). Quite often a microphone is screwed straight onto the cathode-follower to avoid a connecting cable. Figure 24 gives a guide to selection of microphone frequency ranges and sensitivities.

4.2 Measuring Amplifiers

4.2.1 The Sound Level Meter

A sound pressure level of 140 dB may give sufficient microphone voltage output to be measured directly, but if a sound pressure level of only 20 dB must be measured, then only one-millionth of the output voltage given by 140 dB will be obtained. Obviously some kind of amplifier will be required to amplify the weak voltages produced at low sound levels. In addition, it is not possible to display or measure voltages which may vary over a million to one in range according to the sound level, directly on a meter with linear scale length of, say, three inches. The very maximum one may expect to obtain with acoustic readability on a linear scale would be about 20 dB (10:1). The difficulty is one solved by making the amplification variable in steps of, say, 10 dB and calibrating the meter over a scale range of -10dB to +10dB relative to scale datum. Thus a small microphone output (or sound pressure level) may not indicate anything on the meter but, when the amplification (or gain) is adjusted, a reading will be obtained and the sound pressure level (in dB's) will equal the sum of the meter and variable gain readings.

The very wide range of microphone output may require attenuation as well as amplification and some instruments use two separate amplification or attenuation controls. In this case it is very important to check the operating instructions and ensure that the distribution of amplification between the two controls is correct for the level of sound being measured, otherwise there is danger of inadvertently over-loading an amplifier stage and producing an error in reading.

The amplifier of the sound-level meter must be protected from vibration, magnetic fields and intense sound otherwise it may itself act as a microphone and give erroneous output. The apparatus (Figure 25 is typical) should have its mains or battery power supply checked for correct voltage (there may be a built-in test facility for this). Exhausted batteries should be replaced. The equipment should be allowed the recommended time to warm-up before taking any noise readings.

The voltage output of the amplifier is a measure of the sound level and a meter measuring this voltage is calibrated in root-mean-square (r.m.s.) sound pressure level, and is reasonably accurate for most types of sound except impulsive. For the latter a much shorter meter integration time is needed for special grades of meter are especially designed to give a reasonable measure of the sharpest impulses met in most applications. Note that older instruments measured the rectified average pressure but were marked r.m.s. They thus produced errors and only read correctly with certain (usually sinusoidal) sounds.

Very few noises are exactly constant in amplitude over a period of time and hence the sound-level meter pointer will fluctuate over its scale. There is also some evidence that the ear tends to integrate sounds over a duration of 100m sec. This integration or "sluggish" effect in hearing is usually built-in to the indicating meter and also helps the observer estimate the mean of a violently fluctuating sound. Sometimes it is possible to switch from this ("FAST") condition to a more sluggish ("SLOW") one which helps further in obtaining a mean reading of some sounds. Obviously the latter condition could not be used in fluctuating and short duration sounds (e.g. an aircraft fly over) as the meter pointer would not have sufficient time to reach the correct reading before the sound had ceased.

4.2.1.1 Grades of Noise Meters - Noise measuring meters may be classed in the following groups in ascending cost, accuracy and versatility:

- a) Survey meters - light and portable, suitable for preliminary investigations.
- b) Industrial grade sound-level meters - more bulky, often capable of spectrum analysis - useful for most work (British Standard 3489; IEC 123).
- c) Precision sound-level meters - for scientific work and accurate measurement (British Standard 4197; IEC 179)

4.2.2 Microphone Amplifiers

For laboratory work, it is usually more satisfactory to employ a mains powered combined microphone pre-amplifier (cathode-follower), power supply unit, voltage amplifier, and meter display (Figure 26). Such instruments usually also contain filter networks for de-emphasising high, low or high and low frequency sounds, for example the D-weighting and in some countries the A weighting are used to measure aircraft noise levels: the D-weighting permitting an approximation to Perceived Noise Levels.

4.2.3 Calibration

In non-mains equipment battery voltage should be checked regularly (ideally before and after a measurement) and the meter and microphone calibration should be checked and adjusted according to the operating instructions. It is recommended that the instrument is overhauled every year.

The calibration facilities differ considerably between manufacturers and type of instrument.

- a) Electrical calibration - an externally or internally generated electrical signal of known amplitude and frequency is injected into the microphone amplifier circuit. If the output meter deflection is incorrect, slight compensation can be made to the amplification by adjustment of a pre-set control. Although this calibration can check the amplifier, and possibly the weighting networks and filters, the microphone sensitivity is not checked. It is important therefore to supplement this form of calibration with regular acoustic calibration.
- b) Acoustic calibration - a known acoustic sound pressure level is applied to the microphone and compared with the sound level meter reading (usually dB Lin). Any error outside the quoted tolerance may be adjusted by the pre-set gain control (if available), but large errors may indicate damage to the sound level meter or acoustic calibrator and both should be returned to the manufacturer for checking. Briefly, acoustic calibrators fall into the following types:
 - i) Falling Ball Calibrator
These have an accuracy of about ± 2 dB but extreme care is necessary to obtain exact separation and alignment between the calibrator and microphone. The ambient SPL must be at least 10 dB below the calibrator SPL.
 - ii) Cavity Coupled Calibrators (e.g. Pistonphone)
Here the calibrator is attached to the microphone and an accuracy of ± 0.2 dB is possible with care (Figure 27). Pistonphone calibrators should not be left running longer than absolutely necessary to make a calibration reading because considerable mechanical wear and loss of calibrator precision results.

It should be noted that the calibration SPL produced by this form of calibration will depend upon the cavity volume and any leakage of air from the cavity. Hence this form of calibrator is designed for a particular type of microphone.

A technique used for laboratory standardisation calibration of microphones uses the reciprocity principle against a known (secondary standard) microphone periodically checked by the appropriate national standards institute. Also an electrostatically driven actuator can be applied to condenser microphones to induce an equivalent known diaphragm movement to represent a given sound level. This can be driven by a sweep oscillator giving a constant voltage output to check frequency response.

4.3 Filters and Spectrum Analysers

It is often useful to determine the frequency domain version of a noise signal, for example in order to relate discrete tone components with basic features of the machinery or process generating the noise. Also, most of the subjective loudness, speech interference and annoyance ratings of noise are strongly dependent on the frequency composition. We have seen that this may be accomplished through Fourier transformation, and this may be done by a computational method, having firstly represented the signal as a digital sequence, or by analogue devices which have "transfer functions" which copy the mathematical transformation processes.

4.3.1 Analogue Types

- a) Passive filters - the usual analogue signal analysis devices are based on the well-known tuned Resistance, Capacitance and Inductance electronic circuits. By choice of these parameters, and using multiple tuned elements, filters can be devised to accept only signals with frequency components within a certain range called the pass band. Additionally filters can be designed to pass all signals below a certain value (Low Pass) or above a certain value (High Pass). The H.P. filter is particularly useful for avoidance of spurious, but often dominating low frequency components such as from the wind, thus effectively increasing the signal to noise ratio in the frequency range of interest.

Again, the R, C and L values of a filter may be arranged to give either a "single" tuned acceptance band, or a damped "double" band, and with care this double band can come very close to an ideal rectangular acceptance characteristic (see Figure 28).

If the pass bands for a whole series of filters are arranged to take over where the previous filter left off, then the filters are said to be contiguous. Alternatively a single filter may be swept, using the heterodyne principle to filter the signal at any required centre frequency and yet to maintain the same percentage or constant absolute bandwidth. Usually the complete range of frequencies of interest in audio sound cannot be obtained with a single tuning control, and so the sweep is switched in ranges to enable still wider frequency tunings to be obtained. By varying the resistance value, steps of selectivity can be chosen (Figure 28).

Important aspects of filters are the steepness of the boundary zones between acceptance and rejection, and the flatness of the pass zone, particularly for the double pole type. The characteristics of Figure 28 are typical and high grade instruments conform to requirements in respect of skirt steepness according to IEC 225 1966 or ANSI S1.11. Because the skirts cannot be absolutely steep, contiguous filters are arranged so that the energy level for a signal with frequency passing through the transition region remains sensibly constant. In other words the crossing points are arranged to be 3 dB below the average plateau level. The noise bandwidth of the filter is defined as the width of ideal "rectangular" filter which would contain the same noise power level as the real filter, i.e. the areas under the curves are equal.

It is common to find filter sets which have either constant ratios of upper and lower cut-off frequencies, or which have constant pass band intervals. Where the constant percentage type has a ratio of 2 (approximately since there are ISO standardised cross over and centre frequencies with convenient values), the pass bands are designated octave bands. Other fractional bands, such as $1/3$ octaves provide a finer breakdown of the signal in the frequency domain. Some swept single tuned filters can be set such that their skirt characteristics and selectivities range approximately from

1/3rd octave to 1/6th octave or even 1/12 octave bands.

In contrast, filters with constant intervals are not usually found as contiguous sets (at least in analogue form). Constant bandwidths of 3, 5, 10, 30, 50 and 100 Hz are typical, sometimes selectively or with insertion of chosen filter crystals.

For some applications, as with an accelerating gas turbine engine, it is useful to be able to "track" a particular (usually prominent) discrete tone which arises from a process directly associated with the shaft frequencies or some multiple thereof. The tracking is achieved by an automatic gain sensitive loop. Alternatively the tracking may be provided by a specially generated tracking signal, whereby the analyser reverts to a sweep tuned analyser.

b) Active Filters - In the passive filters, the pass band shapes can never be truly rectangular and raises falsified spectra in some circumstances discussed in Section 5.6. With active filter elements, using electronic solid state operational amplifiers to selectively increase the gain of the wanted signal pass bands, much more accurate filtering may be achieved, but at the expense of greater capital outlay.

4.3.2 Real Time Analysers

Fairly recent developments in analyser design have produced a completely new concept of analyser called the Real Time Analyser (RTA). Such analysers can perform all the functions of the types mentioned previously, and with the aid of a small computer several functions hitherto only possible by the use of expensive computer complexes. These analysers are available in two distinct forms: a) third octave (constant percentage) and b) narrow band.

- a) One Third Octave/Octave Real Time Analysers (Figure 29) work on similar lines to any conventional one-third-octave filter, except that instead of switching individual filters, each analyser has a complete set of filters covering the audio frequency spectrum, or where fractional filters are employed, selected parts of the range. The output from each filter is detected, held in an electronic memory and displayed simultaneously, a complete spectrum taking only about 1 ms (1/1000th of a second) to produce. The memory can then be "unloaded" into various display devices at speeds compatible with the device. The memory can be continuously updated with fresh information, or new information added to that already existing to produce an averaged spectrum. More recently, instrument manufacturers have produced completely digital versions of 1/3 octave and octave band RTA (see Section 6 on digital analysers).
- b) Narrow Band or Time Compression Real Time Analysers work on somewhat different techniques. Here the desired audio range is stepped by a constant bandwidth filter in "compressed time" to produce a narrow band spectrum which again can be stored for unloading into many display devices. A typical configuration for such an analysis would be 0 - 2k Hz in 500 steps each having a bandwidth of 6 Hz. As with the other type of analyser, spectra can be averaged, and with additional electronics synthesised into octaves or one-third-octaves.

Both the analysers described above can perform analyses in very short periods of time, hence obviating the need for stable conditions or tape loops. They can be interfaced with a computer to perform very complex tasks and can provide plots on a wide variety of displays. They are, however, considerably more expensive and require more skilled setting up.

4.4 Storage and Display Equipment

Having measured and analysed a signal, it is usually necessary to make some permanent or sometimes temporary or semi-permanent copy of the data for future reference or further processing.

4.4.1. Ultra Violet Light Chart Roll Recorders

This is one of the simplest recording instruments of the type which produces a record of some signal parameter across a chart roll which is fed at uniform rate with time from the device. (figure 30 is an illustration of one type). The marking of the chart is achieved from its sensitivity to Ultra Violet (U.V.) radiation. Each galvanometer channel consists of a finely balanced and suspended coil with a mirror attached. The U.V. radiation is produced by a mercury arc lamp and collimated to a fine beam onto the mirror, motion of the mirror sweeps the beam over the sensitive paper in the direction normal to the chart roll feed. The recordings are invariably multi-channelled. Due to the reflected light principle the beams may cross on the paper trace. Identification of the channels is accomplished by interrupting each beam for a very brief moment with a slight delay on each channel relative to the neighbour.

Main timing marks are available at suitable fractions of a second along the paper feed, whose rate can be varied from about 10mm/sec to about 1.25m/sec. Additionally, finer timing marks are available as a square wave pattern along an edge of the chart, usually at millisecond periods. The signals to be recorded are played into the recorder channels via a suitable variable gain amplifier to ensure the maximum use of the available recorder level scale range for each data channel.

It is usual to use such recorders for displaying signal instantaneous values versus time. Although the light beams can move fairly reponsively, the maximum waveform frequency component which can be accommodated is about 100 Hz. Of course, the instrument can cope with steady signal components or D.C. as well as the fluctuating or A.C. levels associated with noise or vibration signals. Nowadays the papers used in U.V. recorders are self fixing, and as always are easily 'developed' by exposure to daylight or fluorescent lights.

4.4.2 Level Recorders

This term is used for a chart roll recorder which is restricted to a single trace along again a time axis. The chart is marked by a stylus working on waxed paper, or more usually using a special ink cartridge and pen system (see Figure 31). Amplitude of the trace may represent any of the usual signals

obtained from a measuring amplifier meter or sound level meter, viz, R.M.S., Peak or average level. The pen or stylus portion is controlled by a system of drive, comparative and feed back voltages applied to potentiometer coils with an electromagnetic actuator arm. The potentiometer can be changed to provide the desired full scale range, either logarithmically to give, for example, 10, 25 or 50 dB or else a linear scale, for example 10 - 35 mV. Adjustments are provided to control the writing speed of the pen so that adequate response can be set without unacceptable overshoot on rapidly changing signals. Since the writing speed may be set to an unstable condition, whereupon the pen control system goes into oscillation giving erroneous results, the manufacturer's instruction book should be consulted when choosing the writing speed for a given type of data recording, thus ensuring that the correct analysis confidence limits are achieved. The paper chart speed can be varied and usually driven mechanically or electrically in synchronisation with a turntable or a sweep tuned analyser or oscillator. Input range potentiometers and attenuators permit the accurate setting of the pen trace to a reference voltage or to a calibration line using a pre-recorded calibration during the noise measurements.

Since the level recorder detects the A.C. signal voltage, there is a lower limiting frequency at which it will do this correctly with a uniform frequency response. The lower frequency limit is usually selectable. The magnetic field required to drive the pen or stylus is very strong, and therefore care should be exercised not to leave instruments or watches or recorded magnetic tapes close to the level recorder. One make of level recorder permits the use of circular or polar charts in place of the normal chart roll. This is useful for presenting polar traversed data in a form readily appreciated in terms of directivity.

4.4.3 X(t) - Y Plotters

In contrast with chart roll recorders, the X(t) - Y plotter consists of a flat table on which is mounted a suitable paper, usually graphically ruled (figure 32). The pen is moved "upward" on a bridge, which itself is arranged to move "horizontally". The zero position and gain or sensitivity of each scale can be chosen within the available range (typically from 5mV to 5V per cm). Pen movement response is rapid such that the output signal and sweep rates, from analysers etc. can be followed without inaccuracy. Some plotters incorporate their own time base to be used in place of an external X sweep signal and hence effectively provide a level recording capability. Others can have built-in linear or logarithmic scaling circuits as opposed to accepting the form of signal from the analyser recorder output.

4.4.4 X(t) - Y(f) - Z Recorders

By use of fibre optics, a type of recorder can be obtained enabling representation of spectral information as time along the chart roll, frequency normal to the length of the roll, and signal level in a frequency band as density of trace (Figure 33). Naturally it is only possible to qualitatively judge signal band level, but the presentation is very useful in analysing aircraft flyover noise and detecting the Doppler shift of the noise data to the relative source/observer motion. The recorder uses U.V. sensitive paper and can be coupled to the output of an R.T.A.

In an alternative mode, the analyser can be made to output successive frequency analyses to the recorder in successive rapid sweeps of level along the chart roll direction and frequency normal to the roll. The sweep is so rapid that the effect is to produce successive spectral representations in a way permitting Doppler tone shifts or an accelerating machine to be readily observed. Figure 33 gives an example. As usual, paper speed and scale sensitivity is selectable.

Similar displays are obtainable from a type of apparatus known as a sonograph, popularly known for its use in voice printing. In this case, the density of chart colour is produced by a heat sensitive paper, and the chart paper is placed around a special drum designed to channel the frequency and time functions to the drum surface as the drum rotates.

4.4.5 Oscilloscope

This apparatus is familiar to most, since it is used widely in scientific research and engineering testing. A video screen is arranged to have a number of spots scan to a horizontal (X) voltage sweep or time base (t) voltage. The applied voltage is made to deflect the electron beam of the video tube and a further set (or sets) of deflection plates (Y) are used to deflect the sweeping light spot in step with the signal voltage applied to them. Thus the apparatus can be used to examine signals for frequency (since very high sweep rates may be applied) and accurate level of voltage. Hence it is often used as a recording monitor. Oscilloscope scales are set up using calibrated internal signals.

There are a number of refinements which may be used, such as multiple channels, triggered capture, delayed sweep triggering and screen storage so that impulsive signals may be studied relatively easily.

4.4.6 Stored Event Recorders

These are (usually) digital devices. The analogue signal from some short timescale event, such as a sonic boom signature, is converted to digital form in an A to D converter unit. The digital version of the signal is then cycled round a special memory, whereupon it may be recalled and displayed at will on a scope or other suitable device. This is a particularly useful way to produce a spectrum analysis of an impulse sound, since the recall can be analysed by either R.T.A. or by 1/3 octave or octave or 6% narrow band analyser to produce the energy spectrum for a single wave period approximately equivalent to the impulse duration.

4.4.7 Magnetic Tape Recorders

a) Direct Recording - The recording of noise for subsequent analysis is very convenient at times, especially when doing field work, but serious errors are likely to be introduced unless great care is taken.

First of all, expert advice must be obtained for the connection of the recorder input to the microphone or sound level meter output and also from the recorder to the analysing equipment as the electronic characteristics may not be compatible.

The recorder must be of suitable performance, calibrated in terms of input and output levels, and frequency

response (most good and well maintained recorders are within ± 3 dB from 60 Hz to 10 kHz at a tape speed of seven and a half inches/sec.). The performance must be regularly checked with calibrations made before, during and after recording, since dirt can build up on the replay heads and give a partial and unnoticed fall in output. The upper limit in frequency response is approximately proportional to tape speed. Lastly, it is very important that the right recording level is used, otherwise overloading or noise and hum will be produced. A recording level meter gives satisfactory indication of most noise but impulsive noise is not indicated correctly. The peak input should be measured with an oscilloscope and adjusted to the level which is measured when ordinary noise gives a normal recording level. Alternatively the high recording level may be lowered with the impulsive noise applied until the re-produced peak of transient starts to fall in proportion to the fall in recorder input (i.e. if the input to the recorder is halved, the output should also be halved).

Note that only the more expensive scientific recorders are capable of the accurate recording and replay characteristics to permit an overall accuracy better than ± 2 dB, and only then when great care is taken.

A typical recorder response is shown in Figure 34 for the type in which the signal is directly translated into a magnetic flux density pattern on the ferric oxide coated recording tape, and this is known as direct recording or D.R.

If noise must be recorded for subsequent analysis, the recording alone will only yield information about the noise spectrum and will not give absolute sound pressure levels unless the original level is logged at the time when the recording is made. It is good practice to record with speech at the beginning of a recording the following information: microphone position, sound propagation conditions, overall (or weighted) sound pressure level measured with a sound level meter, calibration level, attenuator settings and any other relevant factors such as time of day or night, machine conditions, duration of noise and so on.

b) Frequency Modulated Recording - When very low frequency data must be recorded the D.R. method cannot be used, the electronic and tape magnetisation arrangements fail to respond uniformly at much below 25 Hz. If a higher frequency carrier signal is modulated according to the level of the signal, data right down to the D.C. or average level of a signal can be successfully recorded, and replayed via special recording and demodulation amplifier units. As with D.R. recording a good high frequency response demands high tape speeds and hence tape consumption, and to cover the normal audio range it is necessary to go as high as 60 ips. The available signal to noise of FM recorders is generally somewhat lower than that available from the best D.R. machines at approximately 40 to 45 dB. The amplifier units require special filters to limit the recorded signals according to the tape speed chosen. Since the high tape speeds require time for stabilisation, wait several seconds before initiating data recording.

c) Pulsed Code Modulated Recording - This is a method of essentially recording a series of coded pulses, whose level represents a bit of digital information. Recording levels as such convey no meaning, and inbuilt checks can be included such that even tape speed is not too critical. Vast improvements in effective signal to noise are thus possible with no speed stabilisation or repeatability problems associated with the D.R. and F.M. methods. At present P.C.M. recording is rather specialised and of interest in the radio or T.V. broadcasting fields as well as space communications.

d) Multi-Channel Recordings - Where many channels of data are to be packed onto a single tape, it is advisable to adopt one of the recognised tape head standards, so that other groups may faithfully replay and/or analyse the data. The principle head standards in use are the I.R.I.G. (Inter-Range Instrumentation Group) and the S.B.A.C. (Society of British Aerospace Constructors) systems for $\frac{1}{2}$ " and 1" tapes. The I.R.I.G. code permits 7 or 14 channels (the latter in two interlaced groups of 7 heads) whilst the S.B.A.C. system packs in 16 channels. Some I.R.I.G. recorders permit the use of the edge spaces on the tape as lower grade voice or identification tracks.

e) Multiplexed Recording - Where very many more than 14 data channels must be simultaneously gathered, either several synchronously run recorders must be employed or a multiplexing system may be used. This is an electronic device which intermixes short samplings of the data from a large number of channels and packs these on a single channel of tape. Naturally, it is not possible to avoid loss of some of the data by this method, and normal sampling statistics must be satisfactorily chosen according to the overall accuracy required.

4.4.8 Computer Interfaced

Many modern analysers and correlators which work on a digital, or partially digital-analogue basis, can be interfaced with a computer system. The data can thereby be further refined, such as computing fly-by noise data in complex units such as Perceived Noise Levels (PNL in units of PNdB), and then displaying via the computer's own peripheral graph plotting or line printer tabulation units.

5.0 REAL DATA MEASUREMENTS

5.1 Stationary and Ergodic Signals

Stationary signals have statistical parameters (see Section 3) which are independent of the sample take, whenever a measurement is made. If the mean value of the signal and the auto correlation function are always the same, the signal is said to be weakly stationary. If all other statistics such as the higher order probability moments are also constant, the signal becomes strongly stationary.

Now the determination of the signal statistical parameter values requires signal averaging over a certain time. Thus any measurement is only an estimate of the true value. For stationary signals the estimate tends towards the true value as sampling time increases, and the result should not depend on the actual time of commencement of the measurement. However, for a non stationary signal the statistics do not

tend towards constant values with increased measuring time, and the values obtained depend on the time that the measurement was started.

For stationary signals the time required to measure any statistics to any required degree of accuracy can be predicted. If the difference between different estimates of a signal's statistics is significantly greater than the expected error involved in the measuring time which is used, the signal is non stationary.

It is therefore important to investigate the error involved in various measurements on stationary signals.

A stationary process can be further classified into two categories; ergodic and non-ergodic. A process is ergodic if different samples from the same process have the same statistics. For example, noise from a jet nozzle is ergodic if the noise of all such nozzles built to the same specification have identical statistics. The noise from an engine would be ergodic if it was stationary and its statistics were exactly the same every time the engine was started. The noise produced by an aircraft flyover would be ergodic if each flyover had the same noise statistics.

Thus, to test whether a signal is ergodic, it is also necessary to know the probable error of the measured signal statistics.

5.2 Errors of estimated statistics

The errors involved in measuring signal statistics with known averaging times may be predicted from other statistics of the signal, so that if the general type of signal is known, the probable error may be estimated.

The most usually quoted result is that for the error of filtered white noise. If the filtered signal has components over a bandwidth B the mean square error is given by:-

$$\epsilon = \frac{1}{2\sqrt{BT}}$$

if $B \leq 2f_0$ (f_0 is the filter centre frequency)

T is the integration time of the analysis.

The importance of this result is that it gives the length of integrating time required to obtain the r.m.s. value of a filtered broadband signal to any accuracy. If the signal is a pure tone, the time required to measure the r.m.s. values is simply the transient settling time of the measuring circuit. If the tone is passed through a filter this time is the filter rise time which is approximately the inverse of the bandwidth.

The errors involved in obtaining other signal parameters may be estimated in a similar way. These are discussed more fully in the bibliography and some results are shown graphically in Figure 35.

5.3 Non-stationary Signals

In practice many practical signals are non-stationary to some extent. However, analysis of non-stationary signals is very complicated and stationary signal analysis is often applied in the absence of more relevant techniques. Since the statistics of the signal vary with time, measurements of spectra, for instance, made at different times, but with a BT product correct for stationary signals, will produce completely different results.

Both variations of amplitude and of frequency of components may be regarded as non-stationary effects. However, if the time scale of the variation is less than the integrating time, these appear in the spectrum as amplitude and frequency modulation. This appears as side bands and broadened tones. If the time scale is greater than the integrating time, the non-stationarity appears as different spectra at different times.

In certain cases it is useful to measure the non-stationary correlation function of a signal. This is again obtained from a series of short samples of a signal and is a function of signal time and delay time. Another useful parameter is the double spectrum, which is similar to the cross spectrum between the signal at different times, alternatively the variation of the mean or mean square value may be obtained. When the non-stationarity must be related to other experimental parameter changes, such functions may be usefully measured.

If the non-stationarity cannot be easily related to system changes (e.g. changes of fan noise caused by details of ingested turbulence), it is much more difficult to obtain useful information. In this case it is usual to ensemble average a large number of estimates of the signal statistics in order to obtain a reasonably constant value. More detailed time variations are of little use unless more detail of the cause of the non-stationarity is available (in the above example, the details of turbulence).

5.4 Discrete Sampling

Here we are concerned with inherent problems of inferring knowledge about a whole function from a set of discrete samples of that function. In particular, it is assumed that frequency domain data is required, whilst the samples are taken in the time domain.

5.4.1 Aliasing and the Nyquist Frequency

Suppose $V(t)$ is a continuous function of time, and $V(f)$ is its frequency domain distribution. The two are related by the Fourier transform pair:

$$V(t) = \int_{-\infty}^{+\infty} V(f) e^{2\pi i f t} df$$

$$V(f) = \int_{-\infty}^{+\infty} V(t) e^{-2\pi i f t} dt$$

$V(f)$ exists for both positive and negative values of f , with $V(-f) = V^*(f)$. Clearly $V(f)$ can be calculated if $V(t)$ is known for all time, but can $V(f)$ be deduced from less information i.e. if $V(t)$ is known only at discrete points.

Assume first that $V(t)$ is sampled at regular time intervals, so that the sampling times $t_m = m\Delta t$, $m = 0, \pm 1, \pm 2$. Let the corresponding value of $V(t)$ be written as V_m . If F is written for $1/\Delta t$ (thus F is the sampling frequency), and the sample times substituted in the above equation.

$$\begin{aligned} V_m = V(t_m) &= \int_{-\infty}^{+\infty} V(f) e^{2\pi i f m/F} df \\ &= \sum_{k=-\infty}^{+\infty} \int_{kF}^{(k+1)F} V(f) e^{2\pi i f m/F} df \end{aligned}$$

This latter expression results from splitting up the integration range into many (frequency) intervals of length F . Since $\exp(2\pi i f m/F)$ is periodic (in F) with period F , it can be re-arranged as:

$$V_m = \int_0^F U(f) e^{2\pi i f m/F} df$$

where

$$U(f) = \sum_{t=-\infty}^{+\infty} V(f + kF)$$

The equation can be regarded as a simple integral equation for the unknown function $U(f)$ given the sample values V_m . When solved the function $U(f)$ can be deduced from the values V_m . However generally the true values of $V(f)$ cannot be found, since there is no way of obtaining $V(f)$ from $U(f)$. Thus, all that can be deduced from a set of discrete samples is the distribution $U(f)$.

The nature of the function of $U(f)$ is indicated in Figure 36.

$U(f)$ is the sum of a set of distributions all like $V(f)$ but whose origins are displaced by various multiples of F . It is seen from this figure that if $V(f)$ contains any component at frequencies greater than $F/2$, it contributes to $U(f)$ at a frequency $F-f$, and cannot be distinguished from a genuine component at this lower frequency. This phenomenon, in which a high frequency component makes its presence felt in the sampled data at a lower frequency, is called aliasing, and the critical frequency $F/2$ for which aliasing first occurs is called the Nyquist frequency. A time domain illustration of aliasing is shown in Figure 36.

Although generally it is not possible to determine $V(f)$ from a set of discrete samples because of aliasing, $V(f)$ can be found if it is band limited or low-pass filtered, i.e. $V(f) = 0$ for all $|f| > f_{\max}$. In this case, if the sampling frequency F is greater than $2f_{\max}$ no aliasing occurs, and $U(f)$ in the range $|f| < f_{\max}$ is identical to $V(f)$ in this range.

Thus for band limited signals $V(f)$ can be determined from discrete samples, provided the sampling frequency is greater than $2f_{\max}$.

5.5 Interpretation of Mixed Source Signals

We are in a dilemma if our source contains both random and discrete components. For the random noise, we need to perform a power spectral density analysis or alternatively an analysis of band S.P.L. at a stated bandwidth. For the sinusoidal or discrete tone components however, the concept of bandwidth has no meaning (theoretically tones are entirely at a single frequency and hence of infinitesimal bandwidth - in practice slight variations in frequency and level limits the levels measured by real filters on digital analyses). We can only have one value of a sine wave level, whatever the filter bandwidth chosen. This means that we must use different rules when we observe discrete tone spikes in a spectrum.

The above differences are in fact the reason why averaging of spectrum outputs on Fourier transforms can lead to enhancement of the deterministic portions of the signal. Each time we add two spectra and divide the results by 2, the random levels tend to zero whilst the tones simply add (provided phase is kept in step). Thus the pair of averaged spectra have tones which are 6 dB - 3 dB or 3 dB more protrusive than the individual spectra and repeated averaging continues to enhance the tones. This process is signal averaging in the frequency domain as opposed to the time series averaging discussed earlier.

5.6 Pitfalls

Besides the above, care must be always taken in interpreting seemingly valid spectral data. In narrow band 6% analyses, there can frequently be side bands due to modulation of source amplitudes or frequencies. Sometimes the modulation sideband spikes appear to "climb the skirts" of the 6% filter, where the major tone spike is relatively strong. The levels of the sideband tones are hence in error unless a

correction for the band-spillage is made.

In 1/3 octave and even Octave band analyses, extremely strong tones can appear to pull up the bands either side due to a non negligible overspill of the primary tone signal into the skirts of the filter beyond the adjacent filter cross-over frequencies. Thus when major tone protrusions of order 20dB are present, always check the validity of the adjacent band levels.

In RTA's where a very large signal dynamic range is to be analysed the high frequency data (and sometimes the very low frequency data) normally falls to a level where the discrimination of the binary data words is insufficient to show up fine levels. The analysis thus shows random step changes in level often of 5 or more dB. These are entirely spurious approximations to the noise floor level of the analyser system and the real noise level can only be correctly displayed by chopping the analogue data into several zones as necessary and treating each zone as a separate analysis.

In digital and real time analysers, it is necessary to avoid sampling errors by treating each pass band with a "window function", usually of a Cos form. If no window function is used, spurious frequency spikes can be introduced according to the number of analysis ensembles.

Again, some RTA's derive averaged data and then construct 1/3 octave or octave band data by arithmetically adding the outputs of the narrow bands appropriately. This is fine for the cases where many narrow bands fit into a wide band, but at low frequency the 1/3 octave or octave bands always become comparable to or even smaller than the narrow band width selected.

Additionally, the time compression process means that the effective filter skirts become wider as centre frequency diminishes. Thus a wide band is reached at which the filters no longer comply with standards. It is thus always necessary to check, from manufacturers charts, which of the 1/3 octave and octave bands contain valid data to cover the required range. Even this introduces problems of matching the ends of the ranges since it is never possible to use the same confidence levels of analysis for both samples when ensemble averaging the analysers single sweep data to improve accuracy.

6. COMPUTER BASED DIGITAL ANALYSIS SYSTEMS

The system in use at I.S.V.R.'s Data Analysis Centre forms the basis for this section, since it is the most familiar to the author. Other systems will differ in the manner in which analysis programmes are called in and linked together, but the general principles discussed will be valid.

Figure 37 is a schematic diagram of the system. The Central Process Unit (CPU) is a Digital Systems PDP 11/50 computer. It has linked to it a number of peripheral units for data input, output and display and storage of data and programmes.

6.1 Input and Conversion

Input is via a remotely situated Visual Display Unit (VDU's) which incorporate a typewriter style keyboard under a T.V. tube type of display. The unit also has other useful features such as cursors which can be used to "read off" graphical data values. The VDU console is also equipped with terminals for acceptance of up to four channels of analogue data, either from an on-line experiment, or from recorded experimental data. The data is sent along signal lines to an A.D.C. unit (analogue to digital conversion unit) which can sample the analogue data at up to 40kHz (20 kHz for two channels) continuously or up to 50 kHz in a "short burst". If required data or programmes may also be loaded via a paper type reader.

6.2 Output and Display

Output is via the V.D.U. initially. Under System Control the graph size, portion of interest, scale forms (linear or logarithmic) may be changed and then eventually called up for plotting on a fast single pen plotter located in the computer room. Information in character form may also be screened or commanded to be line printer reproduced for hard copy in the machine room.

6.3 Storage

The input data may be stored on the high capacity disc store units, each with 20 million words. A 1/2 million word fixed head store is available for programme storage etc. There is a back-up storage of the magnetic tape type used to call in systems master program material or long term stored data to the much more instantly accessed disc stores or the main core storage of 96 K capacity.

6.4 System Organisation

The system is organised so that work may be executed by persons having only a basic knowledge of computing. The system permits labelling of data files with convenient user originated names. Then aptly named systems programmes (e.g. ACQUIRE, PSDA, DISPLAY) are called in using simple fortran-like JOB descriptions to operate on the data. Each analysis programme contains parameter lists which need to be selected by the user, either preset or at run time, or alternatively left by default to certain inbuilt values. These parameters describe the file lengths, sampling rates, analysis bandwidths and accuracies etc., as well as graph scales, axis types etc. Filters are available to limit aliasing or to edit low frequency components of irrelevance.

6.5 Specialised Analyses

For users with a more advanced programming capability, special analysis procedures may readily be compiled under the user's reference code for files, and executed by a JOB as if it were a regular systems programme. Job sequences may be controlled in loops with conditional statements if required, so that more complex sets of standard processing routines may be performed on the same initial data string or on selected segments of such a file of data. The bibliography contains more information on the capabilities of such

systems, and Figure 38 is illustrative of an analysis performed on the system. The display facilities include such useful forms as simulated 3 dimensional graphics and contour plotting. The digital computer system has the advantage of total flexibility, but some very specialised operations involving much use of Fourier transforms take more time than specialised analysers and mini-computer systems. However, development of new analysis procedures prior to setting up a specialised analyser is readily accomplished, as are long repetitive analysis procedures, which would involve a lot of technical time if done on a specialised machine.

7. NOISE FIELD SAMPLING

In all branches of acoustics, we make measurements of the sound field in various manners, to a large extent dependent on the purpose of the measurements. Where the data is to be gathered for fundamental research purposes, it is often required to assess the acoustic power emitted and to determine the spectrum of power or power spectral density. On the other hand, we may wish to learn in detail the radiation directivity pattern or the relationship between maximum sound pressure level at a given distance from a source and some appropriate parameters such as jet exhaust velocity and expanded density. In each case we need to consider how best to sample the sound pressures using microphones and the measuring and analysis equipment and techniques described in Section 4.

7.1 Spot Point Measurements

In this case either a single microphone is placed at a known position in the sound field, measurements taken, and then the microphone moved on to the next point; or an array of identical microphone types (or microphones whose relative response characteristics are known) is placed in a suitable pattern in the field.

Frequently with noise measurement schemes, we are presented with a "chicken and egg" situation, since the choice of microphone positions depends on the type of noise source we are dealing with. It is not uncommon to conduct measurements according to a sampling plan and to discover from the results that it would have been preferable to have measured elsewhere or used one of the other survey techniques described later.

With spot sampling points, we have the advantage that a complete time record of the pressures reaching the microphone can be retained if desired, with the disadvantage that the whole of the radiation pattern cannot be sampled in sufficient detail. Often however, by appealing to a theoretical axisymmetry in the sound source radiation, it is possible to sample in a single axial plane, perhaps running spot checks on the assumptions of axisymmetry.

Where the source is expected to have an extremely lobular field pattern it is preferable to use a traversed microphone method (see 7.2) but if this is not possible, it can sometimes be beneficial to concentrate microphones at positions closer to each other where the maximum lobularity is expected to occur.

The lack of a time limitation for spot measurements (subject to such factors as magnetic tape consumption) enables adequate sampling for an acceptable confidence in the measured levels to be used.

The choice between moving a single microphone from point to point, as against an array of channels in parallel, lies on the one hand in the relative complexity and capital cost of the necessary instrumentation and on the other hand with the restriction to an identical response system for all the measurements. Thus for the single microphone, field shapes can be determined without actually knowing the detailed frequency response provided an adequate range of signal to noise is maintained up to the highest frequency of interest. The multi-system approach obviously permits the tests to be completed more rapidly however and does not require absolute stationarity of data. If, for example, an expensive to operate source such as a gas turbine engine is being tested, this advantage has attractions. Thus most aero engine companies use this method nowadays for conducting development and guarantee demonstration measurements on their power plants. Figure 39 is an example of a test facility using the multi-system technique. The acoustically hard ground plane has been chosen in this case so that at least ground interference effects are consistent and to an extent theoretically determinable, and hence correctable.

7.2 Traversing

A microphone traversing arrangement can be used wherever there is a requirement to completely map the directional radiation pattern. It is therefore favoured for multi-lobular sources such as axial flow fans, where the positions and number of lobes and the location of the strongest lobe can lead to interesting conclusions about the modes of the fan duct which are being predominantly excited by the fan blades or fan blade/stator vane noise interaction mechanisms. Also, from a complete pattern of directivity it is possible to compute the total acoustic power spectrum for the source. To do this, it is usual for the traverse to be performed at fixed radius. As with all measurements made with simple microphone arrangements, the radiation has to be monitored at sufficiently large radius to be in the far field, since in the near, or reactive, field the pressures measured do not represent radiated sound energy and falsely high levels of "pseudo sound" can wrongly be attributed to some source parameter variation. The chosen radius should thus be well over $\lambda/2$ where λ is the wavelength at the lowest frequency of interest. In practice, this always means that, for a normal gas turbine engine, the traverse data in the zone close to the jet axis which usually comes very close to the regions in the jet mixing process where the low frequency sources are to be found, must be regarded with some doubt.

When traversed data is gathered, it is always necessary to consider how to deal with the ground interference problem, since the change in geometry for the direct and indirect sound waves must inevitably alter during the traverse, thus leading to interference lobes which might incorrectly be attributed to the source. The anechoic ground plane is not always satisfactory since for waves skimming over the absorbent layer there can be an almost total phase reversal without much of an amplitude change, causing strong interference dips in the received pressure after frequency domain transformation. It has been found that optimally chosen anechoic wedges are necessary to completely avoid this effect for practicable heights of source and receiver microphone.

The traverse rate must always be a compromise. We need a slow enough traverse to allow sufficient time in each angular zone to give good statistical accuracy of the measured data. This in turn, as we have discovered depends critically on the narrowest bandwidth to which we need to resolve the frequency domain or spectral data. On the other hand, too slow a traverse would be complicated by any non-stationarity of the source and would also lead to high testing and tape consumption costs. Let us consider an example:

Supposing we have decided that we wish to traverse at 30ft radius from the source over an arc of -20° to $+160^\circ$ relative to the forward axis of (say) a fan rig. The negative angles are to check symmetry and to ensure smooth data across the axis region of the traverse. We decide we need to analyse the data with a constant 30 Hz bandwidth using effectively 500 contiguous filters spaced at 20 Hz apart using an R.T.A. system. Then the total data frequency range is to be 0 - 10 k Hz in 30 Hz filter bands.

Firstly we expect, for 30ft radius, sources up to wavelengths of $2\pi \times 30\text{ft}$ to be just catered for, or up to $\pi \times 30\text{ft}$ to be well catered for. This means that all data but the 1st 30 Hz band is in the far field, even allowing for higher order source effects, and this is satisfactory.

Supposing we wish to resolve data with a 10° angular variation in level. Then we might wish to traverse only 3° in a data sampling period in order to be able to "plot" a reasonably sharp noise lobe. For 90% confidence that the data is good to within ± 1 dB (based on random noise - thus discrete tonal components will always be more accurately determined), we choose $B \times T = 50$ (100 degrees of freedom). Hence T needs to be 1.67 seconds in order to cover the 3° angular zone. That is the traverse rate must be as low as 1.8 degrees per second. The traverse around the arc from -20° to $+160^\circ$ will thus occupy 324 seconds or 5 minutes and 24 seconds. Over this period of time, the fan unit must essentially remain at the same running conditions and give a constant acoustic output.

In order to record the data at least $7\frac{1}{2}$ ips and preferably 15 ips tape speed would be required, thus needing up to 500 ft of tape for the single traverse after allowing for tape run up etc.

Figure 40 is an example of a test facility using the traversed far field microphone method. Here multi-channel recording is used to record several radii traverses at one time and also to record other relevant parameters such as fan speed, and certain performance transducer outputs. This facility is described in detail in a paper referenced in the bibliography section. A typical result of traversed data for a particular fan discrete tone at Blade Passing Frequency is also shown in Figure 40.

7.3 Polar and Linear Surveys

So far we have assumed that the interest always lies with polar, or constant radius from the source, surveys. In this form we may learn more about the source and its acoustic power level can easily be computed from the results. However, in the context of aircraft and vehicle pass-by tests, the observer effectively "passes along" a line parallel to the direction of flight (in reality he remains fixed whilst the engine's noise field passes over his ears. For this reason, engine manufacturers usually measure noise during development or guarantee proof tests along a linear line or traverse at some fixed distance from the centreline. It is usual, nevertheless for positions along the line (for fixed microphones) to be set at constant angular interval intersections with this line, (see Figure 39). This facilitates conversion by correction from Polar to Linear data and vice versa.

7.4 In duct sampling and traversing

There can sometimes be attractions in measuring the noise field within a fan duct or at least in the near field only just outside the intake flare. Here, the signals from interaction modes are usually more clearly defined and the data obtained can be related in phase to some physical events in the machine. As an example, Figure 41 is taken from reference A and shows how a single traverse arrangement has enabled noise due to inflow distortion to be identified for a low speed research fan. A (now classic) example of fully in-duct traversing is given in reference B., whereby the nature of interacting blade and stator discrete tones were first studied and a theoretical model developed. Note that, in traversing just outside the duct, the former example lessens some of the effects of the microphone in creating fresh disturbances for the fan and sustaining high ambient airflow noise levels.

Wall measurements, using flush mounted transducers, have proved useful on a number of occasions. An example is where data is needed to enable acoustic duct linings to be stressed to withstand the high acoustic fields close to fan blades tips, particularly for supersonics tipspeed fans. For such fans, flush wall mounted transducers have enabled researchers to study the disarray which develops in the shock-wave system responsible for so called buzz-saw noise (reference C) and of course it is possible to assess the level of boundary layer associated noise from such measurements in subsonic fans.

When interaction tones are being studied, it is possible to deduce from the pattern of sound pressures along the axial section of the duct wall (and preferably also with a radial pattern obtained by probe microphones) the distribution of the more important and dominant modes which are being generated. This provides invaluable guidance in the efficient and optimum selection of absorbent duct treatments

7.5 Anechoic Environment

Where it is required to simulate the free field sound radiation conditions such as are applicable to an aero-engine in flight, it is usual either to use open air test stand measurements and make due allowances for the ground plane effect, or to use a suitable anechoic chamber. It is not intended in these notes to enter into the discussion of design requirements, but it should be noted that all anechoic rooms are only echo free over a certain frequency range, governed by the choice of materials and size of the absorbent wedges around its surfaces.

7.6 Semi-Anechoic or Reverberant Environments

In some cases, it is desirable to take sound measurements on a machine for a particular purpose, but

it is not possible to provide a fully anechoic simulation of free field conditions. For example, it might be very important to check the near field noise from a new type of jet engine well before it could be flown or released for regular noise measurements on an open-air test stand. Wherever possible the measuring space should be made as nearly anechoic (or sometimes as nearly reverberant) as possible using foam sound absorbent sheets or blankets of mineral wool fibrous material. The room can be calibrated using some standard source, or else using reverberation time measurements in order to correct the data obtained to the appropriate idealised room conditions. In other words, the calculated reverberant field can be corrected out from the direct field data, or else the reverberant portion can be used to assess the acoustic power.

7.7 Fully Reverberant Environment

It is sometimes, although less often attractive to place aerodynamic sound sources in a fully reverberant chamber and to measure the acoustic power by the usual direct measurement method, using the room calibration or else a substitute standard source of known acoustic output.

An example of this is in the use of reverberant chambers at either end of an aero-acoustic absorptive test facility, such as that shown in Figure 42. The reverberant sections have to be chosen to be large enough to produce multi-modes at the lowest frequency of interest, since below the cut-off condition the measurement field will not be diffuse.

Usually, reverberant field measurements are made with several microphones whose results are averaged before computing the acoustic power spectrum. This is because, even the most sophisticated chamber, with non parallel walls and ceiling, does not produce perfectly random sound fields. As with all chamber measurements, microphones should be kept at least a lowest wavelength away from walls or foam wedges.

7.8 Sound Power Determination

7.8.1 From Transversed Data

Consider diagram 43. The acoustic power spectrum can be assessed by integration of the sound pressure spectrum over all directions of radiation. To do this we use an imaginary spherical (or sometimes hemispherical) surface at a given and sufficient radius from the source. If the source does not radiate axisymmetrically the sound power must be found by smoothing the noise measurements and formally integrating or else summing small areas over which the sound pressure level can be considered uniform. However, it is usually possible to assume axisymmetry, in which case the sound power can be considered uniform over the small zones of the sphere indicated in the figure. Now from the rules of projection, the "zones of latitude" of the sphere, as projected onto the unwrapped cylinder, are equal in area to the true surface area of the zone on the spherical surface. Hence the strip areas are $2\pi R^2 (\cos \theta_n - \cos \theta_{n-1})$ where θ_n and θ_{n-1} are successive angular zones relative to the forward axis of the source, the measurements of sound pressure level being available at the angles mid-way between θ_n and θ_{n-1} . θ_n is taken from 0° to 180° and thus the total area is $4\pi R^2$ as expected.

The acoustic power integration is therefore equivalent to weighting the measured SPL for each zone by $10 \log_{10} (\cos \theta_n - \cos \theta_{n-1})$ and adding each weighted result logarithmically. To this is added the sum $\log_{10} 2\pi R^2$ where R is measured in metres. When the reference units for the soundpower and sound pressures are taken into account the result is that:-

$$PWL_f \text{ re } 10^{-12} \text{ watts} \equiv \overline{\Sigma SPL_0} + 10 \log_{10} (\cos \theta_n - \cos \theta_{n-1}) + 10.9 + 20 \log_{10}(R \text{ metres})$$

where the bar denotes decibel summation over all angular intervals θ .

If the sound pressures are only measured over a hemispherical zone or half space, then the constant becomes 7.9.

From Spot Data it is possible to choose angular intervals θ such that the weightings of $10 \log_{10} (\cos \theta_n - \cos \theta_{n-1})$ are virtually constant. In this case it is only necessary to perform normal decibel addition on all the measured results, add the appropriate constant plus, of course, the other constant terms in the formula. An example of a suitable array of measuring points is given in Figure 44. The procedure is repeated for each frequency band of interest.

7.8.2 From Reverberant Room Data

It was noted above that reverberant chamber measurements were useful for relatively simple determination of sound power.

Firstly it is necessary to calibrate the room. A pistol shot, with sufficient frequency range to suit the test source, is made, (or better still several are made and the results averaged). The shots are recorded using the same measuring microphones as for the source measurements. The data is then analysed by appropriate frequency bands as a trace of level versus time and the equivalent time for the sound to decay 60 dB is determined. Thus using the relationship:

$$t_{60} = \frac{0.161V}{S\alpha}$$

the effective room absorption is determined. Here $S\alpha$ is the mean effective total absorption in the room in Sabins and V is the room volume, both in metric units.

Finally the Reverberant Level is related to the sound power level and measured averaged SPL from the source by:

$$SPL = PWL + 10 \log_{10} \left[\frac{1}{4\pi R^2} + \frac{4}{R} \right]$$

where the source is placed away from the room walls and R is defined by $\bar{S}_a / (1 - \bar{a})$.

As an alternative, the sound power of a source under investigation may be found by simple comparison with a source of known power, by operating each in turn in the same reverberant room. The differences in averaged microphone SPL determinations is used to adjust the power level, and if the test source and comparison source data are analysed into frequency bands, the frequency distribution of sound power is easily found.

8. SPECIAL MEASUREMENT TECHNIQUES

In this section, we discuss some specialised methods of measurements and analysis often useful in aero-acoustic research.

8.1 Phase Locked Averaging and Sampling

This topic has already been touched on in connection with signal or information theory. Supposing we are testing a fan unit, which is subjected to both generally turbulent and grossly distorted inflow velocities. For example the fan might be a buried-in wing VTOL lift fan unit under transitional operating conditions, with both forward flight airflow and turbulence, plus a curved (and perhaps separated flow) entering the fan with "shadows" at the upstream lip and beyond the control bullet to the fan hub.

We can filter the acquired noise data at a narrow band containing the blade passing tone (or any other harmonic tone of interest). Knowing the number of fan blades, it is easy to use the tone signal itself in order to average in the time domain the filtered signal in segments of 1 rotor revolution. After sufficient averaging the data will represent the sound pressure cycle in BPF as modulated by the distorted intake flow mean velocity profile (integrated over the complete blade span). The result in turn could be further analysed to present information on the distortion circumferential spatial harmonics which caused the noise. Alternatively by sampling only when a certain blade is known to be on a certain spatial position (using some form of rotor shaft tachometer signal) short records can be studied to show up the random (turbulent) induced effects and these again could be averaged to present a statistical distribution of sound pressures related to the inflow turbulence/blade interaction response.

8.2 Multi-Transducer Methods

8.2.1 Cross Correlation

Use of two transducers and cross correlation can yield valuable information regarding cause and effect relationships. Supposing in the previous example we wish to examine in detail those portions of the total fan noise output which are directly attributable to the inflow turbulence. Since the turbulence is known to be coherent over a fairly major section of blade span for most practical cases, we can measure the fan noise as before, but also measure the turbulence signal in the inflow via a suitable hot wire anemometer system. The cross spectrum of the noise with the hot wire velocity signal would draw out only those tonal and random noise components which were related to the convected turbulence which had interacted with the blades to produce the noise. By delaying one signal with respect to the other, the effective convection speed could also be determined as well as the phase response of the sound pressures to the turbulent forces.

8.2.2 Duct Wall Impedance

This is a further example of a two transducer measurement, whereby a determination in-situ is possible for the effective impedance of an acoustic duct lining to an applied sound field and surface flow system. A fixed probe microphone is set flush in the near wall of a resonant cavity type laminar absorber layer. A further probe is traversed across the cavity from the flow side of the lining to the back wall. Data from the two probes can simply be processed to yield the resistance and reactive complex impedance components under the actual environment imposed on the lining since it can be shown that:-

$$Z = R + jX = \frac{P_2}{P_1} (\cos \theta + j \sin \theta) \left| \frac{j \cot(kt)}{\cos(kt)} \right|$$

where

Z , R , X are the wall impedance, Resistance and Reactance respectively,

P_1 , P_2 , θ are the two sound pressures and their relative phase angle

k is wave number $= 2\pi f/c = 2\pi/\lambda$, c and λ being the speed of sound and the wavelength, and t is the duct wall liner thickness.

8.3 High Speed Airstreams

8.3.1 Sound Pressure

Measurements of this quantity in airstreams require special care. The microphone calibration and response may alter compared to the static case. The static pressure in the flow and also the air temperature or gas composition may be such that connections are required on account of the changed characteristic impedance of the medium. Finally the presence of stream turbulence and boundary layer growth over the microphone probe may give trouble in attaining an adequate overall signal to noise ratio.

The response change problem is not easy to solve, and most work has assumed that the static response applies. A known source which does not change output under flow conditions, such as a Hartmann whistle, could, in principle be used to check such effects. Otherwise, for high level sounds piezo-electric transducers may be set into wall surfaces or into probes. Care must be taken to obtain exact alignment of the transducer and wall surfaces otherwise extra noise sources will be set up and recorded. The portion of the signal due to turbulence could be ascertained if required by convection speed determination by correlation methods.

8.3.2 Turbulence Velocity

Where required to relate sound characteristics to flow features, it is often necessary to record flow details. Hot wire anemometer probes can be used, either simply, or crossed to isolate a particular component of the turbulence velocity. It is usual to use the constant current compensated hot wire bridge/amplifier which more faithfully reproduces the turbulence velocity waveform than the constant resistance type.

Turbulence velocity spectra can be obtained from the wire signals by transformation, or directly from a laser-doppler velocimeter device. This uses a highly coherent light source to measure doppler scattering spectra from small particles in the flow, and the doppler spectrum directly relates to the instantaneous velocity of the fluid intercepted by the laser beam. If crossed laser beams are used then the data may be processed using cross-correlograms or spectra to give information at a specific section of the beam as opposed to the integrated effects for the single beam method. Suitable lasers have to be chosen to suit the expected turbulence and mean flow velocities, and the available high frequency spectral analysers to be used; also to avoid undue absorption of the scattered light which would make the results less reliable.

8.3.3 Unstable Shock Waves

Whereas steady shock waves in a super critical flow region cannot be responsible for noise generation, instabilities and interaction with turbulence and turbulent eddies can cause shown oscillations. The study of unsteady shock behaviour has been of interest in high speed jet noise research and techniques using special Schlieren systems coupled with high-speed cine-photography have been used successfully. Further reading is to be found in references D and E.

8.4 Measurement in Elevated Temperature Airstreams

Condenser microphones can be used at 150°C but on reversion to lower temperature use their long term stability characteristics are found to be considerably degraded. The cathode follower system for condenser microphones can be cooled using a specially designed flowing water jacket and used up to 250°C. For higher temperatures, cooled probe tubes must be used to separate the sensitive transducer from the hot gas stream, but this imposes severe probe tube response calibration problems on account of the temperature gradient along the tube and multiple resonant response where the tube has necessarily to be much longer than a quarter of a wavelength. Such limitations do not, however, preclude the use of such probe microphones for comparative and diagnostic purposes in problems where it is essential to get even a rough idea of the sound pressures in a hot flow system. Examples of work of this kind are in the main unpublished, but useful results have been acquired from zones near combustion chambers, in gas turbine exhausts and in industrial furnaces. Particularly relevant are comparative measurements as used for the two microphone position method of determining duct wall impedance.

8.5 Measurements for Air-to-Ground and Air-to-Air

Since it is never possible to make a complete simulation of flight conditions, aircraft airframe noise and engine noise testing to confirm the researches from ground based facilities become necessary. Because it is invariably necessary to compare the data at specific radiation field angles, careful measurements of the aircraft speed, track etc. are required. The subject is treated more fully in the subsequent lecture in this series on Aircraft Flyover Measurements. It is worth noting however that methods have been tried which attempt to eliminate some of the difficulties experienced in normal aircraft fly-by recordings. Techniques have been used whereby microphones have been mounted on stings projecting from a wing-root trailing edge in order to record in-flight "on-axis" noise from a development rear fuselage mounted engine, and the data was successful and valuable wherever it could be quite certain that the origination was not from the wing aerodynamic unsteadiness. Obviously attention to the discrete tone levels, which could most emphatically be associated with the engine build and rotational speed details, produced the most reliable data. Other specialised techniques which have been employed are the use of tethered balloons, tall towers, flight towed instrumentation packages and other aircraft in order to gather data on wing and fuselage shielding effects, and sonic boom signatures under realistic flight and atmospheric turbulence conditions.

8.6 Measurements in Wind Tunnels and Ground Based Airspeed Representation Facilities

All flight testing is very expensive and demands very careful analysis treatment of the results. There have of recent years been many attempts to conduct fundamental research with more readily controlled conditions. Methods include the use of open jet wind tunnels, open or atmospheric working section tunnels, closed circuit tunnels (sometimes large enough to accept a modest sized aircraft as in the NASA Ames facility) whirling arm rigs, engine intake cross flow simulation blowers for both conventional and VSTOL research engines and fans, and tracked test stands (either powered by auxiliary means or by the power plant under test). Detailed discussion of the problems involved are the subject of one of the lectures to follow. It has to be appreciated that the elimination of ground effects (acoustic and aerodynamic), proper control of atmospheric turbulence levels and scales, and acquisition of high confidence data at the desired representative geometric scales and airspeeds involve considerable compromise (or ranking of priority) especially when such facilities have to be totally cost effective.

8.7 Measurement of Rotor Blade Wakes

An interesting experimental programme was conducted at ISVR in order to evaluate a method for determining the relative velocity wakes behind a fan stage without recourse to rotating probes. Hot wire anemometers were mounted at various fixed radial stations and at various planes down-stream of the test fan, and the ISVR digital analysis facility used to re-interpret the data in terms of the spinning rotor co-ordinates instead of the fixed frame of reference. The method involved the recording of a pulse from a chosen blade so that the ensembled averaging of many rotor cycles of data could be accomplished. The results, of which Figure 45 is typical, demonstrated by no means the simple flow patterns expected for a 2-dimensional flow situation, there being clear indications of vorticity and wake inclination relative to the blade trailing edge. Further information can be obtained from reference E.

8.8 Correlation Methods

The use of correlation analysis between suitably spaced microphones can obviously provide information on the position of acoustic sources. Again, the subject is covered in other lectures in this series. It is worth noting, however, that work has been conducted over the past two years to demonstrate that, for relatively simple cases of reflection of sound by solid walls on adjacent ground planes, the equivalent free field spectrum of sound from a random source may be recovered using transformations from the autocorrelation function. An interactive technique, or else an exact analytical separation, can be used to eliminate the peaks in the auto correlation function where delayed reflected sound signals constructively interfere with the direct wave in which we are interested. Provided that the time delay for the 1st reflected return is not too small, so that the function for an acceptably narrow (say octave or 1/3 octave) band of the total signal decays fairly rapidly, the relative peak amplitudes can be related to the coefficient of reflection or absorption at the surface in that band. The iterative method uses the digital computer to determine an acceptably accurate synthesis of the overall autocorrelogram from an assumed extrapolation of the direct correlogram decay at low time delays, and the high time delay portion of the reflected wave features. In synthesis, allowance can be made for cross products which tend to zero for the case of well-separated peaks of the correlogram. Finally the iteratively determined direct wave correlogram is forward Fourier transformed to give the power spectral density, which would have been measured but for the interference dips due to the reflecting plane. Figure 46 illustrates the process involved.

REFERENCES

- A. B. Barry and C. J. Moore "Subsonic Fan Noise" 1971 J. S. Vib 17 (2), 207
- B. J. M. Tyler and T. G. Sofrin "Axial Flow Compressor Noise Studies" 1961 S.A.E. Trans. 70, 309
- C. C. L. Morfey and M. J. Fisher "Shock Wave Radiation from a Supersonic Ducted Rotor" 1970 J. R. Ae. S. 74, 579
- D. R. Westley & J. H. Woolley "An Investigation of the Near Noise Fields of a Choked Axi-symmetric Air Jet." 1968 AFOSR - UTIAS Symposium on Aerodynamic Noise - Toronto
- E. P. D. Yardley "Measurement of Noise and Turbulence Generated by Rotating Machinery", 1975 University of Southampton, Institute of Sound and Vibration Research, Theses for Ph.D.
- F. C. A. Mercer "Development of Data Analysis in Sound and Vibration" 1973 J.S. Vib 28 (3), 640

GENERAL BIBLIOGRAPHY

- J. S. Bendatt and A. G. Plesol "Measurement and Analysis of Random Data", Wiley, 1958
- F. H. Large "Correlation Techniques" Iliffe, 1967
- L. J. Chamberlain "A Simple Discussion of Time Series Analysis", Sound and Vibration April 1971
- L. L. Beranek "Acoustic Measurement", Wiley 1967
- T. J. Hargest "Some Experimental Aircraft Engine Noise Facilities in the United Kingdom", 1972 J. S. Vib 20 (3) 359
- J. T. Broch "Acoustic Noise Measurements (Applications Booklet) 1971
- A. G. P. Peterson and E. E. Gross "Handbook of Noise Measurement" 1967 General Radio Company
- Anon "Acoustics Handbook" (Application No. 6 100) 1968 Hewlett Packard

ACKNOWLEDGEMENTS

The Author gratefully acknowledges the consent of the Noise Department, Rolls Royce (1971) Ltd., Derby; Bruel & Kjaer Laboratories Ltd., Sennheiser Electronic, and General Radio to references and research results and reproduction of illustrations.



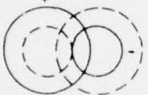

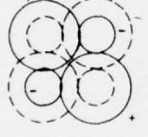
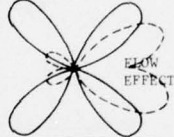
SOURCE TYPE	SOURCE ASSOCIATED WITH:	SOURCE ACOUSTIC REPRESENTATION	DIRECTIVITY PATTERN	SOUND POWER RELATIONSHIP	ACOUSTIC RADIATION EFFICIENCY PROPORTIONAL TO:	EXAMPLES
MONOPOLE	PULSATING FLOW			$\rho L^2 v^4 / a_0$ ($\rho A V^3 M$)	M	DROPLET COMBUSTION - PULSE JETS - INLET & EXHAUSTS OF RECIPROCATING MACHINES
DIPOLE	UNSTEADY FLOWS CLOSE TO SURFACES		DIRECTION OF FORCE FLUCTUATION 	$\rho L^2 v^6 / a_0^3$ ($\rho A V^3 M^3$)	M ³	FAN BLADE NOISE - BOUNDARY LAYER NOISE
QUADRIPOLE	FREE MIXING OF EXHAUST FLOWS INTO ATMOSPHERE		FLOW DIRECTION 	$\rho L^2 v^8 / a_0^5$ ($\rho A V^3 M^5$)	M ⁵	JET NOISE - VALVE NOISE

FIGURE 1 Source Characteristics

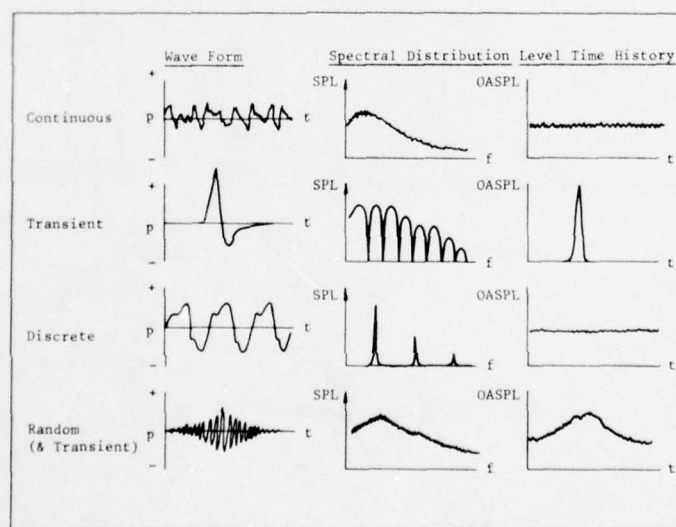


FIGURE 2 Sound Source Characteristics

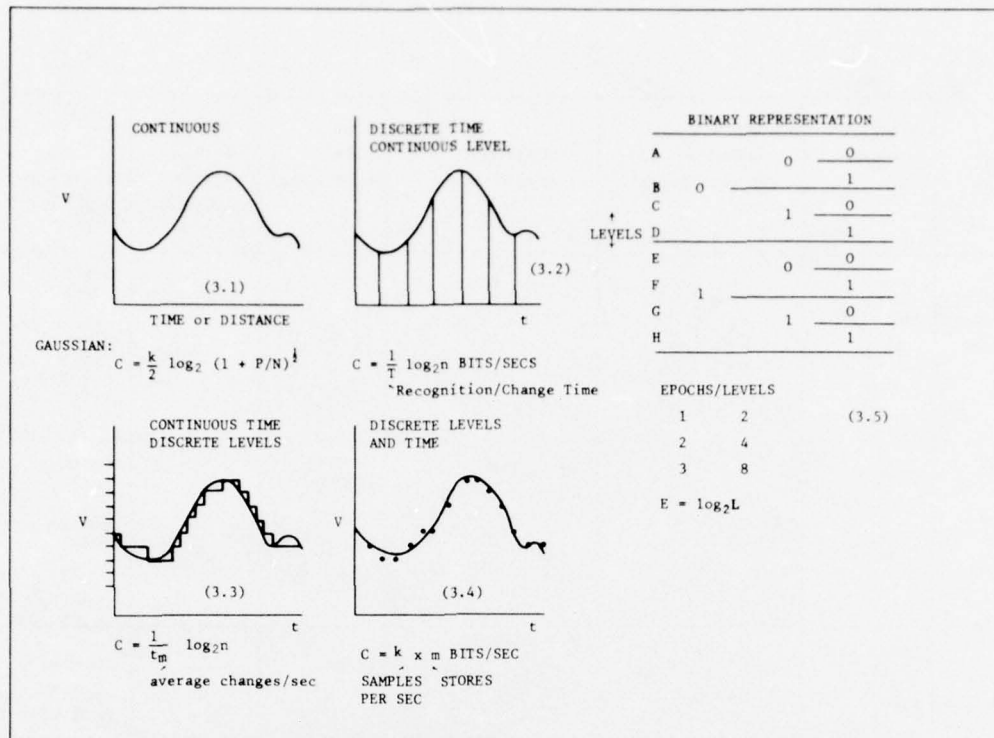


FIGURE 3 Signal Basic Characteristics

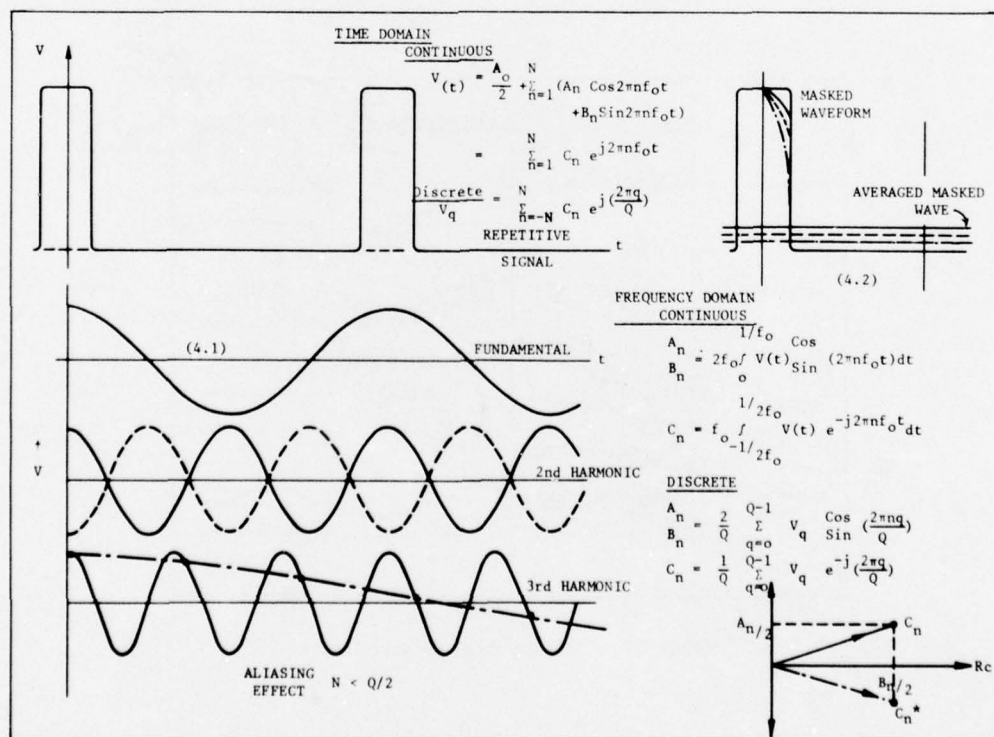


FIGURE 4 Fourier Analysis

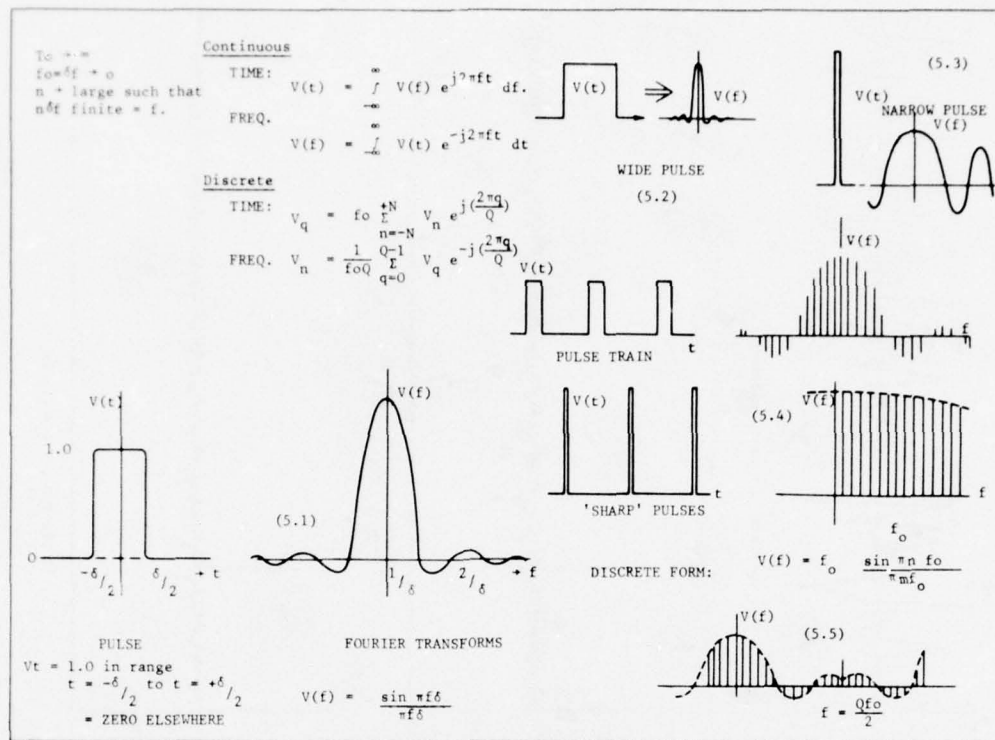


FIGURE 5 Fourier Transformation

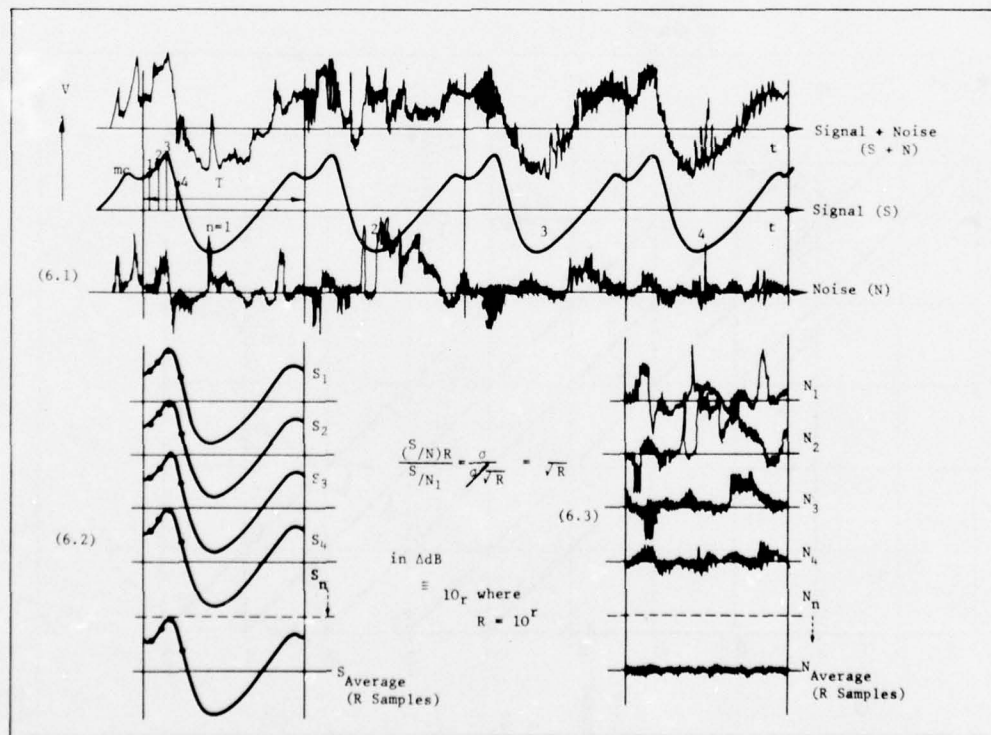


FIGURE 6 Cyclic Averaging and Waveform Education

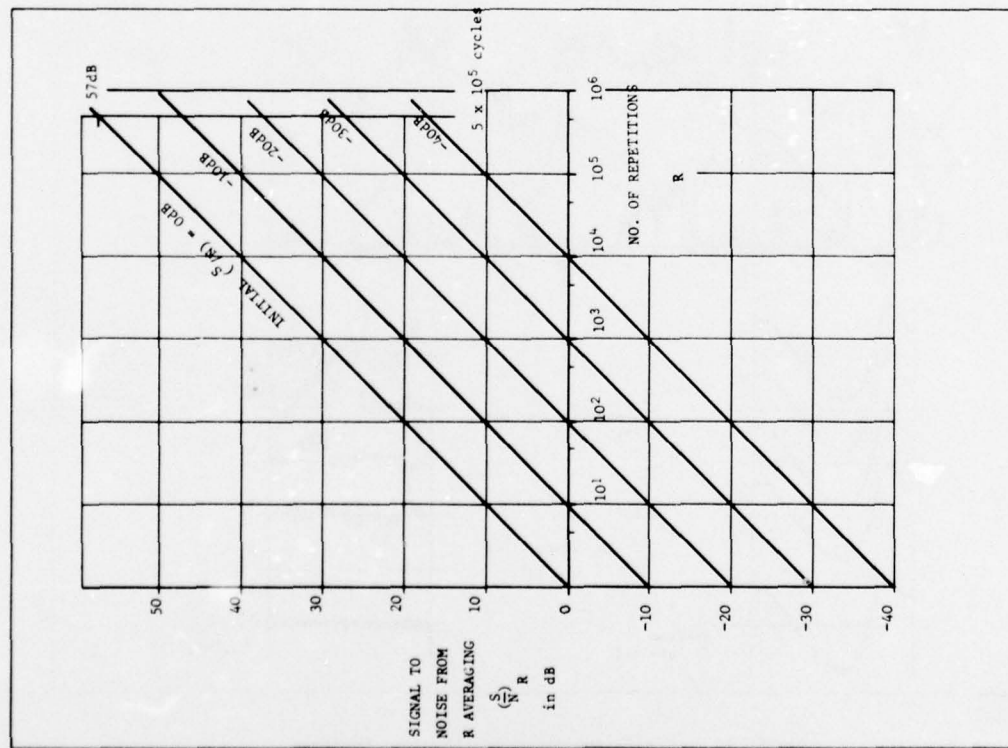


FIGURE 7 Cyclic Averaging

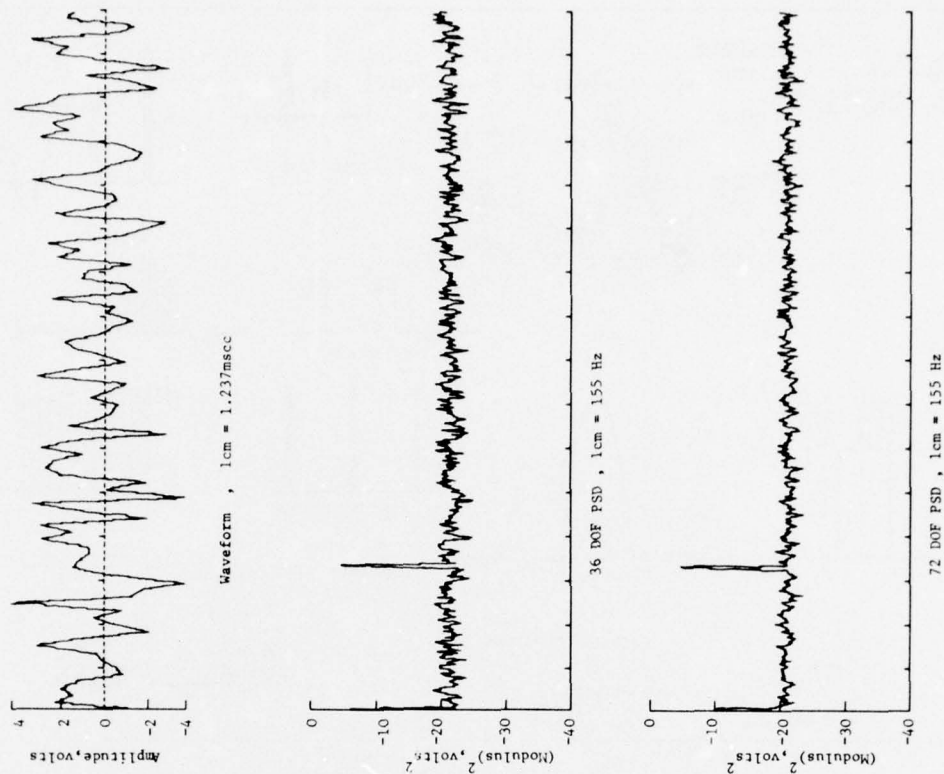


FIGURE 8.1 Waveform and PSD of Tone Buried in White Noise

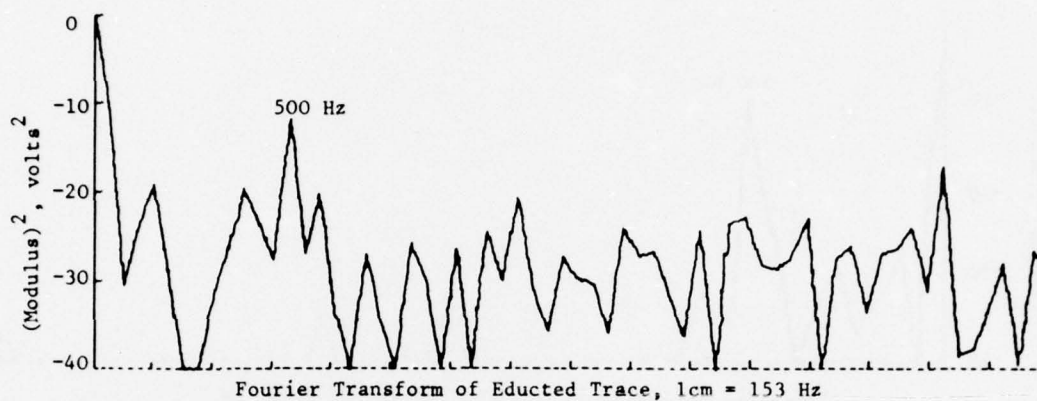
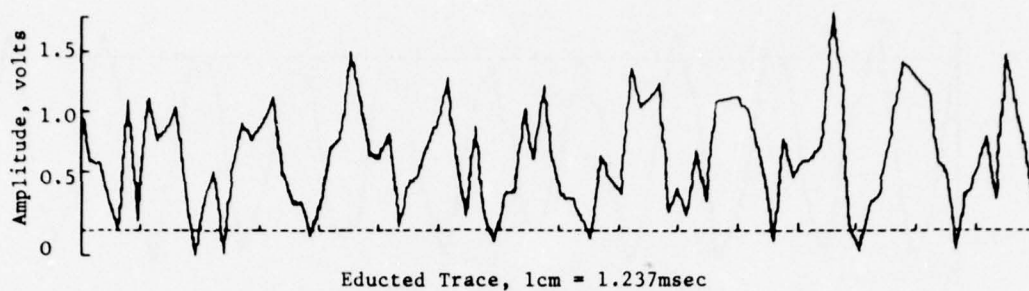


FIGURE 8.2 Eduction of a Sinewave (40 Averagings)

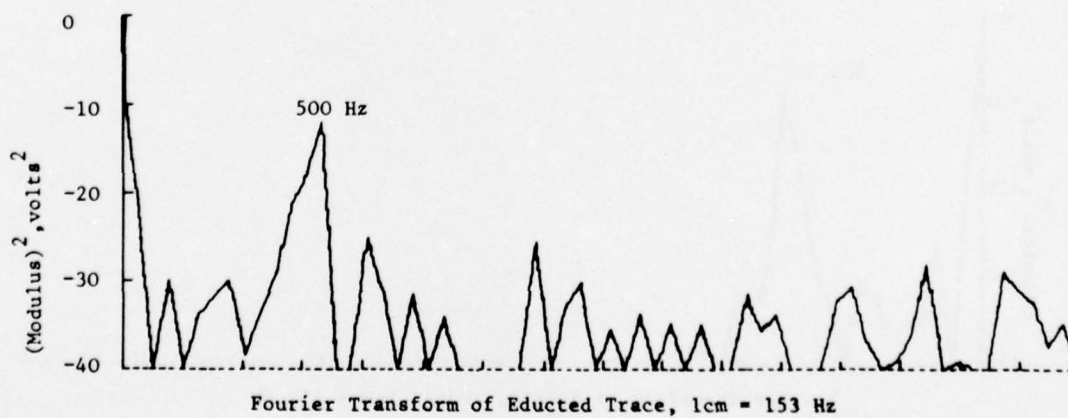
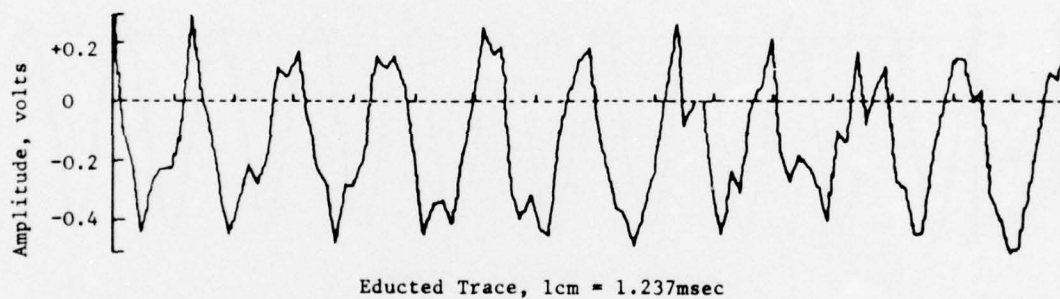
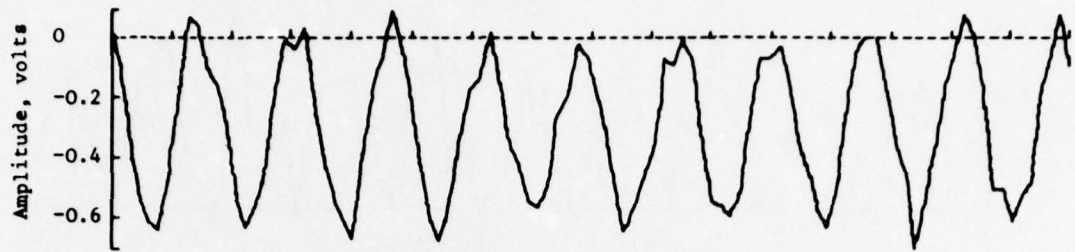
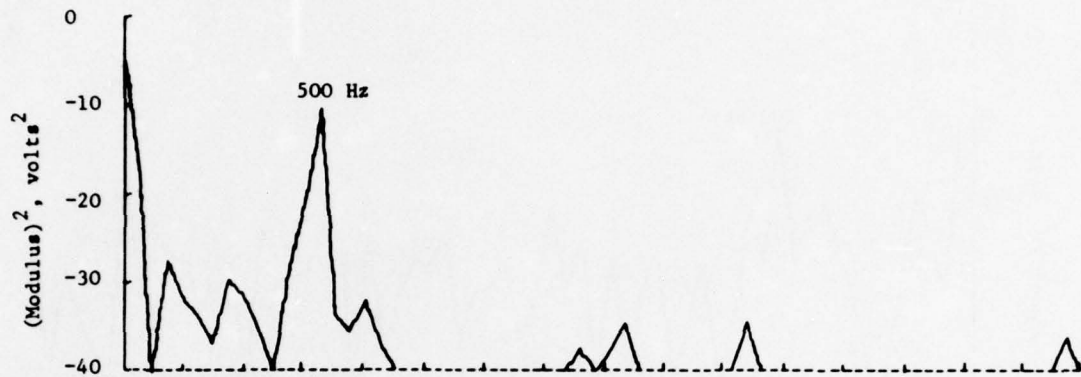


FIGURE 8.3 Eduction of a Sinewave (200 Averagings)

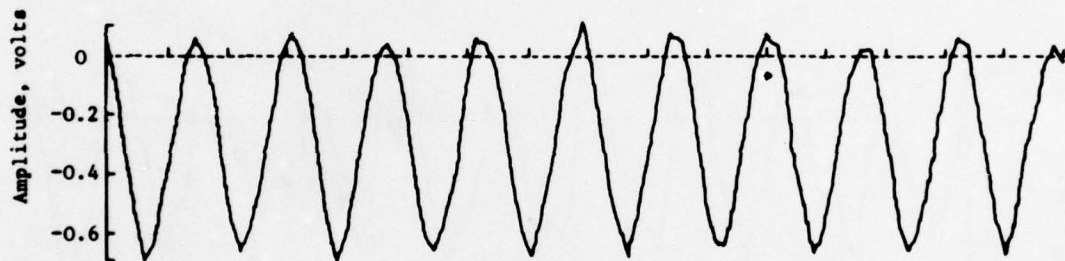


- Educed Trace, 1cm = 1.237msec

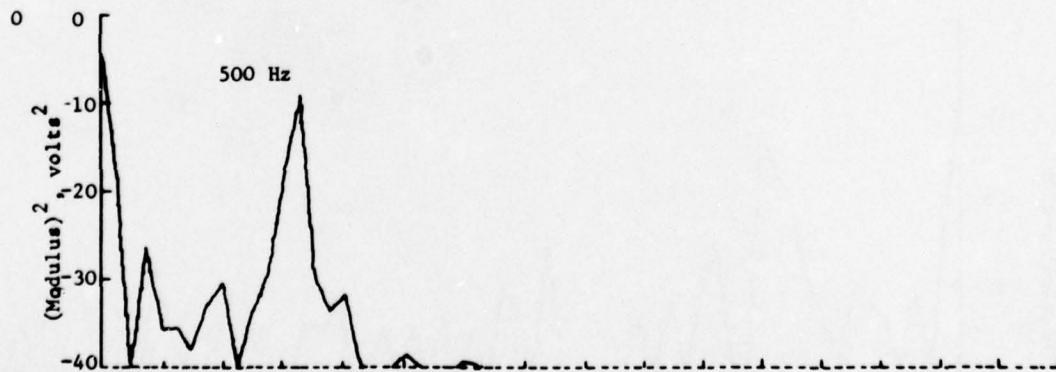


- Fourier Transform of Educed Trace, 1cm = 153 Hz

FIGURE 8.4 Eduction of a Sinewave (1000 Averagings)



Educed Trace 1cm = 1.237msec



Fourier Transform of Educed Trace 1cm = 153 Hz

FIGURE 8.5 Eduction of a Sinewave (5000 Averagings)

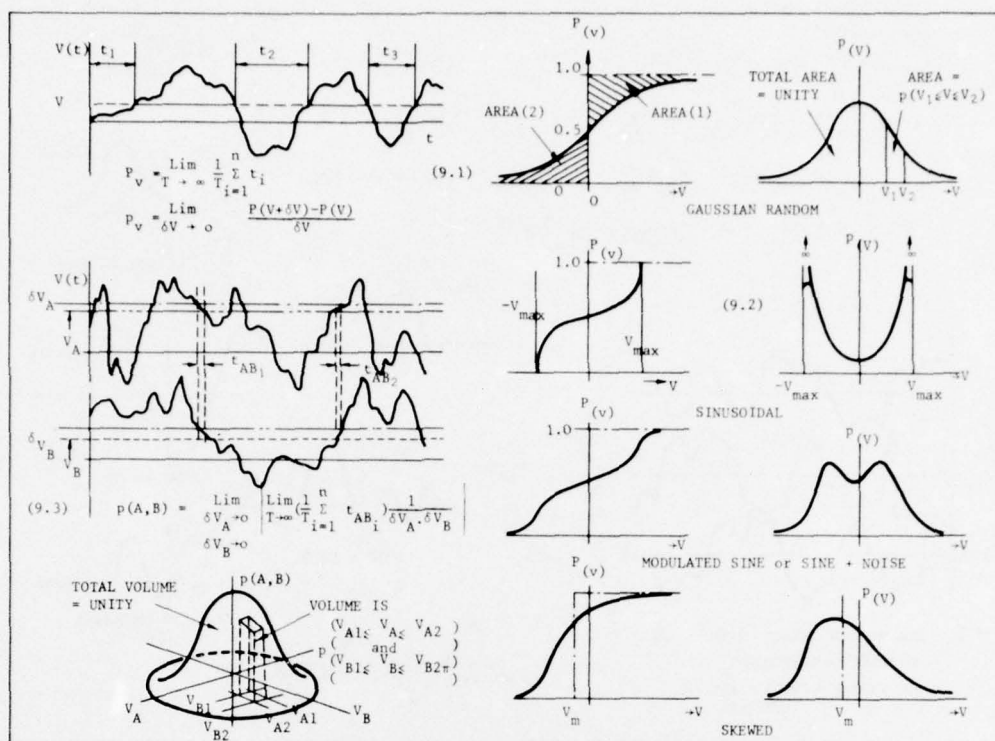


FIGURE 9 Probability Functions

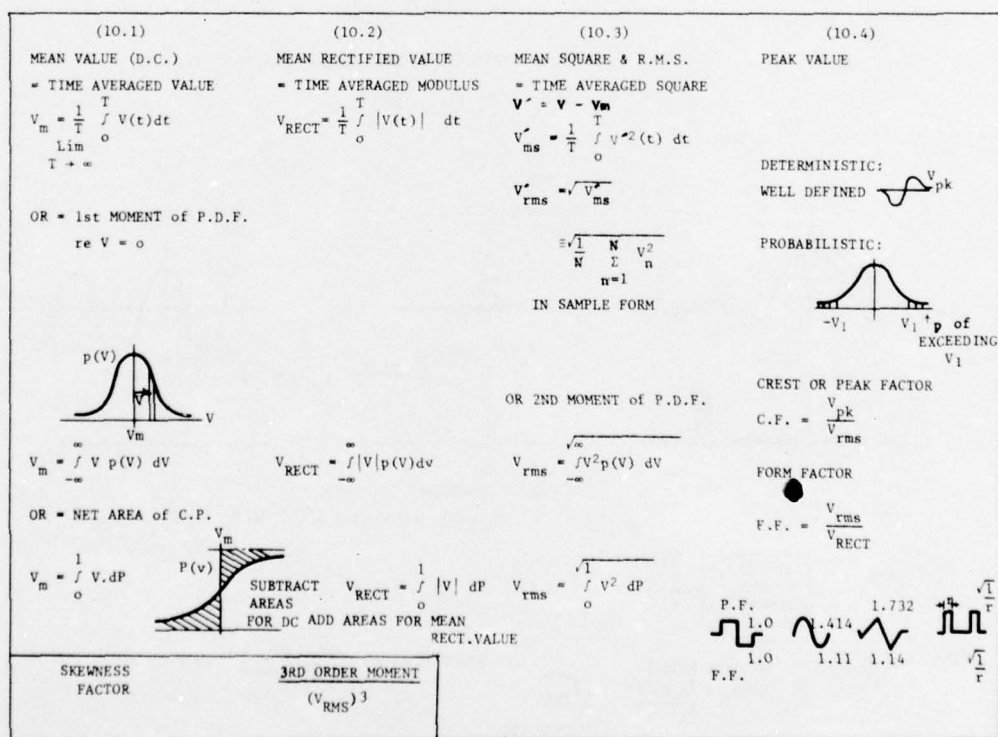


FIGURE 10 Overall Parameters

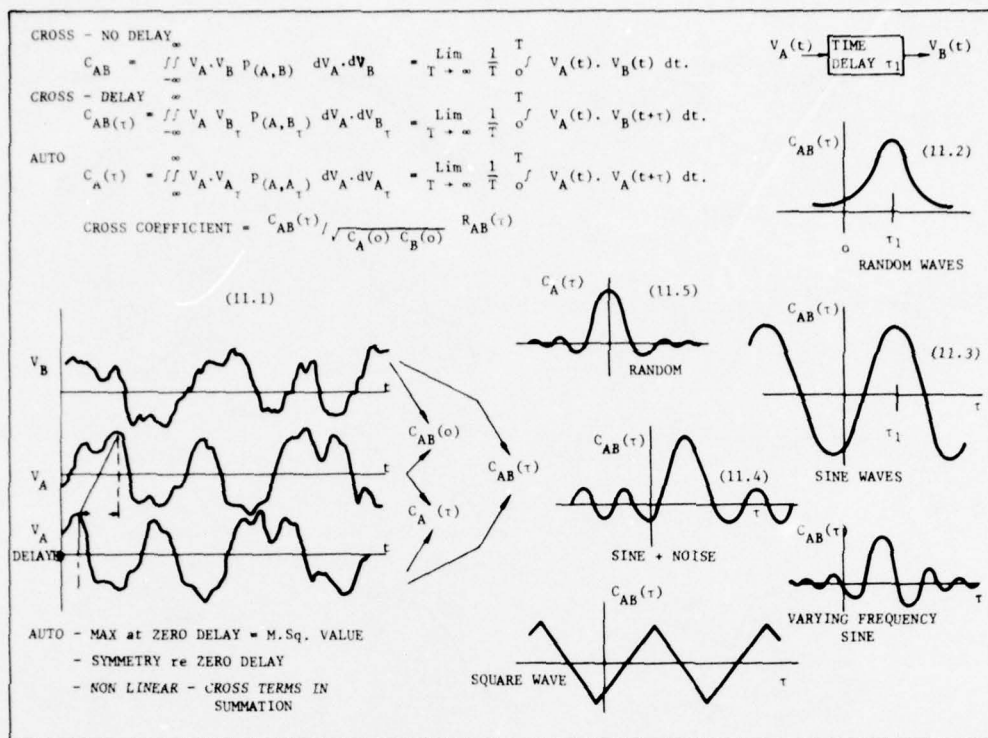


FIGURE 11 Correlation Functions

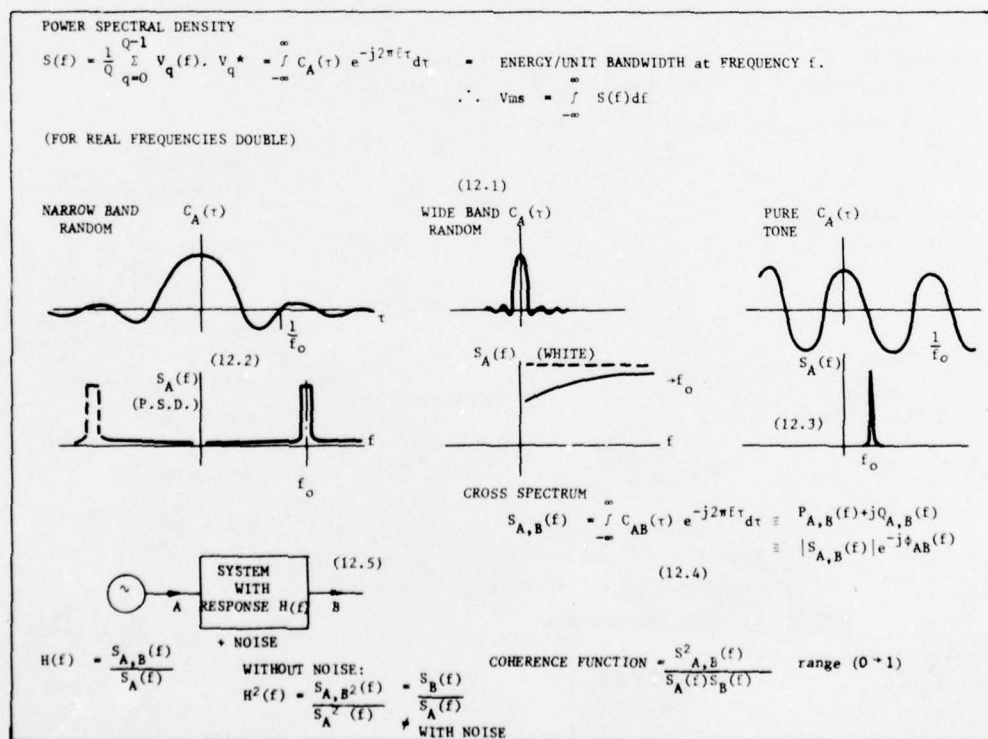


FIGURE 12 Power Spectra and Coherence

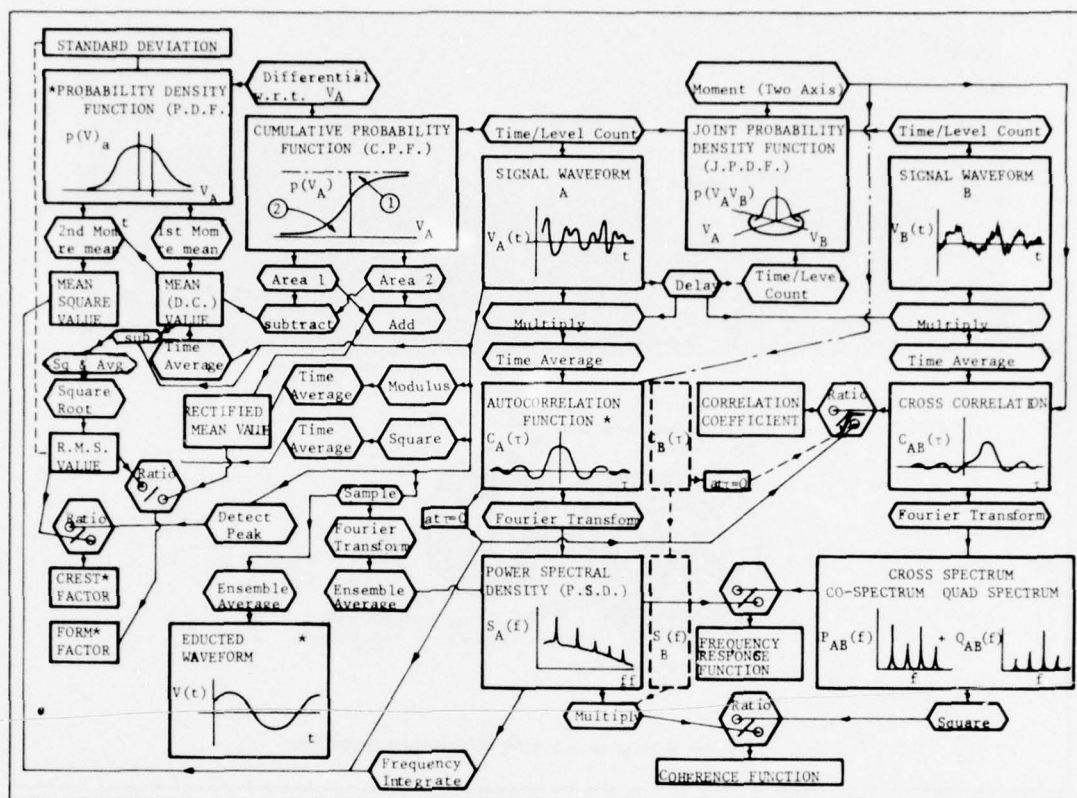


FIGURE 13 Function Relationships

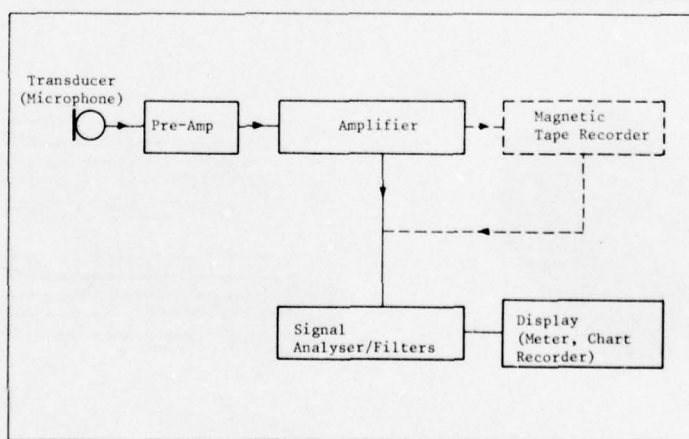


FIGURE 14 Basic Instrumentation Scheme

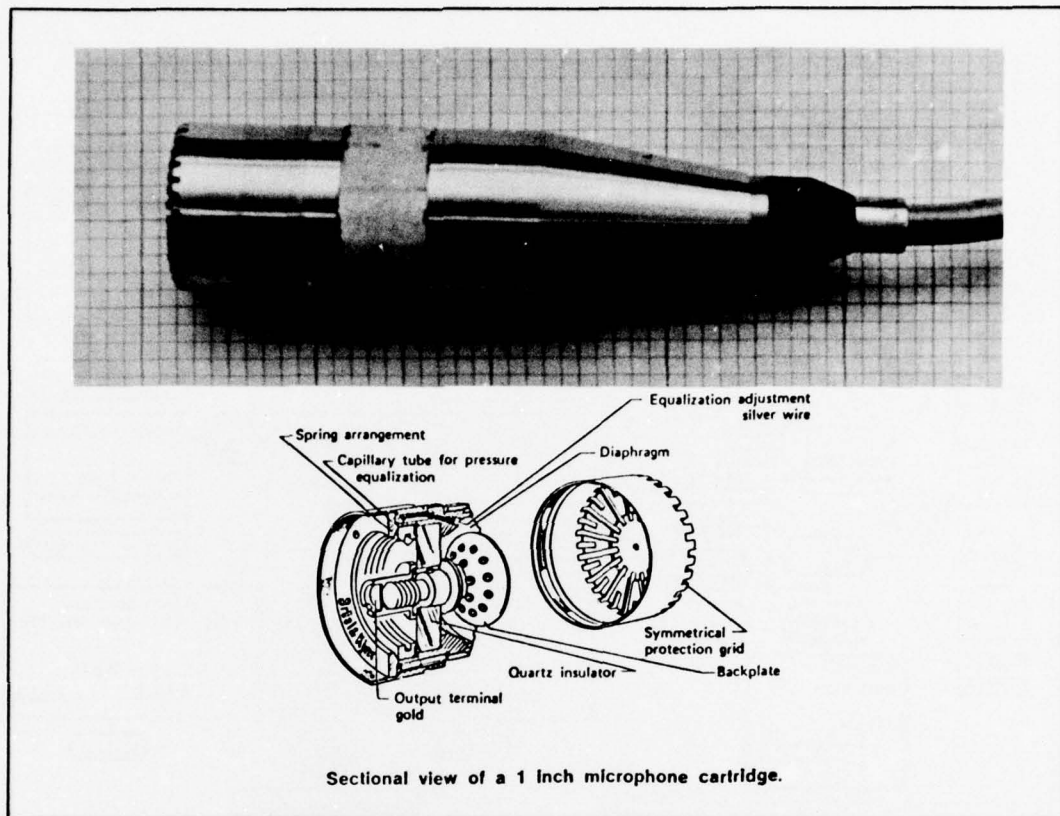


FIGURE 15 Condenser Microphone

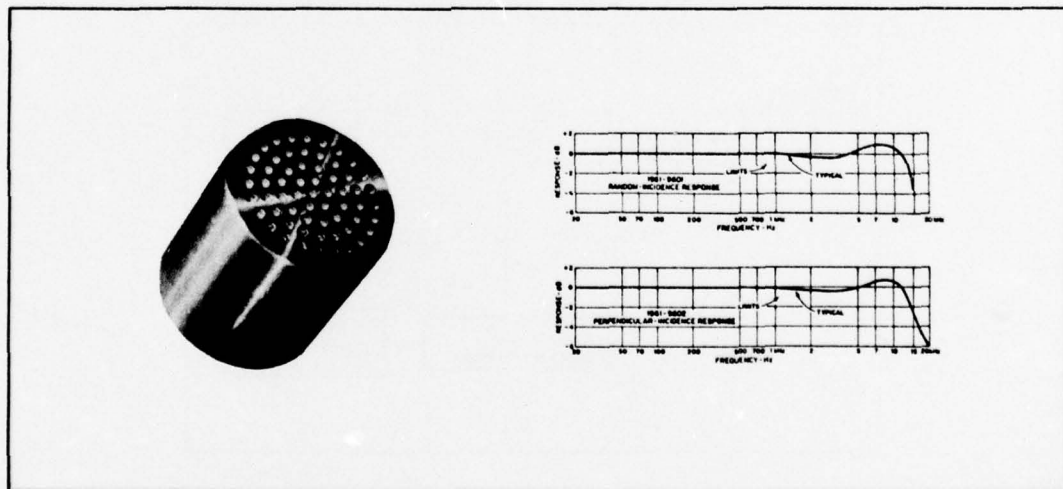


FIGURE 16 Electret Microphones

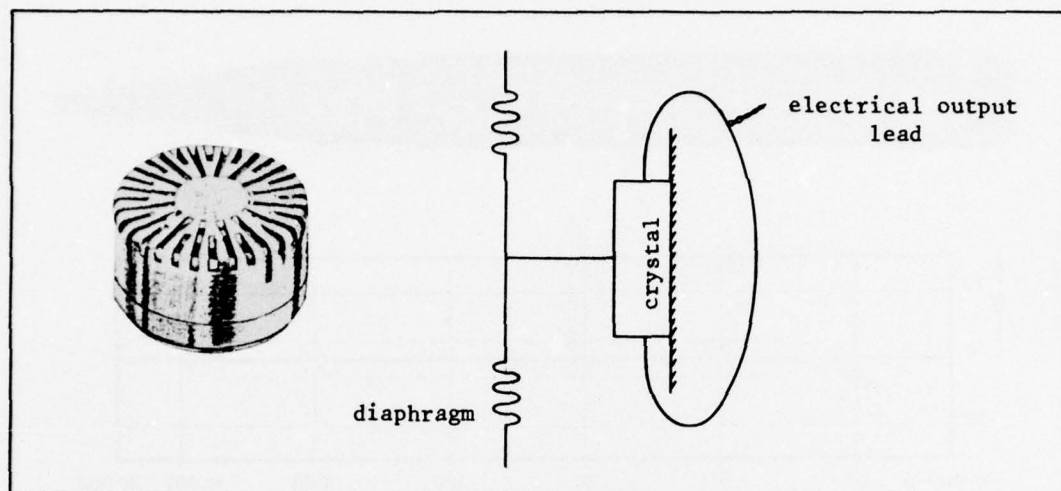


FIGURE 17 Piezo-Electric Microphone

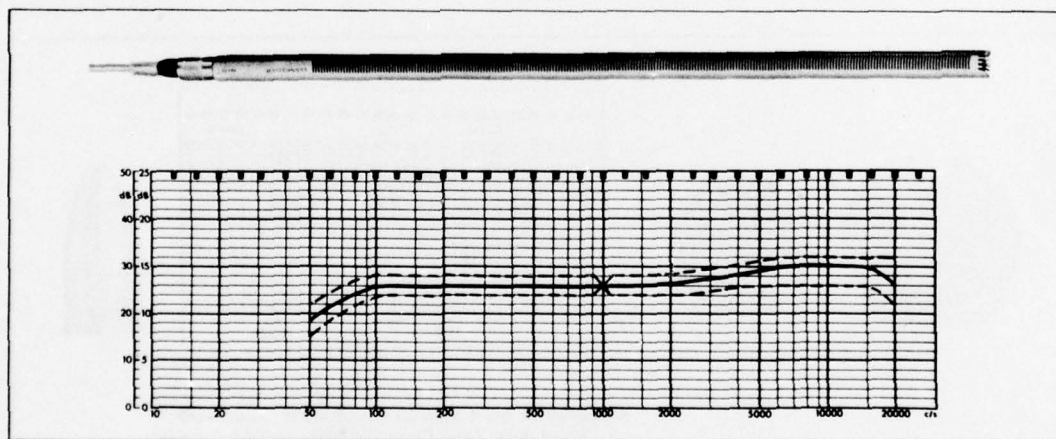


FIGURE 18 Directional Microphone

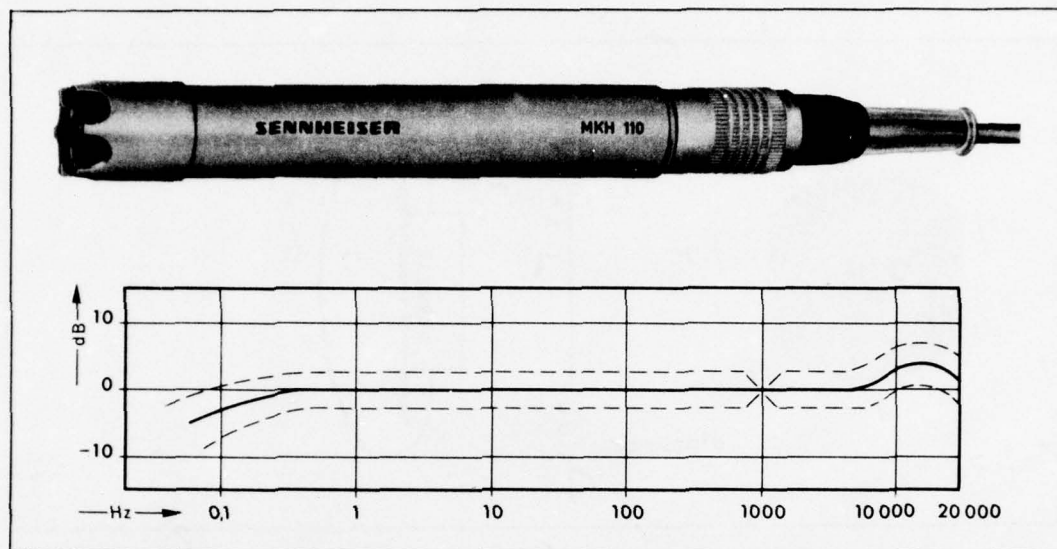
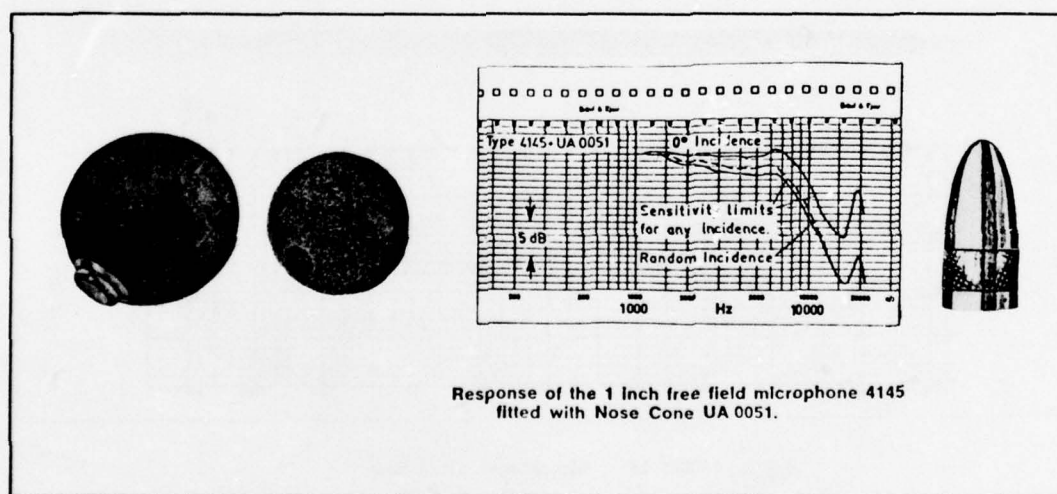


FIGURE 19 Low Frequency Microphone



Response of the 1 inch free field microphone 4145 fitted with Nose Cone UA 0051.

FIGURE 20 Windshields and Nose Cone

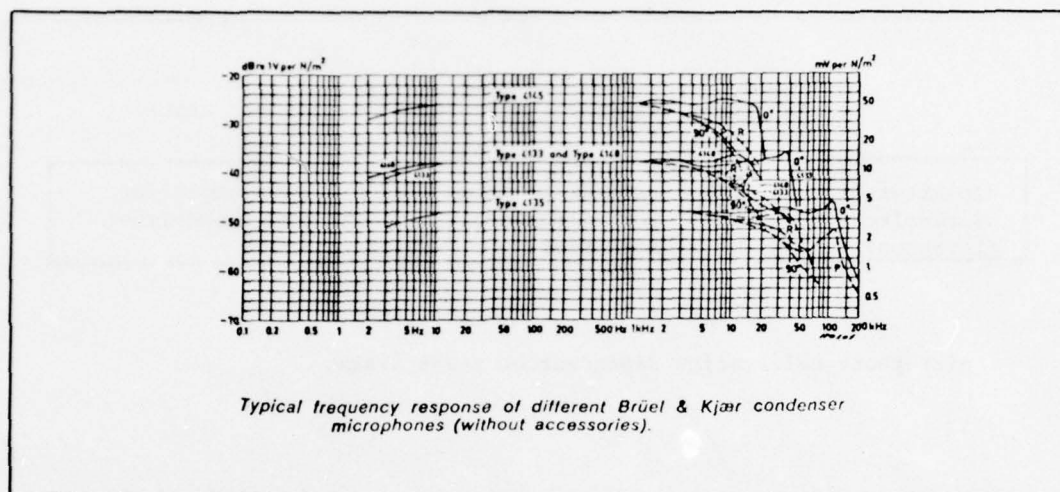


FIGURE 21 Condenser Microphone Response Characteristics

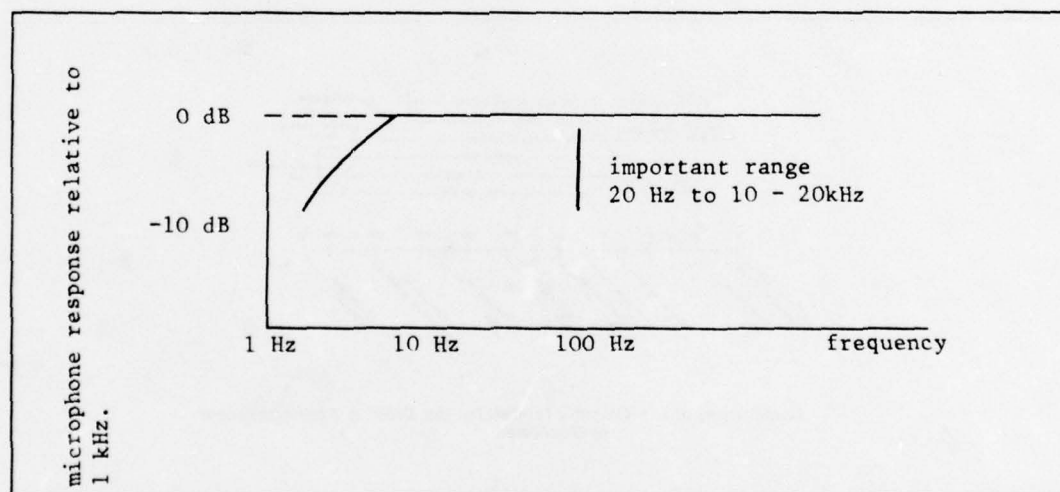


FIGURE 22 Effect of L.F. Capacitor Leakage



FIGURE 25 Sound Level Meter with Octave Band Filters

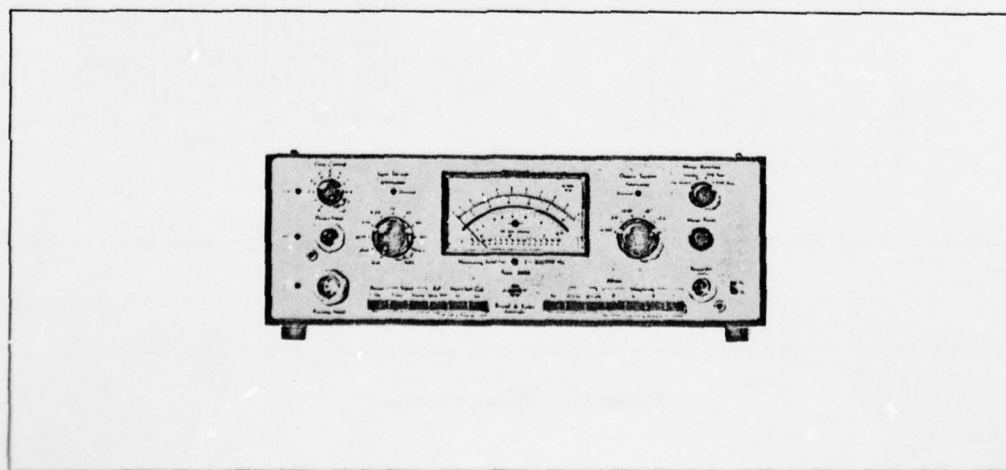


FIGURE 26 Measuring Amplifier

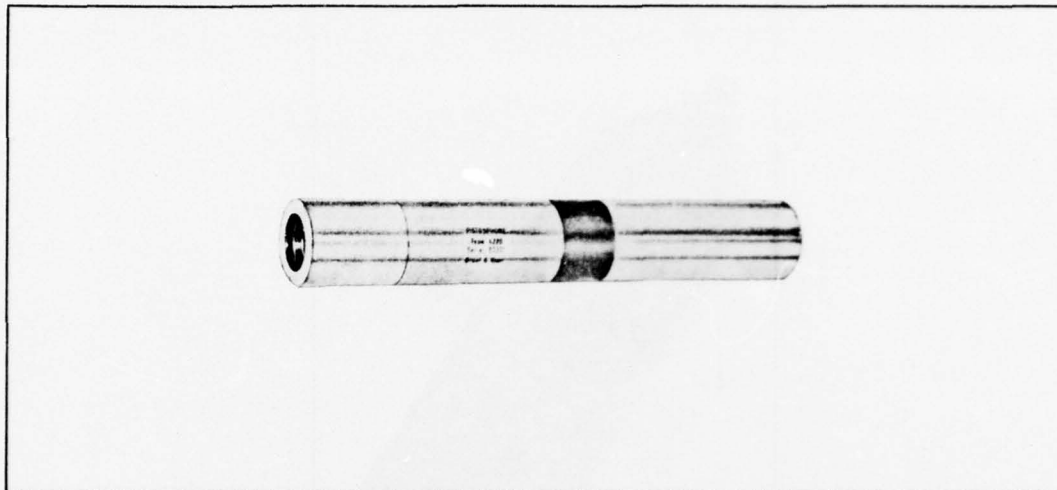


FIGURE 27 Pistonphone Calibrator

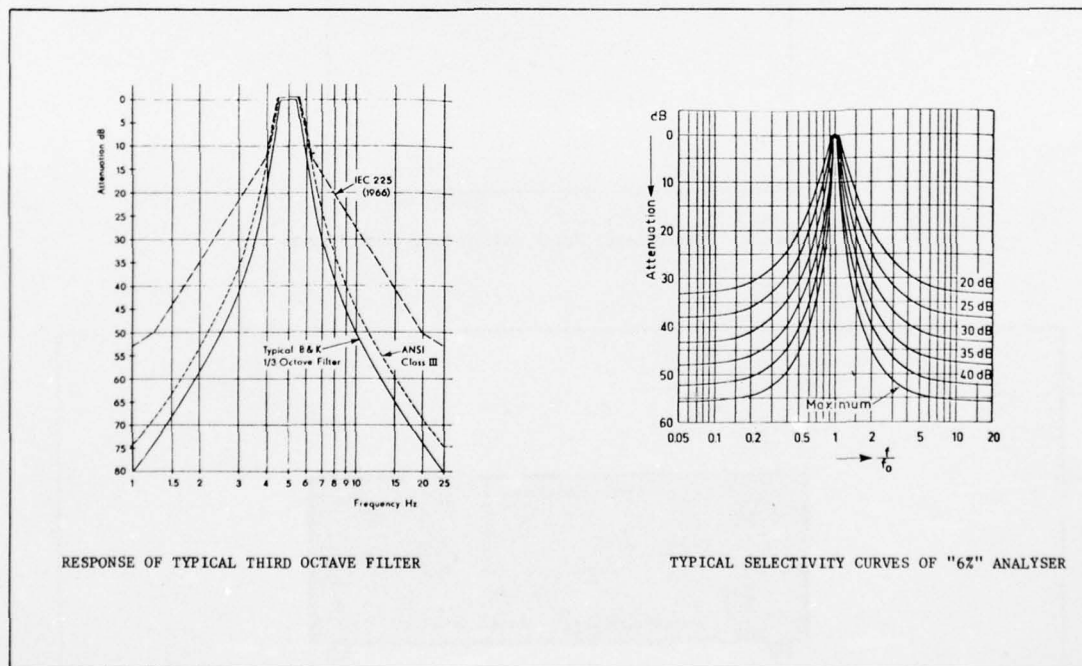


FIGURE 28 Filter Responses

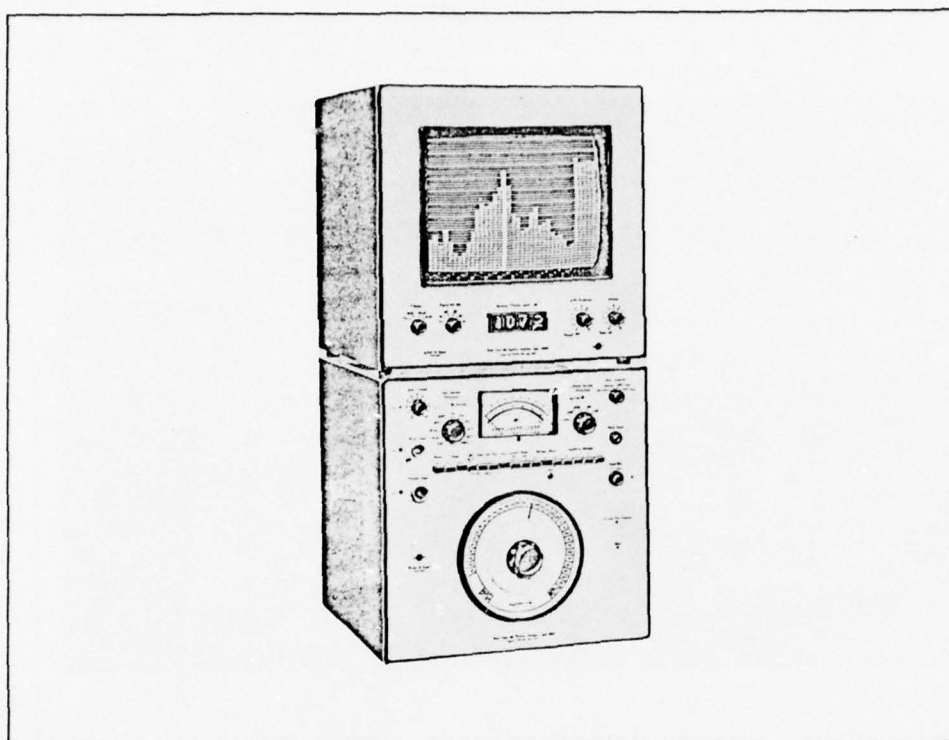


FIGURE 29 A 1/3 Octave Real Time Analyser

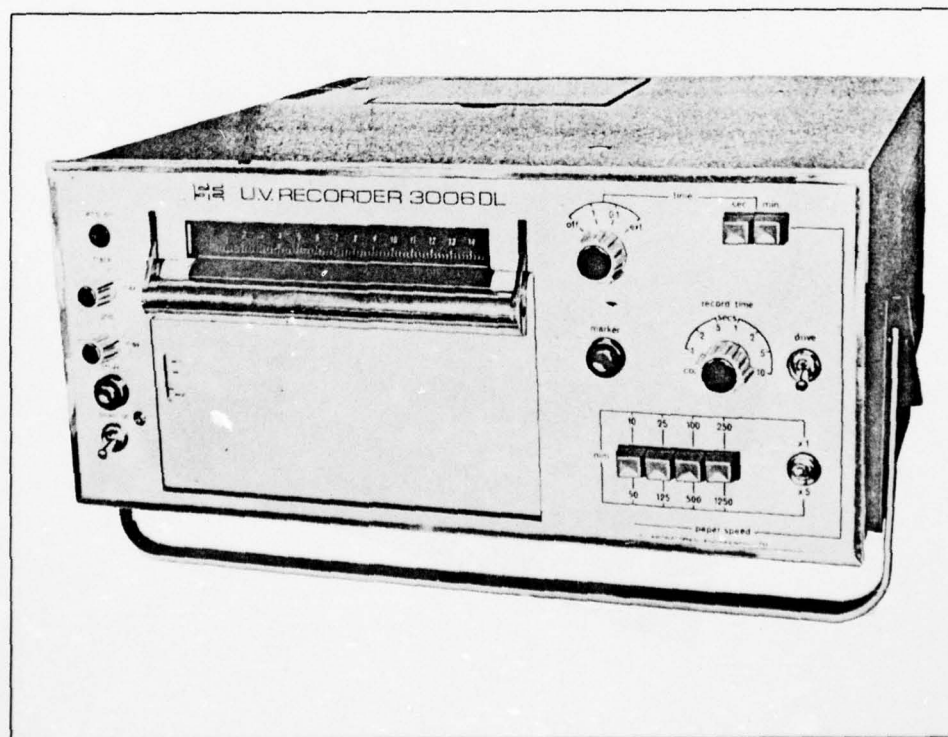


FIGURE 30 U.V. Chart Recorder

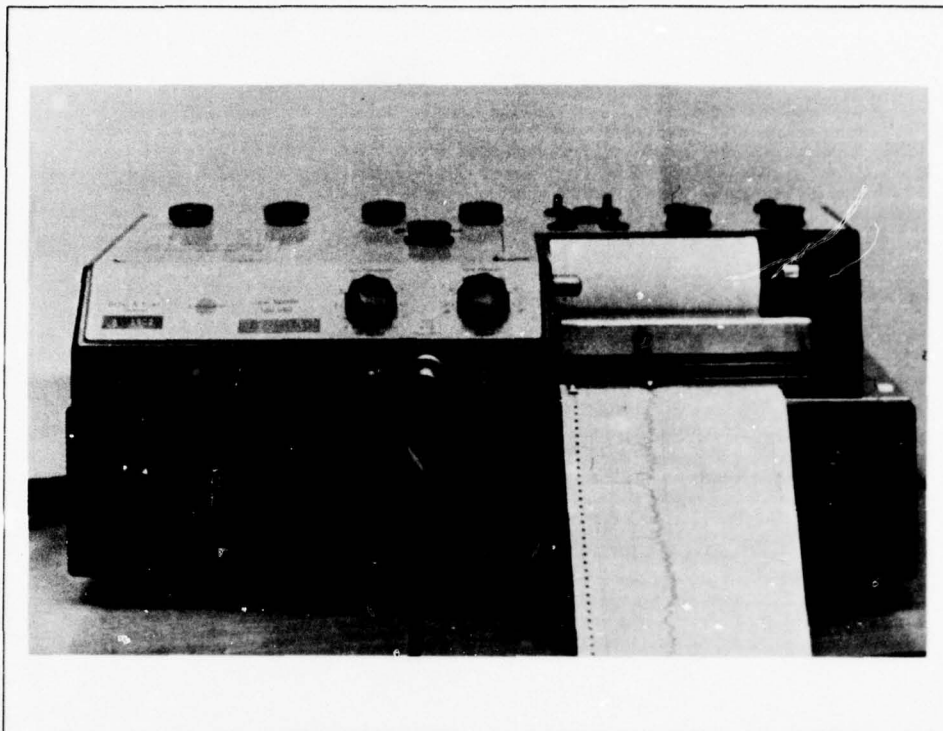


FIGURE 31 Level Recorder

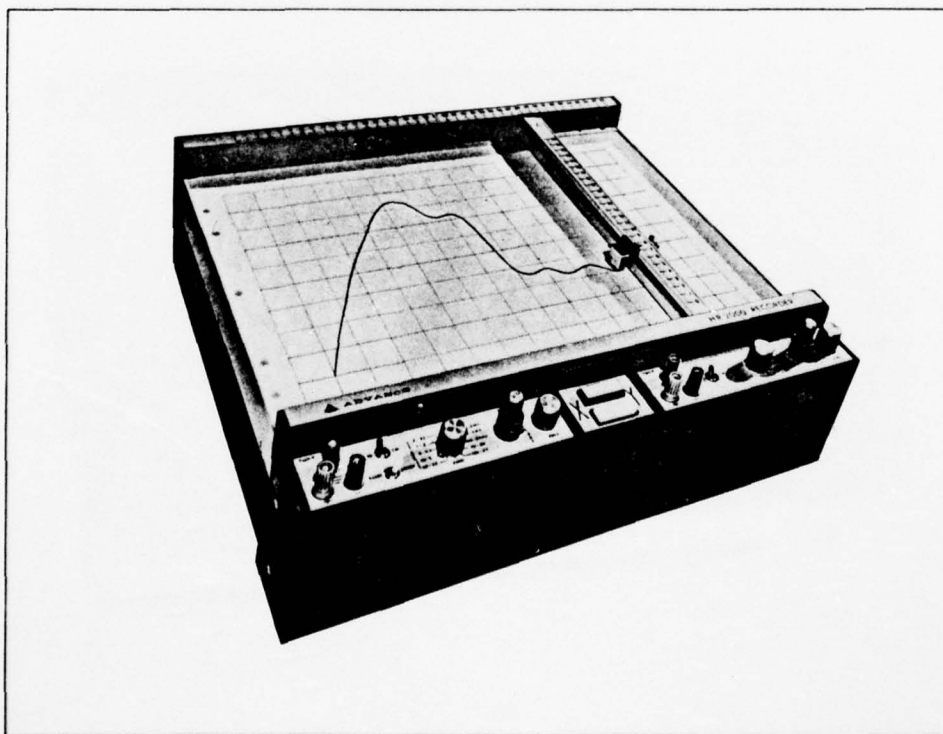


FIGURE 32 X - Y Plotter

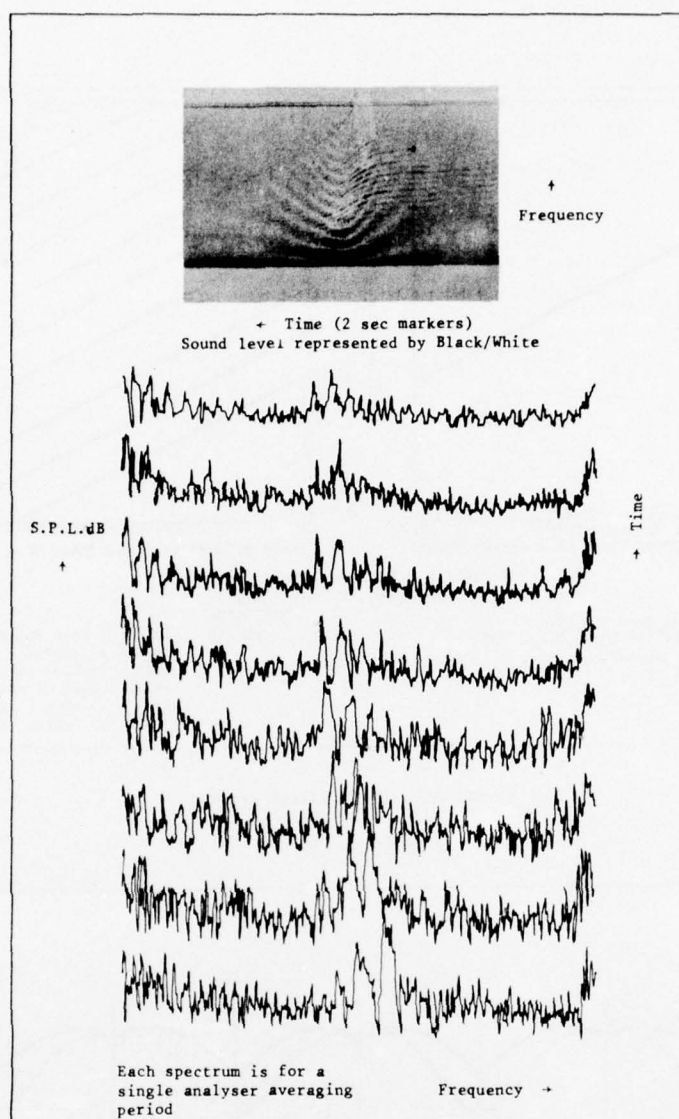


FIGURE 33 3D Representations

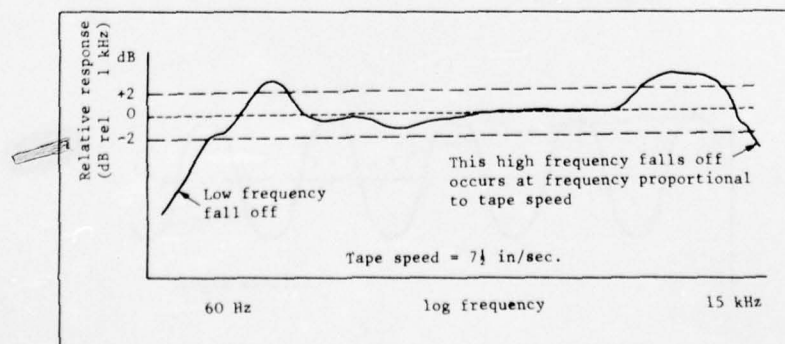


FIGURE 34 Typical D.R. Tape Recorder Frequency Response

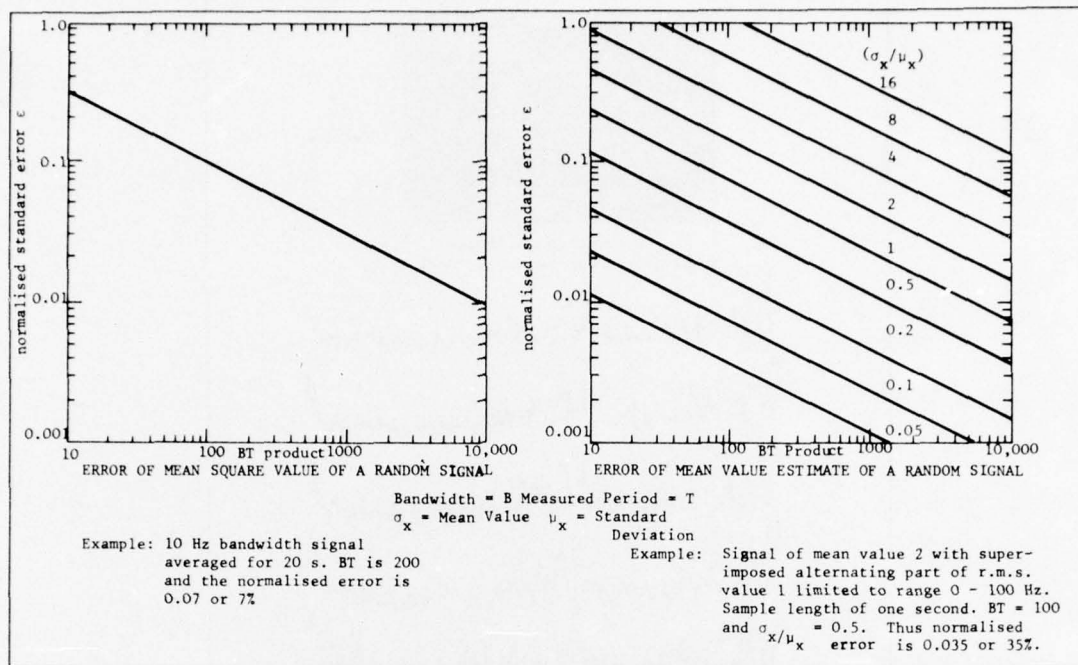


FIGURE 35 Measurement Errors

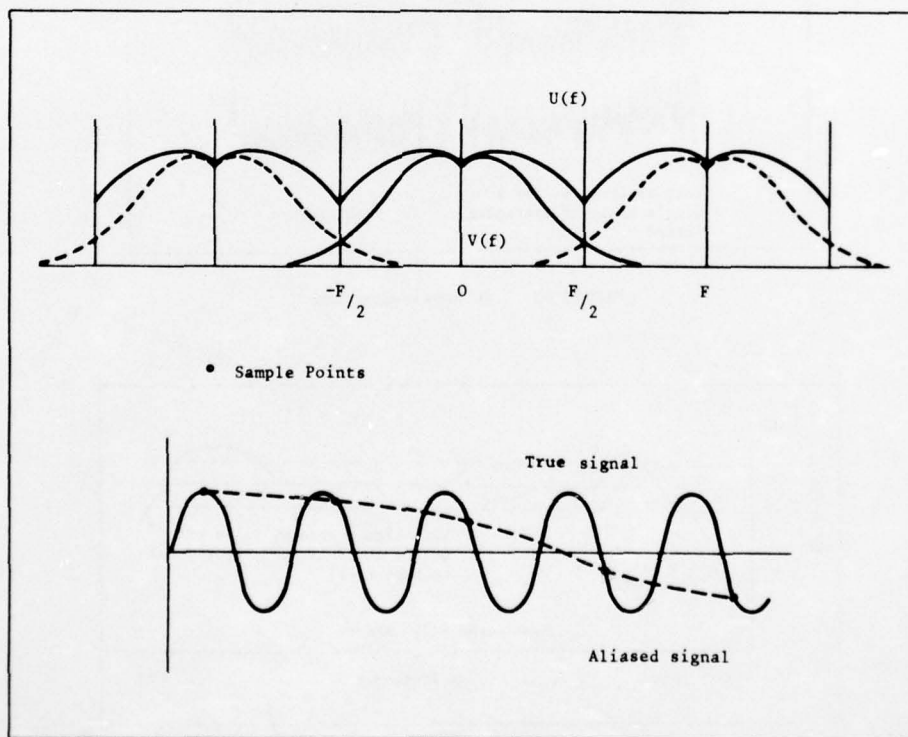


FIGURE 36 Aliasing in Digitally Sampled Analysis

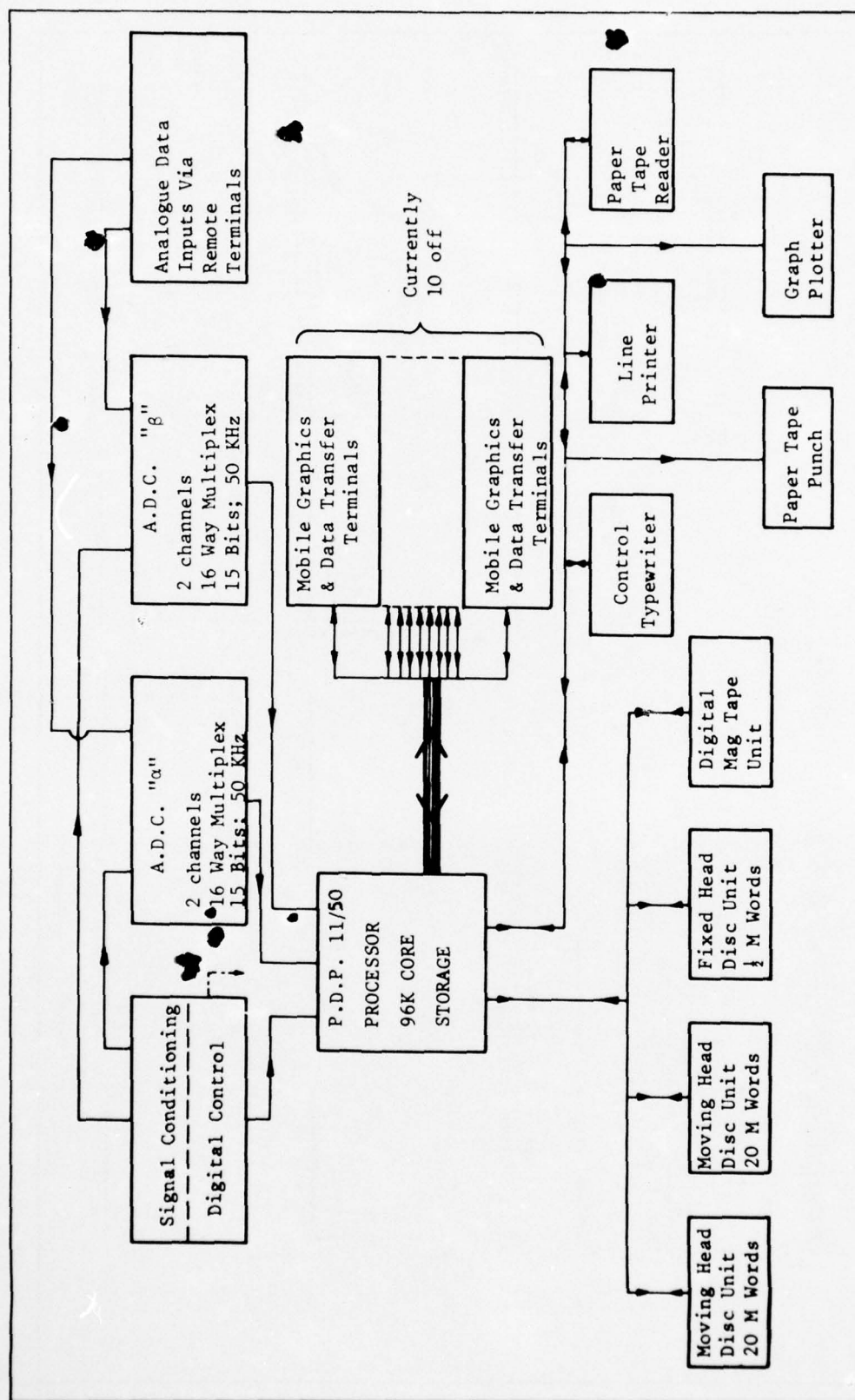


FIGURE 37 Schematic Diagram of Data Analysis Centre
PDP 11/50 Computer

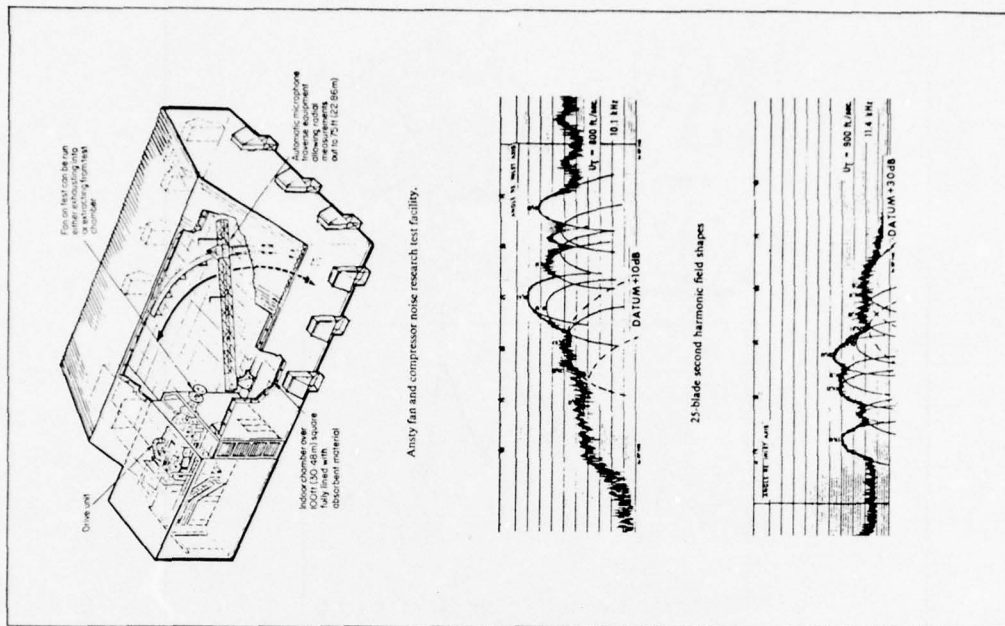


FIGURE 40 Polar Noise Traverse

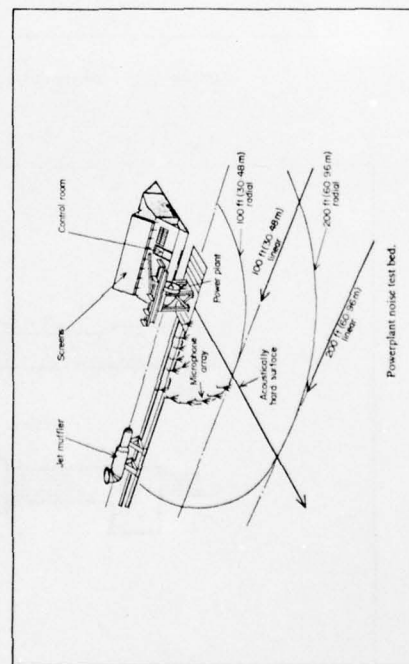


FIGURE 39 Discrete Point Measurements

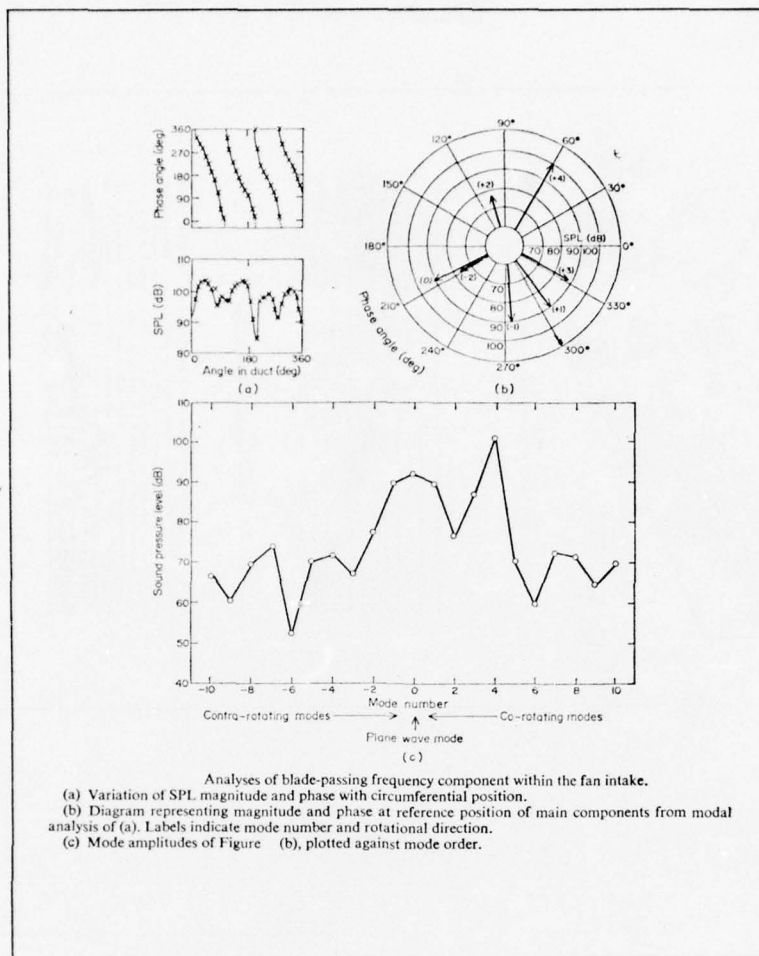


FIGURE 41 Distortion Data from In-Duct Measurements

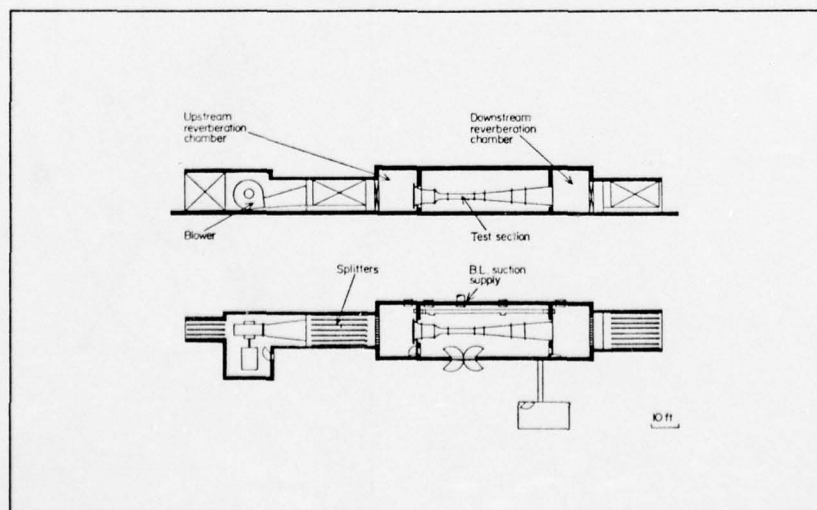


FIGURE 42 Double Reverberation Absorber Test Facility

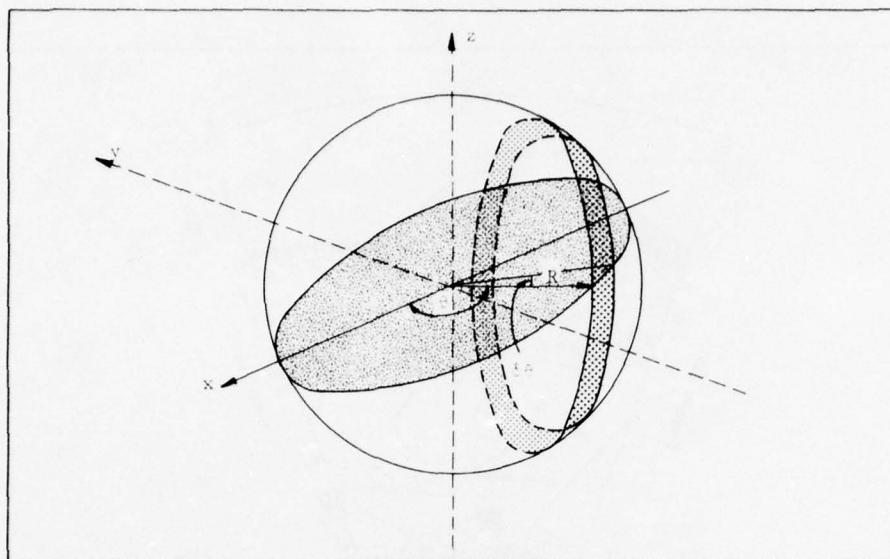


FIGURE 43 Sound Power Integration

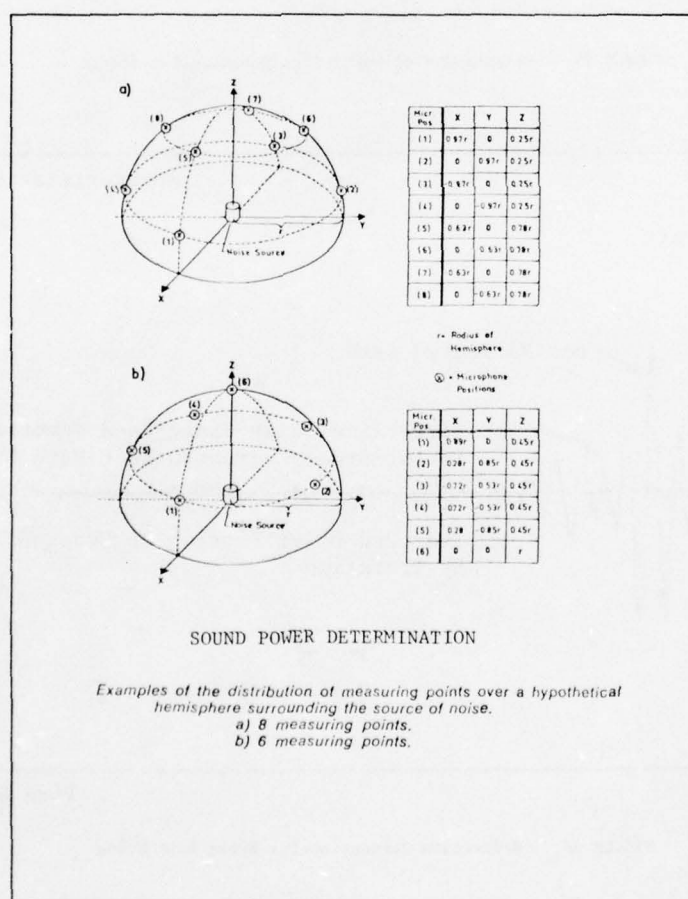


FIGURE 44 Sound Power Determination

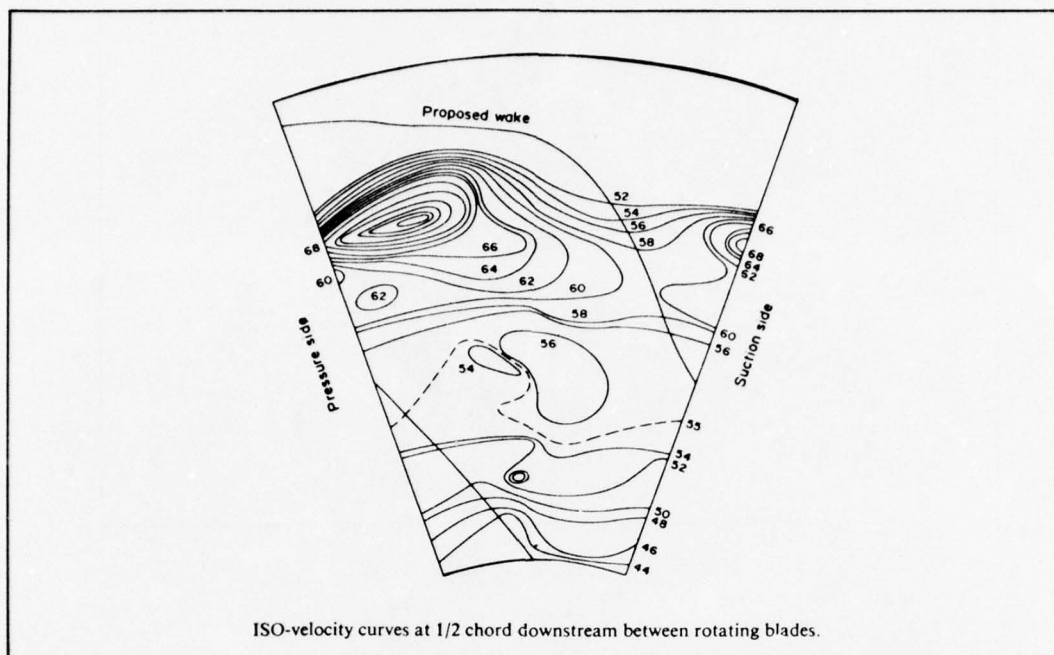


FIGURE 45 Measurement of Wakes from Rotating Fan Blades

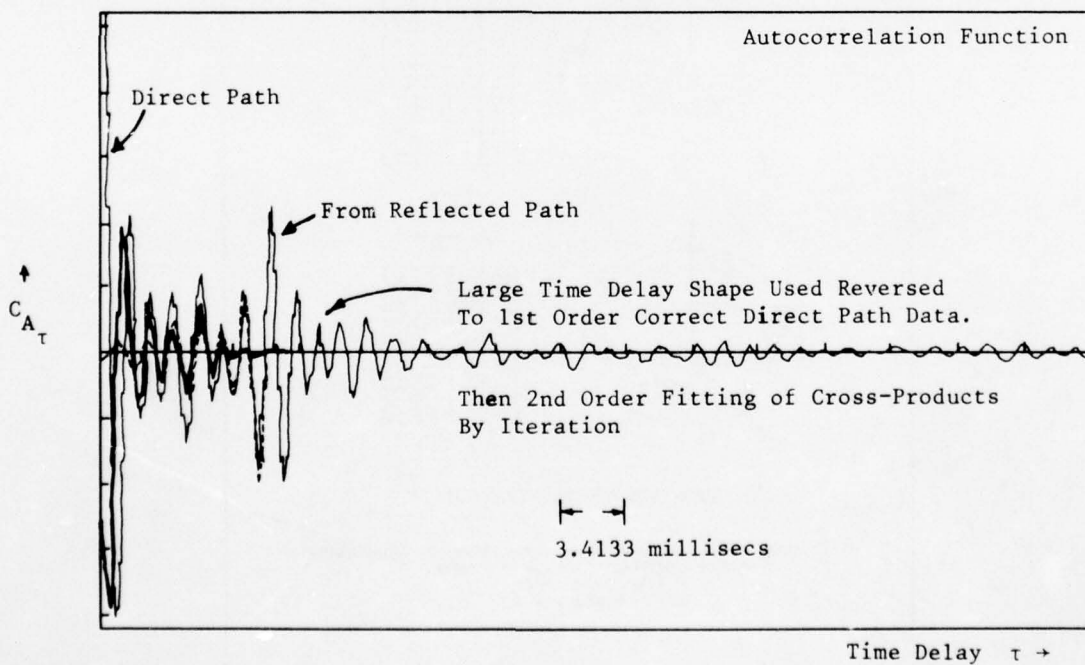


FIGURE 46 Reflection Correction for Broad Band Noise

AIRCRAFT FLYOVER MEASUREMENTS

Michael E. House

1. INTRODUCTION

This lecture specifically deals with the topic of making measurements of the noise from aircraft which are in flight using instruments placed at relevant positions on the ground. It is convenient to treat the subject in two main divisions, namely measurements for specific research purposes, and data collected in order to ascertain whether an aircraft meets noise regulations.

2. RESEARCH MEASUREMENTS

There are a number of aspects of sound propagation from aircraft and engines when in flight which are quite different from ground operations. These relate to engine cycle conditions, intake flow conditions, aircraft and nacelle aerodynamic flow characteristics, convected motion effects, 'Doppler' source-to-receiver effects, aircraft attitudinal and atmospheric or ground propagation effects. As well as this, it is always necessary to be able to determine the aircraft's relative motion and track to the measuring position.

2.1 Basic Influences of In-Flight Conditions on Noise

2.1.1 Engine Cycle Conditions

We will discuss the case of a turbofan engine, although similar arguments apply to pure jet engines, turbopropellers etc. We have seen that the quadrupole sources of jet noise are highly dependent on the jet efflux velocity and in flight, of course, the relative velocity will be relevant to the classical jet noise sources. However, sources due to poor conditions inside the jet pipe, or mixing conditions between the streams of the fan exhaust and the core engine exhaust, will only weakly depend on relative jet velocity. Again, we would expect the fan noise to depend on the rotational velocity relative to the airflow into the fan or more exactly, on the relative velocity distribution over the blades and stationary vanes in the fan stage. Similar arguments hold for turbines.

Intake flow conditions depend upon altitude, day temperatures and aircraft flight Mach Number and thus the fan velocities, jet velocities and even the small additional mass flow due to fuel combustion change to some extent. It is thus never possible to simulate all engine cycle conditions simultaneously even with the most elaborate of artificial altitude test facility. In any case such facilities are most unsuitable for direct measurements of radiated noise levels. As a result, the engineer has to make a choice of engine setting according to the dominant source being studied. Thus he would choose to match relative flight jet efflux velocity with an equivalent ground running condition and accept that the less dominant rotating machinery noise source at full power would be measured at slightly different conditions. To some extent, corrections can be made to those portions of the noise spectrum known to be due to the incorrectly simulated source conditions. In any event, the jet velocity match will not ensure a jet expanded density match between ground running and flight operation. Therefore in ground and flight comparisons of jet noise, it is usual to plot the noise levels corrected for the density and nozzle area terms, as well as for source to receiver distance difference etc.

At low thrust where fan noise is usually the most important source, tests are usually performed at the equivalent fan R.P.M. Again, provided one assumes that enough is known about the jet noise situation, predictive correction can be attempted for the incorrectly simulated jet noise sources.

2.1.2 Engine Intake Condition

Besides the effects of flight speed and atmospheric temperature and pressure altitude, it is now recognised that some sources of fan noise are critically dependent on the turbulence structure of the duct wall boundary layer conditions, and these may alter dramatically between ground running and flight conditions. The general practice of using a flared or bell mouthed intake in ground testing for performance work, and sometimes using flight nacelle hardware for other testing, adds complication in this respect. Experience shows that a well designed flare is more like the "flight nacelle inflight" case since there is a tendency to suppress the moderate scaled eddies which enter the intake due to atmospheric irregularities. It is thus important to understand the in-flight intake flow conditions for proper interpretation of results.

2.1.3 Aircraft and Nacelle Flow

The detailed flow fields around the intake lip and forward part of the flight cowl, also the jet flow behaviour of the fan stream, depend on flight speed and angle of incidence to the free stream flow. Only circumstantial evidence exists to suggest that in some cases it might be wise to keep these effects in mind when interpreting flight test noise data, which through flow gradient differential propagation or refraction and scattering might be responsible for some of the unaccountable ground-to-flight noise differences experienced. Similar conditions over wings and flaps, including vortex flow, have been suggested as important aspects of wing shadow and noise modulation effects in low-wing rear-engined installations.

2.1.4 Convected, Gradient Flow and Doppler Effects

The general difference between engine "flow tube" conditions and the "atmosphere at rest" conditions leads to an expected change in radiation direction for fan discrete tone lobular interference patterns. This is additional to the "in built" engine duct flow effects on noise generation and duct mode wave angles as predicted by the more comprehensive rotor noise theories. The additional directional changes are found from simple refraction theory to behave as:

$$\text{Sec } \theta_s = \text{Sec } \theta_f + M_f$$

Where θ is defined relative to the forward fan axis, subscripts s and f refer to static and flight conditions respectively, and M is the flight Mach number (see Figure 1).

Also illustrated in Figure 1 is the effect of convection relative to the airframe. This can be important where flight and ground comparisons are to be made for noise effects on adjacent structure, or structural transmission of noise into the cabin. There is an apparent translation and hence angular shift, since during the time for propagation of the emitted sound from the jet and intake, the airframe or engine nacelle has moved forward through the atmosphere.

These same effects are also responsible for the so-called Doppler frequency shift due to relative motion between source and observer.

Just outside a notional envelope of air around the engine, the sound waves reach the observer through the general atmosphere (assumed for now at rest and homogeneous). However, in emerging from the envelope the relative motion causes both a shortening of the wavelength ahead of, and a lengthening behind the engine (the effect is a less extreme case of the well-known supersonic Mach cone). As a result, the apparent frequency heard before overhead is higher and that after overhead is lower than the static equivalent case. The downward propagating wave fronts remain undistorted and at the static frequency. Note that also there is a slight redistribution of energy so that sound pressure levels are slightly elevated near the forward axis and reduced near the rearward axis.

Using the digital computer analysis system it is relatively straight-forward to divide the fly-by noise spectrum time history (as received) into small segments, correct for the Doppler and energy distortion effects and if necessary reconstitute the equivalent-to-static wave time-history.

2.1.5 Aircraft Attitude

This is just a simple source re-orientation which can, especially with modern jet aircraft climb-out floor angles, lead to not inconsiderable corrections to the ground observed noise levels.

2.1.6 Atmospheric and Ground Effects on Propagation

As with all noise measurement, it is necessary to recognise that the atmosphere and the ground plane influence the received sound in several respects. Firstly there is molecular relaxational absorption of the upper frequency register at large distances, (typically over 1000 feet range at 1kHz and above). Except under very infrequently encountered very dry conditions, the classical viscous absorption is negligible. Atmospheric absorption is a wide subject, quite a few investigatory exercises having produced rather different data. However the work of Evans and Bazely at the National Physical Laboratory, Teddington, and the SAE ARP 866 data charts are perhaps the most widely used in the aero-acoustic field. Molecular absorption is found to depend on the relative humidity as well as the air temperature. It is important to realise that atmospheric absorption depends on absolute distances from the source along a particular line of wave propagation, and not, as with wave divergence attenuation on the ratio of one range to another reference range. Because the perceived Noise Units generally used for aircraft are particularly sensitively weighted to the moderately high frequencies (2 to 4kHz), the atmosphere has the effect of causing a reduction in PNdB of rather more than 6dB per doubling in range, typically 8 PNdB over the usually encountered ranges for airport noise problems.

The atmosphere also causes the shorter term level of sound from a source to be modulated by interfering multiple propagation paths through the turbulence structure. Naturally this structure is more pronounced during windy and rainy weather than during still air or temperature inversion conditions. Figure 2 is illustrative of some recent measurements using a known steady output from a powerful loud-speaker from well below a tethered balloon. These data are for a 1kHz test tone, but evaluation of the data over a much wider range of frequencies and distances is currently being undertaken at Southampton.

Wind and temperature gradients, of course, also induce the well known ray curvature effects, wind shadow effects, and sound channelling effects which can give rise to freak propagation effects, often sources being discernable over many tens of miles whilst being almost inaudible at close distances, and vice-versa. It is thus important to note all relevant atmospheric data and if possible to perform a vertical meteorological survey over say the 1st 1000 metres of altitude above ground level.

The ground plane affects aircraft noise measurements due to the differing path length between the rays first reaching the microphone (usually mounted on a tripod at 1.2 metres above ground) and that bounced back from the ground. Note that this has the effect of modifying the spectrum such that, at some frequencies, there is an odd multiple of $\frac{1}{2}$ wavelengths difference and hence destructive interference lowering the received level, and at others an even number, leading to constructive elevation of levels by 3 to 6 dB, depending on whether the noise is discrete or random. It is relatively simple to correct for such effects with a perfectly hard reflecting ground plane, but for ordinary terrain the frequency distribution of ground impedance must be known before a reasonably accurate correction can be applied. In the extreme case of propagation of noise from an aircraft at low elevation angle, the rays skim over the ground surface with the result that, even for quite negligible surface absorption coefficients there is almost complete phase reversal compared to the direct wave. This is responsible for the so-called over-ground attenuation effect. For further reading consult the references quoted at the end of the lecture notes.

2.2 Single Microphone Measurements

For research purposes it is usual to arrange for the aircraft to be flown carefully at a constant speed and height over a suitable testing field; although in certain investigations, such as measurements of airframe originating noise this may not always be possible, or some special test involving a manoeuvre might be required.

2.2.1 Microphone Arrangement

The microphone or microphones should always be placed at a standardised height of 1.2 metres above a ground plane with determinable acoustic properties, or else a "perfectly hard" acoustically reflecting surface such as smooth concrete or hot-rolled asphalt.

AD-A037 334

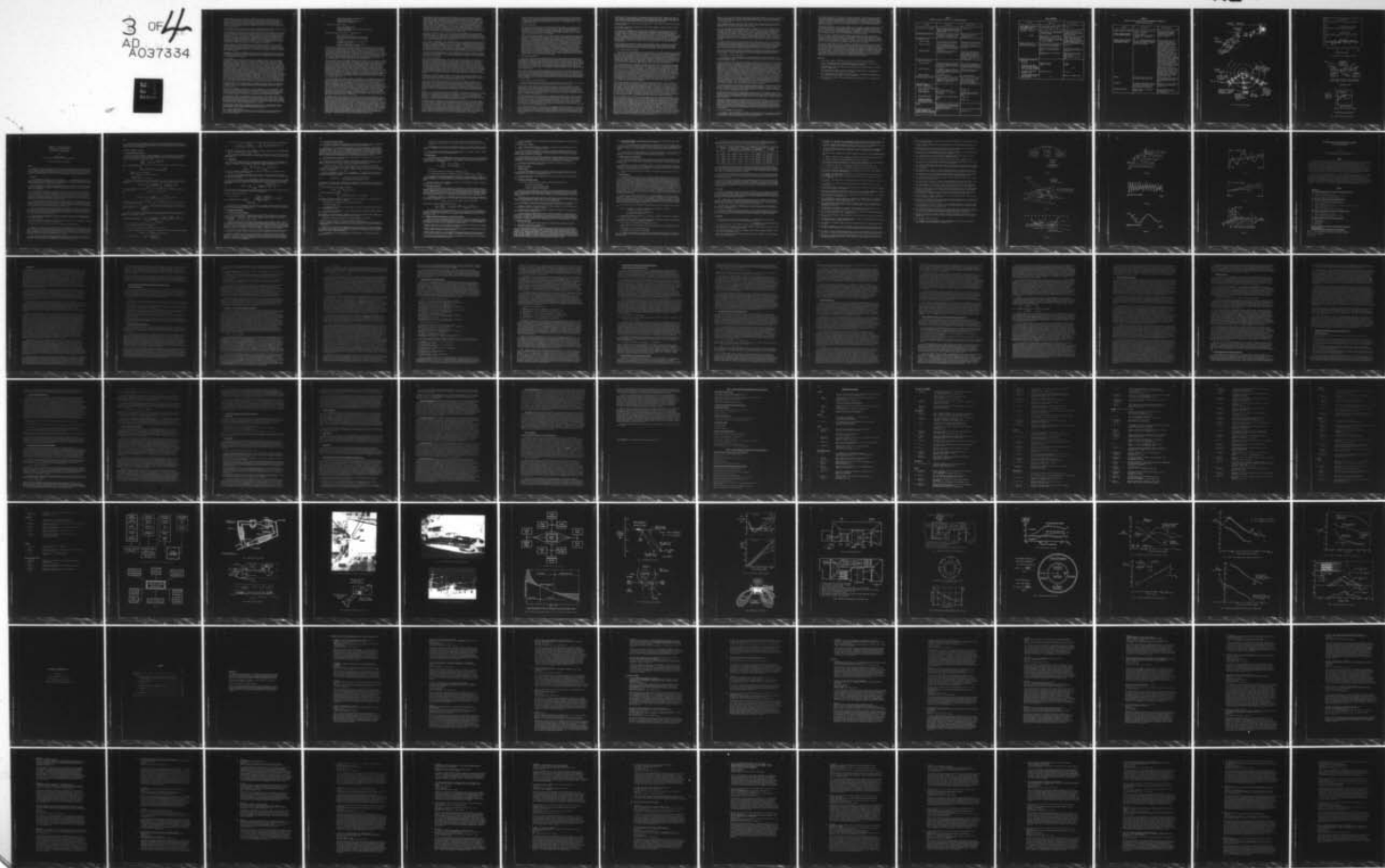
ADVISORY GROUP FOR AEROSPACE RESEARCH AND DEVELOPMENT--ETC F/G 20/1
AERODYNAMIC NOISE.(U)
JAN 77

UNCLASSIFIED

AGARD-LS-80

NL

3 of 4
AD
A037334



The microphone orientation is an important consideration, and practice ranges from those who maintain a fixed orientation (either axis vertical or axis horizontal and in plane of the fly-over) and rely on response corrections where necessary for really accurate results, to those using a grazing incidence situation (or as nearly as possible) for both fly-over and side-line data. In any event, it is most important to know the microphone characteristics and to note the orientation employed. The author prefers the vertical microphone system since this gives utmost signal to noise level in most situations.

The microphone should be situated well away from the recording caravan or personnel conducting the tests, so that stray sounds are minimised and non-idealised reflecting planes are avoided.

The microphone should always be fitted with a suitable wind shield. The foam sphere type is preferred since they maintain good uniform polar and frequency response. For reliable research or development work, the wind at the microphone position should not exceed 4 m/s (8 kts) with occasional gusts to perhaps 5 m/s (or 10 kts). Even so, it may transpire that sharp wind gusts cause momentary overload of the input amplifier to the measuring or recording system and hence will produce spurious data. If the data can be measured with A-weighting or a high-pass filter (125 Hz roll-off had been found in practice to be acceptable) then overloading problems due to wind are largely avoided, but note that the atmospheric propagation effects of the wind may or may not be acceptable at higher speeds than 4m/s depending on whether these effects are to be included in the investigation.

For most purposes a 1" condenser microphone offers a reasonably flat response over the usual audio frequency range defined for aircraft noise work at 45 to 11200 Hz. However, at a loss of basic sensitivity of order 12 dB(A), a 1/2" microphone cartridge can be used when it is necessary to record up to the upper limit of human audibility or to cover smaller scale research engines from which data must be gathered at high enough frequency to scale down to the audio frequency range for a full scale engine of the same type.

Arrangements for powering the microphones range from the use of normal mains driven units, where this is possible, to the use of battery powered sound level meters, or microphone amplifiers operated from 12V vehicle battery supplies. One type of portable recorder now incorporates its own power supplies and input amplifiers for microphones.

2.2.2 Recording

During a flyover, the system is required to cope with a considerable range of levels and frequency distributions. Usually the data has to be recorded for subsequent detailed analysis and, allowing about 10dB for inability to precisely set up for the peak levels which arise, the effective dynamic range for signals using D.R. recorders is a further 40 dB. A typical peak level might be 115 dB LIN against a general background level of 40 to 45 dB LIN. Thus it is impossible to record the peak, and the background level before fly-by, accurately on the same system. Further it must be remembered that, on replay of analysis, it is necessary to cope with a further element of dynamic range imposed by the spectral range of levels. This can easily be a further 30 to 40 dB especially when narrow band analyses are used to distinguish between multiple tonal noises. It should be borne in mind that in measuring systems, gain changes in 10dB steps are desirable, both to ease computation of levels and to avoid obvious errors in noting gains. A way of overcoming this is to use two channel recorders and to feed the same signal into both channels using differently set gains. Then, if the low channel should overload, the data can always be retrieved by switching to the high channel. Since many workers use the second channel as a voice log, the system can always be arranged with a circuit which will permit this unless the signal from the measuring microphone system exceeds a preset value. This is especially useful where a wide range of aircraft events are to be recorded without any accurate prior knowledge of peak levels. Above 800 Hz high frequency pre-emphasis is used to overcome the spectral level range problem. The recorder automatically reduces the high frequency levels again to the correct values on replay.

For some specialised tests, for example where it is desired to record the spread of noise laterally to the flight trackline, a multi-channel system might be preferable, although the author has found that the ability to use up to four synchronised portable twin channel machines for field work eases the power supply problem.

In the main, D.R. equipment is used since it is not often essential to record the very lowest of frequencies, and tape consumption is much less. For highest accuracy research, a tape speed of at least 7 1/2 ips is used, but for operational field work, where indices of community noise are being evaluated and weighting networks are in use, a speed of 3 3/4 ips will cover the frequency range adequately. Of course, if model scale work is being done, then even higher tape speeds might become necessary.

The recording tape should be of the instrumentation grade, capable of a wide dynamic range, and the oxide material should offer low distortion at a high recording level without any drop outs. It should have good long term storage capability, free from static and stray magnetic pick-up. The base material should be robust and relatively non-elastic, and offer good spooling characteristics without snatching. Oxides should be fine in texture giving lower head wear. The tape should be tolerant of the wide range of climatic conditions in which noise measurements have to be made.

Matt backed polyester based tapes with loaded ferric oxide mediums are to be preferred for most precision recordings. A newer range of sandwich materials should soon be available offering a wider dynamic range with higher overload and 3rd harmonic distortion tolerance.

2.3.3 Ancillary Data Measurements

It is necessary to measure or record a number of ancillary parameters during flyover measurements of noise. Of course with research, some data is specific to the purpose of the testing, but it is usual to be able to measure:

Aircraft Altitude over the microphone (array)
 Aircraft Fly-over Speed
 Engine RPM (for each significant rotor)
 Aircraft Actual Track Position

It might also be required to know:

The Aircraft operating weight
 Aircraft Altitude Data
 Aircraft to measuring system range and angular disposition
 throughout the fly-over

We also need to measure the following meteorological data:

Ambient atmospheric pressure
 Wind speed and direction (including gust magnitudes)
 at microphone level and possibly at relevant flight
 altitudes
 Air temperature at microphone level and possibly at
 relevant flight altitudes
 Wet bulb air temperatures at microphone level and
 possibly at relevant flight altitudes

There are several acceptable ways of recording aircraft altitude, remembering that for normal operational flying, it requires as much as 12% error to produce a 1 dB error on this account. One way is to rely on the pressure altimeter of the aircraft being used for the research. More accurately the aircraft could be equipped with radar altimetry. However, it is the usual practice to check the altitude by a ground based independent system. One of the simplest methods is to use a camera fitted with a suitable lens to cater for the ranges involved. A surprisingly reliable way of operating is to have someone pan the camera and to fire the shutter as the aircraft is judged to be at right-angles to the flight path from the observation position. Often features such as the engine intakes can be used as a guide to when this occurs since they are no longer seen as ellipses but as a line; (beware however of aircraft installations with inclined intake face).

Other groups prefer to use a fixed camera system, adjusted by spirit level to point vertically from as close to the microphone as practicable. A refinement is to have two additional cameras, orientated at 30° or so either side of the vertical plane through the flight path, in order to catch the off-track aircraft. With all camera techniques it is preferable to calibrate using a large marked out wall, photographed with the same lens system and from a measured distance typical of the ranges experienced in the flight tests. When using the fixed camera system(s) the calibration can also provide details of off-track distance as well as altitude. Naturally to determine altitude the aircraft size must be known. With focal plane shutters it is preferable to set the camera with the shutter action transverse to the track of the aircraft. Then, if distortion occurs due to the finite blind speed, the fuselage length remains a good basis for the altitude calculations. Wing span can still be used however if any angled appearance is ignored and the projected span perpendicular to the fuselage centre line of the image used instead. The other method of altitude calculation uses the focal length of the camera lens but is less reliable since this must be known or determined to a reasonably high accuracy.

In scaling the image sizes, a large scale print of the negative to a known magnification can be used, but the author prefers to project the original negative material onto a screen in a darkened room (also the calibration negative). With suitable lenses it is then possible to measure image size to better than 1% and thus, if the calibration is over a typical range, to this same accuracy in altitude. Refinements include making allowances in the calculations for aircraft fuselage attitude (from even an approximate knowledge of the aircraft's performance) or judging roll attitude from the ratio of measured span image to fuselage image. With two camera operators equipped with hand-held cameras and built-in devices for projecting a gravitationally determined elevation scale and compass bearing scales into the lens system, researchers at Southampton have successfully determined altitude, track error, and attitudes in pitch or roll. A further simple refinement is to arrange for the camera operation to event mark the tape recording as an indication of the time of the closest fly-by. Other methods of much more accurate altitude (and speed) determination include ground based precision radar and tracking cine-theodolites, preferably two sets in synchrony, used along and normal to the flight path to determine the precise aircraft motion.

An independent check on aircraft speed is also desirable, since the on-board equipment is usually air-speed based, and requires adjustment to give the true ground speed. One method which the author has used is to select suitable points on the ground about 2 to 5 kilometres from the microphone system. Markers are laid out on the ground at these points as an aid to flying the required ground track, which is usually selected on the day of tests to be closely aligned to the wind direction. The ground distance between both markers and the microphone is determined either by identification on suitable ordnance survey maps or by using a precision microwave interferometer instrument, capable of accuracy to much better than 1cm in a kilometer of range. It is then a simple matter for observers (in touch with a control centre by two-way radio) to report marker pass-by, preferably using a simple sighting frame set normally to the expected flight path. The control centre records the times by chronometer or else feeds the audio marks from the outer station observers onto the tapevoice track. It is a simple matter to compute the average ground speed between each marker and the microphone and to calculate the relative times for any required noise propagation path angle from the aircraft to the microphone(s) knowing the flight track and altitude and ambient speed of sound.

Engine parameters, and aircraft weight are usually available in research exercises from on-board data systems, but there are means of deducing the engine speed from the received noise signatures if details of the engine compressors, fans or turbines are available. Account must be taken of the Doppler frequency shift, or the engine speed determined as the aircraft passes with maximum rate of change of Doppler frequency. Note that this does not occur at closest pass-by position due to the finite time taken for sound propagation, during which the aircraft has moved on somewhat. A simple means of achieving this information is to use an $X(t) - Y(f) - Z$ recorder, whereupon the Doppler inflection point can be readily detected, or the extremes of Doppler shift used to calculate the equivalent static frequency. The same shift can be used to provide an independent check on aircraft speed and the rate of change at the inflection can be related to altitude and speed. Doppler corrected frequencies have to be identified with engine rotor frequencies knowing the blade numbers and by deduction of the harmonic series detectable from the analysis trace.

Incidentally, the same $X(t) - Y(f) - Z$ plot can yield very useful information on the ground plane interference problem. It transpires that the constructive and destructive interferences show up as parabolically shaped zones in the frequency versus time plot, minimising at the condition of vertical ray path from the aircraft. This permits the analysed detailed spectra to be more accurately corrected to give "equivalent-to-free-field" data. Again the parabola forms are directly relatable to the source altitude and microphone height above the ground plane.

If the testing is conducted at or near a recognised airfield it is usually simple to collect the hourly data from the local meteorological unit. However the recording team should be equipped with a suitable pole-mounted or hand-held anemometer and also a wet and dry bulb whirling, Mason's, or aspirated hygrometer to determine air temperature and relative humidity. These should be recorded at frequent intervals during the testing. Wind direction is best observed via a weathercock vane, although signs of smoke from local factories, or other indications can be used since it is unusual to use the wind data for elaborate correction of the received noise data. Ambient atmospheric pressure does not vary much over the area used for testing and can usually be obtained from the nearest airfield records of QNH.

If met data at altitudes representative of the aircraft operation are needed, then either the nearest local weather station equipped with balloon ascent equipment may be consulted or else special arrangements made to acquire such data. This is especially important when conducting research into atmospheric propagation from air-to-ground.

2.2.4 Outline Test Procedure

Having set up the measuring systems, the noise channels should be calibrated using a pistonphone or equivalent and this signal recorded at the chosen tape speed, noting the gains used. The calibration also serves to indicate correct working of the system, but it is always wise also to listen with earphones to the ambient noise (birdsong or distant traffic etc.) at a suitably lower gain setting. This can indicate strong hum notes, oscillations or excessive noise and cracking which can be caused by malfunctioning microphones or cathode follower systems and cables. If all is well, the amplifier and recorder gains are set to suitable values for the tests and noted. Measuring systems which provide a frequency encoded gain value or some similar indication onto tape just after switch on to record mode, are very worthwhile for checking that attenuator settings have been correctly documented. Incidentally if the recording system contains a fully variable gain control, make all gain adjustments with the microphone, or S.L.M. amplifier and preferably clamp or retain with adhesive tape the chosen calibration position.

The microphone power supplies must be switched on to allow the system to warm up thoroughly, well before the first flyover is recorded. Where a portable recorder with facilities for direct acceptance of condenser microphones is used, the recorder must be switched to test a standby position. In this setting the microphone signal can be audibly monitored before recording.

The recording process should be started well before the aircraft sound becomes detectable above the ambient noise. This ensures that the ambient can be determined (or at least the system noise floor level) and ensures that enough data is recorded to permit evaluation of duration dependent indices such as EPNL or L_{eq} if these are required. A length of pre and post fly-over tape is also useful for recording the outstation marker timings and for actuation of automatic analysis sequencing systems. These are systems for cycling a fly-over record through a 1/3 octave band analyser and moving through the correct sequence of centre frequencies before switching off - all under operation without supervision.

During the fly-over, besides the marker data and photographic or cine-theodolite activity, it is necessary to keep an eye on the recording level indicator (or preferably an oscilloscope waveform monitor) to check whether suitable recording gains are being used. Most systems will cater for the odd excursion of the needle into the marked overload region on the modulometer, but if the meter stays hard over at high level, or alternatively if the highest level ever recorded is such that the meter hardly indicates, then the gains should be changed by an appropriate number of 10 dB steps.

After the recording, if time permits, it is useful to rewind the tape and to play back the recording for checking purposes, audio monitoring using headphones or using the recorder's monitoring loudspeaker if fitted. Usually the recorder will have a "direct" or "tape" monitoring selection switch for meters and/or audio monitor loudspeaker. Return the recorder to the ready to record status in anticipation of further fly-over recordings. Unless a separate voice channel is available, and even so only if use of the voice mic can be accomplished without airborne sound also reaching the data mic, it is wise to leave all commentary to the beginnings and ends of the tape record. My own practice is to announce all known aspects at the beginning (e.g. Flight Number, Altitude, recording number, gain settings, time at start of data record) and to finish with items which were the result of the test (e.g. maximum level recorded, flight track inaccuracies, time at end of data record and other useful reminders).

At the end of the session, say occupying a morning, a further calibration check should be made and recorded. Systems are usually very stable and more often than not the identical level will be found on re-calibration. However a slight change of say only 0.2 dB is usually ignored, whilst for $\frac{1}{2}$ or 1 dB change an average correction could be made to all the data. It is emphasised that it is rare to have to resort to this.

2.3 Multi Microphone Arrays

Multi microphone arrays have been used for specific research where either it is required to record the spread of noise, say laterally, from all aircraft without repeating flights which might not be identically set up or controllable to the required accuracy. Again, often multi-channel work involves less in the way of costs than a lengthy flying programme. Apart from the multi-recording system necessary, with the need for careful selection of appropriate recording gains over all the channels, the measurement exercise is straightforward.

Where, however, the multi microphone array is chosen to improve accuracy, then there is a slight complication in the analysis procedure. During an aircraft fly-over, the angular radiation region from say 85° to 95° with respect to the forward axis of the engines occupies less than a quarter second in circumstances, when lower altitude and higher speeds are being flown. On analysis therefore, it is impossible to achieve the desired statistical accuracy with an angular resolution of 5° when narrow band information is necessary, or even when using the lower 1/3 octave bands. Therefore accuracy has to be improved either by flying more identical tests, or by averaging data collected from several microphones, receiving essentially the same overflight sequence, but sufficiently apart to make the data unrelated to the next microphone. For the random noise sources of the aircraft, this means spacings of about 2 of the lowest wavelengths to be measured or about 50ft for most aircraft noise work. Some work of this nature conducted in the United States of America has employed arrays up to 500ft separation. The data processing requires that synchronisation between channels (on each separate recorder) is available and a marker pulse assists. Data is digitally or otherwise ensemble averaged to give the required data for frequency analysis, or else the ensembling is performed in the frequency domain. In the case cited, about five or six microphone ensembles would give an acceptable resolution and accuracy over the audio frequency range.

3.0 CERTIFICATION MEASUREMENTS

We will not discuss the detailed background to aircraft noise certification, but basically an internationally agreed scheme was set up by the International Civil Aviation Organisation (ICAO) commencing in 1970 whereby all new subsonic aircraft with engines of by-pass ratio 2 or more requiring a type certificate had to comply with certain noise limitations. In the United States of America a similar scheme was initiated and administered by the Federal Aviation Authority (FAA). Since the initial coverage of aircraft categories, I.C.A.O. and F.A.A. have extended the certification requirement to new production of older types of subsonic jet and in the USA there is a declared programme of progressive coverage of aircraft such as Super-sonic Transports and V.S.T.O.L. types. I.C.A.O. intends to reduce the permitted levels for subsonic aircraft in the very near future.

Both the I.C.A.O. and the F.A.A. schemes follow along very similar lines and each requires the aircraft type to be flown over a prescribed take-off and landing approach procedure whilst noise is recorded at specific points directly under the extended runway centrelines and at a set distance to the side of the runway line. Figure 3 illustrates the procedure and the current maximum permitted levels for the F.A.A. system. Note that the permitted level is a function of the aircraft declared maximum take off weight and that the index chosen, after much discussion and testing against subjective surveys, is the Effective Perceived Noise Level EPNL (in units of EPNdB).

3.1 Analysis of Aircraft Noise to produce EPNL

We will briefly consider the procedure for deriving the EPNL from an aircraft fly-over test, since many of the aspects of Noise Certification testing stem directly from the nature of this index.

We start with the same procedure as for ordinary PNL calculation. That is the instantaneous 1/3 octave band spectrum of noise is firstly converted to NOY values by use of the approved tables or a suitable formulation for computer use. The range of frequency is from the 1/3 octave centred on 50 kHz (lower limit 45 Hz) up to the band centred on 10 kHz (upper limit 11,200 Hz). The NOY values are then summed and the total weighted by a factor 0.15 to which is added 0.85 of the largest NOY value for the spectrum. Then the result is re-converted to decibel form by taking $33.3 \log_{10}$ of its value and adding 40 (the latter to produce numbers of meaningful values apparently).

In the EPNL computational procedure, this process is conducted for the complete fly-over noise time history in $\frac{1}{2}$ second intervals or less. The spectrum is then examined for a given time interval, and a correction procedure applied to allow for irregularities (caused by, for example discrete tones). The procedure is complex and for a complete account the references should be consulted. In essence the slopes of adjacent 1/3 octave bands are computed, and those where adjacent slopes have a change in value outside the range ± 5 dB are noted. If the slope is positive and also algebraically larger than the value at the next 1/3 octave group down, the SPL corresponding is also noted, but if the slope is 0 or negative and the slope below it is positive then the lower band SPL is noted.

The next step computes new SPL's for the noted values by averaging the values below and above. A procedure for the top (23rd 1/3 octave) band, if its SPL was noted computes the new value from the 23rd SPL value and the slope of the 23rd group. The slope procedure is then re-commenced (including an imaginary 25th band value) and the arithmetic average of each group of 3 adjacent slopes calculated. Then new adjusted band SPL's are obtained by starting with the first value and adding the appropriate average slope and proceeding throughout the spectrum.

The adjusted SPL's are then compared to the originals and only those which have increased by at least 3.0 noted. Only for such bands are tone correction values determined from a chart in terms of the actual level difference and the frequency range appropriate. For this purpose the frequency ranges are the bands from 50 Hz to 400 Hz, the bands from 500 Hz to 4000 Hz and the bands at 5000 Hz and above.

The tone correction factors (which can never be greater than $+6^{2/3}$ are added to the PNL values to give the tone corrected PNLT.

The next step is to determine the maximum value of PNLT (called PNLT_M) and to compute a duration correction D, whence EPNL = PNLT_M + D.

D is found by a step integration process for all values of PNLT which are either greater than 90 PNdB or are within 10 PNdB of the PNLT_M level. The summation is performed on a pseudo energy basis, i.e. the individual PNLT's are divided by 10, antilogged to base 10, summed for all relevant time intervals, and divided by a reference or normalising time of 10 seconds. The units are reconverted to decibel form by taking $10 \times \log_{10}$ of the result and subtraction of PNLT_M from this gives the required Duration Correction D. There are refinements for the case where the analysis interval is less than $\frac{1}{2}$ second or to cater for 10 dB down from PNLT_M falling between individual PNLT values. Where two values of peak PNLT occur the maximum duration interval is to be taken. To cater for very quiet aircraft for which the 10 dB down points lie below 90 PNdB, the duration is taken from the time of 1st exceeding 90 PNdB to the last time of falling below this level.

It will be seen from the above that the EPNL is by no means simply related to the overall level (OASPL) or LIN weighted value, and even less so to the A weighted or D weighted values. Thus digital or RTA and computer systems must be used to process noise certification results. However, with the era of micro-processors upon us there may soon be a suitable direct reading meter on the market before very long!

3.2 Test and Data Correction Procedures

Let us now discuss the test procedure in a little more detail. For accuracy and allowance for inabilities to fly precisely accurate flight patterns, the certification procedure calls for at least six sets of data to be averaged. However, the spread of noise data from such a set of flights is not just simply averaged taking into account natural propensities for pilots and aircraft to fly in slightly varying manners each time. Instead, a correction procedure is required to be performed, based on approved data characteristics for the aircraft and its engines, that is to say, data from the aircraft type, accumulated over its development flight programme, which spans more than the required range of experience in respect of noise versus aircraft Take-off and Landing weight, flight speed, engine thrust or reference shaft RPM, meteorological trends etc., etc. In this way a series of trade-offs are established and approved by the certification authority.

Let us take as an example for the approach to land phase of the test results. The certification procedure calls for the aircraft noise to be evaluated under the flight path at 1n.m to the threshold on the extended runway centreline, where under a standard ILS $3^\circ \pm 0.5^\circ$ approach procedure the nominal aircraft altitude would be 370 ft above airfield level at threshold. The noise data has to be that which would have appertained to a sea level equivalent atmosphere at ISA + 10°C and 70% Relative Humidity (RH). Additionally the aircraft, on one of its approaches was found to make the approach at an engine RPM 5% above that which should have been used for the actual day temperature, due to factors such as aircraft weight being higher than anticipated, and a greater than average cross wind component to the runway heading. The aircraft was also found to pass over the measuring station within the permitted tolerance of altitude but at 413 ft above airfield level (aal), a difference of + 43 ft, and moreover at a distance of 98 ft to the left of the runway approach centreline. The tower recorded an air temperature of +18.5°C during the hour occupied by the measurements with a relative humidity of 64% and a wind at 270° (for a runway heading of 235°) and at 6 kts 10 metres aal. The measuring microphone(s) at less than 20ft difference re a.l. required no correction in this respect (a.l. is at 110ft AMSL).

Firstly, having analysed the fly-over data and calculated the measured spectra for $\frac{1}{2}$ second intervals, the spectra must be adjusted to the standard certification atmosphere of ISA + 10°C + 70% R.H. To do this, the slant ranges from the aircraft datum (ILS antenna) to the microphone must be calculated for the time at which the peak value of tone corrected PNL (PNLT_M) was emitted. The absorption, as a function of 1/3 octave band frequency is then interpolated from approved tables, charts or formulations (the SAE ARP 866 method or the simplified methods presented in the certification rules), and applied over the difference between the ranges flown to the ranges had the aircraft passed at the correct nominal altitude of 370 ft. Correction for inverse square law of distance is also made. Note that if the microphone had been outside the 20ft difference from a.l. permitted, the noise level corrections would have been made on a similar basis, i.e. one of correcting the slant ranges. If necessary a directional correction must also be made for the fact that the noise was measured at 134° to the downward vertical rather than right underneath the aircraft.

Because on approach to land, the noise of a turbofan engine aircraft is primarily fan RPM dependent, the noise data must now be corrected for the aircraft performance deviations. From approved aircraft performance data, the engine RPM which should have been used for certifications is known, and also such ancillary parameters as the fan inlet weight flow can be calculated from approved engine performance data. The actually recorded engine RPM's are compared and the mean correction to engine noise level deduced from the attendant change in fan relative velocities and intake airflow. Where it can be established that negligible spectral change results from the changed engine conditions, then simple overall PNdB corrections can be applied, otherwise some modification to the spectral time history might become necessary. Generally speaking most engines will not require elaborate corrections for changes within the permitted tolerances (F.A.A. specify that the correction due to approach weight must not exceed 1 EPNdB and the maximum correction in any 1/3 octave band for the error in passing over the approach datum point is 3 dB. In this way approved correction charts for the influences of aircraft take-off weight, landing weight and angle of approach can be established. Note that there is no correction procedure specified for wind, only a limitation of 10 kts at the airfield measuring location (and a similar condition on the wind local to the microphone position(s)) plus a note that "anomalous" wind conditions or temperature inversions must be avoided.

Likewise, there is no standardised correction procedure for overground attenuation - particularly relevant for the sideline measurement case. Instead, obvious high sound absorptivity sites, such as tall grass or shrubs are to be avoided, also significant obstructions within a cone semi angle of 75° to the vertical at each measuring site.

The above example illustrates the care and scope of data which must be gathered and processed in order to satisfy compliance with noise certification limits. Table I sets out the basic conditions for the F.A.A. scheme and the I.C.A.O. system which differs in minor respects.

For I.C.A.O. the response point for approach at 390 ft is 120 metres (393.7 ft) aal. Sideline noise is measured at 650 metres (.35 nm) from the runway centreline as opposed to the F.A.A. dual system of .35 nm for large aircraft and .25 nm for smaller aircraft. Also there are differences in the trade-offs which are permitted for slight failures to meet the noise limits at a given reference point in exchange for meeting the limits by a margin at other points. The F.A.A. regulations allow excesses at one or two points provided these add up to 3 EPNdB or less and no single excess value is more than 2 EPNdB. Of course the total excess value must balance the total margin available at the other point(s). The I.C.A.O. system allows trade-offs to a total of excesses not greater than 4 EPNdB with a single point excess up to 3 EPNdB provided, as with the F.A.A. requirement, that the excesses and the margins are arithmetically balanced.

On the topic of sideline noise, it must be noted that the relevant peak noise level for calculating EPNL is the maximum which occurs anywhere along the sideline path. Therefore several, usually at least five, measuring stations are needed to establish this fact. The authorities may allow fewer stations provided it can be shown from the aircraft's established noise characteristics that the chosen locations definitely capture the peak sideline levels. Because of ground absorption effects, this will always be where the aircraft has left the runway and subtends an angle above some 10° to 15° to the observers horizon.

The actual recording and basic noise analysis processes for certification are no different from those outlined for research purposes excepting that there are defined instrumentation standards and pen recorder writing speeds etc. to follow. The salient F.A.A. and I.C.A.O. specifications are shown as Table II.

3.3 Some Comments on Certification Problems

In this section, we note a few points about certification measurement methods which either call for eventual improvement, or which need caution if certification derived data is used as a guide for operational suitability of aircraft types.

Just as safety tests for road vehicles are not intended to guarantee road worthiness as far as a potential purchaser is concerned, so the noise certification procedure can only be a test to show that, under fairly representative conditions, the maximum noise levels which the aircraft type could produce at the specified measuring points is within certain limits and tolerances as prescribed for the aircraft type certification weights. To do this, the aircraft manufacturer works out an approved flight procedure which produces the minimum noise at the measuring points by judicious choice of operating thrusts, cut back time after start of take off roll, even advantageous directions of error correction and atmospheric conditions correction if such margins remain open to him under the specified tolerances and approved correction procedures. As an example, it has been found possible to re-establish certification requirements by flying an unmodified aircraft for a new series of tests under differing, but still officially approved and within limitations, atmospheric and ground surface conditions. Within a given application for a certificate, it is required that all data points measured must be included in the overall average, even though results over and above the minimum six samples may have been acquired. Of course points obtained from flights conducted outside the acceptable operation conditions, and data established from agreed freak sound propagating conditions may be discounted by agreement with the certification authorities. It is easy to understand that, at typical operational load factors, on days quite different from the ISA + 10°C , 70% RH atmosphere, and operating to a minimum noise procedure to suit a local community for the airport in question, the noise levels may be quite different, invariably lower, than for the equivalent certification locations.

At extremely high frequencies and extreme but permitted atmospheric conditions, sideline noise corrections may have to be applied to data where already the ambient levels are comparable. Clearly this would lead to erroneous levels and the F.A.A. and I.C.A.O. rules also differ in the methods of limiting such effects. The F.A.A. rule limit for duration correction is that the 80 PNdB level may be used where the 10 dB down point is not clear of the ambient by at least 10dB.

In certification work, the microphone orientations are fixed by F.A.A. to be at grazing incidence for the nominally overhead flights and set at an appropriately similar condition for the sideline conditions. This minimises the extent of microphone response corrections, but since all authorities and companies/corporations conducting such exercises use computerised analysis and correction procedures, there is no great saving in technical complexity.

Certification flying must, of course, be conducted at an airfield not only offering a suitable outfield for the measuring stations (preferably with good visual warning for the noise recording operators) but without conflicting air traffic, noisy local construction noise or other intrusive non-aircraft sources. Such conditions are notoriously difficult to satisfy. The certification rules demand that the aircraft must operate to the full take-off and approach patterns laid down, and after passing the measuring station the aircraft must continue to climb on the permitted cut-back gradient, must have used full take-off thrust up to 1000 ft altitude aal (and at the correct airspeed), and must continue the approach to make a normal landing sequence.

4.0 AIRPORT NEIGHBOURHOOD NOISE MONITORING

The purposes of field measurements at an operational airfield are either for research, for evaluation of certain legalistic measures for compensation or noise insulation of dwellings or schools/hospitals, or for ascertaining whether operators comply with airport noise limit policies.

For the latter, the major point which has not already been covered is, that the siting of microphone needs careful consideration. Some airports site mics at suitable points along specified minimum noise routes and representative community distances. Others use the actual communities from which the bulk of complaints arise and site the transducers on suitable buildings. It might be argued that local acoustic interferences will affect such data, but provided the monitored data is related properly to propensity to complain, via social survey data, then such schemes serve usefully to avoid an ever increasing noise dosage in the community.

The measuring systems have to be "all-weather" capable, and use shielded or rainproof microphones with built in calibration facilities (at cathode follower input). The more sophisticated schemes use noise level actuated recording systems, and some transmit data on-line for immediate processing of data, so that the operator or captain can be informed almost immediately of infringement. Obviously the number of channels must be limited by economic reality and monitoring cannot guarantee that at certain times and locations a greater than desirable noise level was not experienced by an individual resident.

Research and compensation/insulation noise verifications need noise measurements to be made under as realistic listening conditions as possible. Thus portable systems or car based systems are used to record both aircraft operational noise levels, and background levels from all other sources, at "facade" distances from residences or other establishments of interest. Occasionally indoor measurements are made, although there is an over dependence on correction of external data for assumed building noise insulation, since it is not always possible to get agreement to make interior noise recordings.

Very few such environmental noise exercises attempt to record details of flight paths, etc. other than the basic noting of times of principle events, weather conditions and other essentials. However, in the UK, some local authorities check operational details so that contours of NNI can be accepted or disputed as the case may be. Often for general noise work without a statutory basis (as when compensation is not being contested), measurement conditions are necessarily not ideal, wind conditions and light rain being coped with provided there is no obvious disturbance of the measured levels compared to that which would be heard by the local residents. Also, analysis is often simplified, and suitable A or D weighting networks used with adjustment constants instead of using the full PNdB calculation procedures. The I.C.A.O. Document Annex 16 gives, in addition to noise certification information, recommended methods and procedures for monitoring aircraft noise and for calculation of approximate aircraft noise units.

REFERENCES

1. United States of America - Public Law 90-411 Part 36 of the Federal Aviation Regulations
2. I.C.A.O. "International Standards and Recommended Practices - Aircraft Noise - Annex 16 to the Convention of International Civil Aviation (1971 and subsequent editions)
3. Noise Measurement for Aircraft Design Purposes including Noise Certification Purposes, 1970, Board of Trade CAP -35 HMSO London
4. M. E. Delaney and E. N. Bazeley "A Note on the Effect of Ground Absorption in the Measurement of Aircraft Noise" 1969, NPL Aero Report Ac 41 (June 1969)
5. Anon: "Standard Values of Atmospheric Absorption as a Function of Temperature and Humidity for use in Evaluating Aircraft Flyover Noise" 1975 S.A.E. ARP 866
6. M. E. House and P. D. Wheeler "Airborne Public Address", paper presented at I.E.E. Communications '76, Brighton, U.K.

TABLE I

COMPARISON OF SALIENT F.A.A. AND I.C.A.O. CERTIFICATION RULES

FEATURE	FAR Part 36	I.C.A.O. Annex 16
APPLICABILITY (AS AT JANUARY 1976)	All new aircraft types over 5700 Kg weight, excepting supersonic transports (SST) and short take-off and landing aircraft (STOL)	As FAR Part 36
FUTURE PLANNED APPLICABILITY	Older types of aircraft with engines of by-pass ratio less than 2 still operational. SST and STOL types.	As FAR Part 36 (but not to declared timetable of introduction).
MEASUREMENT POINTS:		
TAKE-OFF (FLYOVER)	3.5 nm from start of Take-off-Roll along extended runway centreline	As FAR Part 36 (but defined as 6500 metres from Start of Roll).
TAKE-OFF (SIDELINE)	On a line parallel with runway centreline (extended) and 0.25 nm to the side for the aircraft with two engines and more than two engines respectively.	As FAR Part 36 3.5nm point for all aircraft (but defined as at 650 metres).
APPROACH (FLYOVER)	1 nautical mile from threshold extended runway centreline	At point on the ground on extended runway line 120 metres (394 ft) below glide path of 3° slope originating from a point 300 metres (984 ft) beyond threshold - equivalent to 1.08nm on level ground.
MAXIMUM PERMITTED LEVELS:		
TAKE-OFF (FLYOVER)	108 EPNdB for weights of 600,000 lbs or more, less 5 EPNdB per halving of weight from 600,000 lbs down to 75,000 lbs and under.	108 at 27,200 Kg (599660 lbs) less 5 EPNdB per halving down to 93 EPNdB at 34,000 Kg (74960 lbs) (almost identical to FAR pt 36).
TAKE-OFF (SIDELINE)	108 EPNdB for weights of 600,000 lbs or more, less 2 EPNdB per halving of weight from 600,000 lbs down to 75,000 lbs and under.	Weights defined as above, but otherwise as FAR Part 36.
APPROACH (FLYOVER)	As TAKE-OFF (SIDELINE)	As TAKE-OFF (SIDELINE)
TRADE-OFFS AGAINST EXCESSES	Total of excesses not greater than 3 EPNdB. No one excess greater than 2 EPNdB. All excesses are offset by reductions at other points.	Total of excesses not greater than 4 EPNdB. No one excess greater than 3 EPNdB. All excesses are offset by reductions at other points.
STANDARD ATMOSPHERIC CONDITIONS - MEASUREMENTS:		
RAIN OR OTHER PRECIPITATION	None	As FAR Pt. 36
RELATIVE HUMIDITY	Not above 90% or below 30%	As FAR Pt. 36
AMBIENT TEMPERATURE	Not above ISA + 15°C at 10metres above ground	Not above 30°C (ISA + 15°C) or below 2°C (ISA - 13°C) at 10 metres
AIRPORT REPORTED WIND	Not above 10 kts at 10 metres above ground	As FAR Pt. 36
TEMPERATURE INVERSIONS AND ANOMALOUS WIND CONDITIONS AFFECTING NOISE	None	As FAR Pt. 36
TERRAIN	Relatively flat, no excessive absorption characteristics. No obstructions influencing noise within cone 75° half angle of vertical.	
MAXIMUM MEASUREMENT POINT ALTITUDE DIFFERENCE FROM NEAREST RUNWAY POINT WITHOUT CORRECTIONS	20 ft.	6 metres (20 ft.)

TABLE 1 (CONTINUED)

FEATURE	FAR Part 36	I.A.C.O. Annex 16
MINIMUM NUMBER OF NOISE LEVELS TO BE AVERAGED TO PROVIDE CERTIFICATED LEVELS	6, or sufficient additional to give 90 percent confidence of ± 1.5 dB	As FAR Pt. 36
OPERATIONAL: APPROACH TAKE-OFF	Glide path $3^\circ + 0.5$ at reference speed over measurement point and continued to normal touchdown. Take-off power to at least 1000' Alt above runway, at $V_2 + 10$ kts. After 1000' Alt, thrust may be cut to climb of at least 6% gradient. Take-off flap to be used throughout.	As FAR Pt. 36 but at $1.3 V_a + 10$ kts, speed stabilised over measurement point at max allowable flap settings. Take-off power to at least 210m (700ft) above runway at $V_2 + 10$ kts. Thrust may be cut to climb gradient of at least 4% Constant take-off configuration except for landing gear.
REFERENCE CONDITIONS TO WHICH DATA MUST BE CORRECTED	Max take-off and landing weights for which certification is requested. Approach at 3° glide slope and at 370 ft. above approach measuring point. Atmosphere of 70% RH at temperature of ISA + 10°C .	As FAR Pt. 36 As FAR Pt. 36 but at 120m (394 ft) above approach measuring station. Ambient pressure 1013.25 mb Ambient temperature of 25°C (ISA + 10°C). Relative humidity 70% zero wind.
MAXIMUM ALLOWABLE CORRECTIONS TO NOISE DATA FOR WEIGHT TO SPL (1/3 octave) FOR AIRCRAFT NOT ABOVE MEASURING POINT ON TAKE OFF, OR HEIGHT AND POSITION ERROR ON APPROACH FOR NOISE NOT 10dB ABOVE BACKGROUND LEVELS DIFFERENCES BETWEEN MEASURED EPNL AND CORRECTED TO REF. CONDITIONS EPNL	2 EPNdB at Take-off 1 EPNdB at Approach 3 dB Approved Corrections _____	2 EPNdB 2 EPNdB _____ As FAR Pt. 36 Maximum of 15 EPNdB allowed

TABLE II

COMPARISON OF SALIENT INSTRUMENTATION AND MEASUREMENT REQUIREMENTS FOR
AIRCRAFT NOISE CERTIFICATION

FEATURE	FAR Part 36	I.C.A.O. Annex 16
COMBINED EQUIPMENT CALIBRATION	+ 1dB 45 - 11200 Hz (on axis of calibration of microphone)	Complete recorded time history to be retained. Equipment characteristics to conform to IEC 179 and IEC 225, over range 45 - 11200 Hz
COMBINED EQUIPMENT RESPONSE OF AXIS MICROPHONE RESPONSE	+ 3dB 45 - 11200 Hz + 1dB below 1000 Hz, + 2dB 1000 Hz to 4000 Hz, and + 4dB 4000 Hz to 11200 Hz	
DYNAMIC RESPONSE OF READ OUT DEVICES AND ASSOCIATED AMPLIFIER/DETECTOR SYSTEMS	80 - 100 mSecs/equivalent to level recorder and 50dB log potentiometer, writing speed 16 dB/sec + 10 Hz pen lower limiting frequency	
SAMPLING	Bandwidth x sample time at least 10, with max. sample time 1 sec.	24 x 1/3 octave filters (50 Hz to 10kHz geometric mean frequency) with squared outputs, averaged or integrated and converted to log units. Crest factor capacity of 3 and give + 1dB tolerance of true RMS in each of the 24 bands. (If non-true RMS device, calibrate using time varying non sinusoidal signals.) Analyser dynamic response to inputs at full scale and 20dB below full scale to be 4dB + 1dB less than for steady state equivalent when a sinusoidal pulse of 0.5 secs duration applied at input each 1/3 octave band frequency. Max value to exceed final steady state value by 0.5 + 0.5 dB when sinusoidal input at each 1/3 octave frequency suddenly applied and held constant. Analyser amplitude resolution 0.5dB or less. Outputs + 1.0dB re input levels after all systematic corrections (+ 3dB total systematic error). Adjacent filter systematic error not above 4dB for contiguous filters. Dynamic Range at least 45 dB.
CALIBRATION	In accordance with approved practices corrected for windshields. Acoustic cal immediately before and after each aircraft noise recording.	0.5 sec intervals + 0.01 secs, all 1/3 octave values within 50m secs period omitting no more than 5m secs. Windshield to be used above 6 kts and data corrected accordingly. As FAR Pt. 36.
MICROPHONE ORIENTATION	Grazing incidence to flyovers and sidelin flyby.	Corresponding direction to calibration at time of arrival of maximum sound.

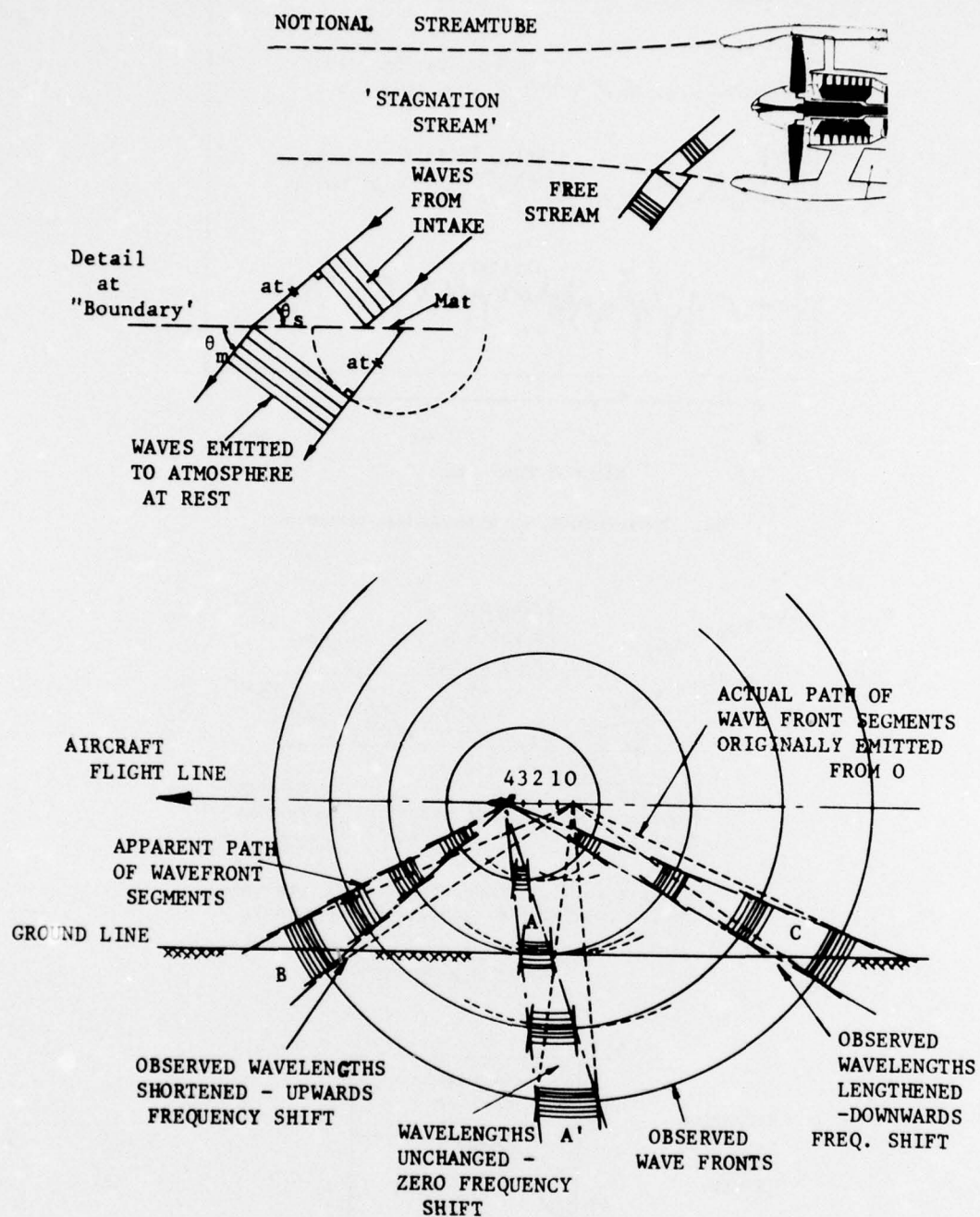


Fig.1 Flight-to-ground propagation

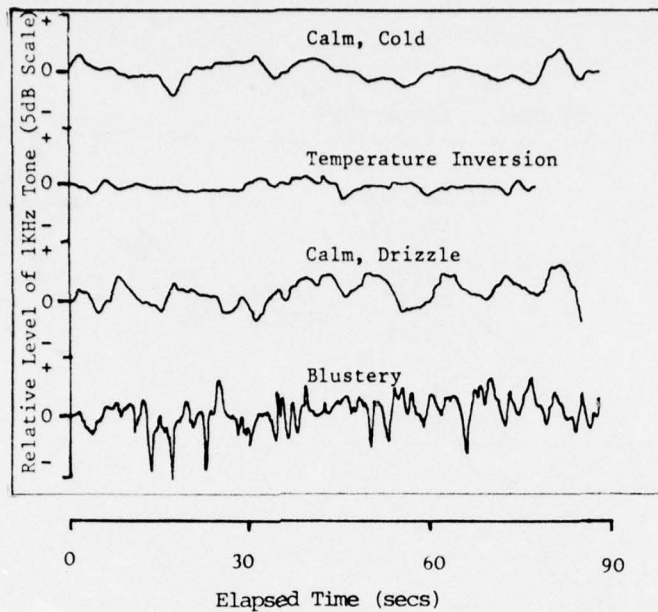
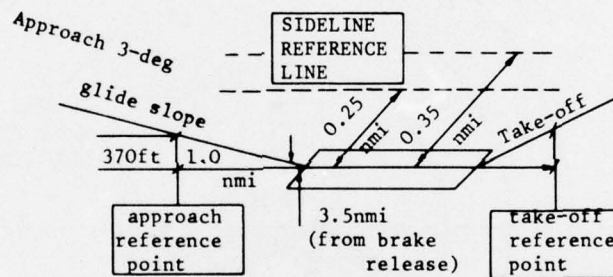
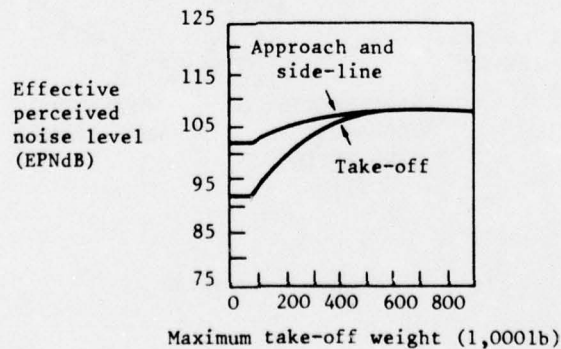


Fig.2 Noise variation due to atmospheric conditions



Cutback thrust allowed to 6% climb gradient above 1,000ft. Altitude, 77°F, sea level.

REFERENCE POINTS



LEVELS RULE FOR NEW AIRCRAFT

Fig.3 Aircraft noise certification (FAA)

COMPARAISON DE DIFFERENTES METHODES DE
LOCALISATION ET D'IDENTIFICATION DE
SOURCES SONORES DE TURBOREACTEURS

par

Mariano Perulli
Office National d'Etudes et de Recherches Aérospatiales
et
Université de Technologie de Compiègne

RESUME

Les études de bruit de turboréacteurs conduisent à développer des techniques particulières de mesure et de traitement du signal. Quelques-unes de ces techniques sont présentées et concernent plus spécialement le sondage du milieu source de bruit ainsi que celui du champ de pression proche et lointain. Elles conduisent le plus généralement à caractériser le milieu source et à fournir une distribution virtuelle de sources de bruit. Dans de rares cas elles conduisent à une distribution réelle des sources de bruit.

1. INTRODUCTION

Dans leurs façons d'être menées, les études de bruits d'origine aérodynamique ont fortement évolué au cours de ces deux dernières décennies du fait de l'augmentation de la variété des aérodynes liée à une forte croissance du trafic, et, surtout, sous l'impulsion d'une mise en application de règlements internationaux de nuisance acoustique (certification acoustique).

Plus particulièrement, l'évolution des études expérimentales est comparable à l'évolution des observations d'un promeneur face à une chaîne de montagnes, qui de très loin ne voit qu'une ligne de crêtes et qui, au fur et à mesure qu'il approche, peut, à loisir contempler plus de détails ... au risque d'en oublier la vue d'ensemble.

Il y a une, voire deux décennies, les études expérimentales d'aéro-acoustique sur le bruit consistaient principalement en des mesures, au point fixe, de "directivité" (évolution, dans le champ lointain, de l'intensité sonore I en fonction de l'angle θ que forme la direction d'observation avec l'axe du moteur), et en des mesures de bruit en survols dans des conditions proches de celles de la certification acoustique. Les informations déduites de ces mesures ont permis, en particulier, de mettre au point des formulations prévisionnelles indispensables aux constructeurs pour connaître la position des différentes générations d'aérodynes (et de moteurs) par rapport aux normes.

Ces études expérimentales, première approche (figure 1), correspondent à un constat global du rayonnement acoustique du moteur en fonction des conditions génératrices moyennes et globales. Cette première approche est représentative de l'esprit avec lequel les travaux théoriques étaient alors menés [1], [2], [3]. Par exemple, dans le cas de jets subsoniques, les grandeurs caractéristiques de turbulence nécessaires à la prévision acoustique sont définies à l'échelle du volume source.

En effet, on considère, dans ces modèles théoriques, sur l'ensemble du volume du jet libre, une valeur unique de vitesse de convection, d'échelle intégrale des longueurs ou des temps, et une valeur unique de l'intensité de turbulence. Les lois phénoménologiques d'évolution du champ sonore lointain ainsi calculé sont "raisonnablement" représentatives de la réalité ([4] par exemple), à des constantes empiriques près, déduites d'essais statiques ou de survols.

De cette approche, il a été possible de déduire des variétés de silencieux et de moteurs, basées sur des considérations globales, atténuant les nuisances acoustiques sans trop diminuer les performances moteurs. Citons par exemple :

- les silencieux multitubes : rejet dans le domaine des hautes fréquences, fortement absorbées par l'atmosphère, des fréquences caractéristiques de turbulence ;
- les moteurs double flux : diminution des effets de cisaillement des termes fluctuants

Rapidement les limites de cette première approche sont apparues, en particulier l'impossibilité de localiser les zones les plus émissives du jet libre. Aussi, un effort très important a été fourni dans de nombreux laboratoires, dont l'ONERA [5], [6] pour développer une seconde approche (figure 1). Celle-ci consiste en une caractérisation locale du milieu source de bruit dans le but d'en déduire le rayonnement acoustique à partir de modèles théoriques et, réciproquement, de pouvoir détecter, de l'extérieur du volume source, le rayonnement acoustique de différents éléments de la source de bruit.

Une telle approche nécessite des moyens de sondage du volume source, à la périphérie, dans son voisinage proche et lointain, auxquels il faut adjoindre des moyens particuliers de traitement du signal, sans oublier des développements théoriques complémentaires ou différents des précédents.

Certains aspects de ces problèmes de mesure et de traitement du signal seront examinés. Au préalable, et afin de bien imaginer les difficultés auxquelles les études expérimentales se confrontent, nous rappellerons quelques concepts théoriques en renvoyant le lecteur aux exposés théoriques [7] de cette série de conférences n° 80 de l'AGARD.

2. RAPPELS D'ELEMENTS DE THEORIES

2.1. Approches théoriques classiques

Suivant l'analogie de Lighthill, l'équation inhomogène des ondes qui représentent les fluctuations locales de l'écoulement d'un jet libre en l'absence de parois et d'injection de matière, se déduit des équations de conservation de la masse (équation de continuité) et de la quantité de mouvement. Toutes transformations effectuées, cette équation s'écrit :

$$(1) \quad \frac{\partial^2 \rho}{\partial t^2} - c_\infty^2 \Delta \rho = \nabla \nabla \cdot \vec{T},$$

où ρ est la densité ; c_∞ la célérité du son en milieu homogène infini, et, \vec{T} , parfois appelé tenseur de Lighthill, est égal à :

$$(2) \quad \vec{T} = \rho \vec{v} \vec{v} - \vec{\sigma} + (p - c_\infty^2 \rho) \vec{I}$$

où $\rho \vec{v} \vec{v}$ est le tenseur de Reynolds,
 $\vec{\sigma}$ le tenseur des contraintes visqueuses,
 p la pression,
 \vec{I} le tenseur unité d'ordre deux.

Formellement, par application du théorème de Kirchhoff [8], ou par double application de la formule d'Ostrogradski, la solution de l'équation (1) calculée en tout point \vec{x} du champ lointain est de la forme :

$$\rho(\vec{x}, t) = \sum_{i,j} \frac{x_i x_j}{4\pi c_\infty^4 x^3} \int_{V(\vec{y})} \left[\frac{\partial^2 T_{ij}}{\partial t^2} \right]_{\hat{t}} d^3 y,$$

ou bien, en adoptant, dans le champ acoustique lointain (hors du volume source $V(\vec{y})$), l'hypothèse de l'acoustique linéaire :

$$(3) \quad p(\vec{x}, t) = c_\infty^2 \rho(\vec{x}, t),$$

$$(4) \quad p(\vec{x}, t) = \sum_{i,j} \frac{x_i x_j}{4\pi c_\infty^2 x^3} \int_{V(\vec{y})} \left[\frac{\partial^2 T_{ij}}{\partial t^2} \right]_{\hat{t}} d^3 y.$$

(L'hypothèse champ lointain implique que $|\vec{x}| = \text{Sup}(\text{plus grandes longueurs d'ondes, plus grande dimension linéaire du volume source})$,

\hat{t} représente le temps retardé égal au temps d'émission t diminué du temps de parcours de l'information qui s'écrit en milieu froid, homogène, en l'absence de vitesse d'entraînement :

$$\frac{|\vec{x} - \vec{y}|}{c_\infty}.$$

De cette expression (4) on peut déduire toutes les grandeurs caractéristiques du champ sonore lointain, à savoir : le spectre et l'intensité sonore. Pour cela, calculons la fonction d'autocorrélation $P(\vec{x}, \tau)$ du champ de pression moyenne :

$$(5) \quad P(\vec{x}, \tau) = \langle p(\vec{x}, t) p(\vec{x}, t + \tau) \rangle = \sum_{i,j,k,l} \frac{x_i x_j x_k x_l}{16\pi^2 c_\infty^4 x^6} \int_{V(\vec{y})} \left[\frac{\partial^2 T_{ij}}{\partial t^2} \right]_{\hat{t}} \left[\frac{\partial^2 T_{kl}}{\partial t^2} \right]_{\hat{t}''} d^3 y d^3 y'',$$

où $\langle \rangle$ représente la valeur moyenne sur les temps
 et τ le retard incrémental de la corrélation.

De cette relation on déduit, en tout point \vec{x} du champ lointain :

- le spectre acoustique, à partir de la transformée de Fourier, de la fonction d'autocorrélation $P(\vec{x}, \tau)$:

$$P(\vec{x}, \omega) = \int_0^\infty P(\vec{x}, \tau) \cos \omega \tau d\tau$$

- l'intensité sonore

$$I(\vec{x}) = \frac{P(\vec{x}, \tau=0)}{\rho_\infty c_\infty}$$

On peut arriver à une forme plus simple de (5) en supposant que le milieu source est stationnaire :

$$(6) \quad \left\langle \left[\frac{\partial^2 T_{ij}}{\partial t^2} \right]_{\vec{t}'} \left[\frac{\partial^2 T_{kl}}{\partial t^2} \right]_{\vec{t}''} \right\rangle = \frac{\partial^4}{\partial \tau^4} R_{ijkl}(\vec{y}', \vec{y}''; \tau + \vec{t}'' - \vec{t}')$$

(où $\vec{t}'' - \vec{t}'$ n'est plus fonction que de la différence des temps de parcours des informations de tous points \vec{y}' et \vec{y}'' du volume source au point d'observation \vec{x}).

Avec cette hypothèse, R_{ijkl} représente la fonction de corrélation du milieu. En donnant une forme particulière à cette fonction de corrélation (forme gaussienne) on aboutit aux formulations prévisionnelles classiques [2], [3].

2.1.1. Alternative

La relation (4) permet d'exprimer le champ de pression acoustique en fonction d'une intégrale de volume sur la source représentée par la double divergence d'un tenseur. Par application du théorème de la divergence, on peut passer d'une intégrale de volume à une intégrale de surface [10], [11] :

$$(7) \quad \int_{V(\vec{y})} \vec{\nabla} \cdot \vec{A} d^3y = \int_{S(\vec{y})} \vec{n} \cdot \vec{A} dS,$$

où S est une surface, par exemple les limites du volume source $V(\vec{y})$, \vec{n} la normale sortante à cette surface, et \vec{A} un vecteur quelconque.

Dans le cas où des surfaces matérielles existent réellement (interactions écoulements-profiles : bruit des machines tournantes, bruit des fuselages et des ailes ...), la relation (7) est clairement définie ([12] à [16] par exemple).

Dans le cas de jets libres on peut considérer ([17], [18]) une surface fictive (ou surface de contrôle) entourant le jet et définir le champ acoustique lointain à partir d'une distribution sur cette surface et ainsi passer de relations volumiques (donc tridimensionnelles) à des relations surfaciques (donc bidimensionnelles) :

$$(8) \quad p(\vec{x}, t) = \frac{1}{2\pi} \int_{S(\vec{y})} \frac{1}{|\vec{x} - \vec{y}|} \left[\frac{\partial p(\vec{y}, t)}{\partial n} \right]_{\vec{t}} dS,$$

où S est la surface fictive entourant le jet libre. (Cette surface sera définie à une dimension suffisante du jet libre afin que les termes de champ proche soient négligeables);

et n est la normale à cette surface.

Avec ce formalisme :

$$(9) \quad \langle p(\vec{x}, t) p(\vec{x}', t + \tau) \rangle = \frac{1}{4\pi^2} \int_{S(\vec{y}')} \int_{S(\vec{y}'')} \frac{\langle \frac{\partial p(\vec{y}, t)}{\partial n} \frac{\partial p(\vec{y}'', t + \tau)}{\partial n} \rangle}{|\vec{x} - \vec{y}'| |\vec{x} - \vec{y}''|} d^2y' d^2y''.$$

La relation (9) est à rapprocher de la relation (5), et, de même, on définit la fonction de corrélation de la surface fictive, cette fonction étant, par le biais du théorème de la divergence, représentative de la fonction de corrélation du milieu source.

2.1.2. Grandeurs représentatives

2.1.2.1. Au sens de la grandeur physique

Le champ acoustique lointain est caractérisé en tout point \vec{x} par le niveau global I (intensité sonore) et le spectre. En fonction de l'angle θ (angle formé par l'axe de la source et la direction d'observation) et à $R = |\vec{x} - \vec{y}|$ grand et fixe, $I = f(\theta)$ représente la directivité de la source avec $I = \frac{\langle p^2(\vec{x}, t) \rangle}{\rho c_\infty}$ (ondes planes en champ lointain).

Le champ de pression instationnaire proche a une structure d'ondes non forcément planes; la détection de la structure spatio-temporelle de ce champ sera explicitée au paragraphe traitement du signal. Dans ce cas, l'intensité sonore n'est plus directement déduite de la valeur quadratique moyenne de la pression, mais se calcule à partir de la densité de flux d'énergie définie dans la direction considérée. Plus spécialement, lorsque l'on utilise le formalisme de "la surface de contrôle" (ou surface fictive) la grandeur physique qui intervient directement est la densité de flux d'énergie normale à l'élément de surface considérée.

Dans le cas d'écoulements libres la situation est infiniment plus complexe. Peut-être que l'idéal serait de disposer d'un traceur de pression utilisable du sein de l'écoulement au champ sonore lointain.

Ainsi, et de même que pour le calcul, en champ lointain, du rayonnement acoustique d'une antenne émettrice d'ondes sonores (sonars par exemple [19]), on pourrait déduire du champ de pression instationnaire, mesuré en amplitude et phase dans le volume source, le champ acoustique rayonné. Ce point de vue, apparemment en contradiction avec l'analogie de Lighthill, est en fait complémentaire et rejoint l'"approche modale" que l'on rappellera au paragraphe 2.2.

2.1.2.2. Au sens du traitement du signal

Les grandeurs représentatives du rayonnement acoustique en champ lointain au sens du traitement du signal se déduisent directement du formalisme mathématique présenté au paragraphe 2.1.

En effet, dans le cas de jets libres chauds réels, la fonction de corrélation du milieu $R_{xj\lambda\ell}$ sous l'hypothèse de ce que le milieu est stationnaire au sens statistique (c'est-à-dire indépendant de l'origine des temps), dépend : du profil des grandeurs moyennes (vitesse, température) couplé aux fluctuations de vitesse, de température et de débit-masse, des moments de tout ordre des grandeurs fluctuantes dans la mesure où l'hypothèse gaussienne n'est pas satisfaite [20]. De ce fait, une description spatio-temporelle expérimentale du champ turbulent est une oeuvre immense dans la mesure où aucun fil directeur théorique ne permet d'établir une hiérarchie entre les différentes grandeurs mises en cause.

La référence [21] est un exemple de travail théorique effectué dans ce sens, il a l'avantage de montrer l'ampleur des difficultés rencontrées.

Ce que l'on peut en déduire est la nécessité de développer des méthodes de diagnostic et de traitement du signal permettant de définir localement, en plus des grandeurs moyennes des échelles de longueurs, de durée de vie, des vitesses de convection, des intensités de turbulence.

Une première approche a consisté à déduire ces grandeurs de corrélations spatio-temporelles.

Considérons une information locale $\Delta(\vec{x}, t)$ mesurée à l'aide d'un moyen approprié. Prenons à titre d'exemple le fil chaud utilisé dans un jet froid de vitesse "raisonnable" afin que les effets de compressibilité soient négligeables.

Dans ce cas simplifié, le tenseur \overline{T} a pour composante $T_{xj} = \rho_0 u_x u_j$. Une description du champ turbulent se déduit de corrélations spatio-temporelles. Dans l'espace cartésien on obtient un coefficient de corrélation en formant :

$$(10) \quad C_{12}(\vec{x}, \tau) = \frac{\langle \Delta_1(x, t) \Delta_2(x + \vec{x}, t + \tau) \rangle}{[\langle \Delta_1^2(x, t) \rangle \langle \Delta_2^2(x + \vec{x}, t) \rangle]^{1/2}}.$$

(La relation (10) est écrite pour la composante x et suppose y et z fixées. Il sera, dans le cas général, nécessaire de considérer les autres composantes). Rappelons que, de ces familles de coefficient, on déduit :

- l'échelle intégrale des longueurs L_x , par exemple :

$$(11) \quad L_x = \int_0^\infty C_{12}(\vec{x}, 0) d\vec{x},$$

- l'échelle intégrale des temps \mathcal{C} :

$$(12) \quad \mathcal{C} = \int_0^\infty C_{12}(\vec{x}, \tau_M) d\tau_M, \text{ par exemple}$$

où τ_M est l'abscisse du maximum de $C_{12}(\vec{x}, \tau)$ et $C_{12}(\vec{x}, \tau_M)$ l'ordonnée, la vitesse de convection est donnée par la pente de la droite $\vec{x} = \vec{f}(\tau_M)$.

Ces grandeurs ne sont représentatives que de moments d'ordre deux.

On se doit de remarquer que :

- les intégrales (11) et (12) ne sont correctement définies que si les coefficients de corrélation sont "raisonnablement" monotones,

- le résultat de ces intégrales a un sens de valeur moyenne sur l'ensemble du spectre caractérisant l'élément de volume détecté :

par définition ce sont des échelles intégrales. Elles ont donc le défaut d'accorder le même poids dans l'espace comme dans le temps à chaque paquet d'ondes élémentaire.

Pour pallier ce défaut, deux techniques de traitement du signal sont utilisables :

- la première consiste à effectuer des corrélations sur des signaux filtrés,
- la seconde consiste à se placer dans l'espace de Fourier et à déduire du module des inter-spectres des échelles de longueurs par bandes de fréquence et de la phase les vitesses de convection de ces bandes de fréquence [22].

Dans le cas des corrélations spatio-temporelles tout se passe comme si le jet libre est décomposé en éléments de volume disjoints dont les dimensions sont définies par les échelles intégrales. Dans l'espace de Fourier, des éléments de volume voisins ont une intersection non forcément vide car de dimensions fonctions de la bande de fréquence considérée.

Ces considérations ne sont pas rassurantes pour l'expérimentateur et de nombreuses questions se posent, telles que :

- quelle est la résolution spatiale la mieux adaptée pour des interprétations acoustiques,
- quelle est la méthode de mesure et de traitement du signal la plus représentative des sources de bruit.

Le formalisme théorique que nous venons d'introduire repose sur l'analogie de Lighthill basée sur une équation inhomogène des ondes déduites des équations de conservation de la mécanique des milieux continus.

Avant de passer à une présentation de moyens de diagnostics et de traitement du signal, nous mentionnerons rapidement deux autres formalismes théoriques.

2.2. Approche modale

B.T. CHU et Leslie S.G. KOVASZNY [23] ont proposé une approche basée sur un concept d'interactions non linéaires. Pour ce faire, ces auteurs utilisent un théorème bien connu qui permet de décomposer tout champ de vecteurs en composantes rotationnelles et en composantes irrotationnelles. En particulier, le champ de vitesse \vec{v} se décompose en

$$\begin{aligned} & \vec{v}_{\text{rot.}} \quad \text{tel que} \quad \vec{\nabla} \cdot \vec{v}_{\text{rot.}} = 0 \\ \text{et en } & \vec{v}_{\text{irrot.}} \quad \text{tel que} \quad \vec{\nabla} \times \vec{v}_{\text{irrot.}} = 0 \end{aligned}$$

De ce fait :

- la turbulence cinématique est rattachée aux composantes de $\vec{v}_{\text{rot.}}$
- les fluctuations d'entropie et de compressibilité sont rattachées toutes deux à $\vec{v}_{\text{irrot.}}$

Les équations de base étant essentiellement non linéaires, il est alors possible de mettre en évidence des couplages entre trois modes élémentaires : cinématique, entropique (ou thermique), sonore, et, en ordre de grandeur, il est alors possible d'établir une hiérarchie entre les différents termes de couplage.

La prise en compte, dans ce formalisme, des interactions entre grandeurs fluctuantes et grandeurs moyennes conduit à des calculs très complexes.

2.3. Mécanismes d'instabilité

Les approches théoriques des paragraphes 2.1 et 2.2 supposent des propriétés statistiques du mélange turbulent du jet libre sans tenir compte d'éventuelles structures quasi-récurrentes. Des expériences de CROW et CHAMPAGNE [24] sur l'excitation d'un jet libre par un champ acoustique ont permis de dégager une notion de structure à grande échelle dans la zone de mélange de jets froids. De nombreuses études ont permis de préciser que, pour un jet non excité, cette structure existait et qu'elle était liée au passage de tourbillons de grande dimension qui se détachent de la région avoisinant la sortie de tuyère [25].

A. MICHALKE [26] a démontré que ces structures peuvent être décrites par un modèle théorique basé sur le calcul de l'instabilité spatiale de la couche limite turbulente. Ces instabilités sont représentées par des solutions périodiques

$$p(x, r, \varphi, t) = F(r) \exp -i(\omega t - \alpha x - m\varphi)$$

d'une équation aux petites perturbations de la forme :

$$\frac{D}{Dt} \left[\frac{D^2 p}{Dt^2} - \Delta (c_\infty^2 p) \right] + 2 \vec{\nabla} U \cdot \frac{\partial}{\partial x} [c_\infty^2 \vec{\nabla} p] = 0.$$

Une étude numérique de ce type d'équation étendue au cas de jets chauds a été effectuée [27] et met en évidence l'existence de modes complexes ($m \neq 0$) dont l'efficacité sonore dans le champ acoustique lointain était théoriquement contestée mais a été expérimentalement démontrée [27], [28], ce que nous verrons par la suite.

2.4. Ensemble des grandeurs représentatives du champ sonore lointain

Compte tenu des différents rappels d'éléments de théories présentés dans ce paragraphe on imagine la difficulté que peut avoir l'expérimentateur à définir les moyens expérimentaux les mieux adaptés à la caractérisation des sources sonores. De façon schématisée on peut présenter cet ensemble de grandeurs caractéristiques, en fonction de choix d'objectifs, de la façon suivante :

- sondage du volume source dans le but de mettre en évidence les grandeurs les plus fortement corrélées à l'émission acoustique sur la base de modélisation théorique ;
- sondage du champ proche pour : soit définir une distribution équivalente de sources sonores sur une surface de contrôle, soit préciser l'objectif précédent ;
- sondage du champ lointain avec le souci d'imaginer des dispositifs permettant de définir une distribution virtuelle de sources sonores équivalentes à la distribution réelle, quant à ses conséquences ;
- enfin, effectuer une combinaison de ces trois types de sondage dans le but de passer d'une distribution virtuelle de sources à une distribution réelle.

Dans le paragraphe suivant nous allons essayer de montrer sur des exemples concrets les efforts qui sont réalisés dans ce sens.

3. QUELQUES MOYENS DE DIAGNOSTIC

Avant de présenter quelques moyens de diagnostics, précisons dans quelles conditions ils doivent être utilisés, c'est-à-dire dans quels moyens d'essais.

Nous nous limitons au cas des études de bruit de jets. Celles-ci peuvent être effectuées lors d'essais en vol à l'aide de microphones au sol. Elles peuvent également être effectuées sur moteur réel, au banc d'essais statiques ou en translation (à l'aide de l'Aérottrain de la Société Bertin par exemple [29]), ou encore en soufflerie à veine guidée.

Nous ne traiterons pas ces différents cas. Nous nous attacherons plutôt à présenter quelques moyens de diagnostics utilisés sur des bancs d'essais de maquettes en chambre anéchoïque, en soufflerie anéchoïque à veine ouverte. Ces différents moyens de diagnostics que l'on présentera sont d'ailleurs le plus souvent transposables au cas d'essais à l'aide de moteurs réels au banc statique, voire en translation.

De plus nous ne mentionnerons pas les moyens de diagnostics classiques tels que fils ou films chauds, striescopie à grand champ, ombroscopie; ...

3.1. Sondage de jets libres

3.1.1. Mesures locales

A part les développements actuels de la mesure de vitesse (D.L.V.) par effet Doppler à l'aide de vélocimètre laser ([31] à [33] et [37], par exemple) il existe peu de méthodes de mesure de grandeurs fluctuantes dont on soit certain de la résolution spatiale.

Dans certains cas et pour des jets généralement de faible vitesse, des sondes microphoniques sont parfois utilisées [35], [36].

3.1.2. Technique de faisceaux croisés

La technique de faisceaux croisés est utilisée couramment dans différents cas :

- striescopie laser [33], [36]
- mesure de l'absorption infrarouge [34]
- mesure de l'émission infrarouge [45].

Dans le cas de la striescopie laser, on mesure des fluctuations de gradient de densité. Le signal détectant l'absorption, dans l'infrarouge, d'un signal par le jet est fortement fonction de la concentration de l'espèce chimique choisie et dépend moins fortement de la température. Le signal détectant l'émission infrarouge propre des jets, par contre, est fortement fonction de la température, et dépend de la concentration.

Les corrélations spatio-temporelles basées sur la technique des faisceaux croisés sont définies dans un volume d'interaction des faisceaux égal à la dimension géométrique de ces faisceaux dans la mesure où les informations détectées le long du trajet optique sont indépendantes.

On a vérifié [41] que dans le cas où une structure à grande échelle (définie au paragraphe 2.3) co-existe avec la turbulence classique, la définition spatiale des volumes corrélés est mal connue.

Néanmoins, on déduit de ces moyens de mesure, des échelles intégrales de turbulence comparables à celles obtenues à l'aide de fils chauds, par exemple.

Des tentatives de reconstitution du champ sonore à partir de ces mesures ont été effectuées sur la base de modèles théoriques simplifiés [47].

Ce genre d'exploitation numérique des résultats de mesure de grandeurs de turbulence se heurte à des difficultés fondamentales liées au parcours des paquets d'ondes de l'élément de volume considéré dans le jet libre, à la position de l'observateur, du fait d'effets de convection par la vitesse moyenne, de réfraction par les profils des grandeurs moyennes (vitesse, température), de diffusion par la turbulence du milieu et d'un glissement Doppler dans la combinaison deux à deux de "sources élémentaires" (figure 2).

3.2. Sondage du champ proche

Le sondage du champ de pression instationnaire a été effectué suivant deux idées directrices.

3.2.1. Corrélations infrarouge - microphones [48]

Le but de ce type de corrélations (dans l'espace cartésien comme dans l'espace de Fourier) est de préciser le diagramme de directivité de l'élément de volume du jet libre, isolé par le moyen de mesure (figure 3). Dans le cas des corrélations entre le signal d'émission infrarouge détecté dans le jet par le radiomètre et les signaux des microphones, on obtient des coefficients de cohérence pouvant atteindre 0,5, ce qui représente un coefficient de forte valeur que l'on n'atteint pas avec des fils chauds. Ce résultat en fait n'est pas surprenant car le signal infrarouge est essentiellement dépendant des fluctuations thermiques elles-mêmes fortement corrélées (à un facteur dimensionnel près) aux fluctuations de pression. Dans la référence [47] on trouvera un exemple typique d'application, couronné de succès.

3.2.2. Corrélations microphones - microphones dans le champ proche [17], [18], [28], [30], [36], [38], [39], [40], [43], [44].

Soit à l'aide de lignes multi-microphoniques placées parallèlement à l'axe du jet ou de la frontière du jet, à une distance radiale de l'ordre de quelques diamètres, soit à l'aide de microphones placés circonférentiellement au jet, cette technique a pour but de définir une distribution virtuelle de sources sonores sur une surface de contrôle, équivalente à la distribution réelle des sources dans le volume source.

Un des résultats des plus remarquables de cette technique [38], [28] est l'identification des structures à grande échelle avec la mesure de la structure azimutale calculée suivant le schéma théorique esquissé en 2.3, à l'aide d'une méthode définie dans la référence [6] de [49].

3.3. Sondage à partir du champ lointain

Les méthodes, dans ce cas, sont basées sur l'utilisation de microphones directifs [34], [42], [44]. On trouve deux sortes de systèmes : soit un microphone placé au centre d'un miroir cylindrique, soit un microphone placé au foyer d'un miroir de forme elliptique, la portion du jet à sonder étant alors placée à l'autre foyer.

Signalons dans ce contexte le développement, à l'ONERA, d'une antenne synthétique acoustique bidimensionnelle [50] dont on montre un exemple d'application sur la figure 4 : pour 4 bandes de fréquences (tiers d'octave centrées sur 0,5 ; 1 ; 1,6 ; 2 et 4 kHz) on a porté la distribution axiale de l'amplitude, le jet maquette étant alors à symétrie de révolution.

Comme nous l'avons déjà mentionné, ces méthodes ne fournissent qu'une distribution virtuelle de sources sonores.

3.4. Technique hybride

À l'ONERA, des essais prometteurs sont actuellement effectués pour mesurer directement une distribution de sources réelles [46], c'est-à-dire pour chiffrer directement par des mesures et non pas par déduction, la contribution d'un élément de volume au rayonnement sonore lointain, dans une bande de fréquences données. Pour cela, on étudie les possibilités d'application de l'échantillonnage conditionnel. Pour illustrer les possibilités d'application de cette méthode, les mesures ont été effectuées dans un jet libre froid issu d'une tuyère de diamètre D égal à 3 cm, la vitesse du jet au niveau du plan de sortie étant de 100 ms^{-1} . Deux fils chauds sont placés dans le jet libre, l'un F_1 à la limite du cône potentiel ($X/D = 2$, $Y/D \approx 0,3$), l'autre F_2 dans la zone de mélange ($X/D = 2$, $Y/D = 0,5$). Un microphone M est placé à $X/D \approx 28$ et $Y/D \approx 15$ soit à $R/D \approx 32$ et $\theta \approx 28^\circ$ (θ représente l'angle que forme l'axe du jet et la direction d'observation). Tout autre moyen de mesure peut être employé pour prélever l'information dans le jet (vélocimétrie laser, strioscopie laser, émission ou absorption infrarouge, capteur de pression, ...); nous avons choisi le fil chaud pour cette première application à la place d'autres diagnostics usuellement utilisés au laboratoire du fait que les corrélations fils chauds-microphones (même après filtrage) sont le plus généralement décevantes.

Le signal de F_1 est choisi comme signal pilote. Sa fonction essentielle est de définir une suite d'instants t_i à chaque fois que le signal de F_1 a une propriété d'amplitude et de phase préchoisies. À chacun de ces instants t_i , une porte électronique de largeur T est ouverte ce qui définit un "bloc" et l'acquisition des signaux de F_2 et de M et du produit $F_2 M$ est alors effectuée. Au préalable, un retard constant est appliqué au signal de F_2 pour tenir compte du temps de parcours de l'information de l'emplacement de F_2 à celui de M . Ce retard intervient comme paramètre dans le traitement du signal puisque la vitesse relative du son dans le milieu est variable.

Sur les figures 5 et 6 sont présentés des exemples typiques de la forme du signal contenu dans un bloc :

Figure 5 : en abscisse : le temps, la longueur du signal est égale à $T = 5,12 \text{ ms}$,
en ordonnée : une amplitude arbitraire

La courbe 5-a est relative au signal de F_2
La courbe 5-b est relative à M .

La figure 6-a représente le signal de F_2 et la figure 6-b représente le signal de M acquis dans un bloc durant le temps $T = 0,64 \text{ ms}$.

À partir de ces acquisitions on peut calculer la moyenne d'ensemble des informations contenues dans chaque bloc, ainsi que la somme de ces moyennes d'ensemble.

Sur les figures 7 et 8 on présente un résultat de ce calcul :

- les courbes 7-a et 8-a représentent la somme des moyennes d'ensemble des informations relatives à F_2 ,
- les courbes 7-b et 8-b, celles relatives à M ,
- les courbes 7-c et 8-c, celles du produit $F_2 M$.

On constate que les courbes 7-a, 8-a, 7-b et 8-b sont pratiquement linéaires, ce qui indique simplement que le nombre de points acquis est représentatif du phénomène isolé dans le signal par les choix effectués sur F_1 .

La courbe 7-c, qui correspond à $T = 5,12$ ms, est oscillante, donc de moyenne quasi nulle, la courbe 8-c, correspondant à $T = 0,64$ ms, est par contre assez monotone donc de moyenne assez élevée. En unités arbitraires, les résultats des calculs sont résumés dans le tableau suivant :

T : durée de l'acquisition (ms)	Moyenne d'ensemble sur F_2 Nombre de blocs	Moyenne d'ensemble sur M Nombre de blocs	Moyenne d'ensemble sur $F_2 M$ Nombre de blocs	Carré du coefficient de cohérence conditionnel
5,12	85,4	67	$-3,92 \cdot 10^{-2}$	$-5,19 \cdot 10^{-4}$
2,56	42	33	$17 \cdot 10^{-2}$	$46 \cdot 10^{-4}$
1,28	20	16	$20 \cdot 10^{-2}$	$111 \cdot 10^{-4}$
0,64	10	8	$13 \cdot 10^{-2}$	$145 \cdot 10^{-4}$
0,32	5	4	$50 \cdot 10^{-2}$	$115 \cdot 10^{-4}$

Sur la figure 9, la variation du carré du coefficient de cohérence conditionnel $C^2(T, S^{\pm}, \hat{C})$ est tracée en fonction de T (temps d'acquisition) et de S^{\pm} (critères de choix sur F_1 : amplitude et forme), dans ce cas, \hat{C} : retard incrémental compensant le temps de parcours de l'information de F_2 à M a été maintenu constant. On constate sur cette courbe un maximum pour $T = 0,64$ dont le maximum maximum n'apparaît pas (à cause d'une limitation des moyens mis en oeuvre).

Aux alentours de ce maximum, la cohérence conditionnelle entre le fil chaud (de $10 \mu\text{m}$ d'épaisseur et environ 5 mm de long) et le microphone est de l'ordre de 12%, ce qui est élevé. En déplaçant le point de mesure F_2 on peut alors tracer des cartes d'iso-amplitude pour différentes valeurs de T (donc différentes bandes de fréquence).

Cette méthode est en cours d'application pour caractériser en plus des sources de bruit de jets, celles de machines tournantes (compresseurs, ventilateurs, hélicoptères, ...), de profils, de mécanismes d'interaction, de structures vibrantes. Elle a l'avantage de permettre de s'affranchir de propriétés statistiques strictes des signaux que l'on voudrait traiter par des procédés classiques (corrélation, transformation de Fourier) en permettant d'être synchrone par rapport à un mécanisme sélectionné par les conditions imposées à F_1 .

4. CONCLUSIONS

On constate actuellement une situation inverse de celle existante il y a 10 ans environ. En effet, les importants investissements, attribués au développement de moyens nouveaux d'investigation, font que l'expérience apporte des résultats forts pour lesquels les modélisations théoriques restent à trouver. Ces résultats sont obtenus à l'aide de moyens de mesure dont la relation dimensionnelle avec la grandeur physique recherchée est parfois difficile à définir.

Dans l'ensemble des résultats expérimentaux retenons, ainsi que le Pr. LAUFER l'a fait lors des conclusions de la 3ème Conférence de l'AIAA sur l'Aéro-Acoustique (Palo-Alto, juillet 1976), les preuves expérimentales de l'existence des structures à grande échelle sur des jets de forte vitesse ainsi que l'évaluation quantitative de leur efficacité acoustique dans le champ lointain.

Ces études sont à approfondir en particulier en ce qui concerne les relations entre structure à grande échelle et turbulence "classique" (ou fine). Dans ce sens les expériences sur l'amplification paramétrique [51] sont prometteuses.

Cet ensemble de moyens de sondage des jets, complété par des systèmes microphoniques directifs et par des méthodes de traitement du signal permettant de donner une distribution réelle des sources dans le jet, met l'expérimentateur en position favorable pour définir des remèdes aux nuisances acoustiques.

5. REFERENCES

1. J.M. Lighthill, "On Sound Generated Aerodynamically. I - General Theory", Proc. Roy. Soc. (London), Ser. A, Vol. 211, No. 1107, pp. 564-587, March 20, 1952.
II - Turbulence as a Source of Sound", Proc. Roy. Soc. (London), Ser. A, Vol. 222, No. 1148, pp. 1-32, February 23, 1954.
2. J.E., Ffowcs-Williams, "The Noise from Turbulence Convected at High Speed", Phil. Trans. Roy. Soc. (London), Ser. A, Vol. 255, pp. 469-503, 1963.
3. H.S., Ribner, "The Generation of Sound by Turbulent Jets", Advances in Applied Mechanics, Vol. 8, pp. 104-182, Academic Press, 1964.
H.S., Ribner, "Quadrupole Correlations Governing the Pattern of Jet Noise", J. Fluid Mech., 38, Part 1, pp. 1-24, August 1969.

4. R.G., Hoch, J.P., Duponchel, P.J., Cocking, W.T., Pryce, "Studies of the Influence of Density on Jet Noise", 1st Int. Symp. on Airbreathing Engines, Marseille (France), 19-23 juin, 1973.
5. J. Taillet, "Méthodes expérimentales d'analyse des sources de bruit des compresseurs et des jets" L'Aéron. et l'Astron., No. 24 (1970-8), pp. 57-67, T.P. ONERA, No. 908, 1970.
6. J. Taillet, "Description et mise en œuvre d'une méthode de caractérisation des sources de bruit dans les jets", 8^{ème} Congrès I.C.A.S., Amsterdam, 28 août-1^{er} septembre, 1972, T.P. ONERA, No. 1122, 1972.
7. H.S., Fuchs, "Basic Aerodynamic Noise Theory", AGARD Lecture Series, No. 80 on "Aerodynamic Noise", 1976.
M.J., Fisher, "Jet-Efflux Noise", AGARD Lecture Series, No. 80 on "Aerodynamic Noise", 1976.
8. J.A., Stratton, "Théorie de l'électromagnétisme", Ed. Dunod, Paris, 1961.
9. H., Viviani, "L'équation fondamentale de la théorie du bruit aérodynamique dans le cas de surfaces en mouvement de translation uniforme", J. de Méc., Vol. 9, p. 335, 1970.
10. D.I., Blokhintsev, "Acoustics of a Nonhomogeneous Moving Medium", NACA TM-1399, 1956.
11. P.M., Morse, H., Feshbach, "Methods of Theoretical Physics", Ed. Mc Graw-Hill Inc, 1953.
12. N. Curle, "The Influence of Solid Boundaries on Aerodynamic Sound", Proc. Roy. Soc. (London), Ser. A, Vol. 231, No. 1187, september 1955.
13. M.V., Lowson, "The Sound Field for Singularities in Motion", Proc. Roy. Soc. (London), Ser. A, Vol. 286, No. 1407, august 1965.
14. Th. von Karman, W.R., Sears, "Airfoil Theory for Non-uniform Motion", J. Aeron. Sci., Vol. 5, No. 10, août 1938.
15. M.V., Lowson, "Theoretical Analysis of Compressor Noise", J. Acoust. Soc. Amer., Vol. 47, No. 1, Part 2, 1970.
16. C.L., Morfey, "Sound Generated in Subsonic Turbomachinery", J. Basic Eng., Ser. D, Vol. 92, september 1970.
17. L., Maestrello, "Acoustic Energy Flow from Subsonic Jets and their Mean and Turbulent Flow Structures", Ph.D, University of Southampton.
18. S.P., Pao, L., Maestrello, "New Evidence of Subsonic Jet Noise Mechanisms", AIAA Paper No. 75-437, Presented at AIAA 2nd Aeroacoustics Conf., Hampton (Virginia), March 24-26, 1975.
19. M.C., Junger, M., Pérulli, "Eléments d'acoustique physique", Cours d'Acoustique No. 1 de l'Université de Technologie de Compiègne, 1976.
20. J.F., de Belleval, O., Leuchter, M., Pérulli, "Simulation of Flight Effects on the Structure of Jet mixing Layers for Acoustical Applications", AIAA Paper No. 76-559, Presented at AIAA 3rd Aero-Acoustics Conf., Palo-Alto, 20-22 July, 1976.
21. P.E., Doak, "Progress toward a Unified Theory of Jet Engine Noise", Ser. "The Generation and Radiation of Supersonic Jet Noise", Vol. III, The Lockheed Georgia Company, Technical Report AFAPL-TR-72-53, july, 1972.
22. P.O.A.L., Davies, M.J., Fisher, M.J., Barratt, "The Characteristics of the Turbulence in the Mixing Region on a Round Jet", J. Fluid Mech., Vol. 15, Part 3, March, 1963.
23. B.T., Chu, L.S.G., Kovaszny, "Non-linear Interactions in a Viscous Heat Conducting Compressible Gas", J. Fluid Mech., Vol. 3, Part 5, february, 1958.
24. S.C., Crow, F.H., Champagne, "Orderly Structure in Jet Turbulence", J. Fluid Mech., Vol. 48, Part 3, august, 1971.
25. G., Neuwerth, "Akustische Rückkopplungserscheinungen am Unter- und Überschall-Freistrah, der auf einen Störkörper Trifft", DLR-FB 72-72, 1972.
26. A., Michalke, "An expansion Scheme for the Noise from Circular Jets", Z. Flugwiss, 20, pp. 229-237, 1972.
27. C., Dahan, "Contribution à l'étude de l'émission acoustique de structures cohérentes dans un jet turbulent", Thèse de Doctorat d'Etat ès Sciences Physiques, Publication ONERA, No. 1976-4, 1976.
28. C., Dahan, G., Elias, "Source Structure Pattern in a hot Jet by Infrared-Microphones Correlation", AIAA Paper No. 76-542, Presented at AIAA 3rd Aero-Acoustics Conf., Palo-Alto, 20-22 July, 1976.
29. R.G., Hoch, M., Berthelot, "Use of Bertin Aerotrain for the Investigation of Flight Effects on Aircraft Engine Noise", AIAA Paper No. 76-534, Presented at AIAA 3rd Aero-Acoustics Conf., Palo-Alto, 20-22 July, 1976.

30. W.D., Bryce, "A Comparison of Engine and Model Jet Noise Measurements in the Near-Field, Colloque I.S.L., 14-16 mai, 1974.
31. B., Koch, "Anwendungsmöglichkeiten des Laseranemometers zur Turbulenzmessung", Colloque I.S.L., 14-16 mai, 1974.
32. P., Ardonneau, "Reflexions sur quelques problèmes posés par l'application de la vélocimétrie laser aux écoulements turbulents", Colloque I.S.L., 14-16 mai, 1974.
33. P.F., Massier, S.P., Parthasarathy, R.F., Cuffel, "Experimental Evaluation of Fluctuating Density and radiated Noise from a high Temperature Jet", AGARD-CP-131, 1973.
34. R.J., Damkevala, F.R., Groschi, S.H., Guest, "Direct Measurement of Sound Sources in Airjets using the crossed Beam Correlation Technique", AGARD-CP-131, 1973.
35. T.E., Siddon, "Noise Source Diagnostics using causality Correlations", AGARD-CP-131, 1973.
36. W.C., Meecham, P.M., Hurdle, "Use of Cross-Correlation Measurements to Investigate Noise Generating Regions of a Real Jet Engine and a Model Jet", AGARD-CP-131, 1973.
37. M.J., Fisher, "Crossed Beam Schlieren Laser Doppler Velocimeter", Ser. "The Generation and Radiation of Supersonic Jet Noise", Vol. III, The Lockheed Georgia Company, Technical Report AFAPL-TR-72-53, July, 1972.
38. R.R., Armstrong, H.V., Fuchs, A., Michalke, "Coherent Structures in Jet Turbulence and Noise", AIAA Paper No. 76-490, Presented at AIAA 3rd Aero-Acoustics Conf., Palo-Alto, 20-22 July, 1976.
39. T.M., Farabee, F.E., Geib Jr., "Measurement of Boundary Layer Pressure Fields with an Array of Pressure Transducers in a Subsonic Flow", ICIASF' 75 Record, Ottawa, September, 1975.
40. P.T., Soderman, "Instrumentations and Techniques for Acoustic Research in Wind Tunnels", ICIASF' 75 Record, Ottawa, September, 1975.
41. J.F., de Belleval, J., Maulard, M., Pérulli, "Caractérisation des sources de bruit dans les jets chauds par la technique des faisceaux croisés", Symposium AGARD, Saint Louis, mai, 1976.
42. S.P., Parthasarathy, "Jet Noise Source Location by Cross-Correlation of Far Field Microphone Signals", AIAA Paper No. 75-456, AIAA 2nd Aero-Acoustic Conf., Hampton (Virginia), March, 1975.
43. C.H., Liu, L., Maestrello, M.D., Gunzburger, "Simulation by Vortex Rings of the Unsteady Pressure Field near the Jet", AIAA Paper No. 75-438, Presented at AIAA 2nd Aero-Acoustic Conf., Hampton (Virginia), March, 1975.
44. J., Laufer, R., Schlinker, R.E., Kaplan, "Experiments on Supersonic Jet Noise", AIAA Paper No. 75-478, Presented at AIAA 2nd Aero-Acoustic Conf., Hampton (Virginia), March, 1975.
45. J.F., de Belleval, M., Pérulli, "Représentation de la turbulence d'un jet chaud à partir de son émission infrarouge", AGARD-CP-131, 1973.
46. M., Pérulli, L., Avezard, A., Guédel, A., Lelarge, C., Malarney, "Application de l'échantillonnage conditionnel à la caractérisation du rayonnement acoustique de sources de bruit", C. R. Ac. Sc. de Paris, 1976, (en cours de publication).
47. J.F., de Belleval, J., Randon, M., Pérulli, J.C., Taillefer, "Influence of Refraction Effects on the Interpretation of a hot Jet Acoustic Radiation", AIAA Paper No. 73-990, Presented at AIAA 1st Aero-Acoustic Conf., Seattle, October, 1973.
48. J.F., de Belleval, "Relation du champ acoustique d'un jet chaud avec sa turbulence et son émission infrarouge", Doctorat de Thèse d'Etat ès Sciences Physiques, Publication ONERA No. 159, 1974, Traduction en langue anglaise par l'European Space Agency, ESA-TT-248, february, 1976.
49. J., Taillet, M., Pérulli, S., Lévy, J., Prieur, "Répartition de pression instationnaire et propagation du bruit dans les manches d'entrée des turbomachines", Xème Congrès I.C.A.S., Ottawa, Octobre, 1976.
50. M., Bodiansky, communication privée.
51. E., Pfizenmaier, "On the Instability of Sound", Influenced Free Jet, Report No. DLR-FB-73-69, 1973, Technical Translation ESRO-TT-122, January, 1975.

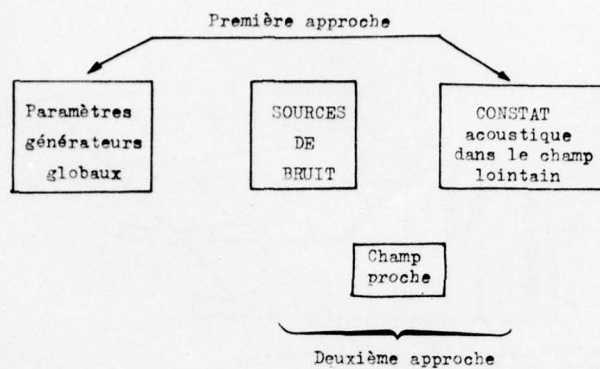


Figure 1

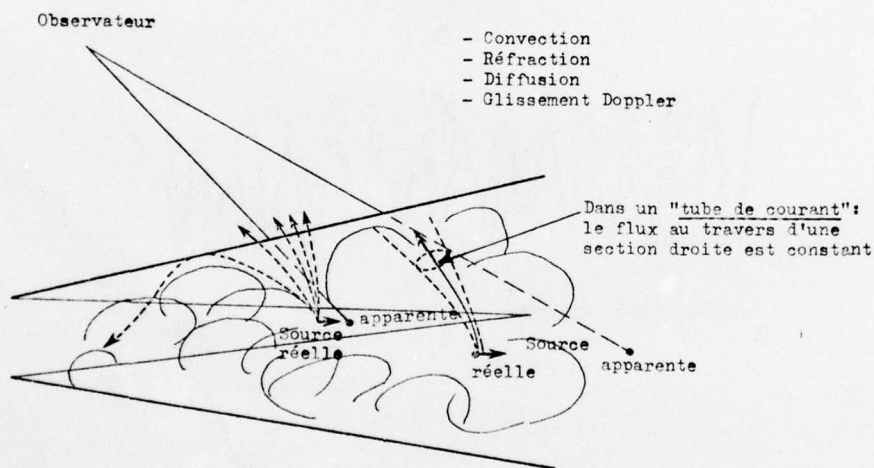


Figure 2

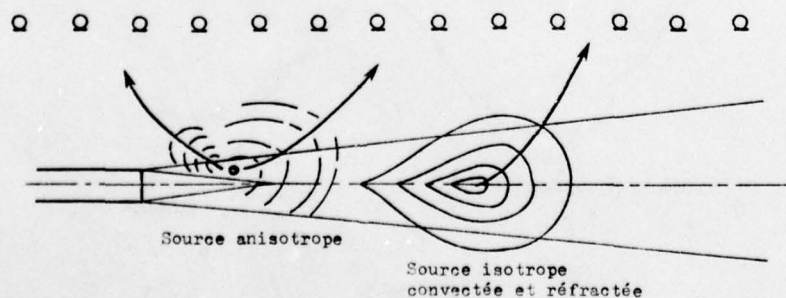


Figure 3

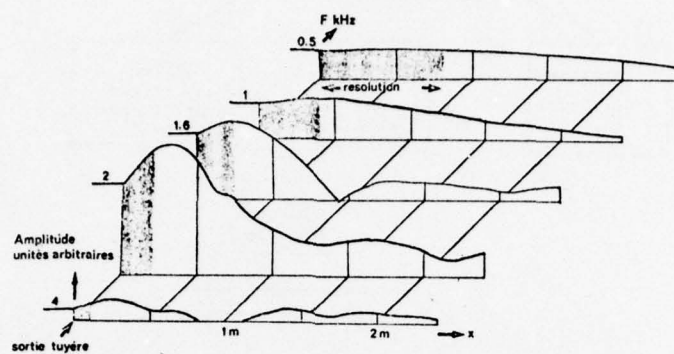


Figure 4

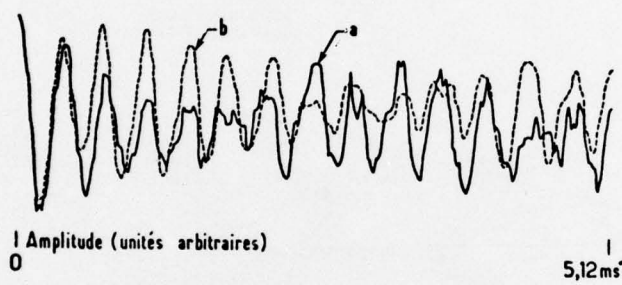


Figure 5

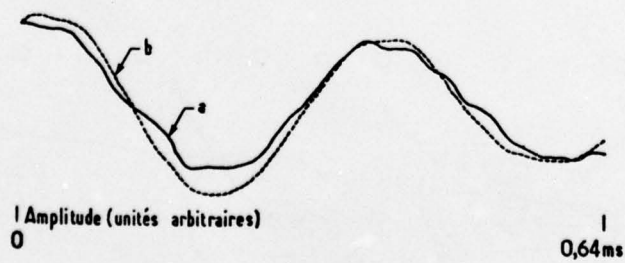


Figure 6

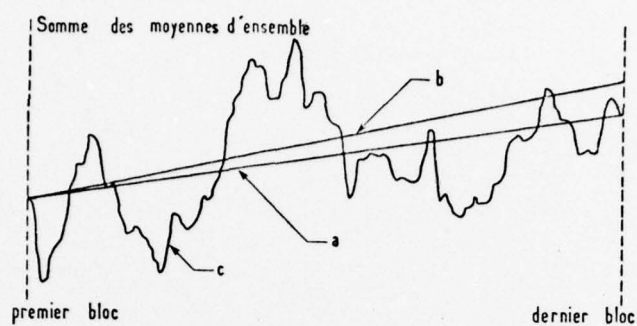


Figure 7

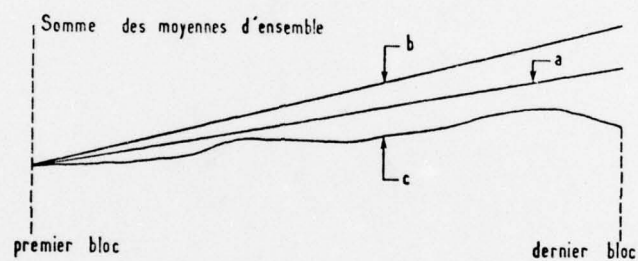


Figure 8

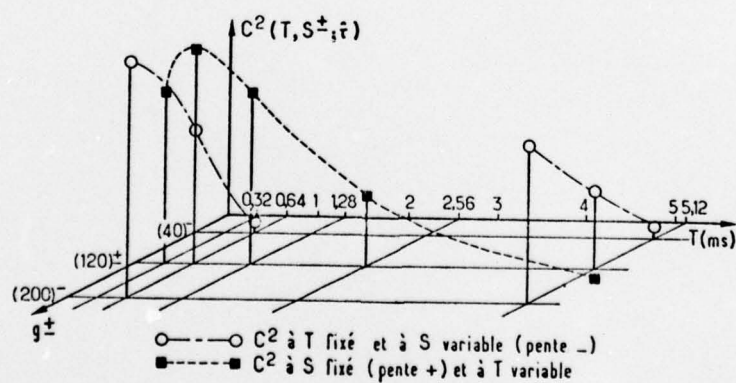


Figure 9

GROUND-BASED FACILITIES WITH FORWARD-SPEED REPRESENTATION
FOR AIRCRAFT NOISE RESEARCH

by

John Williams

Aerodynamics Department, Royal Aircraft Establishment
 Farnborough, Hants, GU14 6TD, England

SUMMARY

The prediction and reduction of aircraft noise for flight conditions is much more complex than for static since, apart from conventional Doppler-shift and flight-path considerations, the relative airflow past the aircraft can have significant effects on both the generation and propagation of the noise from the engine/airframe combination. Ground-based facilities providing adequate representation of forward-speed conditions for noise-model experiments, in a well-defined and controlled environment, are now essential to complement and preferably precede full-scale investigations under static and flight conditions. The special merits, deficiencies and problem areas arising with several particular types of such facilities are analysed and quantified here in basic practical terms. The complementary usage of more than one facility type is shown to be desirable, in view of their inherent limitations individually, to ensure some checks on each other as well as to widen the range of experiments possible.

Acoustic windtunnels, using fixed models in an anechoic working-chamber enclosing a quiet airstream, receive the most detailed analysis here since they have now been the most thoroughly investigated, and can now provide the best experimental approach to noise-model research work (basic and applied). The application of linear-track vehicles is also extensively discussed, as being the most appropriate for providing practical mobile-model experiments using real small engines. Some comments are added about the exploitation of other mobile-model techniques, including rotating arms, road/runway vehicles, aerial-cable runs, and free-flight. The Bibliography should be reasonably comprehensive, in that it lists the titles of over 100 directly relevant papers published by European and North American workers from 1970 to mid-1976.

CONTENTS

1	<u>Introduction</u>
2	<u>Subsonic Windtunnel Development and Operation for Noise-Model Testing</u>
2.1	Nature of tunnel merits
2.2	Tunnel noise-testing considerations
2.3	Microphone location and relative-motion considerations
2.4	Specific tunnels for noise-model testing
3	<u>Special Factors in Acoustic Tunnel Design and Application</u>
3.1	Acceptable frequency range and model-scale
3.2	Acoustic constraints of test-section size and type
3.3	Acoustic constraints of model geometry and type
3.4	Tunnel background noise
3.5	Noise absorption treatment of tunnel circuit and aerodynamic implications
3.6	Tunnel flow quality requirements
3.7	Tunnel airflow drive
3.8	Open-jet nozzle and collector-flow interactions
4	<u>Tracked Vehicle Development and Operation for Noise-Model Testing</u>
4.1	Nature of track merits
4.2	Track noise-testing considerations
4.3	Required microphone locations and track lengths
4.4	Specific tracks for noise testing
5	<u>Other Mobile Ground-Based Facilities for Noise Testing</u>
5.1	General scope
5.2	Rotating arms
5.3	Road/runway vehicles
5.4	Aerial cables
5.5	Free-flight
6	<u>Model-Scale Simulation of Propulsion and Powered-Lift Noise Sources</u>
7	<u>Concluding Remarks -</u>
	<u>Overview of Ground-Based Facilities for Noise Experiments</u>
	Table 1 - Tunnel development considerations for noise-model testing
	Table 2 - Tunnel operational considerations for noise-model testing
	References and Bibliography
	Illustrations

1 INTRODUCTION

The aircraft designer is now faced with significant problems in assessing, predicting and guaranteeing the noise field from future aircraft projects to a much greater accuracy than hitherto, while at the same time meeting the demand for even lower noise levels without significant penalties in respect of economy, safety and performance¹. The prediction of aircraft noise for flight conditions is much more complex than under static conditions, apart from forward speed effects through conventional Doppler-shift and flight path considerations. The relative mainstream flow past the aircraft in flight can have significant influence on the generation and propagation of the source noise from the engine itself, from the airframe, and from the engine-airframe interactions (Fig 1). Forward-speed can affect the perceived noise appreciably through changes not only in the overall sound pressure level but also in the noise spectrum and directivity characteristics. Our fundamental understanding of these effects is still poor. Their practical importance has already been forcibly illustrated by: the difficulties of reconciling static-rig and in-flight measurements on engines - as regards both fan noise and exhaust noise; the recognition of some exhaust noise silencing schemes which worked well statically but proved much less effective in flight; the observation of trailing-vortex refraction effects on engine noise propagation; the significant airframe noise measured in flight with landing-devices deployed and quietened engines; and some impulsive noise of helicopters.

Noise measurements from actual aircraft in flight will always be necessary for confirmation of predictions, for final proving and for type certification. Carefully controlled flight experiments with research-orientated modifications of small aircraft can also play a useful role, as well illustrated by in-flight work directed towards investigation of surface-shielding and airflow refraction of engine noise. In some extreme cases, typified by early airframe self-noise investigations, flight testing of available production aircraft may prove to be the only technique immediately applicable, at least to gain some practical experience rapidly. However, as a primary tool for R&D on forward-speed effects, flight tests on noise - as well as on associated aerodynamics - are relatively restricted in flexibility, measurement accuracy, and productivity.

Thus ground-based facilities providing forward-speed simulation for model experiments in a well-defined and consistent environment are essential to complement full-scale investigations under static and flight conditions (Fig 2). They can be especially profitable not only for research, but also for detailed and safe studies of critical components and special problem areas; thereby expediting comparison of novel project concepts, exploratory development, and guarantees for in-service applications. Naturally, to ensure meaningful evaluation of the effects of forward-speed on aircraft noise characteristics, reliable measurements of related aerodynamic flow conditions as well as noise must be possible, so that correlation of the observed noise changes with variations in aerodynamic behaviour can be achieved.

Acoustic windtunnels, using 'fixed' models in an anechoic working-chamber enclosing a quiet airstream, in principle should provide the best approach to noise-model research work (basic and applied) and ultimately in direct support of specific aircraft projects; analogous to the extensive aerodynamic testing that is general practice nowadays. The special advantages of such tunnels in ensuring a more sheltered and controlled environment than outdoor mobile facilities (Section 2.1) include capability of continuous operation, repeatable test conditions, high productivity, good measurement accuracy, testing-flexibility and the precise alleviation of reflections from neighbouring surfaces. From analytical and experimental studies, most of the problem areas associated with subsonic tunnel design and usage for noise-model experiments have now been identified (Sections 2.2 and 2.3), their magnitudes critically assessed, and the special treatments or limitations involved have become quantifiable in many respects (Section 3). In particular, various parasitic noise fields which could mask the actual model noise measurements can be avoided by acoustic lining of the working-chamber to minimise reverberation effects, by acoustic treatment of the tunnel circuit to substantially reduce the intrinsic background noise associated with the tunnel drive, and by using special microphone and model-rig arrangements to minimise their self-noise and local interference in an airstream. Several acoustic tunnels with equivalent airstream diameters less than 3 m have already been built (eg Figs 3 and 4) and others are nearing completion (Section 2.4). However, apart from the desirability of good quality mainstream flow past the model in the test-section, a large tunnel size is advantageous from acoustic as well as aerodynamic constraint considerations. This has encouraged developments for the application of existing large tunnels, such as the RAE 24 ft diam. open-jet (Figs 5 and 15) and the NASA 40 ft x 80 ft closed-jet (Fig 6), and has influenced design specifications for new large tunnels.

Outdoor Mobile facilities of the Tracked-Vehicle type can be more usefully exploited (instead of flight vehicles) for noise testing of large-scale models or even full-scale investigations, using representative real engines and with simulation of the local airframe surfaces, and in principle with true 'in-flight' motion of the noise generator through a real atmosphere and past a stationary observer. Naturally, a variety of special testing problems have again to be clarified and quantified, such as measurement and analysis requirements under non-stationary conditions, parasitic noise and aerodynamic interference from the vehicle and model rig, and environmental effects (Section 4). Although feasible developments of the Earith Tracked Hovercraft Facility for aircraft noise research in the UK had to be terminated in 1974, much valuable experience was accrued for the critical appreciation and more reliable application of mobile facilities elsewhere and of allied flight testing techniques. The Bertin Aerotrain Vehicle (Model 02) has been developed in France for noise tests on its jet propulsion unit (now J85 engine), with the vehicle supported on a concrete inverted-T rail by air-cushion lift fans driven by a Turbomeca Palouste (Fig 7).

Other types of ground-based facilities (Fig 2) have also warranted serious examination for particular applications, each facility with its individual merits and problems (Section 5). For example, Rolls-Royce have successfully developed a 'Spinning-rig' (rotating arm), self-driven by a tip-jet, for model testing on the noise characteristics of high-speed jet nozzles and silencer arrangements (Fig 8). Road Vehicles, some already developed for aerodynamic model testing, have now been assessed for possible noise-model testing capabilities; they tend to be more limited in the speed and in the size of engine or model that could be carried, compared with linear-track vehicles, but the operating costs could be lower. Aircraft

Taxying (ground-run) along a runway represents another technique which has been the subject of preliminary trials. Aerial-Cable tracks, with a test noise source moving down a cable, have also been studied particularly by NASA. Free-flight model techniques could be further exploited, with noise models projected over a well-instrumented quiet range outdoors or through a large anechoic chamber. Recently, devices for static-rig fan-testing have also been developed in attempts to produce representative forward-speed aerodynamic conditions (distortion-free) at the fan inlet and yet not impede radiation of the acoustic signals.

More generally, for model-scale testing in all facilities, meaningful representation (qualitative and quantitative) of full-scale noise sources and radiation characteristics requires careful appreciation with respect to the specific research task. Fortunately, only partial simulation of propulsive engine or powered-lift noise sources is usually needed for studies of the primary changes due to forward speed. Even so there are significant problems including model-drive and model support implications (Section 6).

2 SUBSONIC WINDTUNNEL DEVELOPMENT AND OPERATION FOR NOISE-MODEL TESTING

2.1 Nature of Tunnel Merits

In view of the continuing demand for lower noise levels for aircraft, the recently established significance of forward-speed effects, and the need for combined acoustic and aerodynamic testing of possible configurations with noise-shielding or engine/airframe interactions, suitable 'acoustic' subsonic windtunnels are now considered essential to help establish reliable noise-testing techniques and some noise technology frameworks which are closer in quality to those already available for conventional aerodynamic investigations. The main advantages of windtunnels over external mobile facilities for such noise research are broadly similar to those often claimed aerodynamically.

Typically

- (a) Continuity of operation, allowing ready acquisition of statistically adequate samples, with steady signals from fixed points and with slow controlled traverses of measuring instruments (eg microphones) to map out fields.
- (b) Relative ease of providing or qualifying free-field conditions, subject to model or tunnel size constraints, while background noise in a well-designed acoustically-treated tunnel need not be higher than the self-noise level of a quiet moving vehicle.
- (c) Precise control and repeatability of the test condition, unaffected by the external environment, in a closed-return tunnel at least. Also the capability of providing controlled and repeatable measurements under transient conditions (eg jet thrust or fan pitch variation).
- (d) Flexibility, measurement accuracy and productivity of tunnel testing programmes, including the capability of making detailed aerodynamic measurements along with and essentially allied to the acoustic experiments.
- (e) The elimination or control of ground reflection effects and of pure Doppler effects arising from relative motion between the measuring point and the noise source simplifies the fundamental analysis of the experimental measurements considerably, though the problems of correction to practical flight conditions remain.

2.2 Tunnel Noise-Testing Considerations

The available experience on noise testing under forward-speed conditions and on associated techniques is still very limited at both model-scale and full-scale, as compared with extensive continuous aerodynamic testing over several decades. However, most of the problem areas associated with tunnel design and usage for noise-model testing (Tables 1 and 2) can now be identified and clarified, to expedite their treatment.

For adequate simulation at model-scale in tunnels or other facilities, the relevant geometrical and constructional features have to be selected for representation in relation to any aerodynamic, elastic and dynamic aspects particularly affecting noise generation, with overall consideration of scaling-factor implications. Some non-dimensional similarity parameters then have to attain values at model scale reasonably close to those of interest full-scale; eg Mach number, Reynolds number, and effective-speed ratios (blade-tip/airstream, or engine-flow/airstream). Essentially, shortfall in some of the parameter values may have to be accepted in practice as of secondary importance, and interpreted in the light of experimental variations of the parameter values and other experience. At the same time, other scaling factors such as selected Strouhal number (frequency parameter) and sound-level coefficients should be validated experimentally as applicable to full-scale practical prediction for the particular aircraft type of interest, for example by comparisons at different model-scales.

To relate the tunnel model experiments directly to conventional flight test conditions, an analytic framework also has to be specified for the appropriate frame-of-reference transformations. This must convert from the relative motions for the fixed model in the tunnel moving airstream with the microphones also fixed inside or outside the airstream, across to the moving aircraft in ambient still air with the microphones fixed on the ground. One current practice is simply to correct tunnel measurements for the absence of elementary Doppler shift effects on sound frequency, for the presence of elementary airstream convection effects on sound directivity angle, and for simple refraction effects through the airstream mixing boundary if external microphone locations are employed (Section 2.3).

Parasitic noise fields can be produced naturally by the testing environment (Fig 9), unless special precautions are taken. For windtunnels in particular, the following sources may be identified and alleviated:-

- (a) intrinsic background noise of the tunnel in operation, associated with the tunnel drive, circuit and mainstream flow (Sections 3.4 to 3.7);
- (b) reverberation caused by reflection of the model noise by the work-chamber boundaries (test-section enclosure) leading to limits on the acceptable frequency range and model-scale (Section 3.1);
- (c) spurious noise associated with flow over the measuring microphones (Section 3.6) and over the model supporting rig;
- (d) supplementary noise generation arising from deficiencies in the quality of the mainstream flow into the test-section and around the tunnel circuit, and from any flow variation with changes of powered model condition (Section 3.6).

For applicable analysis of model noise measurements, including extrapolation to full-scale far-field conditions, reliable noise-measurement should be achievable in the 'free-field' portion of the model-source far-field, where the sound pressure level varies almost inversely as the square of the distance (spherical radiation) apart from atmospheric attenuation (Fig 10). This 'free-field region' is bounded internally by the 'near-field' region of the noise source and externally by the 'reverberation-field' of the working-chamber, thus restricting the maximum permissible size of model and the minimum permissible size of the test-section from acoustic as well as aerodynamic considerations (Sections 3.1 to 3.3). Also, a minimum acceptable size of model can be determined by practical difficulties in achieving adequate microphone response and resolution simultaneously with high frequency noise measurements, as well as from representative-model constructional problems at small-scale.

Such tunnel-testing difficulties while significant can be overcome or alleviated by appropriate tunnel design modifications as discussed later (Sections 3.1 to 3.8) along with careful model specification (Section 6). If meaningful interpretation of the noise measurements for reliable application towards practical developments and improvements full-scale is to be ensured, some near-field noise measurements can often usefully complement extensive far-field measurements. More generally, as regards the investigation of airstream effects on model noise, some correlation of the observed noise changes with probable variations in aerodynamic behaviour should invariably be sought.

2.3 Microphone Location and Relative-Motion Considerations

A preference for microphone locations well inside the test-section airstream of a large windtunnel, for an open-jet such as the RAE 24 ft tunnel as well as inevitably for closed-jet tunnels, can follow from the need to make measurements as close to the noise source as far-field requirements may permit (Sections 3.1 and 3.2), or as near-field studies may require. Simultaneously, the effects of parasitic flow fields at or outside the mainstream jet boundary, ie other than those flows properly associated with the model condition, are then avoided on the model noise propagation characteristics. Thus, choosing for comparative purposes here a frame of reference fixed to a noise-model (Fig 11) there exists an elementary direct correspondence between noise measurements for the model fixed in an ideal tunnel airstream (effectively uniform and unbounded) and for the same model in steady level flight at the same relative velocity to the likewise ideal still air. Naturally for such ideal model test conditions in tunnel and flight, with the identical relative airflow velocity, measurements can directly correspond at the same microphone distance from the model, for the same sound emission angle θ (ie wavefront-normal inclination) to the direction of relative motion; there is then of course identity also of the 'retarded-time' from pulse emission at the model source to pulse reception at the microphone location. This careful distinction here between correlation of results from different test methods at the same value of the emission angle θ rather than of the 'convected' ray angle ψ , while seemingly trivial at first sight, becomes of vital practical significance for the meaningful comparison and physical interpretation of results at different flight and/or tunnel Mach numbers M and under static rig conditions. From simple relative airstream convection arguments

$$\tan \psi = \tan \theta (1 + M \cos \theta)^{-1}.$$

In real flight, this emission angle θ is of course the instantaneous line-of-sight angle from the conventional stationary observer to the aircraft (ie flight model) at the sound pulse emission time; as distinct from the 'convected' ray angle ψ which represents the instantaneous line-of-sight angle at the corresponding pulse reception time, varying with M even for constant source emission characteristics. In real tunnel tests, to ensure measurements for unchanged values of emission angle θ as tunnel airspeed is varied (including static conditions), the datum microphone locations (ψ values for assigned θ values) can be displaced geometrically downstream with increasing airstream Mach number, according to the foregoing convection relationship. With an extensive distributed source (eg jet efflux) the geometric far-field conditions may not be adequately achieved for the allowable microphone distance from the model, when strictly these angles should be related to several prescribed source elements in turn rather than to the model geometrical location. Even some rough checks, with simple source distributions based on theoretical arguments and other experiments (eg static), could usefully indicate the magnitude of possible errors due to the more convenient assumption of a single compact source at or near the model; see also Section 3.3.

To fully complete the practical equivalence (Fig 11), the microphone should not only occupy the same position relative to the model frame-of-reference at pulse reception time (ie identical θ), but ideally the velocity of the microphone relative to the model should also be unchanged. Now in principle, for the same θ , the acoustic pressure amplitude measured by a moving microphone is independent of its velocity relative to the source, though any pulse is then detected over a time period proportional to $(1 + M \cos \theta)$. Hence in practical terms, the stationary microphone with stationary model in the tunnel airstream measures the same proportional-bandwidth mean-square pressures (eg $\frac{1}{3}$ -octave) as the stationary microphone (conventional observer) with flight model (moving aircraft); strictly provided the tunnel airstream and flight Mach numbers are identical, for the same values of θ , and at the same microphone distance. Even so the tunnel-model frequencies then need to be multiplied by the Doppler factor:

$$(1 + M \cos \theta)^{-1}$$

to convert to the flight-model observer conditions with the separation speed Ma . More generally, to allow for essential differences in practice between the tunnel model microphone and the flight model observer distances, it is customary to appeal of course to the far-field inverse-square law, with $\Delta SPL \approx -6$ dB per doubling of distance. Additionally, conventional corrections to allow for atmospheric attenuation may be applied, typically

$$\Delta SPL \approx f/1000 \text{ dB per } 150 \text{ m distance.}$$

To reduce the wind-generated noise at the microphone located within the tunnel airstream, for much higher airspeeds than conventional ambient-wind conditions, a streamlined nose-cone with a circumferential axi-symmetric strip of fine wire mesh is usually substituted for the standard flat grid protecting the microphone diaphragm, replacing also the conventional spherical porous windscreen. The nose-cone and hence the axis of the microphone diaphragm are pointed directly upstream at any microphone location to minimise airflow disturbances. The microphone response corrections needed to give true free-field conditions are a function of both the sound frequency and sound incidence at the microphone. Additional free-field corrections for the presence of the nose-cone are often determined at RAE by datum microphone measurements made with and without nose-cone, for noise generated by the model at zero tunnel airspeed. Fortunately the omni-directional characteristics of the microphone tend to be improved by the addition of the nose-cone, though sound incidence effects are still large at high frequencies and calibration checks are still essential. There is also some justification for the expedient practical assumption that the local airflow over the microphone in the tunnel airstream does not significantly alter the microphone response to the sound received, with of course the nose-cone and streamlined support kept aligned along the local airstream direction.

Nevertheless, the future significance of any residual wind-generated noise at microphones located within the airstream of open-jet tunnels or closed-jet tunnels needs continually to be re-assessed, taking into account possible reductions in or discrimination of other parasitic noises and the available signal strengths from quieter or more complex model-sources. For example early exploratory studies in the RAE 24 ft tunnel implied that the wind-generated noise for microphones at locations well clear of the open-jet mixing boundary can be kept small relative to the existing background noise level of this tunnel, provided the microphone nose-cone is kept aligned within $\pm 10^\circ$ of the local airstream direction, and with careful attention to the microphone support structure. More recent analysis in relation to the provision and application of much quieter tunnels has confirmed that, unless very low turbulence levels are achieved, the pressure fluctuations associated with the turbulence in the airstream can determine the 'apparent' background noise levels of such tunnels, as indicated by a microphone (even with nose-cone) in the airstream. Indeed datum microphone measurements inside a very quiet small tunnel, but for very high turbulence levels (airstream u'/U of order 1% rather than conventional 0.1%), recorded SPL values as much as 20 dB higher than measurements well outside the airstream. Some further comments on this aspect can be found in the subsequent discussion of 'Tunnel flow quality requirements' (Section 3.6).

With an open-jet test-section inside a much larger acoustically-treated working-chamber, the microphones for far-field measurements can alternatively be located external to the airstream and well clear of the mixing boundary (Fig 20) so as to be in nominally still air; though at a greater distance from the noise source giving a correspondingly weaker signal strength relative to the background noise level. Moreover, possible falsification of the noise measurements needs to be assessed and allowed for, because of the intervention of the mixing boundary between the noise source (within the test-section potential core) and the external microphones.

As regards spurious refraction of sound propagated through the mixing boundary, and even possibly through weaker secondary flow regimes outside the mixing boundary, early RAE studies indicated that such effects were tolerably small and adequately assessable by qualitative ray theory arguments, for the low airstream speeds ($M < 0.15$) then feasible with acceptable background noise levels. More recently, precise theoretical treatments have been formulated by Amiet¹¹¹, Jacques⁶⁰ and others, in which the tunnel mixing boundary is modelled simply in terms of a thin vortex sheet of small thickness (compared with the incident-sound wavelength) between the uniform stream and still air without change in density across the shear layer (Fig 12). Essentially Amiet considers a plane interface and uses ray theory to derive equations which, conveniently for our purpose, permit sound pressure measurements p_m made at an apparent directivity angle θ_m and radius r to be corrected in both intensity and angle for 'ideal tunnel' conditions with the microphone immersed in an infinitely large airstream. Note that the effect of the refraction is not merely to change the ray direction from θ'_c inside to θ_c outside the airstream (Fig 12), but also the intensity through effective changes in ray spreading angle as well as distance. Fig 13 shows that the changes to corrected angle θ'_c from visual measurement angle θ_m , and the corresponding SPL changes $20 \log(p_c/p_m)$ for an equal radial distance r from the source, are certainly no longer small when the airstream Mach number is increased from 0.1 to 0.3 (and to 0.5) for $h/r = 0.15$, where h is the separation distance between the source and shear layer. With increasing M , θ'_c essentially reduces over the whole measurement angle range, while the SPL at equal radius increases over the whole of the forward arc (upstream of source) but decreases over most of the rearward arc. It should be observed that small angles to the airstream direction are not allowable in practice for measurements outside the airflow, because of the rapid variations in the corrections there, both in the forward and rear arcs; in the forward arc even at angles somewhat exceeding those for total internal reflection from the mixing boundary (ie even outside the 'zone of silence').

Additionally, the model noise propagation may be subject to frequency and spatial scattering at the test-section mixing boundary, or can augment noise generation from the turbulent mixing itself. Early RAE experiments again implied that the practical effects were small, at least up to the maximum frequency of 10 kHz and for low airstream Mach numbers ($M < 0.15$) then tested. But such scattering effects are envisaged primarily as high frequency phenomena, affecting sound propagation at wavelengths less than the turbulence length scales within the mixing region. Indeed, for $M \approx 0.2$, noticeable broadening of a pure

tone at about 24 kHz has been displayed by measurements made well outside the mixing boundary of the UTRC tunnel¹¹², while as much as half the transmitted intensity across a shear layer at very small wavelengths has been attributed to scattered waves from experiments by ONERA¹⁸.

Overall, the complex nature and larger thickness of the mixing boundary needs to be properly appreciated in practical terms, including the influence of any tabs incorporated round the tunnel nozzle periphery to ensure airflow stability, so that representation by simple thin shear layers seems only an expedient gross approximation to the true airflow conditions. At this stage, the available theories and limited measurements should be used for qualitative guidance rather than precise corrections, preferably towards defining the test conditions for acceptably small corrections on the noise changes with forward speed under investigation.

2.4 Specific Tunnels for Noise-Model Testing

Within the past five years several acoustic windtunnels have been specially built or existing aerodynamic tunnels correspondingly modified, to provide simultaneously an anechoic working-chamber and low background noise at the test-section with the tunnel in operation. But these existing acoustic tunnels are small with equivalent test-section airstream diameters less than 3 m. The test-section and working-chamber measurements, quoted below in metres, refer either to the diameter x length, or to width x height x length; supplementary dimensions quoted in feet signify only the original designation of the tunnel. Sometimes alternative test-sections may be available, either smaller and faster, or both closed and open. The specific references quoted here give more detailed specifications of the particular tunnels. Overall analysis of considerations arising in the design and application of acoustic tunnels is contained in Sections 3.1 to 3.8. The provision of very small 'free-jet' tunnels by simple adaptation of anechoic chambers with existing capability of static noise-testing on jets should also be noted, the major jet efflux of largest available diameter then being employed as a mainstream flow, for example about a model jet co-axially centred but of much smaller diameter (see Section 3.3).

American acoustic tunnels already include:-

- (1) Naval Ship Research and Development Center (NSRDC, 1971)^{101,102}
Open-section 2.4 m diam. x 3.5 m; max airspeed 60 m/s; closed-return.
Working-chamber 7.2 m x 7.2 m x 6.3 m; cut-off 150 Hz.
- (2) United Technologies Research Center (UTRC/UARL, 1971)¹⁰⁸
Open-section 0.8 m x 0.5 m x 4.8 m; max airspeed 200 m/s; atmos-return
Working-chamber 6.7 m x 4.9 m x 5.5 m; cut-off 200 Hz.
- (3) Massachusetts Institute of Technology (MIT 5 ft x 7 ft modified, 1971)¹¹⁵
Open-section 2.3 m x 1.5 m x 2.4 m; max airspeed 35 m/s;
Working-chamber 2.3 m x 1.5 m x 2.4 m; cut-off 600 Hz.
- (4) Bolt, Beranek and Newman (BBN, 1975)¹²⁸
Open-section 1.2 m x 1.2 m x 10 m; max airspeed 45 m/s; atmos-return.
Working-chamber 7.0 m x 6.1 m x 13.2 m; cut-off 160 Hz.
- (5) Lockheed-Georgia (LG, 1975)⁹⁵
Open-section 0.76 m x 1.1 m x 2.9 m; max airspeed 75 m/s; atmos-return.
Working-chamber 3.4 m x 5.2 m x 3.4 m; cut-off 200 Hz.

European acoustic tunnels include:-

- (6) Southampton University (SU 7 ft x 5 ft modified, 1975)⁶²
Closed-section 2.1 m x 1.5 m x 4.4 m; max airspeed 30 m/s; closed-return.
Working-chamber as test-section; cut-off 500 Hz.
- (7) RAE Farnborough (RAE 5 ft modified, late 1976)⁴⁴
Open-section 1.5 m diam. x 2.8 m; max airspeed 65 m/s; closed-return.
Working-chamber 3 m x 3 m x 3 m; cut-off 500 Hz.
- (8) CEPR Saclay (CEPR/ONERA, early 1977)¹⁴
Open-section 2.0 m diam. x 9.0 m; max airspeed 100 m/s; atmos-return.
Working-chamber quarter-sphere 9.6 m radius; cut-off 200 Hz.

Other existing aerodynamic tunnels of small-to-medium size have also been given partial acoustic treatment, either around the test-section boundaries or inside the tunnel circuit. These include:-

- (1) NASA Ames 3.0 m x 2.1 (7 ft x 10 ft) closed-section.
Test-section acoustic lining.
- (2) NASA Lewis 4.6 m x 2.7 m (9 ft x 15 ft) closed-section.
Tunnel circuit acoustic inserts.
- (3) Boeing-Seattle 2.7 m x 2.7 m (9 ft x 9 ft) closed-section.
Test-section acoustic lining.
- (4) VKI Brussels 3.0 m diam. open-section⁶.
Working-chamber acoustic lining.
- (5) DFVLR Porz-Wahn 3.3 m x 2.2 m open-section²⁴.
Tunnel circuit acoustic inserts.

The only large European tunnel currently incorporating acoustic treatment is the RAE 24 ft tunnel with its open test-section 7.3 m diam. x 13 m length, max airspeed 50 m/s, and closed return-circuit. The working-chamber boundaries (13 m x 10 m x 13 m) are now lined with sound-absorbing foam sheet and wedges to provide a cut-off frequency as low as 200 Hz. This 40-year tunnel has been employed successfully since 1971 for a variety of basic noise-model investigations and for the improvement of associated testing

techniques^{35,41}. Nevertheless, it is important to stress that the available maximum airspeed of 50 m/s is not usable for noise-model testing in general, because the tunnel background noise becomes excessive at airspeeds much above 30 m/s. Furthermore, at all airspeeds, the aerodynamic flow quality is considered to be relatively poor by modern tunnel standards, so is unlikely to satisfy future noise research demands. Some acoustic and aerodynamic studies made to assess possible practical modifications to the 24 ft tunnel circuit and the 5 ft scale-model⁴⁴, in order to at least double their usable noise-model testing speeds, can conveniently be referred to later to illustrate some major considerations arising in the design and application of acoustic tunnels more generally.

In the USA, at least two large aerodynamic tunnels have already been used for noise-model testing. The NASA Langley 30 ft x 60 ft tunnel, with its open elliptic test-section 18 m x 9 m x 17 m length, max airspeed 45 m/s, and closed return-circuit, now has its working-chamber boundaries (34 m x 23 m x 21 m) lined with foam sheet providing a cut-off frequency about 500 Hz⁶⁹. Again, the usable airspeeds for noise-model testing in general reasonably cannot much exceed 30 m/s, while the airflow quality must leave much to be desired in this very old tunnel. The NASA Ames 40 ft x 80 ft tunnel, with its closed test-section 24 m x 12 m x 24 m length, max airspeed 95 m/s, and closed return-circuit has rather limited acoustic lining of the test-section boundaries and sometimes none⁸⁵, but special microphone arrays and other schemes are used for discrimination against reverberant field and background noise levels⁸⁶. Planned improvements to this tunnel (Fig 6) include the installation by 1980 of low-noise fans with much greater drive power to provide the existing test-section with higher max speed (24 m x 12 m, 150 m/s), and the incorporation of an additional circuit leg with much larger test-section (36 m x 24 m, 55 m/s).

More generally, research is now being carried out on the possibility of limited noise-model testing in modern aerodynamic tunnels, with minimum or no acoustic treatment of mainly closed test-sections and closed return circuits, but taking advantage of their outstanding airflow qualities (turbulence $u'/U \approx 0.05\%$) and higher maximum airspeeds (>100 m/s). Experimental investigations, for expediency usually in small tunnels at this stage, naturally include the exploitation of directional acoustic receivers and other discrimination/correlation techniques, to extract the true source signal from test-section reverberation effects, tunnel/rig background noise, and instrumentation parasitic noise (in the airstream). Ultimately, other existing aerodynamic tunnels of comparable size to the 24 ft may be profitably employed for aero-acoustic studies on noise-models using such techniques, appreciating that the latter techniques tend to introduce much greater complexity of measurement, and that other noise-field diagnostic capabilities may be impaired.

Such tunnels could for example include:-

- (1) ONERA Modane S1 Ma 8 m diam. closed-section, max airspeed 350 m/s.
- (2) RAE Farnborough 5 m x 4.2 m closed-section, max airspeed 110 m/s.
- (3) NASA Langley 6.6 m x 4.4 m closed or open-section, max airspeed 100 m/s.
- (4) Boeing-Vertol 6.1 m x 6.1 m closed or open-section, max airspeed 130 m/s.
- (5) Lockheed-Georgia 7.1 m x 4.9 m closed-section max airspeed 110 m/s.
- (6) NAE Ottawa 9.1 m x 9.1 m closed-section, max airspeed 60 m/s.

New large subsonic-tunnels, though intended primarily for improved aerodynamic testing, are clearly also of importance for noise testing. In particular, the DNW German-Netherlands windtunnel³⁴ is now to be built by 1980 at MLR (North Polder), with interchangeable closed and open test-sections 8 m x 6 m x 18 m length, max airspeed 100 m/s, and closed return circuit (contraction-ratio 9). For aerodynamic testing, alternative closed test-sections may also be provided, probably $9\frac{1}{2}$ m x $9\frac{1}{2}$ m with max airspeed 55 m/s, and 6 m x 6 m with max airspeed 130 m/s. A 'ventilated' working-chamber acoustically lined will be provided for noise testing with the 8 m x 6 m open test-section configuration. The tunnel is expected to provide a reasonably quiet test-section primarily because the drive-fan has been designed with a lower tip-speed and more moderate aerodynamic loading than previously, presumably accepting other penalties. But acoustic inserts within the tunnel circuit to further reduce background noise at the test-section will probably be limited to absorber treatment of the corner vanes, to preclude large power-factor penalties and other constructional difficulties.

The possible 'European low-speed tunnel' recently studied by the AGARD LaW's Group^{2,4}, was recommended to have a closed test-section of up to 25 m x 19 m and a maximum airspeed of 130 m/s. From a noise-model testing viewpoint the largest possible atmospheric design (with facility for providing an open test-section) would be preferred rather than a smaller pressurised version and restrictive closed test-section, while a quiet drive with some acoustic treatment of the tunnel circuit and test-section would be wanted assuming that the aerodynamic or cost penalties were tolerable. Admittedly, since such a tunnel now seems unlikely to be completed for at least a decade, directional acoustic receivers together with other new discriminatory techniques may by then prove sufficiently practical and flexible to allow substantial relaxation of such acoustic treatments (for special tests at least), though other noise-field study capabilities could become correspondingly impaired and more complex.

While it would be unrealistic to suppose that such a LaW's tunnel (25 m x 19 m) would satisfy all the development requirements of the next two or three decades, the cost-benefit justification of proceeding upwards to the next much larger size (60 m + tunnel) to ensure near full-scale noise testing could be questioned. This could in part depend on the progress made with noise-reduction and testing techniques in the meantime, and on whether much greater reductions than say 10 dB below the current standards of FAR Part 36/ICAO Annex 16 will even then be demanded in view of associated economic penalties. Moreover, it could be argued that, by the time such a very large tunnel (60 m +) could be made available in Europe for extensive noise testing (? 1990 +), the remaining demands from a noise-testing viewpoint could be more reasonably met then by an intelligent combination of other large acoustic and aerodynamic tunnels (then available), complemented by tracks, other ground-based facilities and in-flight testing, all integrated with much more advanced theoretical frameworks (Fig 2).

3 SPECIAL FACTORS IN ACOUSTIC TUNNEL DESIGN AND APPLICATION

3.1 Acceptable Frequency Range and Model-Scale

Anechoic chambers have long been exploited for conventional acoustic research, to provide a controlled and sheltered environment in which the generation and propagation characteristics of noise sources can be studied consistently in the absence of confusing reflections, and where far-field properties (as well as near-field) can be accurately measured if the chamber is sufficiently large relative to the wavelength and spatial extent of the source. In principle, similar techniques can be employed in the anechoic design and application of windtunnel test-sections for aircraft noise research, though a variety of special testing requirements can then arise as discussed throughout this paper.

As a rough working rule for the acoustic treatment of tunnel test-section boundaries, adequate absorption of incident sound energy can be achieved by foam sheet covering (thickness t) for wavelengths up to $\lambda_{\max} \approx 2t$, or by foam wedges (height h) up to $\lambda_{\max} \approx 5h$. Nevertheless in practice there can be significant regions which are not amenable to appropriate acoustic treatment for aerodynamic or structural reasons, including downstream or upstream facing areas in or at the ends of the tunnel circuit; these surfaces can cause troublesome reflections unless they are at relatively large distances away from the model noise source and measurement points. For open-jet tunnels, an adequately anechoic test-section can be provided without appreciable aerodynamic interference on the test-section airflow, simply by appropriate acoustic lining of the large working-chamber well clear of the open-jet boundaries; but acceptable treatment of the collector entry and of any supporting structure for the jet nozzle can be difficult. For closed-jet tunnels, the acoustic lining of the test-section tends to be more limited because the surface presented to the airflow has to be relatively smooth, streamlined and hard-wearing. The outer covering should preclude objectionable aerodynamic interference with the test-section airflow, or the generation of additional airflow noise, while not impairing the sound absorption efficiency of the particular scheme nor allowing deterioration due to long-period scrubbing effects.

The full-scale frequency range (F_{\min} to F_{\max}) of subjective interest for the prediction of perceived noise levels is typically from 50 Hz to 10 kHz. The lower limit on measurement frequency in model tests (f_{\min}) is usually prescribed by the increasing difficulty of providing an adequately anechoic test-chamber at lower frequencies, though the problems are more tractable with an open test-section (cf closed) since the acoustic treatment of the solid boundaries (walls) is then far-removed from the test-section airflow. The upper frequency limit in model tests (f_{\max}) is usually determined by the reductions in microphone size necessary to ensure adequate frequency response and spatial resolution at the higher frequencies, though with reduced signal strength, and by the problems of adequate allowance for atmospheric attenuation and directivity corrections with the higher frequency. Now, from non-dimensional parameter considerations, frequencies should scale inversely as the corresponding linear dimension (full-scale L or model-scale ℓ) at the same airspeed. Hence, to ensure an adequate frequency range at model scale of full-scale subjective interest,

$$f_{\min} \ell \leq F_{\min} L \quad \text{and} \quad f_{\max} \ell \geq F_{\max} L;$$

thus, the permissible model size is correspondingly limited if full-scale needs are to be covered, in that

$$F_{\min}/f_{\min} \geq \ell/L \geq F_{\max}/f_{\max}.$$

For example, to preclude troublesome source-noise reflections at the microphone measurement points in the RAE 24 ft tunnel, some sound absorbing wedges 0.3 m high have now been added over critical areas, on top of the foam sheets 0.075 m thick which already line the boundaries of the chamber housing the open test-section (Fig 15). The results of tone burst tests (Fig 19) have validated estimates that this combined sound-absorption treatment should now be effective for source-noise frequencies down to 200 Hz instead of the earlier 2 kHz with the foam sheets only. Moreover, recent experience from noise-model tests has confirmed that any noise reflections inside the acoustically-treated working-chamber are indeed negligible in practice down to 200 Hz, except possibly in the forward arc which can be affected by the presence of large untreated areas of the corner immediately upstream. The downstream-facing concrete-wall of the corner appears to act as an efficient reflector of low frequency noise (<1 kHz) from models in the test-section, with the corner vanes acting fortunately as a wave guide for the higher frequencies.

The accuracy of measurement using a combination of $\frac{1}{2}$ in and $\frac{1}{4}$ in diameter microphones might also be adequate with extreme care up to about 80 kHz, tolerating some fall-off in precision at high frequencies with low PNL weightings. Thus, using the preceding inequality relation for ℓ/L , with the declared practical frequency ratios

$$F_{\min}/f_{\min} = 50 \text{ Hz}/200 \text{ Hz} \quad \text{and} \quad F_{\max}/f_{\max} = 10 \text{ kHz}/80 \text{ kHz},$$

models of linear scale between $\frac{1}{4}$ and $\frac{1}{2}$ full-scale could be tested over the whole frequency range of practical interest in the 24 ft tunnel test-section; if of course compatible on other aero-acoustic counts, as discussed later. Such arguments are not intended to decry the usefulness of smaller-scale or larger-scale models, particularly over more limited ranges of frequency; but rather to stress the importance of matching the model size and measurement frequency range to the capabilities of the particular anechoic chamber and of the available instrumentation, and to clarify needs to improve the relevant capabilities. More generally, the model size has to be made compatible also on a variety of other aero-acoustic counts, as discussed in the following sections.

3.2 Acoustic Constraints of Test-Section Size and Type

The extent of the near-field region from the noise model depends in general on the noise source type (monopole, dipole, quadrupole) and the intensity. But, for a compact noise, it is roughly of the order of one or two wavelengths. Thus, to ensure that the acoustic far-field noise conditions (spherical radiation) are attained within the test-section airstream (radius R_{air}), the latter must extend to say at least 1.5 times the maximum wavelength λ_{\max} ($= a/f_{\min}$) of interest from the model noise source.

Moreover, to provide measurement conditions free of the boundary near-field interference effects, the measurement points should be located at least a distance (R_{mic}) of say $0.3 \lambda_{max}$ from any acoustically treated wall or airstream 'free-jet' mixing boundary. Hence, as illustrated diagrammatically by Fig 20, for a centrally located compact noise source,

$$R_{air} > 1.5 \times (a/f_{min}) \text{ and } R_{mic} > 0.3 (a/f_{min}) .$$

The advantages of employing a large test-section are clearly evident from this aspect of permitting adequately long wavelengths (low frequencies), appropriate to large model size.

For example, in the RAE 24 ft tunnel the radius of the uniform airstream is at least 3 m, the thickness of the free-jet mixing boundary is about 1 m, and the acoustically-treated walls of the surrounding chamber are more than 2 m distance outside this mixing boundary. Thus, for model noise source locations close to the test-section axis as for example with a centrally-mounted small jet or fan, microphone measurements of far-field noise should be feasible inside the uniform airstream region for source-noise wavelengths up to about 1.7 m ($3 \text{ m}/1.8$); and possibly outside the airstream for wavelengths up to about 2.0 m ($3 \text{ m}/1.5$). On this basis therefore, measurement frequencies down to at least 200 Hz ($340 \text{ m/s} + 1.7 \text{ m}$) could be envisaged without significant restrictions due to far-field and free-field requirements; taking full advantage also of the existing acoustically-treated working-chamber with its acceptable 'anechoic' properties down to 200 Hz, appropriate to models up to $\frac{1}{4}$ scale (Section 3.1). Correspondingly, for aircraft models with a noise source as far out as halfway from the test-section centreline to the airstream boundary or about 1.5 m from both, measurement frequencies down to at least 400 Hz (up to $\frac{1}{8}$ scale) could be tolerated.

An open airstream boundary can also allow some noise measurements well outside the test-section airstream, with the microphones in nominally still air while still remaining within the acoustically-treated working-chamber (Fig 20). Such 'outside' measurements are subject to considerations of relatively weaker signal strength at the more distant measurement points and to some doubts concerning corrections for noise propagation characteristics across the airstream mixing boundary, as discussed in Section 2.3. On the other hand, for a model size prescribed as acceptable from the acoustic wavelength constraints related to airstream size as here and also from aerodynamic constraints, such outside measurements can reduce geometrical far-field corrections associated with spatially large distributions of model noise sources, as discussed in Section 3.3. In the RAE 24 ft tunnel the present acoustic curtain could then be withdrawn, with the whole hangar space cleared and critical parts given acoustic treatment, to provide a large addition to the anechoic working-chamber space to one side of the airstream⁴⁴. In the UTRC acoustic research tunnel, with an airstream equivalent diameter of only about one-tenth the RAE 24 ft, far-field noise measurements are invariably made outside the airstream and typically at distances some three airstream diameters away from a model located on the airstream centre-line¹⁰⁰.

3.3 Acoustic Constraints of Model Geometry and Type

With practical models, as distinct from single compact noise sources, the finite geometry and character of the spatially large distribution of noise source elements across and along the tunnel airstream need to be allowed for to ensure attainment of far-field measurements. For then, the extent of the near-field of the distributed noise source depends strongly not only on the wavelength (or frequency) of interest, but also on the relevant characteristic dimension of the noise source and the possible variation of predominant frequency and sound power along its extent. Indeed, the choice of characteristic dimension itself could vary with the frequency band and noise measurement direction of primary concern. The formal specification of general working rules for predicting the near field limits for practical noise models covering our interests is thus still difficult. Nevertheless, this feature can be of particular concern in the sizing of ground-based testing facilities and of the models to be tested in them.

As a simple example, it could be postulated crudely that adequate geometric far-field measurements could be achieved (say within $\pm 3 \text{ dB}$) at distances from the model source distribution exceeding some multiple of the source characteristic dimension (eg > 5 times); effectively restricting the allowable subtended angle by the source distribution at the measurement microphone location (within $\pm 5^\circ$). Correspondingly, the characteristic dimension for fan-intake noise could reasonably be assumed to be of the order of a fan diameter ($> d_{fan}$) centred geometrically about the intake axis; or, for jet-efflux noise, of the order of several jet exit diameters ($> 5 d_{jet}$) centred geometrically a few jet diameters downstream of the nozzle exit, according to the frequency bandwidth of interest. Then if far-field conditions have to be sensibly achieved within the test-section airstream radius R_{air} (Fig 20), for a simple fan or jet model centrally located

$$D_{air} = 2R_{air} > 10d_{fan} : \text{ or } D_{air} > 50d_{jet} .$$

Again, on these crude arguments, a typical value $D_{air} \approx 6 \text{ m}$ for the 24 ft open-jet tunnel (excluding the mixing boundary) would imply the acoustic model constraints

$$d_{fan} < 0.6 \text{ m} : \text{ or } d_{jet} < 0.12 \text{ m} ;$$

which could well imply models smaller than $\frac{1}{4}$ -scale. Thus such a model 'geometric' size constraint can become as significant as the 'wavelength' constraint of the preceding section. More generally, other relevant factors such as model/rig difficulties and aerodynamic constraints also have to be allowed for at the same time.

For an open-jet tunnel, with the test-section airstream surrounded by a much larger anechoic chamber, it could be argued that full development to such geometric far-field conditions need not be achieved until well outside the airstream jet-mixing boundary. Then, because of the alleviation on the foregoing constraint arguments, relatively larger models might be permitted, assuming of course that other acoustic wavelength constraints, aerodynamic constraints and avoidance of distortion of the airstream boundary are not already limiting factors. Nevertheless, the use of microphone locations outside the airstream mixing boundary can introduce doubts concerning noise propagation characteristics across the

varied and complex flow field between the model source and the microphone (Section 2.3), particularly if the source-noise characteristics are unknown or varied.

An interesting illustration is in the use of a small 'free-jet' tunnel for testing of a model-jet coaxially-centred on the mainstream jet, with the need to achieve a model-scale as large as possible without excessive testing constraints. Here, from turbulent jet-flow development concepts and practical experience, it can be argued that the aero-acoustic interference of the mainstream-jet development on the model-jet source-noise generation is only negligible if the ratio of mainstream-jet diameter to model-jet diameter is at least 10. However, unless this diameter ratio is even much greater (> 50 say), far-field measurement will necessitate microphone locations well outside the mainstream rather than within. Then the noise-propagation corrections associated with refraction effects through the mainstream external mixing boundary can be substantial for realistic Mach numbers; see Section 2.3 and Fig 13. Of course the problem becomes much more complex and the available corrections more questionable if the model-jet is inclined to the mainstream or off-centre, or if airframe installation/interaction effects are to be explored.

Overall, in any practical noise experiments, it is advisable to explore the sound field at different distances as well as different directions from the model, in order to establish that adequate far-field conditions have been reached at the measurement points to the standard of accuracy required. More specifically, further quantification of the type of constraints raised in this and the preceding section could now profitably follow from a declaration and critical analysis of relevant experimental and theoretical results, supplemented by some specially directed and carefully controlled explorations of noise fields during future model testing programmes in acoustically-treated tunnels. There is an urgent need for such reliable guide-lines to expedite more profitable designs of models, facilities and experiments for investigating forward-speed effects on noise. Even static test results for elementary models (if precise) could help the formulation of useful working limits for far-field measurement locations under forward-speed conditions, in the light also of reasonable theoretical concepts; for example from diagnostic field studies on small-scale models in large anechoic chambers.

3.4 Tunnel Background Noise

Typically, the background noise level in the tunnel test-section or working-chamber must be 10 dB or more below the model source noise, over the frequency range of interest at the measurement points, to ensure adequate resolution (within $\frac{1}{2}$ dB) of broadband spectra without reliance on special discriminatory techniques. Large-scale models are of course required for good aero-acoustic similarity and to preclude microphone measurement problems at high frequencies, but tunnel background noise tends to increase at lower frequencies and anechoic chamber demands become more difficult. Furthermore, it is worth noting that the source noise levels available for measurement at acceptable microphone locations may not increase with greater model-scale, if far-field limitations at the correspondingly lower frequencies for similarity necessitate also correspondingly greater microphone distance from the source. The principal factors contributing to the background noise are included in Fig 9 as part of the interacting acoustic/aerodynamic elements associated with model noise measurement in windtunnels.

External ambient noise effects may warrant particular consideration in the design of open-return (straight-through) tunnels and for test-sections not protected by an acoustically-treated working-chamber. Structural transmission of mechanical vibration and motor noise from the tunnel drive system may require special precautions, but problems can be avoided by heavily constructed and damped components with appropriate isolation joints. Minimisation of model rig noise may need special attention when air has to be supplied to model jets and fans, or to resonance-type generators, since internal airflow noise from valves and pipework has to be avoided, along with externally-generated noise from possible vortex shedding and other aerodynamic interference by supporting structure/wires. Spurious noise can likewise be generated by measurement devices and their supports located in the airstream, but the influence of turbulent airstream pressure fluctuations on the noise recorded by the microphone (Section 3.6) or of microphone support vibrations tends to be of more practical concern.

The residual background noise elements, apart also from possible working-chamber boundary constraints on model noise propagation (Section 3.2), may be considered to make up the intrinsic background noise associated with the tunnel-fan and circuit aerodynamics. In general, the design characteristics needed for a good aerodynamic tunnel with uniform low-turbulence flow in the test-section tend also to help towards providing a quiet tunnel, by minimising unsteady separated flow conditions around the circuit and by careful aerodynamic design of the fan-in-duct combination. Again, for aerodynamic reasons, anti-turbulence screens and honeycombs are usually located in low-airspeed regions, so they need not create any significant self-noise problems with a reasonable tunnel contraction-ratio (say > 6). However, the possibility of embarrassing self-noise generation by other tunnel flow-control devices must be kept in mind; for example, essential turning vanes and support struts/wires in the circuit flow must be designed or damped to avoid intrusive noise due to 'singing'. Equally well, any inserts for acoustic treatment should neither promote significant self-noise in the flow (Section 3.5), nor introduce troublesome wakes.

In respect of choice of test-section type, with either free or walled boundaries at the edge of the airstream, the open-jet at first sight would appear the more attractive for low background noise levels. The noise emanating from the contraction nozzle and the collector/diffuser can then radiate freely (at least hemispherically out of the test-section) along with that from the model under test, without significant reflection from the acoustically-treated distant boundaries of the surrounding large working-chamber. In principle the achievable lower limit to background noise may then be expected to be set by the broadband quadrupole-type noise produced by the turbulent mixing at the free-jet boundary, for measurement points well within the airstream or several diameters outside. However, a special feature for most open-jet tunnels is the apparent need for 'tabs' protruding from the jet-nozzle periphery into the airstream, and/or for venting of the collector by a cowl or wall slots, in order to preclude possible mainstream jet instability and low-frequency unsteadiness over the operational speed range (Section 3.8). For very quiet tunnels, aero-acoustic problems may then include the possible excess noise and jet-boundary thickening from such tabs, collector noise from jet impingement and its possible variation with

aerodynamic model testing condition, and adequate sound absorption treatment of the collector-entry/cowl still satisfying aerodynamic and structural needs. Correspondingly for closed test-sections, excess noise can be generated by the high-speed airflow over the test-section walls, especially with acceptable acoustic lining which itself may be of limited effectiveness because of other aerodynamic constraints, while other spurious noise and aero-acoustic constraints can be associated with the essential location of even the far-field microphones in the airstream.

The tunnel airflow-drive represents of course the primary source of background noise in the test-section, unless especially designed to have low noise characteristics (Section 3.7), and located far enough away from the test-section that sufficient circuit length is available in-between to permit adequate in-duct sound-absorption treatment (Section 3.5), with tolerable aerodynamic performance penalties. For example the RAE 24 ft tunnel, with an old design of tunnel fan at the collector end of the test-section (Fig 15), has its usable speed (acceptable background noise) restricted to below 30 m/s for the study of the practical noise sources associated with the low velocity jets (Fig 21) and quiet fans of modern engines, while airframe noise is completely swamped at least in the far-field. As expected for predominantly dipole-type sources, the overall sound-pressure level of the measured background noise increases almost as V_T^6 (Fig 22), being nearly 15 dB higher at $V_T = 50$ m/s (present top-speed) than 30 m/s. To ensure that noise spectra and directivity patterns can be simulated more correctly at model-scale or can be extrapolated with greater confidence to full-scale, tunnel usable speeds and Mach numbers should approach more closely those for take-off and landing, eg at least 50 m/s (100 kn) and preferably up to 100 m/s (200 kn).

Comparison of background noise studies in the RAE 24 ft tunnel (7.3 m diam.) with those in the 5 ft scale-model tunnel (1.5 m diam.) show that the two noise spectra are not only similar in shape (Fig 23), but also yield almost identical sound pressure levels when compared at the same airspeed and the same values of Strouhal number, here defined as the product of frequency and test-section diameter divided by airspeed. Such results have given us considerable confidence to now modify the small 5 ft tunnel, for acoustic tunnel research including some new aspects of quiet fan-in-duct design and circuit acoustic treatments, as well as for direct aerodynamic and acoustic checks on possible profitable improvements to the large 24 ft tunnel (Figs 16 and 17).

As a convenient illustration and measure of the low levels of tunnel background noise which can be achieved in practice, the sound pressure levels for the successful small acoustic tunnels built at UTRC (effective jet diam. 0.7 m) and NSRDC (2.4 m) are as much as 40 dB lower than for the existing untreated tunnels, when compared at the same speed and at the same Strouhal number (Fig 24). Broadly speaking, as regards acceptable standards of background noise levels, representative powered models suitable for far-field noise experiments in such acoustic tunnels can usefully be tested at airspeeds up to 50 m/s at least, without significant background noise problems and without the need for discriminatory techniques. However, spurious noise generated by the model-rig and in-flow microphone support (unless properly streamlined) can now even exceed the intrinsic background noise of the quiet tunnel and also exceed the airframe self-noise from a clean unpowered model, all usually rising together with increase in tunnel airspeed.

3.5 Noise Absorption Treatment of Tunnel Circuit and Aerodynamic Implications

The design of in-duct sound-absorption treatments has progressed considerably for commercial ventilation systems, where airspeeds are usually low (≤ 10 m/s) and airflow quality seems a minor consideration. However, significant unknowns and restraints can arise in attempts to apply efficiently and economically such techniques to substantially reduce tunnel background noise by internal-circuit treatments between the drive-fan and the test-section, especially with the much higher airspeeds involved. Some compromises in wall-lining and splitter designs, are essential because of the following factors:

- Local airspeeds and airstream pressure losses tend to rise with silencing efficiency over a wide range of frequency, because of the more extensive circuit-flow blockage and larger wetted areas, even with careful streamlining. Broadly speaking the absorption of high-frequency noise requires closely-spaced splitters, whereas low-frequency absorption demands greater lengths.
- Low airstream-pressure losses are needed to ensure high airspeeds in the test-section with acceptable power and cooling requirements.
- Objectionable self-noise and reductions in-absorption efficiency can be caused by high speed airflow over the absorber surface areas.
- Reductions of absorber efficiency may be associated with the needs for surface protective covering and structural integrity in high-speed airflows without costly maintenance over a period of several years.

Such considerations suggest that the most favourable tunnel-circuit locations for the application of sound-absorption techniques are where the airspeed is near the minimum, ie in the settling chamber upstream of the contraction and after considerable diffusion well downstream of the test-section, commensurate of course with the fan location, and with the circuit type and geometry. However, for acoustic modifications to existing aerodynamic tunnels, or for the design of new dual-purpose tunnels where aerodynamic-model testing still has much greater priority than noise-model testing, other conflicting practical aspects and economic constraints can be limiting factors.

To illustrate practical acoustic treatment considerations, some design factors of acoustic splitters will be briefly outlined and conveniently quantified in the context of some feasible practical modifications to the RAE 24 ft tunnel circuit, retaining the existing concrete shell and anechoic working chamber (Fig 15). Envisaged modifications to the internal circuit⁴⁴ naturally centre on the provision of a new low-noise fan re-located in the back leg, instead of immediately downstream of the test-section, so that duct length also becomes available upstream and downstream of the fan to enable sound-absorption treatment to be incorporated as required. The two typical schemes shown in Figs 16 and 17 both include uniform blocks of low-frequency and high-frequency splitters as part of the multi-passages diffuser downstream of the fan, but the upstream arrangements are radically different.

The first scheme, essentially maintaining the large test-section size (7.3 m diam.) with the low contraction-ratio (3.5/1), locates similar blocks of low-frequency and high-frequency splitters in the first diffuser because primarily a sufficient straight-length is available only there in practice (Fig 16); then representing a reasonable compromise between acoustic efficiency and duct airflow pressure loss without producing significant airstream distortion. However, since the circuit airspeed is highest in the first diffuser, splitter self-noise there may become a serious design factor, as well as splitter aerodynamic drag which raises appreciably the tunnel drive power required for a prescribed test-section speed. The possibility of making the splitters sinusoidal along their length to achieve increased sound attenuation by elimination of 'line-of-sight' through the block is precluded here by lack of length when adapting this existing facility, but it might be worthwhile to take advantage of the change of duct direction through the first and second corners.

The second scheme, accepting an appreciably smaller test-section size (eg 5.5 m diam.) to provide a worthwhile increase in contraction-ratio and hence improvements in top speed and flow quality, inherently decreases the circuit volume flow rate and likewise the required fan tip-speed (nearly halved). So fan-generated noise and splitter self-noise are also reduced for a given test-section speed, alleviating the acoustic treatment required to achieve the prescribed background noise level in the test section. Thus, in Fig 17, no acoustic treatment is attempted in the first diffuser, but all the duct surfaces through the first and second corners are chosen to be of absorptive material to take advantage of directivity effects, while treatment of the turning vanes in the second corner at least should be beneficial. Perhaps two acoustic splitters of unequal length might also be added between the first and second corners, spaced unevenly in an attempt to equalise the flow pressure loss in the three divided passages; but the extra sound absorption could be outweighed by the extra fan noise resulting from the undispersed splitter wakes directly entering the fan. Again, compared with the first scheme, some reduction in the acoustic treatment at the downstream end of the multi-passage diffusion from the fan may well be possible.

Estimates of the acoustic properties of feasible splitter arrangements can be made using developments of Kremer's theory reported by Beranek and Schultz¹²⁷, where the splitters are considered to be of homogeneous porous material, with the acoustical impedance assumed to be a unique function of the through-flow resistance R_1 (Rayls/m) of the material as demonstrated many years ago by NPL. With the splitter thickness defined as $2d$ (m) and the gap as $2h$ (m) between the splitters, the maximum attenuation is then attained at a particular frequency

$$f_{opt} = 101.6/\sqrt{hd} \quad (\text{Hz})$$

using an absorbent material with the 'optimum' flow resistance

$$R_{opt} = 667.5\sqrt{h/d^3} \quad (\text{Rayls/m})$$

This peak optimum design restricts significant noise attenuation to only a narrow band of frequencies but, as illustrated in Fig 26, attenuation over a much wider band of frequencies can be obtained if material with a higher flow resistance is chosen, though then at the expense of a lower value of peak attenuation. Maximum attenuation for a given splitter length is obtained if $d > h$, but this arrangement can produce excessive drag losses, as in the 24 ft tunnel context, where $d = 0.35h$ proved a better compromise between the acoustic and aerodynamic requirements with some lengthening of the splitters to compensate for the reduced attenuation per unit length.

Some exploratory small-scale tests of splitter acoustic efficiency by Trebble at RAE, with pink noise sources but without airstream flow, have confirmed that the noise attenuation by representative in-duct splitter blocks did increase with the number of splitters much as expected, ie with reduction of air gap between adjacent splitters reduced, while substantial benefits could be achieved by choosing a bulk absorber material of appropriate flow resistance (Fig 26). Although the measured peak attenuation occurred at the predicted frequency, the peak ΔdB was substantially less than the theoretical estimates when $R_1 \approx R_{opt}$, while at the lower frequencies the attenuation was greater than estimates. The measured attenuation varied almost linearly with splitter length l at constant thickness $2d$, over the l/d range 10 to 50 studied and relevant frequency range (1 kHz to 10 kHz here). Protective covering of the absorber material by a perforated plate with small closely-spaced holes of 40% open area had little effect on the splitter noise-attenuation effectiveness. But when this in turn was faced with aircraft linen, to preclude splitter self-noise (perforation howling) in an airstream, there was a noticeable reduction in attenuation effectiveness. Complementary experiments are now being completed on various practical coverings and bonding techniques, in respect not only of the effects on splitter attenuation, but also their resulting self-noise and wearing properties in representative airflows.

The noise absorption treatments adopted and experience gained for other acoustic tunnels can usefully be referenced. In particular, for the elaborate NSRDC tunnel (Fig 3)¹⁰¹, long 'acoustic mufflers' are incorporated in the especially large legs of the closed return circuit immediately upstream and downstream of the quiet axial-fan drive, to reduce fan noise reaching the test-section particularly in the low-frequency range but with only minor aerodynamic penalties. Each muffler comprises two sinuous absorptive splitters mounted vertically in the middle of the tunnel and one along each side-wall; the sinuous bends have a large radius to avoid flow separation, while providing additional high-frequency noise reduction by eliminating an unobstructed linear sound path through the muffler, and also increasing the effective length of the passage for a given geometric length of muffler. The aerodynamic total-head losses for each muffler were only about 15% of the overall loss round the tunnel circuit and about the same as the loss through the cooler or through the anti-turbulence screen section. Moreover, the perforated metal coverings of the absorptive material here causes no troublesome self-noise because the duct airspeed at these muffler locations is so low.

The simpler UTRC tunnel (Fig 4)¹⁰⁸, with its open-return design and extractor-type centrifugal fan at the exit, avoids the need for acoustic treatment of the tunnel inlet upstream of the test-section assuming of course the absence of any external noise problems. Downstream of the test-section, at the end of the conventional straight diffuser and just ahead of the drive-fan, the tunnel circuit incorporates a Z-shaped muffler (absorptive and reactive) comprising two arrays of parallel baffles/splitters and two lined 90°-bends, which serve to attenuate the fan noise by at least 50 dB for frequencies down to 250 Hz in the test-section. Turning vanes were not installed in the bends here, to preclude the possibility of discrete frequency noise due to 'singing' and of broadband noise generation due to their immersion in turbulent flow from the diffuser.

3.6 Tunnel Flow Quality Requirements

The desirability of good uniformity, steadiness, and low turbulence of the flow in the test-section airstream is already well established for aerodynamic-model testing. The possible significance of such flow quality considerations on noise-model testing, either directly or indirectly through the influence of resulting aerodynamic changes on model noise generation and propagation characteristics, still needs to be clarified and quantified. In particular, there appears to be little quantitative appreciation as yet of the influence of intensity and scale of the turbulence in the oncoming mainstream as regards noise generation at the model, except that the influence could be relatively small perhaps for a jet efflux but significant for a fan intake. Nevertheless, these aspects certainly cannot be ignored, not merely for fan-model noise, but also for airframe-model noise and engine installation effects at least for small-scale models; ie when the aerodynamic flow field under the low Reynolds number conditions can vary appreciably with stream turbulence. The declaration and analysis of any existing relevant results is now badly needed, complemented by some exploratory noise measurements and related aerodynamic studies in existing tunnels with known variation of turbulence, particularly on fan-powered models.

Noise measurements employing a microphone inside the tunnel airstream (rather than outside) are frequently required for far-field studies as well as near-field, unavoidably so with closed-jet tunnels and usually with large open-jet tunnels (Section 2.3). However, RAE experimental research by T B Owen has now established that with a very quiet tunnel the tunnel background noise, as measured inside the airstream by a microphone even when fitted with a nose-cone and pointed directly upstream, can still be largely due to the interaction of the airflow with the microphone rather than the true quiet-tunnel noise levels.

More specifically theoretical arguments suggest that, if u' is the rms longitudinal velocity fluctuation and U the airflow mean velocity, then the rms momentum-pressure fluctuation p'_u associated with the turbulence should be $\rho U u'$, while the static-pressure fluctuation should be about $\frac{1}{2} \rho u'^2$. Thus p'_u should give approximately the 'pitot-pressure' fluctuation experienced by a microphone facing upstream without nose-cone or protective grill. Preliminary analysis of RAE experimental results, for $20 \log (p'_u / \rho U u')$ as a function of Strouhal number fD/U where here D is the microphone nominal diameter, confirms that the microphone alone (without nose-cone) measures p'_u as expected over a considerable portion of the Strouhal number range, (Fig 25). The fall-off in microphone response at high frequency is also in line with the reduction in scale of turbulence ($L \propto U/2\pi f$), as expected. However, when a nose-cone is fitted the microphone does not measure $\frac{1}{2} \rho u'^2$ but a fraction of p'_u depending on the Strouhal number, this fraction being dependent on nose-cone shape. Admittedly this apparent primary dependence on p'_u does not in itself provide a clear physical explanation of the microphone response to turbulence, particularly since the spectra of lateral component v' are similar to those of u' in the experiments presently completed. Nevertheless, the practical significance of these results cannot be ignored in respect of acceptable turbulence levels for acoustic tunnels.

More detailed analysis now being undertaken already indicates some important trends. Fig 25 shows the relationship between the apparent noise level indicated by the microphone, the true background noise level deduced from a subsidiary experiment, and the pressure-fluctuation quantities associated with the turbulence for a particularly high turbulence level (about 2%) in a small free-jet quiet tunnel. Reducing the turbulence level does result in the microphone apparent noise levels being unaltered if non-dimensionalised again in terms of p'_u ; $\frac{1}{2} \rho u'^2$ falls and the true background noise (as a fraction of p'_u) rises - though remaining sensibly constant in absolute terms. For this tunnel it appears that the turbulence induced signal at the microphone would fall below the true background noise level if the turbulence were reduced to about 0.1% for frequencies below a Strouhal number of about 0.5. At higher frequencies, however, there would still remain an appreciable signal resulting probably from the airflow over the gauze screen on the nose-cone, which can be regarded as 'microphone self-noise'.

Now for the practical achievement of high quality airflow in tunnel test-sections, closed-return circuit designs are usually preferred to open-return (straight-through) designs. Additionally, the closed circuit helps to isolate the tunnel testing from the nearby outside environment, thus precluding spurious changes in model test conditions due to ambient winds and external noise, while partially shielding the surrounding community from objectionable testing noise. However, for the avoidance of spurious noise generation by models (again particularly fans), it is equally important to ensure that no significant distortion of the test-section airstream can arise from possible persistence of the model wake (or efflux) round the closed-return circuit. Some relevant studies have therefore already been started in the existing fifth-scale replica of the 24 ft open-jet closed-return tunnel (Fig 15); using nozzles with relatively large efflux diameter up to 0.13 of airstream diameter, discharging along wind in the test-section. Despite the small contraction-ratio (3.5:1) and short circuit length of this very old tunnel design, the efflux recirculation was barely apparent in the test-section mean flow up to the maximum ratio (unity) of jet-efflux momentum to tunnel-flow momentum tested, except as a slight lateral gradient of velocity which is not considered significant even for model-fan testing. The turbulence level at high frequencies was again increased by only up to one-third at large values of the momentum ratio, although it should be appreciated that the basic turbulence level is already high by modern aerodynamic standards. In fact the main effect of the large jet efflux was to cause slow variations of velocity in the test-section, with a period typically at least 1 sec when scaled to the 24 ft tunnel size, the amplitude of this unsteadiness being nearly proportional to the momentum ratio and reaching $\pm 5\%$ of the mean airspeed.

Fortunately more modern circuit designs provide much longer distance for the jet efflux to disperse before reaching the tunnel fan remote from the test-section (not immediately downstream), which should reduce recirculation effects. Also slotting of the collector of open-jet tunnels, as then feasible, should reduce the unsteadiness to tolerable values. Nevertheless, further tests are desirable to quantify the effects of high energy efflux inserted in the test-section, particularly if directed at a large angle to the airstream direction or well off-centre, when more severe distortion may make it necessary to devise a scheme to more rapidly diffuse or even remove the jet efflux.

3.7 Tunnel Airflow Drive

For subsonic tunnels, the conventional fan system with its well-developed continuously-running capabilities still tends to be preferred for the tunnel airflow drive; usually of an axial fan type, though not always so for straight-through tunnels where other extractor-type fans can be conveniently exploited. The often contemplated air-injector drive may appear simpler than the fan drive, and probably cheaper if appropriate compressed-air supplies are already available on site. But, even if this pressure/induction system may be made as acceptably quiet as the fan drive, the limitations on running periods then available would often be unacceptable for general low-speed testing.

The tunnel fan itself can contribute a major component of the background noise level in the test-section, especially at low frequencies. Consequently the fan design and the duct length available for acoustic treatment between the fan location and the test-section, both represent critical features as regards background noise limitations and acceptable airspeeds for any noise-model testing. The tunnel fan noise is mainly identifiable as of broadband dipole-type, usually attributed to lift fluctuations on the blades and associated with vortex shedding at the trailing-edges. Typical experimental results are consistent with this, in that the fan sound pressure level tends to increase as the fifth to sixth power of the fan rotational speed; a useful crude working rule when comparing fans of similar design under similar operating conditions is:-

$$(\text{Fan overall sound power}) \propto (\text{Tip speed})^3 \times (\text{Aerodynamic Shaft-Power}).$$

More generally, providing the fan aerodynamic efficiency η [= (pressure-rise power)/(shaft power)] is known, the inclusion of the aerodynamic power dissipation factor $(1 - \eta)$ offers a reasonable basis for comparing the noise of fans of differing design, since the aerodynamic losses and noise generation are closely related. The spectrum at a given rotational speed has a decreasing sound pressure level with rising frequency, but with discrete tones superimposed at the blade passing frequency and harmonics, whose intensities can be a function of inflow turbulence as well as tip-speed. Increase in inflow turbulence to the fan can also aggravate the broad-band noise.

For low noise, the fan should be designed to operate near the condition of maximum aerodynamic efficiency, avoiding significant flow separation regions on blades, but with a low tip-speed - certainly below half the speed of sound. Nevertheless, it must be appreciated that there can be a significant variation of airstream total head across the fan entry section, remaining sensibly axisymmetric if due to boundary effects in the test-section and duct upstream of the fan, but possibly with deviations due to non-axisymmetric acoustic treatments of the upstream ducts. Fortunately the well-designed single fan has proved a powerful and accommodating tool for providing a uniform distribution downstream of the drive section. With modern aerodynamic design methods, essentially involving the choice of an appropriate blade-twist distribution from fan-hub to tip for the expected velocity distribution into the fan and the required pressure rise through the fan, only small adjustments should have to be made to the predicted fan design after appropriate model fan-in-duct checks. Broadly speaking, a tunnel design which incorporates a large contraction-ratio is favourable to low noise, because of resulting reductions in both the aerodynamic power required and fan tip speed, for a prescribed test-section size and speed.

For example, exploratory fan designs for the possible modification to the 24 ft tunnel (Fig 16) imply that the required fan characteristics retaining the 7.3 m diam. test-section should be neither unusual nor unreasonable in respect of existing tunnel experience (Fig 18). The tip speed need not exceed 110 m/s, the section C_p -values lie between 0.5 and 0.7, and the blade angles to the fan disc do not exceed 50° even at the root, despite the unusually large power-factor for the low contraction-ratio available without enlarging the existing circuit. An alternative modification, involving reduction of the test-section size (to 5.5 m diam.), primarily to permit a higher maximum speed, could lead to about 8 dB lower noise levels at the same test-section speed because of the corresponding 45% reduction in fan tip speed (reduced volume flow rate). In addition, even without allowing for the then improved fan conditions of reduced turbulence and lower aerodynamic loading, the shift of noise energy to lower frequencies associated with the lower fan speed could yield about a further 4 dB reduction in noise level over the same frequency range of interest.

The particular fan designs for the NSRDC acoustic tunnel¹⁰¹, for the DNW large low-speed tunnel³⁴ now under construction, and for the planned modification to the NASA 40 ft x 80 ft tunnel⁹⁶ must also be referred to. More generally, although continuous variation of tunnel speed is usually achieved through alteration of fan rpm, fan aerodynamic efficiency and quietness could usefully be further improved especially for large blockage changes, by incorporation of adjustable or variable blade angle, possibly even with some facility to adjust blade twist or effective camber at least during the installation proving stage.

3.8 Open-Jet Nozzle and Collector-Flow Interactions

In most subsonic tunnels, either with open or closed test-sections, careful tailoring of the test-section design as well as of the tunnel circuit and airflow drive is invariably needed to ensure that the test-section flow is steady throughout the required airspeed range. Often, any shortfall or improvement in this respect is manifest also in the degree to which the allied requirements of minimum pressure gradients and minimum energy losses are met. Here, we are primarily concerned about possible low frequency unsteadiness (pulsing) in open-jet tunnels, largely associated with interaction between the jet

nozzle flow and the collector, which could generate excessive background noise and intolerable flow conditions. For preciseness, the primary origins of such flow unsteadiness (and appropriate treatments) can be divided into two different categories, though these can arise simultaneously.

Firstly, mixing at the tunnel airstream boundary, while traversing the space between the nozzle and the collector, results in entrainment of the order of 10% excess volume flow which has to be spilt at the collector entry. With the large-scale eddy sizes arising in this mixing, the instantaneous quantity to be spilt will show appreciable amplitude variations in the very low frequency range, so that tunnels with simple bellmouth collectors have experienced low frequency variations in tunnel airspeed apparently associated with this unsteady entry flow. All modern open-jet tunnels with closed return circuits incorporate some form of ventilation slots downstream of the collector to accommodate this variable spillage and attenuate pressure waves which might otherwise propagate round the tunnel; in some cases extensive ad-hoc tailoring of the slots has been required to obtain satisfactory tunnel flow, eg DFVLR Porz-Wahn²⁴ and VKI, while in others a single peripheral slot has given satisfactory results. Clearly, the aerodynamic design of the collector cowl has to be carefully tailored to the particular test-section and working-chamber configuration, while the cowl must also have acceptable structural and acoustic characteristics.

Secondly, nozzle/collector-edge-tones and related jet-flow oscillations are usually considered to originate from aerodynamic resonance between a disturbance (eg ring vortex) leaving the jet nozzle, impinging on the collector cowl, and then feeding back a new disturbance which arrives back at the nozzle in phase with the creation of another disturbance at the nozzle. The frequency of such edge-tones, (primary and higher-order) tend to increase with greater mean airspeed at the jet nozzle and then decrease with greater separation distance between the jet nozzle and collector. In some closed return-tunnels, severe vibrations of the tunnel structure have arisen when the jet/collector edge-tone frequency coincides with the organ-pipe resonance frequency of the tunnel duct. Two very different designs of wind-tunnels, the RAE 24 ft tunnel (also a fifth-scale model) with 3.5:1 contraction-ratio and the DFVLR Porz-Wahn tunnel with 10:1 contraction ratio experienced these severe organ-pipe resonances; while other tunnels of intermediate design, eg the model of the new DNW tunnel with 5:1 contraction ratio³⁴, show no signs of this phenomenon. Fortunately when it does occur, this type of aerodynamic resonance can be readily suppressed or reduced by the introduction of peripheral tabs in the form of spoilers or discrete vortex generators at the nozzle outlet, to preclude regular formation of the jet ring vortices; there can be some penalty because of possible increases in high frequency noise. It should be noted that in some cases (eg DFVLR Porz-Wahn) venting of the collector alone produced no noticeable attenuation of these organ pipe resonances.

Additionally, with the introduction of sealed anechoic chambers surrounding an open test-section, an alternative type of edge-tone resonance appears possible involving low-frequency standing waves in the chamber, rather than a return-circuit organ-pipe resonance. This supplementary type was apparently present in the UTRC Acoustic Tunnel (open return circuit)¹⁰⁸, there again cured by the use of peripheral tabs, and was probably responsible for initial resonance problems in the NSRDC tunnel but there cured by collector slotting^{101,104}.

In view of wide variations in severity of the unsteadiness problems reported in different open-jet tunnels and the large variety of collector cowl shapes and venting configurations employed, more basic research would still seem worthwhile to further clarify the fundamental causes of the various types of unsteady phenomena and to provide detailed guidance for their avoidance in acoustic tunnels with minimum penalties in other respects. More generally, for dynamic as well as noise testing in open-jet tunnels, it seems essential to establish whether the test-section airflow can really be guaranteed to be as steady as that in good closed test-section tunnels, or whether some low-frequency unsteadiness and relatively higher levels of turbulence will remain despite jet-nozzle and collector treatments. The aerodynamic and acoustic significance of deflection of the open-jet boundary due to the presence of lifting models, particularly with powered high-lift systems, needs also to be explored further.

4 TRACKED-VEHICLE DEVELOPMENT AND OPERATION FOR NOISE TESTING

4.1 Nature of Track Merits

Outdoor linear-track vehicles have in principle significant attractions for forward-speed simulation. Typically,

- (a) 'In-flight' motion of the noise generator through the normal atmosphere and past a stationary observer is properly represented, potentially without excessive self-noise from the facility itself.
- (b) Free-air turbulence levels under true atmospheric conditions are likely to be more representative of low-altitude flight than those provided in wind-tunnels, an aspect particularly of importance for fan noise studies.
- (c) Airflow effects on the stationary measurement microphones under conditions of low ambient windspeed should generate much less pseudo-noise than with microphones inside a tunnel airstream or even in the surrounding working chamber.
- (d) In the absence of objectionable environmental effects, the testing could be precisely controlled, and established flyover noise techniques may be further developed, to ensure adequate measurements and analysis for both research and development purposes.

Such outdoor tracks can most profitably be envisaged as practical development tools and as a means of establishing and comparing practical noise-reduction schemes in almost a true flight environment. Perhaps their major attraction is that they could offer the potential for carrying-out forward-speed tests on real engines and on engine-airframe design features; at much greater size than can be catered for in any existing European tunnel, yet without the necessity to render the engine installation flight worthy -

otherwise a more expensive and time-consuming process. In addition some research investigations can obviously be attempted using outdoor tracks, while particular tests specifically intended for direct selected comparisons with more general tunnel data would be an important aspect of their use.

4.2 Track Noise-Testing Considerations

Naturally, for the proper application of linear-track vehicles in aircraft noise research, some significant problems have to be clarified and related test constraints quantified, several of which already appear in the corresponding application of flight testing but there can be less precisely controlled. The non-stationary nature of the random noise from the rapidly moving sources, when recorded at spatially fixed microphones, demands a long-duration sample for the accurate determination of the spectral characteristics, but much shorter component-samples for accurate resolution of directivity effects. In practice, this apparent conflict is overcome by individual analysis of a large number of short-duration samples from several microphone locations (in-line parallel to the track direction) and from several passes of the vehicle, to ensure statistical adequacy for ensemble averaging of the resulting spectra. The required number of in-line microphones or passes naturally increases for better accuracy and confidence levels, and for the lower frequencies of interest associated with larger-scale models. The spacing between adjacent microphones, to ensure uncorrelated noise samples, may be determined by the required separation of several wavelengths or by the permissible angular resolution (integration time) for the vehicle moving past each measurement point. Directivity analysis for a model source which is non-axisymmetric about its line of travel (eg an aircraft model) demands also distributions of microphones in planes normal to the track at each in-line location. The total track length usually needs to be several times the "measurement length" over which the vehicle test conditions need to be maintained steady, in order to safely accommodate acceleration and deceleration of the vehicle between rest and the test speed.

Other constraints for acceptable noise-model experimental conditions can include again (as with tunnels):-

- (1) Low background noise from the vehicle, equipment and surroundings, relative to the model source level.
- (2) Low aerodynamic interference from the model rig, vehicle proximity, and ground/track.
- (3) Reliable noise measurement techniques over a wide frequency range, taking special account of possible variations of atmospheric conditions spacewise and timewise.

More generally, as discussed elsewhere for flight experiments, adverse weather can significantly affect the test conditions outdoors or severely limit the test periods allowed.

Since the noise measurements at the microphones can be affected by acoustic interference (sound reflections, etc) from the ground, track or vehicle itself, the careful application of correlation techniques is desirable. Moreover, for diagnostic and correction purposes, as well as for analysis of Doppler-shift and near-field conditions, some microphones and associated recording equipment should be carried on the moving vehicle; along with any aerodynamic or performance measurement devices and any auxiliary power sources (eg compressed air or fuel).

4.3 Required Microphone Locations and Track Lengths

The achievement of statistically adequate noise samples for spectrum analysis by 'ensemble averaging techniques' can necessitate the use of an appreciable number of microphone locations along lines parallel to the direction of the linear track. From statistical arguments for sampling of random data, the accuracy level and the associated confidence limit desired from the analysis prescribe together the corresponding number of freedoms or samples N required; eg accuracy within either ± 1 dB or $\pm 2\frac{1}{2}$ dB, with 95% confidence, requires $N \approx 100$ or 20 respectively. N is then identified as the product $2BT$, involving the lowest frequency-bandwidth B at which this level of accuracy is demanded and the total sampling or record time T needed; eg with $T = 1$ sec, for $N = 100$ or 20, $B \approx 50$ Hz or 10 Hz corresponding to $\frac{1}{3}$ -octave band centre-frequencies ($f_c = B/0.231$) of about 200 Hz or 40 Hz respectively.

The maximum time interval δT_m allowable for measurement as the vehicle passes through a plane normal to the track at a particular microphone position ($\theta \approx 90^\circ$) is essentially defined by the minimum time taken by the vehicle to traverse the permitted angular limit $\Delta\theta$ of fore-and-aft resolution, at the particular vehicle speed V and distance d_{mic} from the microphone; namely

$$\delta T_m = 2(d_{mic}/V) \tan(\Delta\theta/2);$$

eg for $\Delta\theta = 10^\circ$ (ie $\pm 5^\circ$), $V = 80$ m/s and $d_{mic} = 50$ m, the measurement interval $\delta T_m \approx 0.1$ sec. The number of in-line microphones n required is then of the order of the number of measurement intervals ($T/\delta T_m$) divided by the number of vehicle-passes p which can be repeated to an appropriate accuracy; eg using the numerical values here, $n \approx 10$ so that 4 microphone locations with 3 vehicle passes should suffice. For propagation directions well away from $\theta = 90^\circ$, without decrease in permitted $\Delta\theta$, the available component-sample times δT_m become much larger.

To ensure that the measured signals at each microphone are indeed statistically independent in order to achieve the designated accuracy up to the maximum wavelength λ_{max} , the microphone spacing ℓ may need to exceed several wavelengths; namely

$$\ell/\lambda_{max} = (\ell f_{min}/340) > 1;$$

eg $\ell \approx 10$ m ensures a spacing of more than $5\lambda_{max}$ or only $1\frac{1}{2}\lambda_{max}$ at frequencies of 200 Hz or 50 Hz respectively. As an alternative criterion, the microphone spacing may need to be large enough so that adjacent microphones do not have to include samples from the same wavefront, and additionally so that the filter output during the prescribed averaging period does not contain significant parasitic contributions from the practical input-response delays. On this basis, it can be argued that:-

$$\ell \approx V (\delta T_m + 2/B) ;$$

eg, with the numerical values already quoted ($V = 80$ m/s, $\delta T_m = 0.1$ sec, $B = 50$ Hz or 10 Hz),
 $\ell \approx 10$ m or 25 m respectively.

Directivity analysis for a model source which is non-axisymmetric about its line of travel, eg an aircraft model, further demands a distribution of microphones in planes normal to the track at each in-line location. Typically these positions would be at a fixed radius d_{mic} from the source and at chosen azimuth intervals $\Delta\phi$ over at least one quadrant; eg with $\Delta\phi = 15^\circ$, at least 7 in each transverse plane making as many as 28 in all if there are 4 in-line locations.

The track 'measurement-length' L_{meas} over which the vehicle test conditions need to be maintained steady (constant vehicle-speed, engine-power, etc) can be expressed crudely in terms of the extent $n\ell$ of the number n of in-line microphone at equal spacings ℓ , the directivity angular range θ_1 to θ_2 measured relative to the direction of travel, and the distance d_{mic} of the line of microphones from the track. Thus, in simple terms,

$$L_{meas} > (n-1)\ell + d_{mic} (\cot \theta_1 + \cot \theta_2) .$$

Thus, with the numerical values already quoted ($n = 4$, $\ell = 10$ m, $d_{mic} = 50$ m) and typically $\theta_1 = 20^\circ$, $\theta_2 = 160^\circ$, the track measurement length $L_{meas} \approx 300$ m. Clearly, this increases with the greater number of microphones required for better accuracy or less repeat runs, and with any greater spacing needed to accommodate larger wavelengths associated with larger-scale models.

The extra track length L_{ad} , prescribed by the distances required for acceleration and deceleration of the vehicle can be much greater than the measurement length; eg $L_{ad} \approx 2500$ m with an equivalent mean value of 0.25 g for both the acceleration and deceleration between rest and a vehicle test speed of 80 m/s. The total track length required, $k(L_{meas} + L_{ad})$, must incorporate some safety factor $k > 1$; eg $L \approx 3500$ m, when $k = 1.5$ for the present example with $V = 80$ m/s. This distance tends to vary roughly as the square of the test-speed assuming small changes in acceleration and deceleration forces.

4.4 Specific Tracks for Noise Testing

The Bertin Aerotrain Vehicle (Model 02) has been developed in France^{19,20} for noise tests on its jet-propulsion unit with a variety of silencer nozzles. The inverted-T single-rail track on which this air-cushion supported vehicle is operated has about 6500 m total length between Gometz and Limours (South-West Paris). But, due to various restrictions, noise measurements are usually limited to a selected mid-track length of about 350 m and made at distances up to 50 m on one side of the track only. The Vehicle is now propelled by a GE J-85 engine, instead of the P&W JT-12 engine used in 1973, both small turbo-jets of about 13 kN max thrust (3000 lb).

Forward-speeds of about 5 m/s (nominally static), 40 m/s and 80 m/s are usually employed for noise testing, with J-85 jet-efflux velocities between 400 m/s and 650 m/s through the 0.3 m diameter nozzle; max pressure ratio ≈ 2.4 , max exhaust temperature $\approx 1000^\circ\text{K}$. Unwanted noise from the J-85 intake is now minimised by acoustic treatment there, while the internally-generated component of the exhaust noise can optionally be reduced (leaving jet-mixing noise predominant) by jet-pipe acoustic lining. Recorded engine-performance parameters include rpm, inlet pressures, turbine exit pressure and temperature, jet-pipe pressure and fuel flow. The air-cushion support for the vehicle is supplied by fans driven by a Turbomeca Palouste (run at constant rpm), whose intake and exit now also have been acoustically treated to make the parasitic noise acceptably low down to the minimum test jet velocity (400 m/s). The vehicle speed is controlled simply to within $\pm 5\%$ of target speed by pilot-operated wooden brakes on the vertical sides of the track-rail, the true speed (within $\pm 1\%$) and location of the vehicle being measured from pulses sensed by a photocell through holes every 6 m length along the rail. Acceptable atmospheric conditions for noise tests are limited usually to temperatures above 5°C , no precipitation, humidity between 40% and 90%, and windspeeds below 5 m/s or 2 m/s for high noise levels or low noise levels respectively.

For the far-field noise measurements, four in-line microphone positions are now usually employed, spaced at 12 m intervals about 50 m distant from the track and at post heights increased to 15 m, with temperature and humidity measured at mid-height to improve atmospheric corrections. Near-field measurements are also made on the modified Vehicle, with flush-mounted microphones in the J-85 ducts and nose-cone microphones at entry and exit. The data acquisition system, developed by ONERA, uses radio links from the measurement points to a central command post located on one of the three bridges crossing the track. Synchronisation at measurement locations is achieved by sequence emitters which start the NAGRA recorders and also transmit synchronisation pulses to the tapes and to on-board recorders used to monitor the engine and vehicle performance parameters.

For $\frac{1}{3}$ -octave analysis, integration times of 0.125 sec are normally employed, with a permissible angular resolution for maximum test speed of $\pm 5^\circ$ at 90° , reducing to $\pm 1^\circ$ at 20° and 160° from track direction, while integration time is increased to 1 sec for nominally zero speed. Corrections are applied for background noise including ambient and electronic contributions, but not Palouste noise or Vehicle self-noise; for signal reflections from the intervening ground between the vehicle and the microphones, but not from the vehicle itself or any nearby trees; and for atmospheric deviations from standard-day conditions. Typically, the scatter of the corrected data over the four in-line microphones and over several runs appears to be within ± 3 dB for $\frac{1}{3}$ -octave spectrum distributions above 200 Hz and within ± 1 dB for PNL, so that reasonable mean values can be arrived at. Possible application of the full-scale Bertin Aerotrain on the Orleans track is also now worth consideration for noise testing at larger scale.

In the UK, feasible development of the Earith 'Tracked Hovercraft' Facility for aircraft noise investigations, using a fast and quiet wheeled vehicle, has been the subject of analytical and experimental studies by HSA in conjunction with ISVR (Southampton University) and RAE. Although this particular development had to be irrevocably terminated in late 1974, much valuable experience has been accrued from extensive design work, model experiments, and exploratory tests with an existing air-cushion supported vehicle on the track. This should now help the critical appreciation and improved application of mobile facilities elsewhere and of allied noise testing techniques.

In the USA, the feasibility of using the 'Sled Track' at Holloman Air Force Base has been studied in relation to engine exhaust noise testing at least. Some conflicting views have been expressed about possible limitations associated with background noise, in particular the vehicle self-noise, and more generally about the cost-effectiveness merits of relevant noise research developments for this particular facility. At NASA Langley, the 'Landing Loads Vehicle Track' could be developed for noise investigations and the 'Landing Loads' area there is said to permit adequate free-field conditions over the time period for which the vehicle is conveyed past the fixed microphone array. The vehicle self-noise is claimed to be negligible for frequencies above 1 kHz, while the impulse propulsion system could provide an adequately large distance over which the vehicle speed and direction remain constant since the vehicle has a high inertia to drag ratio.

5 OTHER MOBILE GROUND-BASED FACILITIES FOR NOISE TESTING

5.1 General Scope

In between the two extremes of windtunnels and linear tracks considered by Sections 2 and 4, there are a variety of other techniques under development or projected for noise testing. Although each can have particular advantages for specific types of noise investigations, they can be expected only to supplement rather than replace windtunnels and linear tracks for basic research and exploratory development. The following sub-sections relate in turn to the possible use of:-

- Rotating Arms (5.2), such as the Rolls-Royce jet-nozzle rig.
- Road/Runway Vehicles (5.3), as envisaged with the NGTE lorry or by aircraft taxiing tests.
- Aerial Cables (5.4), as being studied by NASA Langley.
- Free-Flight (5.5), with models projected outdoors or through a large anechoic chamber.

Naturally since these facilities all involve motion of noise sources and in most cases operate outdoors, many of the problem areas listed for the track vehicles are to some degree relevant here, while some new problems can also arise.

5.2 Rotating Arms

Rotor-type rigs with the test-model at the extremity of an arm, rotating usually about a vertical axis, have not yet been validated for a wide range of noise-model testing. However, Rolls-Royce experience^{57,60} has already established that jet-exhaust noise at least can be investigated profitably in this way, at realistic values of jet parameters (cold and hot) and of tip-speed/jet-speed ratios, with the correct moving-source to fixed-observer relationship. Useful experiments with the noise from a Hartmann generator shielded by a simple wing model attached to the tip of the rotating arm, have also been made by HSA.

The main problems of such rigs can be associated with:-

- (1) The non-stationary noise signal. Since the rate of change of the noise signal at a typical operating condition and microphone position is very high, special time-interval analysis and careful averaging of the data from a number of revolutions must be performed if an acceptable combination of accuracy and angular resolution is to be achieved.
- (2) Rig self-noise. This can restrict noise measurements to large source strengths, eg high-speed jets or intense discrete-tone generators.
- (3) Residual wake interference. The model without a strong downwash field, naturally travels through the wakes of previous revolutions, which can affect both the source noise generation and propagation characteristics as well as the model aerodynamics. These effects seem unlikely to be significant for high-speed jets, but, together with the high acceleration field, probably make such rigs unsuitable for fan noise studies.
- (4) Airfeed design limitations. Mechanical constraints, including the bend in the supply pipe and hub restrictions close to the model, can prevent ideal aero-acoustic conditions being achieved at the entry to the nozzle; this could create significant internal-noise sources (upstream of the nozzle exit), and also create uncertainties in the simulation of jet-efflux characteristics particularly for low-speed jets.
- (5) Ground and rig reflection/scattering interference. When combined with the non-stationary nature of the signal, the resulting parasitic noise effects at the measurement microphones could be troublesome unless minimised by appropriate surface acoustic treatment.

On the Rolls-Royce 'Spinning Rig' at Aston Down⁵⁷, propulsion is by thrust from the actual test nozzle (typically 75 mm diam.) mounted at a tip radius of 10 m and rotating in a horizontal plane nearly 5 m above ground level, with the air supplied by bleed from two Avon gas-turbines located in a quiet enclosure some 30 m away. The tip 'forward-speed' can be varied independently of the jet-efflux speed over the required practical range up to the maximum of 150 m/s, by airbrake variation of the drag of the rotor arm and change of nozzle size. The complete tip-jet assembly comprises three sections - the nose-fairing containing mass balance weights, the combustion chamber with a simple kerosene burner, and the

special test nozzle. The maximum nozzle pressure-ratio is 4:1, the max efflux temperature 1100°K, and the max allowable mass of the nozzle 15 kg (at max rpm). The basic microphone position for 'far-field' noise measurements is located at 20 m radius, with additional microphones in a linear array and one above the axis of rotation for check purposes.

Over the three years of 'spinning-rig' operation, the variety of specific testing problems and data interpretation difficulties have been substantially alleviated by changes in test procedure, cleaning-up the rig, application of sound-absorbing material to critical reflective surfaces on the ground and rig, and by more refined data analysis techniques. From a jet-noise viewpoint, the spinning-rig model with its combustion chamber just upstream of the nozzle exit provides an appreciable level of internal noise compared with the cleaner jet-mixing models often tested in windtunnels. Furthermore, the supporting wing-fairing structure tends to be closer to the nozzle exit on the spinning-rig than on tunnel rigs, so the forward-arc noise-field at least could be more significantly affected by associated reflection/scattering effects. Such aspects have been especially of interest in attempts to explain the noticeable increase with forward speed of the forward-arc noise from exhaust nozzle models on the spinning rig, rather than the reduction in both forward and rear arcs found from tunnel tests on simple jets.

5.3 Road/Runway Vehicles

Vehicles developed originally for aerodynamic testing could now usefully be assessed for possible noise-testing capabilities, accepting similar and additional constraints to those discussed for track vehicles (Section 4.2). The NGTE lorry⁴⁸ already extensively employed for testing circulation-control rotors and investigation of jet-engine installation aerodynamics represents one possibility considered but not yet proceeded with in the UK for noise testing. The maximum speed capability is restricted to 45 m/s on the RAE Farnborough runway used (3000 m length), primarily by acceleration and deceleration requirements, using an Avon-engine for thrust and reverse thrust. Smaller 'car-type' vehicles are understood to be under development for noise-source testing up to similar forward speeds by NASA Langley and by Bertin. If higher speeds were demanded, tyre heating, vehicle stability problems and other safety aspects would need to be examined. Although compared with possible tracks such vehicles tend to be more limited in speed and in the size of engine or model that could be carried, the operating costs should be lower.

Taxying of an aircraft along a runway represents another possibility which has been the subject of preliminary trials by Rolls-Royce (BED) to assess the prospects and limitations for engine noise studies under forward-speed conditions.

5.4 Aerial Cables

NASA Langley has begun exploratory investigations towards the exploitation of their 'Lunar Lander' rig, with a test noise source moving along a cable suspended between two points about 75 m and 35 m above ground level, the speed being maintained constant down a nearly-straight slope length of about 50 m. An array of fixed microphones suspended above and parallel to this noise source 'flight path', as well as array near ground level, is intended to allow evaluation of both the non-stationary and stationary noise spectra, so as to provide proper interpretation of the moving-source sound field. Further information is awaited.

5.5 Free-Flight

Following extensive aerodynamic testing experience, noise-models could be projected likewise outdoors; from the ground, or from aircraft/helicopters possibly taking advantage of established free-dropping techniques. Additionally, small models could be projected indoors across large anechoic chambers already used for static noise tests. However, the only experience yet available on the practical applicability of such free-flight model techniques for noise studies under forward-speed conditions seems to be from a NASA preliminary investigation⁹⁴ of remotely piloted vehicles for airframe noise research.

6 MODEL-SCALE SIMULATION OF PROPULSION AND POWERED-LIFT NOISE SOURCES

For clarification of relevant in-flight conditions, selective representation of the primary noise contributions from engine operation is required including engine-airframe interactions, with particular emphasis here on the possible changes in source noise generation and propagation characteristics resulting from the addition of the relative external airflow. Complete aero-acoustic simulation of a practical engine at model-scale is hardly feasible (Fig 14), nor is it necessarily desirable for research aimed towards clarification and evaluation of individual major noise components and possible alleviation. For example, it has already proved both expedient and profitable to simulate separately such specific noise generators of interest as nozzle with jet efflux and fan with intake under forward-speed as well as static conditions. Further engine-components of interest for simulation as 'internal' noise generators include other turbo-machinery (compressors and turbines) and combustion systems, while noise reduction devices and airframe interference also need to be represented. For completeness, it should be appreciated that many of the difficulties now raised in respect of model-scale simulation and relevant rig features apply not only to windtunnel facilities ('fixed'-model), but often even more acutely to mobile facilities and particularly if equally reliable results are required.

The relative airstream effects to be expected, even for studies of noise from a particular engine-component, are not simple. They can comprise:-

- (1) Changes in the source noise characteristics arising from the different local airflow and neighbouring surface areas, both internal and external to the engine-nacelle duct.
- (2) Modified acoustic near-field development through the local flow field or from local airframe installation interference; including refraction, diffraction, reflection, absorption, scattering and possibly augmentation in the vicinity of the nacelle installation.

- (3) Unpredictable development from the acoustic near-field to the aircraft noise far-field, again particularly across practical non-uniform airflow regions or solid surface areas, and with extended sources of a complex nature.

Fortunately, if acoustic and aerodynamic behaviour of the engine-component under static conditions is well understood or can be thoroughly explored, only partial simulation at model-scale may be needed for comparative studies of the primary changes due to forward speed, including the clarification and formulation of basic prediction methods.

Special noise generators whose sound emission characteristics at source are unaffected when placed in an airstream (or change in a known manner) can be profitably applied from at least two aspects, for noise tests in most facilities. Firstly, the validity of conventional or novel noise measurement techniques can be checked when employed within or outside the tunnel airstream, or with a mobile model. Secondly, the particular influence of neighbouring surfaces (eg shields) or of flow velocity gradients (eg vortex refraction), affecting the near-field and far-field propagation in the relative airstream, can be isolated and diagnosed more readily without simultaneous unknown changes at the source due to the airstream. Some electrodynamic noise sources, (eg loudspeakers), jet-resonators (eg Hartmann-type), and sirens have already proved useful and are being further developed for such work, particularly with a view to improving their performance in respect of power and frequency range, and to permit controlled variation of their directivity characteristics. However, for acceptable installations in close proximity to surfaces, inside or outside engine nacelles, more compact sources are needed avoiding significant aerodynamic interference on the local airflow.

Aero-Engine Jet-efflux development and the associated external jet-mixing noise-source distributions can be investigated at model scale, in principle simply by a geometrically similar jet nozzle, with an appropriate airfeed arrangement providing a quiet air supply to the model (negligible internally-generated rig noise) and an acceptable jet-flow profile. For static testing, this now usually presents a straightforward tailoring problem for the particular experimental configuration, involving the incorporation of a silencer, burners (for hot jets), plenum chamber, and substantial contraction often in close proximity to the nozzle. However, when forward-speed representation is required, such bulky bluff rigs become unacceptable because of their spurious aerodynamic and acoustic effects arising from their interaction with the external airstream. The introduction of conventional aerodynamic fairings to streamline or shield the rig in the airstream can generate its own problems (acoustic, aerodynamic and mechanical), particularly because of the relatively large sizes involved. Such rig problems are naturally tending to become more acute with advances beyond isolated single cold-jet models. Previous experience with jet aerodynamic testing in windtunnels is helpful, but alone is completely inadequate for noise-model and airfeed rig design, since good aerodynamic and acoustic simulation is simultaneously required without the introduction of parasitic noise sources. For example, while compactness of the external airfeed arrangement can be achieved in aerodynamic testing by very high pressure air-feeds to the jet nacelle, the controlled expansion (with pressure drop and turning) inside the nacelle to provide a representative flow at the nozzle must now not generate unwanted noise internally, or such excess noise must be controlled by internal absorptive treatment. The difficulties become aggravated with the demand for typical nacelle installations, heated jets, and coaxial or multiple jet arrangements.

The combustion system, in addition to producing steady-state temperature effects, can generate noise in at least three other ways; directly from the combustion processes, from interaction with the turbine systems downstream, and from interaction with the jet flow. For noise shielding investigations, the first two types (internally-generated noise) may be simulated crudely by incorporating prescribed noise sources within the feed-pipe, for example from internal loudspeakers, a jet hitting a target plate, or even multiple air injectors. But further investigations seem necessary to develop other more suitable devices for installation near to or within model nacelles. The third type, involving essentially the interaction of the unsteady combustion processes with the jet development, probably can be simulated adequately only by producing representative unsteady temperatures in the flow from actual combustion within the model. If this noise generating mechanism is indeed of practical significance, then careful investigations are required to guarantee reliable and controllable simulation of such source characteristics, particularly since external airflow can also affect the characteristics simultaneously.

Aero-Engine ducted-fan representation by small-scale powered-nacelle units generally cannot be expected to offer direct simulation and prediction of full-scale noise levels under forward-speed conditions, in respect of relevant discrete-tones and broadband spectra. For engineering reasons, some important full-scale geometric features such as the number of rotor and stator blades may not easily be duplicated at small scale, the boundary-layer flow characteristics over the duct walls and the blades can be unrepresentative at the low Reynolds numbers, and even the inlet-flow turbulence can differ significantly in intensity and relative length. Nevertheless, such models can be useful at least for diagnostic studies and design guidance, particularly in respect of specific model-configuration changes for which results can be interpreted using theoretical frameworks and thereby applied to estimate the corresponding influence full-scale. The required experimental measurements can then necessitate not only the incorporation of a relatively quiet fan drive, but also the ability to make both acoustic-pressure and aerodynamic-flow studies inside as well as outside the powered nacelle. Separately from noise-source generation considerations, the engine-nacelle flow characteristics and geometrical shape can of course affect the near-field acoustic development in the forward and rear arcs. In principle, for the investigation of such effects, simple high-frequency noise sources of broadband or discrete-tone types can be located within a representative nacelle-duct flow, with the location and directionality characteristics biased as appropriate; naturally, the influence of any variation in duct flow on the noise-source properties must be appreciated. Again, a combination of complementary experimental and theoretical modelling on particular noise aspects is especially important here for analysis of model-scale results and relevant full-scale interpretation.

Noise reduction devices which influence primarily the acoustic propagation towards the measurement point, rather than effecting reduction of sound energy or other changes in characteristics at source, can be subdivided conveniently here into noise absorbers and noise shields. Dissipative-type absorbers whose acoustical performance is determined mainly by viscous flow resistance can often be simply scaled, though the levels of accuracy achievable in the presence of different airflows and at very small scale are not clear, particularly if substantial protective covering has also to be simulated. Resonant-type absorbers currently in use, with perforated sheet facing, are especially subject to significant Reynolds number effects, and it has been suggested that model scaling down below about one-third full-scale requires very careful justification. Indeed, some lack of confidence has been expressed in the practical usefulness of modelling liners in engine ducts at well below full-scale and without detailed engine component representation, for other than basic comparative tests. Shield-type devices usually need to be several wavelengths in size to be effective, so tend to be reasonably large and in principle can be readily modelled if the noise source frequencies are also properly scaled. However, the possible interactions of any aerodynamic flow field with the acoustic field and shield have to be taken into account; in particular the shield boundary conditions should be adequately represented at the shield trailing-edge or the effect of possible variations investigated. Thus, further research on how to model absorption treatment of airframe surface and special shields does seem justified, taking note also of the airframe/engine interference considerations referred to next.

The airframe, apart from providing direct shielding or absorption/reflection properties, can also affect the engine noise characteristics by aerodynamic interactions with the exhaust or inlet flows, and by influencing the acoustic near-field development. Correspondingly, engine airflow in the vicinity of airframe surfaces or edges can introduce excess noise from the airframe (even statically). The external airstream associated with flight conditions may radically modify these effects, while simultaneously generating noise from the airframe which can be significant with landing devices deployed and quiet engine conditions. Here again, the complexities of the related acoustic and aerodynamic effects are so marked that careful selective modelling from both aspects is essential with realistic and well-defined goals. Because of the small amount of experience yet accumulated, any flight research on aircraft noise should invariably be complemented by appropriate model tests, to take full advantage of the possible correlation and clarification of experimental results and the mutual improvement of measuring and analysis techniques. Such complementary experimental programmes have now been undertaken in the UK and USA at least. Moreover, NASA Ames have attempted with some success a few direct tunnel-flight comparisons on small full-scale aircraft, even though handicapped by the high background noise and reverberation effects in the closed test-section of their existing '40 ft x 80 ft' tunnel.

7 CONCLUDING REMARKS -

Overview of Ground-Based Facilities for Noise Experiments

Encouragingly successful noise experiments in ground-based facilities with forward-speed representation have already included research studies on single and co-axial jets, jet interaction with airframe surfaces, airframe shielding of engine noise, sound refraction by wing vortex flows, airframe self-noise, engine-fan and helicopter rotor noise. This is not to dispute that, as in the past with aerodynamic and aero-elastic testing, difficulties of model-simulation, experimental measurement and analytical interpretation of results will continue to arise with aero-acoustic testing. For example, there have been apparent disagreements and lack of understanding because some forward-speed effects from flight tests on engine exhaust noise and from spinning-rig tests on exhaust nozzle models with internal combustion systems have exhibited a noticeable increase in noise over the forward arc, rather than the reduction expected from tunnel tests on simple pure jets. Such discrepancies tend to be aggravated by the individual limitation of the particular testing facilities, model installation and techniques which can be provided, taking practical account of complexity and cost constraints. Overall, in order to ensure adequate and reliable R&D on aircraft noise under flight conditions, a judicious combination of a wide range of ground-based facilities must be utilised, complemented by continual re-evaluation of tractable theoretical frameworks and by carefully-controlled flight research experiments. Nevertheless the critical comments made earlier should be taken to signify realism not pessimism, already implying the attainment of a much greater practical appreciation of viable techniques and of potential improvements than would have been possible a few years ago.

Modified windtunnel type facilities, incorporating acoustic treatment, should provide the best experimental approach for both basic and applied research work on noise models. Applications of tracked-vehicle facilities appear most appropriate (without actual flight) for providing exploratory development tests, using real small engines at least in the simulation of practical engine nacelle installations. Taken together, windtunnels and tracks are essentially complementary, with the inherent capability of ensuring some overlap and hence important checks on each other for specific configurations, as well as to widen the range of experiments possible. Road/runway vehicles could provide some useful support for some mobile noise-model testing, rotating arms should continue to be exploited for jet-noise model work in particular, the aerial cable rigs may prove especially useful for clarifying some fundamental aspects of moving-source sound fields, while the possible practical application of free-flight model testing techniques should certainly not be ignored. It should also be stressed that, even for the meaningful application of static testing rigs at model-scale and full-scale, special devices may have to be incorporated to ensure acceptable free-air conditions, without unrepresentative distortions of a fan inlet flow at least.

Following on the rapid developments in various ground-based facilities with forward-speed representation and the further advances now technically achievable, the provision of noise-models with better simulation of engine noise sources (in flight) is next of vital importance. Here the term model is intended in its broadest sense of both experimental and theoretical frameworks, for the complementary interpretation of results for small-scale and full-scale conditions. This task presents problems perhaps at least comparable with the complex developments in aircraft aero-elastic models some 40 years ago or in

powered-lift aerodynamic models some 20 years ago. Simultaneously, the development and exploitation of directional acoustic receivers and of other discrimination/correlation techniques should also be expected, to help diagnosis of the changes in noise characteristics with forward speed, and to help isolation of true model propagation characteristics from 'environmental' background-noise interference.

Although the foregoing discussion of ground-based experimental facilities with forward-speed representation for aircraft noise research is quite extensive (see List of Contents), detailed consideration of several aspects has had to be omitted in limiting the scope and length of the present paper. Naturally, some of the topics mentioned only briefly here fall equally or more within the province of other Lecturers, such as special items associated with aero-acoustic measurement and analysis techniques (see Table 2), and the selective simulation of aircraft noise sources at model-scale (see Section 6). Another topic I would hope to discuss more extensively concerns the aero-acoustic exploitation of modern aerodynamic tunnels, taking full advantage of their good flow quality and extensive speed range, but without costly acoustic treatment of the existing tunnel circuit and test-section to overcome background-noise and partial-reverberation problems.

Finally I must recall that, under the auspices of the AGARD Fluid Dynamics Panel, informal two-day 'Workshops' involving a small number of specialists have been held on this lecture subject, in both Europe and North America; the first pair was held during October 1974^{4,5}, the second pair during April/May 1976. The resulting stimulating exchanges of up-to-date experience, often accompanied by debates on controversial issues, proved timely and constructive towards expediting a more integrated and thorough appreciation of relevant technical difficulties and possible solutions. The updated Bibliography included here lists over 100 papers (issued between 1970 and mid-1976), which were declared then to be of direct technical relevance, though many were not available for reference during the preparation of this lecture paper. A tabulation of the primary features of relevant windtunnels, both existing and proposed, is also being completed. In view of the still rapidly growing experience in this relatively new field and to help resolve some of the important controversial issues still existing, a further pair of similar 'Workshops' would be well worthwhile in late 1977.

The opinions expressed by the author in this lecture are personal and do not necessarily represent official views.

TABLE 1 - TUNNEL DEVELOPMENT CONSIDERATIONS FOR NOISE-MODEL TESTINGTunnel-Flight Simulation Needs

Significance of aerodynamic/geometric representations and of aero-acoustic similarity parameters.

Significance of different relative motions of 'fixed' noise-measuring devices, with respect to both ambient air and noise generator, between tunnel and flight test conditions.

Significance of tunnel flow quality (flow uniformity, steadiness and turbulence).

Limitations from Acoustic and Geometric ConstraintsOpen Test-Section Design

Open test-section utilisation and acoustic treatments.

Jet nozzle and collector flow effects.

Free-jet limitations.

Closed Test-Section Design

Reverberant field considerations with conventional test-sections.

Limited acoustic treatments and aerodynamic implications.

Tunnel Circuit Design

Closed-return type.

Straight-through type.

Free-jet limitations.

Intrinsic Tunnel Background Noise

Low-Noise drive-fans and inflow turbulence effects.

Quiet practical alternatives to fan-drive systems.

Open-jet mixing-boundary and collector noise.

Closed-jet wall boundary-layer noise.

Noise absorption treatment of tunnel circuit and aerodynamic implications.

Noise of airflow improvement devices.

Discrimination and correction for background noise.

Target background noise levels for new or improved tunnels.

TABLE 2 - TUNNEL OPERATIONAL CONSIDERATIONS FOR NOISE-MODEL TESTINGModel-Rig Generation of Parasitic Noise, and Alleviation

Influence of model on tunnel background noise.

Model-rig self noise.

Model source noise transmission round tunnel circuit.

Model-airfeed noise.

Measurement-device noise.

Discrimination and correction possibilities.

Model Aero-Acoustic Measurement and Analysis Techniques

Sound measurements inside test-section airflow.

Sound measurements outside open-jet airflow.

Model far-field definition and full-scale flight estimation.

Tunnel/Model general constraints.

Near-field measurements and interpretation.

Microphone calibration and corrections under test conditions.

Special pressure-fluctuation measurement techniques.

Directional acoustic receivers.

Discrimination/Correction techniques for eliminating reverberation and parasitic noise.

Source noise discrimination and location techniques with airflow.

Special data acquisition and reduction methods.

REFERENCES AND BIBLIOGRAPHYGeneral

1. - The impact of economics on the design and operation of quieter aircraft. Proc. Roy. Aero. Soc. Sympos. (April 1975).
2. AGARD (MiniLaWs) A review of current research aimed at the design and operation of large windtunnels. AGARD Advisory Report 68 (March 1974).
3. - Problems in windtunnel testing techniques. AGARD Report 601 (April 1973). See Paper 8.
4. AGARD (MiniLaWs) A further review of current research aimed at the design and operation of large windtunnels. AGARD Advisory Report 83 (Sept 1975). See Appendix 4.
5. AGARD (FMP) Flight/Ground testing facilities correlation. AGARD CP 187 (June 1975). See Paper 7B.

Belgium

6. Oetting R B Preliminary noise measurements in the open-jet of the VKI low speed wind tunnel, L-1. von Karman Instit. TN 89 (May 1973).
7. Oetting R B Preliminary wind tunnel noise measurements of a semi-span wing with an upper-surface blown-flap. AIAA Paper 74-191 (Jan 1974).

Canada

8. Cockshutt E P
Chappell M S
Mair G E Proposal for an engineering acoustic research laboratory. NAE Quart. Bull., pp 15-36, Oct-Dec 1971.
9. - A resumé of some acoustic laboratories. NRC Internal Report (Aug 1972).
10. Krishnappa G
Schaub U W Aerodynamic and acoustic characteristics of an experimental lifting fan under crossflow conditions. AGARD CP , Paper (Sept 1973).
11. Krishnappa G Acoustic tests on a fan-in-wing model: effects of an extended inlet. NRC Ae. Rep. LR-576 (Feb 1974).
12. Krishnappa G Background noise levels at the open efflux from a VTOL cross-flow facility. NRC Mech. Eng. Rep. LTR-Eng-33 (Jan 1975).

France/ONERA and CEPr

13. Broll C Noise measurements in the large Modane windtunnel. La Recherche Aérospatiale, No 1972-1, pp 47-51, (Jan-Feb 1972); RAE Lib. Transl. 1683 (1972).
14. Lienard P
Bongrand J Developpement des moyens d'essais acoustiques en France. Paper 3, Institute St Louis Colloq., May 1974.
15. de Belleval J F
Chen C Y
Perulli M Investigation of in-flight jet noise based on measurements in an anechoic windtunnel. ONERA TP 1975-80 (Sept 1975).
16. Candel S
Guedel A
Julienne A Refraction and scattering of sound in an open windtunnel flow. ONERA TP 1975-79 (Sept 1975).
17. de Belleval J F
etc Analysis of problems posed by simulation of flight effects in anechoic open windtunnels. AIAA 76-533 (July 1976).
18. Candel S M
Guedel A
Julienne A Radiation, refraction and scattering of acoustic waves in a free shear flow. AIAA 76-544 (July 1976).

France/Bertin and SNECMA

19. Alliou J P
Doyotte C L'Aerorail grande vitesse, moyen d'experimentation acoustique des tuyères silencieuses.
Revue d'Acoustique, Vol 22, pp 199-206 (1972).
20. - Essais de bruit en transition sur un Aerorail Bertin à grande vitesse.
Air et Cosmos, No 464, pp 11-13 (Jan 1973).
21. Hoch R G
Berthelot M Use of the Bertin Aerorail for the investigation of flight effects on aircraft engine noise.
AIAA 76-534 (July 1976).
22. Drevet P
Duponchel J
Jacques J R Effect of flight on the noise from a convergent nozzle as observed on the Bertin Aerorail.
AIAA 76-557 (July 1976).

Germany/DFVLR

23. Schulz G
Viehweiger G Noise measurements on bodies in the flow in subsonic windtunnels.
Part 1 - DFVLR Rep. FB 68-43 (July 1968); RAE Lib. Transl. 1352
Part 2 - DFVLR Rep. FB 69-89 (1969); RAE Lib. Transl. 1465.
24. Schulz G
Viehweiger G The low-speed windtunnel of the DVL in Porz-Wahn: Improvements and developments in properties and equipment.
DFVLR Rep. FB 65-66 (July 1965); RAE Lib. Transl. 1224.
25. Schulz G Considerations of an aero-acoustic windtunnel project.
DFVLR Rep. 74-27 (July 1974); RAE Lib. Transl. 1843.
26. Niese W The influence of flow around a microphone on noise measurements of fan in duct.
DLR-FB 74-04 (1974).
27. Grosche F R
Stiewitt H
Binder B Sound source location and discrimination from background noise in windtunnel tests.
Proc. ICIASF 75, pp 301-310, Ottawa (Sept 1975).
28. Grosche F R
Holst H
Wulf R Experimente zur Möglichkeit von aeroakustischen Messungen im 3 m - Niedergeschwindigkeitswindkanal der DFVLR - AVA.
DLR-FB75-52 (1975).
29. Dobrzynski W Freistrahlsprüfstand zur Durchführung von akustischen Modellversuchen.
DLR - Mitt. 75-22 (1975).
30. Neise W The change of microphone sensitivity under mean flow conditions.
DLR-FB 75-23 (1975).
31. Fuchs H V Turbulent pressure data relevant to airframe noise sources.
DLR-FB 76-09 (Jan 1976).
32. Grosche F R
Stiewitt H
Binder B On aero-acoustic measurements in windtunnels by means of a highly directional microphone system.
AIAA 76-535 (July 1976).
33. Heller H H
Dobrzynski W Sound radiation from wheel-well/landing-gear configurations:- a lower bound to airframe noise.
AIAA 76-552 (July 1976).

Netherlands

34. van Ditschuijzen J C A Design and calibration of the 1/10 scale model of the NLR Low-speed Windtunnel LST 8 m x 6 m.
AGARD CP 174, Paper 8 (Sept 1975).

UK/RAE

35. Holbeche T A
Williams J Acoustic considerations for noise experiments at model scale in subsonic windtunnels.
Paper 8, AGARD-R-601; RAE TR 72155 (July 1972).
36. Williams J Some noise requirements for large subsonic windtunnels.
Proc. Amer. Hel. Soc. Mid-East Symp. (Oct 1972).
37. Holbeche T A
Williams J Basic acoustic considerations for model noise experiments in windtunnels.
Paper 73 ANA5, Proc. British Acoust. Soc. Mtg (March 1973).
38. Williams J
Crabtree L F Exploratory analysis of testing facilities for the investigation of aircraft noise at forward speeds.
AGARD LaW Paper 136 (June 1973); RAE Unpublished.

39. Butler G F
Holbeche T A
Fethney P Some experimental observations of the refraction of sound by rotating flow.
AGARD CP 131, Paper 9 (March 1974).
40. Jeffery R W
Holbeche T A An experimental investigation of noise-shielding effects for a delta-winged aircraft in flight, wind-tunnel and anechoic room.
AIAA Paper 75-513 (March 1975).
41. Williams J
Armstrong F W Some research towards quieter aircraft.
RAE TM Aero 1627 (April 1975); also NGTE Note NT 966.
42. Fethney P An experimental study of airframe self noise.
AIAA Paper 75-511 (March 1975).
43. Williams J Problems of noise-testing in ground-based facilities with forward-speed simulation.
RAE TM Aero 1639 (May 1975); also AGARD AR 83 - App. 4.
44. Williams J
Owen T B Some acoustic and aerodynamic analysis for proposed improvements to the RAE 24 ft low-speed tunnel.
RAE TM Aero 1669 (March 1976).
45. Williams J Aero-acoustic requirements for forward-speed simulation in aircraft noise research.
Proc. Inter-Noise '76, pp 79-84 (April 1976).
46. Jeffery R W
Broadbent E G
Hazell A F A windtunnel investigation of vortex refraction effects on aircraft noise propagation.
AIAA Paper 76-558 (July 1976).
47. Edwards J B W Comparative measurements of the noise of cold air jets from three nozzles under static and forward-speed conditions.
RAE TM Aero (1976).

UK/NGTE

48. Smith M C G The use of a runway vehicle for testing lifting rotors in simulated forward flight.
Aeron. Journ. Roy. Aero. Soc., Vol 74, pp 548-560 (July 1970).
49. Armstrong F W Recent developments in noise research at NGTE.
9th ICAS Conf. (Aug 1974)
Aeron. Journ. Roy. Aero. Soc., Vol 77, pp 15-27 (Jan 1975).
50. Cocking B J
Bryce W D An investigation of the noise of cold air jets under simulated flight conditions.
NGTE Rep. R334 (Sept 1974).
51. Cocking B J
Bryce W D Subsonic jet noise in flight based on some recent windtunnel results.
AIAA Paper 75-462 (March 1975).
52. Cocking B J An experimental study of co-axial jet noise.
NGTE Rep. R333.
53. Martlew D L
etc The design, construction and operation of the noise test facility at the National Gas Turbine Establishment.
Aeron. Journ. Roy. Aero. Soc., Vol , pp 1-19 (Jan 1976).
54. Armstrong F W
Williams J Some research towards quieter aircraft.
NGTE Note NT 966 (April 1975); also RAE TM Aero 1639.
55. Cocking B J The effect of flight on subsonic jet noise.
AIAA 76-555 (July 1976).
56. Pinker R A
Bryce W D The radiation of a plane-wave duct noise from a jet exhaust, statically and in flight.
AIAA 76-581 (July 1976).

UK/RR, CNRU, SU

57. Smith W The use of a rotating arm facility to study flight effects on jet noise.
Proc. 2nd Intern. Sympos. on Air Breathing Engines, Paper (March 1974).
58. Lowrie B W Simulation of flight effects on aero-engine fan noise.
AIAA Paper 75-463 (March 1975).
59. Bushell K W Measurement and prediction of jet noise in flight.
AIAA Paper 75-461 (March 1975).
60. Brooks J R
Woodrow R J The effects of forward speed on a number of turbo-jet silencers.
AIAA Paper 75-506 (March 1975).

61. Jacques J The noise from moving aircraft; some relevant models.
Chap 4 - "Windtunnel simulation of the effects of flight"
on radiated sound.
Cambridge University Thesis (1975).
62. Frichard B The new 7 ft x 5 ft closed-section, closed-return acoustic windtunnel
Cheeseman I C at Southampton University, England.
SU Dept of Aeron., Unpublished Report (May 1976).
63. Crighton D G The outlook for simulation of flight effects on aircraft noise.
Pf. Williams J E AIAA 76-530 (July 1976).
Cheeseman I C
64. Morfey C L Noise measurements in a free-jet flight simulation facility:
Tester B shear layer refraction and static-to-flight corrections.
AIAA 76-531 (July 1976).

USA/NASA (including Contractor Reports)

65. Cox C R Full-scale helicopter rotor noise measurements in the
Ames 40- by 80-foot windtunnel.
Bell Helic. Rep. 576-099-052 (Oct 1967).
66. Cox C R Rotor noise measurements in windtunnels.
Proc. 3rd CAL/USAVLabs Symposium Vol. 1 (June 1969).
67. Hickey D H Noise measurements in windtunnels.
Soderman P T NASA SP-207, pp 399-408 (July 1969).
Kelly M W
68. Bies D A Investigation of the feasibility of making model acoustic measurements
in the NASA Ames 40 ft x 80 ft windtunnel.
NASA-CR-114352 (July 1970); BBN Report
69. Ver I L Acoustical evaluation of the NASA Langley full-scale windtunnel.
Malme C L NASA CR-111868 (Jan 1971); BBN Report 2100.
Meyer E B
70. Scheimann J Acoustical measurements of the vortex noise for a rotating blade
Hilton D A operating with and without its shed wake blown downstream.
Shivers J P NASA TN D-6364 (Oct 1971).
71. Ver I L Acoustic modelling of the test-section of the NASA Langley
Research Center's full-scale windtunnel.
NASA CR- (Nov 1971); BBN Report 2280.
72. Ver I L Acoustic evaluation of the NASA Langley V/STOL windtunnel.
NASA CR- (Dec 1971); BBN Report 2288.
73. Palarski M D Large-scale windtunnel investigation of the noise characteristics
of a semi-span wing equipped with an externally blown flap.
NASA TMX-62154 (1972).
74. Palarski M D Aspects of investigating STOL noise using large-scale
Koenig D G windtunnel models.
Soderman P T NASA TMX-62164 (June 1972).
75. Atencio A J Comparison of windtunnel and flyover noise measurements of the
Soderman P T YOV-10A STOL aircraft.
Hall L P NASA TMX-62166 (June 1972).
76. v Glahn U Forward flight effects on mixer nozzle design and noise considerations
Sekas N for STOL externally blown flap systems.
etc AIAA Paper 72-792 (Aug 1972).
77. Scheimann J Rotating blade noise.
Letko W Proc. Amer. Hel. Soc. Mid-East Symp. (Oct 1972).
Shivers J P
78. Atencio A J Comparison of flight and windtunnel experiments of jet noise
Solderman P T for the XV-5B aircraft.
Hall L P NASA TMX-62182 (Oct 1972).
79. Arndt R E A A State-of-the-art report on aeroacoustic testing in
Boxwell D A conventional windtunnels.
Paper, 84th Meeting Acoust. Soc. America (Nov 1972).
80. Bender J Aeroacoustic research in windtunnels: a status report.
Arndt R E A NASA CR 114575 (Feb 1973); Penn State Univ. Report

81. v. Glahn U
Groesbeck D
Goodykoontz J H
Velocity decay and acoustic characteristics of various nozzle geometries in forward flight.
AIAA Paper 73-629 (July 1973).
82. Hodder B K
Investigation of the effect of inlet turbulence length scale on fan discrete tone noise.
NASA TMX-62300 (Sept 1973).
83. Atencio A J
Soderman P T
Comparison of aircraft noise measured in flight test and in the Ames 40- by 80-foot windtunnel.
AIAA Paper 73-1047 (1973).
84. Wilcox F A
Comparison of ground and flight test results using a modified F106B aircraft.
AIAA Paper 73-1305 (Nov 1973).
85. Hickey D H
Kelly M W
Aspects of large-scale, subsonic, windtunnel design for propulsion noise research.
AIAA Paper 73-1279 (Nov 1973).
86. Soderman P T
Noble S C
A four-element end-fire array for acoustic measurements in windtunnels.
NASA TMX-62231 (Jan 1974).
87. Beulke M R
Clapper W S
etc
A forward-speed effects study on jet noise from several suppressor nozzles in NASA 40 x 80 tunnel.
NASA CR-114741 (May 1974); General Electric Report
88. Soderman P T
Noble S C
A directional microphone array for studies of windtunnel models.
AIAA Paper 74-640 (July 1974).
89. Hodder B K
The effects of forward speed on fan inlet turbulence and its relation to tone noise generation.
NASA TMX-62381 (Aug 1974).
90. Scheimann J
Further analysis of the vortex noise of a rotating blade operating with and without its shed wake blown downstream.
NASA TND-7623 (Sept 1974).
91. Kasper P K
Pappa R S
Acoustical characteristics of the NASA-Langley full-scale windtunnel test section.
NASA CR to be issued; Wylie Lab Report.
92. Davis S S
Measurements of discrete vortex noise in a closed throat windtunnel.
AIAA 75-488 (March 1975).
93. Shearin J
Block P J
Airframe noise measurements in a quiet open-jet facility.
AIAA 75-509 (March 1975).
94. Fratello D J
Shearin J G
A preliminary investigation of remotely piloted vehicles for airframe noise research.
AIAA 75-512 (March 1975).
95. Plumblee H E
etc
A study of the effects of forward velocity on turbulent jet mixing noise.
NASA CR- (July 1975). Lockheed-Georgia Report
96. Mort K W
Kelly M W
Hickey D H
The rationale and the sign features for the 40- by 80-/80- by 120-foot windtunnel.
AGARD CP 174, Paper 9 (Sept 1975).
97. Strout F G
Flight effects on noise generated by the JT8D-17 Engine in a quiet nacelle and a conventional nacelle as measured in the Ames 40 ft x 80 ft windtunnel. Summary report.
NASA CR-2576 (March 1976). Boeing Report
98. Ahtye W F
Kojima G K
Correlation microphone for the measurement of airframe noise in large scale windtunnels.
AIAA 76-553 (July 1976).
99. Diedrich J H
Luidens R W
Measurement of model propulsion system noise in a low-speed windtunnel.
NASA TMX-71845 (Jan 1976).
100. Hodder B K
An investigation of possible causes for reduction of fan tone noise in flight.
AIAA 76-585 (July 1976).

USA/NSRDC

- 101 Brownell W F
An anechoic test facility design for the Naval Ship Research and Development Center, Carderock.
NSRDC Rep. 2924 (Sept 1968).
- 102 Franz G J
O'Donnell J F
Shen J T C
Anechoic test facility at NSRDC 2nd USA/FRG Hydro-acoustics Symposium.
Vol. 1, pp 278-298 (Jan 1971).
- 103 Mathews T C
Bowers B E
Brown R W
The anechoic flow facility at NSRDC Carderock.
Acoust. Soc. America, Miami Mtg (Nov 1972).
- 104 Bowers B E
The anechoic flow facility - Aerodynamic calibration and evaluation.
NSRDC Evaluation Rep. SAD-48E-1942 (May 1973).
- 105 Brown R W
Sound pressure spectrum level of background noise in NSRDC anechoic flow facility.
Unpublished Communication (Nov 1974).
- 106 DeMetz F C
Casarella M J
An experimental study of the intermittent properties of the boundary layer pressure field during transition on a flat plate.
NSRDC Rep 4140 (Nov 1973).

USA/UTRC (UARL)

- 107 Paterson R W
Vogt P G
Pink M R
Vortex noise of isolated airfoils.
J. Aircraft Vol 10 (4), pp 296-302 (May 1972).
- 108 Paterson R W
Vogt P G
Foley W M
Design and development of the United Aircraft Research Laboratories acoustic research tunnel.
J. Aircraft Vol 10 (7), pp 427-433 (July 1973).
- 109 Mathews D C
Nagel R T
Inlet geometry and axial Mach number effects on fan noise propagation.
AIAA Paper 73-1022 (Oct 1973).
- 110 Paterson R W
Amiet R K
Munch C L
Isolated airfoil-tip vortex interaction noise.
J. Aircraft Vol 12 (1), pp 34-40 (Jan 1975).
- 111 Amiet R K
Correction of open jet windtunnel measurements for shear layer refraction.
AIAA Paper 75-532 (March 1975).
- 112 Foley W
Paterson R W
Development of the United Technologies Research Center Acoustic research tunnel and associated test techniques.
AGARD CP 174, Paper 7 (June 1975).
- 113 Packman A B
Ng K W
Paterson R W
Effect of simulated forward flight on subsonic jet exhaust noise.
AIAA 75-869 (June 1975).
- 114 Paterson R W
Amiet R K
Acoustic radiation and surface pressure characteristics of an airfoil due to incident turbulence.
AIAA 76-571 (July 1976).

USA/MIT

- 115 Hanson C E
The design and construction of a low noise, low turbulence windtunnel.
Mass. Instit. Tech. Rep. DSR 79611-1 (Jan 1969).
- 116 Bauer P
Widnall S
The development of a windtunnel facility for the study of V/STOL noise.
Mass. Instit. Tech. FTL Rep. R-72-6 (Aug 1972).
- 117 Widnall S
Bauer P
Lee A
Experimental results of rotational noise in forward flight.
Proc. Amer. Hel. Soc. Mid-East Sympos. (Oct 1972).
- 118 Spinka N J
Acoustic levels in a low turbulence windtunnel.
Mass. Instit. Tech., M.Sc. Thesis (Jan 1974).
- 119 Harris W L
Lee A
The development of experimental techniques for the study of helicopter rotor noise.
AIAA 75-455 (March 1976).

- 120 Lee A
Harris W L
Widnall S E
An experimental study of helicopter rotational noise in a windtunnel.
AIAA 76-564 (July 1976).

USA/Boeing

- 121 Sternfeld H
Acoustical modelling of the heavy lift helicopter.
Proc. Amer. Hel. Soc. Mid-East Symp. (Oct 1972).
- 122 Roundhill J P
Schaut L A
Model and full scale test results relating to fan-noise in-flight tests.
AIAA 75-465 (March 1975).
- 123 Bhat W V
Rosso D G
The effect of forward speed on jet wing/flap interaction noise.
AIAA 75-475 (March 1975).
- 124 Bohn A J
etc
Model and full-scale large transport airframe noise.
AIAA 76-550 (July 1976).
- 125 Strout F G
Atencio A
Flight effects on JT8D Engine jet noise as measured in the 40 x 80 foot windtunnel.
AIAA 76-556 (July 1976).

126

USA/BBN

- 127 Beranek L L
Schultz T J
Noise and vibration control: Chapter 15.
McGraw Hill (1971).
- 128 Kadman Y
Hayden R E
Design and performance of a high-speed free-jet acoustic windtunnel.
AIAA 75-531 (March 1975).
- 129 Ver I
etc
Acoustic studies on some NASA windtunnels.
BBN Reports

USA/GE, Lockheed, Douglas

- 130 Clapper W S
Banerian G
Mani R
Development of a technique for in flight jet noise simulation.
Parts I and II.
AIAA 76-532 (July 1976).
- 131 Tanna K H
Morris P J
In-flight simulation experiments on turbulent jet mixing noise.
AIAA 76-554 (July 1976).
- 132 Merriman J E
Low K C
Yee P M
Forward motion and installation effects on engine noise.
AIAA 76-584 (July 1976).

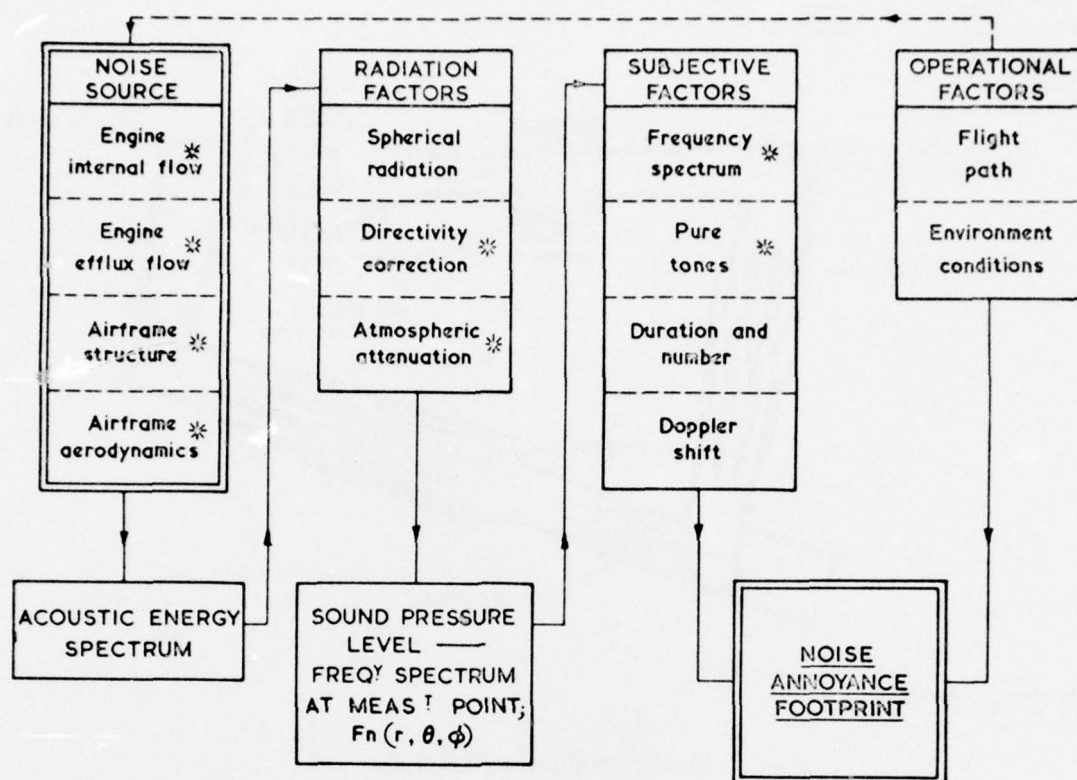


Fig.1 Noise factors affected directly by mainstream flow (*)

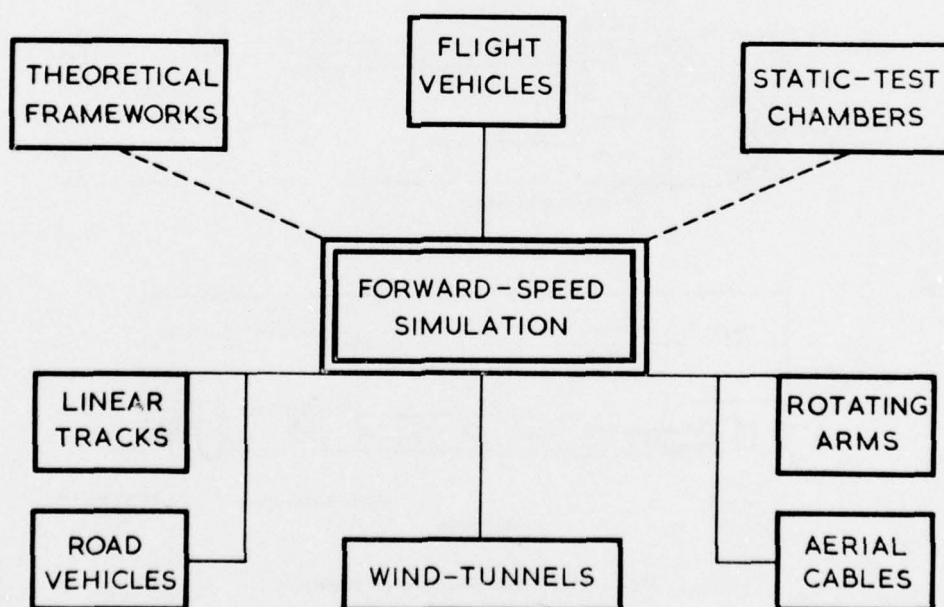


Figure 2

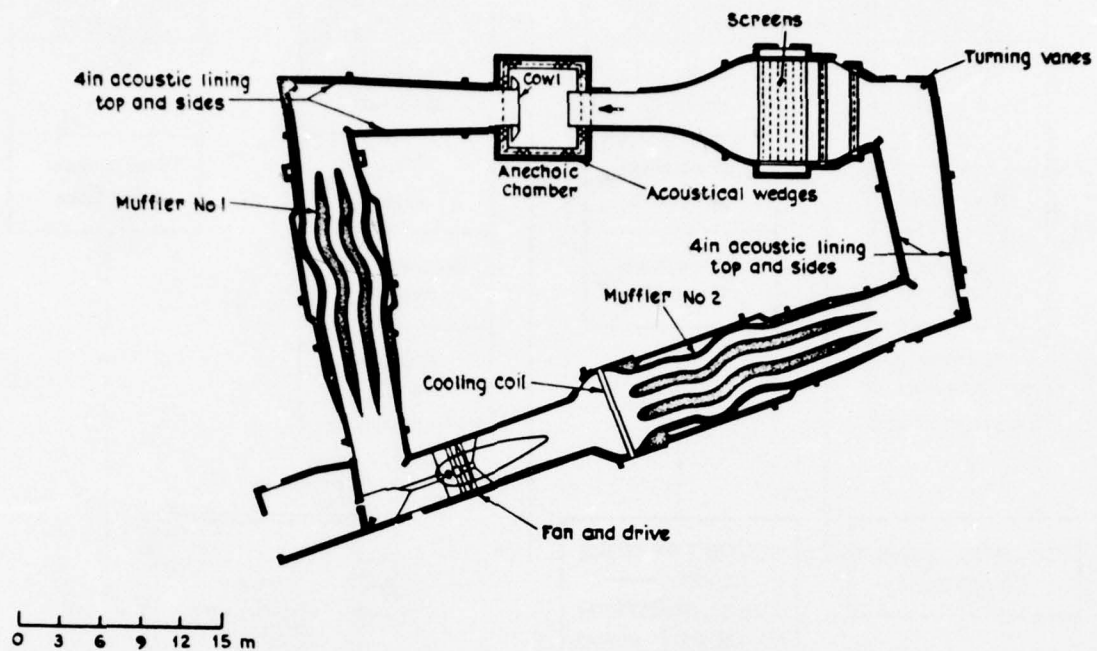


Fig. 3 NSRDC anechoic test facility

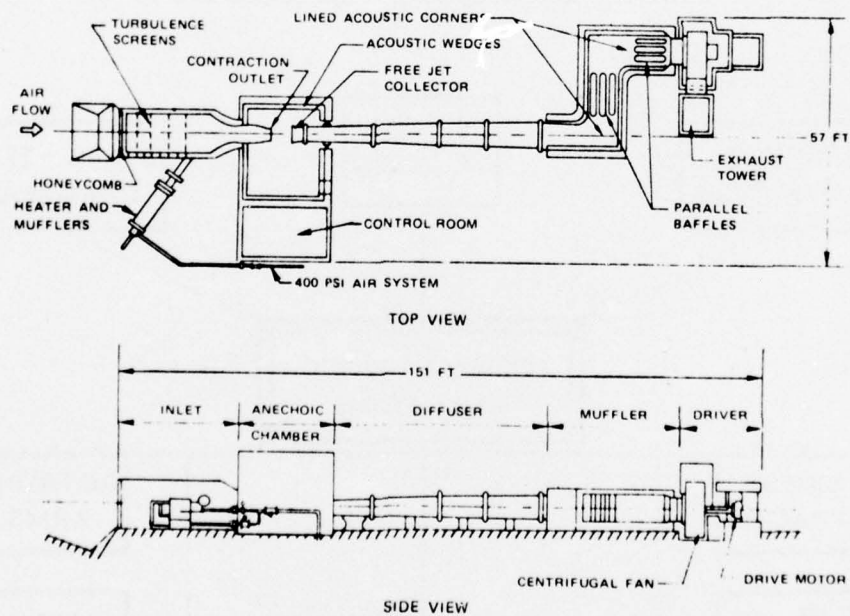


Fig. 4 UTRC acoustic research tunnel

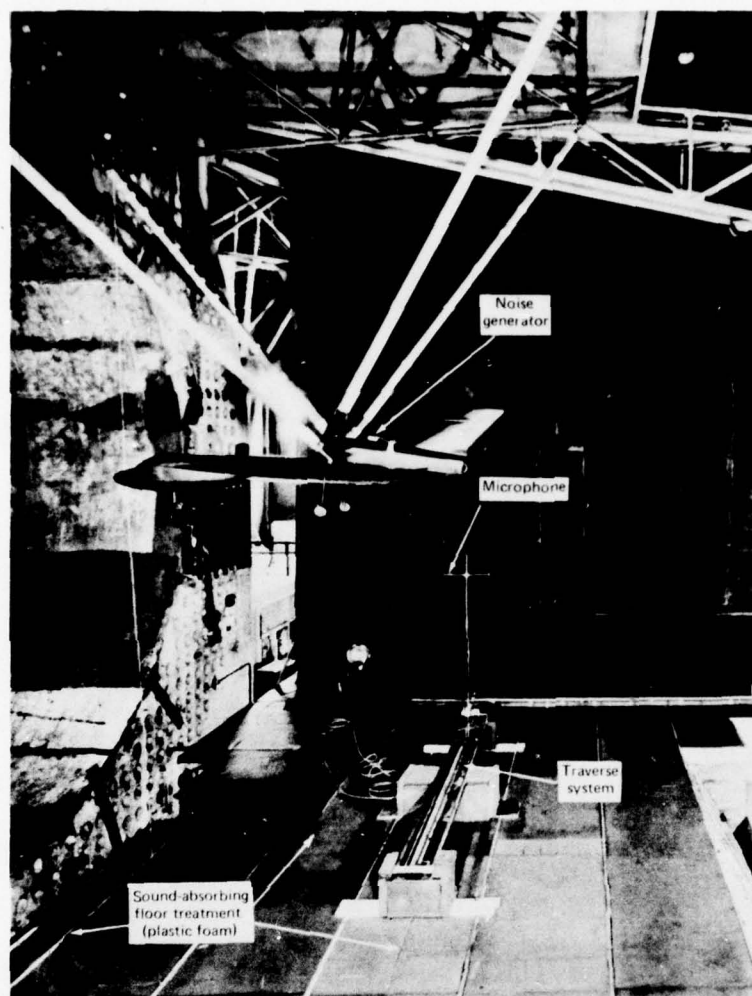


Fig.5 HP 115 model installed in the RAE 24 ft diameter wind tunnel

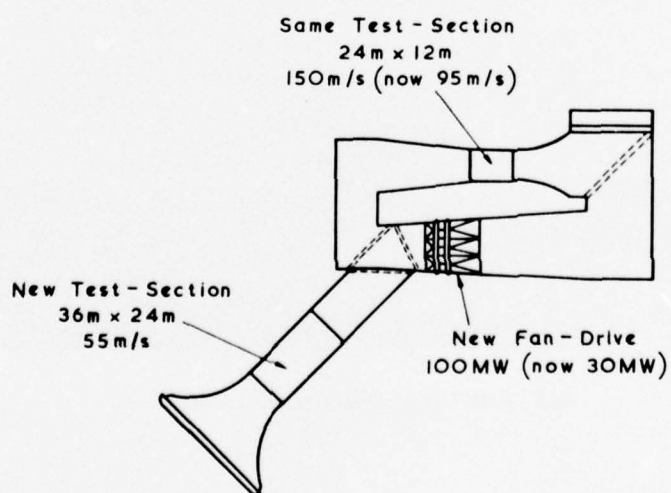


Fig.6 Modifications to NASA 40 ft x 80 ft tunnel

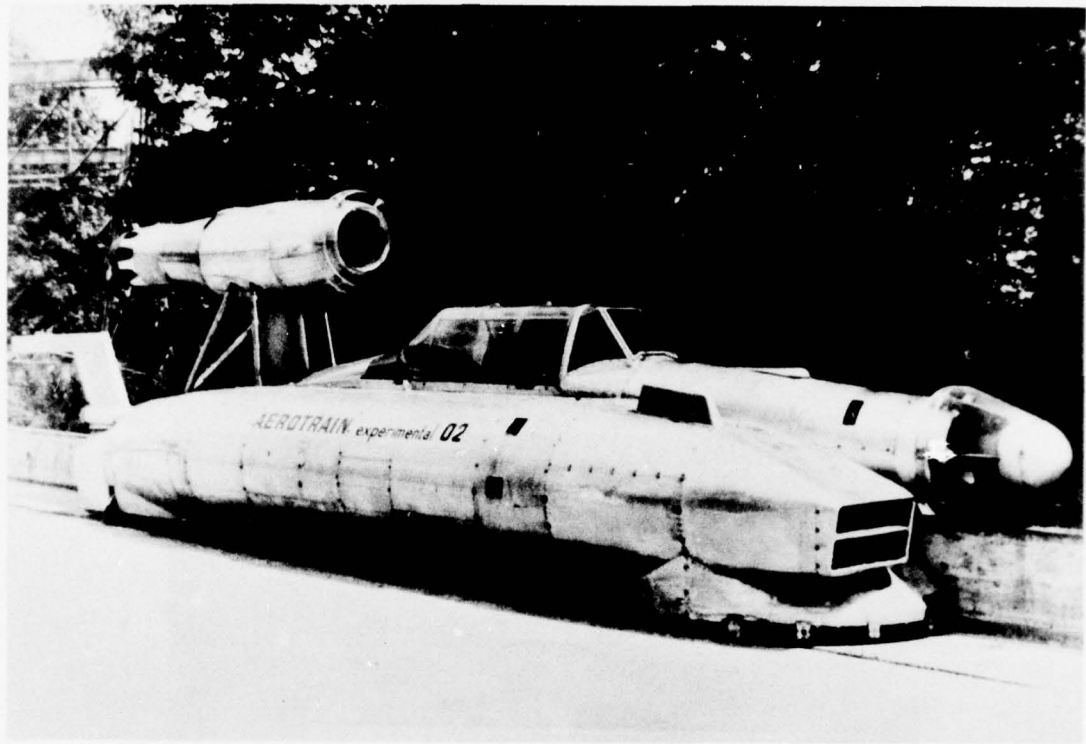


Fig.7 Bertin Aerotrain vehicle (02) with J-85 jet engine

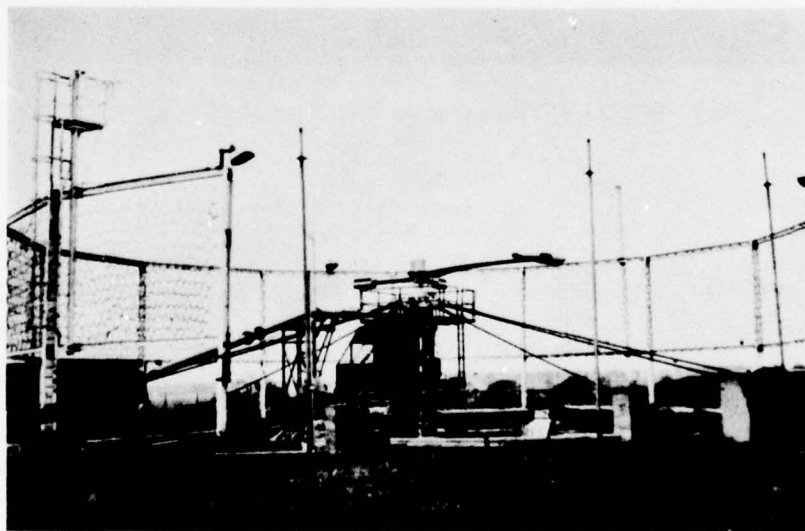


Fig.8 Rolls-Royce spinning rig with tip-jet nozzle

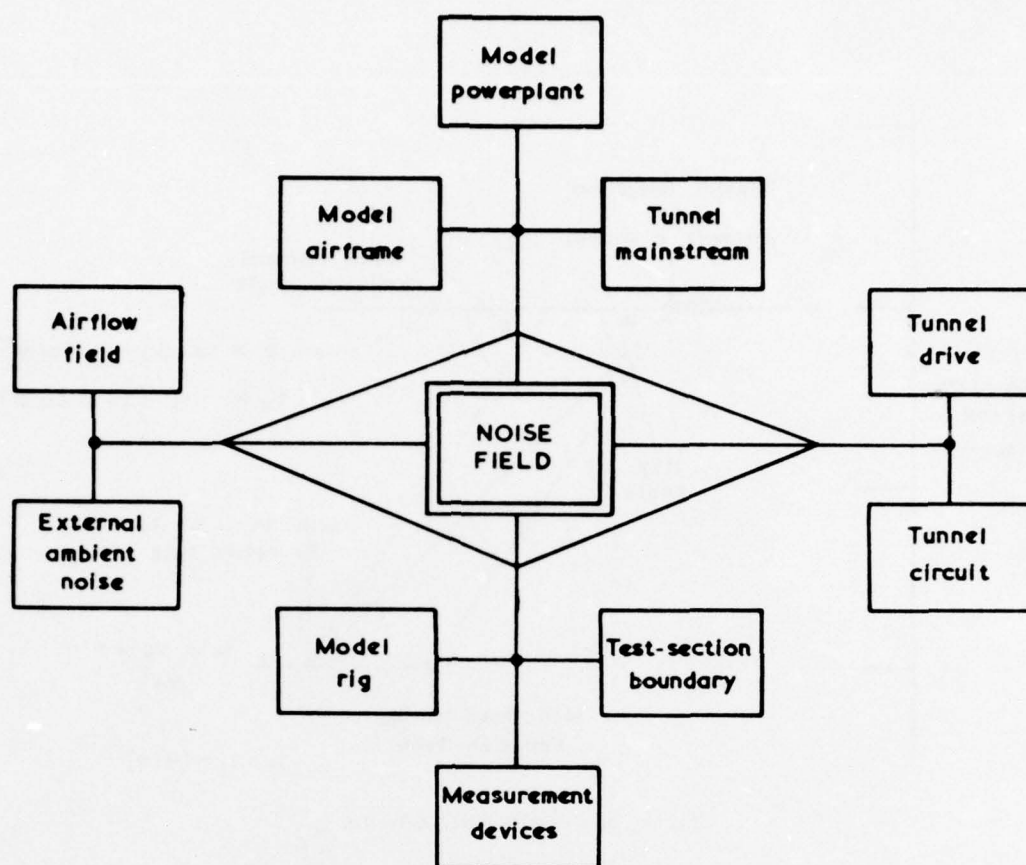
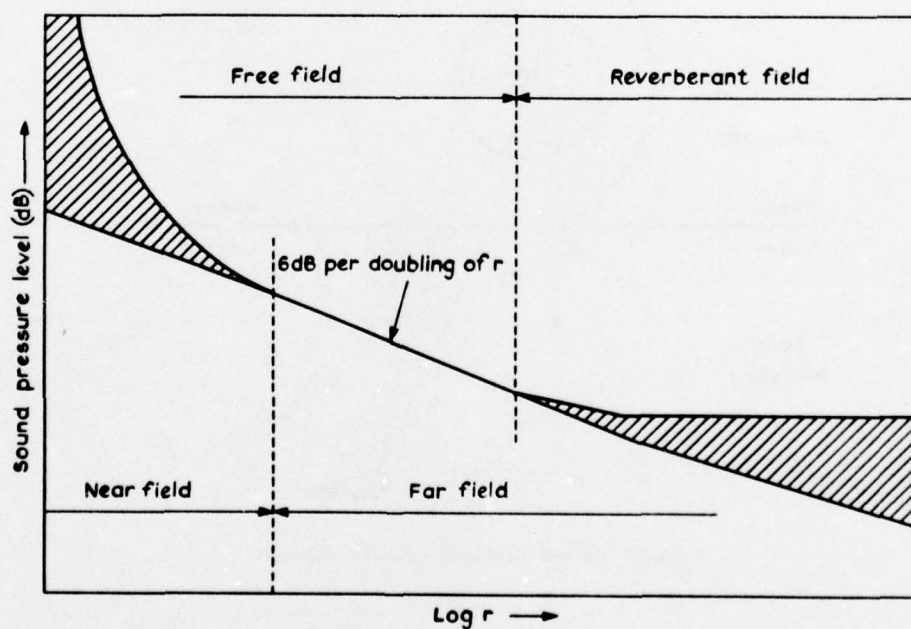


Fig.9 Simplified interaction element diagram



Large fluctuations of SPL with distance occur within shaded areas

Fig.10 Domains of measurement at distance r from a noise source in a reverberant enclosure

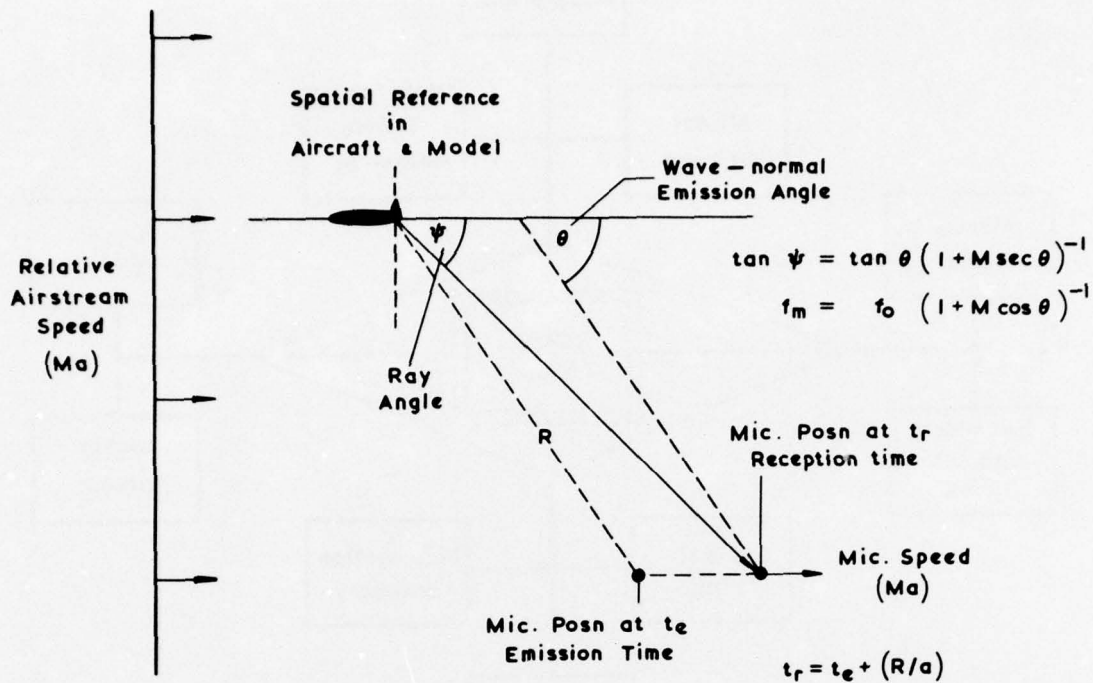


Fig.11 Ideal flight/tunnel equivalence

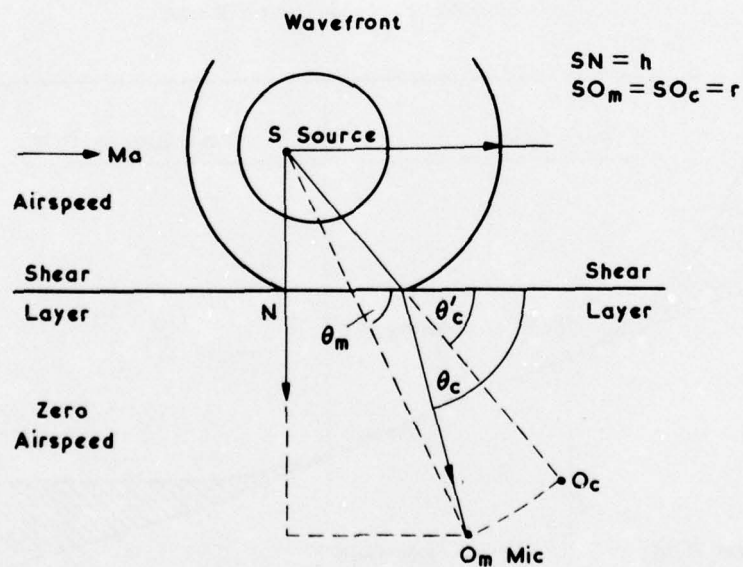


Fig.12 Tunnel shear-layer refraction principle

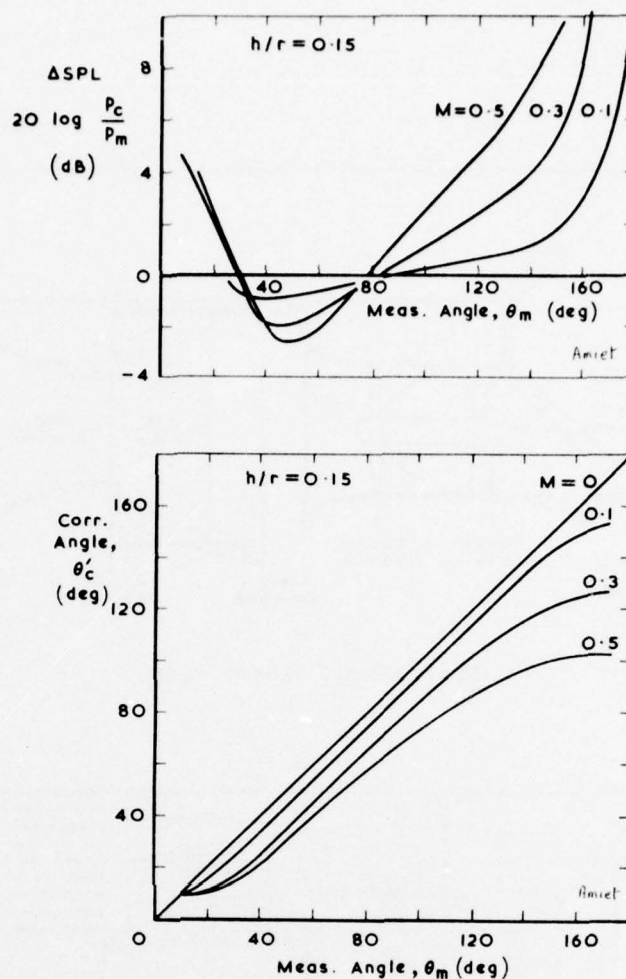


Fig.13 Tunnel-shear-layer refraction corrections

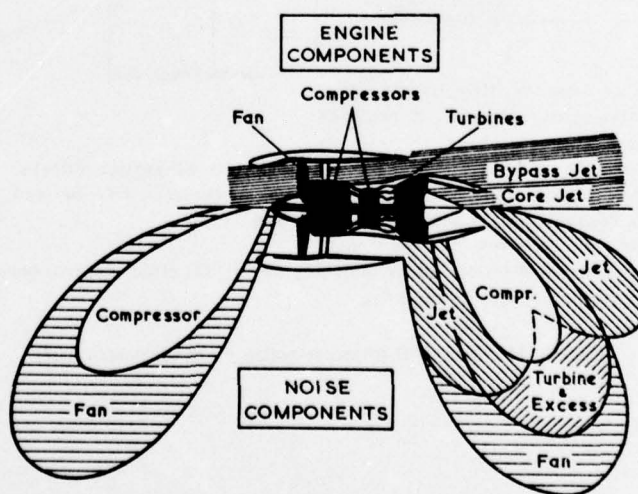


Fig.14 High bypass ratio fan-engine

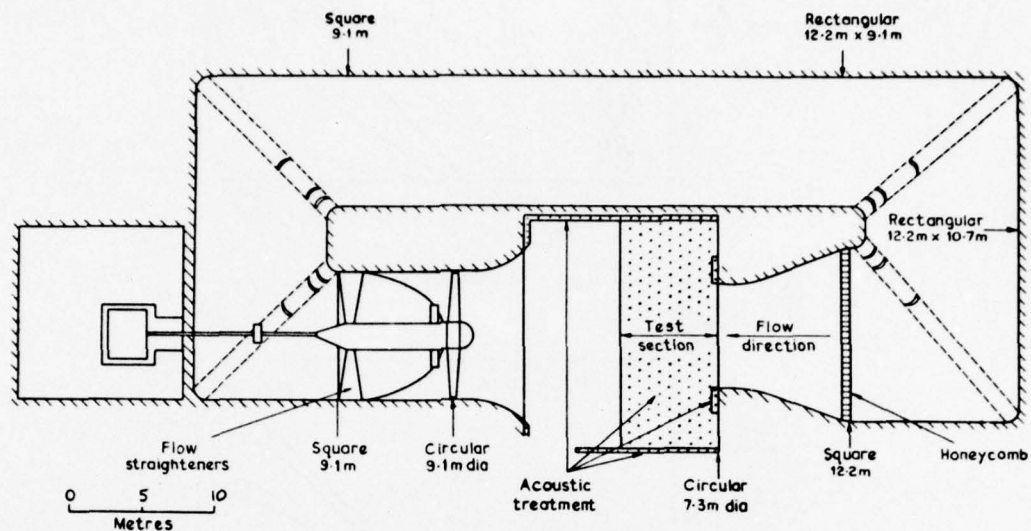
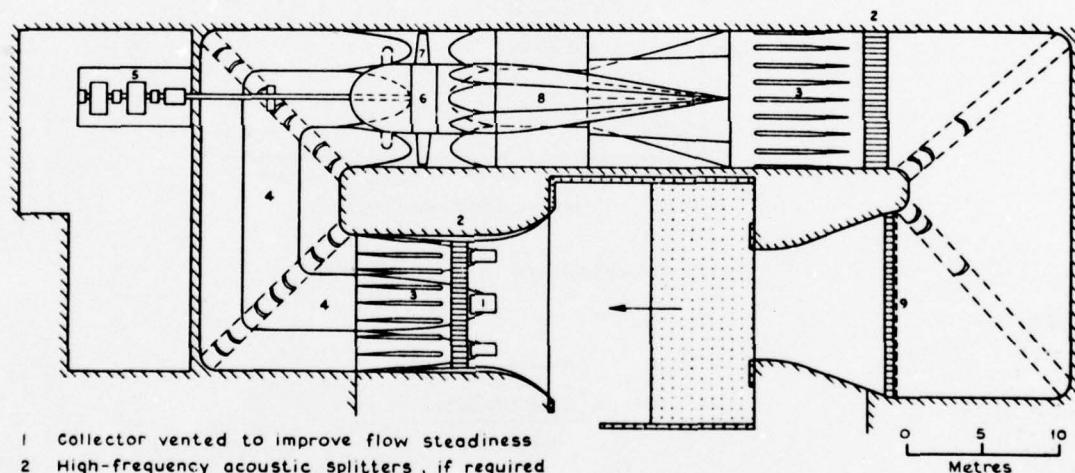


Fig. 15 Present 24 ft tunnel circuit



- 1 Collector vented to improve flow steadiness
- 2 High-frequency acoustic splitters, if required
- 3 Low-frequency acoustic splitters
- 4 Square section converted to octagonal by the addition of corner fillets
- 5 Surplus 3000 kW fan drive system in new motor house replaces life-expired 1500 kW system
- 6 Tunnel drive-fan repositioned to tunnel return leg
- 7 New low-noise fan of improved design
- 8 Multi-passage wide-angle diffuser within existing shell installed downstream of the fan
- 9 Gauze screen to reduce flow turbulence

Fig. 16 Modified 24 ft tunnel retaining 7.3 m diameter nozzle

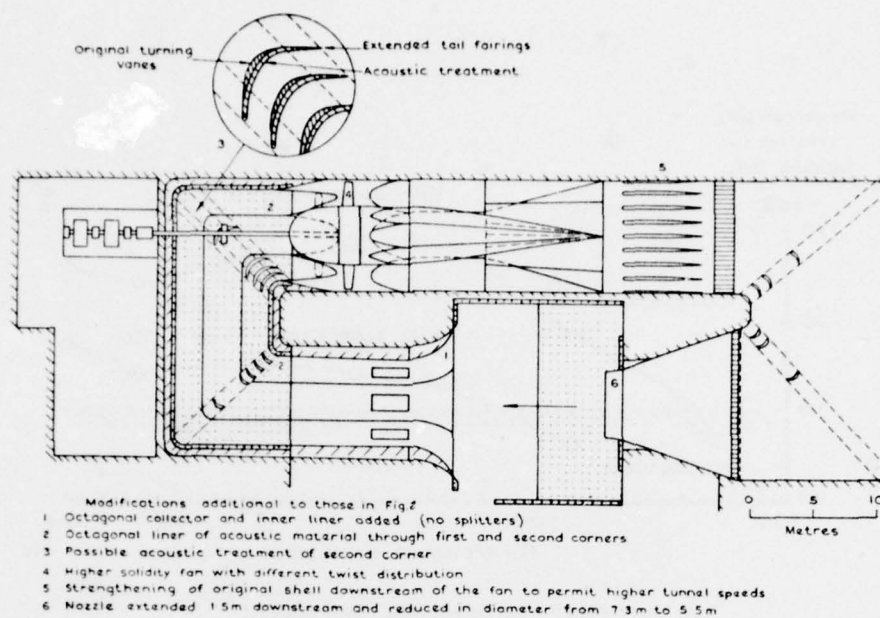
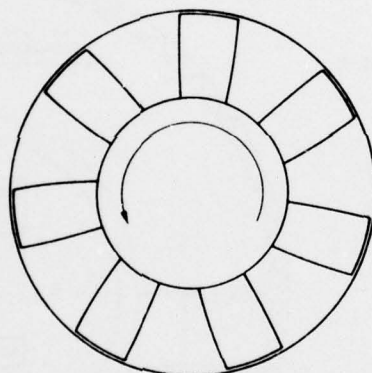


Fig.17 Modified 24 ft tunnel with 5.5 m diameter nozzle



Fan diameter = 8.9 m Centrebody diameter = 4.65 m
7 blades, chord = 1.67 m

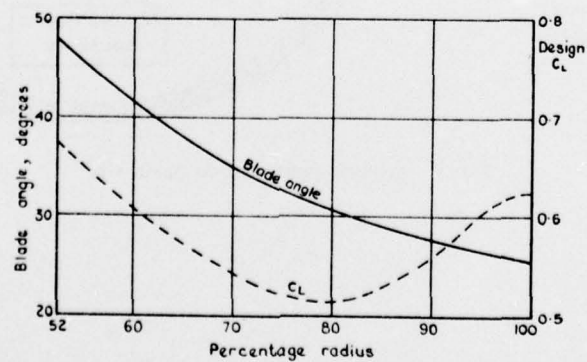


Fig.18 Proposed fan for modified 24 ft tunnel with 7.3 m nozzle

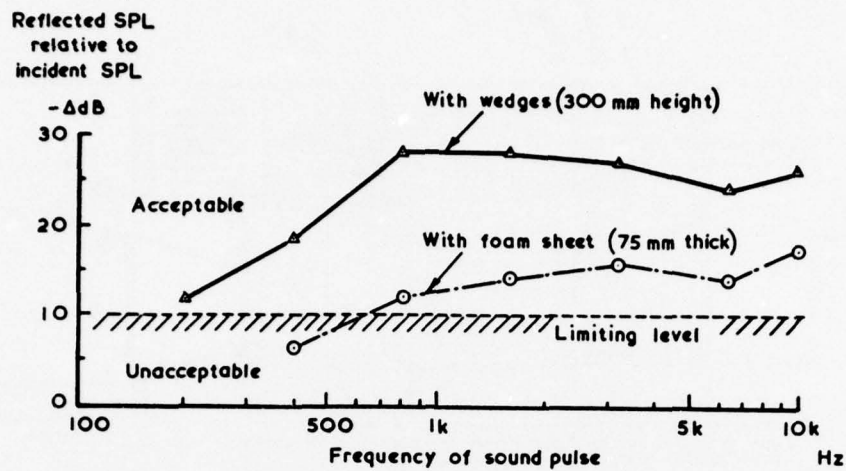


Fig.19 Reflection tests: 24 ft tunnel

For minimum frequency f_{min}
 Far-Field in Airstream if
 $R_{air} > R_{far} = k_{far} \times (a/f_{min})$
 eg $R_{air} > 1.5 \times \frac{340 \text{ m/s}}{200 \text{ Hz}}$
 $\approx 2.5 \text{ m}$

Free-Field at Mic. if
 $B_{mic} > k_{mic} \times (a/f_{min})$
 eg $B_{mic} > 0.3 \times \frac{340 \text{ m/s}}{200 \text{ Hz}}$
 $\approx 0.5 \text{ m}$

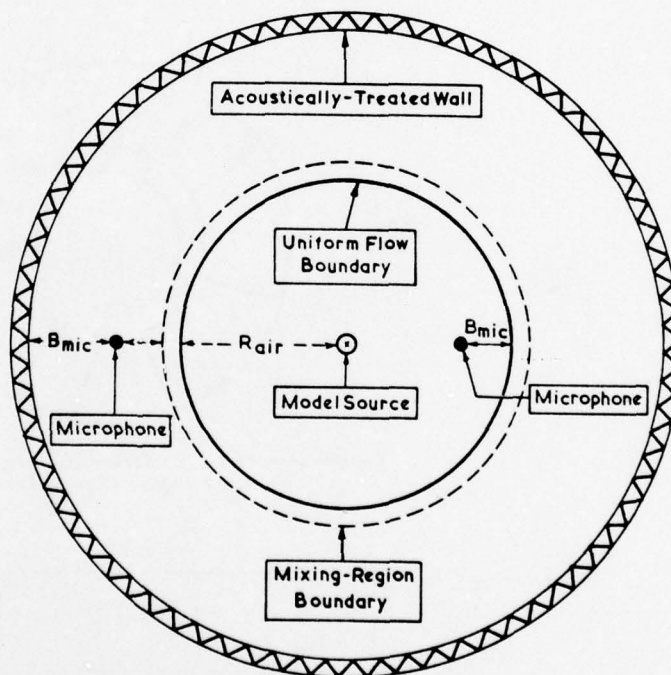


Fig.20 Acoustic constraints on tunnel size

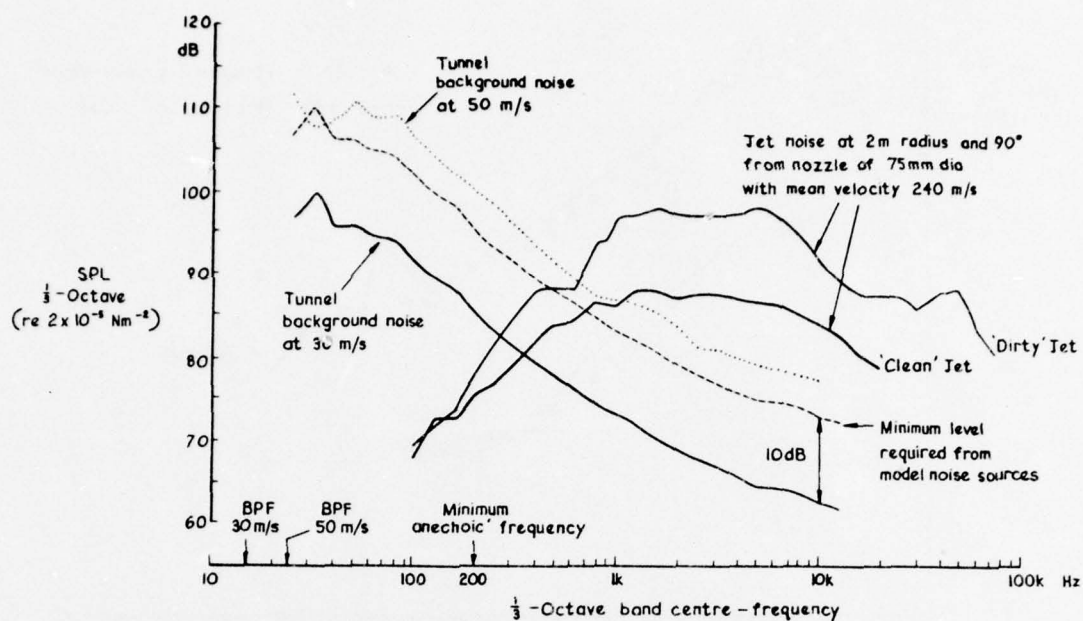


Fig.21 Comparison of background noise and jet-model noise spectra

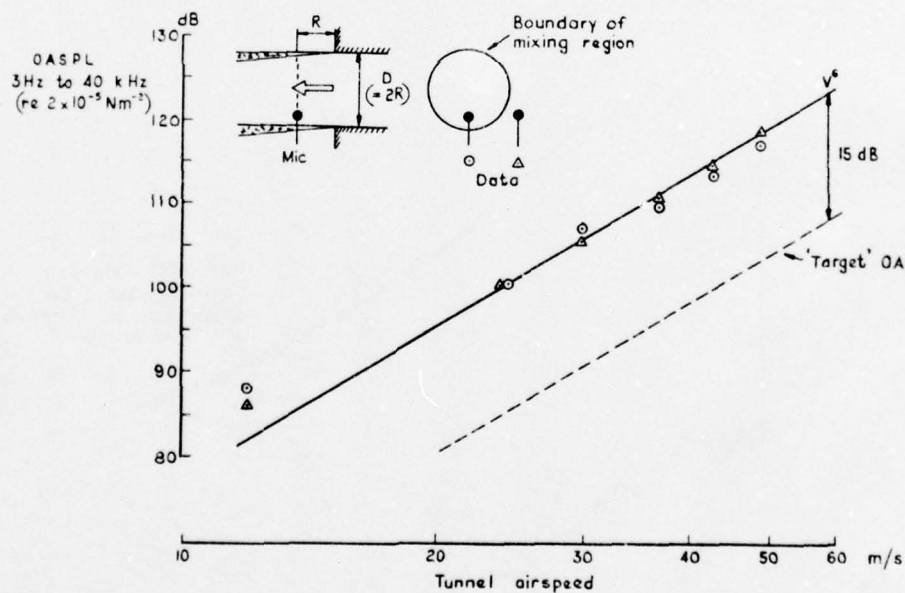


Fig.22 Variation of background noise with tunnel airspeed

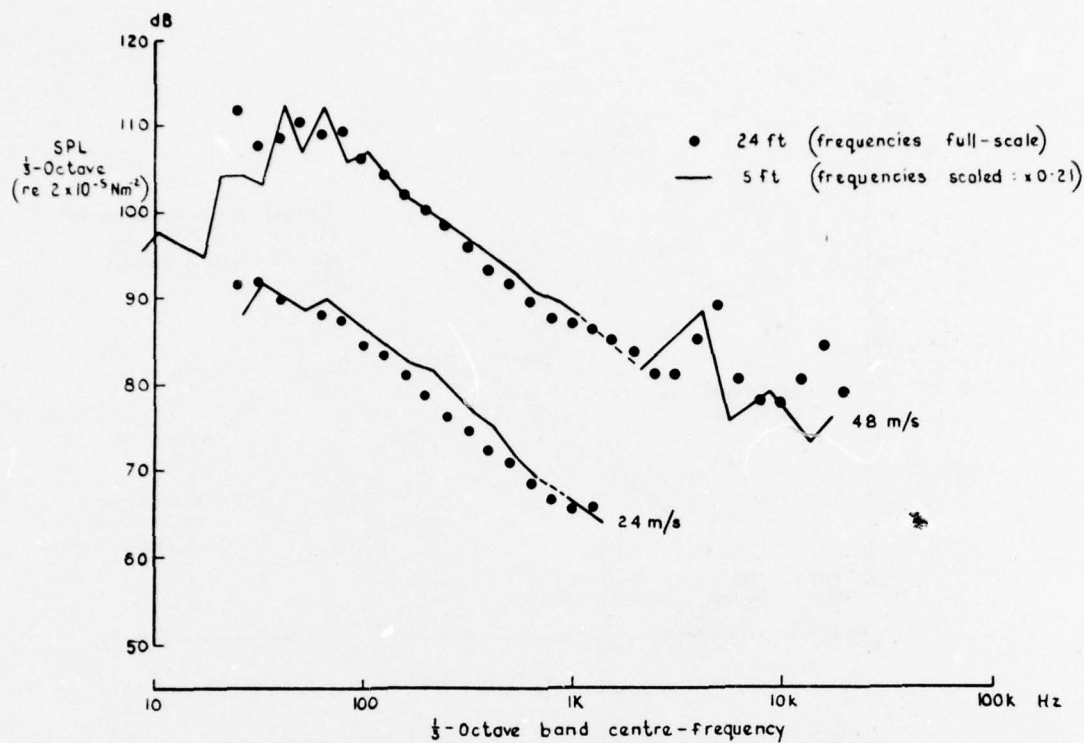


Fig.23 Comparison of background noise of RAE 24 ft and 5 ft tunnels

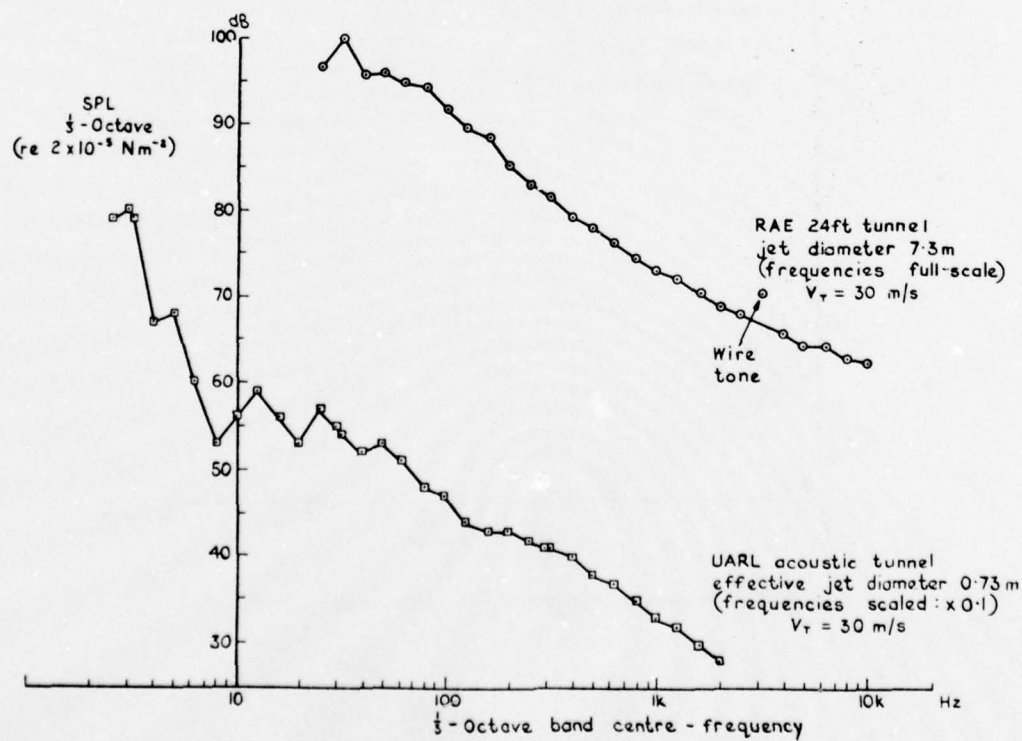


Fig 24 Comparison of background noise of RAE 24 ft and UARL tunnels

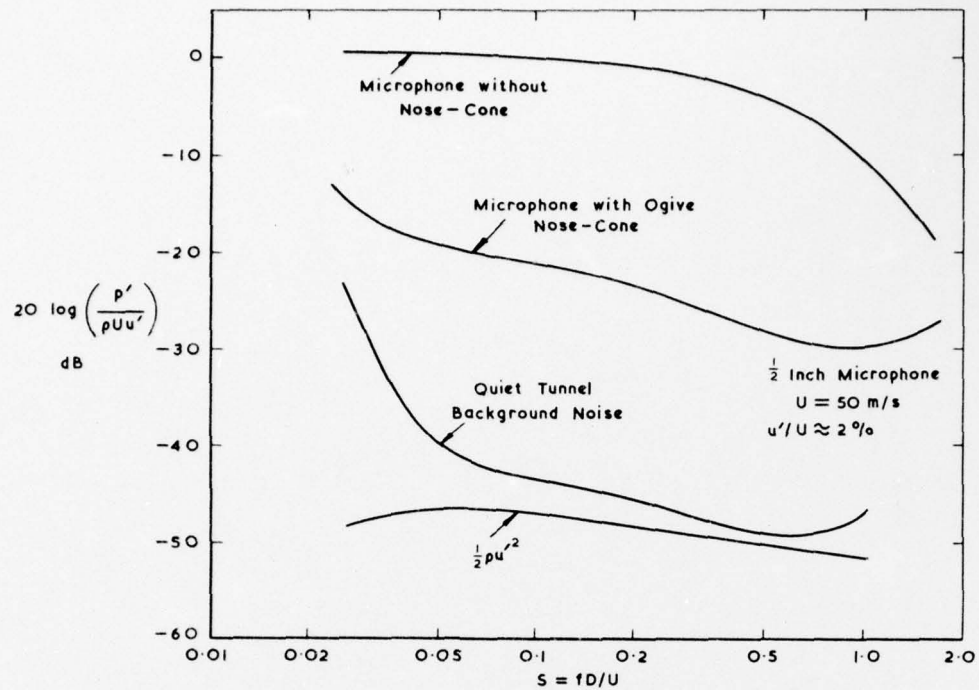


Fig.25 Comparison of microphone output and equivalent turbulence

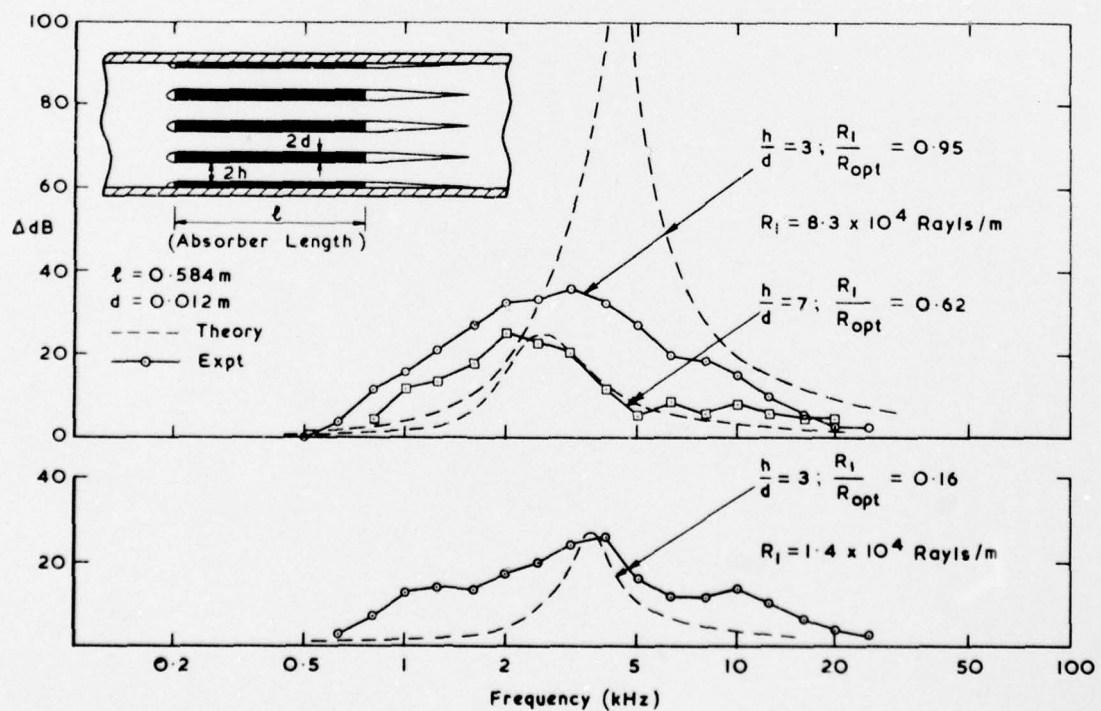


Fig.26 Noise attenuation produced by splitters

BIBLIOGRAPHY ON AERODYNAMIC NOISE

Compiled by

Miss E.H. Ridler B.Sc F.I.Inf.Sc.

Defence Research Information Centre

Ministry of Defence Procurement Executive U.K.

CONTENTS

	Page
Introduction	B-2
Bibliography	
1. Aerodynamic sound. General reviews and studies not included in later sections	B-3
2. Measurement techniques	B-6
3. Jet noise	B-8
4. Noise associated with lift augmentation devices	B-20
5. Airframe noise	B-30
6. Fan noise	B-33
7. Noise prediction	B-40
Author Index	B-47

INTRODUCTION

This bibliography is a selection of the literature published between 1973 and 1976, with emphasis on experimental studies. All references have been taken from NASA Scientific and Technical Aerospace Reports (STAR) and the American Institute of Aeronautics and Astronautics publication International Aerospace Abstracts (IAA).

The citations are presented in alphabetical order of first author within each section. An author index is concluded.

Sources and availability of references listed:

Items of the type beginning N74-28505 were obtained from STAR and copies of these reports are generally obtainable from national libraries or information centres, usually in microfiche form. Items of the type beginning A75-27943 were obtained from IAA. These are of published literature and the source is quoted in the reference.

1. Aerodynamic Sound. General Reviews and Studies not included in later sections

- 1 N74-28505 Scientific Translation Service, Santa Barbara, Calif.
EXPERIMENTAL STUDY OF THE AERODYNAMIC NOISE OF AIRFOILS
Bridelance, J.P., Quziaux, R.
Washington NASA Jul. 1974. 32 p refs Transl. into English from 10th Colloq.
d'Aerodynamique Appl., France, No 7-9, 1973 19 p.
(Contract NASw-2483)
(NASA-TT-F-15732) Avail: NTIS HC \$4.75

Analysis of the noise intensity level generated by a flow with a low back-ground noise past an airfoil or a blade cascade. A particular effort is made in this study to separate the respective influences of pure sounds and turbulence noise and to indicate possible applications of the findings obtained to the design of a low-noise turbofan. It is confirmed that the Strouhal number is the fundamental parameter in the cases studied. It is shown that the characteristic length which must be chosen for calculating the Strouhal number is the chord in the case of turbulence noise and the airfoil thickness in the case of pure sounds.

- 2 A75-27943
CLASSIFICATION PROBLEMS OF AIRCRAFT NOISE (KLASSIFIZIERUNGSPROBLEME DES FLUGLARMES)
Chalupova, V.
Hungarian Optical, Acoustical and Filmtechnical Society, Conference on Noise Abatement, 2nd, Budapest, Hungary, May 6-10, 1974, Paper 7. 7 p. In German

Some aspects of far-field measurements of the noise generated by a stationary source are examined. Particular attention is given to the determination of the acoustic power, noise level, and acoustic pressure level in the individual frequency bands to identify the noise characteristics of an engine operating in a specific mode. The determination of the directional pattern of an aircraft, involving the determination of the maximum noise level, is also studied.

- 3 A75-18385
EXPERIMENTAL EVALUATION OF TRAILING EDGE AND INCIDENCE FLUCTUATION NOISE THEORIES
Fink, M.R.
American Institute of Aeronautics and Astronautics, Aerospace Sciences Meeting, 13th, Pasadena, Calif., Jan. 20-22, 1975, Paper 75-206, 10 p. 13 refs.
Contract No. NAS3-17863

Tests were conducted to evaluate conflicting theories for trailing edge noise and for incidence fluctuation noise. A flat-plate airfoil with flush-mounted surface pressure transducers was tested in an anechoic wind tunnel at velocities from 31.5 to 177 m/sec and nominal 4 and 6% grid-generated turbulence levels. In one series of runs, the airfoil was faired into the tunnel nozzle and extended beyond the nozzle lip for studies of trailing edge noise without a leading edge and with flow on only one side. Such noise was found to vary with velocity to the fifth power and turbulence level squared as predicted by Ffowcs Williams and Hall (1970) and by Chase (1972). Power spectral density at high frequencies decayed approximately inversely with frequency to the 10/3 power as predicted by Chase. The data were poorly predicted by Hayden's correlation (1969, 1972).

- 4 N74-34482 Lockheed-Georgia Co., Marietta
NON-ENGINE AERODYNAMIC NOISE INVESTIGATION OF A LARGE AIRCRAFT - Final Report
Gibson, J.S.
Washington NASA Oct. 1974 56 p refs
(Contract NAS1-12443) Avail: NTIS HC \$3.75

A series of flyover noise measurements have been accomplished utilizing a large jet transport aircraft with engine power reduced to flight idle. It was determined that the aerodynamic (non-engine) noise levels did occur in the general range that had been predicted by using small aircraft (up to 17,690 kg gross weight) prediction techniques. The test procedures used are presented along with discussions of the effects of aerodynamic configuration on the radiated noise, identification of noise sources, and predicted aerodynamic noise as compared with measurements.

- 5 N75-11982 Lockheed-California Co., Burbank
MEASUREMENT AND ANALYSIS OF AIRCRAFT FAR-FIELD AERODYNAMIC NOISE - Final Report
Healy, G.J.
Washington NASA Dec. 1974 71 p refs
(Contract NAS1-12440)
(NASA-CR-2377; LR-26195) Avail: NTIS HC \$4.25

A systematic investigation of aircraft far-field radiated, aerodynamically generated noise was conducted. The test phase of the original program involved the measurement of the noise produced by five gliding aircraft in an aerodynamically clean configuration during low altitude flyovers. These aircraft had gross weights that ranged from 5785 to 173925N (1300 to 39,000 pounds), fly-by velocities from 30 to 98.5 m/sec (58 to 191.5 knots or 98 to 323 ft/sec) and wing aspect ratios from 6.59 to 18.25. The results of these measurements were used to develop an equation relating aerodynamic noise to readily evaluated physical and operational parameters of the aircraft. A non-dimensional frequency spectrum, based on the mean wing thickness, was also developed.

- 6 N75-14763 Cranfield Inst. of Technology (England). Coll. of Aeronautics
SUBSONIC JET TRANSPORT NOISE: THE RELATIVE IMPORTANCE OF VARIOUS PARAMETERS
Howe, D.
Jul. 1974 22 p refs
(Cranfield-Aero-25) Avail: NTIS HC \$3.25

The area of the 80 PNdB noise footprint of subsonic jet transport aircraft was evaluated using a simple expression for powerplant noise level. The parameters varied were the bypass ratio, field strength, climb out and descent angle, installed thrust, standard of engine acoustic treatment, and the rate of noise attenuation. Curves are presented for typical ranges of the variables. It was concluded that the bypass ratio is the most important influence on the footprint area. The attenuation rate also has a very significant effect but it is outside the control of the designer. Field length has only a secondary effect on noise footprint.

- 7 N73-31253 Illinois Univ., Urbana. Mechanical Engineering Dept.
A STUDY OF THE LOCAL PRESSURE FIELD IN TURBULENT SHEAR FLOW AND ITS RELATION
TO AERODYNAMIC NOISE GENERATION Status Report, 31 Jul. 1972 - 31 Jan. 1973
Jones, B.G., Planchon, H.P.
31 Jan. 1973 35 p refs
(Grant NGR-14-005-149)
(NASA-CR-134493; SR-5) Avail: NTIS HC \$3.75

Work during the period of this report has been in three areas: (1) pressure transducer error analysis, (2) fluctuating velocity and pressure measurements in the NASA Lewis 6-inch diameter quiet jet facility, and (3) measurement analysis. A theory was developed and experimentally verified to quantify the pressure transducer velocity interference error. The theory and supporting experimental evidence show that the errors are a function of the velocity field's turbulent structure. It is shown that near the mixing layer center the errors are negligible. Turbulent velocity and pressure measurements were made in the NASA Lewis quiet jet facility. Some preliminary results are included.

- 8 A75-28518
AERODYNAMIC SOUND GENERATION DUE TO THE INTERACTION OF AN UNSTEADY WAKE WITH
A RIGID SURFACE
Smith, C.A., Karamchet, K. (Stanford University, Stanford, Calif.)
American Institute of Aeronautics and Astronautics, Aero-Acoustics Conference,
2nd, Hampton, Va., Mar. 24-26, 1975, Paper 75-454, 41 p 14 refs.
Grants No. NGL-05-020-275; No. NSG-2007

Some aspects of sound generation by the interaction between a wedge and the wake of a circular cylinder in a uniform incompressible stream are studied experimentally. There is a minimum separation distance between the cylinder and the wedge when a tone is first generated. As the separation distance increases beyond the minimum, the frequency increases and asymptotically approaches the frequency normally present in the free wake. The Strouhal number defined as the ratio fd/U where f is the frequency, d is the cylinder diameter and U the free-stream speed is found to be in general a function of the Reynolds number (based on d) and h/d , where h is the separation distance. The minimum distance is in general a function of the Reynolds number. Flow visualization studies show that considerable differences exist between the flow below the minimum separation distance and just above it.

- 9 N76-13090 Federal Aviation Administration, Washington, D.C.
EFFECT OF TEMPERATURE AND HUMIDITY ON AIRCRAFT NOISE PROPAGATION - Final Report
McCollough, J.B., True, H.C.
Sept. 1975 105 p refs
(AD-A014644/9; FAA-RD-75-100) Avail: NTIS HC \$5.25

The results are presented of a test program conducted to measure the effect of varying meteorological conditions on aircraft flyover noise levels. Detailed temperature and humidity data were obtained using an instrument system carried by a light aircraft. High and low altitude inversions as well as standard lapse rate atmospheres were investigated. Level flyovers were conducted, using a DC-9-10 aircraft operated at a thrust of 6,000 lbs., as a constant noise source. Measured noise levels varied up to 4 EPNdB depending upon the absorptive properties of the atmosphere. Several analysis procedures were investigated in an effort to correct noise data for weather conditions. A layered analysis procedure normalized all flyover noise levels to those levels taken under near reference conditions. The layered analysis procedure incrementally adjusts the measured peak spectra based on the acoustic absorption in each increment. These results indicated that noise certification testing under nonuniform temperature and humidity conditions could, if allowed, be conducted provided that frequent and detailed meteorological data is available and the layered weather correction procedure is used.

- 10 N74-11804 Stanford Univ., Calif.
AERODYNAMIC SOUND GENERATION DUE TO VORTEX-AEROFOIL INTERACTION Ph.D. Thesis
Parthasarathy, R.
1973 150 p
Avail: Univ. Microfilms Order No. 73-14954

The aerodynamic sound produced by a vortex passing past an airfoil in uniform motion is studied. Following the procedure proposed by Lighthill to study how aerodynamic flows produce noise, the complete flow field is broadly divided into two separate regions: (1) a region of sound generation in the neighborhood of the airfoil, and (2) a uniform medium at rest where sound, due to the fluid fluctuations in the region (3) is being propagated. The vortex-airfoil interaction problem is formulated as a vortex of strength K being released ahead of an airfoil of chord C , at a specific location, at time $t = 0$. Classical two dimensional incompressible, inviscid, unsteady potential airfoil theory has been employed to determine the trajectory of the vortex, the forces acting on the airfoil, and the complete flow field around the airfoil.

- 11 N75-32119 National Aeronautics and Space Administration. Flight Research Center, Edwards, Calif.
REVIEW OF AIRCRAFT NOISE PROPAGATION
Putnam, T.W.
Sept. 1975 61 p refs
(NASA-TM-X-56033) Avail: NTIS HC \$4.25

The current state of knowledge about the propagation of aircraft noise was reviewed. The literature on the subject is surveyed and methods for predicting the most important and best understood propagation effects are presented. Available empirical data are examined and the data's general validity is assessed. The methods used to determine the loss of acoustic energy due to uniform spherical spreading, absorption in a homogeneous atmosphere, and absorption due to ground cover are presented. A procedure for determining ground induced absorption as a function of elevation angle between source and receiver is recommended. Other factors that affect propagation, such as refraction and scattering due to turbulence, which were found to be less important for predicting the propagation of aircraft noise, are also evaluated.

- 12 A75-25759
TRAILING EDGE NOISE
TAM, C.K.W. (Florida State University, Tallahassee, Fla.), Yu, J.C. (George Washington University; NASA Langley Research Center, Hampton, Va.)
American Institute of Aeronautics and Astronautics, Aero-Acoustics Conference, 2nd, Hampton, Va., Mar. 24-16, 1975, Paper 75-489, 13 p 16 refs. Grant No. NSG-1021

Shadowgraphic observations of the flow structure of a wall jet downstream of the trailing edge of a flat plate were carried out. Shadowgraphs obtained at jet exit Mach Number 0.3 to 0.8 consistently showed an orderly large oscillatory flow structure. It is believed that these large scale disturbances are the result of flow instabilities. It is also believed that these orderly disturbances are responsible for generating the dominant part of trailing edge noise either directly or indirectly. The interaction of sound generated by these coherent oscillatory flow disturbances and the plate was investigated theoretically. It is found that the farfield noise directivity is strongly influenced by diffraction of sound at the leading edge of the plate.

- 13 A75-35226
ACOUSTIC EMISSION OF TURBULENCE IN MOTION (SCHALLABSTRAHLUNG VON BEWEGTER TURBULENZ)
Zimmermann, G. (Max-Planck-Institut für Strömungsforschung, Göttingen, West Germany).
(Gesellschaft für angewandte Mathematik und Mechanik, Wissenschaftliche Jahrestagung,
Bochum, West Germany, Apr. 1-5, 1974)
Zeitschrift für angewandte Mathematik und Mechanik, vol. 55, Apr. 1975, p T170, T171.
In German.

Aspects of acoustic emission in the case of a limited region of turbulent flow are considered, taking into account the theory of aerodynamically generated sound developed by Lighthill (1952, 1954). A transformation of the obtained integral in relation to the system in motion provides an approach for separating the integrand into two factors. Attention is given to the results obtained for a constant convection velocity.

- 14 N75-30166 Advisory Group for Aerospace Research and Development, Paris (France)
AIRCRAFT NOISE GENERATION, EMISSION AND REDUCTION
Jun. 1975 188 p refs Presented at Lecture Series, Belgium, 16-17 Jun. 1975 and
West Germany, 19-20 Jun. 1975 and Great Britain, 23-24 Jun. 1975; sponsored by AGARD
(AGARD-LS-77) Avail: NTIS HC \$7.00

The physical properties of aircraft noise are summarized, with special emphasis on jet noise and fan-compressor-propeller-rotor noise. Topics discussed include acoustic fundamentals, noise source characteristics and interactions, atmospheric propagation, airframe noise, sonic boom, duct liner, and muffler theory. Research and technology activities related to jet engine noise and its control are discussed, and the impact of this noise on people and communities and aircraft operational procedures for noise minimization are reviewed.

2. Measurement techniques

- 15 N76-11393 European Space Agency, Paris (France)
OPTICAL COMPENSATION MEASUREMENTS ON THE NONSTATIONARY EXIT CONDITION AT A NOZZLE
DISCHARGE EDGE. AN INVESTIGATION IN CONNECTION WITH SOUND TRANSMISSION THROUGH
NOZZLES WITH FLOW
Bechert, D., Pfizenmeier, E.
Sept. 1975 77 p refs Transl. into English of "Opt. Kompensationsmessungen zur
instationären Abflussbedingung an einer Duesenaustrittskante. Eine Untersuchung im
Zusammenhang mit dem Schalldurchgang bei durchstroemten Duesen", DFVLR, Berlin
Report DLR-FB-73-93, 30 Jul. 1973. Original German report available from DFVLR,
Porz, West Ger. 27.70 DM
(ESA-TT-191; DLR-FB-73-93) Avail: NTIS HC \$5.00

The exit conditions at the trailing edge of a nozzle with a slightly nonstationary flow were investigated experimentally. These conditions play a major role in the theory of sound transmission through such nozzles. The measurements were carried out for a range of the Reynolds number R (relative to the nozzle diameter) between 10,000 and 100,000 and for a range of Strouhal numbers so that, for R equal to 10,000, the entire spectrum of amplified waves in the boundary layer was included. The technique used was based on the synchronization of a small laser beam with the wave motion of a small smoke filament in the boundary layer leaving the nozzle. The measurements of the jet flow deflection had a resolution between one and three microns. No singularity in the velocity near the edge was found. The flow problem therefore remains linear for small oscillating velocities in that area.

- 16 N74-14383 Scientific Translation Service, Santa Barbara, Calif.
REPRESENTATION OF HOT JET TURBULENCE BY MEANS OF ITS INFRARED EMISSION
De Belleval, J.F., Perulli, M.
Washington NASA Dec. 1973 24 p refs Transl. into English from Office Natl. d'Etudes
et de Rech. Aéropatiales (France), report tp-1277, 17-21 Sept. 1973 10 p
(Contract NASw-2483)
(NASA-TT-F-15233; TP-1277) Avail: NTIS HC \$3.25

The theoretical description of a jet acoustic radiation is characterized by turbulence data, defined at the scale of the total emissive volume. These data have average values, in time, i.e. representing the whole spectrum. A representation of a hot jet turbulence by means of crossed spectral densities is presented. It is possible to define at any point of the source volume the characteristics turbulence data by frequency bands.

- 17 N73-26247 Royal Aircraft Establishment, Farnborough (England). Aerodynamics Dept.
ACOUSTIC CONSIDERATIONS FOR NOISE EXPERIMENTS AT MODEL SCALE IN SUBSONIC WIND TUNNELS
Holbeche, T.A., Williams, J.
In AGARD Probl. in Wind Tunnel Testing Tech. Apr. 1973 30 p refs (AGARD-R-601)

Acoustic considerations for noise experiments at model scale in subsonic wind tunnels are presented. Emphasis is placed on similarity to flight test conditions, noise measurement constraints on model and tunnel sizes, the parasitic effects of back-ground noise, and the various factors contributing to the generation of noise. The specific contributions to tunnel noise from the tunnel drive fan, the tunnel circuit, the test section mainstream flow, and the particular test section boundary conditions are discussed.

- 18 N75-10928 McDonnell-Douglas Corp., Long Beach, Calif.
EFFECTIVE DATA MONITORING DURING AIRPLANE FLYOVER NOISE TESTS
Lowder, E.M.
In Soc. of Flight Test Engr. Advan. in Flight Test Eng. 1974 6 p

The parameters to be considered when conducting flyover tests to measure aircraft noise are discussed. The basic areas considered are: (1) the airplane/engine configuration, (2) airplane/engine performance, (3) flight procedures, (4) weather, (5) terrain, and (6) microphone installation. Emphasis is placed on noise recording validity monitoring and on-site records and measured data displays. It is stated that adjustments to the planned data sample should be made on the basis of preliminary normalized data. Comprehensive data monitoring requires automated data normalization involving a near-real time flyover noise evaluation system.

- 19 A74-39970
THE USE OF A ROTATING ARM FACILITY TO STUDY FLIGHT EFFECTS ON JET NOISE
Smith, W. (Rolls-Royce/1971/, Ltd., Bristol, England)
In International Symposium on Air Breathing Engines, 2nd, Sheffield, England, March 24-29, 1974, Proceedings. (A74-39964 20-28) London, Royal Aeronautical Society, 1974, 13 p

Description of the design, instrumentation, and operation of a rotating arm facility for the study of flight effects on jet noise, and review of the capabilities and limitations of the facility. Noise data acquisition and analysis techniques are outlined, and the results obtained from recent tests are shown to indicate the repeatability and accuracy of the data.

- 20 N73-22387 National Aeronautics and Space Administration. Langley Research Center, Langley Station, Va.
INSTRUMENTATION FOR MEASUREMENT OF AIRCRAFT NOISE AND SONIC BOOM Patent Application
Zuckerwar, A.J. inventor (to NASA) Filed 25 Apr. 1973 15 p
(NASA-Case-LAR-11193-1; US-Patent-Appl.-SN-354408) Avail: NTIS HC \$3.00

Instrumentation suitable for measuring both aircraft noise and sonic boom is described. It is comprised of a converter that produces an electric current proportional to the sound pressure level at a condenser microphone. The electric current is transmitted over a cable, amplified by a zero drive current amplifier, and recorded on a magnetic tape recorder. The converter consists of a local oscillator, a dual-gate field-effect transistor (FET) mixer, and a voltage regulator/impedance translator. The local oscillator generates a carrier voltage that is applied to one of the gates of the FET mixer. The mixer mixes the microphone signal with the carrier to produce an electrical current at the frequency of vibration of the microphone diaphragm. The voltage regulator/impedance translator regulates the voltage of the local oscillator and mixer stages, eliminates the carrier at the output, and provides a low output impedance at the cable terminals. Diagrams are included.

- 21 A74-26345
A SOLID-STATE CONVERTER FOR MEASUREMENT OF AIRCRAFT NOISE AND SONIC BOOM
Zuckerwar, A.J. (Youngstown State University, Youngstown, Ohio), Shope, W.W. (Ford Motor Co., Dearborn, Mich.)
IEEE Transactions on Instrumentation and Measurement, vol. IM-23, Mar. 1974, p 23-27, 8 refs. Grant No. NGR-36-028-004

A solid-state converter, used in a system of instrumentation for measuring aircraft noise and sonic boom, features a dual-gate FET mixer and an output stage designed for compatibility with a zero drive amplifier. With a half-inch condenser microphone the converter itself has an operating frequency range from dc-28 kHz (-3 dB), a dynamic range of 72 dB, and a noise floor of 50 dB in the band from 22.4 Hz to 22.4 kHz; the system requires no impedance matching networks and is insensitive to cable length up to at least 3000 ft.

3. Jet Noise

- 22 A75-15404
AN EXPERIMENTAL STUDY OF THE EFFECTS OF UPSTREAM OBSTRUCTIONS UPON SUBSONIC JET NOISE
Ahuja, K.K. (Syracuse University, Syracuse, N.Y.)
Journal of Sound and Vibration, vol. 37, Nov. 22, 1974, p 205-234, 37 refs

Results obtained for noise produced by two obstructions - one circular (1 inch diameter by 2.84 inch long) and another rectangular (0.4 inch thick by 1 inch wide by 2.84 inch long) in shape - immersed in both 'clean' and turbulent flows 4.8 inches upstream of the nozzle exit are described. Variations of overall sound pressure levels (OASPL's) and power watt levels with jet exit velocity and the directivities of OASPL's are considered in detail. Considerable care was taken to ensure that any comparison of the obstruction generated noise with the 'clean' jet noise is for the same mean jet exit velocity and thrust. The mean jet exit velocity was derived from the measured velocity profile at the nozzle exit in each case.

- 23 N74-27505 Pennsylvania State Univ., University Park
INVESTIGATION OF THE LARGE SCALE COHERENT STRUCTURE IN A JET AND ITS RELEVANCE TO JET NOISE
Arndt, R.E.A., George, W.K.
[1974] 20 p refs
(Grant NGR-39-009-270)
(NASA-CR-138908) Avail: NTIS HC \$4.00

A study was conducted to determine the causes of aircraft noise in large jet aircraft. It was determined that jet noise varies strongly with velocity and that significant pure tones are generated by rotor-stator interaction in the jet engines. An objective method for deducing the large eddy structure in a large jet is described. The provisions of Lighthill's theory are analyzed and applied to investigating the nature of jet noise. There is considerable evidence that a large scale coherent structure exists in a jet and that this structure can play a major role in sound radiation. Mathematical models are developed to define the parameters of orthogonal decomposition, finite extent velocity field, homogeneous fields, and periodic velocity fields.

- 24 A75-25754
AMBIENT AND INDUCED PRESSURE FLUCTUATIONS IN SUPERSONIC JET FLOWS
Barra, V, Slutsky, S., Panunzio, S. (New York University, Westbury, N.Y.)
American Institute of Aeronautics and Astronautics, Aero-Acoustics Conference, 2nd, Hampton, Va., Mar. 24-26, 1975, Paper 75-482. 14 p 29 refs. Grant No. NGR-33-016-177

An experimental investigation of the ambient static pressure fluctuations and induced acoustic fields in supersonic jet flows has been undertaken to identify possible noise sources and the mechanisms involved in the propagation of disturbances within the flows. The axisymmetric cold air jet under investigation exhausted from a 7-in. exit diameter C-D nozzle run in two conditions: one yielding a fully expanded flow and the other an overexpanded flow. The survey of static pressure fluctuations consisted of measurements of the overall levels and spectra of the fluctuations along the centerline of the two flows and the variation in level across various transverse sections. The second aspect of the study involved the development of a procedure for tracing the propagation of externally induced periodic pressure disturbances inside the jet.

- 25 N74-21898 General Electric Co., Philadelphia, Pa.
 A FORWARD SPEED EFFECTS STUDY ON JET NOISE FROM SEVERAL SUPPRESSOR NOZZLES IN THE
 NASA/AMES 40- BY 80-FOOT WIND TUNNEL Final Report
 Beulke, M.R., Clapper, W.S., McCann, E.G., Morozumi, H.M.
 3 May 1974 264p refs
 (Contract NAS2-7457)
 (NASA-CR-114741) Avail: NTIS HC \$16.25

A test program was conducted in a 40 by 80 foot wind tunnel to evaluate the effect of relative velocity on the jet noise signature of a conical ejector, auxiliary inlet ejector, 32 spokes and 104 tube nozzle with and without an acoustically treated shroud. The freestream velocities in the wind tunnel were varied from 0 to 103.6 m/sec (300 ft/sec) for exhaust jet velocities of 259.1 m/sec (850 ft/sec) to 609.6 m/sec (2000 ft/sec). Reverberation corrections for the wind tunnel were developed and the procedure is explained. In conjunction with wind tunnel testing the nozzles were also evaluated on an outdoor test stand. The wind tunnel microphone arrays were duplicated during the outdoor testing. The data were then extrapolated for comparisons with data measured using a microphone array placed on a 30.5 meter (100 ft) arc. Using these data as a basis, farfield to nearfield arguments are presented with regards to the data measured in the wind tunnel. Finally, comparisons are presented between predictions made using existing methods and the measured data.

- 26 A75-27929
 AN INVESTIGATION OF THE NOISE FROM A SCALE MODEL OF AN ENGINE EXHAUST SYSTEM
 Bryce, W.D., Stevens, R.C.K. NGTE, Farnborough, Hants, England
 American Institute of Aeronautics and Astronautics, Aero-Acoustics Conference,
 2nd, Hampton, Va., Mar. 24-26, 1975, Paper 75-459. 16 p. 14 refs.

To assist in the identification and understanding of the noise sources which contribute to the exhaust noise of aircraft gas-turbine engines, controlled experiments have been carried out to study the noise characteristics of a model turbojet exhaust system. The noise data have been related to measurements of the aerodynamic conditions in the model and, with the aid of specific diagnostic tests, the predominant noise mechanisms are considered to have been recognized. The noise radiation, above that of the jet, is attributed primarily to dipole sources generated by the turbine outlet struts, the transmission of this noise being modified by duct propagation and nozzle impedance effects.

- 27 N74-28240 National Aeronautics and Space Administration, Lewis Research Center,
 Cleveland, Ohio
 FLIGHT VELOCITY EFFECTS ON THE JET NOISE OF SEVERAL VARIATIONS OF A 104-TUBE
 SUPPRESSOR NOZZLE
 Burley, R.R.
 Washington Jul. 1974 53 p refs
 (NASA-TM-X-3049; E-7901) Avail: NTIS HC \$3.75

At the relatively high takeoff speeds of supersonic transport aircraft, an important question concerns whether the flight speed affects the noise of suppressor nozzles. To answer this question, flyover and static tests using a modified F-106B aircraft were conducted on a 104-tube suppressor nozzle. Comparison of adjusted flyover and static spectra indicated that flight velocity had a small adverse effect on the suppression of the 104-tube suppressor. The adverse effect was larger with the acoustic shroud installed than without it.

- 28 N75-26292 Stanford Univ., Calif.
 AN EXPERIMENTAL STUDY OF THE STRUCTURE AND ACOUSTIC FIELD OF A JET IN A CROSS STREAM
 Ph.D. Thesis
 Camelier, I.de A.
 1975 135p
 Avail: Univ. Microfilms Order No 75-13493

In order to understand the noise generated and radiated by a high speed circular jet issuing normally into an otherwise uniform stream, such as in the case of V/STOL aircraft, experimental studies were carried out in 7 x 10 foot wind tunnel. The jet is 1.5 inches in diameter and is operated at a fixed Mach number equal to .58. The tunnel velocity is changed to vary the ratio of the speed of the jet to that of the uniform stream in the range from 3.7 to 9.4. Measurements for zero crossflow were also included. A survey of the plane of symmetry of the jet was performed to measure the mean and turbulent velocity fields by using constant temperature hot wire anemometry. The intensity of the noise radiated from the jet was determined in the tunnel test section by utilizing the cross-correlation at a particular time delay between the signals of two microphones suitably located along a given direction.

29 A75-41800

DISCRETE ACOUSTIC RADIATION FROM A HIGH-SPEED JET AS A SINGULAR PERTURBATION PROBLEM

Chan, Y.Y. National Research Council, High-Speed Aerodynamics Lab., Ottawa, Canada
Canadian Aeronautics and Space Journal, vol. 21, June 1975, p. 221-227. 12 refs

The directional radiation of acoustic waves generated by the shear layer instability of a high-speed jet has been analyzed as a singular perturbation problem. Solutions up to the first order are obtained by the technique of matched asymptotic expansion. The zero order solution is the viscous mixing of the jet. The first order outer expansion yields the acoustic wave equation and the inner expansion the small disturbance equations for the jet instability. The analysis is applied to a small helium jet emanating into the surrounding air. The calculated radiation frequencies and wave numbers are in good agreement with experimental data.

30 N74-18669

INVESTIGATION OF FAR-FIELD AND NEAR-FIELD JET NOISE Ph.D. Thesis

Chen, C.Y. Cincinnati Univ., Ohio

1973 167p

Avail: Univ. Microfilms Order No 74-95167

A method is presented for estimating jet noise in terms of the details of the turbulent field. The acoustic characteristics of a jet are obtained by evaluating contributions from the distribution of sound sources represented as small volume elements of turbulence. Each volume element is regarded as an elementary sound generator emitting acoustic energy at a characteristic frequency. Several models for far- and near-field calculations based on various extensions of Lighthill's quadrupole theory are formulated and evaluated by comparing with experimental data. It is shown that quantitative estimates are obtainable for both the far and near field. The strength distribution of sound sources in a jet obtained in the present calculation is in agreement with the generally accepted theory. It is also shown that an increase of initial turbulence level causes a more pronounced increase of sound at high frequencies than at low frequencies for the far and near field.

31 A75-18302

CALCULATIONS OF FAR-FIELD AND NEAR-FIELD JET NOISE

Chen, C.Y. United Aircraft Research Laboratories, East Hartford, Conn.

American Institute of Aeronautics and Astronautics, Aerospace Sciences Meeting, 13th, Pasadena, Calif., Jan. 20-22, 1975, Paper 75-93. 18p 60 refs

A method is presented for estimating the noise produced by both cold and hot, shock-free round jets in terms of the details of the turbulent field. The acoustic characteristics of the jet are obtained by evaluating contributions from distributed sound sources represented as small volume elements of turbulence. Each volume element is regarded as an independent sound generator emitting acoustic energy at a characteristic frequency. Several models for far-field and near-field noise calculations based on various extensions of Lighthill's quadrupole theory are formulated and evaluated by comparing with experimental data. It is shown that quantitative estimates are obtainable for both the far and near fields. The strength distribution of sound sources in a jet obtained in the present calculation is in agreement with generally accepted theory. The initial turbulence level of a jet is shown to significantly affect far and near field noise levels and the high frequency portion of the noise spectra.

32 A75-27930

SUBSONIC JET NOISE IN FLIGHT BASED ON SOME RECENT WIND-TUNNEL TESTS

Cocking, B.J., Bryce, W.D. NGTE, Farnborough, Hants, England

American Institute of Aeronautics and Astronautics, Aero-Acoustics Conference 2nd, Hampton, Va., Mar. 24-26, 1975, Paper 75-462 20 p. 24 refs

The mixing noise produced by a cold subsonic air jet has been measured under simulated flight conditions in a large open-jet wind tunnel which has been modified for acoustic work. At a noise emission angle of 90 degrees to the jet axis, the overall sound pressure level reduces approximately in proportion to the fifth power of the relative jet velocity and the noise reductions in the rear arc increased steadily as the jet axis is approached. These results are compared with theory, and together with some limited data obtained from a coaxial jet, are used as the basis for a discussion on the prediction of jet noise in flight.

- 33 A75-37901
COHERENT STRUCTURE IN A LOCALLY SUBSONIC HOT JET
(STRUCTURE COHERENT DANS UN JET CHAUD LOCALEMENT SUBSONIQUE)
Dahan, C., Elias, G., Lelarge, A.
(Societe Francaise de Physique, Congres, Dijon, France, June 30-July 4, 1975) ONERA, TP no. 1975-69, 1975. 22 p. 13 refs. In French
- Near-field microphonic exploration and infrared radiometry of a subsonic free jet indicate the presence of large-scale turbulence structures in the mixing zone of the jet. A linear hydrodynamic instability approach to the locally stratified flow forms the basis for a second-order analysis of the radiometric signals. An approach oriented toward the dynamics of the turbulent motions is used to characterize the mixing mechanism; it is shown that the large coherent structures, formed between one and two diameters downstream, reach the end of the potential cone without being severely degraded, having traveled at a constant mean velocity. A transition is then initiated at this point.
- 34 N73-28177 Michigan State Univ., East Lansing. Div. of Engrg Research
PRELIMINARY RESULTS FOR A LARGE ANGLE OBLIQUE JET IMPINGEMENT AND FLOW AND FOR THE EFFECT OF INITIAL CONDITIONS ON THE NEAR FIELD OF AN AXISYMMETRIC JET
Foss, J.F., Kleis, S.J.
25 May 1973 61 p refs
(Grant NGR-23-004-068)
(NASA-CR-121257; SAR-3) Avail: NTIS HC \$5.25

The structure of an axisymmetric jet in the near field is discussed for jet noise and for jet impingement schemes for STOL aircraft. It is inferred from previous studies, and the inference is supported by analysis, that the scale and intensity of the turbulence structure at the jet exit plane are the important boundary conditions which effect the development of the flow in the near field. The techniques to study these effects while maintaining a uniform mean flow and the results which document the range of the initial conditions are presented. The large angle, oblique jet impingement conditions is of interest in terms of the jet/flap interaction. Detailed turbulence data can be obtained with the specially constructed facility. The development of the flow and instrumentation system and initial data from the new facility are presented.

- 35 N75-11950 Tennessee Univ. Space Inst., Tullahoma
SOME RESULTS OF AEROACOUSTIC RESEARCH
Goethert, B.H.
In Tech. Hochschule Aachen Short Course on STOL Aircraft Technol. and the Community Vol. 2 1974 13 p refs
- Research on special noise producing characteristics of unconventional exhaust nozzles such as multicircular nozzles, slot nozzles, and nozzles with flaps as noise shields, is reported. Studies have been initiated on exhaust jets, which mix with secondary air underneath a shroud. Such a configuration has a region of high turbulence, and thus also of intense noise shielded from the outside, and discharges the exhaust jet into the atmosphere at greatly reduced velocities, leading to overall exhaust noise reduction. Some calculations were carried out in order to determine the potential of these configurations. Initial test results with shrouds equipped with internal noise attenuating liners confirmed the predicted potential.
- 36 N75-21281 Tennessee Univ. Space Inst., Tullahoma
SOME RESULTS OF AEROACOUSTIC RESEARCH
Goethert, B.H.
(1974) 13 p refs
Avail: NTIS HC \$3.25

Fundamental and applied research in the field of exhaust jet noise, emphasizing the special noise producing characteristics of unconventional exhaust nozzles as multicircular, slot, and those with noise flap shields are reported. Studies were initiated on exhaust jets, which mix with secondary air underneath a shroud. The guiding idea of such configurations is to have the region of high turbulence and thus also of intense noise shielded from the outside, and have the exhaust jet discharged into the atmosphere at greatly reduced velocities. At such reduced velocities, the externally generated noise is greatly reduced, and in conjunction with the internal shielding of the primary jet, a significant reduction of the total exhaust noise can be expected.

- 37 A75-43741
THE LOW FREQUENCY SOUND FROM MULTIPOLE SOURCES IN AXISYMMETRIC SHEAR FLOWS, WITH APPLICATIONS TO JET NOISE
Goldsmith, M.E. NASA, Lewis Research Center, Cleveland, Ohio
Journal of Fluid Mechanics, vol. 70, Aug. 12, 1975, p. 595-604. 18 refs

A closed-form solution for the sound radiation from multipole sources imbedded in an infinite cylindrical jet with an arbitrary velocity profile is obtained. It is valid in the limit where the wavelength is large compared with the jet radius. Simple formulae for the acoustic pressure field due to convected point sources are also obtained. The results show (in a simple way) how the mean flow affects the radiation pattern from the sources. For convected lateral quadrupoles it causes the exponent of the Doppler factor multiplying the far-field pressure signal to be increased from the value of 3 used by Lighthill to 5.

- 38 N74-16728 Graham Associates, Shaw Island, Wash.
THEORETICAL STUDY OF THE EFFECTS OF REFRACTION ON THE NOISE PRODUCED BY TURBULENCE IN JETS Final Report
Graham, E.W., Graham, B.B.
Washington NASA Mar. 1974 104p refs
(Contract NAS1-11533)
(NASA-CR-2390) Avail: NTIS HC \$4.50

The production of noise by turbulence in jets is an extremely complex problem. One aspect of that problem, the transmission of acoustic disturbances from the interior of the jet through the mean velocity profile and into the far field is studied. The jet (two-dimensional or circular cylindrical) is assumed infinitely long with mean velocity profile independent of streamwise location. The noise generator is a sequence of transient sources drifting with the surrounding fluid and confined to a short length of the jet.

- 39 N76-13883 Graham Associates, Shaw Island, Wash.
THEORETICAL STUDY OF REFRACTION EFFECTS ON NOISE PRODUCED BY TURBULENT JETS Final Report
Graham, E.W., Graham, B.B.
Washington NASA Dec. 1975 92p refs
(Contract NAS1-12834)
(NASA-CR-2632) Avail: NTIS HC \$5.00

The transmission of acoustic disturbances from the interior of a jet into the ambient air is studied. The jet is assumed infinitely long with mean velocity profile independent of streamwise location. The noise generator is a sequence of transient sources drifting with the local fluid and confined to a short length of the jet. In Part 1, supersonic jets are considered. Numerical results for mean-square pressure versus angle in the far-field show unexpected peaks which are very sharp. Analysis of simplified models indicates that these are complex quasi-resonant effects which appear to the stationary observer in a high frequency range. The peaks are real for the idealized model, but would be smoothed by mathematical integration over source position, velocity, and frequency. Subsonic jets were considered in part 2, and a preliminary study of the near-field was attempted. Mean-square radial displacements (or mean radial energy flow or space-time correlations of radial pressure gradient) are first found for very simple cases. The most difficult case studied is a sequence of transient sources at the center of a uniform-velocity circular cylindrical jet. Here a numerical triple integration is required and seems feasible although only preliminary results for mean square radial displacement are now available. These preliminary results show disturbances decreasing with increasing radial distance, and with increasing distance upstream and downstream from the source. A trend towards greater downstream disturbances appears even in the near field.

- 40 N75-24161 Illinois Univ., Urbana
AN EXPERIMENTAL INVESTIGATION OF THE TURBULENT CHARACTERISTICS OF CO-AXIAL JET FLOWS AND THEIR ROLE IN AERODYNAMIC NOISE GENERATION Ph.D. Thesis
Hammersley, R.J.
1974 214p
Avail: Univ. Microfilms Order No 75-11777

An experimental and analytical study of the velocity and pressure fields in the turbulent mixing regions of a co-annular jet was conducted. These results were applied to the prediction of the aerodynamic noise by jet flows. The work was performed on an isothermal, subsonic flow system; the co-annular nozzle configurations provided area ratios of 2.2 and 7.4 and velocity ratios ranging from 0.0 to 0.8 were examined. The turbulence measurements utilized standard constant temperature hot-wire anemometry techniques and a pressure transducer. The narrow-band space-time correlation model was applied to the prediction of the jet's far-field noise. The model was used to specify the source term in Ribner's formulation of the sound radiated by a turbulent pressure field. The results were compared to measured noise levels and the dependence upon the several input parameters was discussed.

- 41 N73-21573 NASA, Langley Research Center, Langley Station, Va.
ANALYSIS OF NOISE PRODUCED BY AN ORDERLY STRUCTURE OF TURBULENT JETS
Hardin, J.C.
Washington Apr. 1973 31 p refs
(NASA-TN-D-7242; L-8834) Avail: NTIS HC \$3.00

The orderly structure which has been observed recently by numerous researchers within the transition region of subsonic turbulent jets is analyzed to reveal its noise-producing potential. For a circular jet, this structure is modeled as a train of toroidal vortex rings which are formed near the jet exit and propagate downstream. The noise produced by the model is evaluated from a reformulation of Lighthill's expression for the far-field acoustic density, which emphasizes the importance of the vorticity within the turbulent flow field. It is shown that the noise production occurs mainly close to the jet exit and depends primarily upon temporal changes in the toroidal radii. The analysis suggests that the process of formation of this regular structure may also be an important contribution of the high-frequency jet noise. These results may be helpful in the understanding of jet-noise generation and in new approaches to jet-noise suppression.

- 42 N74-17004 California Univ., Los Angeles
PRESSURE CROSS-CORRELATIONS IN THE INVESTIGATION OF AERODYNAMIC NOISE FROM JETS
Ph.D. Thesis
Hurdle, P.M.
1973 178p
Avail: Univ. Microfilms Order No 73-28714

Cross correlation techniques were employed to investigate the noise generating source distribution for a subsonic free jet. The cross correlation measurement was the basis for the calculation of a Q-function, which is defined as the fraction (per unit volume) of the mean square far field sound pressure originating in a particular region within the turbulent volume. Employing this Q-function, the source distributions of a free jet at two different jet exit velocity are quantitatively described. To examine the validity of this technique employed, the Q-function was integrated over a reasonable turbulent volume. The integration showed good agreement with the theory. The results of this experiment showed that the turbulent volume mainly responsible for the noise generated is confined to a rather limited cylindrical volume centered about the jet axis in the vicinity of the end of the potential core region with a length of approximately six jet diameters.

- 43 N74-27487 NASA, Lewis Research Center Cleveland, Ohio
ACOUSTIC TESTS OF A 15.2 CENTIMETER-DIAMETER POTENTIAL FLOW CONVERGENT NOZZLE
Karchmer, A.M.; Dorsch, R.G.; Friedman, R.
Washington Jun. 1974 19 p refs
(NASA-TM-X-2980) Avail: NTIS HC \$3.00

An experimental investigation of the jet noise radiated to the far field from a 15.2-cm-diam potential flow convergent nozzle has been conducted. Tests were made with unheated airflow over a range of subsonic nozzle exhaust velocities from 62 to 310 m/sec. Mean and turbulent velocity measurements in the flow field of the nozzle exhaust indicated no apparent flow anomalies. Acoustic measurements yielded data uncontaminated by internal and/or background noise to velocities as low as 152 m/sec. Finally, no significantly different acoustic characteristics between the potential flow nozzle and simple convergent nozzles were found.

- 44 N73-24697 Lockheed Missiles and Space Co., Palo Alto, Calif
HIGH-FREQUENCY SPECTRUM DOMAIN OF TURBULENT JET NOISE
Krasilnikov, V.A.; Shikhlińskaia, R.E.
(1973) 3 p refs Transl. into ENGLISH from Vestn. Mosk. Univ. Ser. 3-Fiz-Astron (Moscow) v 12, no 5, 1972, p 626-628
Avail: NTIS HC \$3.00 National Translations Center John Crerar Library, Chicago, Illinois 60616

The expression for the dependence of the noise power spectral density on the radiation frequency is found by using similarity and dimensional analysis. The expression is then used to find the high frequency part of the turbulent jet noise spectrum where viscosity is essential.

- 45 A75-25751
EXPERIMENTS ON SUPERSONIC JET NOISE
Laufer, J., Schlinker, R., Kaplan, R.E. Southern California, University, Los Angeles, Calif. American Institute of Aeronautics and Astronautics, Aero-Acoustics Conference, 2nd Hampton, Va., Mar. 24-26, 1975, Paper 75-478. 16p 26 refs.
US Department of Transportation
Contract No OS-00002
- Certain aspects of the noise generation by a supersonic jet were investigated at jet Mach numbers 1.5, 2.0 and 2.5. In particular, the axial source strength per unit length, w , was determined using a specially developed directional microphone system. The integrated value of w along the jet axis was found to be consistent with the sound intensity obtained by conventional direction microphone confirming the a priori assumption that the jet consists of independent, spatially compact acoustic sources. The main finding of the investigation is the presence of two distinct intense noise producing regions in a jet having supersonic source velocities, the upstream region radiating in the form of Mach waves. An estimate of the fraction of the radiated intensity associated with the Mach waves is also made.
- 46 A75-26234
DEVELOPMENT OF ACOUSTIC DISTURBANCES IN SUPERSONIC ANNULAR JETS
(RAZVITYE AKUSTICHESKIKH VOZMUSHCHENII V SVERKHZVUKOVYKH KOL'TSEVYKH STRUIAKH)
Lebedev, M.G., Telenin, G.F. Moskovskii Gosudarstvennyi Universitet, Institut Mekhaniki, Nauchnye Trudy, no. 30, 1973, p. 182-199. In Russian
- The present work investigates theoretically the interaction of a supersonic jet issuing from an annular nozzle with an external acoustic field. The sound waves are taken to be traveling towards the nozzle, and the analysis concerns in particular the effect of the interior region between the nozzle end and the area where the ring jet comes together to form a single jet on the sound field. This interior region has certain resonating properties. The analysis is carried out in a linear approximation for both planar and cylindrical models and for the two cases when the disturbances on opposite sides of the jet are either in phase or antiphase. Expressions are derived for certain characteristic frequencies at which disturbances in the jet and the interior region significantly exceed those in the external field.
- 47 N75-28021 Old Dominion Univ, Research Foundation, Norfolk Va. School of Engng
ANALYTICAL SIMULATION OF THE FAR-FIELD JET NOISE AND THE UNSTEADY JET FLOW-FIELD
BY A MODEL OF PERIODIC SHEDDING OF VORTEX RING FROM THE JET EXIT Final Technical Report
Liu, C.H.
Aug. 1975 4 p
(Grant NsG-1144)
(NASA-CR-143211; TR-75-T10) Avail: NTIS HC \$3.25
- The construction of a theoretical flow field due to shedding of vortex rings, the identification of the controlling parameters, and the determination of whether the theoretical model successfully simulated the unsteady pressure field near jet (and consequently the far field noise) was studied. The basic parameters contained in the analytic solutions were the epoch at which a vortex ring was shed near the jet exit and the eddy viscosity coefficient. These parameters were identified from the experimental data for the real-time pressure and from the spread of the mixing layer of the jet. Results of the theoretical analysis show good qualitative agreement with the experimental data.
- 48 A75-33067
EXPERIMENTS ON THE INSTABILITY WAVES IN A SUPERSONIC JET AND THEIR ACOUSTIC RADIATION
McLaughlin, D.K., Morrison, G.L., Troutt, T.R. (Oklahoma State University, Stillwater, Okla). Journal of Fluid Mechanics, vol. 69, May 13, 1975, p. 73-95. 26 refs.
NSF Grant No GK-32686

The instability and acoustic radiation of an axisymmetric supersonic jet of low Reynolds number are studied experimentally. Hot-wire measurements in the flow field and microphone measurements in the acoustic field are obtained from different size jets at Mach numbers of about 2. Hot-wire measurements indicate that the instability process in the perfectly expanded jet consists of numerous discrete frequency modes around a Strouhal number of 0.18, where the waves grow almost exponentially and propagate downstream at a velocity greater than the ambient speed of sound. Microphone measurements show that the wavelength, wave orientation, and frequency of the acoustic radiation generated by the dominant instability agree with the Mach wave concept. The sound pressure levels measured in the low Reynolds number jet extrapolate to values approaching the noise levels measured by other investigators in high Reynolds number jets, so that noise generation in high Reynolds number jets is attributed mainly to large-scale instability. The agreement of experimental results with Tam's theoretical predictions is discussed.

- 49 N73-33181 NASA, Langley Research Center, Langley Station, Va.
ON THE RELATIONSHIP BETWEEN ACOUSTIC ENERGY DENSITY FLUX NEAR THE JET AXIS AND FAR
FIELD ACOUSTIC INTENSITY
Maestrello, L.
Washington Oct. 1973 64 p refs
(NASA-TN-D-7269; L-8871) Avail: NTIS HC \$3.00

By measurement and analysis, the relationship between the distribution of the outflow of acoustic energy over the jet boundary and the far-field intensity is considered. The physical quantity used is the gradient of the pressure evaluated on a geometrical plane at the smallest possible radial distance from the jet axis, but outside the vortical region, in the area where the homogeneous wave equation is reasonably well satisfied. The numerical and experimental procedures involved have been checked out by using a known source. Results indicate that the acoustic power output per unit length of the jet, in the region from which the sound emanates, peaks approximately 9 diameters downstream. The acoustic emission for a jet Strouhal number of about 0.3 exceeds the emission for all other Strouhal numbers nearly everywhere along the measurement plane. However, the far-field peak intensity distribution obtained from the contribution of each station was found to depend on the spatial extent of the region where sound emanates from the jet, which, in turn, depends more on the far-field angle than on the Strouhal number.

- 50 A75-41349
ON THE DEVELOPMENT OF NOISE-PRODUCING LARGE-SCALE WAVELIKE EDDIES IN A PLANE
TURBULENT JET
Merkine, L.O., Liu, J.T.C. (Brown University, Providence, R.I.)
Journal of Fluid Mechanics, vol. 70, July 29, 1975, p. 353-368, 28 refs
NSF Grants No GK-10008; No ENG-73-04104; Grant No NsG-1076

The paper studies the development of large-scale wavelike eddies in a two-dimensional turbulent jet, extending earlier work on the mixing regions (Liu, 1974). The basic mean flow develops from one of mixing-region type with an initially specified boundary-layer thickness into a fully developed jet. This study brings out the role of the varicose and sinuous modes as they develop in a growing mean flow. In general, it is found that, for a given frequency parameter, the varicose mode has a shorter streamwise lifetime than the sinuous mode. For lower frequencies, the latter persists past the end of the potential core only to become subject to dissipation by the enhanced fine-scale turbulent activity in that region.

- 51 A75-40209
ON TURBULENCE AND NOISE OF AN AXISYMMETRIC SHEAR FLOW
Michalke, A., (Berlin, Technische Universität, Berlin, West Germany)
Fuchs, H.V. (Deutsche Forschungs- und Versuchsanstalt für Luft- und Raumfahrt, Institut für Turbulenzforschung, Berlin, West Germany) Journal of Fluid Mechanics, Vol. 70 July 15, 1975, p. 175-205, 32 refs. Research supported by the Deutsche Forschungsgemeinschaft.

The noise produced by mean flow-turbulence interaction of a circular subsonic jet is investigated theoretically, and expanded in azimuthal constituents of the turbulent pressure fluctuations. It is found that the low-order azimuthal constituents are the most efficient sound sources. On the basis of pressure correlation measurements, the azimuthal constituents are determined in a low Mach number jet. It is found that, in a range of Strouhal numbers between 0.2 and 1, the first three to four azimuthal constituents clearly dominate over the rest of the turbulent source quantity. A strictly axisymmetric ring vortex model for the coherent structure of the turbulence is, however, shown to be inappropriate.

- 52 N75-30187 Toronto Univ. (Ontario) Inst. for Aerospace Studies
CORRELATION OF JET NOISE DATA IN TERMS OF A SELF NOISE SHEAR NOISE MODEL
Nosseir, N.S.M.
Jan 1975 44 p
(Grant AF-AFOSR-1885-70; AF Proj. 9781)
(AD-A008899; UTIAS-TN-193; AFOSR-75-0496TR) Avail: NTIS

The theoretical formalism of Ribner (1964 and 1969) was applied in the analysis of a large body of experimental jet noise data. It was found that the basic directivity which results on excluding convection and refraction effects could be decomposed unambiguously into self noise and shear noise. The basic self noise spectrum peaked approximately one octave higher than the shear noise spectrum, and the peak amplitudes were roughly in the ratio two to one. Upon frequency shifting and normalizing alignments, the two spectra were found to match well in shape. All these properties are in accord with the theory. The self noise-shear noise spectral similarity was applied in a formalism for jet noise prediction utilizing the theory.

- 53 A75-44821
SOUND GENERATION BY HEATED SUBSONIC JETS
Obermeier, F.
(Max-Planck-Institut für Strömungsforschung, Göttingen, West Germany)
Journal of Sound and Vibration, vol. 41, Aug. 22, 1975, p.463-472 15 refs

The noise generation by the turbulent mixing of a heated subsonic jet and its cold surroundings is discussed, with the help of the method of matched asymptotic expansions, separately for an inner region where hydrodynamical characteristics dominate and for an outer region where sound fields prevail. The actual calculations then can be confined to the inner region since the first approximation of the outer solution depends only on the multipole-character of the inner solution. For a first inner approximation compressibility effects are negligible, and the flow field can be described by the incompressible approximation of the flow equations. Monopole-like sources are possible only if there is a mass flow between the heated and the cold gasflow due to the diffusion caused by temperature gradients. This effect can be included by disregarding the usually applied assumption dS/dt equals 0 (S being the entropy). A qualitative assessment of the order of magnitude of these effects is given.

- 54 A74-21599
JET NOISE FROM COAXIAL NOZZLES OVER A WIDE RANGE OF GEOMETRIC AND FLOW PARAMETERS
Olsen, W., Friedman, R. (NASA, Lewis Research Center, Cleveland, Ohio)
American Institute of Aeronautics and Astronautics, Aerospace Sciences Meeting, 12th, Washington, D.C., Jan. 30-Feb. 1, 1974, Paper 74-43. 30 p. 12 refs.
Members, \$1.50; nonmembers, \$2.00

Free field pure jet noise data were taken for a large range of coaxial nozzle configurations. The core nozzles were circular (1 to 4 in diam.) and plug types. The fan to core area ratio varied from 0.7 to 43.5, while the velocity ratio typically varied from 0 to 1. For most cases the two nozzles were coplanar but large axial extensions of either nozzle were also tested. Correlation of the data resulted in a simple procedure for estimating ambient temperature subsonic coaxial jet noise spectra over a wide range of geometric and flow parameters.

- 55 A75-25724
NEW EVIDENCE OF SUBSONIC JET NOISE MECHANISMS
Pao, S.P., Maestrello, L. (NASA, Langley Research Center, Hampton, Va.)
American Institute of Aeronautics and Astronautics, Aero-Acoustics Conference 2nd, Hampton, Va., Mar. 24-26, 1975 Paper 75-437. 10p

Measurements of sound gradient near a subsonic jet have shown that coherent sound is emanated from the flow in the form of narrow beams. Within any given short period of time, sound appears to come from small volumes in the jet with a preferred direction of propagation for that particular moment. These conclusions are drawn from a large data base using correlation techniques, and are further confirmed by additional experiments.

- 56 A75-27934
DENSITY FLUCTUATIONS AND RADIATED NOISE FOR A HIGH-TEMPERATURE SUPERSONIC JET
Parthasarathy, S.P., Massier, P.F., Cuffel, R.F., Radbill, J.R. (California Institute of Technology, Jet Propulsion Laboratory, Pasadena, Calif.)
American Institute of Aeronautics and Astronautics, Aero-Acoustics Conference 2nd, Hampton, Va., Mar. 24-26, 1975, Paper 75-483. 18 p. 5 refs
Contract No. NAS7-100.

Experimental data on density fluctuations were obtained by the laser Schlieren method in a supersonic jet which at the nozzle exit had a Mach Number of 1.43 and a stagnation temperature of about 1090 K. The jet emerged into the ambient atmosphere in an anechoic chamber, correctly expanded from a nozzle which had an exit diameter of 10.8 cm. Using the information on the density fluctuations and the meanshear obtained by probes, the autocorrelation of the radiated noise was calculated by a theory that is suitable for Mach wave emission. This theory is a modification of that developed by Ffowcs, Williams and Maidanik (1965). The calculated noise field agrees well with that obtained by using microphones outside the jet.

- 57 N75-13867 University of Southern Calif., Los Angeles. Dept of Aerospace Engineering
ORDERED STRUCTURES AND JET NOISE
Petersen, R.A., Kaplan, R.E., Laufer, J.
Oct 1974 58p
(Contract NAS3-17857)
(NASA-CR-134733) Avail. NTIS HC \$4.25

A series of measurements of near field pressures and turbulent velocity fluctuations were made in a jet having a Reynolds number of about 50,000 in order to investigate more quantitatively the character and behaviour of the large scale structures, and to ascertain their importance to the jet noise problem. It was found that the process of interaction between vortices can be inhibited by artificially exciting the shear layers with periodic disturbances of certain frequency. The turbulent fluctuation amplitudes measured at four diameters downstream decreased considerably. Finally, it was observed that the passage frequency of the structures decreased with x in a similar manner as the frequency corresponding to the maximum intensity radiation emanating from the same value of x .

- 58 A75-18303
JET NOISE ANALYSIS UTILIZING THE RATE OF DECAY OF KINETIC POWER
Pinkel, B.
American Institute of Aeronautics and Astronautics, Aerospace Sciences Meeting, 13th, Pasadena, Calif., Jan, 20-22, 1975, Paper 75-94. 11p 13 refs

A simple model of the noise generated from a gas jet discharging into the atmosphere is presented to facilitate calculation of the effects of nozzle flow and geometric parameters on jet noise. Equations are derived for the overall sound power and the sound generated per unit length of the jet. The application of these equations is illustrated by computations of the effects on noise of (1) jet temperature and (2) velocity of the nozzle relative to the ambient air. Good agreement between the computed values and published experimental results is noted.

- 59 N73-28989 National Aeronautics and Space Administration, Flight Research Center, Edwards, Calif.
INVESTIGATION OF COAXIAL JET NOISE AND INLET CHOKING USING AN F-111A AIRPLANE
Putnam, T.W.
Washington Aug 1973 32p refs
(NASA-TN-D-7376: H-685) Avail: NTIS HC \$3.00

Measurements of engine noise generated by an F-111A airplane positioned on a thrustmeasuring platform were made at angles of 0 deg to 160 deg from the aircraft heading. Sound power levels, power spectra, and directivity patterns are presented for jet exit velocities between 260 feet per second and 2400 feet per second. The test results indicate that the total acoustic power was proportional to the eighth power of the core jet velocity for core exhaust velocities greater than 300 meters per second (985 feet per second) and that little or no mixing of the core and fan streams occurred. The maximum sideline noise was most accurately predicted by using the average jet velocity for velocities above 300 meters per second (985 feet per second). The acoustic power spectrum was essentially the same for the single jet flow of afterburner operation and the coaxial flow of the nonafterburning condition. By varying the inlet geometry and cowl position, reductions in the sound pressure level of the blade passing frequency on the order of 15 decibels to 25 decibels were observed for inlet Mach numbers of 0.8 to 0.9.

- 60 N73-27923 Bolt. Beranek and Newman Inc., Cambridge, Mass.
SUPERSONIC JET NOISE INVESTIGATION USING JET FLUCTUATING PRESSURE PROBES
Scharton, T.D., White, P.H., Rentz, P.E.
1973 131p refs
(Contract F33615-71-C-1661)
(AD-762296: BBN-2220: AFAPL-TR-73-35) Avail: NTIS

Various mechanisms of jet noise generation are modeled using the fluctuating jet pressures to characterize the sources. The subsonic mixing mechanism is shown to dominate for sonic and mildly supersonic jets. An input-output relation between the jet pressure and sound pressure spectral densities is derived and verified. Fluctuating pressure probes are developed to measure sources of noise generation in sonic and supersonic jet exhausts. Jet exhausts with total temperatures as high as 3500F may be measured. Definitive data are obtained regarding the percentage of the sound radiated at a given angle and frequency by each region of the jet exhaust. Simple laser refraction experiments support the fluctuating pressure measurements.

- 61 A75-34256
PRESSURE FLUCTUATIONS IN AN ANNULAR JET IN WAKE FLOW (KOLEBANIYA DAVLENIIA V KOL'TSEVOI STRUE V SPUTNOM POTOKE)
Shvets, A.I.
Akademiia Nauk SSSR, Izvestiia, Mekhanika Zhidkosti i Gaza,
Mar-Apr 1975, p 42-46 21 refs In Russian

The influence of wake flows on the discrete component of the base-pressure pulsation spectrum of jets expelled from supersonic annular nozzles is studied experimentally. Evidence is obtained for the existence of two types of discrete components: the first type is induced by resonance excitation of the ejector, and the second type by acoustic feedback. The critical frequency is plotted against the wake Mach number for a cold cylindrical jet.

- 62 N73-21929 General Electric Co., Cincinnati, Ohio. Aircraft Engine Group
EFFECT OF CROSSFLOW VELOCITY ON THE GENERATION OF LIST FAN JET NOISE IN VTOL AIRCRAFT
Stimpert, D.L., Fogg, R.G.
Feb 1973 43p refs
(Contract NAS2-5462)
(NASA-CR-114571) Avail: NTIS HC \$4.25

Analytical studies based on a turbulent mixing noise prediction technique indicate that jet noise power levels are increased when a jet is situated in a crossflow. V/STOL model transport acoustic test data obtained in the NASA Ames 40 ft x 80 ft wind tunnel confirmed this jet noise power level increase due to crossflow, increases up to 6 db at a Strouhal number of 2.5 and crossflow velocity to jet velocity ratio of 0.58 were observed. The power level increases observed in the experimental data confirm the predicted power level increases.

- 63 N76-12066 National Aeronautics and Space Administration, Lewis Research Center, Cleveland, Ohio
ON THE EFFECTS OF FLIGHT ON JET ENGINE EXHAUST NOISE
Stone, J.R.
1975 26p refs Presented at 90th Meeting of the Acoust. Soc. of Am.,
San Francisco, 4-7 Nov 1975
(NASA-TM-X-71819: E-8518) Avail: NTIS HC \$4.00

Differences between flight data and predictions of jet engine exhaust noise were reconciled by considering the combined effects of jet mixing noise and internally generated engine exhaust noise. The source strength of the internally generated noise was assumed to be unaffected by flight, as experiments demonstrated. The directivity of the internally generated noise was assumed to be the same statically as that given in the NASA interim prediction method for core engine noise. However, it was assumed that in flight internally generated noise is subject to the convective amplification effect of a simple source. The absolute levels of internally generated noise were obtained from an empirical fit of some typical engine data. The static and flight jet noise were predicted using the above prediction method. It was shown that in many cases much of the flyover noise signature is dominated by internally generated noise.

- 64 A75-31086
THE INFLUENCE OF TEMPERATURE ON SHOCK-FREE SUPERSONIC JET NOISE
Tanna, H.K., Dean, P.D., (Lockheed-Georgia Co., Marietta, Ga.) Fisher, M.J.,
(Southampton University, Southampton, England)
Journal of Sound and Vibration, vol 39, Apr 22, 1975, p 429-460 12 refs
Contract No F33615-73-C-2032

The effect of flow temperature on the sound field of supersonic shock-free jets is studied experimentally by measuring the turbulent mixing noise in the far-field from four 2-inch diameter nozzles situated in an anechoic room that provides a free-field environment. To minimize additional problems of convective amplification and refraction, the effects of temperature on mixing noise source strengths are evaluated by examining the data at 90 deg to the jet axis only. It is shown that there are in general two sources of noise: a source which results from Reynolds shear stress fluctuations, and a source which is attributed to density or temperature fluctuations promoted by the turbulent mixing of streams with dissimilar temperatures. Highly correlated scaling laws for the velocity and temperature dependencies of the spectra of these noise components are obtained and verified.

- 65 A75-22363
 SUPERSONIC JET NOISE GENERATED BY LARGE SCALE DISTURBANCES
 Tam, C.K.W. (Florida State University, Tallahassee, Fla.)
 Journal of Sound and Vibration, vol 38, Jan 8, 1975, p 51-79 26 refs
 NSF Grant No GK-35790

A body of experimental evidence is now available which tends to suggest that the dominant part of supersonic jet noise is produced by large scale flow disturbances. A mathematical model of large scale disturbances in a supersonic jet is presented in this paper. It is believed that the presence of large scale disturbances not only enhances the unsteady entrainment of ambient gas into the jet flow but also causes the jet to vibrate laterally. These unsteady processes in turn induce the emission of acoustic waves from the jet. Numerical calculations of the far field noise directivity pattern of a 2.2 Mach number cold jet according to the proposed model compare favorably with experimental measurements.

- 66 N75-30170 Center for the Study of Noise in Society, Glastonbury, Conn
 JET ENGINE NOISE AND ITS CONTROL
 Tyler, J.M.
 In AGARD Aircraft Noise Generation, Emission and Reduction
 Jun 1975 25p refs (AGARD-LS-77)

The noise of turbojet and turbofan engines is described and presented in a form useable by engine and aircraft designers; it deals primarily with the practical aspects of aircraft powerplant noise. Noise from the wakes of turbojet and turbofan engines, the effects of engine cycle on wake noise, and the possibilities for noise reduction using exhaust noise suppressors are discussed. Methods for exhaust noise prediction are presented. Fan and compressor noise, including a description of the mechanisms of fan and compressor noise generation, was investigated. Design practices to minimize fan and compressor noise are presented. A discussion of turbine and combustion noise, and a summary of the state of the art in the research and development stage are included.

- 67 N73-32968 National Aeronautics and Space Administration, Lewis Research Center, Cleveland, Ohio
 FORWARD VELOCITY EFFECTS ON JET NOISE WITH DOMINANT INTERNAL NOISE SOURCE
 Von Glahn, U., Goodykoontz, J.
 1973 17p refs
 Presented at 86th Meeting of Acoustical Soc. of Am., Los Angeles.
 30 Oct-2 Nov 1973
 (NASA-TM-X-71438: E-7694) Avail: NTIS HC \$3.00

Acoustic data, with and without forward velocity, were obtained with a circular nozzle using a quiet flow system and one dominated by a low frequency internal noise source (analogous to combustion noise). Forward velocity effects were obtained by installing the test nozzle in a free jet. Farfield noise data were obtained at jet pressure ratios from 1.3 to 1.7 and forward velocities up to 260 ft/sec. With a quiet flow system, jet noise is reduced by forward velocity. With a dominant low frequency core noise source, the portion of the noise spectra dominated by this source was not appreciably affected by forward velocity.

- 68 N75-22606 Illinois Univ., Champaign
 TURBULENT VELOCITY FIELD STRUCTURE IN A ROUND JET AND ITS RELATION TO FLUCTUATING PRESSURE FIELDS Ph D THESIS
 Weber, D.P.
 1974 327p
 Avail Univ Microfilms Order No 75-464

An experimental examination of the turbulent velocity field structure in a 2.5 inch cold jet was performed. Primary emphasis was given to the description of the structure within the driven shear layer to five diameters downstream. Both single point and two point correlation measurements were made with a special emphasis on the modeling of the two point covariance function with axisymmetric tensor forms. A higher order stochastic analysis of the velocity field was performed using an extended version of the single variate Gram-Charlier expansion of the probability density function. A qualitative examination of the stochastic structure of the velocity field was performed using the Wiener Hermite expansion theory for turbulence in an extended version to include the effect of mean velocity gradients. Results were to be used in the prediction of fluctuating pressure fields, as in the problem of aerodynamic noise generation, or in the more general shear flow dynamic equations.

- 69 N75-10088 New York Univ., NY. Aerospace and Energetics Lab.
 FLUID DYNAMIC ASPECTS OF JET NOISE GENERATION
 Final Report 1 Oct 1973-30 Sep 1974
 30 Sep 1974 110p refs
 (Grant NGR-33-016-177)
 (NASA-CR-140673) Avail: NTIS HC \$5.25

The location of the noise sources within jet flows, their relative importance to the overall radiated field, and the mechanisms by which noise generation occurs, are studied by detailed measurements of the level and spectral composition of the radiated sound in the far field. Directional microphones are used to isolate the contribution to the radiated sound of small regions of the flow, and for cross-correlation between the radiated acoustic field and either the velocity fluctuations or the pressure fluctuations in the source field. Acquired data demonstrate the supersonic convection of the acoustic field and the resulting limited upstream influence of the signal source, as well as a possible increase of signal strength as it propagates toward the centerline of the flow.

- 70 N75-29104 Engineering Sciences Data Unit, London (England)
 AN INTRODUCTION TO GAS TURBINE EXHAUST NOISE
 Jun. 1973 10p refs
 Sponsored in part by Ministry of Defense (Procurement Executive) and the Roy. Aeron. Soc.
 (ESDU-74001) Copyright. Avail: NTIS HC \$50.50

Various noise sources associated with gas turbine exhausts are described. The data are applicable to methods for estimating the magnitude of exhaust noise sources for far field noise, which is assumed to be at distances greater than 50 jet diameters.

4. Noise Associated With Lift Augmentation Devices

- 71 A75-27932
 EFFECT OF FORWARD SPEED ON JET WING/FLAP INTERACTION NOISE
 Bhat, W.V., (Boeing Commercial Airplane Co., Seattle, Wash.), Rosso, D.G. (Aeritalia S.p.A., Naples, Italy)
 American Institute of Aeronautics and Astronautics, Aero-Acoustics Conference, 2nd, Hampton, Va., Mar. 24-26, 1975, Paper 75-475. 8p 10 refs

A series of model tests has been conducted to assess the problem of jet wing/flap interaction noise for low-aspect-ratio D-shaped nozzles located on the upper surface of a wing. The measurements have been made using far-field and near-field wing-mounted flush microphones. A prediction procedure for static interaction noise has been formulated from far-field low-frequency interaction-noise measurements obtained under static conditions. The effect of forward speed on interaction noise has been investigated experimentally using an open-jet tunnel. These test data show that both far-field noise and the near-field wing trailing-edge pressure fluctuations are reduced by the simulated forward speed.

- 72 N73-26030 Linguistic Systems, Inc., Cambridge, Mass.
 NOISE CHARACTERISTICS OF A JET AUGMENTED FLAP CONFIGURATION
 Burrand, A.
 Washington NASA. Jun 1973 20p refs
 Transl into ENGLISH from l'Aeronautique et l'Astronautique (France) no 39 1973 p 44-54 Presented at the 3rd Colloq. on Aeronautic Acoustics. Toulouse 6-7 March 1972
 (Contract NASw-2482)
 (NASA-TT-F-14951) Avail: NTIS HC \$3.00

The STOL-type aircraft lift augmenting requires the use of very efficient devices which, however, are likely to be sources of noise themselves or may modify the noise generated by the jet-engines. Among these devices is the internal-flow jet augmented flap wherein a jet from auxiliary generators is directed onto the wing flap upper-surface. The noise of this device is to be added to that produced by the engines. Static tests recently performed in an anechoic chamber have made it possible to investigate the various possible configurations and to appraise the effect of numerous parameters. The application of results at full scale allows the noise level of this STOL type to be evaluated.

- 73 N74-17752 Boeing Commercial Airplane Co., Seattle, Wash.
 DESIGN INTEGRATION AND NOISE STUDIES FOR JET STOL AIRCRAFT, TASK 7C:
 AUGMENTOR WING CRUISE BLOWING VALVELESS SYSTEM. VOLUME 1: STATIC
 TESTING OF AUGMENTOR NOISE AND PERFORMANCE
 Campbell, J.M., Herkonen, D.L., O'Keefe, J.V.
 Nov. 1973 45 p refs
 (Contract NAS2-6344)
 (NASA-CR-114622; D6-41216-Vol-1) Avail: NTIS HC \$5.25

Static performance and acoustic tests were conducted on a two-dimensional one-third-scale augmentor flap model that simulated a cruise blowing augmentor system designed for a scale augmentor flap model that simulated a 150-passenger STOL air-plane. The cruise blowing augmentor, which offers a degree of simplicity by requiring no fan air diverter valves, was simulated by fitting existing lobe suppressor nozzles with new nozzle fairings. Flow turning performance of the cruise blowing augmentor was measured through a large range of flap deflection angles. The noise suppression characteristics of a multilayer acoustic lining installed in the augmentor were also measured.

- 74 N74-14761 National Aeronautics and Space Administration, Lewis Research Center, Cleveland, Ohio.
 EFFECT OF CONFIGURATION VARIATION ON EXTERNALLY BLOWN FLAP NOISE
 Dorsch, R.G., Goodykoontz, J.H., Sargent, N.B.
 1974 33p refs Presented at 12th Aerospace Sci. Meeting, Washington, D.C.
 30 Jan - 1 Feb. 1974; sponsored by AIAA
 (NASA-TM-X-71495; E-7858) Avail: NTIS HC \$3.75

The sensitivity of flap interaction noise to variations in engine-under-the-wing externally blown flap geometry was investigated with a large cold-flow model. Both 2- and 3-flap wing sections (7-ft chord) with trailing flap angles up to 60 deg were employed. Exhaust nozzles included coaxial, plug, and 8- and 13-inch diameter conical configurations. These nozzles were tested at two positions below the wing. The effects of these geometry variations on noise level, directivity, and spectral shape are summarized in terms of exhaust flow parameters evaluated at the nozzle exit and at the flap impingement station. The results are also compared with limited flap noise data available from tests using real engines.

- 75 N73-18041 National Aeronautics and Space Administration, Ames Research Center, Moffett Field, Calif.
 ACOUSTIC CHARACTERISTICS OF A SEMISPAN WING EQUIPPED WITH AN EXTERNALLY BLOWN JET FLAP INCLUDING RESULTS AT FORWARD SPEED
 Falarski, M.D.
 Washington Mar. 1973 84 p refs Prepared in cooperation with Army Air Mobility R and D Lab., Moffett Field, Calif.
 (NASA-TM-X-2749; A-4469) Avail: NTIS HC \$3.00

A wind-tunnel investigation was made of the noise characteristics of a 14.5-ft semispan, externally blown jet flap model. The model was equipped with a single 30-in. diameter, ducted fan with a 1.03 pressure ratio. The effects of flap size, fan vertical location, and forward speed on the noise characteristics were studied. With the ducted fan mounted 0.79 or 1.24 diameters below the wing and a flap chord greater than 50 percent, the peak perceived noise level increased 2 to 3 Pndb when the flap was deflected to 90 deg. The jet scrubbing noise increased 3 to 4 db when the flap was deflected 90 deg. Installation of the fan on the wing was responsible for 1 to 2 db of this change. Forward speed did not have a significant effect on the perceived noise level, although it did cause a reduction in the sound pressure levels of the first and second fan harmonics.

- 76 A75-10278
COMPARISON OF THE ACOUSTIC CHARACTERISTICS OF LARGE-SCALE MODELS OF SEVERAL PROPULSIVE-LIFT CONCEPTS.
Falarski, M.D. (U.S. Army, Air Mobility Research and Development Laboratory, Moffett Field, Calif.).
Aiken, T.N., Aoyagi, K., Koenig, D.G. (NASA, Ames Research Center, Moffett Field, Calif.).
American Institute of Aeronautics and Astronautics and Society of Automotive Engineers, Propulsion Conference, 10th, San Diego, Calif., Oct. 21-23, 1974, AIAA Paper 74-1094 10 p. 10 refs. Research supported by the Department of National Defence and DeHavilland Aircraft of Canada, and NASA.

Wind-tunnel acoustic investigations were performed to determine the acoustic characteristics and the effect of forward speed on the over-the-wing externally blown jet flap (OTW), the under-the-wing externally blown jet flap (UTW), the internally blown jet flap (IBF), and the augmentor wing (AW). The data presented represent the basic noise generated by the powered-lift system without acoustic treatment, assuming all other noise sources, such as the turbofan compressor noise, have been suppressed. Under these conditions, when scaled to a 100,000-lb aircraft, the OTW concept exhibited the lowest perceived noise levels, because of dominant low-frequency noise and wing shielding of the high-frequency noise. The AW was the loudest configuration, because of dominant high-frequency noise created by the high jet velocities and small nozzle dimensions. All four configurations emitted noise 10 to 15 PNdb higher than the noise goal of 95 PNdb at 500 ft.

- 77 N74-10052 National Aeronautics and Space Administration, Ames Research Center, Moffett Field, Calif.
ACOUSTIC CHARACTERISTICS OF A LARGE-SCALE AUGMENTOR WING MODEL AT FORWARD SPEED
Falarski, M.D., Koenig, D.G.
Washington Nov. 1973 42 p refs. Prepared in cooperation with Army Air Mobility R and D Lab., Moffett Field, Calif.
(NASA-TM-X-2940: A-4964) Avail: NTIS HC \$3.00

The augmentor wing concept is being studied as one means of attaining short takeoff and landing (STOL) performance in turbofan powered aircraft. Because of the stringent noise requirements for STOL operation, the acoustics of the augmentor wing are undergoing extensive research. The results of a wind tunnel investigation of a large-scale swept augmentor model at forward speed are presented. The augmentor was not acoustically treated, although the compressor supplying the high pressure primary air was treated to allow the measurement of only the augmentor noise. Installing the augmentor flap and shroud on the slot primary nozzle caused the acoustic dependence on jet velocity to change from eighth power to sixth power. Deflecting the augmentor at constant power increased the perceived noise level in the forward quadrant. The effect of air-speed was small. A small aft shift in perceived noise directivity was experienced with no significant change in sound power. Sealing the lower augmentor slot at a flap deflection of 70 deg reduced the perceived noise level in the aft quadrant. The seal prevented noise from propagating through the slot.

- 78 A76-18778
CORRELATION OF INTERNAL SURFACE TURBULENCE WITH FAR-FIELD NOISE OF THE AUGMENTOR WING PROPULSIVE-LIFT CONCEPT.
Falarski, M.D. (NASA, Ames Research Center; U.S. Army, Air Mobility Research and Development Laboratory, Moffett Field, Calif.).
Wilby, J.F. (Bolt Beranek and Newman, Inc., Canoga Park, Calif.).
Aiken, T.N. (NASA, Ames Research Center, Moffett Field, Calif.).
American Institute of Aeronautics and Astronautics, Aerospace Sciences Meeting, 14th Washington, D.C. Jan 26 - 28, 1976, Paper 76-79, 11 p 5 refs.

A wind tunnel investigation was conducted to determine the nature, strength, and variation with airspeed of the acoustic sources of the augmentor wing propulsive-lift concept. The augmentor wing overall noise is dominated by the high frequency jet mixing noise characteristic of the lobed primary nozzle. The augmentor modifies the intensity and propagation characteristics of the jet sources, especially those that exist inside the augmentor. The interaction of the turbulent flow with the augmentor creates low-frequency, low-intensity surface noise and trailing edge noise. These sources dominate any jet mixing noise that is present at the low frequencies and could become significant if the jet noise was suppressed by treating the augmentor with a lining tuned to the jet noise source location. The far-field noise of the untreated augmentor is unaffected by airspeed; however, this may not be the case when the jet noise is suppressed, because the trailing edge surface pressure and correlations with far-field noise do show a reduction with forward speed.

79 AD-25745

SCRUBBING NOISE OF EXTERNALLY BLOWN FLAPS.

Fink, M.R. (United Aircraft Research Laboratories, East Hartford, Conn.).
 American Institute of Aeronautics and Astronautics, Aero-Acoustics Conference,
 2nd, Hampton, Va., Mar. 24-26, 1975, Paper 75-469, 12p, 22 refs.
 Contract No. NAS3-17863.

An experimental study was conducted to examine the aero-acoustic mechanism that produces externally blown flap (EBF) scrubbing noise, i.e. a surface-radiated noise which is generally strongest normal to UTW deflected flaps. Scrubbing noise was not radiated from portions of the surface adjacent to strong, locally coherent turbulent eddies. Instead, scrubbing noise seemed to come from weak loading fluctuations that were coherent along the scrubbed span. These loading fluctuations probably were induced by the convected large-scale vortex structure of the attached exhaust jet. Deflecting a UTW flap would reduce the distance between the vortex trajectory and the flap surface, increasing the resulting dipole noise and rotating its directivity. In contrast, deflecting a USB flap would increase this distance, so that observable scrubbing noise would be radiated only from the undeflected forward portion of the wing.

80 N73-24059 National Aeronautics and Space Administration, Lewis Research Center, Cleveland, Ohio.

NOISE TESTS OF A MIXER NOZZLE-EXTERNALLY BLOWN FLAP SYSTEM

Goodykoontz, J.H., Dorsch, R.G., Groesbeck, D.E.
 Washington May 1973 56 p refs
 (NASA-TN-D-7236: E-7288) Avail: NTIS HC \$3.00

Noise tests were conducted on a large scale model of an externally blown flap lift augmentation system, employing a mixer nozzle. The mixer nozzle consisted of seven flow passages with a total equivalent diameter of 40 centimeters. With the flaps in the 30 - 60 deg setting, the noise level below the wing was less with the mixer nozzle than when a standard circular nozzle was used. At the 10 - 20 deg flap setting, the noise levels were about the same when either nozzle was used. With retracted flaps, the noise level was higher when the mixer nozzle was used.

81 N74-16715 National Aeronautics and Space Administration, Lewis Research Center, Cleveland, Ohio.

ACOUSTIC CHARACTERISTICS OF EXTERNALLY BLOWN FLAP SYSTEMS WITH MIXER NOZZLES

Goodykoontz, J.H., Dorsch, R.G., Wagner, J.M.
 (1974) 26 p refs Presented at the twelfth Aerospace Sciences Meeting, Washington, D.C.,
 30 Jan 1 Feb 1974; sponsored by AIAA
 (NASA-TM-X-71499) Avail: NTIS HC \$4.50

Noise tests were conducted on a large scale, cold flow model of an engine-under-the-wing externally blown flap lift augmentation system employing a mixer nozzle. The mixer nozzle was used to reduce the flap impingement velocity and, consequently, try to attenuate the additional noise caused by the interaction between the jet exhaust and the wing flap. Results from the mixer nozzle tests are summarized and compared with the results for a conical nozzle. The comparison showed that with the mixer nozzle, less noise was generated when the trailing flap was in a typical landing setting (e.g. 60 deg). However, for a takeoff flap setting (20 deg), there was little or no difference in the acoustic characteristics when either the mixer or conical nozzle was used.

82 N75-15653 National Aeronautics and Space Administration, Lewis Research Center, Cleveland, Ohio.

FORWARD VELOCITY EFFECTS ON UNDER-THE-WING EXTERNALLY BLOWN FLAP NOISE

Goodykoontz, J., VonGlahn, U., Dorsch, R.
 1975 21 p refs Proposed for presentation at 2d Aero-Acoustics Specialists Conf.,
 Hampton, Va., 24-26 Mar. 1975; sponsored by AIAA
 (NASA-TM-X-71656) Avail: NTIS HC \$3.25

Noise tests were conducted with small-scale models of externally blown-flap powered-lift systems that were subjected to simulated takeoff and landing free-stream velocities by placing the nozzle-wing models in a free jet. The nozzle configurations consisted of a conical and an 8-tube mixer nozzle. The results show that the free-stream velocity attenuates the noise from the various configurations, with the amount of attenuation depending on the flap setting. More attenuation was obtained with a flap setting of 20 degrees than with a flap setting of 60 degrees. The dynamic effect on the total attenuation caused by aircraft motion is also discussed.

- 83 N75-11948 Motoren- und Turbinen-Union Muenchen G.m.b.H. (West Germany)
 PROPULSION CONCEPTS FOR STOL AIRCRAFT
 Grieb, H., Klussman, W., Weist, G.
 In Tech. Hochschule Aachen Short Course on STOL Aircraft Technol and the Community
 Vol 2 1974 58 p refs

In view of the possibility of applying STOL capabilities to jet transport aircraft, the technical scope for developing high bypass cruise engines and for designing air supply systems for wings with internally blown flaps are identified and dealt with. The effect of bypass ratio on static and takeoff thrust and on general dimensioning is considered. Engine noise and technical problems are elucidated. Experimental results on air supply requirements and noise emission of airfoils with externally blown flaps and various concepts for internally blown flaps are depicted. Various air supply systems are reviewed and compared.

- 84 N74-32438 Boeing Commercial Airplane Co., Seattle, Wash.
 STATIC PERFORMANCE AND NOISE TESTS ON A THRUST REVERSER FOR AN AUGMENTOR WING AIRCRAFT
 Herkonen, D.L., Marrs, C.C., O'Keefe, J.V.
 July 1974 86 p refs
 (Contract NAS2-7641)
 (NASA-CR-137561; D6-41926) Avail: NTIS HC \$7.50

A 1/3 scale model static test program was conducted to measure the noise levels and reverse thrust performance characteristics of wing-mounted thrust reverser that could be used on an advanced augmentor wing airplane. The configuration tested represents only the most fundamental designs where installation and packaging restraints are not considered. The thrust reverser performance is presented in terms of horizontal, vertical, and resultant effectiveness ratios and the reverser noise is compared on the basis of peak perceived noise level (PNL) and one-third octave band data (OASPL). From an analysis of the model force and acoustic data, an assessment is made on the stopping distance versus noise for a 90,900 kg (200,000 lb) airplane using this type of thrust reverser.

- 85 N74-11813 National Aeronautics and Space Administration, Lewis Research Center, Cleveland, Ohio.
 NOISE TESTS ON AN EXTERNALLY BLOWN FLAP WITH THE ENGINE IN FRONT OF THE WING
 Karchmer, A.M., Friedman, R.
 Washington Dec. 1973 17 p refs
 (NASA-TM-X-2942; E-7564) Avail: NTIS HC \$2.75

Noise tests were conducted with a nozzle exhausting over a small scale model of an externally blown flap (EBF) lift-augmentation system, with exhaust impingement on the wing leading edge. Two series of tests were conducted with wing leading edge inside the nozzle; and with leading edge set back from the nozzle exit plane 1 diameter on the jet axis. The results indicated no significant differences in spectral shape, level, or directivity pattern. Static lift and thrust tests were conducted on the same model indicated considerable flow attachment on both configurations, with slightly greater attachment and turning for the wing outside the nozzle. Finally, a comparison with engine-above and engine-below-the-wing EBF's tested by previous investigators shows the acoustic performance of the configurations tested for this report to lie between the other two.

- 86 N75-15399 National Aeronautics and Space Administration, Lewis Research Center, Cleveland, Ohio.
 ANALYSIS OF NOISE PRODUCED BY JET IMPINGEMENT NEAR THE TRAILING EDGE OF A FLAT AND A CURVED PLATE
 McKinzie, D.J., Burns, R.J.
 Washington Jan 1975 32 p refs
 (NASA-TM-X-3171; E-8080) Avail: NTIS HC \$3.75

The sound fields produced by the interaction of a subsonic cold gas jet with the trailing edge of a large flat plate and a curved plate were analyzed. The analyses were performed to obtain a better understanding of the dominant noise source and the mechanism governing the peak sound-pressure-level frequencies of the broadband spectra. An analytical expression incorporating an available theory and experimental data predicts sound field data over an arc of approximately 105 deg measured from the upstream jet axis for the two independent sets of data. The dominant noise as detected on the impingement side of either plate results from the jet impact (eighth power of the velocity dependence) rather than a trailing-edge disturbance (fifth or sixth power of the velocity dependence). Also, the frequency of the peak SPL may be governed by a phenomenon which produces periodic formation and shedding of ring vortices from the nozzle lip.

- 87 N74-33455 Boeing Commercial Airplane Co., Seattle, Wash.
 STATIC NOISE TESTS ON AUGMENTOR WING JET STOL RESEARCH AIRCRAFT (C8A BUFFALO)
 Marrs, C.C., Herkonen, D.L., O'Keefe, J.V.
 May 1974 102 p refs
 (Contract NAS2-7641)
 (NASA-CR-137520; D6-41324-1) Avail: NTIS HC \$8.25

Results are presented for full scale ground static acoustic tests of over-area conical nozzles and a lobe nozzle installed on the Augmentor Wing Jet STOL Research Aircraft, a modified C8A Buffalo. The noise levels and spectrums of the test nozzles are compared against those of the standard conical nozzle now in use on the aircraft. Acoustic evaluations at 152 m (500 ft), 304 m (1000 ft), and 1216 m (4000 ft) are made at various engine power settings with the emphasis on approach and takeoff power. Appendix A contains the test log and propulsion calculations. Appendix B gives the original test plan, which was closely adhered to during the test. Appendix C describes the acoustic data recording and reduction systems, with calibration details.

- 88 N74-16714 National Aeronautics and Space Administration, Lewis Research Center, Cleveland, Ohio.
 RATIONAL FUNCTION REPRESENTATION OF FLAP NOISE SPECTRA INCLUDING CORRECTION FOR REFLECTION EFFECTS
 Miles, J.H.
 1974 30 p refs Presented at 12th Aerospace Sci. Meeting, Washington D.C. 30 Jan. - 1 Feb 1974; sponsored by AIAA
 (NASA-TM-X-71502; E-7869) Avail: NTIS HC \$3.50

A rational function is presented for the acoustic spectra generated by deflection of engine exhaust jets for under-the-wing- and over-the-wing versions of externally blown flaps. The functional representation is intended to provide a means for compact storage of data and for data analysis. The expressions are based on Fourier transform functions for the Strouhal normalized pressure spectral density, and on a correction for reflection effects based on the N-independent-source model of P. Thomas extended by use of a reflected ray transfer function. Curve fit comparisons are presented for blown flap data taken from turbofan engine tests and from large scale cold-flow model tests. Application of the rational function to scrubbing noise theory is also indicated.

- 89 A75-25747
 FLUCTUATING PRESSURES ON AIRCRAFT WING AND FLAP SURFACES ASSOCIATED WITH POWERED-LIFT SYSTEMS.
 Mixson, J.S., Schoenster, J.A., Willis, C.M.
 (NASA, Langley Research Center, Hampton, Va.). American Institute of Aeronautics and Astronautics, Aero-Acoustics Conference, 2nd, Hampton, Va., Mar. 24-26, 1975, Paper 75-472, 11 p 7 refs.

The present work presents results from two research studies that provide information on the fluctuating pressures generated by the use of powered-lift systems in STOL aircraft. Data are given for several chordwise and spanwise locations on large-scale models of an externally blown flap (EBF) configuration and an upper surface blown flap (USB) configuration in which actual jet engines were used. Pressure levels were high enough to indicate that special design effort will be required to avoid acoustic fatigue failures of wing and flap structures. The observation that pressure levels did not decrease very much with increased distance from the engine exhaust center line suggests that a STOL aircraft fuselage, which is in relatively close proximity to the engines for aerodynamic reasons, will be subjected to unusually high external overall fluctuating pressure levels (OAFPLs) that may cause difficulty in control of the cabin noise level.

- 90 N75-11951 Technische Hochschule, Aachen (West Germany)
 NOISE OF JETS WHICH ARE IMPINGING ON OBSTACLES (FOR EXAMPLES EXTERNALLY BLOWN FLAPS) AND POSSIBILITIES OF NOISE ATTENUATION
 Neuwarth, G.
 In Tech. Hochschule Aachen Short Course on STOL Aircraft Technol. and the Community, Vol. 2 1974 16 p refs

The acoustic mechanism of the noise radiation caused by a subsonic (or supersonic) free jet impinging on an obstacle was studied. The natural orderly structure of turbulence of a subsonic free jet at Mach numbers between 0.5 and 1.0 was examined, and the reinforcement of the first harmonic of the axisymmetric structure by the feedback mechanism established. The interaction noise was amplified by an externally blown flap as an obstacle. The ring vortices reinforced by feedback can be destroyed if they are cut off at one point of their periphery and the total sound power level can be reduced about 10 db. Results show that the natural orderly structure cannot be destroyed but only weakened.

- 91 N73-27897 National Aeronautics and Space Administration, Lewis Research Center, Cleveland, Ohio.
 NOISE TESTS OF A MODEL ENGINE-OVER-THE-WING STOL CONFIGURATION USING A MULTIJET NOZZLE WITH DEFLECTOR
 Olsen, W.A., Friedman, R.
 Washington Aug. 1973 26 p refs
 (NASA-TM-X-2871: E-7459) Avail: NTIS HC \$3.00

Noise data were obtained with a small scale model stationary STOL configuration that used an eight lobe mixer nozzle with deflector mounted above a 32-chord wing section. The factors varied to determine their effect upon the noise were wing flap angle, nozzle location, deflector configuration, and jet velocity. The noise from the mixer model was compared to the noise from a model using a circular nozzle of the same area. The mixer nozzle model was quieter at the low to middle frequencies, while the circular nozzle was quieter at high frequencies. The perceived noise level (PNL) was calculated for an aircraft 10 times larger than the model. The PNL at 500 feet for the mixer nozzle turned out to be within 1 db of the PNL for the circular nozzle. For some configurations a highly directional broadband noise, which could be eliminated by changes in nozzle and/or deflector location, occurred below the wing.

- 92 A75-25748
 ACOUSTIC CHARACTERISTICS OF A LARGE UPPER-SURFACE BLOWN CONFIGURATION WITH TURBOFAN ENGINES.
 Preisser, J.S., Fratello, D.J.
 (NASA, Langley Research Center, Hampton, Va.). American Institute of Aeronautics and Astronautics, Aero-Acoustics Conference, 2nd, Hampton, Va., Mar. 24-26, 1975, Paper 75-473, 9 p 19 refs.

This paper presents acoustic results from static and simulated low forward velocity tests of a large-scale model of an aircraft configuration with two turbofan engines in the full-scale tunnel at the Langley Research Center. The turbofan engines were integrated into the model and equipped with rectangular nozzles to provide the upper-surface blowing. Results indicate that the upper-surface-blowing noise problem can be characterized, primarily, by the unsymmetrical radiation pattern due mainly to shielding of the high-frequency engine noise and the production of low-frequency noise by jet-surface interaction. The directivity of the low-frequency noise was found to depend on the trailing-edge flap angle when the thrust levels were low. Normalized sound pressure level spectral density data showed good agreement at low Strouhal number with other small and large-scale model data from tests using simulated wing-flap systems. Forward speed effects were undetectable at the low tunnel speeds used during the tests.

- 93 A75-27931
 PROPULSIVE-LIFT NOISE OF AN UPPER SURFACE BLOWN FLAP CONFIGURATION
 Reddy, N.N.
 (Lockheed-Georgia Co., Marietta, Ga.). American Institute of Aeronautics and Astronautics, Aero-Acoustics Conference, 2nd, Hampton, Va., Mar. 24-26, 1975, Paper 75-470, 7 p 7 refs.

The radiated sound and the flow characteristics of a scaled model of an upper surface blown-flap configuration are experimentally investigated. The acoustic results consist of the radiation pattern and spectral distribution of radiated sound in two planes. The two planes considered are the nozzle exit plane and the plane perpendicular to the wing surface passing through the jet centerline. The flow measurements include mean flow and the turbulence intensity distribution on the wing/flap (wall jet) and in the trailing-edge wake. These results indicate that a dominant noise is generated in the vicinity of the trailing edge. Radiated sound in the direction perpendicular to the flap trailing edge correlates with the trailing-edge velocity raised to the power 5, and the spectra correlate with the wall-jet thickness and velocity at the trailing edge. Turbulence close to the surface is amplified as the flow is convected past the trailing edge, while more distant turbulence is not affected by the surface.

- 94 A75-18383
 ACOUSTIC CHARACTERISTICS OF AN UPPER-SURFACE BLOWING CONCEPT OF POWER-LIFT SYSTEM.
 Reddy, N.N., Brown, W.H.
 (Lockheed-Georgia Co., Marietta, Ga.). American Institute of Aeronautics and Astronautics, Aerospace Sciences Meeting, 13th, Pasadena, Calif., Jan. 20-22, 1975, Paper 75-204, 9 p 14 refs.

The noise characteristics of a typical upper-surface-blowing (USB) configuration are studied experimentally using a small scale model. The directivity and the spectral distribution of the radiated noise measured in the free field environment and the mean flow profiles measured around the wing/flap indicate that the dominating noise generating mechanisms of USB are: free jet mixing, wall-jet mixing, secondary mixing (trailing edge wake), and boundary layer turbulence near the flap trailing edge. The wall-jet 'roll-up' at the edges also may contribute to the radiated noise. The relative significance of each source to community noise is discussed.

- 95 N75-27855 National Aeronautics and Space Administration, Langley Research Center, Langley Station, Va.
 RADIATED NOISE FROM AN EXTERNALLY BLOWN FLAP
 Reddy, N.N., Yu, J.C. (George Washington Univ.)
 Washington Jul. 1975 36 p refs
 (NASA-TN-D-7908; L-9895) Avail: NTIS HC \$3.75

The far field noise from subsonic jet impingement on a wing-flap with a 45 deg bend was experimentally investigated. The test parameters are jet Mach number and flap length. For long flaps, the primary source mechanisms are found to be turbulent mixing and flow impingement. For short flaps, the interaction of turbulent flow with the flap trailing edge appears to strongly influence the radiated noise.

- 96 N73-30015 National Aeronautics and Space Administration, Lewis Research Center, Cleveland, Ohio.
 ACOUSTIC INVESTIGATION OF THE ENGINE-OVER-THE-WING CONCEPT USING A D-SHAPED NOZZLE
 Reshotko, M., Friedman, R.
 1973 18 p refs Proposed for presentation at Aero-Acoustic Specialists Conf., Seattle, Wash., 15-17 Oct. 1973; sponsored by AIAA.
 (NASA-TM-X-71419) Avail: NTIS HC \$3.00

Small-model experiments were conducted of the engine-over-the-wing concept using a D-shaped nozzle in order to determine the static-lift and acoustic characteristics at two wing-flap positions. Configurations were tested with the flow attached and unattached to the upper surface of the flaps. Attachment was obtained with a nozzle flow deflector. In both cases, high frequency noise shielding by the wing was obtained. Configurations using the D-shaped nozzle are compared with corresponding ones using a circular nozzle. With flow attached to the flaps, the static lift and acoustic results are almost the same for both nozzles. Without the nozzle flow deflector, (unattached flap flow), the D-nozzle is considerably noisier than a circular nozzle in the low and middle frequencies.

- 97 N73-24070 National Aeronautics and Space Administration, Lewis Research Center, Cleveland, Ohio
 ENGINE-OVER-THE-WING NOISE RESEARCH
 Reshotko, M., Goodykoontz, J.H., Dorsch, R.G.
 1973 23 p refs Proposed for presentation at 6th Fluid and Plasma Dyn. Conf., Palm Springs, Calif., 16-18 Jul. 1973; sponsored by AIAA
 (NASA-TM-X-68246; E-7429) Avail: NTIS HC \$3.25

Acoustic measurements for large model engine-over-the-wing (EOW) research configurations having both conventional and powered lift applications were taken for flap positions typical of takeoff and approach and at locations simulating flyover and sideline. The results indicate that the noise is shielded by the wing and redirected above it, making the EOW concept a prime contender for quiet aircraft. The large-scale noise data are in agreement with earlier small-model results. Below the wing, the EOW configuration is about 10 PNdb quieter than the engine-under-the-wing externally-blown-flap for powered lift, and up to 10 db quieter than the nozzle alone at high frequencies for conventional lift applications.

- 98 N74-17751 Boeing Commercial Airplane Co., Seattle, Wash.
 DESIGN INTEGRATION AND NOISE STUDIES FOR JET STOL AIRCRAFT. TASK 7A: AUGMENTOR WING CRUISE BLOWING VALVELESS SYSTEM. VOLUME 1: SYSTEM DESIGN AND TEST INTEGRATION
 Roepcke, F.A., Nickson, T.B.
 Apr. 1973 47 p refs
 (Contract NAS2-6344)
 (NASA-CR-114621; D6-40950-Vol-1) Avail: NTIS HC \$5.50

Exploratory design studies conducted to establish the configuration of an augmentor wing cruise blowing (valveless) system in a 150-passenger STOL airplane were reported in NASA CR-114570. Those studies have been updated to incorporate the results of static rig, flow duct, and wind tunnel tests. Minor adjustments in duct flow velocity, flap length, and blowing nozzle geometry were incorporated to provide airplane characteristics that minimize takeoff gross weight and achieve sideline noise objectives for an advanced commercial STOL airplane.

AD-A037 334

ADVISORY GROUP FOR AEROSPACE RESEARCH AND DEVELOPMENT--ETC F/G 20/1
AERODYNAMIC NOISE.(U)

JAN 77

UNCLASSIFIED

AGARD-LS-80

NL

4 OF 4
AD
A037334



- 99 N74-17753 Boeing Commercial Airplane Co., Seattle, Wash.
 DESIGN INTEGRATION AND NOISE STUDIES FOR JET STOL AIRCRAFT. TASK 7C: AUGMENTOR WING
 CRUISE BLOWING VALVELESS SYSTEM. VOLUME 2: SMALL-SCALE DEVELOPMENT TESTING OF
 AUGMENTOR WING CRITICAL DUCTING COMPONENTS
 Runnels, J.N., Gupfa, A.
 Nov. 1973 77 p refs
 (Contract NAS2-6344)
 (NASA-CR-114623: D6-40879-Vol-2) Avail: NTIS HC \$7.00

Augmentor wing ducting system studies conducted on a valveless system configuration that provides cruise thrust from the augmentor nozzles have shown that most of the duct system pressure loss would occur in the strut-wing duct y-junction and the wing duct-augmentor lobe nozzles. These components were selected for development testing over a range of duct Mach numbers and pressure ratios to provide a technical basis for predicting installed wing thrust loading and for evaluating design wing loading of a particular wing aspect ratios. The flow characteristics of ducting components with relatively high pressure loss coefficients were investigated. The turbulent pressure fluctuations associated with flows at high Mach numbers were analyzed to evaluate potential duct fatigue problems.

- 100 N74-10042 National Aeronautics and Space Administration, Lewis Research Center, Cleveland, Ohio.
 EFFECT OF EXHAUST NOZZLE CONFIGURATION ON AERODYNAMIC AND ACOUSTIC PERFORMANCE OF AN
 EXTERNALLY BLOWN FLAP SYSTEM WITH A QUIET 6:1 BYPASS RATIO ENGINE
 Samanich, N.E., Heidelberg, L.J., Jones, W.L.
 1973 32 p refs Presented at the Propulsion Joint Specialist Conf., Las Vegas, Nev.,
 5-7 Nov. 1973; sponsored by AIAA and SAE
 (NASA-TM-X-71465) Avail: NTIS HC \$3.75

A highly suppressed TF-34 engine was used to investigate engine and flap interaction noise associated with an externally blown flap STOL powered lift system. Noise, efficiency, and velocity decay characteristics of mixed and separate flow exhaust systems including convergent, co-annular, and lobed designs were determined with the engine operating alone. Noise data were then obtained for several of the exhaust configurations with the engine blowing a wing-flap segment. Noise for both the engine alone and the engine with blown flaps showed substantial differences for the various exhaust configurations tested. The differences in observed noise are related primarily to nozzle effective exhaust velocity, flap impingement velocity, and noise spectral shape.

- 101 N74-17756 Tennessee Univ. Space Inst. Tullahoma.
 NOISE CHARACTERISTICS OF JET FLAP TYPE EXHAUST FLOWS - Final Report
 Schrecker, G.O., Maus, J.R.
 Washington NASA Feb. 1974 135 p refs
 (Grant NGR-43-001-075)
 (NASA-CR-2342) Avail: NTIS HC \$4.75

An experimental investigation of the aerodynamic noise and flow field characteristics of internal-flow jet-augmented flap configurations (abbreviated by the term jet flap throughout the study) is presented. The first part is a parametric study of the influence of the Mach number (subsonic range only), the slot nozzle aspect ratio and the flap length on the overall radiated sound power and the spectral composition of the jet noise, as measured in a reverberation chamber. In the second part, mean and fluctuating velocity profiles, spectra of the fluctuating velocity and space correlograms were measured in the flow field of jet flaps by means of hot-wire anemometry. Using an expression derived by Lilley, an attempt was made to estimate the overall sound power radiated by the free mixing region that originates at the orifice of the slot nozzle (primary mixing region) relative to the overall sound power generated by the free mixing region that originates at the trailing edge of the flap (secondary mixing region). It is concluded that at least as much noise is generated in the secondary mixing region as in the primary mixing region. Furthermore, the noise generation of the primary mixing region appears to be unaffected by the presence of a flap.

- 102 N74-10037 National Aeronautics and Space Administration, Lewis Research Center, Cleveland, Ohio.
 NOISE TESTS OF A HIGH-ASPECT-RATIO SLOT NOZZLE WITH VARIOUS V-GUTTER TARGET THRUST REVERSERS
 Stone, J.R., Gutierrez, O.A.
 1973 22 p refs Presented at 86th Meeting of the Acoustical Soc. of Am. Los Angeles, 30 Oct - 2 Nov. 1973
 (NASA-TM-X-71470: E-7771) Avail: NTIS HC \$3.25

The results of experiments on the noise generated by a 1.33 by 91.4 cm slot nozzle with various V-gutter reversers, and some thrust measurements are presented. The experiments were conducted with near-ambient temperature jets at nozzle pressure ratios of 1.25 to 3.0, yielding jet velocities of about 190 to 400 m/sec. At pressure ratios of 2 or less, the reversers, in addition to being noisier than the nozzle alone, also had a more uniform directional distribution and more high-frequency noise. At pressure ratios above 2, the nozzle alone generated enough shock noise that the levels were about the same as for the reversers. The maximum overall sound pressure level and the effective overall sound power level both varied with the sixth power of jet velocity over the range tested. The data were scaled up to a size suitable for reversing the wing-flap slot nozzle flow of a 45 400-kg augmentor-wing-type airplane on the ground, yielding perceived noise levels well above 95 PNdB on a 152-m sideline.

- 103 N75-10948 National Aeronautics and Space Administration, Lewis Research Center, Cleveland, Ohio.
 NOISE OF MODEL TARGET TYPE THRUST REVERSERS FOR ENGINE-OVER-THE-WING APPLICATIONS
 Stone, J.R., Gutierrez, O.A.
 1974 24 p refs Presented at the 88th Meeting of the Acoust. Soc. of Am., St Louis, 5-8 November 1974
 (NASA-TM-X-71621: E-8142) Avail: NTIS HC \$3.25

The results of experiments on the noise generated by V-gutter and semicylindrical target reversers with circular and short-aspect-ratio slot nozzles having diameters of about 5 cm are presented. The experiments were conducted with cold-flow jets at velocities from 190-290 m/sec. The reversers at subsonic jet velocities had a more uniform noise distribution and higher frequency than the nozzles alone. The reverser shape was shown to be more important than the nozzle shape in determining the noise characteristics. The maximum sideline pressure level varied with the sixth power of the jet velocity, and the data were correlated for angles along the sideline. An estimate of the noise level along the 152 m sideline for an engine-over-the-wing powered-lift airplane was made.

- 104 N75-33056 National Aeronautics and Space Administration, Lewis Research Center, Cleveland, Ohio.
 INSTALLATION AND AIRSPEED EFFECTS ON JET SHOCK-ASSOCIATED NOISE
 Von Glahn, U., Goodykoontz, J.
 1975 26 p refs Presented at 90th Meeting of the Acoustical Society of America, San Francisco, 4-7 Nov. 1975
 (NASA-TM-X-71792: E-8469) Avail: NTIS HC \$3.75

Experimental acoustic data are presented to illustrate, at model scale, the effect of varying the nozzle-wing installation on shock-associated noise, statically and with airspeed. The variation in installations included nozzle only, nozzle under-the-wing (with and without flaps deflected), and nozzle over-the-wing (unattached flow). The nozzles used were a conical and a 6-tube mixer nozzle with a cold-flow nozzle pressure ratio of 2.1. A 33-cm diameter free jet was used to simulate airspeed. With the nozzle only, shock wave noise dominated the spectra in the forward quadrant, while jet mixing noise dominated in the rearward quadrant. Similar trends were observed when a wing (flaps retracted) was included. Shock noise was attenuated with an over-the-wing configuration and increased with an under-the-wing configuration (due to reflection from the wing surface). With increasing flap deflection (under-the-wing configuration), the jet-flap interaction noise exceeded the shock noise and became dominant in both quadrants. The free jet results showed that airspeed had no effect on shock noise. The free jet noise data were corrected for convective amplification to approximate flight and comparisons between the various configurations are made.

- 105 N75-33812 National Aeronautics and Space Administration, Lewis Research Center, Cleveland, Ohio.
ACOUSTICS OF ATTACHED AND PARTIALLY ATTACHED FLOW FOR SIMPLIFIED OTW CONFIGURATIONS WITH 5:1 SLOT NOZZLE
Von Glahn, U., Groesbeck, D.
1975 21 p refs Presented at 19th Meeting of The Acoustical Society of America, San Francisco, Calif., 4-7 Nov. 1975
(NASA-TM-X-71807: E-8497) Avail: NTIS HC \$3.25

The acoustics of simple engine over-the-wing configurations, with complete and partially attached jet flow to the shielding surface were studied with scale models. The nozzle used consisted of a 5:1 slot nozzle operated at a nominal jet Mach number of 0.6, with the flow directed parallel to and at angles up to 10 deg toward the shielding surface. The flow field at the trailing edge of each nozzle/surface configuration was mapped, the results indicate that, with attached flow, the jet flow field is stretched in the flow direction resulting in locally higher velocities than those for partially attached flow or nozzle only flow. The stretching of the flow field increases the noise levels for the attached flow cases compared to those with only partially attached flow. With attached flow, the shielding benefits are substantially reduced compared with fully detached flow.

- 106 N76-13882 Bolt, Beranek, and Newman, Inc., Canoga Park, Calif.
A STUDY OF NOISE SOURCE LOCATION ON A MODEL SCALE AUGMENTOR WING USING CORRELATION TECHNIQUES
Wilby, J.F., Scharton, T.D.
10 Nov. 1975 67 p refs
(Contract NAS2-8382
(NASA-CR-137784: BBN-2955) Avail: NTIS HC \$4.50

An experimental investigation, conducted on a model-scale augmentor wing to identify the sources of far-field noise, is examined. The measurement procedure followed in the investigation involved the cross-correlation of far field sound pressures with fluctuating pressures on the surface of the augmentor flap and shroud. In addition pressures on the surfaces of the augmentor were cross-correlated. The results are interpreted as showing that the surface pressure fluctuations are mainly aerodynamic in character and are convected in the downstream direction with a velocity which is dependent on the jet exhaust velocity. However the far field sound levels in the mid and high frequency ranges are dominated by jet noise. There is an indication that in the low frequency range trailing edge noise, associated with interaction of the jet flow and the flap trailing edge, plays a significant role in the radiated sound field.

5. Airframe Noise

- 107 N74-19668 National Aeronautics and Space Administration, Lewis Research Center, Cleveland, Ohio.
PRELIMINARY MEASUREMENT OF THE AIRFRAME NOISE FROM AN F-106B DELTA WING AIRCRAFT AT LOW FLYOVER SPEEDS
Burley, R.R.
Mar. 1974 42 p refs
(NASA-TM-X-71527: E-7928) Avail: NTIS HC \$5.25

To establish a realistic lower limit for the noise level of advanced supersonic transport aircraft will require knowledge concerning the amount of noise generated by the airframe itself as it moves through the air. The airframe noise level of an F-106B aircraft was determined and was compared to that predicted from an existing empirical relationship. The data were obtained from flyover and static tests conducted to determine the background noise level of the F-106B aircraft. Preliminary results indicate that the spectrum associated with airframe noise was broadband and peaked at a frequency of about 570 hertz. An existing empirical method successfully predicted the frequency where the spectrum peaked. However, the predicted OASPL value of 105 db was considerably greater than the measured value of 83 db.

- 108 A75-16805
SUPPRESSOR NOZZLE AND AIRFRAME NOISE MEASUREMENTS DURING FLYOVER OF A MODIFIED F106B AIRCRAFT WITH UNDERWING NACELLES.
Burley, R.R. (NASA, Lewis Research Center, Cleveland, Ohio)
American Society of Mechanical Engineers, Winter Annual Meeting, New York, N.Y., Nov. 17-22, 1974, Paper 74-WA/Aero-1. 14 p 21 refs, Members, \$1.00; nonmembers, \$3.00.

The effect of flight velocity on the jet noise and thrust of a 104-tube suppressor nozzle was investigated using an F-106B delta wing aircraft modified to carry two underwing nacelles each containing a turbojet engine. The nozzle was mounted behind one of the nacelles. Flight velocity had a large adverse effect on thrust and a small adverse effect on suppression when correlated with relative jet velocity. The clean airframe noise of the aircraft was measured at Mach 0.4 and was compared with that predicted from an empirical expression. The 83-dB measured value was considerably below the predicted value.

109 A75-25777

AN EXPERIMENTAL STUDY OF AIRFRAME SELF-NOISE.

Fethney, P. Royal Aircraft Establishment, Aerodynamics Dept., Farnborough, Hants., England.

American Institute of Aeronautics and Astronautics, Aero-Acoustics Conference, 2nd, Hampton, Va., Mar. 24-26, 1975, Paper 75-511, 12 p, 9 refs.

Some results are given of an investigation into the level of the airframe self-noise of four aircraft, ranging from a slender delta to a long-range transport. These aircraft, with their engines at flight idle, flew over a ground array of measuring microphones arranged to cover the noise directly beneath the flight path and on the side-line. The flight programme included a range of airspeeds and aircraft configurations. The intrinsic statistical error in the measurements was reduced by ensemble averaging the outputs of the several microphones for a number of overflights. Measurements of engine noise for the static aircraft were used to correct the flight data for the residual engine contribution. The experimental and analytical techniques are described, the measured airframe noise levels and spectra are presented and the relative contributions of some of the airframe components identified. Comparisons with empirical methods of estimation show only moderately good agreement and do not support the hypothesis that the dominant noise source is a vertically aligned dipole.

110 A75-25778

A PRELIMINARY INVESTIGATION OF REMOTELY PILOTED VEHICLES FOR AIRFRAME NOISE RESEARCH.

Fratello, D.J., Shearin, J.G. (NASA Langley Research Center, Hampton, Va.)

American Institute of Aeronautics and Astronautics, Aero-Acoustics Conference, 2nd, Hampton, Va., Mar. 24-26, 1975, Paper 75-512, 7 p 6 refs.

Aircraft noise encountered in the community is caused predominantly by the aircraft engines. However, expected advances in engine noise technology combined with recent experimental evidence indicate that airframe (nonpropulsive) noise, may be a significant aircraft noise component in the future. Thus, methods for research into control of this type of noise are being evaluated and a technique based on the remotely piloted vehicle (RPV) concept appears to overcome some of the difficulties encountered with other test techniques. In particular, this paper presents sample experimental data, gathered during a preliminary RPV experiment, which illustrate the high signal-to-noise ratio attainable with this technique. Further, since the data are recorded as transients or nonstationary signals, a method of measurement and analysis is presented which increases statistical confidence in the results.

111 A75-25755

DIAGNOSTIC CALCULATIONS OF AIRFRAME-RADIATED NOISE.

Hayden, R.E., Kadman, Y., Bliss, D.B., Africk, S.A. (Bolt Beranek and Newman, Inc., Cambridge, Mass.). American Institute of Aeronautics and Astronautics, Aero-Acoustics Conference, 2nd, Hampton, Va., Mar. 24-26, 1975, Paper 75-485, 13 p 22 refs. NASA-supported research.

Methods of calculating airframe noise due to the following components are presented: wings and stabilizers, flaps, landing gear 'self-noise', landing gear bay (wheel well) oscillations, separated flow interaction with edges of cavities, and doors associated with gear deployment. The predominant source mechanisms were dipole-like in nature, being related to the local fluctuating aerodynamic forces on struts, airfoil edges, cavity edges, etc. Available data are converted into semiempirical prediction methods to enable a tentative rank ordering of noise sources. A sample application of these prediction procedures is carried out for a typical CTOL passenger jet using actual aircraft parameters, where available.

112 A75-37538

THEORY OF AIR FRAME NOISE.

Meecham, W.C. (California, University, Los Angeles, Calif.).

Acoustical Society of America, Journal, Vol. 57, June 1975, Pt.2, p 1416-1420, 10 refs.

Airframe noise is examined using Curle's theory for noise from rigid surfaces interacting with turbulence. Measured 'airframe noise' often is open to question because of engine contribution. A large number of examples are considered: model airfoil in a jet, glider noise, jet wing in atmospheric turbulence, boundary layer noise on trailing wing edge, flap-generated noise, landing gear noise, noise from jet impinging on flap, and some others. Of all of these estimated noise sources it appears that for commercial jets the noises from jets on flaps (when present) and from landing gear may be the only sources of possible practical significance.

113 A75-25776

MEASUREMENTS AND ANALYSIS OF AIRCRAFT AIRFRAME NOISE

Putnam, T.W., Lasagna, P.L. (NASA, Flight Research Center, Edwards, Calif.)
 White, K.C. (NASA, Ames Research Center, Moffett Field, Calif.)
 American Institute of Aeronautics and Astronautics, Aero-Acoustics Conference,
 2nd, Hampton, Va., Mar 24-26, 1975, Paper 75-510. 8p. 8 refs.

Flyover measurements of the airframe noise of Aero-Commander, JetStar, CV-990, and B-747 aircraft are presented. Data are shown for both cruise and landing configurations. Correlations between airframe noise and aircraft parameters are developed and presented. The landing approach airframe noise for the test aircraft was approximately 10 EPNdB below present FAA certification requirements.

114 A75-25757

INDUCED DRAG EFFECT ON AIRFRAME NOISE

Revell, J.D. (Lockheed-California Co., Burbank, Calif.)
 American Institute of Aeronautics and Astronautics, Aero-Acoustics Conference,
 2nd Hampton, Va., Mar. 24-26, 1975, Paper 75-487. 18 p. 28 refs.

In a companion paper (75-539) and previous work in 1974, the author has predicted the non-engine aerodynamic noise (airframe noise) by expressing the acoustic energy as being proportional to the mechanical energy dissipated by each major drag component. Empirical constants are derived from flyover noise test data. Wing profile drag noise and wing induced drag noise are thus identified as important components at typical landing approach lift coefficients (1.3 to 1.5). This paper shows how trailing vortex wake turbulence causes extra wing pressure fluctuations. The associated force fluctuations radiate dipole noise whose strength is related to the induced drag. The theory gives explicit but approximate expressions for narrowband SPL. Numerical results are shown for one-third octave band SPL. The levels compare well with the empirically derived spectra in AIAA Paper 75-539; however, the present one-third octave spectra have a flatter shape.

115 N75-30167 Toronto Univ. (Ontario). Inst. of Aerospace Studies.

JET AND AIRFRAME NOISE

Ribner, H.S.

In AGARD Aircraft Noise Generation, Emission and Reduction June 1975 17 p. refs
 (AGARD-LS-77)

Basic notions of acoustics (wave equation, plane and spherical waves, sources, dipoles, quadrupoles) are discussed along with an account of jet noise theory, from the dilatation (simple source) point of view, and from the equivalent quadrupole point of view. The quadrupole sources are shown to dictate a basic directional pattern (self noise and shear noise) which is powerfully modified by convection and refraction effects. The refraction by mean flow velocity gradients is illustrated by laboratory experiments. Jet noise suppression theory examines the role of bypass ratio, the mechanisms of multiple jet shielding, and of reflective shielding by a surface or a gas layer. Airframe noise, distinct from jet noise and other engine noise, is traced to a number of sources on the aircraft. Methods for estimating levels, spectra, and directivity are described.

116 A75-25775

AIRFRAME NOISE MEASUREMENTS ON A TRANSPORT MODEL IN A QUIET FLOW FACILITY

Shearing, J.G., Block, P.J. (NASA, Langley Research Center, Hampton, Va.)
 American Institute of Aeronautics and Astronautics, Aero-Acoustics Conference, 2nd
 Hampton, Va., Mar. 24-26, 1975, Paper 75-509. 6 p. 8 refs.

An experimental investigation was conducted in an anechoic flow facility to explore problems and methods of measuring the airframe (nonpropulsive) noise associated with a 1/20-scale model of a B-737 transport. The test model geometry simulated the cruise and a landing configuration. Nonpropulsive model noise was detected at various flow velocities and at various angles of attack when turbulent flow was induced over the model. Discrete tones, associated with the extended undercarriage and wheel cavities, and an increase in broadband sound pressure level were observed with the model in a landing configuration.

6. Fan Noise

- 117 N73-32975 National Aeronautics and Space Administration Ames Research Center, Moffett Field, Calif.
NOISE MEASUREMENTS FROM A LARGE-SCALE LIFT FAN TRANSPORT IN THE 40 BY 80-FOOT WIND TUNNEL
Atencio, A. (Army Air Mobility R and D Lab)
Mar. 1973 77p refs
(NASA-TM-X-62284) Avail: NTIS HC \$6.00

Noise data measurements from a large scale lift fan transport model aircraft were made in the 40- by 80-foot wind tunnel. The model had two lift fans in deep inlets in the forward fuselage and two lift-cruise fans in pods on the aft fuselage. The noise data measurements are presented as listings and plots of sounds pressure level versus 1/3 octave center frequency.

- 118 N76-13878 National Aeronautics and Space Administration, Lewis Research Center, Cleveland, Ohio
INLET NOISE ON 0.5-METER-DIAMETER NASA QF-1 FAN AS MEASURED IN AN UNMODIFIED COMPRESSOR AERODYNAMIC TEST FACILITY AND IN AN ANECHOIC CHAMBER
Gelder, T.F., Soltis, R.F.
Washington Dec 1975 99p refs
(NASA-TN-D-8121: E-8201) Avail: NTIS HC \$5.00

Narrowband analysis revealed grossly similar sound pressure level spectra in each facility. Blade passing frequency (BPF) noise and multiple pure tone (MPT) noise were superimposed on a broadband (BB) base noise. From one-third octave bandwidth sound power analyses the BPF noise (harmonics combined), and the MPT noise (harmonics combined, excepting BPF's) agreed between facilities within 1.5 db or less over the range of speeds and flows tested. Detailed noise and aerodynamic performance is also presented.

- 119 N74-25534 National Aeronautics and Space Administration, Lewis Research Center, Cleveland, Ohio
SOUND RADIATION FROM A HIGH SPEED AXIAL FLOW FAN DUE TO THE INLET TURBULENCE QUADRUPOLE INTERACTION
Goldstein, M.E., Rosenbaum, B.M., Albers, L.U.
Washington Jun 1974 49p refs
(NASA-TN-D-7667: E-7741) Avail: NTIS HC \$3.25

A formula is obtained for the total acoustic power spectra radiated out the front of the fan as a function of frequency. The formula involves the design parameters of the fan as well as the statistical properties of the incident turbulence. Numerical results are calculated for values of the parameters in the range of interest for quiet fans tested at the Lewis Research Center. As in the dipole analysis, when the turbulence correlation lengths become equal to the interblade spacing, the predicted spectra exhibit peaks around the blade passing frequency and its harmonics. There has recently been considerable conjecture about whether the stretching of turbulent eddies as they enter a stationary fan could result in the inlet turbulence being the dominant source of pure tones from nontranslating fans. The results of the current analysis show that, unless the turbulent eddies become quite elongated, this noise source contributes predominantly to the broadband spectrum.

- 120 N74-14379 Connecticut Univ., Storrs.
THE SPECTRUM OF TURBOMACHINE ROTOR NOISE CAUSED BY INLET GUIDE VANE WAKES AND ATMOSPHERIC TURBULENCE Ph.D THESIS
Hanson, D.B.
1973 142p
Avail: Univ. Microfilms Order No 73-24404

A theoretical methodology is developed to calculate the partially coherent acoustic radiation of propellers, helicopter rotors and axial flow fans due to inflow turbulence. The methodology is applied to two important cases, in the first case the rotor inflow contains non-homogeneous turbulence in the wakes of inlet guide vanes (IGV's) and in the second case it contains the turbulence ingested from the atmosphere which is highly anisotropic at low or zero forward flight speed.

- 121 A74-21565
 UNIFIED ANALYSIS OF FAN STATOR NOISE
 Hanson, D.B. (United Aircraft Corp., Hamilton, Standard Div., Windsor Locks, Conn)
 Acoustical Society of America, Journal vol 54 Dec 1973, p 1571-1591. 27 refs
 Research supported by the United Aircraft Corp.

A theory is developed which predicts the acoustic radiation of an axial-flow fan stator due to interaction with rotor viscous wakes. Calculations are compared in detail with experimental data. Both the harmonic and broadband noise-spectrum components are calculated from a unified model using methodology from the theories of random pulse amplitude modulation, PAM, and pulse position modulation, PPM. The stator is modeled as a circular array of pulsed dipoles. The amplitude and arrival time of each pulse are random variables whose means correspond to the values calculated from harmonic rotor-stator interaction theory. The standard deviations of these random variables are measures of the turbulence levels in the blade wakes.

- 122 N75-30866 Hamilton Standard, Windsor Locks, Conn.
 STUDY OF NOISE SOURCES IN A SUBSONIC FAN USING MEASURED BLADE PRESSURES AND ACOUSTIC THEORY
 Final Report
 Hanson, D.B. Washington NASA Aug 1975 138p refs
 (Contract NAS1-12505)
 (NASA-CR-2574) Avail: NTIS HC \$5.75

Sources of noise in a 1.4 m (4.6 ft) diameter subsonic tip speed propulsive fan running statically outdoors are studied using a combination of techniques. Signals measured with pressure transducers on a rotor blade are plotted in a format showing the space-time history of inlet distortion. Study of these plots visually and with statistical correlation analysis confirms that the inlet flow contains long, thin eddies of turbulence. Turbulence generated in the boundary layer of the shroud upstream of the rotor tips was not found to be an important noise source. Fan noise is diagnosed by computing narrowband spectra of rotor and stator sound power and comparing these with measured sound power spectra. Rotor noise is computed from spectra of the measured blade pressures and stator noise is computed using the author's stator noise theory. It is concluded that the rotor and stator sources contribute about equally at frequencies in the vicinity of the first three harmonics of blade passing frequency. At higher frequencies, the stator contribution diminishes rapidly and the rotor/inlet turbulence mechanism dominates. Two parametric studies are performed by using the rotor noise calculation procedure which was correlated with test in the first study, the effects on noise spectrum and directivity are calculated for changes in turbulence properties, rotational Mach number, number of blades and stagger angle. In the second study the influences of design tip speed and blade number on noise are evaluated.

- 123 A75-27926
 THEORETICAL AND EXPERIMENTAL STUDIES OF DISCRETE-TONE ROTOR-STATOR INTERACTION NOISE
 Hornicz, G.F., Ludwig, G.R., Lordi, J.A. (Calspan Corp., Buffalo, NY).
 American Institute of Aeronautics and Astronautics, Aero-Acoustics Conference,
 2nd, Hampton, Va, Mar. 24-26 1975, Paper 75-443. 19p 37 refs
 Contract No F33615-73-C-2046

A theoretical and experimental study is conducted on the discrete-tone noise caused by interaction between rotor and stator blade rows of subsonic axial-flow fans and compressors. A compressible two-dimensional analysis of the generated aerodynamic forces is matched, on a strip-theory basis, to the three-dimensional annular duct acoustic modes. Expressions are derived for both the mean square pressure at any position in the duct, and for the total power radiated at harmonics of blade passage frequency in terms of the fan/compressor operating conditions and geometry. The sound pressure level at the outer wall is calculated theoretically, and the resulting predictions are compared with the acoustic data for two different rotor-stator configurations. The discrepancy between theoretical and experimental findings is discussed in detail.

- 124 N74-20426 National Research Council of Canada, Ottawa (Ontario). Div. of Mechanical Engineering
 NOISE CHARACTERISTICS OF AN EXPERIMENTAL LIFTING FAN UNDER CROSSFLOW CONDITIONS
 Krishnappa, G.
 In AGARD V/STOL Propulsion Systems Jan. 1974 14p refs (AGARD-CP-135)

The results of acoustic tests conducted on a 12-in diameter model lifting fan, to find the effect of crossflow on its noise radiation characteristics are presented. The broadband noise levels increased with the velocity of the crossflow. The fundamental blade passing frequency and its second harmonic tones showed moderate changes in the field shapes and levels for low crossflows. At high crossflow velocities due to the presence of a partial stalled region the tone levels increased drastically. The tones generated by the rotor blades due to inflow distortions were believed to dominate over the rotor and stator interaction levels. At fan speeds close to the design point, there were only slight changes in the tone levels and field shapes at the blade passing frequency as the blade incidence excursions became less severe and rotor and stator interaction was much stronger. However, at the higher crossflow velocities the second harmonic tones showed substantial reductions in tone levels with different field shapes.

- 125 N74-29376 National Research Council of Canada, Ottawa (Ontario). Div. of Mechanical Engineering
 ACOUSTIC TESTS ON A FAN-IN-WING MODEL: EFFECTS OF AN EXTENDED INLET
 Krishnappa, G.
 Feb. 1974 58p refs
 (NRC-13898: LR-576) Avail: NTIS HC \$6.00

The aerodynamic noise generated by the lifting fan in the fan-in-wing configuration of vertical takeoff aircraft is discussed. The effect of increasing the depth of the inlet on the noise characteristics of the fan at static and crossflow conditions is analyzed. The causes for aerodynamic noise under crossflow conditions are explained. The changes in noise tonal signature under crossflow conditions were investigated in a wind tunnel.

- 126 A75-25728
 FAN AEROACOUSTICS - THE EFFECT OF STATOR BLADE NUMBER AND SPACING ON IN-DUCT NOISE SIGNATURES
 Krishnappa, G. (National Research Council, Engine Laboratory, Ottawa, Canada)
 American Institute of Aeronautics and Astronautics, Aero-Acoustics Conference
 2nd, Hampton, Va., Mar 24-26 1975, Paper 75-444. 12p 9 refs

Experimental work is reported aimed at determining the relative importance of the rotor blade row and the stator blade row in generating blade-passing frequency tones and broadband noise. Results suggest that the blade-passing frequency tone and its higher harmonics were generated by rotor-stator interaction at low subsonic speeds. The rotor-stator interaction tone was strong when there was a smaller number of stator blades than rotor blades. However, at higher subsonic speeds when the stator blade number exceeded the rotor blades, the tone at the blade-passing frequency was apparently generated by the rotor alone, while the higher harmonics showed the presence of rotor-stator interaction tones. With a smaller number of stator blades the rotor-stator interactions produced the blade passing frequency tone. The severe attenuation of the contrarotating modes during their upstream propagation through the rotor blade appears to be responsible for the relatively weak rotor-stator interaction tones at the fan inlet with a larger stator blade number.

- 127 N73-26014 National Aeronautics and Space Administration, Lewis Research Center, Cleveland, Ohio
 EFFECT OF ROTOR DESIGN TIP SPEED ON NOISE OF A 1.21 PRESSURE RATIO MODEL FAN UNDER STATIC CONDITIONS
 Loeffler, I.J., Lieblein, S., Stockman, N.O.
 1973 21p
 Proposed for presentation at 1973 Winter Ann. Meeting of the ASME, Detroit, 11-15 Nov 1973
 (NASA-TN-X-68243: E-7555) Avail: NTIS HC \$3.25

Preliminary results are presented for a reverberant-field noise investigation of three fan stages designed for the same overall total pressure ratio of 1.21 at different rotor tip speeds (750, 900 and 1050 ft/sec). The stages were tested statically in a 15-inch-diameter model lift fan installed in a wing pod located in the test section of a wind tunnel. Although the fan stages produced essentially the same design pressure ratio, marked differences were observed in the variation of fan noise with fan operating speed. At design speed, the forward-radiated sound power level was approximately the same for the 750 ft/sec and 900 ft/sec stages. For the 1050 ft/sec stage, the design-speed forward-radiated power level was about 7 db higher due to the generation of multiple pure tone noise.

- 128 A75-41693
 DC-9 FLIGHT TESTING OF THE REFANNED JT8D ENGINE
 Lowder, E.M., Hanwell, R.C. (Douglas Aircraft Co., Long Beach, Calif.)
 American Institute of Aeronautics and Astronautics, Aircraft Systems and Technology
 Meeting, Los Angeles, Calif., Aug 4-7, 1975, Paper 75-998. 9p 7 refs

Two refanned JT8D engines, each equipped with a larger single-stage fan and an acoustically treated nacelle, were installed and tested on a DC-9-30 airplane. The primary noise tests consisted of takeoff and approach-related flyover runs that were consistent with FAR test procedures. Survey-type flyovers were also conducted to obtain data to complete a basic map of flyover noise as a function of engine power and airplane height. Other noise measurements were obtained to evaluate the relative strengths of the various engine-noise components. Considerable testing was done to assess the effect of the refanned engine and its installation on flightworthiness and basic airplane/engine performance. The results indicate that significant noise reduction was achieved and that flight characteristics and structural integrity were acceptable

- 129 A75-25739
 SIMULATION OF FLIGHT EFFECTS ON AERO ENGINE FAN NOISE
 Lowrie, B.W. (Rolls-Royce 1971 Ltd, Derby, England)
 American Institute of Aeronautics and Astronautics, Aero-Acoustics Conference,
 2nd Hampton, Va., Mar 24-26, 1975, Paper 75-463. 9p 9 refs

It is now widely recognized that in flight an element of aero engine fan noise, ie distortion tones, reduce significantly compared to static conditions. Since these tones dominate on static tests it is difficult to carry out meaningful research and development testing using ground facilities. In an effort to study and overcome this problem a number of possible solutions have been tried and are described including the effects of using intake screens, 'conditioning' the air before it is drawn into the fan intake, and using a moving vehicle. From these experiments the requirements for forward speed simulation are being derived.

- 130 N73-27207 Hamilton Standard, Windsor Locks, Conn
 NOISE AND WAKE STRUCTURE MEASUREMENTS IN A SUBSONIC TIP SPEED FAN: TABULATION AND PLOTS OF TEST DATA
 Magliozzi, B., Johnson, B.V., Hanson, D.B., Metzger, F.B.
 23 July 1973 284p
 (Contract NAS1-11670)
 (NASA-CR-132259) Avail: NTIS HC \$16.25

Noise and wake structure measurements in a ducted fan were conducted. The tip speed was kept at subsonic levels. The anechoic platform used during the test is described. The following conditions are reported: (1) one third octave band analyses of the fan noise data. (2) narrow band analyses of the fan noise for selected test conditions. (3) narrow band sound power level data for all fan test conditions, and (4) velocity and air angle evaluation of blade wake data.

- 131 A75-25740
 EFFECT OF FORWARD MOTION ON FAN NOISE
 Merriman, J.E., Good, R.C. (Douglas Aircraft Co., Long Beach, Calif.)
 American Institute of Aeronautics and Astronautics, Aero-Acoustics Conference,
 2nd, Hampton, Va., Mar 24-26, 1975, Paper 75-464. 11p 19 refs

A test program was conducted to investigate the effect of forward motion on the fan noise generated by a CF6-6 turbofan engine installed on a McDonnell Douglas DC-10-10 airplane. Acoustic measurements were made with nine microphones mounted internally in the inlet and the fan-discharge ducts, one fuselage-mounted microphone, and an array of ground microphones. The results of the test program indicated that the primary difference between static and flight data is the reduced inflight level of the fan fundamental tone for fan rotor speeds below cutoff. Under static test conditions, there is sufficient inlet flow turbulence to cause the generation of a strong blade-passage-frequency tone at approach power setting. With forward motion however, these noise-generating mechanisms are minimized, and the level of the fan tone is reduced. This result suggests that the use of static engine noise data to design acoustically treated nacelles may result in unnecessary weight and performance penalties for the required inflight noise reductions.

- 132 N73-18011 Hamilton Standard, Windsor Locks, Conn
ANALYTICAL PARAMETRIC INVESTIGATION OF LOW PRESSURE RATIO FAN NOISE
Metzger, F.B., Hanson, D.B., Menhe, R.W., Towle, G.B.
Washington NASA Mar. 1973 118p refs
(Contract NAS1-10896)
(NASA-CR-2188: HSER-5990) Avail: NTIS HC \$3.00

The results of an analytical study are reported which shows the effect of various physical and operating parameters on noise produced by low pressure ratio propulsive fans operating at subsonic tip speeds. Acoustical duct lining effects are included in the study. The concepts used to develop the noise theory used in the study, as well as the correlation between the theory and model test results are also presented. It is shown that good correlation has been established between theory and experiment. Using the theory, it is shown that good aerodynamic design, maximum acceptable fan solidity, low tip speed operation and use of few blades and vanes leads to the lowest noise levels. Typical results of the study indicate that a fan operating at 1.2 fan pressure ratio and 700 ft/second tip speed with 12 blades and 7 vanes and including modest acoustic treatment on the duct wall would produce levels allowing a 100,000 lb. STOL aircraft to meet a noise level objective of 95 Pndb at 500 ft at takeoff.

- 133 A75-37127
AXIAL FLOW FAN NOISE CAUSED BY INLET FLOW DISTORTION
Mugridge, B.D. (Southampton University, Southampton, England)
Journal of Sound and Vibration, vol 40, June 22, 1975, p 497-512. 21 refs
Research supported by the Ministry of Defence (Procurement Executive).

Flow distortion at the inlet of an axial flow fan will cause discrete tone noise generation at shaft rotational frequencies. Controlled experiments have been carried out to check the validity of existing theories to predict these tone levels. The results have shown satisfactory agreement at low frequencies for a concentrated force representation of the blade chordwise load distribution. Both tone and broadband noise predictions have been used to calculate the total 1/3 octave spectrum for the type of fan used in cooling flow applications.

- 134 A76-13611
APPLICATION OF SIMILARITY LAWS TO THE BLADE PASSAGE SOUND OF CENTRIFUGAL FANS
Neise, W. (Deutsche Forschungs und Versuchsanstalt für Luft und Raumfahrt, Institut für Turbulenz-forschung, Berlin, West Germany). Journal of Sound and Vibration, vol 43, Nov 8, 1975, p 61-75 18 refs
Research supported by the Deutsche Forschungsgemeinschaft.

This paper is concerned with similarity laws governing the harmonic components of the sound radiated from centrifugal fans. Measurements are made with two precisely similar fans having impellers of 140-mm and 280-mm diameter. The experimental apparatus used is in accordance with the in-duct method suggested in a recent proposal by the International Organization for Standardization. The present experimental results verify Weidemann's (1971) formulation of similarity laws, which describes the radiated sound pressure as a product of nondimensional terms. The experiments also prove that it is possible to extrapolate data from a model fan to other geometrically similar fans of different size.

- 135 A76-16494
CALCULATION OF THE TURBULENCE NOISE OF A RADIAL FAN (BERECHNUNG DES TURBULENZGERÄUSCHES VON RADIALVENTILATOREN).
Neuhauser, H. (Wien, Technische Universität, Vienna, Austria).
Ingenieur-Archiv, vol 44, no 5, 1975, p 301-315 16 refs. In German

An equation which can easily be applied to the calculation of the turbulence noise of a centrifugal fan is developed. Besides data on the turbulence itself, the only data necessary for the calculation of the sound power is the parameters characterizing the working condition and the geometrical dimensions of the rotor. A relation between the turbulence and the fluctuating lift of the individual airfoil is developed and with it the sound power is determined. The results are then applied to the airfoil in the radial cascade.

- 136 A75-27927
THE ROLE OF ROTOR BLADE BLOCKAGE IN THE PROPAGATION OF FAN NOISE INTERACTION TONES
Philpot, M.G. (National Gas Turbine Establishment, Farnborough, Hants., England)
American Institute of Aeronautics and Astronautics, Aero-Acoustics Conference,
2nd, Hampton, Va., Mar 24-26, 1975, Paper 75-447, 12p 15 refs

Experimental studies indicate that forward propagation of the tone noise caused by rotor/OGV combinations is inhibited by the blocking effect of the rotor - in some cases to a considerable extent. The physics of this mechanism and the available two-dimensional theoretical treatments of it are reviewed. To enable fans of low hub/tip ratio to be analyzed, a method, based on strip-theory principles, of extending such treatments to three dimensions is outlined. This is used in conjunction with one of the simpler theories to predict the blockage effects for four different research fans. Generally good agreement with experiment is obtained and it is concluded that the approach forms a viable basis for prediction. The implications of the findings are discussed briefly in the context of turbofan engine design.

- 137 N75-14764 Rao and Associates, Inc., Palo Alto, Calif.
THEORETICAL STUDIES ON TONE NOISE FROM A DUCTED FAN ROTOR
Rao, C.V.R., Chu, W.T., Digumarthi, R.V., Agarwal, R.K.
Sep 1974 69p refs
(Contract NAS2-6401)
(NASA-CR-137620) Avail: NTIS HC \$4.25

The method of computing radiated noise from a ducted rotor due to inflow distortion and turbulence are examined. Analytical investigations include an appropriate description of sources, the cut-off conditions imposed on the modal propagation of the pressure waves in the annular duct, and reflections at the upstream end of the duct. Far field sound pressure levels at blade passing frequency due to acoustic radiation from a small scale low speed fan are computed. Theoretical predictions are in reasonable agreement with experimental measurements.

- 138 N73-30952 Rao (G.V.R.) and Associates, Sherman Oaks, Calif. Aerodynamics and Propulsion Technology
ANALYTICAL LIFT FAN NOISE STUDY - INTERIM REPORT 13 Apr. 1971-13 June 1972
Rao, G.V.R., Chu, W.T., Digumarthi, R.V.
13 July 1973, 78p refs
(Contract NAS2-6401)
(NASA-CR-114576) Avail: NTIS HC \$6.00

Based on reasonable estimates of flow conditions occurring in an axial fan, acoustic radiation from various noise sources is evaluated. Results of computations on two specific fans are presented, and relative significance of the various sources is examined.

- 139 A76-10248
BLADE-WHEEL NOISE CAUSED BY RANDOM INHOMOGENEITIES OF AN INCOMING FLOW (SHUM LOPATOCHNOGO KOLESA, VYZYVAEMYI SLUCHAINYMI NEODNORODNOSTIAMI NABEGAIUSHCHEGO POTOKA)
Rimski-Korsakov, A.V. In: Acousto-aerodynamic studies, (A76-10238 01-02)
Moscow, Izdatel'stvo Nauka, 1975, p 72-77 7 refs. In Russian

The noise spectrum is evaluated which arises from the interaction of the blades in an axial-flow fan with random inhomogeneities (velocity fluctuations) of the incoming flow. It is shown that a series of maxima are located in this spectrum near the frequencies that are multiples of the rotation frequency of the blade wheel and that the bandwidth of these maxima depends on the rotation time and the dimensions of the inhomogeneities in comparison with the rotation period and the blade dimensions. The maximum estimate gives 110 dB of sound pressure at a distance of 10 meters for a 100-kW fan with 20 blades rotating at 3000 rpm and a 2% effective fluctuation of flow velocity.

- 140 A75-25741
MODEL AND FULL SCALE TEST RESULTS RELATING TO FAN NOISE IN-FLIGHT EFFECTS
Roundhill, J.P., Schaut, L.A. (Boeing Commercial Airplane Co., Seattle, Wash.)
American Institute of Aeronautics and Astronautics, Aero-Acoustics Conference,
2nd, Hampton, Va., Mar 24-26, 1975, Paper 75-465. 11p 8 refs

Full scale high bypass ratio engine noise comparisons are shown that indicate fan noise in-flight is lower than would be estimated from static data extrapolations. This effect is most prevalent at subsonic fan tip speeds and is attributed to the static test inflow turbulence conditions aggravating the rotor-alone noise generation. A model scale fan test was conducted in which the fan inflow turbulence was minimized using a large screened inlet and the results compared with conventional bellmouth inlet measurements. In addition, tests were conducted with and without exit guide vanes to determine the significance of the rotor and stator sources with controlled fan inflow. Both full scale and model test results indicate that fan inflow changes from static to flight conditions significantly affect fan source noise and extrapolating normal uncontrolled static data to flight can be misleading. The results also indicate that the screened inlet approach is a promising method to better simulate in-flight fan noise in static tests.

- 141 N73-21928 General Electric Co., Cincinnati, Ohio. Aircraft Engine Group
EFFECT OF CROSSFLOW VELOCITY ON VTOL LIFT FAN BLADE PASSING FREQUENCY NOISE
GENERATION
Stimpert, D.L.
Feb 1973, 56p refs
(Contract NAS2-5462)
(NASA-CR-114566) Avail: NTIS HC \$5.00

Analysis of noise measurements taken during tests of a remote lift fan wing installation, a V/STOL model transport with both lift and lift/cruise fans, and XV5B research aircraft flight tests has indicated a definite increase in pure tone sound pressure level due to crossflow over the face of the lift fans. The fan-in-wing and V/STOL model transport tests were conducted in the NASA Ames 40 ft by 80 ft wind tunnel and the XV5B flight tests at Moffett Field. Increases up to 10 db were observed for the lift fan installation tested at crossflow to fan tip velocity ratios up to 0.25. Cruise fan noise levels were found to be unaffected by the external flow. The noise level increase was shown to be related to an increase in fan distortion levels.

- 142 N75-14761 General Electric Co., Cincinnati, Ohio
ACOUSTIC RESULTS FROM TESTS OF A 36-INCH (0.914 m) DIAMETER STATORLESS LIFT FAN
Stimpert, D.L. Jun. 1973 114p refs
(Contract NAS2-5462)
(NASA-CR-137621: R73AEG360) Avail: NTIS HC \$5.25

A statorless, turbotip lift fan was tested statically outdoors to determine its acoustic characteristics. Spectral and directivity results are presented with comparison to data from the same family of lift fan designs having stator vanes. Modifications to the fan were tested to evaluate circular inlet guide vanes and exhaust treatment. A comparison was made of results obtained at General Electric Edwards Flight Test Center and NASA Ames Research Center with regards to test data and differences in site characteristics.

- 143 N75-14765 National Aeronautics and Space Administration, Lewis Research Center, Cleveland, Ohio
ACOUSTIC AND AERODYNAMIC PERFORMANCE OF A 1.83 METER (6 FOOT) DIAMETER 1.2 PRESSURE RATIO FAN (QF-6)
Woodward, R.P., Lucas, J.G., Stakolich, E.G.
Washington Dec 1974 117p refs
(NASA-TN-D-7809: E-7996) Avail: NTIS HC \$5.25

A 1.2-pressure-ratio, 1.83-meter (6-ft-) diameter experimental fan stage with characteristics suitable for use in STOL aircraft engines was tested for acoustic and aerodynamic performance. The design incorporated features for low noise, including absence of inlet guide vanes, low rotor-blade-tip speed, low aerodynamic blade loading, and long axial spacing between the rotor and stator rows. The stage was run with four nozzles of different area. The perceived noise along a 152.4 meter (500-ft) sideline was rear-quadrant dominated with a maximum design-point level of 103.9 PNdb. The acoustic 1/3-octave results were analytically separated into broadband and pure-tone components. It was found that the stage noise levels generally increase with a decrease in nozzle area, with this increase observed primarily in the broadband noise component. A stall condition was documented acoustically with a 90-percent-of-design-area nozzle.

- 144 N74-30239 General Electric Co., Cincinnati, Ohio. Aircraft Engine Group
CONCEPTUAL DESIGN STUDIES OF LIFT/CRUISE FANS FOR MILITARY TRANSPORT Final Report
6 Aug. 1974 264 p refs
(Contract NAS3-17850)
(NASA-CR-134636; R74AEG283) Avail: NTIS HC \$16.25

A study program for conceptual design studies of remote lift and lift/cruise fan systems to meet the requirements of military V/STOL aircraft was conducted. Parametric performance and design data are presented for fans covering a range of pressure ratios, including both single and two stage fan concepts. The gas generator selected for these fan systems was the J101-GE-100 engine. Noise generation and transient response were determined for selected fan systems.

7. Noise Prediction

- 145 N75-25883 Lockheed-Georgia Co., Marietta
A METHOD FOR PREDICTING ACOUSTICALLY INDUCED VIBRATION IN TRANSPORT AIRCRAFT,
APPENDIX Final Report
Bartel, H.W., Schneider, C.W.
Sep. 1974 54p refs
(Contract F33615-73-C-3638; AF Proj. 1370)
(AD-A004215; LG74ERO121-App-1; AFFDL-TR-74-App-1)
Avail: NTIS

A method is set forth for predicting the acoustically induced structural vibration in transport category aircraft. Charts are presented which correlate third-octave random noise and vibration levels at various confidence levels, for the frequency range of 50 to 2500 Hertz. The prediction charts are based on measured data from modern transport aircraft and are presented for the normal direction, ground operation, and a reference structural mass and rigidity. Shell-type structure (fuselage, pods, fairings) and box-type structure (wing, horizontal/vertical stabilizer) are treated separately. Means are provided for predicting lateral and tangential vibration, vibration in pressurized cruise flight, and for correcting for changes in structural mass and rigidity. Application of the method to a hypothetical airplane design case is illustrated in an example.

- 146 N76-12062 Illinois Univ., Urbana
PREDICTING AXIAL FLOW FAN SOUND PRESSURE SPECTRUMS Ph.D Thesis
Bates, K.C.
1975 282 p
Avail: Univ. Microfilms Order No 75-24255

The aerodynamic sound pressure produced by axial flow engine cooling fans is examined. An analytical solution that described the sound pressure radiated at distances less than one fan radius from the fan was developed. The solution consisted of theoretically derived periodic sound pressure components superimposed upon an empirically derived random sound pressure component. The solution was manipulated to render complete time and frequency sound pressure spectrums and overall sound pressure levels (unweighted, A-weighted and B-weighted). A computer program, written in the computer language FORTRAN 4, was developed to evaluate the analytical solution.

- 147 A74-18722
NOISE FROM NONUNIFORM TURBULENT FLOWS
Berman, C.H. (Boeing Commercial Airplane Co., Seattle, Wash.,) American Institute of Aeronautics and Astronautics, Aerospace Sciences Meeting, 12th, Washington, D.C., Jan. 30-Feb. 1, 1974, Paper 74-2.
11 p. 26 refs Members, \$1.50; nonmembers, \$2.00

The effects of a nonuniform mean flow on turbulence noise generation and propagation are treated analytically. A special form of an equation studied by Lilley is applied to a parallel flow model possessing arbitrary mean velocity and temperature profiles. Solutions of the resultant ordinary differential equation show that inviscid attenuation of sound occurs at very high frequencies, while a boost in sound level is present at very low frequencies. A new interpretation of shear and self noise generation terms is presented. The applicability of these results to jet noise prediction is discussed.

- 148 A75-25738
MEASUREMENT AND PREDICTION OF JET NOISE IN FLIGHT
Bushell, K.W. (Rolls-Royce/1971/ Ltd, Derby, England)
American Institute of Aeronautics and Astronautics, Aero-Acoustics Conference
2nd, Hampton, Va., Mar. 24-26, 1975, Paper 75-461, 10 p. 12 refs

The most difficult problem facing the aircraft noise engineer is the determination of the level of jet mixing noise in flight. Recent measurements of a range of aircraft are compared with measurements of static engine noise. These comparisons show a reduction in noise close to the jet axis as predicted by theory and shown in wind tunnel investigations, but at 90 deg to the engine axis no reduction is observed in complete contrast to both theory and wind tunnel measurements. At forward angles, an increase in absolute noise level is often observed. The implications to jet noise prediction in flight are discussed.

- 149 N73-32969 National Aeronautics and Space Administration, Lewis Research Center, Cleveland, Ohio
FLAP NOISE PREDICTION METHOD FOR A POWERED LIFT SYSTEM
Clark, B., Dorsch, R., Reshotko, M.
1973 15 p refs Presented at the Aero-Acoustic Specialists Conf., Seattle, 15-17 Oct. 1973, sponsored by AIAA
(NASA-TM-X-71449; E-7717) Avail; NTIS HC \$3.00

A method is presented for estimating the noise generated by deflection of the engine exhaust for under-the-wing and over-the-wing versions of an externally blown flap configuration for powered lift. Correlation equations and curves are given for the overall sound pressure level and directivity and for spectra scaled to a high bypass 25,000-pound thrust size engine. Data are taken from TF34 engine tests and from large cold flow model tests. The correlations are empirical, and thus application of this prediction procedure is limited to geometrically similar configurations. Application of the method is illustrated by calculated sample footprints.

- 150 N73-31946 Boeing Commercial Airplane Co., Seattle, Wash.
AIRCRAFT NOISE SOURCE AND COMPUTER PROGRAMS - USER'S GUIDE
Crowley, K.C., Jaeger, M.A., Meldrum, D.F.
Jul. 1973 112 p refs
(Contract NAS2-6969)
(NASA-CR-114650; D6-60234) Avail NTIS HC \$7.75

The application of computer programs for predicting the noise-time histories and noise contours for five types of aircraft is reported. The aircraft considered are (1) turbojet, (2) turbofan, (3) turboprop, (4) V/STOL and (5) helicopter. Three principle considerations incorporated in the design of the noise prediction program are core effectiveness, limited input, and variable output reporting.

- 151 N75-30176 National Aeronautics and Space Administration, Lewis Research Center, Cleveland, Ohio
INTERIM PREDICTION METHOD FOR EXTERNALLY BLOWN FLAP NOISE
Dorsch, R.C., Clark, B.J., Reshotko, M.
1975 51 p refs
(NASA-TM-X-71768; E-8423) Avail; NTIS HC \$4.25

An interim procedure for predicting externally blown flap (EBF) noise spectra anywhere below a powered lift aircraft is presented. Both engine-under-the-wing and engine-over-the-wing EBF systems are included. The method uses data correlations for the overall sound pressure level based on nozzle exit area and exhaust velocity along with OASPL directivity curves and normalized one-third-octave spectra. Aircraft motion effects are included by taking into account the relative motion of the source with respect to the observer and the relative velocity effects on source strength.

- 152 N73-31945 Boeing Commercial Airplane Co., Seattle, Wash.
 AIRCRAFT NOISE SOURCE AND CONTOUR ESTIMATION
 Dunn, D.G., Peart, N.A.
 Jul. 1973 233p refs
 (Contract NAS2-6969)
 (NASA-CR-114649; D6-60233) Avail; NTIS HC \$13.75

Calculation procedures are presented for predicting the noise-time histories and noise contours (footprints) of five basic types of aircraft; turbojet, turbofan, turboprop, V/STOL, and helicopter. The procedures have been computerized to facilitate prediction of the noise characteristics during takeoffs, flyovers, and/or landing operations.

- 153 A75-29465
 PREDICTION OF AIRFOIL TONE FREQUENCIES
 Fink, M.R.
 Journal of Aircraft, vol. 12, Feb. 1975, p. 118-120. 10 refs.

Recent experiments on the prediction of airfoil tone frequencies are compared with boundary layer theory. It is concluded that measured tone frequencies for airfoils radiating vortex shedding noise (airfoil wake-generated noise) can be predicted directly from that theory without the use of empirical constants. Such noise can be eliminated by tripping the laminar boundary layer at model scale or by increasing the Reynolds number toward full scale.

- 154 N75-33054 United Technologies Research Center, East Hartford, Conn.
 PREDICTION OF EXTERNALLY BLOWN FLAP NOISE AND TURBOMACHINERY STRUT NOISE
 Fink, M.R.
 Aug. 1975 142 p refs
 (Contract NAS3-17863)
 (NASA-CR-134883) Avail; NTIS HC \$5.75

Methods were developed for predicting externally blown flap (EBF) noise and turbomachinery strut noise. Noise radiated by under-the-wing and upper-surface-blowing EBF configurations is calculated as a sum of lift dipole noise, trailing edge noise, and jet quadrupole noise. Resulting predictions of amplitudes and spectra generally were in good agreement with data from small-scale models. These data cover a range of exhaust velocity, flap deflection, exhaust nozzle position, exhaust nozzle shape, and ratio of exhaust nozzle diameter to wing chord. A semi-empirical method for predicting dipole noise radiation from a strut with incident turbulence was in good agreement with data. Leading-edge regions made of perforated plate backed by a bulk acoustic absorber achieved up to 7 db reduction of strut noise caused by incident turbulence at high frequencies. Radial turbulence in a turbofan exit duct was found to have a relatively high level associated with the mean velocity defect in the rotor blade wakes. Use of these turbulence spectra and a dipole noise radiation equation gave general prediction of measured aft-radiated sound power caused by a splitter ring in a full-scale fan exit duct.

- 155 N75-18182 National Aeronautics and Space Administration, Langley Research Center, Langley Station, Va.
 PREDICTION OF AIRFRAME NOISE
 Hardin, J.G., Fratello, D.J., Hayden, R.E., Africk, S.
 (Bolt, Beranek, and Newman, Inc., Boston) Washington Feb. 1975 115 p refs
 (NASA-TN-D-7821; L-9912) Avail; NTIS HC \$5.25

Methods of predicting airframe noise generated by aircraft in flight under nonpowered conditions are discussed. Approaches to predictions relying on flyover data and component theoretical analyses are developed. A nondimensional airframe noise spectrum of various aircraft is presented. The spectrum was obtained by smoothing all the measured spectra to remove any peculiarities due to airframe protrusions normalizing each spectra by its overall sound pressure level and a characteristics frequency, and averaging the spectra together. A chart of airframe noise sources is included.

- 156 N76-14134 ARO Inc., Arnold Air Force Station, Tenn.
 JET NOISE: A SURVEY AND A PREDICTION FOR SUBSONIC FLOWS Final Report
 Jul. 1973 - Sep. 1974
 Harsha, P.T.
 AEDC Aug. 1975 78 p refs
 (ARO Proj. RF438; ARO Proj. R32P)
 (AD-A013794; ARO-ETF-TR-74-115; AEDC-TR-75-85) Avail; NTIS

The state-of-the-art of the prediction of turbulent jet noise is surveyed. This survey includes a description of the available experimental data on subsonic and supersonic, cold and hot jets, and of present theoretical treatments of the mechanisms of turbulent jet noise production. A detailed analysis of the production of subsonic cold jet noise, based on the acoustic analogy formulation, is described, and results of computations using this analysis and a turbulent kinetic energy analysis of the jet flow field are presented and compared with representative experimental data.

- 157 A75-25756
 AIRCRAFT FAR-FIELD AERODYNAMIC NOISE - ITS MEASUREMENT AND PREDICTION
 Healy, G.J.
 (Lockheed-California Co., Burbank, Calif.).
 American Institute of Aeronautics and Astronautics, Aero-Acoustics Conference, 2nd,
 Hampton, Va., Mar. 24-26, 1975, Paper 75-486. 9 p 13 refs

The material presented in this paper is a synopsis of what is believed to be the first systematic investigation of far-field radiated, aerodynamically generated noise from 'clean' configured aircraft during low altitude unpowered flight. Five aircraft, ranging in weight from 5785 to 173,925N (1300 to 39,000 pounds) and having wing aspect ratios ranging from 6.59 to 18.25, were tested at flight velocities ranging from 30 to 98.5 m/sec (58 to 191.5 knots or 98 to 323 ft/sec). An equation relating far-field aircraft aerodynamic noise to readily evaluated physical and operational parameters of the vehicle was developed from the results of these measurements. In addition, a slight modification to this equation is herein proposed which permits accurate computation of the recently published far-field aerodynamic noise from the Lockheed Jet Star and the Convair F-106B delta wing Mach 2 aircraft.

- 158 N75-25948 National Aeronautics and Space Administration, Lewis Research Center,
 Cleveland, Ohio
 INTERIM PREDICTION METHOD FOR FAN AND COMPRESSOR SOURCE NOISE
 Heidmann, M.F. Jun. 1975 83 p refs
 (NASA-TM-X-71763; E-8398) Avail; NTIS HC \$4.75

A method is presented for interim use in assessing the noise generated by fans and compressors in turbojet and turbofan engines. One-third octave band sound pressure levels consisting of broadband, discrete tone, and combination-tone noise components are predicted. Spectral distributions and directivity variations are specified. The method is based on that developed by other investigators with modifications derived from an analysis of full-scale single-stage fan data. Comparisons of predicted and measured noise performance are presented, and requirements for improving the method are discussed.

- 159 N75-12950 National Aeronautics and Space Administration, Lewis Research Center,
 Cleveland, Ohio
 INTERIM PREDICTION METHOD FOR LOW FREQUENCY CORE ENGINE NOISE
 Huff, R.G., Clark, B., Dorsch, R.G.
 Nov. 1974 25 p
 (NASA-TM-X-71627; E-8154) Avail; NTIS HC \$3.25

A literature survey on low-frequency core engine noise is presented. Possible sources of low frequency internally generated noise in core engines are discussed with emphasis on combustion and components scrubbing noise. An interim method is recommended for predicting low frequency core engine noise that is dominant when jet velocities are low. Suggestions are made for future research on low frequency core engines noise that will aid in improving the prediction method and help define possible additional internal noise sources.

160 A75-25730

NONCOMPACT SOURCE EFFECT ON THE PREDICTION OF TONE NOISE FROM A FAN ROTOR
Kaji, S. (NASA, Ames Research Center, Moffett Field, Calif., Tokyo Univ., Tokyo, Japan)
American Institute of Aeronautics and Astronautics, Aero-Acoustics Conference, 2nd, Hampton, Va., Mar. 24-26, 1975, Paper 75-446. 13 p 12 refs.

A comparison is made between the conventional compact source prediction for airfoil sound radiation and the rigorous prediction based on distribution sources along the airfoil chord. The theoretical analysis performed is for a single airfoil and cascaded airfoils immersed in a sinusoidally varying convected gust field. The pressure field around a single airfoil in supersonic gust flows is also studied. In subsonic flows the phase change of unsteady lift along the chord of a single airfoil reduces the sound radiation significantly in the upstream direction and increases the downstream radiation compared to the compact source prediction. In supersonic flows the compact source prediction gives substantial error in the region just behind the Mach wedge originating from the leading edge, while it approaches the noncompact source results far downstream from the airfoil. In the case of cascaded airfoils the compact source prediction over-estimates the upstream radiation by as much as 20 dB depending on frequency and interblade phase.

161 A74-18723

JET NOISE MODELING - EXPERIMENTAL STUDY AND MODELS FOR THE NOISE AND TURBULENCE FIELDS

Moon, L.F., Zelazny, S.W. (Bell Aerospace Co., Buffalo, N.Y.)
American Institute of Aeronautics and Astronautics, Aerospace Sciences Meeting, 12th Washington, D.C., Jan. 30-Feb. 1974, Paper 74-3. 11 p 33 refs.
Members, \$1.50; nonmembers, \$2.00. Research sponsored by the Bell Aerospace Co; Contract No F44620-70-C-0116

Detailed turbulence profiles were measured at 28 axial locations extending from the nozzle exit to twelve nozzle diameters downstream for a circular jet exhausting into an ambient environment. Measurements include mean velocity, turbulence intensity, shear stress as well as sound intensity, spectral distribution and directivity. A noise model was developed which accurately predict sound amplitude, spectral distribution and directivity pattern in terms of self and shear noise components. A turbulence model was also developed which accurately predicted mean velocity, turbulence intensity, and shear stress in subsonic and supersonic axisymmetric jets with predictions starting in the potential core. Turbulence and noise models were computationally coupled and the sensitivity of noise predictions to inaccuracies in the predicted turbulence field studied. It is shown that errors of only 20% in predicted peak turbulence intensity level in the core region results in up to a 5 dB difference in the predicted overall sound pressure level.

162 N73-30054 United Aircraft Corp., Stratford Conn. Sikorsky Aircraft Div.,

PREDICTION OF V/STOL NOISE FOR APPLICATION TO COMMUNITY NOISE EXPOSURE

Final Report Jun. - Dec. 1972

Munch, C.L.

May 1973 280 p refs

(Contract DOT-TSC-438; DOT-OS-207)

(PB-221140/7; DOT-TSC-OST-73-19) Avail; NTIS HC \$6.75

A computer program to predict the effective perceived noise level (EPNL) the tone corrected perceived noise level (PNLT) and the A-weighted sound level (dBA) radiated by a V/STOL vehicle as it flies along a prescribed takeoff, landing, or cruise flight path is described and a complete users guide for the program is presented. The procedures used to predict the noise radiated by helicopter rotors, propellers, turboshaft engines, lift and cruise fans, and jets are described in detail. Helicopter rotor noise and jet noise are theoretically predicted with some empirical modifications while propeller, fan, and turboshaft engine noise is calculated with primarily empirical procedures.

163 A75-25723

TESTS OF A THEORETICAL MODEL OF JET NOISE

Nosseir, N.S.M., Ribner, H.S. (Toronto Univ., Downsview, Ontario, Canada)

American Institute of Aeronautics and Astronautics, Aero-Acoustics Conference, 2nd, Hampton, Va., Mar. 24-26, 1975, Paper 75-436. 11 p 35 refs. Research sponsored by the General Electric Co. and National Research Council of Canada, Grant No. AF-AFOSR-70-1885

The present study establishes the approximate invariance with frequency of a certain parameter beta formed from experimental measurements of jet noise. The parameter beta, essentially a shear noise/self noise spectral ratio, is a construct of Ribner's theory and this invariance is predicted by the theory. The experimental data also confirm the prediction that the shear- and self-noise spectra match in shape, and that they exhibit a relative shift of close to one octave. The theoretical model as used herein provides a simple closed-form framework for the prediction of jet noise excluding the refraction valley. The main empirical input is the spectrum at 90 deg to the jet axis.

164 A75-25773

NOISE RADIATION FROM TURBULENT FLOWS OVER COMPLIANT SURFACES

Pan, Y.S. (NASA, Langley Research Center, George Washington Univ. Hampton, Va.)
 American Institute of Aeronautics and Astronautics, Aero-Acoustics Conference, 2nd,
 Hampton, Va., Mar. 24-26, 1975, Paper 75-507. 14 p 34 refs.
 Grant No. NGR-09-010-085

The present study is based on Lighthill-Curle's theory of aerodynamic noise. Using a correlation approach and the image concept of Powell, the volume contribution of turbulent flow over a large surface is approximated by a surface contribution of pressure fluctuations. Far-field noise intensities are expressed in terms of the surface pressure fluctuations and surface impedance. Based on available experimental measurements, numerical examples are performed for noise radiated from a turbulent boundary layer and from a normal jet impingement over rigid surfaces. Comparisons with available noise measurements are made. For general turbulent flows over compliant surfaces, measurements are suggested to obtain useful data for noise predictions.

165 N76-13099 National Aeronautics and Space Administration, Langley Research Center, Langley Station, Va.

RESEARCH NEEDS IN AIRCRAFT NOISE PREDICTION

Raney, J.P.

Nov. 1975 38 p refs Presented at 3d Interagency Symp. on Univ. Res in Transportation Noise

(NASA-TM-X-72787) Avail; NTIS HC \$4.00

Progress needed in understanding the mechanisms of aircraft noise generation and propagation is outlined using the focus provided by the need to predict accurately the noise produced and received at the ground by an aircraft operating in the vicinity of an airport. The components of internal engine noise generation, jet exhaust, airframe noise and shielding and configuration effects, and the roles of atmospheric propagation and ground noise attenuation are presented and related to the prediction problem. The role of NASA in providing the focus and direction for needed advances is discussed, and possible contributions of the academic community in helping to fulfill the needs for accurate aircraft noise prediction methods are suggested.

166 A75-18541

NEW COMPUTER SYSTEM FOR AIRCRAFT NOISE PREDICTION

Raney, J.P., Zorunski, W.E. (NASA, Langley Research Center, Acoustics and Noise Reduction Div., Hampton, Va.).

In: Inter-Noise 74; Proceedings of the International Conference on Noise Control Engineering, Washington, D.C., September 30-October 2, 1974. (A75-18530 06-07)
 Poughkeepsie, N.Y., Institute of Noise Control Engineering, 1974 p. 183-186 10 refs.

The purpose of the Aircraft Noise Prediction Office (ANOPO) at Langley Research Center is to provide a focal point for NASA's aircraft noise prediction activities and an appropriate interface with other agencies and industry. An interim prediction system is now in operation, which includes a program for source modeling leading to noise prediction for a single event, two complementary multiple event prediction programs, which predict NEF contours on the basis of interpolation of noise, thrust and altitude data, and the FAA data base for the commercial fleet. An integrated multimode aircraft noise prediction program has been designed, and a mechanism for continuously providing current prediction technology to be incorporated in the program has been implemented.

167 A75-25801

METHODS FOR THE PREDICTION OF AIRFRAME AERODYNAMIC NOISE

Revell, J.D., Healy, G.J., Gibson, J.S. (Lockheed-Georgia Co., Marietta, Ga.)

American Institute of Aeronautics and Astronautics, Aero-Acoustics Conference, 2nd,
 Hampton, Va, Mar. 24-26, 1975, Paper 75-539. 16 p 30 refs

There are three basic methodologies for the prediction of airframe (non-engine) aerodynamic noise: (1) the whole aircraft method; (2) the aircraft drag element method and (3) the individual component distributed source method. A brief review of all three methodologies is presented with prediction methods covering the first two categories detailed. The whole aircraft method is based entirely on measured airframe noise whereas the aircraft drag element method is formulated from knowledge of the drag coefficients of the major airframe noise contributors with a number of constants evaluated from measured airframe data.

- 168 N75-18976 Air Force Flight Dynamics Lab., Wright-Patterson AFB, Ohio
 NEAR FIELD NOISE PREDICTION FOR A LINEAR ARRAY OF TURBOJET ENGINES Final Report
 Smith, D.L., Paxson, R.P., Talmadge, R.D., Pizak, G.A.
 Jul. 1974 79 p refs
 (AF Proj. 1471)
 (AD-A001329; AFFDL-TM-74-139-FYA) Avail; NTIS

A computer program is presented for calculating the sound pressure level (SPL) in the jet near field which accounts for ground reflection and multiple engine operation. The prediction method is a modification of the semi-empirical technique presented in AFFDL TR-67-43 'Near Field Noise Analysis of Aircraft Propulsion Systems with emphasis on Prediction Techniques for Jets'. The modifications in addition to accounting for ground reflection allow the prediction of the SPL for the overall and three octave bands at any point in the field and require data inputs of jet exit temperature, Mach number and diameter. A brief description is presented of a noise measurement program conducted on the XB-70 aircraft during which one-third octave band noise spectra were obtained for a range of engine conditions and for various combinations of linear arrays of engines.

- 169 A75-27933
 DEVELOPMENTS IN JET NOISE MODELING - THEORETICAL PREDICTIONS AND COMPARISONS WITH MEASURED DATA
 Tester, B.J., (Lockheed-Georgia Co., Marietta, Ga.) Morley, C.L.
 (Southampton, University, Southampton, England) American Institute of Aeronautics and Astronautics, Aero-Acoustics Conference, 2nd, Hampton, Va., Mar. 24-26, 1975, Paper 75-477. 14 p 21 refs
 Contract No. F33615-73-C-2032

Spectral information on the sound radiated from turbulent shock-free jets is now available over a wide range of Strouhal numbers, for jet densities ranging from 0.3 to 2 times the ambient sound speed. The unexpected nature of some of the data has led to a fundamental re-examination of aerodynamic sound theory in general, by Lilley (1972) and Morfey (1973), and jet-noise modeling in particular. Two areas of significant progress are described: (1) the effects of nonuniform density which arise with hot jets, and (2) the effects of high Mach number on the radiation from 'isothermal' jets (density ratio = 1). The jet-noise models presented are based on solutions to Lilley's equation.

- 170 N75-29103 Engineering Sciences Data Unit, London (England)
 ESTIMATION OF SUBSONIC FAR-FIELD JET-MIXING NOISE
 Jun. 1973 14 p
 (ESDU-74002) Copyright. Avail: NTIS HC \$74.50

A method is described for estimating far-field jet mixing noise emanating from gas turbine exhaust for fly-over, and side-line noise level of jet aircraft. The method is applicable to the far-field (distances greater than 50 jet diameters from the exit), for subsonic jets with temperature ratios between 1 and 3.2, and pressure ratios between 1.1 and 1.9.

- 171 N74-22638 Alabama Univ., Huntsville. Div. of Graduate Programs and Research
 INVESTIGATION OF THE JET NOISE PREDICTION THEORY AND APPLICATION UTILIZING THE PAO FORMULATION Final Technical Report
 Nov. 1973 159 p refs
 (Contract NAS8-28588)
 Avail: NTIS HC \$11.00

Application of the Phillips theory to engineering calculations of rocket and high speed jet noise radiation is reported. Presented are a detailed derivation of the theory, the composition of the numerical scheme, and discussions of the practical problems arising in the application of the present noise prediction method. The present method still contains some empirical elements, yet it provides a unified approach in the prediction of sound power, spectrum, and directivity.

REPORT DOCUMENTATION PAGE			
1. Recipient's Reference	2. Originator's Reference AGARD-LS-80	3. Further Reference ISBN 92-835-0180-2	4. Security Classification of Document UNCLASSIFIED
5. Originator	Advisory Group for Aerospace Research and Development North Atlantic Treaty Organization 7 rue Ancelle, 92200 Neuilly sur Seine, France		
6. Title	AERODYNAMIC NOISE		
7. Presented at	the von Kármán Institute, Rhode St Genèse, Belgium in December 1976.		
8. Author(s) Various	9. Date January 1977		
10. Author's Address Various	11. Pages 316		
12. Distribution Statement	This document is distributed in accordance with AGARD policies and regulations, which are outlined on the Outside Back Covers of all AGARD publications.		
13. Keywords/Descriptors	<div style="display: flex; justify-content: space-between;"> <div style="width: 45%;"> Aerodynamic noise Aircraft noise Engine noise </div> <div style="width: 45%;"> Sound generators Acoustic measurement </div> </div>		
14. Abstract This Lecture Series 80 on 'Aerodynamic Noise' was co-sponsored by the Fluid Dynamics Panel of AGARD and by the von Kármán Institute for Fluid Dynamics, and implemented by the Consultant and Exchange Programme of AGARD together with VKI. It was presented at the VKI, Rhode St Genèse, Belgium, 6-9 December 1976. The aim is to provide an up-to-date account and authoritative appraisal of aerodynamic noise concepts, theory and experiments. Particular emphasis is given to practical methods for the prediction, measurement and reduction of external noise from jet/fan aircraft. Following a brief overview of relevant aircraft design and operational considerations, the main lectures include detailed presentations on the fundamental theory of aerodynamic noise generation and propagation, basic aero-acoustics of jet efflux noise, engine exhaust noise characteristics, fan noise, airframe self-noise, airframe/engine interaction effects, aero-acoustic measurement and analysis techniques, aircraft flyover noise measurement, noise-source identification and location methods, and ground-based facilities with forward-speed representation. A bibliography of 171 items is included in the publication.			

<p>AGARD Lecture Series No.80 Advisory Group for Aerospace Research and Development, NATO AERODYNAMIC NOISE Published January 1977 316 pages, including Bibliography</p> <p>This Lecture Series 80 on 'Aerodynamic Noise' was co-sponsored by the Fluid Dynamics Panel of AGARD and by the von Kármán Institute for Fluid Dynamics, and implemented by the Consultant and Exchange Programme of AGARD together with VKI. It was presented at the VKI, Rhode St Genèse, Belgium, 6-9 December 1976.</p> <p>The aim is to provide an up-to-date account and authoritative appraisal of aerodynamic noise concepts, P.T.O.</p>	<p>AGARD-LS-80</p> <p>Aerodynamic noise Aircraft noise Engine noise Sound generators Acoustic measurement</p>	<p>AGARD Lecture Series No.80 Advisory Group for Aerospace Research and Development, NATO AERODYNAMIC NOISE Published January 1977 316 pages, including Bibliography</p> <p>This Lecture Series 80 on 'Aerodynamic Noise' was co-sponsored by the Fluid Dynamics Panel of AGARD and by the von Kármán Institute for Fluid Dynamics, and implemented by the Consultant and Exchange Programme of AGARD together with VKI. It was presented at the VKI, Rhode St Genèse, Belgium, 6-9 December 1976.</p> <p>The aim is to provide an up-to-date account and authoritative appraisal of aerodynamic noise concepts, P.T.O.</p>	<p>AGARD-LS-80</p> <p>Aerodynamic noise Aircraft noise Engine noise Sound generators Acoustic measurement</p>
<p>AGARD Lecture Series No.80 Advisory Group for Aerospace Research and Development, NATO AERODYNAMIC NOISE Published January 1977 316 pages, including Bibliography</p> <p>This Lecture Series 80 on 'Aerodynamic Noise' was co-sponsored by the Fluid Dynamics Panel of AGARD and by the von Kármán Institute for Fluid Dynamics, and implemented by the Consultant and Exchange Programme of AGARD together with VKI. It was presented at the VKI, Rhode St Genèse, Belgium, 6-9 December 1976.</p> <p>The aim is to provide an up-to-date account and authoritative appraisal of aerodynamic noise concepts, P.T.O.</p>	<p>AGARD-LS-80</p> <p>Aerodynamic noise Aircraft noise Engine noise Sound generators Acoustic measurement</p>	<p>AGARD Lecture Series No.80 Advisory Group for Aerospace Research and Development, NATO AERODYNAMIC NOISE Published January 1977 316 pages, including Bibliography</p> <p>This Lecture Series 80 on 'Aerodynamic Noise' was co-sponsored by the Fluid Dynamics Panel of AGARD and by the von Kármán Institute for Fluid Dynamics, and implemented by the Consultant and Exchange Programme of AGARD together with VKI. It was presented at the VKI, Rhode St Genèse, Belgium, 6-9 December 1976.</p> <p>The aim is to provide an up-to-date account and authoritative appraisal of aerodynamic noise concepts, P.T.O.</p>	<p>AGARD-LS-80</p> <p>Aerodynamic noise Aircraft noise Engine noise Sound generators Acoustic measurement</p>

theory and experiments. Particular emphasis is given to practical methods for the prediction, measurement and reduction of external noise from jet/fan aircraft. Following a brief overview of relevant aircraft design and operational considerations, the main lectures include detailed presentations on the fundamental theory of aerodynamic noise generation and propagation, basic aero-acoustics of jet efflux noise, engine exhaust noise characteristics, fan noise, airframe self-noise, airframe/engine interaction effects, aero-acoustic measurement and analysis techniques, aircraft flyover noise measurement, noise-source identification and location methods, and ground-based facilities with forward-speed representation. A bibliography of 171 items is included in the publication.

ISBN 92-835-0180-2

theory and experiments. Particular emphasis is given to practical methods for the prediction, measurement and reduction of external noise from jet/fan aircraft. Following a brief overview of relevant aircraft design and operational considerations, the main lectures include detailed presentations on the fundamental theory of aerodynamic noise generation and propagation, basic aero-acoustics of jet efflux noise, engine exhaust noise characteristics, fan noise, airframe self-noise, airframe/engine interaction effects, aero-acoustic measurement and analysis techniques, aircraft flyover noise measurement, noise-source identification and location methods, and ground-based facilities with forward-speed representation. A bibliography of 171 items is included in the publication.

ISBN 92-835-0180-2

theory and experiments. Particular emphasis is given to practical methods for the prediction, measurement and reduction of external noise from jet/fan aircraft. Following a brief overview of relevant aircraft design and operational considerations, the main lectures include detailed presentations on the fundamental theory of aerodynamic noise generation and propagation, basic aero-acoustics of jet efflux noise, engine exhaust noise characteristics, fan noise, airframe self-noise, airframe/engine interaction effects, aero-acoustic measurement and analysis techniques, aircraft flyover noise measurement, noise-source identification and location methods, and ground-based facilities with forward-speed representation. A bibliography of 171 items is included in the publication.

ISBN 92-835-0180-2

theory and experiments. Particular emphasis is given to practical methods for the prediction, measurement and reduction of external noise from jet/fan aircraft. Following a brief overview of relevant aircraft design and operational considerations, the main lectures include detailed presentations on the fundamental theory of aerodynamic noise generation and propagation, basic aero-acoustics of jet efflux noise, engine exhaust noise characteristics, fan noise, airframe self-noise, airframe/engine interaction effects, aero-acoustic measurement and analysis techniques, aircraft flyover noise measurement, noise-source identification and location methods, and ground-based facilities with forward-speed representation. A bibliography of 171 items is included in the publication.

ISBN 92-835-0180-2

AGARD

NATO  OTAN

7 RUE ANCELLE · 92200 NEUILLY-SUR-SEINE
FRANCE

Telephone 745.08.10 · Telex 610176

**DISTRIBUTION OF UNCLASSIFIED
AGARD PUBLICATIONS**

AGARD does NOT hold stocks of AGARD publications at the above address for general distribution. Initial distribution of AGARD publications is made to AGARD Member Nations through the following National Distribution Centres. Further copies are sometimes available from these Centres, but if not may be purchased in Microfiche or Photocopy form from the Purchase Agencies listed below.

NATIONAL DISTRIBUTION CENTRES

BELGIUM

Coordonnateur AGARD - VSL
Etat-Major de la Force Aérienne
Caserne Prince Baudouin
Place Dailly, 1030 Bruxelles

CANADA

Defence Scientific Information Service
Department of National Defence
Ottawa, Ontario K1A 0Z2

DENMARK

Danish Defence Research Board
Østerbrogades Kaserne
Copenhagen Ø

FRANCE

O.N.E.R.A. (Direction)
29 Avenue de la Division Leclerc
92 Châtillon sous Bagneux

GERMANY

Zentralstelle für Luft- und Raumfahrt-
dokumentation und -information
Postfach 860880
D-8 München 86

GREECE

Hellenic Armed Forces Command
D Branch, Athens

ICELAND

Director of Aviation
c/o Flugrad
Reykjavik

ITALY

Aeronautica Militare
Ufficio del Delegato Nazionale all'AGARD
3, Piazzale Adenauer
Roma/EUR

LUXEMBOURG

See Belgium

NETHERLANDS

Netherlands Delegation to AGARD
National Aerospace Laboratory, NLR
P.O. Box 126
Delft

NORWAY

Norwegian Defence Research Establishment
Main Library
P.O. Box 25
N-2007 Kjeller

PORTUGAL

Direcção do Serviço de Material
da Força Aérea
Rua de Escola Politécnica 42
Lisboa
Attn: AGARD National Delegate

TURKEY

Department of Research and Development (ARGE)
Ministry of National Defence, Ankara

UNITED KINGDOM

Defence Research Information Centre
Station Square House
St. Mary Cray
Orpington, Kent BR5 3RE

UNITED STATES

National Aeronautics and Space Administration (NASA),
Langley Field, Virginia 23365
Attn: Report Distribution and Storage Unit

THE UNITED STATES NATIONAL DISTRIBUTION CENTRE (NASA) DOES NOT HOLD
STOCKS OF AGARD PUBLICATIONS, AND APPLICATIONS FOR COPIES SHOULD BE MADE
DIRECT TO THE NATIONAL TECHNICAL INFORMATION SERVICE (NTIS) AT THE ADDRESS BELOW.

PURCHASE AGENCIES

Microfiche or Photocopy

National Technical
Information Service (NTIS)
5285 Port Royal Road
Springfield
Virginia 22151, USA

Microfiche

Space Documentation Service
European Space Agency
10, rue Mario Nikis
75015 Paris, France

Microfiche

Technology Reports
Centre (DTI)
Station Square House
St. Mary Cray
Orpington, Kent BR5 3RF
England

Requests for microfiche or photocopies of AGARD documents should include the AGARD serial number, title, author or editor, and publication date. Requests to NTIS should include the NASA accession report number. Full bibliographical references and abstracts of AGARD publications are given in the following journals:

Scientific and Technical Aerospace Reports (STAR),
published by NASA Scientific and Technical
Information Facility
Post Office Box 8757
Baltimore/Washington International Airport
Maryland 21240, USA

Government Reports Announcements (GRA),
published by the National Technical
Information Services, Springfield
Virginia 22151, USA



Printed by Technical Editing and Reproduction Ltd
Harford House, 7-9 Charlotte St, London W1P 1HD

ISBN 92-835-0180-2